Rift Architecture and Caldera Volcanism in the Taupo Volcanic Zone, New Zealand

A thesis submitted in fulfilment of
the requirements for the degree of

Doctor of Philosophy in Geology

at the
University of Canterbury
By

Karl D. Spinks

1. Text & References

University of Canterbury
2005

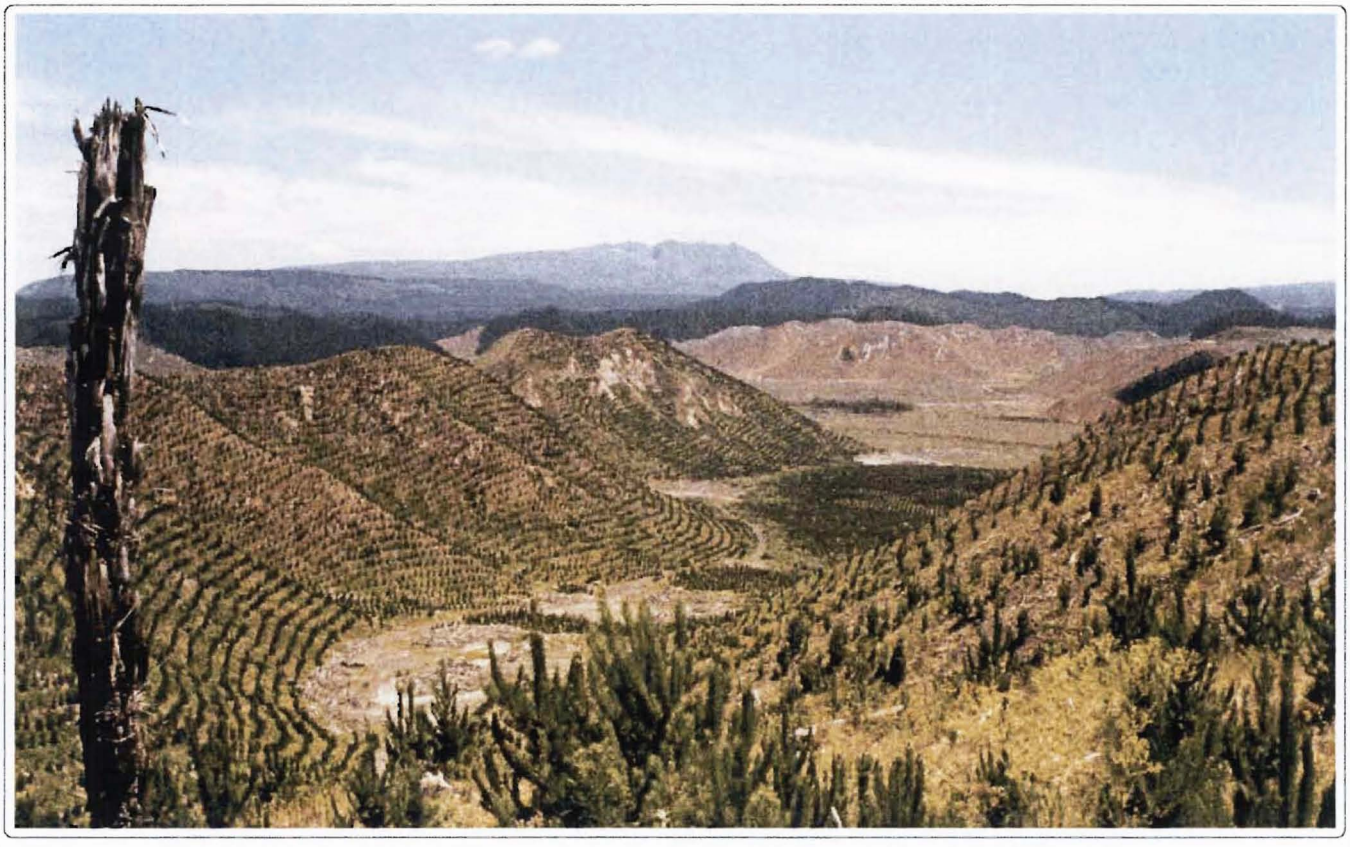

Looking southwest from Puhipuhi basin toward Mt Tarawera, Okataina Caldera Complex, Taupo Volcanic Zone. The 1886 basaltic rift is visible as a cleft in the skyline on top of the Tarawera Rhyolite dome complex. Puhipuhi basin forms a subsidiary volcano-tectonic basin filled with young pyroclastic flows. It formed adjacent to the caldera where the local rift segment axis and caldera intersect; the Tarawera rift is the intra-caldera expression of this rift axis.

Abstract

The Taupo Volcanic Zone (TVZ) is investigated to determine the interaction of regional structure and volcanism. A three-tiered approach is employed involving (i) analysis of rift geometry and segmentation in Modern TVZ (<300 ka) from remote sensing and digital topographic data; (ii) fault kinematic data collected along the length of TVZ; and (iii) combining new and existing volcanological data for TVZ. Modern TVZ is a NNE-SSW trending intra-arc rift zone, subject to dextral transtension, and characterised by a segmented axial rift zone with a number of offset and variably oriented rift segments. These segments are subject to varying degrees of extension, and a general correlation exists between the amount of extension and the volume and style of volcanism in each segment. Segments with the highest degrees of extension correspond to the Okataina and Taupo Caldera Complexes in the central rhyolitic zone of Modern TVZ, while segments with a higher degree of dextral transtension correspond to the volumetrically-subordinate andesitic extremities.

The influence of the structural framework on the shape and formation of calderas in Modern TVZ has been inferred from remote sensing and ground-based structural analysis. Detailed analysis of caldera structure and geometry in Modern TVZ indicates that caldera evolution is largely a function of caldera location relative to the axial rift zone. Calderas peripheral to the rift are simple, single-event structures, while those located within the axial rift zone are multiple-event caldera complexes with geometries dictated by their coincidence with rift faulting. These results show that in Modern TVZ the type, volume, and spatial distribution of magmatic activity is strongly influenced by rift structure and kinematics.

The inter-relationship between rift geometry and caldera-complex development is particularly clear at the intra-rift Okataina Caldera Complex (OCC). OCC is located at a step-over in the rift where local rotation of the extension direction accompanies the development of a major transfer zone. Three main collapse events are spatially concentrated in a zone of orthogonal extension within the transfer zone. The 28 x 22 km OCC is elongate parallel to the extension direction, with a complicated topographic margin largely controlled by regional faulting. Major embayments occur on each side of OCC where it is intersected by adjacent rift segments. These are contiguous with two intra-caldera dome complexes forming two overlapping linear

vent zones, which transect the caldera complex. The development of volcanism at OCC records the progressive interaction between offset rift segments and the propagation of overlapping rift segment axes. As rift propagation proceeded, a diffuse zone of volcanism progressively concentrated in the centre of the transfer zone then divided into two spatially restricted eruptive centres as through-going faults became established.

Field investigations at OCC reveal a major revision to the eruptive stratigraphy that has implications for the development of the caldera and for hazard assessment in northern TVZ. Kawerau Ignimbrite is a partially welded pumice-rich ignimbrite that fills Puhipuhi Basin on the eastern side of the caldera complex and forms a thick terrace in and around the Kawerau township area. Within Puhipuhi Basin it is ~100 m thick, exposed on clear-felled knolls and locally forms jointed bluffs in thickest sections where it is valley ponded. Originally mapped as Kaingaroa Ignimbrite, it was subsequently considered distinct and renamed Kawerau Ignimbrite by Beresford & Cole (2000) with an accepted age of 240 ka.

In Puhipuhi basin the Kawerau Ignimbrite overlies both the ~280 ka Matahina and ~65 ka Rotoiti ignimbrites and also the older tephras of the 43-31 ka Mangaone Subgroup. Whole-rock and glass geochemistry tie the ignimbrite specifically to the 33 ka Unit I eruptive phase of the subgroup, vastly increasing the eruptive volume of that unit and implying caldera collapse in this recent phase of OCC activity. Two pumice compositions are identified, reflecting eruption of two distinct magma bodies. Vertical variation in the ignimbrite records rapid depletion of a subordinate dacitic magma such that pumices of this composition are rare beyond proximal exposures. Lithic and pumice size distribution data indicate a source within OCC to the west of Puhipuhi basin. The residual volume of the ignimbrite is <15 km^3, but estimates of the original volume approach 50 km^3 when intra-caldera volumes are considered. Kawerau Ignimbrite thus represents the largest eruption from OCC in the last 65 ka since the Rotoiti event, and is the youngest partially-welded ignimbrite in TVZ.

CHAPTER 1
Introduction & Thesis Outline

CHAPTER 2
The Architecture, kinematics & volcanism of Modern TVZ

CHAPTER 3
Caldera volcanism in TVZ: influence of regional structure

CHAPTER 4
Effect of regional structure on 3D caldera geometry: a Review

CHAPTER 5
Structure and development of the Okataina Caldera Complex

Chapter Seven
Conclusions

CHAPTER 1 Introduction & Thesis Outline

1.1 GENERAL INTRODUCTION

The Taupo Volcanic Zone (TVZ) is the late-Pliocene–Quaternary locus of volcanism related to subduction of the Pacific plate beneath the North Island of New Zealand. Current estimates of erupted magma volumes in TVZ exceed 10,000 km^3. The vast majority is contributed by the central rhyolitic portion, which has been documented as the most frequently active and productive Quaternary silicic system on Earth (HOUGHTON *et al.*, 1995). Numerous papers have been published on the evolution, history, and structure of the zone, though many uncertainties remain. This study addresses several aspects of the volcanic and structural development of the zone, in light of new data on the architecture and kinematics of the zone and the relationship to volcanism.

Surprisingly few studies have considered the TVZ as a tectonic feature, or at least considered the structural and volcanic aspects together as one system. Relatively little is known about fault displacement and kinematics, the geometry of regional fault systems, and in particular, the relationship between regional deformation and volcanism. The origin of the marked compositional segmentation, and with it the disproportionate volume of silicic magma erupted from the central portion relative to the andesitic extremities, is contended by TVZ researchers, and remains poorly understood. Similarly, no model has sufficiently explained the restricted nature of active silicic vents. The relationship between the location and characteristics of calderas and the structure of the zone as a whole has not been explored. Specifically, the link between regional fault patterns and caldera-bounding fractures has not been investigated.

Many of the difficulties in elucidating the development of TVZ reflect its frequently active and productive nature. Older deposits and structures are rapidly buried or destroyed by regional faulting, caldera collapse and the voluminous products of younger eruptions. The abundant vegetation throughout TVZ and the prevalence of unconsolidated deposits makes outcrop exposure generally poor and mainly confined to road-cuts, quarries, and drainage channels. While many units are poorly exposed, there is excellent preservation of geomorphic surfaces. These range from shallow dipping ignimbrite plateau, to complex associations of silicic lava domes, caldera wall scarps, and regional faults. The segmented

nature of the rift system and the location and geometry of calderas and of the entire zone can be easily recognised from aerial and satellite images.

There is thus a need for a broad understanding of the structural-volcanic-magmatic associations and their relationships to the entire TVZ in space and time. This thesis considers TVZ on a variety of scales and by various methods, including the architecture, kinematics and geometry of the zone, the structure, geometry, and location of its calderas, and the volcanic and structural evolution of an active intra-rift caldera complex. By employing techniques not previously used in TVZ research, and by extensive investigation of the literature concerning structural-volcanic systems and calderas, a model of rift architecture and caldera volcanism is developed.

1.2 Research Objectives

The general aims of this thesis are to (a) document rift architecture and kinematics in TVZ, (b) model caldera volcanism in TVZ, and (c) derive a model for the evolution of Okataina Caldera Complex. To achieve these aims this thesis addresses the following ten objectives, with the relevant chapters in parentheses:

1. Determine rift structure, geometry and segmentation in TVZ (2).
2. Determine the kinematics of rifting in TVZ (2).
3. Investigate the relationship between rift architecture and kinematics, and the volume, composition, age and nature of volcanism in TVZ (2).
4. Determine the geometry and structure of Rotorua, Reporoa, Taupo and Okataina calderas in Modern TVZ (3).
5. Combine new morphotectonic data and existing geological and geophysical data to characterise TVZ calderas and evaluate the relationship between caldera volcanism and rift architecture in Modern TVZ (3).
6. Review the controls on the geometry and structure of calderas in a variety of tectonic regimes and in analogue modelling, and apply this to the model of caldera volcanism in TVZ (4).
7. Review and update the geology and eruptive history of Okataina Caldera Complex (5).
8. Delineate the margins of individual collapse events at Okataina Caldera Complex and provide a model for its development (5).

9. Determine the role of tectonics and regional structure in the evolution of Okataina Caldera Complex, and compare them with other examples in TVZ and elsewhere (5).

10. Investigate the distribution, lithology, geochemistry, stratigraphy, and emplacement of the Kawerau Ignimbrite at Okataina, and place it the the context of the evolution of Okataina Caldera Complex (6).

In addition to these ten objectives are more detailed objectives for each specific research area; these are outlined at the beginning of the relevant chapters.

1.3 Introduction to Research Methods

The methods employed in this thesis reflect a desire to understand TVZ at a variety of scales, for instance using field mapping and physical volcanology in combination with remote sensing and structural analysis. Perhaps the most beneficial was fieldwork at overseas volcanoes and volcanic regions, and learning the alternative methods used successfully outside TVZ. In this way the project was able to evolve with experience gathered during overseas fieldwork, particularly on a CEV 'inside calderas' field workshop to Glencoe, Scafell and Snowdon calderas in the UK in 1999, and a fieldtrip around the Campi Flegrei caldera and other volcanoes along the Tyrrhenian margin of central Italy in 2000. Field experience was also gained during visits to Crater Lake, Newberry and Mt St Helens in Oregon and Washington respectively, the various Hawaiian volcanoes, and on a field workshop through the southern central Andes in late 2004.

To determine the relationships between volcanism and tectonics in TVZ, two approaches have been taken (1) on a morphotectonic basis using remote sensing and Digital Elevation Model (DEM) data, and (2) ground-based structural analysis of fault kinematics. The influence of the structural framework on the location, geometry and development of calderas and caldera complexes is examined using morphotectonic mapping and field analysis combined with existing geologic data. An extensive critical literature review investigates the relationships between geodynamic setting and calderas worldwide as a basis for understanding the TVZ model. Geomorphic mapping and ground based structural analysis at Okataina Caldera Complex are used to reconstruct the collapse history and link the main geomorphic and structural features with its volcanic evolution.

Fieldwork investigates the distribution and character of pyroclastic deposits that are significant to understanding the eruptive history of Okataina Caldera Complex. Physical volcanological techniques establish the eruptive and depositional processes and constrain a source. Whole-rock and glass geochemistry are used to determine magmatic characteristics and correlate the deposits within the eruptive stratigraphy and development of the caldera complex.

1.4 THESIS OUTLINE

This thesis is a collection of connected studies that together provide a model for rift architecture and caldera volcanism in TVZ. Each chapter reflects a different aspect of this research and is largely independent. Some of the material is already published (the contents of chapters two and three, see appendices); since the thesis format is less restrictive it invariably contains more detail and is wider in its approach than are the published articles. Some of the data were also reconsidered and modified *after* manuscript submission, so this thesis contains the most recent analysis and interpretation. Adaptation of chapters five and six into manuscript form for publication is in progress.

This thesis is presented as three volumes: (I) text & references; (II) figures; and (III) appendices. This division is thought to promote ease of use and follows the common conventions of manuscript preparation. The contents of each volume are outlined in the following sections.

1.4.1 Volume I: Text & References

Volume I comprises seven chapters:

Chapter One gives a general introduction to the thesis, summarises the reasons for and objectives of the study, introduces the research methods, and provides a thesis outline.

Chapter Two describes rift architecture in TVZ through an original detailed analysis of remote sensing and Digital Elevation Model (DEM) data, and combines this with field studies and structural data to consider the relationship between regional structure and volcanism in TVZ.

Chapter Three combines morphotectonic mapping and field work at TVZ calderas to describe their structure and geometry. These data are combined with existing geological and geophysical data to develop a model for caldera volcanism in TVZ.

Chapter Four considers the controls on caldera geometry and structure through an extensive literature review. The results of modern caldera research are applied to the results of chapters two and three.

Chapter Five makes a detailed analysis of one specific TVZ caldera – Okataina Caldera Complex. The eruptive history of the caldera and surrounding centres are reviewed and revised, the caldera morphology, structural characteristics and collapse history are established, and a model is generated for its structural and volcanic evolution.

Chapter Six describes the physical and chemical characteristics of the Kawerau Ignimbrite from Okataina, and discusses the implications of a considerable age change requiring a major revision to the eruptive stratigraphy at Okataina.

Chapter Seven presents the conclusions of the thesis, and makes suggestions and comments regarding future work.

1.4.2 Volume II: Figures

Volume II of the thesis contains the figures, arranged by chapter.

1.4.3 Volume III: Appendices

Volume III contains a number of additional documents associated with this research, and the data collected during this research and reported in this thesis. The authors contribution to each paper is outlined at the beginning of each appendix.

Appendix A

The early results and analysis of the rift architecture and kinematics work presented in this thesis (chapter two) were compiled in a paper published in 2003 in *Tectonics*:

> ACOCELLA, V.A., **SPINKS, K.D.**, COLE, J.W. & NICOL, A. (2003) Oblique back-arc rifting of Taupo Volcanic Zone, New Zealand. *Tectonics*, 22 (4), 1045, doi: 10.1029/2002TC001447

Appendix B

Aspects of the rift architecture and caldera structure research (chapters two and three) were combined with existing volcanological data and constrained by the previously published structural data in an invited manuscript for a special volume of the *Journal of Volcanology and Geothermal Research* in 2003:

SPINKS, K.D., ACOCELLA, V.A, COLE, J.W. & BASSETT, K.N. (2005) Structural control on volcanism and caldera development in the transtensional Taupo Volcanic Zone, New Zealand. *Journal of Volcanology and Geothermal Research*, Special Volume: Tectonics & Physics of Volcanoes; vol. 144: 7-22

Appendix C

This major review paper on calderas was compiled over the last four years as part of a major University of Canterbury research program into the structure and development of calderas.

COLE, J.W., MILNER, D.M. & **SPINKS, K.D.** (2005) Calderas and caldera structures: a review. *Earth Science Reviews* 69: 1-26

Appendix D

In December 2004 a three-day field trip was organised to immediately follow the annual Geological Society of New Zealand (GSNZ) conference in Taupo, New Zealand. The field guide material was generated largely from this thesis.

SPINKS, K.D., COLE, J.W. & LEONARD, G.S. (2004) Caldera volcanism in the Taupo Volcanic Zone. *In*: MANVILLE, V. (ed.) Field Trip Guides, *Geological Society of New Zealand Miscellaneous Publ*ication 117B, 111-135

Appendix E

In late 2000 I.A. NAIRN of 'Geological Investigations Ltd' commissioned a research project to examine the recently exposed breccias of the Waiohau Pyroclastics, Tarawera Volcanic Centre. This was part of a major research program, led by I.A. NAIRN, studying the eruptive history and hazards associated with the Tarawera Volcanic Complex. Fieldwork was carried out in January and February 2001, alongside ongoing work in the Puhipuhi Basin of Okataina Caldera Complex.

SPINKS, K.D. (2001) Block and ash flows of the Waiohau Eruptive Episode. *Unpublished report prepared for* 'Geological Investigations Ltd'. pp 1-15

CHAPTER 2 The architecture, kinematics & volcanism of Modern TVZ

2.1 INTRODUCTION

Understanding the interaction of regional structure and volcanism is a major task in defining the evolution of rift zones and magmatic provinces. Such an understanding requires a sufficient knowledge of the overall structural and volcanic features of a region as well as their mutual relationships. Of particular importance are the geometry (general architecture and segmentation) and kinematics (direction and magnitude of extension) of a rift zone. Primary volcanic parameters to consider include the volume, composition, and age of eruptive products, and the type of volcanic edifice (stratovolcanoes, calderas, domes, vents and fissures). Analysis of rift geometry and fault kinematics allows a greater understanding of the relationships between the formation and evolution of rifts, magmatic activity, and regional plate tectonics.

Of principal interest is the effect of tectonics on the rise, emplacement and eruption of magmas under conditions of pure and oblique convergence (NAKAMURA, 1977; GLAZNER, 1991; TIKOFF & MICHEL DE SAINT BLANQUAT, 1997; ACOCELLA & ROSSETTI, 2002). In these settings, the rise of magmas forming a volcanic arc is typically controlled by strike-slip structures, such as observed in the central Andes (DE SILVA, 1989), NE Japan (SATO, 1994), and Mexico (TIBALDI, 1992). Nevertheless, localised areas of rifting may also form within convergent settings, as observed along the Taupo Volcanic Zone of New Zealand (COLE, 1990) or the Tyrrhenian margin of Italy (MALINVERNO & RYAN, 1986). To study these situations, specific consideration must be given to the interaction between strain rates and magmatism (e.g. PATERSON & TOBISCH, 1992; PETFORD *et al.*, 2000), and how tectonics influences magma composition and eruption styles (e.g. GROCOTT *et al.*, 1994; RILLER *et al.*, 2001). The evolution of continental extensional fault systems has been the focus of much recent research (e.g. ROSENDAHL *et al.*, 1986; COWARD *et al.*, 1987; MORLEY *et al.*, 1990; ROBERTS *et al.*, 1991; GUDMUNDSSON *et al.*, 1993; MCCLAY & WHITE, 1995; ACOCELLA *et al.*, 1999; ACOCELLA *et al.*, 2000), and an improved understanding of rift zone structure and kinematics may also further constrain the mechanisms of extensional systems at convergent margins and the dynamics of plate convergence in general (*e.g.* TAYLOR *et al.*, 1994; UPTON *et al.*, 2003, and references therein).

Within this framework, the structure and kinematics of TVZ are examined using satellite and shaded relief imagery and field structural data throughout TVZ. Two principal questions drive this research: 1) what is the style of rifting in TVZ, and in particular, has TVZ formed in association with orthogonal or oblique rifting; 2) is there an observable relationship between rift geometry and kinematics and volcanism?

2.2 TVZ AND ITS TECTONIC SETTING

The Tonga, Kermadec, and Taupo arcs are segments of a relatively contiguous 2000 km long arc – back-arc system developed at the convergent plate boundary between the Pacific and Australian plates (Fig. 4.1a). The Lau Basin – Havre Trough back-arc basin and the associated intra-continental rifting of Taupo Volcanic Zone (TVZ) has long been recognised as an active back-arc system (e.g. KARIG, 1970a, b) related to westward subduction of the Pacific plate, and is a rare case where arc – back-arc processes and structure can be studied across an oceanic-continental crust transition. Westward subduction of the Pacific Plate beneath the Australian Plate has formed the Taupo-Hikurangi arc-trench system (COLE & LEWIS, 1981), and this is largely contiguous with the Kermadec Arc - Havre Trough system to the north; the boundary between active back-arc extension in TVZ and that of the Havre Trough however is offset in a complex *en echelon* style north of New Zealand (CARTER, 1980; WRIGHT, 1992; Fig. 4.1a). Oblique subduction along the Hikurangi Margin began during the early Miocene (BALLANCE, 1976; RAIT *et al.*, 1991) with the current orientation resulting in relative plate motion trending between 40° and 70° to the strike of the margin at c. 38-50 mm/yr (DEMETS *et al.*, 1994) (Fig. 1a). Many geologic and geodetic studies have helped to define the dynamics of the margin and its expression across the plate boundary zone (e.g. WALCOTT, 1978; COLE & LEWIS, 1981; COLE, 1990; CASHMAN *et al.*, 1992; DEMETS *et al.*, 1994; DARBY & MEERTENS 1995; DAVEY *et al.*, 1995; BEANLAND *et al.*, 1998; BEANLAND & HAINES, 1998; NICOL & BEVAN 2003; UPTON *et al.*, 2003). Oblique convergence across this part of the plate boundary zone is believed to be partitioned into contractional and strike-slip components of deformation in the over-riding plate (CASHMAN et al., 1992; BEANLAND & HAINES, 1998; WEBB & ANDERSON, 1998), manifest as three main active fault provinces: imbricate reverse faulting associated with the accretionary wedge at the subduction interface; a belt of dextral faulting at the back of the forearc; and predominantly normal faulting within the intra-arc TVZ.

TVZ is a volcano-tectonic zone of Quaternary calk-alkaline volcanism and intra-arc rifting in the North Island of New Zealand (Fig. 1b), associated with a highly thinned crust of 15 km (BIBBY *et al.*, 1995). Volcanic activity in TVZ began at ~2 Ma (HOUGHTON *et al.*, 1995) and was accompanied by rifting at c. 1.1 Ma (WILSON *et al.*, 1995). WILSON *et al* (1995) emphasise that the early geological record is concealed by the eruptives of the Whakamaru Caldera (c. 0.32 Ma). Data for the volcanic and structural evolution of TVZ following the Whakamaru events are considerably more complete and thus this study considers only this time frame of TVZ evolution. In the last 300 ka (HOUGHTON *et al.*, 1995) active volcanism and extension has been focused in a 250 km long NNE-SSW trending zone extending from Ruapehu in the south to White Island in the north. This zone is referred to as 'modern TVZ' (Fig. 2.1; ACOCELLA *et al.*, 2003; SPINKS *et al.*, *in press*; Appendix I & II respectively), and represents a temporal-spatial zone for which we can study both structural and volcanological aspects of its evolution. This definition differs from the use of 'modern TVZ' in WILSON *et al* (1995) and more closely corresponds to their 'young TVZ'. Modern TVZ is divided into three parts along its length (Fig. 1b): (a) a central part (from Okataina to Taupo) dominated by rhyolitic caldera volcanism responsible for at least 34 ignimbrite eruptions (WILSON *et al.*, 1984, 1995; COLE, 1990; HOUGHTON *et al.*, 1995; GRAHAM *et al.*, 1995); (b) two lateral parts characterised by andesite-dacite stratovolcanoes (WILSON *et al.*, 1995, WILSON, 1996; HOUGHTON *et al.*, 1995). This central section is an extraordinarily productive region of rhyolitic volcanism (~0.28 m^3s^{-1}) and geothermal fluxes (~4200 MW) unparalleled on the planet (WILSON, 1996).

Geodetic and geophysical data dominate our current understanding of the kinematics of extension in TVZ (e.g. SISSONS, 1979; STERN & DAVEY, 1987; DARBY & MEERTENS, 1995). Reported surface faults in TVZ have been described as steeply dipping normal faults that vary in strike between 040° and 080° (COLE, 1990). Relative displacement of tephras shows that many of the faults have moved within the last 10,000 years (e.g. NAIRN, 1971), yet structural observations are impeded by poor exposure. Existing fault maps are typically produced by fault trace mapping using aerial photo analysis (GRINDLEY, 1960; HEALY *et al.*, 1964; NAIRN *et al.*, 1998; maps published by the Institute of Geological and Nuclear Sciences (IGNS)) and constitute the largest structural dataset (ROWLAND & SIBSON, 2001).

Extensional strain is thought by most researchers to be accommodated by steeply dipping normal faults. Data presented by BERRYMAN & VILLAMOR (1999) suggest that deformation may young towards the axis of the extensional system. No strike-slip faulting has previously been documented, although there has been some controversy regarding the existence of strike-slip faulting within TVZ. The main arguments in support of strike-slip motion in TVZ are: 1) steeply-dipping faults (e.g. GRINDLEY *et al*, 1994); 2) *en echelon* fractures and eruptive fissures (NAIRN & COLE, 1981; COCHRANE & TIANFENG, 1983; COLE, 1990); 3) intersection of dextral faults within the North Island Dextral Fault Belt (NIDFB) with TVZ basement (COLE, 1990); and 4) first motion studies on focal mechanisms of microearthquakes indicating strike slip components (SMITH & WEBB, 1986). A regional strike-slip component has also been proposed for TVZ (COLE & LEWIS, 1981; WALCOTT, 1984; COLE, 1990); however recent work in TVZ (ROWLAND & SIBSON, 2001) suggests predominantly normal dip-slip faulting. Recent results from geological mapping (ROWLAND & SIBSON, 2001) and GPS surveys (DARBY & MEERTENS, 1995; DARBY *et al.*, 2000) suggest predominantly orthogonal rifting in TVZ, and give an extension rate of 8 ± 4 mm/yr along an azimuth of 124 ± 13° (DARBY & MEERTENS, 1995). Significantly, prior to this study, structural evidence at the surface for significant strike slip faulting had not been documented.

2.3 PHYSIOGRAPHY AND STRUCTURE OF TVZ

2.3.1 General Physiography

Figure 2.2 provides an oblique aerial perspective of onshore TVZ looking SSW down the axis of the arc from the Bay of Plenty toward the Tongariro volcanoes. TVZ comprises an intra-arc axial rift zone flanked by extensive ignimbrite plateau. Four main tectonic units may be defined (Fig. 2.2b): the axial rift zone; Taupo-Reporoa Basin; Mamaku Plateau; and Kaingaroa Plateau. In the north and west, the Mamaku Plateau extends to the Hauraki Rift northwest of TVZ and in the east the Kaingaroa Plateau extends toward the axial ranges. Both eastern and western sides of TVZ are bound by ranges of basement rocks although structural boundaries are poorly defined at the surface. While the general trend of TVZ is northeast, the axial rift is not a straight or continuous feature, but forms a number of sub-parallel segments. The central and widest part of TVZ from Taupo to Okataina is particularly complex; it contains the rhyolitic calderas, numerous rhyolite domes and dome complexes, and is formed by a series of offset rift segments. Some of the recognised calderas are conspicuous while older structures (i.e. those not part of modern TVZ) are obscured by overprinting of younger volcanism and tectonic activity. The two

monogenetic and smallest calderas, Rotorua and Reporoa, are notably located within modern TVZ but outside of the central rift axis, while the oldest caldera (Mangakino) occurs west of modern TVZ.

2.3.2 Satellite Imagery

Landsat images have been a key component in analysis of volcanic terrains both terrestrially and on the planets (e.g. FRANCIS *et al.*, 1978; FRANCIS & BAKER, 1978; FRANCIS & DE SILVA, 1989; DE SILVA & FRANCIS, 1991; MOUGINIS-MARK & ROWLAND, 2001). The availability of Landsat Multispectral Scanner (MSS) data in 1972 also directly led to discovery of volcanic structures in the Central Andes e.g. Cerro Galan caldera (FRANCIS & BAKER, 1978), and the introduction of Landsat Thematic Mapper (TM), with improved spatial and spectral capabilities, enhanced the use of satellite images as a geological tool. The synoptic view provided by Landsat imagery allows regional mapping of structural and physiographic patterns over a large area, and aspects of caldera evolution and magma storage systems (e.g. MOUGINIS-MARK & ROWLAND, 2001).

OLIVER (1978) used Landsat MSS imagery in a survey of broad structural characteristics of New Zealand, including the Taupo – Hawke Bay area as part of the major NASA Landsat II investigation. The majority of lineaments identified were in the heavily dissected Mesozoic basement rocks of the NISB, with very few defining TVZ structure. COCHRANE & TIANFENG (1983) reinterpreted the same image used by OLIVER (1978), adding lineaments and providing structural interpretation for faulting in Taupo Volcanic Zone (Fig. 2.3). Using both the satellite image and aerial photos they provide evidence for horizontal shear displacement at several key localities, suggesting that faults in TVZ, widely interpreted as normal, may have a significant component of dextral strike-slip motion. They also identify several major NW-trending 'basement' faults which are continuous across the TVZ (Fig. 2.3b) and which they observe as consistent with HOCHSTEIN & HUNT'S (1980) map of gravity anomalies.

A Landsat 7 TM image covering the entire TVZ and extending east to Hawke Bay (Fig. 2.3a) was analysed in an attempt to assess the structural architecture of the central North Island, and to compare with previously collected datasets. An increase in resolution from 80 m pixel size (MSS: OLIVER, 1978; COCHRANE & TIENFENG, 1983) to 30 m pixel size (TM: this study) justifies this reassessment. While other studies incorporating satellite data have been very successful in volcanic terrains, the central North Island of New Zealand is

densely vegetated, in contrast to the arid and unvegetated environments typical of other examples of studies using satellite imagery. The image presented in figure 2.4a is a colour composite image created from a combination of spectral bands 7, 5, and 4, which provided the clearest image of regional structure. Figure 2.4a highlights the contrasting physiographic and land-use terrains in the central North Island. Mesozoic basement rocks constitute a major structural element of the image, forming the dissected NNE-trending ranges extending from bottom-centre to top-right of the image, and to the west of Lake Taupo. Their yellow-brown colour contrasts with the varied appearance of the agricultural land and plantation forest that dominate the low-lying areas. Sharp colour changes reflect the boundaries of plantation forest; the brown and blue colours relate to forested and deforested land respectively.

Lineaments

A lineament map was generated from the Landsat image (Fig. 2.4b). Lineaments are lines or edges of presumed geologic origin, visible on remotely sensed images (CAMPBELL, 1987). CAMPBELL (1987, p. 439) notes that controversy may arise when judging the geological significance of these features. For this reason, a conservative approach is taken, and only clearly discernible lineaments are shown, in line with other studies (e.g. NOVAK & SOULAKELLIS, 2000).

The lineaments observed (Fig. 2.4b) are largely consistent with those of OLIVER (1978) and COCHRANE & TIANFENG (1983), although there is no evidence for the major NW-trending faults identified by COCHRANE & TIANFENG (1983). The main features are thus a curvilinear belt of N-S – NE-SW trending lineaments within the NISB, and the few lineaments that define the NNE-trending TVZ. Lineaments of the NISB vary in trend along the length of the image from predominantly N-S east of central TVZ, to NE-SW in the Kaimanawa Ranges east of Tongariro Volcanic Centre in the south. While they do not continue through TVZ, it is notable that these structures intersect TVZ at its northern and southern extremities, the portions of TVZ restricted to andesitic volcanism. Within TVZ itself, scattered NE-trending lineations reflect the major fault scarps with significant topographic expression. The major vent lineations of Tongariro and Tarawera volcanic centres are conspicuous; other features are too subtle and/or masked by vegetation cover.

2.3.3 Shaded-Relief and Surface Imagery

Digital topographic data enables morphotectonic analysis through a variety of easily manipulated image types. *Shaded relief images* indicate the local orientation of a surface relative to a light source direction, and rotating the light source highlights geomorphic features of various orientations. *Surface images* are three-dimensional surface renderings of topographic grid data and provide a unique visual interpretation of the data. Detailed shaded relief and surface images generated for segments of TVZ have been analysed as a series of small segments and as mosaics covering large parts of TVZ. An accurate Digital Elevation Model (DEM) produced by Landcare Research New Zealand Ltd was used to generate these images. The DEM was produced from the Land Information New Zealand 1:50,000 scale topographic database and has a grid separation of 25 m. The DEM has vertical precision of 1 m, and preliminary estimates of DEM accuracy suggest an RMSE of approximately 7-8 m (LANDCARE RESEARCH, *writ. comm.*, 2002).

The physiography and structure of onshore TVZ is described in four sectors from south to north (Fig. 2.5). Sector boundaries are arbitrary, but placed to divide TVZ into four major geomorphic zones of roughly equal size. While extremely detailed studies have been made using digital topographic data to map lineaments (e.g. SOENGKONO, 1999, 2000), WISE (1982) warns against such 'over-analysis'. Only clearly discernible lineaments with an effective surface length greater then 2 km are delineated in this study, reflecting the desire for an entire-rift scale analysis. Lineaments are classified as either: (1) 'faults', where relative displacement is clear, generally across well-developed topographic escarpments; (2) 'tectonic lineaments', all other regional scale lineaments of supposed tectonic origin; and (3) 'vent lineaments', lines or linear zones connecting volcanic eruptive vents. The lineament dataset generated in this study is entirely independent of existing fault maps and known surface geology. All shaded relief images in this chapter relate to an apparent light source direction from the northwest (N45°W), at 55° from the horizontal, although mapping has incorporated the use of multiple images using a systematic rotation in lighting direction.

2.3.4 Tongariro Sector

The Tongariro Sector (Fig. 2.6) is characterised by the juxtaposition of the Kaimanawa Ranges in the east with the Quaternary composite volcanoes of the Tongariro Volcanic Centre (TgVC). The Kaimanawa Ranges consist of Mesozoic basement greywacke (GRINDLEY, 1960) forming the main axial ranges of the North Island. A thin covering of

Tertiary marine sediments (GRINDLEY, 1960) overlies basement rock to the southeast, south and west of Ruapehu.

Volcanic Morphology

TgVC is a complex of four andesite composite volcanoes: Kakaramea, Pihanga, Tongariro and Ruapehu, and forms the southern portion of TVZ (Fig. 2.6; COLE, 1978). Ruapehu volcano (2797 m) has a cone volume of 110 km^3 (HACKETT & HOUGHTON, 1989) and is a roughly symmetrical composite volcano with an extensive ring plain that forms a rectilinear southern terminus to TVZ. The c. 2.5 km x 1 km N-S elongate summit area of Ruapehu contains several craters and gives the volcano a truncated appearance from the ground. Four cone-building phases over at least 250 ka (HOUGHTON *et al.*, 1987) are represented on the flanks of the volcano as lava flows with varying stages of dissection; the smooth surfaces of geomorphically youthful lavas contrasting with the eroded surfaces of older lavas. Much of the summit area is permanently glaciated and the upper flanks of the volcano are cut by steep-walled glacial valleys. West of Ruapehu, the isolated Hauhungatahi plateau comprises andesitic lavas and pyroclastics overlying Tertiary sediments, and represents the remains of a significantly older volcanic complex (~ 0.8 Ma, CAMERON *et al.*, 2003).

Tongariro massif is only slightly smaller than Ruapehu with a similar sized ring plain and a broad summit area consisting of several coalescing cones forming a NNW-elongate summit region. The largest component of the complex is the geomorphically youthful Ngauruhoe cone, located at the head of oppositely directed glacial valleys, and considered to have formed over the last 2.5 ka (COLE *et al.*, 1986). Growth of the massif has been steady since at least 275 ka, with several intervals of vigorous cone growth (HOBDEN *et al.*, 1996), and intervening periods of extensive glaciation and dissection. Youthful topographic profiles of the summit area contrast with the dissected older flows on the flanks of the massif. A young (3400-9700 yr b.p.) lava flow on the east side of the massif extends from its source at Red Crater area 6.5 km down an old glacial valley, with a volume of c. 371-640 km^3 calculated from airborne interferometric radar data (STEVENS, 2002).

Kakaramea is heavily dissected by NNE-trending faults and possible vent features can only be identified towards the east of the massif. Pihanga massif, to the southeast of Kakaramea, has well-formed cones and craters, with conspicuous vents concentrated in a

NNE-trending graben on the northwestern flank of the symmetrical Pihanga cone. Lake Rotoaira occupies the depression between Pihanga and Tongariro massifs.

The main (<50 ka) vents for Ruapehu and Tongariro define a strong NNE-trending continuous lineation; in detail however vents are scattered over a narrow (2-3 km wide) NNE-trending zone. NAIRN *et al* (1998) suggest that post-glacial (<15 ka) vents are arranged in a left-stepping en echelon pattern with discontinuous NE-trending segments. Young vents of Pihanga occur on the same trend as those for the Ruapehu and Tongariro massifs.

Tectonic morphology

The extensive ring plain of the TgVC volcanoes is constrained to the east by the Kaimanawa Ranges, where the linear range-front reflects down-faulting of basement to the west along regional NNE-trending faults. This essentially defines the east side of a ~30 km wide graben defined by NNE-trending regional faulting and filled with Quaternary volcanics. ESE-trending tectonic lineaments form a linear southern margin to the TgVC ring plain forming a rectilinear southern terminus of TVZ. The western margin is less constrained, where volcaniclastics of the TgVC ring plain intersect and partially infill valley systems in basement rocks west of TVZ.

Faulting within the graben defines a NNE-trending ~18 km wide axial rift zone, parallel to the major linear vent zone of Ruapehu and Tongariro volcanoes. Faults dip towards the eruptive centres, and graben-bounding fault zones on the flanks of Tongariro converge to the SW in the saddle between Tongariro and Ruapehu; to the NE they bound a low area containing Lake Rotoaira. A 4 km wide NNE-NE trending fault zone dissects Kakaramea and continues northeast as the major east-facing Waihi Fault scarp along the western shore of Lake Taupo. Extensive faulting at the southwest end of Lake Taupo is concurrent with hydrothermal activity and has been the site of at least two fatal landslides in historical time (HEGAN *et al.*, 2001). The timing of faulting is poorly constrained, but NAIRN *et al* (1998) suggest most TgVC faults have been active in post-glacial time.

The parallel fault and vent patterns, and location of vents axial to major grabens strongly indicates a tectonic influence on vent location. Alignment of older vents is less constrained, and early eruptive centres appear more widely spaced, suggesting recent volcanic vent alignments are in response to a young tectonic stress pattern. The traces of

NE-trending tectonic lineaments in the Kaimanawa Ranges do not extend into the TgVC, but it is likely they intersect with the TgVC at depth.

2.3.5 Taupo Sector

Northeast of the Tongariro sector the boundaries of TVZ are less well defined, and form a wide shallow basin with Lake Taupo filling the axial rift zone. Topographic relief in this sector is subtle, and positive topographic features relate mainly to a basement high west of Lake Taupo and volcanic domes and cones in and around the Taupo Volcanic Centre.

Volcanic Morphology

Lake Taupo is the largest lake in TVZ, and New Zealand, with an area of 620 km^3 and a volume of ~60 km^3 (MANVILLE *et al.*, 1999). Its geometry reflects infilling of a large volcano-tectonic depression formed during multiple collapse of the Taupo Caldera in the north part of the lake (COLE *et al.*, 1998). The largely planar surfaces east and west of Lake Taupo reflect the shallow dip of non-welded ignimbrite surfaces dipping back towards the source caldera. Lake margins are broadly rectilinear and comprise a series of roughly parallel NNE-trending scarps; in the north these control a scalloped caldera margin. The early history of Taupo volcanic centre (prior to 65 ka) is poorly constrained by age data but is thought to have been active over ca. 300 ka, represented by rhyolite and dacite domes and associated pyroclastics (SUTTON *et al.*, 1995; Fig. 2.7) which surround Lake Taupo. The eruptive morphology of rhyolite lavas is poorly preserved along the north margin of Lake Taupo; the Tauhara andesite-dacite complex to the east of Taupo city comprises a number of well-preserved cones and lava flows. Inferred vent locations for both domes and cones around the Taupo volcanic centre define NNE-trending lineations.

Tectonic morphology

The fault zone extending from Kakaramea through the NE block-faulted margin of Lake Taupo and continuing northeast towards Waiotapu was named the Taupo Fault Belt by GRINDLEY (1960). The precipitous southwestern shore of Lake Taupo extends NE from Kakaramea and represents a major volcano-tectonic fault forming the west side of a half-graben associated with caldera collapse in the north of Lake Taupo. NNE-trending faults are conspicuous on the northern shore of Lake Taupo where they bound a series scalloped embayments and there is a marked orientation change of ~15° between those intersecting the northern and southwestern shores of the lake. Parallel fault and vent lineaments indicate that eruptive vents are strongly influenced by regional structure, and the geometry

of the lake suggests the structural influence of similar trending features. A major scarp to the west of Lake Taupo effectively forms the western margin to TVZ where volcanics are juxtaposed against basement rocks forming the western graben wall.

2.3.6 Whakamaru Sector

The Whakamaru sector encompasses the width of modern TVZ and in particular, highlights the restricted zone of active volcanism and tectonism comprising the axial rift zone.

Volcanic Morphology

Within the area of figure 2.8 two main volcanic domains are identified: 1) the axial rift zone, and 2) the variably dissected ignimbrite plateau extending as the flanks of TVZ toward the axial ranges. The axial rift zone is characterised by dissected ignimbrite surfaces and rhyolite domes of the Maroa Dome complex and the Western and Northwestern dome belts. The Maroa complex comprises a coalescing series of well-preserved domes arranged mainly along a series of NE-trending lineaments. Domes are generally small (commonly <3 km) and form stubby steep-sided protrusions, with few lateral flows. Western dome belt lavas are conspicuously truncated on their eastern sides and many of these may originally have been much larger dome structures. East of the axial rift zone, the surface is largely planar and undissected. The Taupo-Reporoa Basin extends northeast from Taupo to Waiotapu where it sits between the eastward-dipping Paeroa block and the westward facing Kaingaroa Fault scarp. The northern part of the basin constitutes the 0.24 Ma Reporoa Caldera (NAIRN *et al.*, 1994) and the Waiotapu geothermal field, bounded to the north by Maungaongaonga and Maungakakaramea dacite cones. The caldera is notable for its well preserved eruptive morphology and simple geometry, in contrast to the poorly-defined intra-rift Whakamaru caldera to the west within this sector and Taupo caldera to the southwest. To the east of the Taupo-Reporoa Basin, the Kaingaroa plateau extends eastward towards the axial ranges. East and southeast of the Reporoa Caldera, the Kaingaroa Ignimbrite (0.24 Ma, BERESFORD & COLE, 2000a) caps the plateau with clear fan-like geomorphic expression. The variably dissected surfaces to the east represent older ignimbrites extending toward the axial ranges. STAGPOOLE (1994) shows the Kaingaroa Plateau consists of 650 m of ignimbrites overlying 'greywacke' basement. The plateau represents a subsided block of sub-volcanic basement relative to the axial ranges in the east, but clearly has not been part of the active TVZ rifting. Minor

dome and lavas are exposed at the surface within the Taupo-Reporoa Basin (TRB) adjacent to the Reporoa Caldera.

Tectonic Morphology

The Paeroa Fault scarp has considerable relief (400+ m) and it defines the southeast margin of the ~18 km wide NNE-trending Taupo Fault Belt, a heavily faulted transtensional graben (ACOCELLA *et al.*, 2003, Appendix A) with an axis defined by opposite verging scarps. Visible deformation is restricted to the zone between the Paeroa and Horohoro fault scarps. Surface fault traces are laterally discontinuous but extend into the Maroa dome complex. Typically planar ignimbrite surfaces are strongly tilted and displaced vertically by NE-trending faults. The Paeroa scarp appears to comprise a number of structural elements that form a left-stepping en echelon pattern that may indicate dextral shear. Many domes of the Maroa complex are cut by faults parallel to the vent lineations, consistent with the NE-trending regional structure. The N-S trending Western Dome Belt (c. 250-320 ka, HOUGHTON *et al.*, 1991) to the west of Maroa Dome Complex is cut by a segmented N-S trending fault, forming a number of step-over like geometries. The Horohoro Fault scarp, 16 km to the northwest, is not as continuous as the Paeroa scarp, but defines the northwest structural margin of the Taupo Fault Belt. East of this scarp, the 0.22 Ma Mamaku Ignimbrite, erupted from Rotorua Caldera to the north, is down-faulted and is not exposed in the graben, although present in drill core (MILNER *et al.*, 2003). A less obvious set of discontinuous NNW-trending lineaments also dissect this region of the axial rift. To the north, NE-trending faults of the axial rift zone show a systematic easterly rotation in strike with proximity to the Okataina Volcanic Centre.

2.3.7 Okataina Sector

This sector of TVZ (Fig. 2.9) highlights the contrast between the narrow axial rift zone and the adjacent ignimbrite plateau, and contains two clearly different caldera structures, Okataina and Rotorua, located within and outside from the axial rift zone respectively.

Volcanic Morphology

The area west of the axial rift zone and surrounding Lake Rotorua is dominated by the Mamaku Plateau, the largest preserved ignimbrite plateau in TVZ. The Mamaku Plateau is capped by the welded Mamaku Ignimbrite, covering an area of >3200 km^2 (MILNER *et al.*, 2003). Mamaku Plateau is boarded in the north by the Kaimai Range and Tauranga Basin, in the south by the Horohoro lavas and fault scarp on the west side of the axial rift zone,

and by the Hauraki rift in the northwest. The plateau dips northwards at c. 2° and northwest and west at c. 3° (BRIGGS *et al.*, 1996). The ignimbrite surface northwest of the lake dips toward the caldera due to downsagging during caldera formation (MILNER *et al.*, 2002). The planar surface of the ignimbrite plateau contrasts with lava flows and domes within and around Rotorua Caldera.

The axial rift zone SE of Lake Rotorua is dominated by lava domes and flows. The NE-elongate Tarawera and Haroharo dome complexes fill much of the floor of the Okataina Caldera Complex (chapter five) defining linear vent zones that transect the caldera. The 1886 fissure eruption of Tarawera comprises numerous craters that are aligned in a left-lateral en echelon pattern along a NE trend. Domes and flows exhibit clear eruptive morphology in contrast to the surrounding flat-lying and dissected surfaces. Ridges and furrows are visible on the surface of many lava flows and domes attesting to their youthful morphology. The two complexes exhibit subtly different eruption morphology: Haroharo dome complex in particular displays extensive development of coulee's, and flow directions have been controlled by the pre-existing topography of older lavas. The presence of many lateral flows on Haroharo compared to Tarawera may reflect a difference in magma eruptive viscosity. An absence of block and ash flow deposits in the eruptive stratigraphy of the Haroharo complex, in contrast with Tarawera (I.A. NAIRN, *pers. comm.* 2003), may also be consistent with the eruption of less viscous magmas from Haroharo. The partially eroded and dissected surfaces of older domes and lava complexes are visible around the caldera complex and together with those on the caldera floor bound a series of lakes, effectively forming a moat around the western and northern rim of the caldera floor. The irregular boundary between older surfaces and lavas with a youthful morphology effectively marks the caldera boundary, a complex N-S elongate structure. The surface extending north of the caldera complex toward the coast is more dissected than much of the Mamaku Plateau, reflecting the more rapid incision of unwelded ignimbrite which caps the plateau north of Okataina.

Tectonic Morphology

Lineaments are in general scarce in the Rotorua area, illustrating its spatial separation from the axial rift zone. Within the axial rift zone, faults rotate by as much as 30° south of the OCC to trend NE along the southern caldera margin. Faulting within the caldera is rare, but northeast of the caldera faults trend NNE such that the rift forms a conspicuous right-stepping bend or offset at OCC. The major vent lineaments of Tarawera and Haroharo also

trend NE, and appear to coincide with the axes of rift segments to the north and south of OCC respectively. The intersection of faulting within the axial rift zone and the caldera coincides with embayments in the caldera margin, particularly on the NE and SW caldera margins. Faults here are defined by a series of scarps; some of these are continuous with caldera margin faults such that caldera collapse scarps are not differentiated from regional faults.

North of Okataina a zone of intense faulting defines the western margin of the axial rift zone. The eastern margin is marked only by the edge of the axial ranges, where predominantly N-S-trending faults within the NISB have rotated and intersect the Whakatane Graben. No surface deformation is exhibited between the margins of the axial rift zone in this part of TVZ, although the alluvial plains of the Tarawera and Rangitaiki rivers obscure any sub-surface structure. About 9 km east of the Tarawera volcanic complex a NNE-trending linear zone divides two opposing drainage networks. Deep valleys on the western side trend roughly N-S and drain into the eastern part of the caldera complex, while in the east drainage networks are directed ESE toward the axial ranges. This feature is continuous with the fault bordering the west side of the Whakatane Graben.

2.3.8 Regional Structure and Lineament Geometry

Shaded relief images have been used to determine the location and trend of faults and tectonic lineaments defining the structure of modern TVZ, and the distribution and type of volcanic edifice. Data from the analysis of four sectors of the central North Island are compiled in figure 2.10. Lineaments are scattered over a broad area but concentrated in two tectonic domains; TVZ itself is dominated by an array of NNE to NE-trending faults with minor tectonic lineaments both parallel and oblique to the faults, while the axial ranges east of TVZ are characterised by tectonic lineaments that are NNW to NE-trending. This spatial separation in lineament type reflects the scarp-forming predominantly normal faulting in TVZ, and most lineaments in modern TVZ are therefore inferred to be the morphological expression of active faults. The structure of TVZ is thus characterised by a system of NNE-NE-trending faults that extend from Ruapehu in the south to the Bay of Plenty coast with a 15-20 km wide axial rift zone characterised by the highest fault density. Within this zone sub-parallel scarps are generally arranged towards an axial symmetry where opposite verging scarps define a complex graben structure. Current deformation is therefore largely restricted to within the axial rift zone, consistent with the view that this axial zone is the focus of strain accumulation. Minor N-S and E-W-trending lineaments

may relate to caldera margins oblique to the regional trend, pre-existing structures inherited from older tectonics or may be influenced by structures intersecting with TVZ. To the east of TVZ, faults of the North Island Shear Belt (NISB) generally strike N-S but intersect TVZ in the southern and northernmost sectors, east of TgVC and Whakatane Graben respectively.

The distribution of volcanic vents in TVZ is strongly associated with regional structure. Vents are concentrated along the axial rift zone and most lie within linear zones parallel with regional faults. Distinct groupings of vents relate to dome complexes (e.g. Maroa & Tarawera) or to volcanic massifs (e.g. Tongariro & Ruapehu). A number of major vent lineations exist where vents are aligned sub-parallel and contiguous with faulting or directly continuous with faults; often domes aligned along the regional trend are cut by later faulting along the same orientation (e.g. Maroa dome complex). Rhyolite dome lavas and rhyolitic calderas are restricted to the central and widest portion of TVZ while absent from the extremities, consistent with the common division of TVZ into a central rhyolitic portion and andesitic extremities (e.g. COLE, 1990). Four calderas are located within modern TVZ; two, Okataina and Taupo, are located within the axial rift zone while two smaller calderas, Rotorua and Reporoa, are located some distance from the axial rift zone.

The trend and magnitude (length) of lineaments is illustrated in figure 2.11. Tectonic lineaments are considerably more variable in trend than faults, with faults showing a strong preferred orientation that constitutes a general TVZ trend (Fig. 2.11A). Figures 2.11a & b plot the length of tectonic lineaments and faults respectively as a function of their trend; these consider the variation in trends of longer lineaments as compared to shorter lineaments; this may provide some proxy for the importance of lineament length in defining regional structure. Figure 2.11a shows that the longer of the tectonic lineaments are only slightly more restricted in their trend variation than shorter lineaments, indicating there is significant variation in the trend of even the largest of these structures along the length of the axial ranges. Faults are also scattered over a considerable range (~70% of faults trending between 30° and 70°) but longer faults cluster more tightly. Considerable variation in fault trend is visible in figure 2.11; this occurs mainly as variation in the overall trend of specific rift segments rather then significant variation within segments of the axial rift zone. The entire lineament population has a mean resolvable length of 7.7 km, while faults alone have a mean resolvable length of 6.3 km.

Analysis of the shaded relief imagery reveals that the overall rift structure is not continuous and figure 2.12 presents the lineament population divided into 10 structural domains based on the perceived continuity and variation in trend of lineaments. The trend of local rift axes is also plotted; the axes of these domains are located where the predominant downthrow direction changes polarity. The axial ranges, which constitute the main tectonic lineament population, are divided into northern and southern domains, while TVZ is divided into eight domains along its length. These TVZ domains are characterised by a dominant fault trend, and are separated by distinct bends or offsets in the rift system. The Okataina domain in particular represents a major bend in the axial rift zone where ENE-trending faults link the offset sub-parallel and NNE-trending Kapenga and Whakatane domains. Most domains are in structural continuity (i.e. hard-linked) with adjacent domains, while the Nth-Taupo domain appears soft-linked (without evident structural continuity) with the Sth-Taupo domain and with the Maroa domain where a major left step occurs. Rose diagrams of lineament trend illustrate the variation in lineament trend in TVZ as a function of structural domain, indicating the trends of all lineament and fault-only populations for each domain. These also highlight the preferred orientation of faults in each domain compared with the entire lineament population.

Figure 2.13 provides further analysis of the seven domains that constitute the axial rift zone within modern TVZ. The length of faults is plotted as a function of fault trend for each of these domains and compared with the total lineament population (i.e. including tectonic lineaments). The mean orientation and length of faults and tectonic lineaments is given for each domain, where appropriate. Neither the fault trend suggested by clustering of data on rose diagrams, or the calculated mean values in figure 2.13, give a precise picture of the trend of each rift segment. It has been noted that faults comprising a rift segment are not necessarily parallel with the rift segment axes, particularly in cases of oblique extension (e.g. McCLAY & WHITE, 1995). In figure 2.12 the trends of each rift segment (i.e. pertaining to the axis of each of the 7 domains) are based on a visual estimate of broad scale morphologic features more representative of the overall trend of each related segment. The significance of figure 2.13 is that the data show considerable variation in trend between each domain with mean trend values ranging from 22° in the Tongariro domain to 54° in the Okataina domain.

2.4 STRUCTURAL DATA

The precise tectonic setting and type of fault motion in TVZ remains poorly understood, so the kinematics of TVZ is addressed here as part of constraining the relationship between structure and volcanism in TVZ. Early results of this study are also presented in a paper in Appendix A (ACOCELLA *et al.*, 2003) based on fieldwork by the author and V. ACOCELLA during February 2002. The topics addressed as the main aims of the kinematic study are: 1) what is the relationship between fault geometry and kinematics, and volcanism in TVZ; and 2) can the kinematics of the TVZ rift be reconciled with the kinematics of the plate boundary zone in the North Island?

While all faults within TVZ are considered normal by most researchers, very few fault slip vector data have previously been collected and a component of strike slip motion could not be discounted. This section presents structural data consisting of both fracture measurements and offset stream channel displacements along the length of TVZ. Fault orientation and slip direction, and joint and dike orientations, were collected over a distance of 200 km, from Ruapehu in the south to Whakatane in the north. Data were collected predominantly from bedded pyroclastic deposits (< 300 ka), exposed in road cuts throughout TVZ and subordinately from lake sediments (< 200 ka) exposed within parts of Kapenga graben and Rotorua Caldera (Fig. 2.14).

Fault plane striation measurements were made to constrain the kinematics of TVZ faults. Careful excavation of fault plane surfaces revealed mechanical striations, the pitch of which could be measured in order to calculate the relative components of dip-slip and strike-slip shear and the extension direction (Fig. 2.14b). In addition, slip vectors were derived from offset stream channels abandoned between 15 and 25 ka (Fig. 2.15; VILLAMOR & BERRYMAN, 2001). These offset channels provided piercing points with which slip vectors could be estimated on seven faults with displacements > 10 m. Displacements were calculated by locating the stream channel axis on each side of the fault and projecting these onto the fault plane (Fig. 2.15b). In most, the channels trend at high angles to the faults, and are typically eroded. Channel axes were projected onto the fault plane and piercing points calculated using GPS and tape measure. These measurements involved some error and the trends of these slip vectors are considered less precise than those measured from fault planes striations.

2.4.1 Fault and Fracture Geometry

The acquired data comprises faults (68%), joints (31%) and dikes (1%). The general term fracture is used for any type of mechanical discontinuity, and includes faults (fractures with motion parallel to the failure surface) and joints (fractures with extension normal to the failure surface). Data are presented in figure 2.16 on Schmidt lower hemisphere nets. Joints are typically subvertical and characterised by small (<5 cm) dilations, while faults are high-angle (~60°) to sub-vertical (80°-90°) with displacements from a few centimetres to a few hundred metres, and with predominantly extensional motion. Figure 2.17a-c summarises the geometry of the measured fractures. Preferred fracture orientations are 31° and 217° for east and west-dipping fractures respectively, with a roughly equivalent number of data in each dip direction. Figure 2.17b illustrates the strike from -90° to +90°; 36% cluster around 33° ± 23° (general TVZ trend), while 19% cluster around 70° ± 26 (mostly in the Okataina domain) and 10% around 329° ± 23° (mostly in the Kapenga domain, Figure 2.12). The measured fractures are mainly subvertical, with a mean dip of 83° (Fig. 2.17c). The collected structural data are consistent with the lineament data in section 2.3, in terms of both fracture density and strike, indicating that lineaments observed in shaded relief and satellite imagery along TVZ relate to tectonic activity.

2.4.2 Fault Kinematic Data

The pitch of slip vectors from both faults and offset stream channels is presented in figure 2.17d. Pitch values can range from 0° to 180°; 0° and 180° correspond to pure strike slip motion, while 90° corresponds to pure dip-slip motion. The pitches of slip vectors on faults subparallel to the TVZ trend are presented as a function of displacement (Δ, m) in figure 2.17d. The entire fault population clusters around a mean pitch of 102° which becomes more oblique with increasing displacement, with 103° for selected faults with $\Delta >$ 1 m, and 119° for faults with large ($\Delta >$ 10 m) displacement. Data spread decreases with increasing fault displacement, with a mean pitch value > 90° suggesting a dextral shear component.

ACOCELLA *et al* (2003; Appendix A) assign a weighting system to the fault population, suggesting that faults with larger displacements provide more reliable slip vector data: small faults ($\Delta <$ 1 m) = weight 1, medium faults (1 < Δ <10) = weight 10, large faults ($\Delta >$ 10 m) = weight 100. The mean pitch derived from such a weighting system = 115°, and averaging this value with unweighted data (102°) gives 109°, from which the dextral (D) and extensional (E) components of displacement are calculated.

$$D / E = \sin(109-90) / \cos(109-90) = 0.34$$

This shows that the strike slip component D = 34% of the vertical displacement (E) or D = sin19° = 33% of the total displacement. The strong weighting system used by ACOCELLA, *et al* (2003; Appendix A) means however that the D/E value is heavily influenced by the few large displacement fault data, and the relatively low-quality offset stream data, included in the large displacement fault population. To assess the affect of this weighting system, two other weighting systems are also considered here. The two additional weighting systems (0.5, 5, 20; 1, 2, 3; small, medium, large faults respectively) produce mean pitch values of 106° and 103°, corresponding to D/E values of 0.29 and 0.23 (29% and 23% of the vertical displacement, and 28% and 22% of the total displacement respectively). While both values also suggest a dextral shear component, they are significantly less, and highlight the affect of the strong weighting system used by ACOCELLA *et al* (2003; Appendix A) on the fault pitch population.

ACOCELLA *et al* (2003; Appendix A) use the stereographic procedure of MARRETT & ALLMENDINGER (1990) to evaluate extension directions from the collected fault data (Fig. 2.18a). Figure 2.18b plots the extension directions of faults subparallel to the TVZ trend as a function of their distance from rift axis and their displacement. Most of the faults have an extension direction between 300° and 340°, and in particular, all data for the Ruapehu and Whakatane segments, and most for the Kapenga segment (especially those with larger displacements) are above the line representing orthogonal extension. This suggests these segments have a dextral component of motion. Data from the Taupo and Okataina segments however show predominantly orthogonal extension. The angle β is defined as between the direction perpendicular to the trend of the rift segment and the extension direction (Figure 2.19); this angle is proportional to the component of horizontal shear along the segment; $\beta = 0°$ corresponds to pure orthogonal extension; $\beta > 0°$ and $\beta < 0°$ correspond to components of dextral and sinistral shear respectively. When the evaluated extension directions are considered in combination with rift domain trends (Figure 2.19) the data obtained show that TVZ domains are characterised by different components of dextral shear ranging from ~0° (Taupo and Okataina segments) to 23° (Whakatane Segment).

2.5 Eruptive Volume Data

Structural data suggest that five rift segments comprising TVZ (Acocella *et al.*, 2003; Appendix A) have different amounts of dextral shear. For each of these segments, an attempt has been made to constrain the volume of eruptives based on published volumetric data (Table 2.1). Volumes are Dense Rock Equivalent (DRE) taken from a large number of published data; the calculation of such volumes from both lavas and pyroclastics therefore may involve some significant error. In all cases, a standard 25% error margin is used; however, quoted volumes are thought to be underestimates of true volumes, particularly where they include largely unknown volumes of caldera fill. Only the volumes erupted in the last 300 ka are considered, for consistency with the collected structural data. The volumes erupted in the last 300 ka by the Rotorua and Reporoa calderas are not considered as these are located outside the axis of TVZ and cannot be specifically related to any of the identified rift segments.

In order to compare volumes in different segments, the total eruptive volume of a segment is divided by its length, obtaining a volume per km value. The values of β (Fig. 2.19) and the related volume estimates for each segment are reported in Table 1. Figure 2.20 shows the relationship between the obliquity of extension (β) and the erupted volumes per km for each segment. Despite the associated errors, the inverse correlation indicates that segments with the larger extensional components ($\beta \sim 0°$) are associated with larger eruptive volumes; in contrast, segments with the larger components of dextral shear ($\beta > 0°$) are associated with lower eruptive volumes. Figure 2.20 thus shows the focusing of eruptive activity at the purely extensional Okataina and Taupo segments. In general, the segments with higher β values are also associated with stratovolcanoes (Whakatane and Tongariro), whereas the segments with smaller β are associated with calderas, indicating that, within the axial zone of TVZ, calderas relate to the highest tensile conditions.

2.6 Discussion

2.6.1 Rift Architecture

Shaded relief imagery has enabled analysis of the architecture and segmentation of the intra-arc rift zone of modern TVZ, through the mapping of lineaments on a regional scale, both within and outside modern TVZ. Specifically, the location, trend, length, and density of faults and tectonic lineaments have been used to evaluate the along-strike continuity, graben symmetry, and rift axis location and orientation. These data are combined with field data providing details on the geometry and kinematics of fractures within TVZ. A

summary of TVZ structure is presented in figure 2.21. Modern TVZ is a NNE-SSW trending intra-arc rift zone, is narrowest at its extremities (< 20 km) and up to 50 km wide across the central portion. The axial part of the rift is 15-25 km wide and appears to be symmetric with a central graben axis. Axis orientation along the length of TVZ (left-stepping *en echelon* rift axes) is broadly consistent with dextral transtension; the central five domains rotate to a more easterly trend between the sub-parallel Tongariro and Whakatane domains (Fig. 2.22). Domains are distinguished based on structural characteristics, and importantly, these are consistent and often coincident with major volcanic systems and structures (e.g. Okataina and Taupo Caldera complexes comprise the Okataina and Nth Taupo domains respectively).

Rift axis orientation varies considerably (c. 42°) between the Whakatane and Kapenga domains where these two axes are offset by at least 20 km across the Okataina domain (Fig. 4.21). Other moderate changes in orientation in rift axes occur between the Sth and Nth Taupo domains (c. 14°) and between Sth Taupo and Tongariro domains (c. 5°); these record a broad orientation change in the axial rift zone of 19° over a rift length of <40 km. Moderate changes in orientation also occur between the Kapenga and Maroa domains (11°), and a major axis-normal offset (c. 10 km offset; 6° axis variation) occurs between the Maroa and Nth Taupo segments. The TVZ rift system is therefore a series of offset and variably oriented rift segments. ROWLAND & SIBSON (2001) interpret the major offsets and variations in rift axes in TVZ as transverse 'accommodation zones'. Observing that mechanical and geometric continuity must exist between offset rift segments, they argue that the absence of transfer faults between offset segments indicates displacement transfer must occur by soft-linkage of interlocking extensional faults.

2.6.2 TVZ Kinematics

Normal dip-slip is clearly the predominant fault mechanism in TVZ, however a component of dextral strike-slip occurs in 4 of the 7 segments along the length of TVZ (Fig. 2.22). The Okataina and Nth Taupo segments show, on average, an orthogonal extension direction, which reflects their more easterly orientation with respect to the rift (70° and 41° respectively). With a uniform regional extension direction, these changes in segment orientation would increase the proportion of segment-normal extension. The Maroa domain also has a more easterly segment trend, but no structural data was acquired from this part of the rift. ACOCELLA *et al* (2003; Appendix A) suggest that variability in segment orientation is not sufficient to account for all of the observed rotation in the

extension direction, and propose a local rotation in the extension direction citing similar rotations in analogue models and in other rifts (e.g. ACOCELLA *et al.*, 1999; GUDMUNDSSON *et al.*, 1993).

ACOCELLA *et al* (2003; Appendix A) estimated dextral shear in TVZ as 34% of the total displacement but this was strongly influenced by the few large displacement faults and offset stream channel data. Further analysis of pitch data indicates that dextral shear may account for between 22% and 28% of the total displacement. A dextral component of shear indicates that TVZ is an oblique intra-arc rift. Assuming a mean extension rate of ~7 mm/yr in TVZ (DARBY & MEERTENS, 1995; VILLAMOR & BERRYMAN, 2001; DARBY *et al.*, 2000), and a conservative 25% component of dextral shear (of total displacement), pure extension and dextral shear account for ~6.8 and ~1.68 mm/yr of deformation, respectively.

2.6.3 Implications for Volcanism in TVZ

The distribution of volcanic types is consistent with the petrological division of TVZ recognised by HOUGHTON *et al* (1995). The active Okataina and Taupo caldera complexes bound the central predominantly rhyolitic portion of TVZ while andesitic and dacitic volcanism dominates the segments to the northeast and southwest. Figure 2.20 shows an inverse correlation between the dextral component of transtension and the volume of erupted magma along the segmented modern TVZ. The largest eruptive volumes from the caldera complexes in the Okataina and Taupo segments are associated with the highest degree of extension; conversely, lower erupted volumes from the andesitic volcanoes in the Ruapehu and Whakatane segments are associated with the highest degree of dextral shear.

The major implication of this correlation is a genetic link between the degree of extension and the eruptive volume and style. As a first approximation, we can consider two main possibilities to account for this relationship. 1) Upper crustal tectonic processes have controlled the location of magma storage and extrusion. Crustal extension relaxes the least horizontal compressive stress $\sigma 3$, enhancing the rise of magma through the crust mainly by dike propagation (e.g. GUDMUNDSSON, 1988, 2002). 2) The presence of large volumes of magma at specific locations in the upper crust has controlled the structural evolution of the rift system. Magmatism may have an important role influencing the structural style and evolution of rifts (e.g. LYNCH & MORGAN, 1987; MORLEY, 1999; VIGNERESSE *et al.*, 1999).

Four points suggest that the first model is most likely. 1) Enhanced dike propagation within crust subject to crustal extension is the simplest way in which to accommodate the rise and storage of magma at shallow crustal levels; greater extension at specific localities will lead to accumulation of large magma volumes. 2) Eruptive vents for all styles of volcanism in TVZ, including Taupo and Okataina, are typically aligned parallel to regional structure. 3) The geometry of Taupo and Okataina calderas indicates strong tectonic influence on caldera formation and evolution. 4) The extension axes for the Taupo and Okataina segments are consistent with the evaluated overall N46°W extension direction for TVZ (ACOCELLA *et al.*, 2003; Appendix A).

2.6.4 Implications for compositional segmentation in TVZ

The presented data have provided some insight into the structural control on volcanic activity both within the axial zone of TVZ. However, a classical issue in TVZ studies is the conspicuous segmentation into andesitic extremities and a central zone dominated by rhyolitic calderas (e.g. COLE, 1990; WILSON, *et al.*, 1995). The presented data allow this broad compositional segmentation in TVZ, at least in the last 300 ka, to be considered as reflecting upper crustal processes rather than deeper dynamics. The dominance of rhyolite in the central zone has been attributed to partial melting of basement CVZ lavas (COLE, 1990). However, chemical data suggest a more complex petrogenetic model involving some combination of fractionation of basaltic parent magmas with crustal assimilation (e.g. GRAHAM *et al.*, 1995). No petrogenetic model has been able to sufficiently account for the anomalously high thermal flux in central TVZ.

The increased component of crustal extension in the central zone may account for the restricted distribution of rhyolitic volcanism by inducing extreme thinning, a decrease in pressure, and partial melting of mantle asthenosphere, generating an anomalous heat source for (1) partial melting of suitable crustal materials (e.g. COLE, 1990) or (2) high rates of mafic magma production below the crust (leading to fractionation). Regardless of the precise petrogenetic model, the selective presence of voluminous rhyolitic volcanism in the central part of TVZ in the last 300 ka can be explained as a function of rift zone architecture, by (1) creating an area of preferred rhyolite generation at depth, where CVZ lavas are likely to form part of the basement; and (2) focusing the rise and accumulation of magma at high levels in the crust. The proposed model therefore shows how TVZ constitutes an example of rift architecture influencing the characteristics of magma generation and emplacement, and the type of volcanism observed at the surface.

In addition, the intersection of NISB faults with the TVZ may have influenced volcano spacing through their role in providing conduits for rising magma. Primitive, density-bound magma may have utilised these pre-existing structures to reach the surface; this may provide a partial explanation for the dominant presence of andesitic volcanism in the southern and northern segments of TVZ.

2.6.5 Implications for plate boundary deformation

The observed dextral strike-slip component of shear in TVZ indicates that dextral shear is *not restricted* to the NIDFB and is therefore *not completely partitioned* within the plate boundary zone. Oblique slip on faults in TVZ indicates that a component of dextral shear is distributed across this zone. Based on fault slip data the mean dextral shear in TVZ is estimated to be 1.68 mm/yr (section 2.6.2). In the NIDFB, 3-6 mm of margin-parallel slip is occurring at the latitude of TVZ fault slip data (BEANLAND, 1995; MOUSOLOPOLO, *unpublished data*, A. NICOL *writ. comm.* 2004). Therefore, the total margin-parallel slip in the upper plate is at least ca. 5-8 mm/yr; however, this minimum value will rise if the faults east of the NIDFB also carry a component of strike slip.

The relative plate motion vector at this latitude gives a total convergence rate of 45 ± 0.2 mm/yr, with margin normal and margin-parallel motion values of 35 ± 0.2 and 27 ± 0.2 mm/yr, respectively (DEMETS *et al.*, 1994). Comparison of the dextral components observed on the overriding plate with the margin-parallel component of plate motion indicates a disparity in values, leaving up to 22 mm/yr margin-parallel motion unresolved. It is unlikely that major strike-slip structures remain unidentified, but it is possible that a component of strike slip is distributed across the margin on oblique slip faults outside TVZ. It is also possible that some margin-parallel slip has accrued on the plate interface. The recognition that strike slip motion occurs on faults outside the NIDFB suggests, however, that less of the total margin-parallel relative motion may be accommodated on the plate interface than previously thought.

CHAPTER 3 Caldera volcanism in TVZ: influence of regional structure

3.1 INTRODUCTION

Central TVZ is the most frequently active and productive Quaternary silicic system on Earth (HOUGHTON *et al.*, 1995) characterised by intense and volumetrically dominant rhyolitic volcanism that is expressed largely as major calderas and caldera complexes. Caldera-forming silicic volcanism in TVZ began at c. 1.6 Ma, and at least thirty-four caldera-forming eruptions have occurred since then during three main periods: 1.68-1.53 Ma, 1.21-0.68 Ma, and 0.34-present (HOUGHTON *et al.*, 1995). Developing an evolutionary model for large, multiple-source silicic volcanic fields such as central TVZ requires a reliable stratigraphic and structural framework. A regional stratigraphy of major ignimbrite units is fairly well established (e.g. HOUGHTON *et al.*, 1995), and the eruptive history of some calderas is known in some detail, particularly for the last 65 ka (e.g. NAIRN, 1989, 2003; WILSON, 1993). Despite numerous studies of both individual calderas (e.g. WILSON *et al.*, 1986; BROWN *et al.*, 1998; COLE *et al.*, 1998; BERESFORD & COLE, 2000a; MILNER *et al.*, 2002;), and those of the zone as a whole (e.g. COLE, 1990; BIBBY *et al.*, 1995, 1998; GRAHAM *et al.*, 1995; WILSON *et al.*, 1995; HOUGHTON *et al.*, 1995; ROWLAND & SIBSON, 2001) there remain aspects of volcanic and structural evolution of TVZ that are unclear. Significantly, prior to this study, no considered attempt has been made to relate regional deformation and caldera location, geometry, and development in TVZ, with regard to the structural evolution of caldera sources.

This chapter focuses on assessing the structural influence on caldera volcanism within modern TVZ (<300 ka), in terms of the regional structural framework established in chapter two (Fig. 3.1c, d). Four of the calderas identified in central TVZ (Okataina, Taupo, Rotorua and Reporoa) have formed in the last 300 ka. These comprise both multiple event caldera complexes (Okataina and Taupo) and single event calderas (Reporoa and Rotorua). The Okataina and Taupo caldera complexes, located at the boundaries of the central part (Fig. 3.1) are the most productive rhyolitic volcanoes on earth, with eruption rates of c. 0.1 m^3s^{-1} and c. 0.2 m^3s^{-1} respectively, averaged over the last 65 ka (WILSON, 1993). Remote sensing and structural data obtained on deposits younger than 300 ka along TVZ (chapter two) show that it comprises a number of segments with variable dextral components of shear, and significantly that pure extension is restricted to those segments containing the Okataina and Taupo caldera complexes (Fig. 3.1d;

ACOCELLA *et al.*, 2003; Appendix A). The diversity of calderas within modern TVZ thus provides an opportunity to examine the role of rift architecture in controlling the location and development of caldera volcanism.

3.1.1 Volcanic Centres vs. Calderas in TVZ

Rhyolitic volcanism in central TVZ is traditionally divided into a number of 'volcanic centres' or less commonly 'caldera centres', that typically represent calderas or caldera complexes and their spatially associated vents (e.g. WILSON *et al.*, 1995). COLE (1990) describes four composite rhyolitic volcanic centres in TVZ (Fig. 3.1a) while more recently (e.g. HOUGHTON *et al.*, 1995; WILSON *et al.*, 1995) eight caldera centres have been recognised in central TVZ (Fig. 3.1b). These terms are used interchangeably in the literature while none are suitably defined. In particular, a 'volcanic centre' is a rather subjective concept based on some arbitrary spatial association of vents and adjacent caldera structures (e.g. Okataina Volcanic Centre, NAIRN, 1989, 2002). In some situations (as in COLE, 1990) the term is used for broad areal groups of extrusive and explosive volcanics, and are thus larger than calderas. In other situations the term is used for a constrained group of volcanics associated with one volcano, often within a caldera (e.g. Maroa Volcanic Centre; Tarawera Volcanic Centre). In this study, the terms 'caldera' and 'caldera-complex' are used following BURT *et al* (1998), where the former describes the structure from which an individual ignimbrite erupted and the latter describes a number of spatially and structurally associated nested or overlapping calderas. The term 'volcanic centre' is used for a specific spatial-temporal association, typically within a caldera or caldera-complex.

3.2 CALDERA RECOGNITION IN TVZ

The eight documented calderas in TVZ are expressed at the surface by clustering of known or inferred vent locations and/or at depth by geophysically defined basement depressions. High production rates in TVZ and concomitant rapid burial makes caldera delineation in TVZ difficult, and only four of the currently recognised calderas (Taupo, Okataina, Rotorua and Reporoa, i.e. those corresponding to modern TVZ) are sufficiently exposed to enable analysis of surface morphology. Other collapse structures have been buried and/or destroyed by subsequent activity. Specifically, 'Kapenga volcanic centre' was first postulated entirely on geophysical evidence (ROGAN, 1982; WILSON *et al.*, 1984), and while at least seven ignimbrites are attributed to it (HOUGHTON *et al.*, 1995), no deposits are unequivocally related to any proposed caldera-forming events or documented collapse

structures. The Mangakino and Whakamaru calderas also have effectively no surface expression, and recent work within the proposed Maroa Caldera does not indicate any separate caldera-forming event or caldera structure associated with the Maroa Dome Complex (LEONARD, 2003). Further calderas may be implied by extensive ignimbrite deposits exposed at the surface (e.g. Ohakuri Ignimbrite; GRAVLEY, 2005), and in drillhole samples (e.g. Rautawhiri Breccia; BROWN, 1994) but indications of source areas do not amount to evidence of caldera structure at the surface. Even where calderas are exposed at the surface, caldera structure is often obscured by caldera infill, including both intra-caldera ignimbrite and post-caldera volcanism. In addition, coincidence with intense regional faulting at some calderas forms complex structures where the relative contributions of volcanism and tectonism in landscape development are intimately associated and potentially difficult to resolve.

3.2.1 Geophysical Analysis

Geophysical techniques, particularly gravity analysis (e.g. PAKISER, 1961; KANE *et al.*, 1976) may help elucidate the geometry and extent of caldera structures at depth. Gravity response is a function of density contrasts between lithologies, and for calderas, where dense basement rocks are deeper within the caldera than outside the caldera margins, burial by a potentially thick succession of intra-caldera, low-density pyroclastic material leads to a negative gravity anomaly (KANE *et al.*, 1976). A caldera is therefore expected to have a negative gravity anomaly that will reflect the shape of the collapse structure at depth.

TVZ is characterised by a broad gravity low, and superimposed on this are several large negative residual gravity anomalies up to 75 mGal which indicate the presence of thick sequences of low-density volcaniclastic sediments and effectively mark the location of the rhyolitic calderas (ROGAN, 1982; DAVY & CALDWELL, 1998). Major well-defined negative gravity anomalies are coincident with the Okataina and Taupo caldera complexes, and an extensive region of gravity lows extends between these structures (Fig. 3.2). These partly coincide with documented calderas (i.e. comparing b & c in Fig. 3.1) and as such may provide a more accurate depiction of the buried caldera structures such as Whakamaru and Mangakino. While it is somewhat justifiable to consider much of the basement depression in the central TVZ (inside the -40 mGal contour for example) representative of caldera collapse, the gravity signal records zones of relatively low-density material, and these could similarly be accounted for by the accumulation of volcaniclastic material in structural depressions within the rift.

The 3D distribution of P-wave velocity (Vp) also exhibits strong lateral variation within the upper crust of central TVZ (SHERBURN *et al.*, 2003). Several intense low Vp anomalies occur in central TVZ, which approximate the locations of the calderas, and are largely consistent with the residual gravity lows. The largest anomaly is coincident with Okataina Caldera Complex, where a low Vp anomaly is clearly discernible at a depth of 4 km, effectively indicating the minimum depth of the collapse structure (Fig. 3.2b; SHERBURN *et al.*, 2003). Geophysical data allows us to consider the shape and extent of basement depressions and accumulations of low density, low Vp volcaniclastic material at depth, and thus provide further control on the geometry and structure of collapse structures identified at the surface.

3.2.2 Remote Sensing / Morphotectonic Analysis

Some of the most impressive landforms on the shaded relief image of TVZ (Fig. 3.3) are the large caldera volcanoes within modern TVZ. They dominate the physiography of the central part of TVZ, controlling the distribution of lakes and drainage systems, with broad ignimbrite fans extending from their margins and flanking the axial rift zone. The close spatial and temporal juxtaposition of destructive and constructive volcanism in TVZ complicates the surface expression of some calderas, resulting in the impressive coincidence of caldera scarps and youthful silicic domes and flows (e.g. at Okataina). Many attempts have been made to classify calderas on Earth and other planets based on their structure and morphology (e.g. MACDONALD, 1972; WILLIAMS & MCBIRNEY, 1979; FRANCIS, 1993; MOUGINIS-MARK & ROWLAND, 2001), and these elements are crucial to a thorough caldera description (e.g. COLE, MILNER & SPINKS, 2005, *appendix* C).

Remote sensing and morphotectonic studies show the relationship between volcanic complexes or caldera location, morphology and tectonics (THOURET, 1999), and these studies may therefore enable us to infer how the structural setting controlled the location and geometry of a caldera. The remote sensing and morphotectonic approach to the analysis of volcanic geology (THOURET, 1999) and in particular to sea-floor (e.g. WRIGHT, 1996, 1997; WRIGHT *et al.*, 1996, 2003; HAMMOND, 1997) and planetary volcanism (e.g. MOUGINIS-MARK & ROWLAND, 2001) has revealed an appreciable amount about volcano evolution. The location, geometry, and nature of volcanism at the surface, and in particular the spatial distribution of vents and relative volumes of eruptives, provide information concerning the transport and storage of magma through the crust, and therefore may infer

the crustal lithospheric stress-field and local stress-field configurations (CAS & WRIGHT, 1988).

3.3 CALDERAS IN MODERN TVZ

In the following sections, the Modern TVZ calderas (Rotorua, Reporoa, Okataina, Taupo) are considered in light of existing volcanological, geochemical and geophysical data. In addition, new morphological and structural data derived from DEM analysis and field studies are used to assess the influence of the structural framework on caldera shape and development.

3.3.1 Rotorua Caldera

The Rotorua caldera is perhaps the most conspicuous caldera in TVZ, accentuated by its large, sub-circular caldera lake, Lake Rotorua (Figs. 3.2, 3.5). The caldera is located 15-20 km NW of the junction between Okataina and Kapenga rift axes (Fig. 3.1), and formed during and immediately following the eruption of the c. 225 ka Mamaku Ignimbrite (WILSON *et al.*, 1984; SHANE *et al.*, 1994; HOUGHTON *et al.*, 1995; BLACK *et al.*, 1996; MILNER *et al.*, 2002), with a minimum eruption volume (including intra-caldera ignimbrite) of 145 km^3 DRE (MILNER *et al.*, 2003). Some authors have proposed earlier events at Rotorua caldera to account for older ignimbrites in the area (WOOD, 1992; LYNCH-BLOSSE, 1998), or that Rotorua is not a caldera at all (HUNT, 1992), but a detailed study by MILNER *et al* (2002, 2003) confirmed Rotorua as a single-event caldera, and the source of the Mamaku Ignimbrite.

Eruptive History

A number of pre-caldera rhyolite domes are exposed in the vicinity of Rotorua Caldera (Fig. 3.5b, d). MILNER (2001) showed that those on the rim of the caldera are geochemically distinct from each other and from the Mamaku magma system. The post-caldera rhyolite dome complexes are geochemically similar to the Mamaku Ignimbrite system and may reflect a final eruptive phase from the Mamaku magma system (MILNER *et al.*, 2002). Smaller rhyolite domes are geochemically distinct (MILNER, 2001) and thought to be much younger (NAIRN & WOOD, 1987).

Stratigraphic evidence outlined by MILNER *et al* (2002) indicates caldera collapse occurred throughout the eruption and emplacement of the Mamaku Ignimbrite during a single eruptive episode. MILNER *et al* (2002) describe asymmetric caldera collapse deepest in the

southwest of the caldera, with a component of downsag expressed in the overlying Mamaku Ignimbrite. Mamaku Ignimbrite geochemistry indicates the eruption of a single, compositionally zoned magma reservoir, represented by three petrogenetically related pumice types. An andesitic juvenile component in the upper parts of the Mamaku Ignimbrite is thought to reflect a discrete magma injected into the residual silicic chamber and tapped during later phases of the eruption during advanced stages of caldera collapse (MILNER *et al.*, 2003).

Geophysical Response

The Rotorua Caldera is characterised by an N-S elongate negative residual gravity anomaly to the west and southwest of Lake Rotorua, including Rotorua city and the post-caldera rhyolite dome of Ngongotaha (ROGAN, 1982; HUNT, 1992; DAVY & CALDWELL, 1998; Fig. 3.3, 3.5c). The surrounding gravity contours are not specifically concentric to the caldera margin, defining an asymmetric rise in basement towards the northeast and northwest caldera margins. The basement gradient is shallowest towards the east and steepest around the south-western margin. HUNT (1992) concludes that Rotorua is not a caldera collapse structure based on gravity anomalies that are not concentric or parallel to the caldera margins; however, MILNER (2001) argues that many recognized calderas have a gravity response that varies from an ideal concentric pattern, and the Rotorua gravity anomaly is not incompatible with caldera collapse. Basement highs clearly separate it from the adjacent negative gravity anomalies (Fig. 3.3). Although relatively indistinct, a low P-wave velocity (Vp) anomaly is consistent with the negative gravity anomaly and a collapse structure filled with low density, low Vp volcaniclastic material (SHERBURN *et al.*, 2003; Fig. 3.4).

Physiography and Structure

DEM and field data show that Rotorua Caldera is located several km westwards from the present area of active tectonism within TVZ, with most of the active faults restricted to the junction between the Kapenga and Okataina segments (chapter 2; Fig. 3.1). To the south and east of the caldera, the Mamaku Ignimbrite surface is downfaulted and has been largely overprinted by volcanism and faulting (Fig. 3.5). This is in contrast with the extensive ignimbrite surface to the north and west of the caldera reflecting the location of Rotorua Caldera west of the actively rifting portion of TVZ.

Morphotectonic mapping of DEM data reveals a sub-circular approximately 20 x 16 km structure (Fig. 3.5) with an eccentricity $E = L_{min}/L_{max} = 0.78$ (where L_{min} and L_{max} are the shorter and longer axes respectively). The caldera floor is dominated by the ~9 km diameter caldera lake and the youthful morphologies of post-caldera rhyolite dome complexes. Pre- and post-caldera rhyolite domes form prominent topographic features against the flat-lying ignimbrite plateau to the west of the caldera. The topographic margin is semi-continuous around the caldera and best expressed where formed by arcuate scarps in pre-caldera rhyolite domes or Mamaku Ignimbrite (Fig. 3.5b, e); elsewhere the margin is marked by the limit of the inwards dipping Mamaku Ignimbrite, referred to as the limit of deformation by MILNER *et al* (2002). The southeast margin of the caldera roughly parallels NE-trending regional faults in the adjacent Okataina segment. The caldera margin does not truncate any regional structures and only in the NE is dissected by younger faulting. Other lineaments in the caldera are arcuate and relate to caldera bounding scarps and associated deformation, rather than to regional structure. In the northwest of the caldera several low scarps sub-parallel to the caldera margin are located within the area defined by MILNER *et al* (2002) as having deformed by downsag into the caldera during collapse. The vents for post-caldera rhyolite domes define several lineations within the caldera, interpreted by MILNER *et al* (2002) as reflecting eruption along major dislocations bounding the area of deepest basement collapse.

Discussion

At Rotorua Caldera, lineaments relate to caldera bounding scarps and associated deformation, rather than to regional structure. Based on the collected data, little interpretation can be made regarding the structure of the caldera floor. The extent of the topographic margin appears to overstate the dimensions of the caldera indicated by geophysical evidence. NW-trending structures discussed by MILNER *et al* (2002) are not identified here, and while this does not preclude their existence, it would appear difficult to resolve their lack of surface expression with their suggested control on caldera collapse. It is also difficult to accommodate the lack of NE-trending structures at the surface with the invasive block-faulting collapse processes inferred by MILNER *et al* (2002). Rotorua caldera is clearly a simple caldera within Modern TVZ, and from geomorphic evidence, the lack of structures with a regional trend indicates a general lack of coupling between caldera structure and regional structure.

3.3.2 Reporoa Caldera

Reporoa Caldera (NAIRN *et al.*, 1994) is located at the northern end of the Taupo-Reporoa depression ~15 km E of the Kapenga segment axis (Fig. 3.1), and was originally interpreted as part of a large fault angle depression between the Taupo Fault belt and the Kaingaroa fault belt (MODRINIAK & STUDT, 1959). It was redefined by NAIRN *et al.* (1994) as a caldera and the source of the 0.23 +/- 0.01 Ma (HOUGHTON *et al.*, 1995) Kaingaroa Ignimbrite, with a total eruptive volume of 100 km^3 (NAIRN *et al.*, 1994; BERESFORD & COLE, 2000a). Kaingaroa Ignimbrite extends radially for 20-30 km beyond the caldera, mostly to the east of Reporoa Caldera where it caps the Kaingaroa Plateau (Fig. 3.6).

Eruptive History

Pre-caldera volcanism in the Reporoa area comprises rhyolite lavas unrelated to the Kaingaroa magma system or the formation of Reporoa caldera (BERESFORD & COLE, 2000a; Fig. 3.6) and older ignimbrites from caldera sources to the west (WILSON *et al.*, 1986; RITCHIE, 1997; BERESFORD & Cole, 2000a). Minor (<2 km^3) post-caldera rhyolite domes are geochemically and isotopically distinct from the Kaingaroa magma system (BERESFORD et al., 2000). Lithic componentry data for the Kaingaroa Ignimbrite presented by BERESFORD & COLE (2000a) identify multiple stages in the eruption event: 1) an initial single vent phase; 2) a multiple vent or ring fracture phase on the eastern side with asymmetric caldera collapse leading to eastward-directed pyroclastic flows; 3) piston collapse accompanied by radially directed pyroclastic flows.

Chemical and isotopic data for the Kaingaroa Ignimbrite indicate a weakly zoned magma chamber, with four dominant pumice types related by minor plagioclase-dominated fractionation (BERESFORD *et al.*, 2000). An additional unrelated pumice type is considered by BERESFORD *et al* (2000) to represent incorporation of a discrete magma batch into the resident magma chamber during eruption.

Geophysical Response

The caldera has a small but clear negative gravity anomaly (NAIRN *et al.*, 1994; STAGPOOLE, 1994; STAGPOOLE & BIBBY, 1999; Fig. 3.3, 3.6c) and a low Vp anomaly consistent with low density, low Vp caldera fill (SHERBURN *et al.*, 2003; Fig. 3.4). The gravity anomaly corresponds well with the topographic expression of the caldera, with a gentle and largely open western margin and a steep eastern margin (Fig. 3.6), consistent with asymmetric collapse (BERESFORD & COLE, 2000a). Gravity data partly define the

buried southern margin, which NAIRN *et al* (1994) consider to coincide with a small rhyolite dome. NAIRN *et al* (1994) also interpret post-caldera rhyolite domes and a buried dome complex inferred to exist by magnetic studies (SOENGKONO & HOCHSTEIN, 1996) to have erupted along fractures related to the caldera rim and a supposed inner caldera ring fault.

Physiography and Structure

New DEM and field data (Chapter 2; Fig. 3.6) show that the Reporoa caldera is located several km eastwards from the eastern boundary of the area of active tectonism within TVZ, most of the active faults being restricted to the Kapenga graben (Fig. 3.1). The Kaingaroa Ignimbrite extends eastward from the caldera, capping the Kaingaroa Plateau and forming a clear geomorphic fan on a sequence of older ignimbrites extending to the axial ranges. The asymmetry of the Kaingaroa Ignimbrite distribution is partially an artefact of the heavily faulted terrain to the west of the caldera. Distribution of the Kaingaroa Ignimbrite in this area is strongly controlled by normal faulting (BERESFORD, 1997) and the situation is analogous to that for the Mamaku Ignimbrite from the Rotorua Caldera, which is poorly exposed within the adjacent active rifting zone.

DEM and field data depict a simple sub-circular geometry, with approximate dimensions of 11 x 13 km and well-preserved 250 m high collapse scarps along the northern boundary. The N-S long axis of the caldera (eccentricity E = 0.81) is oblique to the regional trend of faults to the west; in the east a NE-trending fault scarp merges with the N-S trending eastern caldera margin. The flat-floored caldera has a well defined topographic margin in the north and east, but is open to the west and south. The caldera margin is neither dissected by younger faults nor does it truncate older structures. The Reporoa Caldera has contained lakes at various stages in its history, evidenced by lacustrine sediments and terraces above the current basin floor (MANVILLE, 2001 *and refs within*). Minor lineaments within the caldera may record modern subsidence or reflect the lacustrine history of the basin.

BERESFORD & COLE (2000a) interpret the eastern margin of the Reporoa Caldera as coinciding with the Kaingaroa fault forming the eastern margin of the Taupo-Reporoa Basin. In fact, this fault is much more likely to continue sub-parallel to regional structure and pass obliquely beneath the Kaingaroa Plateau (Fig. 3.6g). BERESFORD (1997) inferred a 'hole' in the pre-caldera stratigraphy where proximal flows of the Kaingaroa Ignimbrite

were restricted; middle and upper units of the ignimbrite maintain a near uniform thickness across the plateau. This 'hole' likely represents the down-faulted area west of the NE-trending Kaingaroa Fault, restricting early flows, and explaining the lack of early flow units of the Kaingaroa Ignimbrite. A NE-trending structure is visible northeast of the Kaingaroa plateau, dividing two opposing drainage networks, and may be reflected in a subtle elevation change (west side downthrown) across the plateau (Fig. 3.6g).

Discussion

The Reporoa is a morphologically simple caldera, and its surface expression reveals little information regarding its internal structure. A complex origin may be concealed by its morphological youthfulness; however the combination of known eruptive history, geophysical response, and surface morphology indicate a simple structure. Even though regional structures may have played a limited role in controlling the asymmetric collapse of Reporoa Caldera (BERESFORD & COLE, 2000a), the overall morphology of the caldera has remained largely unaffected by regional fault geometry.

3.3.3 Okataina Caldera Complex

The Okataina Caldera Complex (OCC) is a complex of overlapping and nested collapse structures, largely filled by the products of post-caldera rhyolite volcanism. The composite structure is the result of two main collapse events associated with the 0.28 ± 0.01 Ma Matahina Ignimbrite (BAILEY & CARR, 1994; date from HOUGHTON *et al.*, 1995) and the 65 ka Rotoiti eruption (NAIRN, 1981, 1989; date from HOUGHTON *et al.*, 1995), and modified by substantial intra-caldera rhyolite volcanism (e.g. JURADO-CHICHAY & WALKER, 2000; NAIRN, 1989, 2002). Further older (>300 ka) and younger (>65 ka) collapse events are likely (see chapter 4), but potential deposits, and precise collapse margins are obscured and/or overprinted by subsequent activity. Magmatic volume estimates for the Matahina and Rotoiti events (including intra-caldera estimates) are 150 km^3 (BAILEY & CARR, 1994) and 120 km^3 (FROGGATT & LOWE, 1990) respectively; other eruptives from within and adjacent to OCC account for at least 150 km^3 (e.g. NAIRN, 1989; FROGGATT & LOWE, 1990; BELLAMY, 1991; JURADO-CHICHAY & WALKER, 2001). The Matahina and Rotoiti ignimbrites extend predominantly to the east and north, and appear related to overlapping but distinct sources in the southern and northern parts of the caldera complex respectively (NAIRN, 1989, 2002; this study; Fig. 3.7).

Eruptive History

A number of rhyolite dome lavas scattered around the rim of the caldera-complex record volcanism in the Okataina area predating the first collapse event (NAIRN, 1989, 2003; Fig. 3.7). No precise dates exist for these lavas, but BOWYER (2001) showed that they are chemically distinct and relate to discrete magma batches. Geochemical variation is small however, and no significant variability exists between pre-caldera lavas adjacent to the Okataina and Rotorua calderas; this would imply that these lavas are not related specifically to a Rotorua or Okataina 'volcanic centre'. Only one pre-caldera magma batch has a similar chemistry to the Matahina magma system (e.g. NAIRN, 1981; BOWYER, 2001). NAIRN (1989, 2002) attributes poorly exposed ignimbrites and pyroclastics to the south of the caldera to an Okataina source but this is yet to be substantiated; the first caldera-forming event is thus considered that associated with the Matahina Ignimbrite. Various pyroclastic units (predominantly plinian airfall sequences) exposed beneath and overlying the Matahina Ignimbrite may record additional eruptions at Okataina, but their source is not established with any certainty due to limited exposure.

Lavas and associated pyroclastics erupted between the major caldera-forming events are predominantly exposed to the southwest of the caldera (Fig. 3.7) and relate to multiple magma batches (BELLAMY, 1991; BOWYER, 2001). Following the second caldera collapse event, a major phase of explosive volcanism ensued from sources within the caldera complex prior to the development of the two large rhyolite lava massifs that currently fill the caldera. Considerable studies of eruptive activity since the Rotoiti event (e.g. JURADO-CHICHAY & WALKER, 2000, 2001a, b; BOWYER, 2001; LEONARD *et al.*, 2002; SMITH *et al.*, 2002; SMITH *et al.*, 2004) indicate the eruption of multiple discrete magma batches. Two main magma types were erupted during the explosive phase, generating multiple eruptions, while during more recent effusive activity multiple magmas were often involved with a single eruptive episode.

The two documented caldera-forming events at Okataina are spatially overlapping but are significantly temporally separated (> 200 ka) and reflect geochemically distinct magma systems (BURT *et al.*, 1998). Both the Matahina and Rotoiti ignimbrites exhibit minor geochemical variation (CARR, 1984; DAVIS, 1985; SCHMITZ, 1995; BURT *et al.*, 1998) as likely products of weakly zoned magma chambers or late stage contamination by subordinate discrete magmas (e.g. SHANE *et al.*, 2005). Volcanism in the Okataina area from the earliest to the most recent eruptives, including the caldera forming events,

therefore records the eruption of multiple discrete magmas rather than the progressive tapping of a single large chamber.

Geophysical Response

A distinct large negative residual gravity anomaly (ROGAN, 1982; DAVY & CALDWELL, 1998; Fig. 3.3, 3.7C) and low Vp anomaly (SHERBURN *et al.*, 2003; Fig. 3.4) define an N-S elongated depression consistent with the mapped caldera margin and filled with a large volume of low Vp, low density, volcaniclastic sediment. Modelling of gravity and magnetic data gives conflicting depths to the basement of 5 km and 1-2 km, respectively (ROGAN, 1982). However, a clear low Vp anomaly at 4km effectively corresponds to a minimum depth extent of the collapse structure (SHERBURN *et al.*, 2003; Fig. 3.4). Gravity data presented by Nairn (2003; Fig. 3.7C) clearly depicts a N-S elongate negative gravity anomaly roughly concentric to the topographic margin, and centered beneath Tarawera Volcanic Complex and the southern part of Haroharo Volcanic Complex. The contours open on the west side of the structure but clear relative gravity highs separate the structure from basement highs to the east and Rotorua Caldera to the west. Topographic embayments in the caldera complex margin are also peripheral to the main basement depression indicated by gravity and Vp data.

Physiography and Structure

New DEM and field data show that Okataina is located along the major ENE-WSW trending bend of the axial rift zone of TVZ (Fig. 3.1). The OCC is a complex structure delineated by morphologically youthful intra-caldera volcanic features in juxtaposition with the older and more dissected terrain of pre-caldera lavas and ignimbrites forming the caldera margin (Fig. 3.7). The caldera-bounding scarps are partially eroded and many segments are obscured by post-caldera eruptives or by ignimbrites from adjacent sources. The 28 x 15 km caldera complex is strongly rectangular with an eccentricity E = 0.54 (Fig. 3.7e) and a long axis trending N8°W, roughly perpendicular to the Okataina rift axis (Fig. 3.1d). Intra-caldera rhyolite massifs obscure the structure of the caldera floor and the current margin is thus a composite feature.

The topographic margin at Okataina is variably manifest as scalloped slump scars in pre-caldera rhyolite domes and ignimbrites, eroded caldera walls, rectilinear fault scarps often coincident with regional faulting, and in the SW by the steep margins of post-caldera constructional rhyolite domes (Fig. 3.7). As such, the topographic margin merely defines a

depression considerably modified from the original collapse structure. Distinct embayments in the topographic margin occur where zones of intense ENE-WSW-trending regional faulting of the axial rift within the Okataina segment intersect the caldera. The caldera-bounding scarps in the south and southwest are parallel to and often coincident with these regional faults and to NE-trending faults along the western caldera margin (Fig. 3.7e). The embayments form subsidiary tectonic depressions to the main N-S trending caldera structure, and are contiguous with two intra-caldera dome complexes forming the conspicuous linear vent zones, which transect the caldera complex. The boundaries of individual collapse events are complex and largely buried or destroyed by subsequent volcanism and tectonism, but caldera reconstructions (chapter five) suggest the major collapses are centred on the axes of the intersecting rift segments. Lakes at Okataina exhibit a moat pattern where they have ponded between the topographic rim of the caldera and caldera-filling post-caldera constructional volcanism; earlier lakes may have been much larger.

Discussion

The Okataina Caldera Complex is a composite structure where voluminous volcanic activity spanning the caldera-forming events has largely obscured individual collapse structures. The volcanic evolution of the Okataina area is clearly complicated by its intersection with the axial rift zone of Modern TVZ. The influence of regional deformation at Okataina is marked by the conspicuous linear zones of volcanism and tectonism that transect the caldera complex. These are roughly axial to the adjacent Kapenga and Whakatane rift segments, and as such they mark their continuation in the Okataina area, herein recording a ~20 km offset of the rift axis (Figs. 3.1, 3.9).

3.3.4 Taupo Caldera Complex

The Taupo Caldera Complex (COLE *et al.*, 1998) has been frequently active in the past ca. 65 ka (WILSON *et al.*, 1986; HOUGHTON *et al.*, 1995), while its poorly constrained early eruptive history indicates activity over ca. 300 ka (WILSON *et al.*, 1986; COLE *et al.*, 1998). The caldera-forming Oruanui eruption at 26.5 ka (calibrated; WILSON, 1993) generated a ca. 500 km^3 fall deposit, a 300 km^3 bulk volume non-welded ignimbrite (SELF, 1983; WILSON, 1991) and with significant volume of caldera-fill material erupted ~400 km^3 of magma (SELF, 1983; WILSON, 1991; SUTTON *et al.*, 1995). The Oruanui event is thus largely responsible for the modern caldera morphology. WILSON (1993) has identified 28 separate eruptions since the Oruanui eruption, the most recent and largest of these, the

caldera forming 35 km^3 Taupo ignimbrite eruption, occurred about 1800 years ago from vents near the Horomatangi Reefs in the eastern part of the lake (WILSON & WALKER, 1985; SMITH & HOUGHTON, 1995).

Eruptive History

The early history (>65 ka) of volcanism in the vicinity of modern Lake Taupo is represented mainly by domes and limited pyroclastics scattered around the lake (SUTTON *et al.*, 1995; Fig. 3.8). Two ignimbrites exposed on the margin of the caldera are commonly attributed to a Taupo source (SUTTON *et al.*, 1995; COLE *et al.*, 1998), although their limited extent means their relationship to the current caldera complex is ambiguous. Pre-caldera rhyolite lavas form a series of headlands along the northern caldera margin and to the southwest of the caldera, while the large caldera-filling domes and flows characteristic of OCC are noticeably absent. Post-Oruanui activity has been studied in detail, and a sequence of 28 eruptions is now recognized (WILSON, 1993; SUTTON *et al.*, 1995). Vents for the post-Oruanui explosive eruptions are inferred by isopach data to be concentrated along a NE-trending lineation in the eastern part of modern Lake Taupo (WILSON, 1993; Fig. 3.8d). Construction of a dome complex in this area during the post-Oruanui phase is suggested by lithic componentry data for the Taupo Ignimbrite (COLE *et al.*, 1998) with its likely destruction during the Taupo eruption. Lithic componentry analysis of both the Oruanui and Taupo ignimbrites identifies different lithic suites, interpreted by COLE *et al* (1998) as reflecting dissimilar sub-caldera geology beneath mutually exclusive collapse structures.

Petrological studies (e.g. SUTTON *et al.*, 1995; 2000) show a complex magmatic system, involving the stepwise appearance of compositionally distinct magma batches with short crustal-residence times. Eruptives prior to the Oruanui eruption form distinct compositional and spatial groups, while a large isotopically homogeneous magma body was generated prior to the Oruanui caldera-forming eruption (SUTTON *et al.*, 1995). Some of the pre-Oruanui domes exposed on the northern caldera margin (Fig. 3.8d) and widespread tephras erupted between 65 ka and the Oruanui eruption are the same composition as the Oruanui magma, and thus record the coalescence of a large magma chamber. SUTTON *et al* (1995) also point out that compositionally distinct magmas were erupted during the same period from different areas around Taupo, and that ignimbrite pumice chemistry indicates additional magma batches may have been eviscerated during the Oruanui eruption. Eruptives of the post-Oruanui sequence form four temporally

grouped magma types and are compositionally distinct from the Oruanui magma. The youngest magma, associated with the Taupo eruption, represents the largest homogeneous magma accumulation in the post-Oruanui sequence (SUTTON *et al.*, 1995).

Geophysical Expression

A large trapezoidal-shaped negative Bouguer gravity anomaly is documented over the northern part of the lake (DAVY & CALDWELL, 1998) consistent with earlier onshore investigations (ROGAN, 1982). It is the most intense negative gravity anomaly in TVZ (DAVY & CALDWELL, 1998), and indicates a collapse structure filled with volcaniclastics of relatively low-density. The gravity anomaly is consistent with a caldera collapse structure elongate NW-SE, perpendicular to the axial rift zone in this segment. The gravity data do not facilitate identification of individual collapse structures, and Davy & Caldwell (1998) consider the structures are nested, with the Taupo eruption producing additional subsidence in the northeast part of the modern lake. Geophysical data also demonstrate differential subsidence towards the caldera in the southern part of the lake, and a NW-SE-trending structural boundary marking the southern caldera margin (DAVY & CALDWELL, 1998). Seismic reflection, gravity and magnetic data presented by DAVY & CALDWELL (1998) all suggest that a line dividing the northern and southern parts of the lake marks a major structural boundary perpendicular to the trend of TVZ (Fig. 3.8C).

Physiography & Structure

New DEM and field data (Fig. 3.8) show that Taupo is located within the axial rift zone of TVZ. The 28 x 16 km caldera complex is rectangular, with an eccentricity E = 0.57 and a long axis trending N63°W, roughly perpendicular to the Taupo North rift segment (Fig. 3.1). The northern caldera margin intersects NE-trending regional faults controlling a series of peninsulas and embayments in the topographic margin. Pre-caldera lavas to the southwest and north of the modern lake are aligned along regional trends. To the east and west of the caldera, the planar ignimbrite surface is gently tilted toward the lake (Fig. 3.8f) where the eastern and western margins are partially eroded but generally NE-trending linear features (Fig. 3.8).

The southern part of Lake Taupo occupies a NE-trending fault-bounded depression intersecting the southern caldera margin; the western margin of this structure is a continuation of fault systems dissecting the Tongariro Volcanic Centre to the south. A prominent structural feature is the divergence in fault trend (~20°) to the south and north of

the caldera complex (Fig. 3.8e). This bend effectively forms the boundary between the Tongariro and Taupo South rift segments (chapter two). Vents for pre-caldera lavas to the south and north of the caldera complex lie along NE-trending lineaments (Fig. 3.8b, e); the vents for post-Oruanui eruptions mostly occur along the eastern edge of the caldera complex (WILSON, 1993; Fig. 3.8d).

Discussion

Lake Taupo fills a multiple collapse structure and an associated structural depression in the axial rift zone of Modern TVZ. Individual collapse structures are obscured by Lake Taupo and remain unresolved in geophysical data. However, the composite collapse structure is rectangular and elongate perpendicular to the axial rift zone, equivalent to the situation at Okataina. The predominantly linear margins of the caldera complex and rectilinear subsidiary structures suggests that the coincidence with pervasive faulting of the axial rift zone at Taupo would attest to rectilinear fault-bounded caldera collapse, as opposed to sub-circular structural margins inferred by COLE *et al* (1998). Pre-and post-caldera vent lineations are parallel to regional deformation; post-Oruanui vents form a corridor in the eastern part of the lake that is off-axis but likely represents control by a pre-existing structure, possibly related to a zone of structural weakness manifest by an earlier rift-axis configuration.

3.4 OTHER CALDERA SOURCES IN TVZ

3.4.1 Kapenga

ROGAN (1982) postulated the existence of the Kapenga Volcanic Centre based on geophysical evidence. Gravity and magnetic data identified a 2.5 km deep depression filled with low-density magnetized rocks, which ROGAN (1982) correlated with a collapse structure. WILSON *et al* (1984) further described the centre, suggesting there were at least two *distinct* (my emphasis) collapse structures and potentially attributed several ignimbrites to it. WILSON *et al* (1995), citing new age data in HOUGHTON *et al* (1995), suggested that Kapenga is a composite structure where geographically overlapping volcanic centres relate to independent and temporally separate magmatic events.

Potential Eruptive Products

At present no ignimbrites are unequivocally identified with a caldera source in the Kapenga area. Despite this, many ignimbrites proximal to the proposed caldera have no

assigned source. The 0.71 Ma Waiotapu Ignimbrite (RITCHIE 1997) is exposed both to the southeast and northwest of the Taupo fault belt, and in the northwest overlies a series of older ignimbrites (0.77 Ma Rahopaka Ignimbrite, SPINKS, 1998; 0.89 Ma Tikorangi Ignimbrite, HILDYARD 1997, HILDYARD et al., 1998; dates from HOUGHTON *et al.*, 1995) with no positive caldera source. The exposure of these ignimbrites is restricted to within Matahana Basin, and no clear indications of source have been established (HILDYARD *et al.*, 1998; SPINKS, 1998, SPINKS *et al., in prep*).

Geophysical Response

Although a large negative gravity anomaly exists in this area, the data resolution is not sufficient to elucidate separate collapse centres such as WILSON *et al* (1984) indicate. Resistivity data for the axial rift zone indicate highly resistive material to a depth of 7 km suggestive of unaltered ignimbrite and volcaniclastics overlying some basement structure at an unknown depth (BIBBY *et al* 1998; RISK *et al* 1999). SHERBURN *et al* (2003) identify a prominent contrast in Vp at depths of 6-8 km, between the axial rift zone and the Taupo-Reporoa depression. The axial fault zone is characterized by low seismic velocity, low gravity, high resistivity, numerous active faults and high seismicity. These features are largely consistent with, but not exclusive to, a collapse structure. Similar geophysical response could be generated by predominantly tectonic subsidence with pyroclastics infilling from adjacent caldera sources.

Physiography

Kapenga caldera cannot be delineated based on surface morphology. The proposed structure sits in one of the most highly faulted areas in New Zealand (WOOD, 1994; Fig 3.1), between the 600 m high Paeroa Fault scarp and the opposing Horohoro Fault scarp, the margins of the axial rift zone in the Kapenga rift segment. Faulting within the Kapenga segment constitutes a series of NE-trending faults, the opposing scarps of which define the rift axis in this part of the axial rift zone. To the northeast a marked ENE rotation of faults occurs with proximity to the Okataina rift segment. Other lineaments preserved in the landscape constitute roughly N-S trending lineaments which span the width of the graben, and are concentrated in an area just east of Lake Ohakuri, and extending north into Matahana Basin.

3.4.2 Whakamaru Caldera and Maroa Dome Complex

The proposed Whakamaru Caldera has no clear topographic margin and was proposed by WILSON *et al* (1986) on the basis of the thickness and distribution of the Whakamaru-group ignimbrites that are exposed east and west of central TVZ. The proposed Whakamaru structure is defined to the west by the Western Dome Belt, a 32 km long curvilinear chain of simple and compound silicic domes inferred from field evidence to post-date the Whakamaru eruptions (WILSON *et al.*, 1986; Figs. 3.1c). The Western Dome Belt was divided into 1) the Western Dome Complex (WDC), comprising the domes south of the Waikato River, and 2) the North-western Dome Complex (NWDC), north of the Waikato River, by WILSON *et al* (1986). WILSON *et al* (1986) and subsequent authors (e.g. BROWN, 1994) regard the domes as the result of post-collapse volcanism localised along the western caldera margin.

WILSON *et al* (1986) recognise that the oldest lavas are truncated by a fault which also displaces Whakamaru Ignimbrite >1 km to the east (SOENGKONO *et al.*, 1992), suggesting domes may be synchronous with or predate these ignimbrites. Based on field evidence however, they conclude that most of the domes postdate the ignimbrites. Eruption of the domes has clearly been controlled by an N-S-trending fault system which has subsequently ruptured to displace the domes. Domes immediately east of the faults are probably younger features. Given that the domes and faults are aligned along a lineation oblique to the regional trend, if the lavas of the WDC are post-collapse features, then faulting likely relates to continued movement along the margins of the Whakamaru Caldera.

Maroa Dome complex is an accumulation of youthful simple and composite silicic domes. Domes are strongly aligned along NNE trends and extensively faulted along the same lineation, indicating the same regional structure is responsible for controlling vent locations and subsequent deformation. Vent and fault lineations are sub-parallel with faulting in the Kapenga graben to the NE.

Eruptive History

The volume of eruptives inferred to have a Whakamaru source indicates several episodes of collapse likely occurred, with sufficient scope for dome emplacement between events. Other caldera boundaries are defined based on drillhole thickness of Whakamaru ignimbrite i.e. thick inside the structure (Wairakei, Mokai, Tauhara, Rotokawa) and thin outflow sheets outside the structure (Broadlands, Waiotapu) (BROWN 1994).

Whakamaru group ignimbrites constitute the largest eruptive episode in TVZ history, with an exposed volume of at least 1000 km^3. These ignimbrites extend north to the southern margin of OVC, east and west to the boundaries of TVZ and south to partially form the eastern walls of Taupo Caldera. Post Whakamaru-caldera western dome belt lavas are geochemically distinct from the Whakamaru magma, and represent separate magma batches (BROWN, 1994).

3.4.3 Mangakino caldera complex

Early workers (e.g. MARTIN, 1961; BLANK, 1965) in TVZ associated several caldera forming ignimbrites to a source west of Modern TVZ. Five welded ignimbrites, in addition to several large phreatomagmatic airfall deposits, non-welded ignimbrites, and minor lava domes are now attributed to the Mangakino volcanic centre (BRIGGS *et al.*, 1993). Eruptive history of the Mangakino centre is divided into two concentrated periods of caldera-forming eruptions from 1.6 to 1.53 Ma, and 1.21 to 0.95 Ma (HOUGHTON *et al.*, 1995). The caldera complex is effectively defined by a major gravity anomaly (Fig. 3.3) where depth to basement is estimated to be 4 km (ROGAN, 1982; WILSON *et al.*, 1984). WILSON *et al* (1995) interpret 280 metres of lacustrine sediment in drillhole data between Mangakino and younger Whakamaru eruptives to indicate the composite caldera was initially buried by sediment and subsequently by Whakamaru-group ignimbrites. Minor surface expression is observed in the form of a basin lying 200-400 m below the surrounding ignimbrite plateau (BRIGGS *et al.*, 1993), but no surface features can be identified on DEM imagery.

A geochemical study of pumices within the Mangakino ignimbrites by BRIGGS *et al* (1993) indicates significant compositional variation compared with other TVZ ignimbrites. Ignimbrites with pumices recording continuous compositional trends and those with pumices of contrasting compositions are documented, interpreted to reflect fractional crystallisation and mixing of multiple magmas respectively as the magmatic processes responsible for the compositional zoning.

3.4.4 Ohakuri Caldera

The Ohakuri caldera is a newly recognised eruptive centre in the Whangapoa basin, 25 km SSW of Rotorua, which is considered to be the source of the c. 240 ka Ohakuri pyroclastic deposits (GRAVLEY, 2005). It overlies the northern margin of the older Whakamaru

caldera and lies adjacent to the axis of the Kapenga axial rift segment. Topographic or structural caldera margins are obscured by subsequent deposition of volcaniclastic sediments, but its presence is inferred from distribution of air fall deposits, distribution of and transport directions within the Ohakuri ignimbrite, and from geophysical data.

3.5 DISCUSSION

3.5.1 Characteristics of Modern TVZ Calderas

The collected data show that Modern TVZ is characterised by four calderas, located both outside (Reporoa, Rotorua) and within (Okataina and Taupo) the axial rift zone. The characteristics of these calderas are clearly bimodal, corresponding with their location relative to the axial rift zone.

Eruptive history

Silicic domes and groups of domes that predate the major collapse events are randomly scattered around the rims of the four Modern TVZ calderas, although their quantity varies significantly (c.f. Okataina and Reporoa). No absolute ages are published or known to exist, but many domes form precipitous cliffs along the caldera margins (e.g. along the northern margin at Reporoa; Fig. 3.6), commonly ascribed to landsliding during and following caldera collapse. Indirect evidence indicates that further domes existed prior to caldera collapse (dome lavas form a large proportion of the lithic assemblage in some caldera-forming ignimbrites, e.g. COLE *et al.*, 1998), and the current circum-caldera outcrop pattern at many calderas is considered largely a function of selective preservation, rather than any real correlation between caldera rim and eruptive vent. Pre-caldera silicic domes are in total isotopically and geochemically diverse but often occur in small spatially associated groups with common characteristics suggesting a common source or magma chamber.

Reporoa and Rotorua are monogenetic calderas, related to the emplacement of a single ignimbrite during one main phase of caldera collapse. Conversely, Okataina and Taupo are multicyclic caldera complexes, responsible for at least two ignimbrites during spatially and temporally distinct caldera collapse events. Some ignimbrite magmas exhibit limited association with selected pre-caldera eruptives (e.g. at Taupo and Okataina), but in general they are distinguished from previous eruptives. The ignimbrites also record varying amounts and styles of compositional zoning in the magma chambers. Distinct yet petrogenetically related pumice populations in the Kaingaroa and Mamaku Ignimbrites

record significant gradational zonation of the magma chambers at Reporoa and Rotorua Calderas respectively, while both also record the incorporation of additional distinct magmas during the eruption. Zoning is much less evident in the caldera forming ignimbrites of Taupo and Okataina caldera complexes, where the bulk of the erupted magma is homogeneous (Fig. 3.9).

The contribution of post-caldera volcanism at Modern TVZ calderas is diverse. Relatively minor post-caldera volcanism at Rotorua and Reporoa contrasts with voluminous activity at Taupo and Okataina. Post-caldera volcanism is geochemically distinct from earlier magmas, and eruptives largely relate to multiple discrete magma bodies; only at Rotorua caldera are some post-caldera domes possibly related to the magma associated with caldera formation. Vent lineaments for post-caldera volcanism at Okataina and Taupo are strongly influenced by regional structural trends, and at Okataina reflect major structures that extend beyond the caldera margins.

Geophysical Expression

Modern TVZ calderas are clearly bimodal in their geophysical expression, with much smaller (both in intensity and extent) negative gravity and Vp anomalies at off-axis calderas compared with intra-rift caldera complexes. Poorly defined anomalies at Rotorua and Reporoa are consistent with an approximately circular collapse structure but they are smaller than, and not entirely coincident with, the caldera margins. Large rectangular gravity anomalies (-700 mgal) at the intra-rift caldera complexes of Taupo and Okataina record the net effect of multiple collapse events, and individual collapse structures are not delineated. The anomalies at these calderas therefore represent composite structures that are strongly elongate normal to the axial rift. The extent and geometry of basement collapse is clearly delineated and while consistent with the mapped caldera margin, does not include the subsidiary lateral embayments. Vp data clearly shows a deeper basement collapse at Okataina in comparison to Reporoa and Rotorua Calderas.

Physiography and Structure

DEM data depict two types of structure in Modern TVZ (Fig. 3.10). Those within the axial rift zone are large, complex collapse structures, defined by generally linear margins and a rectangular geometry elongate perpendicular to regional structure (Fig. 3.11). In contrast, the calderas located outside the axial rift zone are smaller, sub-circular collapse structures, characterised by a series of arcuate scarps. The complexity of circum-caldera geology is

highly variable but is particularly evident at intra-rift caldera complexes where pre-caldera lava domes are more abundant and additional pre-caldera geology is exposed. Caldera wall scarps at all four calderas are highest and best developed where formed in pre-existing rhyolite lavas; variably welded ignimbrites exposed on the caldera rims form low and transient scarps or dip gently toward the caldera without any scarp development. The structure of the caldera floor is everywhere obscured, but all four are or have been deep lacustrine depocentres in their post-collapse history and Okataina is singular in that it is almost entirely filled by young silicic lavas. Both Okataina and Taupo are characterised by their widespread coincidence with regional tectonic structures within the axial rift zone. Here the intersection of regional faults with the caldera margin has formed subsidiary collapse structures extending beyond the structural depression outlined by geophysical data, forming an oversized, complex topographic margin. At Rotorua and Reporoa calderas, regional tectonic structures are scarce or absent.

3.5.2 Across-axis relationship between tectonism and magmatism

The characteristics of Modern TVZ calderas clearly elucidate the complex eruptive and structural history of Okataina and Taupo in relation to Rotorua and Reporoa. These data therefore show that caldera structures of Modern TVZ can be divided into two groups (1) extra-rift calderas (Reporoa and Rotorua) are simple, relatively small, sub-circular, monogenetic structures, without significant coupling to active regional structure, and where caldera-forming ignimbrites are associated with zoned magma chambers, and (2) intra-rift caldera complexes (Okataina and Taupo) are large, multiple collapse structures, with rectangular geometries and clear coupling to regional structure; here largely homogeneous magmas are erupted during caldera-forming events. This distinction demonstrates the role of active regional tectonics in influencing the location, structure and development of caldera systems within a rift zone (Fig. 3.12).

Accounting for extra-rift calderas

The presence of a major caldera within an active axis of a rift zone is a common situation worldwide. In a model of caldera volcanism in TVZ however, the presence of calderas outside the axial rift zone also has to be accommodated. Among the possible explanations, the alignment of Rotorua and Reporoa Calderas with the southern continuation of the Miocene-Pleistocene Coromandel Volcanic Zone (CVZ; SKINNER, 1986; Fig. 2.1) is considered here. Pre-existing structures related to the NNW-SSE trending CVZ likely extend beneath the central portion of TVZ, and may constitute preferred pathways for the

rise of magmas both inside and outside the axial rift zone. This hypothesis is supported by the common appearance of minor ~NW-SE fractures in the Kapenga and Rotorua area (ACOCELLA *et al.*, 2003; Appendix A). These fractures may be a weak surface expression of an inherited structure, reactivated during the evolution of modern TVZ.

CHAPTER 4 Effect of regional structure on 3D caldera geometry: a Review

4.1 INTRODUCTION

Calderas of varying size and geometry are documented from almost all volcanic environments, ranging from localised collapse features on the summits of oceanic islands to the large silicic systems typical of convergent margins and continental rift zones. They are recognised throughout geologic time on Earth and are conspicuous on other planets. Across the range of volcanic environments, calderas are often multiple collapse structures, can be geometrically complex, and collapse events may involve a variety of subsidence mechanisms.

The three-dimensional geometry of calderas and caldera structures and their relationship to collapse processes have been controversial (e.g. LIPMAN, 1984, 1997, 2000b; BRANNEY & KOKELAAR 1994; FERGUSON *et al.*, 1994). Modern caldera research, with the benefit of extensive direct subsurface and geophysical data, analogue modelling, and an ever-increasing database of calderas and related features, has revealed a complexity in caldera structures that was largely unrecognised in early models (e.g. WILLIAMS, 1941; SMITH & BAILEY, 1968).

There are many review papers (e.g. WILLIAMS, 1941; WILLIAMS & MCBIRNEY, 1979; WALKER, 1984; LIPMAN, 1997, 2000b; BRANNEY, 1995; COLE, MILNER & SPINKS 2005) that discuss caldera features and their formation processes. This chapter specifically examines the influence of regional tectonics on caldera geometry and structure based on a number of key examples in the literature. The following discussion is divided into three sections, dealing first with the relationship between magma chamber geometry and caldera geometry, secondly with the surface geometry of calderas, and thirdly with the collapse or cross-sectional caldera geometry.

4.2 MAGMA CHAMBER GEOMETRY

4.2.1 Magma Chamber geometry as a proxy for caldera geometry

The common correlation between caldera size and eruption volume should seemingly extend to a strong relationship between the shape and size of the chamber and that of the surface collapse structure. Analogue modelling of caldera collapse by ROCHE *et al* (2000) clearly shows that the depth, shape, and size of the 'magma chamber' directly controls the

shape of the collapse structure at the surface. The growth of a magma chamber may also contribute to the collapse geometry, as shown by the reactivation of 'inflation' ring faults during simulation of magma withdrawal in analogue modelling of ACOCELLA *et al* (2000). The mode of magma emplacement into the upper crust is likely important in establishing the stress conditions in the upper crust. While the emptying of a magma chamber during a caldera-forming eruption causes the localised loss of support in the overlying crust, existing crustal defects will affect the exact nature of the collapse, to either localise collapse or extend the area over which deformation takes place. In this way the analogue modelling of caldera collapse by various authors (e.g. MARTI *et al.*, 1994; KENNEDY *et al.*, 1999; ACOCELLA *et al.*, 2000; ROCHE *et al.*, 2000; ACOCELLA *et al.*, 2001; WALTER & TROLL, 2001; TROLL *et al.*, 2002) only consider the nature of caldera collapse purely as a function of the void space formed during evacuation of a magma body; they are 'ideal' models of caldera collapse, but in the field must be considered along with the tectonic setting and regional stress patterns around calderas.

The nature of the magma chamber also affects eruptive mechanisms, which may have an influence on caldera development (BOWER & WOODS, 1998). Mathematical modelling shows that variations in the depth, volume, and aspect ratio of magma chambers have a significant impact on the erupted volume and the eruption duration. These results indicate that extensive shallow chambers of any volume tend to produce longer-duration and more voluminous eruptions, in contrast to deeper chambers or chambers of smaller cross-sectional area. The formation of calderas is often attributed to collapse associated with the eruption of voluminous ignimbrite-forming Pyroclastic Density Currents (PDC) along arcuate ring-faults, however LEGROS *et al* (2000) argue that large volume PDC are significantly easier to generate from pipe-like conduits. Numerical simulations indicate that for a given conduit volume, discharge rates are an order of magnitude smaller in ring-fissure eruptions due to higher friction, and hence LEGROS *et al* (2000) suggest that ring fissure vents do not favour the formation of PDC. Data presented by LEGROS *et al* (2000) indicates that large ignimbrites generated during caldera-forming events do not necessarily imply ring-vent style eruptions.

Based on a number of reservoir shapes, ROCHE *et al* (2000) show that chamber shape has a strong influence on the stress regime around the chamber and on the initiation of collapse. GUDMUNDSSON (1988) and MARTI *et al* (1994) have both considered the stress field generated by the accumulation of magma in a shallow chamber and have indicated that

uplift and the generation of tensile stresses at the surface are important in initiating ring-faulting and permitting caldera collapse. GUDMUNDSSON (1998) suggests that stress concentrated along the margins of sill-shaped magma chambers leads to slip on faults that control (and generate) collapse at the surface above the chamber.

4.2.2 Tectonic control of chamber location and shape

Since analogue modelling shows that the shape of the magma chamber is one of the main controls on the collapse geometry (ROCHE *et al.*, 2000), it is important to consider the controls on chamber location and geometry. Extension inherently permits the accumulation of magma (e.g. HUTTON & REAVY, 1992; CAMBRAY *et al.*, 1995) and may influence the timing of eruption. While eruption may be promoted by a reduction in lithostatic pressure during continued extension, or initiated by tectonic events, the reverse must also be considered, i.e. where rates of magma accumulation simply exceed the rate at which space is created, such that magmatic pressure is no longer accommodated by further extension resulting in eruption.

BOSWORTH *et al* (2000, 2003) consider that the shape of elliptical calderas in the axial part of the Kenya rift valley (Fig. 4.1) reflect stress-induced stretching of originally circular magma chambers, suggesting that magma chambers developed a long axis parallel to the minimum horizontal stress (Fig. 4.2). While vent lineations and faults in the inner rift-zone are rift-parallel, the calderas are typically oblique to the rift, elongate NW-SE, interpreted by BOSWORTH *et al* (2000, 2003) as resulting from rotation of the stress field from the rift-forming E-W extension to NW-SE extension. The presence of NE-trending volcanic alignments in the youngest units of the axial rift volcanoes also supports a new stress-field orientation. BOSWORTH *et al* (2000) consider the elongate calderas to result from compressive shear fracturing adjacent to the minimum horizontal stress, causing spalling of the chamber walls and resulting in an elliptical chamber. The onset of caldera collapse in the axial rift volcanoes is thought by BOSWORTH *et al* (2000, 2003) to relate to the timing of stress field rotation.

Three Quaternary calderas of the Ethiopian rift alternatively illustrate the affect of pre-existing structures on magma chamber and caldera development (Fig. 4.3; ACOCELLA *et al.*, 2002). The axial zone of the rift is characterised by several Quaternary elliptical calderas, whose E-W caldera elongation and vent alignments are oblique to NW-SE extension and NNE-trending rift structures. ACOCELLA *et al* (2002) suggest that stretching

of an originally sub-circular caldera or magma chamber during regional extension (e.g. BOSWORTH *et al.*, 2000) is unlikely since the caldera long axes are oblique to the NW-SE extension direction in the Ethiopian rift (ACOCELLA & KORME, 2002). They propose instead that caldera elongation is due to pre-rift E-W trending structures largely absent within the rift but present on the borders of the rift. Reactivation of these pre-rift structures as left-lateral transtensional strike-slip faults occurred during NW-SE extension. ACOCELLA *et al* (2002) suggest that rift structures have controlled the rise of magma at mid-crustal depths, while E-W transverse structures have controlled the emplacement and geometry of magma chambers in the upper crust and the geometry of calderas at the surface.

ACOCELLA *et al* (2004) incorporate an extensional tectonic regime into analogue modelling of caldera collapse and show that pre-caldera extension produces elliptical collapse structures with long axes parallel to the extension direction; resurgence forms with a long axis perpendicular to the extension direction. ACOCELLA *et al* (2004) suggest that the elliptical collapse and resurgent structures form by reactivation of pre-existing structures, such that elliptical calderas may form even from circular magma chambers in an area undergoing extension.

Source Migration

MARTI & GUDMUNDSSON (2000) interpret overlapping collapse structures at Las Cañadas caldera complex on Tenerife as the result of stepwise chamber evacuation and migration. The 16 x 9 km caldera complex comprises the scalloped margins of three collapse centres (Fig. 4.4), formed 0.4 – 0.5 Ma apart, relating to an alternating sequence of phonolitic and mafic magmatism. MARTI & GUDMUNDSSON (2000) suggest that emptying of an initial magma chamber during a caldera-forming eruption changed the local stress field such that magma supply to the initial chamber area was impeded, encouraging magma accumulation in new magma chambers either side of the old chamber. At Las Cañadas, collapse occurred at the end of c. 200 ka phonolitic magma cycles (MARTI & GUDMUNDSSON, 2000) recording the successive growth, destruction, and migration of shallow magma chambers.

Conspicuously offset collapse structures on flank volcanoes of the Juan de Fuca Ridge are interpreted as a function of source migration (FIG. 4.5; HAMMOND, 1997). The physiography of these flank volcanoes reflects a two-phase process of constructive volcanism (edifice formation) and caldera development, since all cones are circular and

exhibit no evidence of progressively offset calderas (HAMMOND, 1997). The ridge-facing calderas and craters form as a function of the plate motion produced by seafloor spreading (HAMMOND, 1997), reflecting the relative motion between a stationary magma source and the overriding lithosphere. Calderas represent the final phase in the evolution of these short-lived volcanoes, when magma conduits are abandoned generating ridgeward collapse structures.

Summary

Since calderas form primarily because of magma chamber evacuation (COLE *et al.*, 2005), the controls on chamber location and geometry are clearly important in determining the nature of caldera collapse. Analogue and numerical modelling of caldera collapse show that the magma chamber dimensions and depth are controlling factors; however this is largely based on simple structures that clearly have only broad and restricted correlation with actual caldera structures. ROCHE *et al* (2000) acknowledge that their models do not take into account pre-existing structures. Recent work by ACOCELLA *et al* (2004) incorporating deformation of crustal materials in analogue modelling shows that chamber geometry becomes less of a controlling factor in areas of crustal extension. As inherent crustal heterogeneities and structural complexity increases in the upper crust, the disparity between caldera and chamber geometry likely increases acting to complicate the surface expression of the source chamber at depth. Many examples presented in the following sections reveal that regional structure has a significant control on the resultant caldera morphology, in both plan-view geometry and sub-surface geometry.

4.3 CALDERA GEOMETRY

Caldera definitions typically refer to circular or sub-circular structures (e.g. WILLIAMS & MCBIRNEY 1979) formed during collapse along postulated ring faults. Even a short literature search however, reveals that many caldera collapse features show significant variation from an ideal circular shape (e.g. ACOCELLA *et al.*, 2002; BERESFORD & COLE 2000; FERGUSON *et al.*, 1994; MARTI & GUDMUNDSSON, 2000; MILNER *et al.*, 2002; MOORE & KOKELAAR, 1997; DE SILVA & FRANCIS, 1991), and that many caldera margins do not attest to a simple ring-fault model. With detailed study and the availability of extensive geophysical and drill-hole data, some previously well-documented calderas show evidence of a more complex structure. The following examples illustrate the diversity of caldera geometry and morphology at the surface.

Calderas and active tectonism

At Turkey Creek caldera, evidence suggests the caldera formed within an extensional fault-controlled basin, and that regional extension was ongoing during development of the caldera (DU BRAY & PALLISTER, 1991). This evidence includes outflow rocks ponded in fault-controlled basins, and regional NW-trending faults that offset early caldera derived rocks but are later buried by subsequent rhyolites. The regional faults are part of a regional horst and graben system that trends northwest across the caldera and extends for more than 20 km to the south (DU BRAY & PALLISTER, 1991).

BODEN (1986) attributes NW-elongate calderas of the Toquima caldera complex, central Nevada, to a WNW structural grain present prior to NNE Quaternary basin and range faulting (Fig. 4.6). Toquima caldera complex sits near the centre of the 800 km long, 200 km wide belt of mostly silicic volcanics extending from Utah to California. Within this zone, there is a general NW alignment of regional structural and physiographic features including high-angle faults, magnetic and gravity anomalies, and NW-elongate calderas (BODEN, 1986). The Toquima caldera complex is itself elongate NW, with progressive younging of individual calderas to the southeast, suggesting fundamental structural control of caldera development (BODEN, 1986). Based on field and age relations, BODEN (1986) indicates that faulting commenced or resumed synchronously with formation of the caldera complex, and may have facilitated the rise and eruption of magma.

Rectilinear Caldera Margins

The south-western Nevada volcanic field (SWNVF) is an excellent example of a multi-caldera silicic volcanic field. It is well exposed and has been the subject of intensive study, largely because of underground nuclear testing at the Nevada Test Site (SAWYER *et al.*, 1994). More than six major calderas formed between >15 and 7.5 Ma, the youngest of which are well preserved topographic features (CHRISTIANSEN *et al.*, 1977). CHRISTIANSEN *et al* (1977) consider major tectonic intersections controlled the location and development of various structural features of the major calderas that dominate the SWNVF. Volcanism in the SWNVF coincided with the peak of extensional deformation in the Great Basin, although SAWYER *et al* (1994) unconvincingly suggest that while faulting preceded, accompanied, and followed evolution of the volcanic field, magmatism and regional extension were not genetically linked.

A study of the Silent Canyon caldera complex (SCC) by FERGUSON *et al* (1994) reveals that caldera margins were influenced by regional structure, and often coincident with regional faults (Fig. 4.7). The Silent Canyon caldera complex is one of the most extensively drilled calderas, with the structure defined by FERGUSON *et al* (1994) on a combination of drillhole and geophysical data. In contrast to previous depictions of the SCC, they find that the caldera is bounded by high angle rectilinear faults, and suggest the structure "has more the appearance of an asymmetric graben than of a classical caldera" (FERGUSON *et al.*, 1994 p.4336), consistent with development within the Basin-Range rifting.

ACOCELLA *et al* (1999) consider the relationship of regional tectonics to the Campi Flegrei Volcanic District (CFVD) on the southern Tyrrhenian margin in Italy. NW-SE trending extension has occurred along the Tyrrhenian margin since the upper Pliocene, forming a NW-SE trending belt of volcanism. In detail however, volcanic activity is consistently associated with NE-SW trending transverse systems. The CFVD includes the Campi Flegrei caldera and the islands of Ischia and Procida, which together constitute the surface features of a NE-SW transverse horst like structure on the southern part of the Campania Plain (ACOCELLA *et al.*, 1999). Regional structure is dominated by both NW-SE and NE-SW trending normal faults (ORSI *et al.*, 1996; ACOCELLA *et al.*, 1999). Two nested caldera-forming events at Campi Flegrei caldera (Fig. 4.8) are associated with an erupted magma volume totalling 190 km^3 (ORSI *et al.*, 1996). Formation of both calderas reactivated pre-existing regional faults, forming a complex structure (ROSI *et al.*, 1983). The margins of the outer caldera, related to the Campanian Ignimbrite eruption of 37 ka (BARBERI *et al.*, 1978), in particular are controlled by reactivated NE-trending regional faults, forming a complex geometry with conspicuous linear segments (Fig. 4.8; ORSI *et al.*, 1996). ACOCELLA *et al* (1999) suggest that the CFVD is located along a NE-SW trending transfer zone connecting the NW-SE regional faults. They also suggest that the rise of magma in the upper crust is enhanced by such sub-vertical transfer structures, consistent with the eruption of primitive magmas preferentially along NE-SW trending fractures. The NE-SW trending transfer faults appear important for much of the Tyrrhenian margin, and may constitute structural control at other volcanoes such as Vulsini, Sabatini, Colli Albani, and Roccamonfina.

Large silicic volcanic-tectonic systems

Many of the large caldera structures in the Central Andes are nested caldera complexes and are among the largest identified on Earth, with long axes up to 100km (Fig. 4.9; DE SILVA & FRANCIS, 1991). The arid climate and high altitude has produced excellent exposure although these factors and the size of the region have precluded much detailed field study. Extensive study of Landsat TM data space shuttle photography by DE SILVA & FRANCIS (1991) show that many of the calderas have irregular profiles closely linked with regional tectonic structures.

The Altiplano-Puna Volcanic Complex (APVC) consists of several large nested caldera complexes (Fig. 4.9) of which La Pacana Caldera is the largest (DE SILVA & FRANCIS, 1991). The resurgent La Pacana caldera formed during the eruption of the Atana Ignimbrite at about 4 Ma (GARDEWEG & RAMIREZ, 1987) but is thought to be associated with at least three other major ignimbrites (DE SILVA & FRANCIS, 1991), indicating a multiple collapse history. This large (60 x 35 km) caldera complex is in an area of the central Andes where N-S, NW-SE, and NE-SW fault systems have controlled the vent distribution (Fig. 4.9; LAHSEN, 1982, in GARDEWEG & RAMIREZ, 1987). From Satellite image interpretation, GARDEWEG & RAMIREZ (1987) indicate that conspicuous regional lineaments may have controlled both the location and the shape of the caldera complex. The elliptical caldera complex (defined by the topographic rim) has its longest axis oriented N-S, parallel to the 180 km Miscanti Lineament that has also controlled pre-caldera and post-caldera cones and domes. The other lineaments also parallel the caldera walls, and the NE-SW regional structure has also controlled recent lava flows (GARDEWEG & RAMIREZ, 1987).

Most of the described calderas of the central Andes have similar tectonic settings to that of La Pacana caldera, with their longest axis trending N-S paralleling the regional trend of the Andes. The close spatial association between volcanic centres and major fault zones in the central Andes is not well understood. RILLER *et al* (2001) undertook research to establish the kinematic link between major faults and caldera structures, to determine if these faults acted as magma conduits or if displacement could have induced caldera collapse and magma accumulation in the upper crust. RILLER *et al* (2001) show that most calderas in the southern part of the central Andes are associated with NW-SE striking first-order fault systems (Fig. 4.9), indicating a close genetic relationship between faulting and caldera formation. RILLER *et al* (2001) demonstrate that the Negra Muerta Caldera, located on the

NW-SE striking Olacapato-El Toro fault zone (Fig. 4.9), and eroded down to sub-volcanic basement, formed in response to regional left-lateral transtension. Kinematic data from second-order exposed normal and oblique-normal faults within the basement rocks of the caldera establish genetic links to the major left-lateral faults of the zone and indicate NNW-SSE stretching. At Negra Muerta Caldera, temporal relationships between rhyolite and andesitic dike emplacement respectively, and faulting, suggests a 2-phase tectono-magmatic evolution. RILLER *et al* (2001) conclude that normal faulting controlled the ascent and eruption of rhyolite magma, after which andesitic volcanism was associated with strike-slip faulting.

Other calderas in the central Andes exhibit features consistent with NNW-SSE extension associated with left-lateral transtension within large fault zones. The western and eastern margins of Cerro Galan caldera coincide with N-S trending faults (SPARKS *et al.*, 1985). FRANCIS *et al* (1981) report that the Kari Kari Caldera is similar in appearance to the Cerro Galan Caldera in northwest Argentina, with an elliptical shape and the longest axis (32 km) parallel to the regional tectonic trend.

The Great Sumatran Fault (GSF) represents the strike-slip component of oblique convergence of the Indo-Australian and Eurasian plates along the Java-Sumatran trench system (Fig 4.10a). The 1650 km long right-lateral fault is parallel to the trench and follows the Sumatran magmatic arc. BELLIER & SEBRIER (1994) argue that initiation and evolution of Sumatran calderas (eg Toba, Ranau) is tectonically controlled by the Great Sumatran Fault Zone (Fig. 4.10b,c). In a study of the geometry of the strike slip zone, BELLIER & SEBRIER (1994) document the relationship between calderas and the evolution of pull-apart grabens in releasing stepovers. The asymmetric and irregular shaped calderas develop when normal and strike slip faults within a pull-apart basin convert to collapse-bounding fractures (Fig. 4.10b,c).

The relationship between releasing step-overs and caldera formation is clearest in south Sumatra where two major NW trending faults are linked by a releasing step-over fault zone. The rectangular Ranau caldera (12 x 16.5 km) formed in a releasing step-over and was initially the site of geothermal and minor volcanic activity before incremental collapse occurred on normal faults at the boundaries of the pull-apart (Fig. 4.10c; BELLIER & SEBRIER, 1994). The pull-apart became extinct with the development of a through-going

strike-slip fault (BELLIER *et al.*, 1999), which represents one of the currently active fault segments (Fig. 4.10c).

The asymmetric 100 x 30 km Toba caldera is also parallel to the Great Sumatran Fault and likely formed in a large step-over (Fig 4.10b). A huge pull-apart structure hosted progressively larger calderas in zones of crustal weakness until the paroxysmal eruption of the Toba Tuffs at 73,000 +/- 3000 ka (CHESNER *et al.*, 1991) which formed the present Toba Caldera (BELLIER & SEBRIER 1994).

Caldera collapse on Deception Island, at the northern end of the Antarctic Peninsula, has commonly been considered as occurring on arcuate ring faults (WALKER, 1984; NEWHALL & DZURISIN, 1988), generally supported by the volcano's morphology. A study of the volcano's tectonic structure by MARTI *et al* (1996) however reveals that this model is inconsistent with observed tectonic features. Based on fieldwork and remote sensing, MARTI *et al* (1996) describe a dense network of tectonic lineations, with a prominent NE-SW tectonic trend, parallel to the axis of the back-arc Bransfield Strait (Fig. 4.11). Where identified, most faults are normal and cut both pre-caldera and post-caldera rocks. The postulated caldera-bounding ring-fault appears to have formed by intersection of an orthogonal set of linear faults, rather than by arcuate faults. MARTI *et al* (1996) indicate that post-caldera volcanism is associated with these fractures, and not with any ring fault system. Seismic profiles obtained both offshore and within the harbour identify fractures consistent with those present on the island. Tectonic lineaments identified on Deception Island clearly relate to regional structure, and MARTI *et al* (1996) suggest this is inconsistent with the expected stress field around a shallow magma chamber (GUDMUNDSSON, 1998). Without any deposits unequivocally identified to a caldera-forming event, the authors conclude that the central depression formed by volcano-tectonic collapse following extensive hydrovolcanic activity and associated fracturing in an extensional environment.

A complex interplay between caldera development and tectonics has also been described from Vulcano Island in the Aeolian Archipelago (Fig. 4.12; VENTURA, 1994; GIONCADA *et al.*, 2003). Two volcano-tectonic caldera structures occur in the central part of the island, however no products related to a caldera-forming event have been identified (GIONCADA & SBRANA, 1991). Vulcano is dominated tectonically by two systems of NW-SE-trending dextral strike slip faults bounding the eastern and western flanks of the island, with

subsidiary NE-SW and N-S trending normal faults. Extensive structural analysis by VENTURA (1994) indicates the NW-SE and N-S trending faults relate to the regional stress field, while the NE-SW structures relate to a local stress field. The system of faults on Vulcano depicts an evolving system of pull-apart basins between two right-stepping dextral strike slip faults (Fig 4.12a). NE-SW extensional structures between the strike slip faults develop in response to the stretching events, and are responsible for magma ascent in the inner parts of the island. VENTURA (1994) concludes that the 'caldera-type' structures may be explained as a consequence of tectonic processes acting in response to a particular stress regime, and emphasises the importance of regional tectonics in caldera formation.

Active arc volcanism in the central part of Kyushu Island has formed an area of volcano-tectonic depression known as the Hohi volcanic zone (ITOH *et al.*, 1998). Depocentres have migrated NE within the zone to Beppu Bay, a late Quaternary rhomboidal basin surrounded by active faults and filled with volcanic material. There is no suggestion of caldera collapse having occurred, but most features are consistent with those identified as associated with caldera collapse at other locations (e.g. fault-bounded basins filled by volcanic material, geophysical response similar to documented calderas). This example highlights the point that the purely magmatic and tectonic components which produce volcano-tectonic structures often may be difficult to resolve, and as such demonstrate the complex interaction of tectonics and volcanism which produce such structures.

Summary

The examples outlined above range from calderas which superficially appear simple, to volcano-tectonic structures where the volcanic and tectonic components of collapse are difficult to resolve. The Valles and Long Valley calderas are traditionally cited as examples of arcuate ring faults bounding coherent caldera floors, but an increase in subsurface data indicates the influence of pre-existing regional structure. Other examples show distinct rectilinear margins contiguous with regional tectonic faults. The boundaries of some large silicic calderas are controlled by the margins of localised extension in pull-apart basins, forming collapse structures which are very much volcano-tectonic in origin. Volcano-tectonic deformation produced by reactivation of regional structures during caldera volcanism significantly affects collapse geometry and the surface geometry of some well-documented examples of calderas is shown to be as closely related to collapse induced by the regional structural setting as to the withdrawal of magmatic support. The examples highlight the need to consider the role of tectonics in caldera development.

4.4 COLLAPSE GEOMETRY

Most silicic calderas, but particularly those in the western United States, are modelled as simple piston collapse structures, with largely coherent floors and arcuate bounding ring-faults, independent of regional structure. Recent work has highlighted the complexities of caldera structure, in well-exposed examples or where significant sub-surface data is available, and has revealed that the internal structure of many of these calderas is more complex than the initial model of SMITH & BAILEY (1968) suggested. These complexities include components of downsag in the caldera margin (e.g. WALKER, 1984; MILNER *et al.*, 2002), differential and asymmetric collapse (e.g. NIELSON & HULEN, 1984, HEIKEN *et al.*, 1986; BRANNEY & KOKELAAR, 1994) and coupling with regional tectonic systems (e.g. SELF *et al.*, 1986; KOKELAAR, 1988; FERGUSON *et al.*, 1994).

Coherent ring-fault bounded collapse?

Long Valley Caldera is a 17 x 32 km structure on the eastern side of the Sierra Nevada range, California. The caldera is elongate E-W, oblique to NW-trending regional faults related to the frontal Sierra Nevada range and active prior to and following collapse (BAILEY *et al.*, 1976). Post-caldera vents are aligned along NW-trending lineaments, and NW-trending pre-caldera faults control the location of a contemporaneous resurgent dome in the west part of the caldera. While the caldera margins are not clearly coincident with regional faults, asymmetric subsidence of the caldera floor is indicated by gravity (KANE *et al.*, 1976) and seismic refraction data (HILL, 1976). BAILEY *et al* (1976) indicates that a NW-trending gradient in the gravity maps of KANE *et al* (1976) likely represents differential displacement along a Sierra Nevada frontal fault, resulting in asymmetric 'trapdoor' collapse.

Many of the ideas regarding the formation of resurgent calderas are based on work at Valles caldera complex in New Mexico (e.g. SMITH & BAILEY, 1968). Extensive subsurface data obtained at Valles caldera since the development of these early models of piston collapse and central resurgence however, indicate a more complex structure (Fig 4.13; SELF *et al.*, 1986; HEIKEN *et al.*, 1986, 1990). The Jemez volcanic field, which contains Valles caldera complex, coincides with the intersection of the western boundary faults of the N-trending Rio Grande rift and the NE-trending Jemez lineament, the local expression of a precambrian basement feature (Fig 4.13a; SELF *et al.*, 1986). Drill-hole control on caldera fill, and gravity data, reveal that the collapse structure is strongly asymmetric, with deepest subsidence in the east, and is broken by N-NE-trending normal

faults (Fig 4.13b; GOFF, 1983; NIELSON & HULEN, 1984; HEIKEN *et al.*, 1986). Caldera fill abruptly thickens from 1500 m beneath Redondo Dome to 3400 m beneath Valle Grande in the east. Asymmetric collapse during at least two main caldera-forming events is bounded in the east by a major NE-trending rift-related fault, consistent with caldera collapse across the western margin of the Rio Grande Rift (HEIKEN *et al.*, 1986). More than 1 km of resurgence has occurred to form Redondo Dome, dissected by a complex NE-trending apical graben parallel to the Jemez lineament to the southwest. Valles is a clear example of where pre-existing faults have strongly influenced the nature of collapse, with subsurface data recording differential and strongly asymmetric collapse controlled by pre-existing structures. The largely circular surface expression of the caldera obscures the rather more linear collapse margins at depth.

Exhumed calderas and exposed caldera floors

The calderas that constitute the Stillwater caldera complex in west-central Nevada have particularly good three-dimensional exposure due to extensive tilting after their formation (JOHN, 1995). Caldera collapse occurred along subvertical ring fractures; however, several faults dissect the caldera floor forming highly asymmetric subsidence (JOHN, 1995). A fault separating the two structural blocks of the Job Canyon caldera was later reactivated forming the northern walls of both the Poco Canyon and Elevenmile Canyon calderas. Another fault forming the southern rim of the Job Canyon caldera separated the Poco Canyon and Elevenmile Canyon calderas into blocks which subsided to different depths, indicated by the vastly different thicknesses of caldera-related deposits. JOHN (1995) indicates that between major faults, collapse occurred as large piston-like blocks, with no evidence for chaotic collapse.

The Ordovician Snowdon Caldera in Wales formed in a transtensional regime which KOKELAAR & BRANNEY (1999) compare to TVZ, with similar rates of extension and production. Volcanism was concentrated in locations along faults striking NW-SE (HOWELLS *et al.*, 1987; KOKELAAR, 1988; KOKELAAR & BRANNEY, 1999). This faulting affected both caldera location and collapse, with subsidence proposed to have occurred in a trapdoor style with the margins controlled by regional structure (KOKELAAR & BRANNEY, 1999; CAMPBELL *et al.*, 1987). Caldera collapse occurred during the eruption of the Lower Rhyolitic Tuff Formation, which thickens into volcanically and tectonically controlled basins (CAMPBELL *et al.*, 1987; KOKELAAR, 1988; KOKELAAR & BRANNEY, 1999), reflecting active tectonic control. Differential collapse of the caldera floor along regional

structures produced a 'piano-key' style collapse morphology (B.P. KOKELAAR *pers. comm.* 1999). Post-caldera volcanism is aligned along the same regional trend. Resurgence occurred but was less than that of contemporaneous subsidence due to extension, resulting in net subsidence (KOKELAAR & BRANNEY, 1999).

A reinvestigation of Glencoe Caldera in Scotland by MOORE & KOKELAAR (1997; 1998) challenges the common assertion that Glencoe Caldera formed by collapse of a coherent block along a bounding ring fault (CLOUGH *et al.*, 1909; LIPMAN, 1984; WALKER, 1984; WILLIAMS, 1941). MOORE & KOKELAAR (1998) show that caldera collapse was complex, and cannot be reconciled with subsidence of a coherent block along a ring fault. Glencoe caldera formed within a system of orthogonal faults and associated grabens reflecting extension and/or transtension focussed at the intersection of two major discontinuities in metamorphic basement rocks (Fig. 4.14a; MOORE & KOKELAAR, 1997). The dominant NW-trending Glencoe Graben controlled the general location and form of major caldera depocentres. Tectonic faults were active prior to, during, and after caldera collapse, and some were reactivated during eruption as volcano-tectonic faults (Fig. 4.14b). Detailed study of the caldera floor reveals thickness variations of successive eruptive units and buried fault scarps indicating that collapse occurred incrementally and involved multiple vent positions and depocentres (MOORE & KOKELAAR, 1997; 1998). Incremental piecemeal subsidence occurred prior to development of any ring fault. The features described by MOORE & KOKELAAR, 1997; 1998) reveal a complex collapse history reflecting a strong coupling between regional tectonism and volcano-tectonic collapse.

Collapse of Ordovician Scafell Caldera in the English Lake District was also the result of complex interaction between volcanism and tectonics. Rapid lateral thickness changes of ignimbrites at Scafell record an irregular and abruptly changing caldera floor, which reflects fragmentation of the caldera floor into 100 to 2000 m size blocks (BRANNEY & KOKELAAR, 1994). Eruption and collapse at one location may have induced instability at another, leading to multiple collapse and distinct depocentres. Some faults reversed their sense of motion during the eruption. BRANNEY & KOKELAAR (1994) indicate that these extreme stratigraphic and structural complexities characterise successions formed during piecemeal collapse. Pre-existing faults controlled spatially separate eruptions from distinct magma chambers, observed through interfingering tuffs of different composition (BRANNEY & KOKELAAR, 1994). Volcano-tectonic faults active during the collapse event are parallel to the regional northwest trend of tectonic faults.

Resurgence

Resurgence is a common feature in the evolution of many calderas, and often exhibits evidence of structural control. Like the structure of calderas, the structure of resurgent domes reflects both regional structure and the local stresses induced by the magmatic system. The morphology of resurgent blocks may therefore reflect the controls on the original collapse feature in which it has formed. The island of Ischia is located in the westernmost portion of the Campi Flegrei district in southern Italy, and is characterised by a resurgent dome uplifted at least 800 m in the last 33 ka (GILLOT *et al.*, 1982). NE-SW and NW-SE faults relating to regional structural trends, and subsidiary N-S and E-W faults relating to the local stress field, were reactivated during resurgence, forming the boundaries of the polygonal shaped resurgent block (ACOCELLA & FUNICIELLO, 1999). The rectilinear margins of the resurgent block at Pantelleria also relate to volcano-tectonic faults which coincide with the trends of pre-existing faults (ORSI *et al.*, 1991). The combination of NW-SE trending strike slip faults and N-S trending normal faults on the island formed pull-apart basins and likely influenced caldera collapse and subsequent resurgence. Pre-resurgent evidence for structural control on volcanism on the island is present in the form of polygonal margins to the Monastero caldera, and strongly N-S aligned vents (ORSI *et al.*, 1991). Differential uplift of fault bounded blocks in the resurgent block at both locations caused asymmetric resurgence.

Summary

With extensive study of the caldera literature, there exists a clear relationship between the relative level of dissection and exposure of a caldera, and the mechanisms proposed as responsible for caldera formation. The structural (caldera-floor) geometry remains largely unknown at most morphologically youthful calderas, and a simple surface expression may conceal potentially complex caldera structure beneath caldera fill material. Early models of coherent collapse along ring faults are challenged by both increased subsurface data at young calderas and detailed studies of caldera floor successions at exhumed calderas. Many uplifted and well-exposed structures (e.g. FERGUSON *et al.*, 1994; JOHN, 1995) and exhumed structures (e.g. MOORE & KOKELAAR, 1998; BRANNEY & KOKELAAR, 1994) reveal extreme stratigraphic and structural complexity with rapid changes in the thickness of caldera fill material. Differential and often strongly asymmetric subsidence of the caldera floor is consistent with reactivation of pre-existing structures and a clear interaction between volcanism and tectonism.

4.5 DISCUSSION

The examples used in the previous three sections reflect the significant diversity among caldera structures and in particular highlight the evidence for coupling between calderas and regional tectonic systems. Eruptive morphology often obscures caldera structure at the surface, inherently leading to a general perception of calderas as roughly circular structures. Extensive drilling at Valles and Silent Canyon calderas, and less direct evidence at calderas such as Toquima caldera complex, Campi Flegrei, caldera structures of the central Andes, and volcano-tectonic structures in Sumatra, indicate that these calderas are at least in part bordered by linear fault structures rather than circular collapse features. Caldera dimensions in Sumatra appear to be a function of pull-apart basin geometry rather than a function of any perceived magma chamber geometry, and represent areas of volcano-tectonic collapse largely independent of chamber volume or size.

Further geomorphic development of calderas generally approaches a roughly circular profile compounding the perception of calderas as circular structures. Models of coherent collapse along arcuate ring faults are heavily influenced by this surface morphology, but with modern geophysical techniques and stratigraphic evidence from high resolution drilling programs, we are able to define the collapse geometry of calderas more clearly. Calderas are generally either preserved close to their eruptive state, or deeply eroded to expose their caldera floor structure; exposure through the volcanic sequence into sub-caldera rocks is very rare. While we thus have two 'end-members' of preservation, applying observations at exhumed calderas where internal structure is clear to the surface expression of youthful calderas and vice versa is risky. The geometry of a caldera provides information on the regional tectonic setting, and this relationship to regional structure is important in establishing the controls on caldera formation and development.

CHAPTER 5 Structure & Development of the Okataina Caldera Complex

5.1 INTRODUCTION

The Okataina Caldera Complex (OCC) is located 20 km east of Rotorua City (chapter three). Okataina is one of eight rhyolitic calderas recognized in Taupo Volcanic Zone (e.g. WILSON et al., 1995), and one of two active multicyclic caldera complexes in the axial rift zone of Modern TVZ. It is the northernmost caldera in TVZ and conspicuously forms the northern boundary to the central silicic portion of Modern TVZ; the other axial caldera complex, Taupo, similarly forms the southern boundary. Okataina is the site of voluminous activity over at least 300 ka, and remains highly active with an eruptive output of c. 0.1 m^3 s^{-1} over the last 65 ka (WILSON *et al.*, 1995). Okataina Volcanic Centre has previously been associated with up to six caldera-forming eruptions (NAIRN, 1981) while HOUGHTON *et al* (1995) and WILSON *et al* (1995) attribute only the 280 ka Matahina and 65 ka Rotoiti ignimbrite eruptions to caldera-forming events (ages from HOUGHTON *et al* 1995) and BERESFORD & COLE (2000) infer at least four collapse events. Three collapse events are recognised in this study, including an eruption at 33 ka based on a major change to the ignimbrite stratigraphy. While Okataina has been mapped in detail, the existing model for its structure and development (NAIRN, 1989, 2002) is incomplete and insufficient to explain many of the observed features.

Morphotectonic techniques applied to both terrestrial and planetary calderas elsewhere have revealed a significant amount of data on caldera evolution and the nature of magmatic-volcanic-structural associations at volcanoes. Morphotectonic analysis at Okataina using DEM and Remote Sensing data reveals that it is significant in its location at a major transfer in the axial rift zone where adjacent segments are offset by ~25 km. This major ENE-trending bend in the transtensional rift accompanies local rotation of the extension direction resulting in a zone of orthogonal extension. The complex relationship between rift architecture and caldera development (including a major change to the ignimbrite stratigraphy) at Okataina is described here for the first time, in light of recent advances in understanding rift architecture (chapter two) and caldera volcanism (chapter three) in Modern TVZ, and modern caldera research (chapter four).

5.2 PREVIOUS WORK

5.2.1 Mapping the Okataina district

In 1937 L.I. Grange produced an extensive bulletin on the Rotorua-Taupo region that included maps and descriptions of geologic structures and eruptive units (GRANGE, 1937). Additional mapping by HEALY (1962) and MARTIN (1961) further differentiated the various ignimbrites and established their succession across a large part of TVZ. Compiling previous work and with new data, HEALY *et al* (1964) produced a comprehensive geological map at 1:250,000 scale of the Rotorua region that included Okataina (Sheet 5; FIG. 5.2). In 1981 I.A. Nairn completed a detailed geologic map of the Okataina area as part of his PhD research at Victoria University (NAIRN, 1981). He compiled existing data with new detailed studies of OVC eruptives and new interpretations of volcanic and structural features to make a huge contribution in terms of the volcanic history of OVC. This mapping was partially published in his 1989 map of Tarawera Volcano (NAIRN, 1989), and in its entirety in his recent geological map and bulletin for Okataina Volcanic Centre (FIG. 5.4; NAIRN, 2002). The 2002 bulletin includes revisions to both map and stratigraphy generated from Nairn's ongoing work in Okataina since 1981, and contributions from other studies, including the major stratigraphic revision from this thesis. The discussion of caldera structure and evolution is however largely unchanged from his previous work.

5.2.2 Geology of Okataina Volcanic Centre

HEALY (1962) first defined the Okataina Volcanic Centre (OVC) and surrounding structures including the young intra-caldera rhyolite complexes of Haroharo and Tarawera. The OVC was considered the probable source for the Matahina and Kaingaroa ignimbrites, with additional collapse accompanying the eruption of the Rotoiti Breccia (HEALY *et al.*, 1964; NAIRN, 1989).

Subsequent work concentrated on the petrography of OVC eruptives. BAILEY (1965) and BAILEY & CARR (1994) described the physical volcanology of the Matahina Ignimbrite, and considered it to have been erupted during caldera collapse in OVC, consistent with earlier studies. Ewart and co-workers (*e.g.* EWART, 1967, 1968; EWART & HEALY, 1965; EWART *et al.*, 1968) described the petrography and geochemistry of various TVZ rhyolites, while COLE (1970a,b,c,d) made an extensive study of the structure and history of the Tarawera Volcanic Complex. EWART *et al* (1975) further discussed and summarised the rhyolites of Okataina, particularly those of Haroharo Volcanic Complex. Okataina

rhyolites were grouped into four complexes based on mineralogy and location (EWART, 1968). NAIRN (1981, *and subsequent studies*) modified this division, assigning rhyolites to either the Rotorua, Okataina, or Kapenga 'volcanic centres'. More recent work attempting to establish the geochemical boundaries of these centres (BOWYER, 2001) has shown that these rhyolites form groups that do not correspond to their division into volcanic centres and are unrelated to caldera-forming magmas. NAIRN *et al* (1994) showed that the Kaingaroa Ignimbrite was sourced from Reporoa Caldera to the south of Okataina (*section 3.3.2*). BERESFORD & COLE (2000b) reinterpreted the Kaingaroa Ignimbrite exposed inside Okataina as a separate Okataina-sourced 'Kawerau Ignimbrite' of the same age.

Tephrostratigraphic research in the Rotorua district correlated units within and across volcanic centres, elucidating the complex eruptive history of local and distal sources. The distribution, chronology, and source areas for late-Quaternary pyroclastic fall deposits surrounding Okataina were initially documented by VUCETICH & PULLAR (1964, 1969), who confirmed an Okataina source for many of the eruptives. BRIGGS (1973) summarised the characteristics and stratigraphy of TVZ pyroclastics including OVC eruptives. Further mapping delineated new formations (HOWORTH, 1975; HOWORTH *et al.*, 1981) and defined a major sequence of Okataina tephras, the Mangaone Subgroup, stratigraphically bracketed by regional tephras associated with the ~65 ka Rotoiti and 26.5 ka Taupo ignimbrite eruptions from Okataina and Taupo respectively. PULLAR *et al* (1973) summarised ^{14}C ages for Okataina eruptives, while KOHN (1973) presented fission-track dates for the Matahina and Kaingaroa ignimbrites.

With a detailed stratigraphic framework largely in place, modern research at Okataina has focussed on the detailed study of eruptive and magmatic processes of individual eruptive episodes. The Earthquake Flat Breccia, Rotoehu Tephra, and Matahi Basalt pyroclastic deposits and their relationships with the Rotoiti Breccia eruptions were described by NAIRN (1971, 1972), PULLAR & NAIRN (1972), and NAIRN & KOHN (1973). Detailed physical volcanological investigations (JURADO-CHICHAY & WALKER, 2000, 2001) and geochemistry (SMITH, 2002) have further constrained the distribution and characteristics of the Mangaone Subgroup tephras. This thesis makes an important revision to that subgroup stratigraphy, adding a ~20 km^3 partially-welded ignimbrite previously considered ~220 ka older by BERESFORD & COLE (2000b).

Recent work has focussed on the detailed characteristics of specific eruptions. This includes the physical volcanology of young post-collapse plinian sequences and dome building episodes (e.g. JURADO-CHICHAY & WALKER, 2000, 2001; NAIRN *et al.*, 2001, 2004; SPINKS, 2001; SPEED *et al.*, 2002; DARRAGH, 2004), geochemical characteristics of regional tephras, ignimbrites, and lithic fragments in pyroclastic deposits (e.g. BURT *et al.*, 1998; BERESFORD & COLE, 2000b; BOWYER, 2001; SMITH *et al.*, 2002; CHARLIER *et al.*, 2003; SHANE *et al.*, 2005) and magmatic triggering of rhyolite eruptions (LEONARD *et al.*, 2002; SMITH *et al.*, 2004).

5.2.3 Caldera Structure

No studies have ventured any significant new information related to the structure and development of the Okataina region, and the structure and collapse history of the caldera complex, since NAIRN (1981). Early studies considered the OVC to lie within a large ring complex in which cauldron subsidence had occurred during multiple ignimbrite eruptions (HEALY, 1962). The margins of the 'Haroharo Caldera' (*c.f.* Okataina Caldera Complex, this study) and a surrounding 'Ring Structure?' were based on physiographic features by means of smoothed contours (HEALY, 1964; FIG. 5.3). HEALY'S (1964) 'ring structure?' was thought to link vent positions that reflected the location of a circular structure at depth that controlled magma rise in the upper crust. EWART & HEALY (1965) further used the physiography of rhyolite lavas to define the caldera margin based on 'outer-older' and inner-younger' divisions.

The caldera margin defined by HEALY (1964) remains largely unchanged on NAIRN'S (1989, 2002) regional tectonic map of OVC. NAIRN (1989, 2002) describes a topographic margin, inner and outer ring structures, and two linear vent zones that transect the caldera. Embayments on each side of the caldera margin at Rotoma and Okareka were believed to have formed by subsidence caused by magma withdrawal during the 65 ka Rotoiti caldera-forming event. NAIRN (1981) defines the supposed outer ring structure as the OVC margin. The implication of Nairn's and others work is that OVC is the surface expression of a single large magma chamber. Recent research however points to a multitude of discrete, independent magmas in the development of Okataina, indicating that the inferred structural model for Okataina is incorrect. The validity of these features and their relationship to the structural evolution of the caldera complex is discussed in section 5.4.

ROGAN (1980, 1982) presented regional geophysical data for Okataina and for TVZ. A large negative gravity anomaly at Okataina was interpreted as a basement depression infilled with low density rocks. Her gravity model suggests a maximum depth of 5 km, with only the top 1-2 km of caldera fill consisting of magnetised rocks. Alternatively, ROGAN (1982) suggests the gravity anomaly may in part be due to low-density upper crustal rocks, with only 1-2 km of caldera subsidence. NAIRN (2002) presents Bouguer gravity data from R. Wood (Institute of Geological & Nuclear Sciences) for the Okataina region (Fig. 3.7c). Limited data within the caldera define a single major gravity low in the southern part of the caldera. SHERBURN *et al* (2003) consider that a clear low Vp anomaly at 4 km effectively corresponds to a minimum depth extent of the collapse structure.

5.2.4 Key Theses

A number of MSc and PhD theses have considered various aspects of the geology of Okataina region. The greatest contribution is almost certainly that of NAIRN (1981), the main results of which are largely unchanged in his published work. Subsequent research has involved re-mapping specific geographic areas (e.g. LOWTHER, 1997; CROSBY, 1998) or deposits adjacent to Okataina (e.g. BELLAMY, 1991; BERESFORD, 1997), but has typically focused on specific eruptions or groups of eruptions to determine eruption characteristics (e.g. SPEED, 2001; SPINKS, 2001; KILGOUR, 2002; DARRAGH 2004), fingerprint the magmatic history (DAVIS, 1985; SCHMITZ, 1995; LEONARD, 1999; BEGGS, 2000; SMITH, 2001; HIESS, 2004) and assess the modern day hazards of similar eruptions (BARNARD, 2004; BLUMENTHAL, 2004). In addition, MANNING (1995) investigated late Pleistocene tephras in the eastern Bay of Plenty region including some that likely had an Okataina source, while BOWYER (2001) considered the geochemical and isotopic characteristics of rhyolite lavas that are exposed in the vicinity of Okataina and Rotorua calderas.

5.2.5 Terminology

OVC was originally defined by HEALY (1962) as a 20 km by 30 km depression containing the young rhyolitic complexes of Tarawera and Haroharo. Most workers (e.g. WILSON *et al.*, 1995; NAIRN, 1989, 2002; COLE *et al.*, 1998; BERESFORD & COLE, 2000b;) continued and developed the tradition established by HEALY (1962, 1964), of OVC comprising a composite caldera ('Haroharo caldera') with surrounding vents. The grouping of these features as a 'volcanic centre', as elsewhere in TVZ, is misleading. Their spatial relationship is expected since rhyolite domes are present throughout central TVZ (chapters

two & three), are concentrated in the axial rift zone, and caldera collapse will thus inherently generate a depression surrounded by vents that may be wholly unrelated to the caldera.

In this thesis, the term 'Okataina Caldera Complex' refers to the system of spatially and structurally associated overlapping calderas. Similarly, a 'caldera' is the collapse structure formed during a specific eruption, *e.g.* the Matahina ignimbrite was erupted from the Matahina caldera within the Okataina Caldera Complex. No genetic link is made between the caldera and spatially associated vents, thus eliminating the need for the term 'OVC'. Alternatively, and more accurately, both the caldera complex and associated vents are shown to directly relate to regional structure within the Okataina transfer zone.

5.3 Eruptive History

Okataina Caldera Complex formed during three caldera-forming eruptions that produced welded and unwelded ignimbrites and associated widespread regional tephras. In addition, many vents inside and on the margins of the caldera complex that were active prior to, between, and following the caldera forming eruptions have erupted widespread pumice-fall deposits, localised pyroclastic flows and voluminous effusive lavas. Figure 5.4 illustrates the key geology of OCC and its location within the TVZ. The stratigraphy and characteristics of deposits exposed in and around OCC are known in some detail (e.g. Nairn, 2002 *and references therein*). Here they are discussed with reference to a model of the eruptive history of OCC (Fig. 5.5), with particular regard to the caldera-forming eruptions and their temporal-spatial relationships to smaller eruptive centres and vents within and on the periphery of the caldera.

5.3.1 Pre-caldera geology

Whakamaru Group ignimbrite basement

The Rangitaiki Ignimbrites form the southern caldera margin and the heavily incised plateau on which the Matahina and Kaingaroa Ignimbrites were deposited. Originally mapped here by Grindley (1959) and Healy *et al* (1964; Fig. 5.1), they extend over 100 km south to Lake Taupo (Healy *et al.*, 1964). Wilson *et al* (1986, 1995) included the Rangitaiki Ignimbrites in the 'Whakamaru-group Ignimbrites', a group of ignimbrites totalling more than 1000 km^3 erupted at 0.34 Ma during formation of the Whakamaru Caldera (chapter three). The Rangitaiki Ignimbrites are moderately welded, dark grey, crystal-rich tuffs (Martin, 1961) and include underlying coarse tuffs that contain biotite

and hornblende rich units, in contrast to the overlying 'type' Rangitaiki Ignimbrites (MARTIN, 1961). NAIRN (1989; 2002) describes these 'quartz-biotite' tuffs from exposures south of Puhipuhi Basin as non-welded to weakly-welded pumice-rich breccias and airfall beds. Extensive vegetation cover meant that only a single exposure was located in this study, on Tukuhu Road (V16/268146). At this location the coarse pumice- and crystal-rich unwelded ignimbrite underlies welded and coarsely-jointed bluffs of Rangitaiki Ignimbrite although the contact is obscured. Devitrified pumices are consistently 50-60 mm across (Mp = 150 mm) and are particularly quartz-rich, with crystals commonly >4 mm in diameter.

Based on a dissimilar mineralogy to 'type' Rangitaiki Ignimbrite, and the coarseness of the tuffs, NAIRN (1989, 2002) considers the 'quartz-biotite tuffs' as eruptives relating to an early Okataina caldera-forming event. The lack of exposure present during this study inhibits any determination of the distribution, volume and/or spatial variation of the tuffs, thus there is no indication whether they represent part of an extensive ignimbrite sequence related to some earlier phase of caldera collapse at Okataina, or indeed if they are related to the Whakamaru-group ignimbrites. Their mapped distribution and proximity to a large rhyolite dome complex of similar age suggests however, that they may more likely be associated with smaller volume eruptions such as those associated with episodes of silicic dome growth (e.g. BELLAMY, 1991; LEONARD, 2003). Localised deposits with similar characteristics occur in other locations around the caldera in various stratigraphic positions, suggesting that they are typical of small eruptive centres that have characterised the activity between major caldera-forming eruptions. Currently, there is insufficient evidence for a caldera-collapse event associated with these deposits prior to the Matahina event.

Pre-caldera lavas

Prior to the 280 ka Matahina event, several domes had developed that are now exposed surrounding the caldera complex and as partial dome remnants on the rim (Fig. 5.5a-h). The temporal progression of dome extrusion remains unknown, but BOWYER (2001) shows that these relate to at least four discrete magma batches, suggesting they were independently active. Further domes are inferred to have existed in the area now occupied by the caldera, based on the number of remnant pre-caldera domes, the high proportion of rhyolite dome lithics in the Matahina Ignimbrite, and the common occurrence of domes within the axial zone elsewhere in TVZ.

5.3.2 280 ka - Matahina caldera collapse event

The 0.28 ± 0.01 Ma Matahina Ignimbrite (MARTIN, 1961; Ar/Ar age from HOUGHTON *et al.*, 1995) is exposed mainly to east and north of OCC, where it ranges in thickness from 5 to 150 m and covers an area of ~2000 km^2 (BAILEY & CARR, 1994). Detailed description is given in BAILEY & CARR (1994), who identify a basal fall deposit and three overlying flow deposits. The ignimbrite represents a magmatic volume of at least 150 km^3 (BAILEY & CARR, 1994). The thickest part of the ignimbrite notably occurs some distance from OCC in the Rangitaiki River valley to the east, but lithic size variation clearly indicates it has an OCC source (BAILEY & CARR, 1994). The ignimbrite is a buff-brown partially to strongly welded tuff, with characteristic rhyolite and vesicular obsidian lithics. Several lithic lag deposits within the upper parts of the ignimbrite, near the margins of Puhipuhi Basin (V16/308354, V16/300302), are dominated by dense flow-banded rhyolite lithics up to 200 mm but consistently around 60 mm in diameter. A new road-cut (January 2002) on Ohakiri Road (V16/296285) reveals a lithic lag with 40-50 vol. % angular lithics that average 50 mm with a maximum of 270 mm. The assemblage is dominated by purple-grey to light-grey flow-banded rhyolite, but almost 10 wt. % (n = 100) are quartz-rich densely-welded Rangitaiki-type ignimbrite. The location of these lithic lag breccias near the southern margin of the caldera show that the Matahina Ignimbrite was erupted from vents within the caldera complex (Fig. 5.5b), where they are now buried by young post-caldera lavas.

Few geochemical data are available to constrain the magmatic history of the Matahina Ignimbrite, but it is geochemically and mineralogically distinct from other OCC deposits (BAILEY & CARR, 1994; BURT *et al.*, 1998) and is weakly compositionally zoned (74-76%, BAILEY & CARR, 1994). BOWYER (2001) suggests a similar magma fed one group of pre-caldera lava domes on the eastern side of the complex, while BURT *et al* (1998) suggest a partially-molten isolated cupola of Matahina Ignimbrite magma remained after eruption to be erupted more than 200 ka later as granitoid lithics in the Rotoiti eruption.

5.3.3 280-65 ka - peripheral volcanism

South-western eruptive centre

Several exposures of pyroclastic flow and airfall deposits are located outside and on the south-western margin of the modern caldera complex. Deposits are found only locally, suggesting relatively small distributions. These deposits are coincident with a lava dome field and their collective vents are concentrated at the intersection of OCC with the axial

rift zone (Fig. 5.5c-f). These eruptives are stratigraphically interbedded between the major OCC-sourced and other major ignimbrites, and record the development of an eruptive centre southwest of OCC.

A sequence of pyroclastic flow and fall deposits is exposed beneath the Mamaku Ignimbrite on the western caldera margin (Pokopoko Pyroclastics, THOMPSON, 1974; NAIRN, 2002; Fig. 5.5c). Largely buried by later lava extrusions, the pyroclastics are up to 120 m thick near Lake Okareka (BELLAMY, 1991). Drill cores through the same stratigraphic horizon have identified similar but finer-grained pyroclastics near Lake Rotoiti (THOMPSON, 1974) and on the Mamaku Plateau (W. ESLER, *pers comm.* 2005). NAIRN (1981) also suggests the pyroclastics may have correlatives in a sequence of tephras between the Matahina and Kaingaroa ignimbrites to the south of the caldera (the Onuku Pyroclastics, NAIRN, 1989). Coarse pumiceous breccias and their thickness at Lake Okareka are consistent with a source near the southwest margin of OCC. Their volume (<10 km^3) indicates that some collapse likely occurred during the eruption.

A welded ignimbrite exposed immediately beneath Mamaku Ignimbrite is described from the same area (Millar Road Ignimbrite, BELLAMY, 1991). BELLAMY (1991) considers it may correlate with an older regional ignimbrite (e.g. the Rangitaiki Ignimbrite), while NAIRN (2002) suggests it may reflect a precursory eruption to the Mamaku Ignimbrite eruption from Rotorua Caldera. Its location within the axial rift zone where older units are invariably not exposed, and its restricted distribution, is here interpreted as more likely resulting from a localised, small-volume pyroclastic eruption during a dome building episode (Fig. 5.5c). Similar low-volume welded ignimbrites are documented by LEONARD (2003) from the Maroa Dome Complex.

These pyroclastic deposits in the southwest of OCC coincide with the location of a major group of younger coalescing domes that span the width of the axial rift zone where it intersects OCC (Fig. 5.5e). Earlier but now buried domes and related vents may have fed the earlier pyroclastic eruptions. The lavas represent at least two magma types according to BOWYER (2001). Several small (<1 km^3), compound, and poorly-exposed ignimbrites (Te Wairoa pyroclastics, *modified from* THOMPSON, 1974 *by* BELLAMY, 1991) onlap some of the domes and form a fan spreading northwestward from the domes between lakes Okareka and Rotorua. These deposits are spatially and chemically linked to nearby domes

by BELLAMY (1991), who also notes petrological and chemical similarities to the older Pokopoko Pyroclastics.

Kaingaroa and Mamaku ignimbrites

The 240 ka Kaingaroa ignimbrite erupted during the formation of Reporoa Caldera to the south of OCC. Northward directed pyroclastic flows reached at least the southern rim of OCC (Fig 5.5c) and may have overtopped the low-profile southern caldera margin (Fig. 5.5c). Continued incision of the plateau has removed much of the Kaingaroa Ignimbrite in this area, leaving only welded remnants as the peaks of small hills in the Rerewhakaaitu area. The 220 ka Mamaku Ignimbrite erupted during formation of Rotorua Caldera to the west of OCC (Fig. 5.5d), and significant volumes entered the caldera, now destroyed or obscured except for the western OCC margin and an outlying peninsula in southern Lake Tarawera (Fig 5.5e).

Minor eruptive centres

Additional lavas were extruded from a number of vents around OCC during this time. The Puhipuhi Dacite (NAIRN, 1989) comprises a small cone and lavas that are intruded in to lake sediments that cover and were deformed by the emplacement of lava. NAIRN (2002) suggests the lavas are 'considerably older' than the 65 ka Rotoiti Pyroclastics, but only younger (<43 ka) Mangaone Subgroup tephras are observed overlying the massif, indicating it may be older than the preceding Mangaone Subgroup tephras and temporally correlate with this later eruptive phase. Two dacitic volcanic cones formed to the southwest of OCC on the edge of the axial rift zone. One cone is Ar/Ar dated at 0.18 Ma (B.F. Houghton unpublished data, *in* NAIRN, 2002), and NAIRN (1973) notes that the 65 ka Earthquake Flat pyroclastics flowed around them. The dacitic cones are notably located at the outside of the axial rift zone.

5.3.4 65 ka - Rotoiti caldera collapse event

The 65 ka Rotoiti Pyroclastics (Fig. 5.5f) include a 50-100 m thick, compound, non-welded ignimbrite and an associated airfall deposit (NAIRN, 2002) with a combined minimum magma volume of 100 km^3 (CHARLIER *et al.*, 2003). The age estimates for the Rotoiti Pyroclastics ranges from 35.1 ± 2.8 ka to 71.6 ka and are strongly contended, but an age of 65 ka is currently accepted, based on recent K/Ar dates on enclosing lavas at Mayor Island (NAIRN, 2002). The ignimbrite forms a large fan (>850 km^3) that extends mainly north of OCC to the Bay of Plenty coastline, with smaller exposures on the eastern

side of the caldera in the Puhipuhi basin and in the axial rift zone to the northeast. The restricted ignimbrite distribution and location of lithic lag breccias near the northern margin are consistent with a source in the northern part of the caldera complex.

Weak chemical variation in the Rotoiti Pyroclastics has been variably attributed to xenocrystic contamination (DAVIS, 1985), magma mixing (SCHMITZ, 1995), and to a weakly zoned magma chamber (BURT *et al.*, 1998). More recently, systematic geochemistry through the Rotoiti sequence (SHANE *et al.*, 2005) indicates that chemical diversity was generated by contamination of a dominant homogeneous magma by several smaller discrete magmas during the eruption. Thus the bulk of the Rotoiti deposits (~90%) were derived from a single large homogeneous magma (SHANE *et al.*, 2005) that is distinct from those erupted to the southwest of OCC (BOWYER, 2001).

Earthquake Flat Pyroclastics

Non-welded pyroclastic flows and widespread tephra erupted from a NW-trending series of vents to the southwest of OCC immediately following the Rotoiti eruption (NAIRN, 2002; Fig 5.5f). The Earthquake Flat Pyroclastics are up to 120 m thick, form a ~110 km^2 fan and have a volume approaching 10 km^3 (CHARLIER *et al.*, 2003). BOWYER (2001) groups the deposits with some of the lavas southwest of OCC based on chemical and isotopic data, while CHARLIER *et al* (2003) use ^{238}U - ^{230}Th disequilibrium age dating of juvenile material to confirm that despite the close temporal association, the Rotoiti and Earthquake Flat magmas were independent and unconnected. The Earthquake Flat deposits share some physical characteristics with the older Pokopoko Pyroclastics (thickness, distribution, character of the deposit) suggesting the older deposits may have formed in a similar style.

5.3.5 65 ka onward - caldera modification and infilling

Mangaone Subgroup eruptions

The Mangaone Subgroup comprises silicic plinian tephras and pyroclastic flow deposits (81 km^3 bulk volume, JURADO-CHICHAY & WALKER, 2000) that are stratigraphically bracketed by the Oruanui deposit from Taupo Volcanic Centre (c.26 ka), and the Rotoiti Pyroclastics (65 ka), and erupted from vents within the OCC (HOWORTH, 1975; JURADO-CHICHAY & WALKER, 2000; chapter six). Twelve plinian fall deposits dominate the sequence, with two thin, unwelded, pyroclastic flow deposits associated with specific plinian eruptions (JURADO-CHICHAY & WALKER, 2000). SMITH *et al* (2002) add two thin,

poorly exposed airfall units based primarily on geochemical data and identify two compositional-stratigraphic groups related to the eruption of two main magmas that are distinct from the Rotoiti magma. No lavas are recognised from this eruptive phase, but many of the pyroclastic deposits are rich in rhyolite lava lithics, and any lava piles that developed may have been destroyed during larger explosive events. In any case, the young (<22 ka) intra-caldera lavas have buried any evidence for previous dome-building episodes.

Source vents for the Mangaone Subgroup were established by JURADO-CHICHAY & WALKER (2001) based on lithic isopleth maps. Constraining vents within the caldera is inherently difficult since proximal deposits are now buried by the intra-caldera lava dome complexes. The vents for the older of the two compositional groups of SMITH *et al* (2002) are scattered more widely than the younger group, with vents in the northern, central and southern parts of the caldera complex. JURADO-CHICHAY & WALKER (2000) suggest that these eruptions migrated through a north-south zone in the caldera, while the second compositional group was more tightly constrained and erupted from an east-west trending zone in Puhipuhi Basin. Thorough examination of Puhipuhi Basin and its deposits (chapter six) discounts any eruptive vents within the basin, so these are more likely to be sited farther west within the caldera complex. Accounting for the wide distribution of early vents (erupted from an area of >500 km^2) from a single magma body that produced only ~35 km^3 of eruptives (~10 km^3 DRE; JURADO-CHICHAY & WALKER, 2000) is difficult. A small, deep magma body could potentially have fed widely spaced vents at the surface, but this is inconsistent with the spatially-restricted vents of distinct magma batches recognised elsewhere around OCC and throughout TVZ. SMITH *et al* (2002) note some distinctive characteristics for the oldest two units (one of which conspicuously was erupted from the farthest south vent) that may suggest a further discrete magma was involved. Vent locations in addition to those in Puhipuhi Basin may also be in error, compounded by tephra dispersals that are strongly controlled by wind. Noticeably however, all the vent locations of JURADO-CHICHAY & WALKER (2000) are within error of the two linear vent zones transecting the caldera defined by later (<20 ka) eruptions.

33 ka Kawerau event

An ignimbrite filling the Puhipuhi embayment on the eastern side of OCC was originally mapped as an outlier of the widespread 240 ka Kaingaroa Ignimbrite (NAIRN, 1981), which was later assigned a Reporoa Caldera source (NAIRN *et al.*, 1994). BERESFORD & COLE

(2000b) differentiated the ignimbrite near Okataina and renamed it the Kawerau Ignimbrite. They retained the 240 ka date and recognised the ignimbrite as an early OCC eruptive. This work finds the Kawerau Ignimbrite is in fact a 33 ka eruptive of the Mangaone Subgroup at Okataina, associated chemically with the younger of the two Mangaone Subgroup magmas of SMITH *et al* (2002). The ignimbrite is linked with the largest of the Mangaone Subgroup eruptions, unit I, drastically increasing its volume (by between 50 and 200%, chapter six), making it the largest eruption since the Rotoiti event, and very likely associated with a third phase of caldera collapse at OCC. It is particularly significant since it alters the well-documented post-65 ka eruptive history of OCC, and revises the caldera-forming history of OCC. Chapter six of this thesis discusses the ignimbrite in detail. The distribution of Kawerau Ignimbrite, its greatest thickness and westward coarsening lithic component in Puhipuhi Basin, suggest a southern OCC source to the west of the basin (Fig. 5.5g). A similarly located source for the airfall unit of the same eruptive phase has been calculated from isopachs by JURADO-CHICHAY & WALKER (2000). Kawerau Ignimbrite records the eruption of two discrete magmas, a dominant rhyolitic magma equivalent to the young Mangaone Subgroup magma of SMITH *et al* (2002) and a subordinate dacitic magma, which underwent limited mingling during eruption (section 6.4), and provides further evidence for the existence of multiple discrete magmas in the Okataina region.

Intra-caldera volcanic centres

Recent intra-caldera eruptive activity has been concentrated at two intra-caldera dome complexes, the vents of which define two sub-parallel NE-trending vent zones that transect the caldera complex (Fig. 5.5h). Haroharo Volcanic Centre in the north of OCC developed in the last 22 ka during at least four main eruptive episodes, comprising rhyolite lava domes and flows with interbedded pyroclastic flow and fall deposits. Tarawera Volcanic Complex is a similar rhyolite dome complex occupying the southern part of OCC. Its ~18 ka evolution is a result of five recognised eruptive episodes, culminating with the 1886 AD basaltic eruption (NAIRN, 2002). Eruptive vents within the same linear vent zones also occurred on the periphery of OCC, associated with embayments in the caldera margin. Vents at Okareka and Rotoma lie on the Haroharo linear vent zone, while vents at Puhipuhi and Rotomahana similarly lie on the Tarawera linear vent zone.

Temporal trends indicate intra-caldera eruptives since the Rotoiti event at OCC tapped progressively more evolved, shallower, and cooler magmas (SMITH *et al.*, 2004a-c). SMITH

et al (2004c) further note distinct magmatic properties and a lack of temporal (fractionation) trends which suggest multiple source magmas for these eruptives. Vents in the Okareka Basin to the southwest of OCC were active at 25 ka and 15.8 ka, and erupted magmas that were mineralogically and compositionally distinct from those of the Haroharo complex. The deposits have magmatic characteristics consistent with both rhyolite lavas and the Earthquake Flat Pyroclastics previously erupted in the southwest of OCC (V. SMITH, *writ. comm.* 2005). The 15.8 ka Rotorua eruptive episode, from vents in the Okareka basin, involved the mingling and eruption of two rhyolite magmas batches (SMITH *et al.* 2004b). A high-level stagnating magma was intersected and reactivated by a rising hotter magma which triggered the eruption (SMITH *et al.*, 2004b). Mafic triggering of the 1305 AD Kaharoa eruption from Tarawera Volcanic Complex has also been documented (LEONARD *et al.*, 2002; NAIRN *et al.*, 2004).

5.4 CALDERA STRUCTURE AND MORPHOLOGY

A characteristic feature of the axial calderas in Modern TVZ, which is particularly relevant at Okataina, is the complex interaction of constructive and destructive episodes. Constructive episodes involve the accumulation of volcanic material, typically in the form of lava dome complexes along specific linear zones, while destructive episodes include caldera collapse and lateral embayments in the caldera margin where intersection with the axial rift zone occurs. While the occurrence of both of these processes can be demonstrated, their significance in the development of TVZ calderas and the causes leading to such events are not well understood.

Several key questions relating to caldera development are addressed using the synoptic view provided by DEM and remote sensing data. (1) What is the relationship between regional structure and the morphology and structure of the caldera complex? (2) What is the architecture of the caldera complex? (can individual calderas be delineated?) (3) What is the nature of magma storage beneath the caldera, and how does the pattern of collapse features and eruptive vents at the surface provide an insight into this subsurface structure? (3) Can the stress field orientations of the edifice and/or region be determined? (4) How does the stress field orientation relate to caldera geometry and the location and orientation of eruptive fissures?

5.4.1 Physiography of the OCC

The physiography of the area encompassing the OCC is characterised by a clustering of domes and cones and their remnants within the axial rift zone, flanked on both sides by planar ignimbrite plateau in various states of incision (Fig. 5.6a-c; 5.7). In Figure 5.6 (a-c) a clear correlation exists between the age and type of deposits and their morphology and degree of dissection. The youngest lavas for instance, exhibit well-preserved features (such as clear dome shapes, lava flow paths and surface ribbing in figures 5.6a-c), whereas the morphology of older lavas is obscured. Lava flow morphology is particularly clear in satellite analysis of OCC (Fig. 5.7). Pre-caldera domes are cut or bisected by the caldera margin, and are dissected by fault scarps. Some are heavily eroded with no preserved eruption morphology and only preserved as areas of high relief adjacent to the caldera (e.g. on the eastern side in Fig. 5.6a-c; 5.7). The preservation of ignimbrite surfaces reflects their varying emplacement ages and degrees of welding. The deeply incised regions occur where non-welded ignimbrite and pyroclastics have been stripped off to expose older, more-welded ignimbrites (to the southeast of OCC); least incised surfaces are typically capped by the youngest non-welded deposits that have been subjected to less erosion (Fig. 5.6c). The largest (vertical and lateral extent) constructional forms relate to the two intra-caldera lava massifs. The summit of the southern complex (1111 m a.s.l - Tarawera) is the highest point in figure 5.6b, several hundred metres above the highest rim elevation. These morphologically youthful intra-caldera lavas contrast with the surrounding dissected lavas and ignimbrite and effectively define the caldera margin (Fig. 5.6a-c; Fig. 5.7).

The maximum topographic subsidence from the highest point on the caldera margin to the deepest lake basin is 800 m. Lakes form a moat around the western and northern sides of the caldera floor where they pond between the caldera margin and intra-caldera lavas (Fig. 5.6a-c; 5.7) The area southwest of OCC within the axial rift zone is dominated by a complex series of domes while the axial rift zone on the eastern side of the caldera is topographically subdued. The topographic margin at Okataina is variably manifest as precipitous scalloped slump scars in pre-caldera domes, erosion-modified ignimbrite caldera walls, rectilinear scarps that often continue beyond the caldera margin, and by post-caldera lava domes. Many segments of the margin are obscured by post-caldera eruptives or by ignimbrites from adjacent sources (particularly the western margin). Intra-caldera lava massifs obscure the caldera floor and thus the outlines of individual collapse structures. The topographic margin is thus a composite feature that reflects the net effect of multiple caldera collapse and additional tectonic and volcanic processes within the axial

rift zone. Large embayments in the topographic margin are notably not represented in the basement collapse depicted by gravity (Fig. 5.6d), while the overall N-S trend is consistent.

5.4.2 Morphology and Development of the Caldera Margin

Documenting the morphology of the caldera margin contributes to the reconstruction of the collapse history, and is the principal approach at young calderas where the caldera floor may be obscured by caldera infill and post-collapse volcanism. Through the analysis of Satellite remote sensing data and DEM imagery, the components (*e.g.* multiple collapse scarps, intra-caldera benches, embayments in the caldera margin) and characteristics (*e.g.* extent, geometry) of a caldera can be established.

Southern margin

The southern topographic rim of the caldera (Fig. 5.8) is an 8 km long scarp comprising nearly-vertical ~100 m high cliffs of Rangitaiki Ignimbrite (section 5.3.1). This ENE-trending scarp is progressively buried to the east by pyroclastics and lavas extending south from Tarawera that have ponded against and partially overtopped the caldera wall. These post-caldera deposits thus obscure any caldera collapse scar that existed farther along the south-eastern margin. In the opposite direction the scarp is also buried by younger pyroclastic deposits, but appears to continue on a trend that would eventually merge with the border of the axial rift to the south. Thus the southern topographic margin extends beyond the caldera as a regional fault.

The Rangitaiki Ignimbrite surface south of OCC is capped by the Onuku pyroclastics and the Kaingaroa Ignimbrite but these are largely eroded off close to the southern caldera margin. Matahina Ignimbrite forms the surface immediately inside the southern caldera margin, but was also eroded off the heavily incised surface to the south and southeast of the caldera. It thus forms a bench inside the caldera, on which the Tarawera massif was partly constructed. Matahina Ignimbrite is seen nowhere else inside the caldera, presumably destroyed by the subsequent Rotoiti caldera collapse. It partially filled the Matahina caldera, forming a distinct surface onto which subsequent pyroclastics and the Mamaku Ignimbrite ponded within the caldera. In areas contiguous with the axial rift zone it was faulted down, and during the Rotoiti caldera collapse was destroyed north of where the Tarawera Volcanic Centre is located.

Eastern margin

Pre-caldera Maungawhakamana rhyolite massif dominates the eastern margin (Fig. 5.9). The heavily dissected cluster of domes and lava flows are in clear juxtaposition with intra-caldera lavas of the Haroharo Volcanic Complex (Fig. 5.6, 5.7). The northernmost dome was bisected during caldera collapse based on its semi-circular topography, and other flows likely extended at least several km to the west and south prior to caldera collapse. No clear escarpment is identified, however an N-S-trending linear scarp is likely to be buried by subsequent infilling of the caldera, consistent with the steep eastern collapse margin indicated by the gravity profile (Fig. 5.6d; 3.7c). The eroded nature of the margin here suggests collapse occurred during the Matahina event rather than younger collapse events. Regional fault scarps cutting across the massif noticeably curve toward the caldera with increasing proximity.

South of this lava complex is the rectilinear flat-floored Puhipuhi basin, open to the caldera on its western side, and the area of lowest elevation adjacent to OCC. It extends 8 km north-east of the N-S-trending caldera margin, forming a major embayment. The 8 km x 6 km basin has a maximum topographic relief of 150 m and is partially filled by the proximal deposits of the 33 ka Kawerau Ignimbrite. A small dacitic lava pile protrudes through the basin floor on the western side. Isolated exposures of older caldera-forming ignimbrites indicate they previously filled the basin, recording a long history of infilling and erosion within the basin. Deeply incised channels feed into the basin from the south and have removed much of this fill material. These streams drain northward in the basin into the Tarawera River which exits through a ~1 km wide channel in the north-east corner of the basin. JURADO-CHICHAY & WALKER (2000) speculate that the path of the Tarawera River may indicate the location of vents and partial collapse during certain Mangaone Subgroup eruptions. No proximal deposits or evidence for any vents or collapse related to these eruptions was found within the basin during extensive field work during this study (see chapter six).

Northern margin

In the north the topographic rim is formed by a clear 250 m high scarp in the pre-caldera Matawhaura lava massif (Fig. 5.10). These lavas, which form part of the northern margin of Lake Rotoiti, dip away from the caldera suggesting they represent only a small remnant rim of a larger edifice that was almost completely destroyed by caldera collapse. If it were assumed to be roughly circular and a similar size to the Whakapoungakau dome to the

west, it would extend roughly 5 km south of the current margin. On each side of the lava dome the scarp is poorly developed in unwelded Rotoiti Ignimbrite, and there is no clear topographic connection with the eastern and western margins. Here the topographic margin is enlarged and obscured by flat-floored lakes impounded against the modified northern caldera wall, dammed by post-caldera Haroharo lavas to the south. The north-western arm of Lake Rotoiti occupies a breach in the caldera margin where Lake Rotorua drained into the caldera.

Western margin

The western and south-western portion of the caldera is the most complex. In the west the Whakapoungakau rhyolite dome was truncated by the Matahina caldera collapse. A large, steep scarp on the Whakapoungakau rhyolite dome (Fig. 5.11) is parallel and continuous with NNE-trending faults extending to the southwest. This scarp records two phases of collapse, with Mamaku Ignimbrite from Rotorua Caldera ponding against the initial scarp created by the Matahina Caldera. Later collapse during the Rotoiti collapse event formed a second scarp in Mamaku Ignimbrite and left a small bench of the ignimbrite in front of the older scarp (Fig. 5.11b). Subsequent erosion has partially removed the bench. Mamaku Ignimbrite and the underlying pyroclastics (section 5.3.3) form much of the western topographic margin north and south of the dome. The general trend of the topographic escarpment is north-northeast, parallel with faulting in this part of the axial rift zone. A major fault cuts the Whakapoungakau dome, and Haroharo lavas abut against a further linear fault scarp in Mamaku Ignimbrite north of the dome. The ignimbrite surface dips very gently toward OCC, interpreted as the original dip slope of the ignimbrite as it flowed eastward from Rotorua Caldera into OCC. This suggests that the underlying Matahina Ignimbrite was similarly dipping, and therefore outside the Matahina collapse structure, since a major scarp farther west would be reflected in the morphology of overlying deposits. Enhanced scarp retreat and incision in this area reflects the more easily eroded ignimbrite relative to the well preserved scarp in the Whakapoungakau lava dome. Mamaku Ignimbrite is not exposed within the caldera except in a small fault-bounded peninsula in the south of Lake Tarawera. Thus the ignimbrite flowed at least 10 km and probably 15 km beyond the current western margin, to fill much of the Matahina collapse structure.

In the southwest where OCC intersects the Kapenga segment of the axial rift is a cluster of at least ten domes and associated lava flows that record volcanism in this area active over

more than 200 ka. Domes and their remnants reflect at least three main phases of volcanism (section 5.3) and lava packages overlap slightly suggesting a complex temporal progression. Intense NE-trending faulting transverse to the main collapse structure creates a series of scarps that intersect the current topographic margin of OCC. No clear caldera scarp is present in the south-west; this area of the caldera contiguous with the axial rift zone is faulted down forming a major embayment in the caldera margin. The embayment is bound on its southern side by a linear fault scarp in pre-caldera rhyolite. A scalloped edge to this rhyolite along the southern margin of Lake Tarawera may be a primary collapse scar of the Matahina caldera. The northern border of the embayment is obscured but is likely a stepped feature controlled by the continuation of NE-trending faults to the west of Lake Okataina. Lava extrusion after the Matahina collapse largely filled the south-western embayment, but a smaller nested zone of secondary collapse occurred during the formation of the Rotoiti caldera, which defines the current embayment in the topographic margin. A peninsula of Mamaku Ignimbrite extends into the southern part of Lake Tarawera bound on its northern side by a clear NE-trending fault scarp. This scarp effectively borders the main zone of faulting that has occurred since Mamaku Ignimbrite was emplaced inside the caldera. The bathymetry of the lake edge off the end of the peninsula records a distinct NNW-trending scarp which is interpreted as the border of the main Rotoiti collapse structure. The caldera margin in the south-west is thus significantly modified by intersection with regional faulting and an eruptive centre on the periphery of the caldera.

5.4.3 Structural Characteristics

Morphotectonic mapping of DEM and satellite data (Figs. 5.6 & 5.7) is used here to analyse the relationship between structural and volcanic features, and the structural factors contributing to the three-dimensional collapse geometry.

Architecture of OCC

New DEM, satellite, and field data show that the OCC is coincident with a major ENE-WSW trending bend in the axial rift zone of TVZ (Fig 5.11; see also Fig. 5.4, 3.9). The 28 x 15 km caldera complex is strongly rectangular with an overall eccentricity E = 0.55 ($E = L_{min}/L_{max}$ where L_{min} and L_{max} are the shorter and longer axes respectively; Fig. 5.11) and a long axis trending N8°W, perpendicular to the trend of the Okataina axial segment (N71°E; Fig. 3.10). The main scarps bordering the caldera are generally parallel to or coincident with regional faults outside OCC. The shape of the western and southern sides

is controlled by pre-existing NNE- and ENE-trending faulting respectively, possibly reactivated during collapse. The shape of the northern and southern sides of the caldera complex is controlled by curved faults at the margins of the axial rift zone. The individual Matahina and Rotoiti calderas at OCC are delineated on the basis of caldera wall geology and morphology (sections 5.3 & 5.4), and regional structural constraints, and is consistent with the geometry of basement collapse outlined by gravity data (Fig. 5.6d; see also Fig. 3.7c). The structures are each elongate along the axis of the overall caldera complex (with E = 0.69 and 0.71 for the Matahina and Rotoiti calderas respectively) and overlap by ~70%, which is considerably more than indicated by NAIRN (1989, 2002) on the basis of the distribution of caldera-forming ignimbrites. No evidence exists on the caldera margin for the proposed collapse event during the 33 ka Kawerau Ignimbrite eruption, and it is considered to be wholly nested within the existing caldera complex. The distribution of the ignimbrite indicates a source near Puhipuhi Basin, suggesting caldera collapse within the central part of the Matahina Caldera.

Topographic margin

In Nairn's regional tectonic maps of Okataina (NAIRN, 1989, 2002) the 'topographic margin' often has no surface expression and in a number of places is well inside the escarpment that bounds the caldera. The topographic rim of a caldera, according to LIPMAN (2000), encloses both the area of subsidence and area of scarp retreat due to mass wastage. Figure 5.12 shows that the topographic margin at OCC is a complex feature that encompasses both the zone of caldera collapse and the embayments in the caldera margin. This area thus defines the zone of subdued topography related to caldera collapse, but also to tectonic subsidence, volcanic activity on the periphery of OCC, and erosion, which have all modified the margin of the caldera complex. NAIRN (2002) also includes a topographic margin for the supposed Kapenga caldera (section 3.4.1) for which there is poor evidence and, most notably, a distinct lack of any topographic margin.

The distinct embayments in the topographic margin occur where zones of intense ENE-WSW-trending regional faulting within the Okataina rift segment intersect the caldera (Fig. 5.12). The two largest embayments (Puhipuhi and Okareka) occur within the rift on the middle of each side of OCC; smaller embayments (Rotomahana and Rotoma) occur along strike on the diametrically opposite side of OCC respectively. The larger embayments are rectilinear and are bordered by regional faults, while the smaller embayments have irregular geometries and are not as clearly coincident with faulting at the surface. Two sets

of embayments are thus present: (1) embayments at Okareka and Rotoma occur on the trend of the Kapenga axial rift segment; (2) the Puhipuhi Basin and Rotomahana embayments occur along the trend of the Whakatane axial rift segment (Fig. 5.12a,b).

Distribution of extra- and intra-caldera vents

Vents are scattered around the margin of the caldera, interpreted by NAIRN (1989, 2002) as reflecting the location of an underlying ring structure (Fig. 5.3). In detail however, the vents all lie on, or are parallel with, regional faults within the axial rift segments (Fig. 5.12). The fewer eruptive centres in the south and north sides of the caldera compared with the east and west sides is consistent with the preferential extrusion of domes within the axial rift zone. The oldest exposed domes are notably located on the periphery of the axial rift segments. The vents for domes and other eruptives southwest of OCC are concentrated in the structurally complex area where OCC intersects the axial rift zone. This south-western eruptive centre (section 5.3.3) spans the width of the rift zone, thus forming an overall NW-trending group of coalescing domes. Vents are located on NE-trending regional structures that are slightly oblique (rotating clockwise toward OCC) to faulting farther south, and several of the domes are NE-elongate.

The central part of OCC is dominated by the morphologically youthful rhyolite lavas that comprise the Haroharo and Tarawera Volcanic Centres. The vents for these centres define two ~4 km wide NE-trending zones (50° and 58° respectively, Fig. 5.12) that transect the caldera complex and extend beyond the caldera margin to include vents within the embayments on the periphery of OCC. These two linear vent zones are therefore the intra-caldera expression of the same structure which controls the embayments on each side of the caldera, and thus they are interpreted as the intra-caldera expression of the two offset rift segments at OCC.

The basaltic dikes of the 1886 Tarawera eruption have a left-lateral en-echelon configuration (inset in Fig. 5.12), interpreted by NAIRN & COLE (1981) to imply dextral shear. Considering the model of orthogonal extension for the Okataina rift segment (chapter two), the dextral shear results from the acute angle between the extension direction in the Okataina segment (N19°W) and the general trend of the Tarawera linear vent zone (N58°E; inset Fig. 5.12b). The acute angle thus gives a β of 13° (see also inset Fig. 2.19), resulting in localized dextral shear along the Tarawera rift, consistent with the en echelon fractures.

Some vent arrangements in the southwest of OCC appear to define local north-west trends, which have been used by NAIRN (1981, 1989, & 2002) to indicate underlying NW-trending structures. The vents for lavas filling the current Okareka embayment are typically referred to as NW-trending (NAIRN, 1989, 2002; BOWYER, 2001; SMITH *et al.*, 2004), which NAIRN (2002) considers to reflect the rim of the 'Kapenga caldera' in this area. In fact, while these vents form a local north-west trend, they remain consistent with the Haroharo vent zone, in a region of intense NE-trending faulting. The nearby NW-trending scarp forming the north-eastern margin of Lake Okareka probably records caldera collapse during the eruption of the Pokopoko Pyroclastics (section 5.3.3; Fig. 5.5c). While specific evidence for such an event is largely obscured by later activity, it suggests a NW-elongate collapse structure (Fig. 5.5c), with a long-axis transverse to regional structure. The Earthquake Flat Pyroclastics similarly erupted from a NW-trending 5 km long vent zone dominated by a NW-elongate elliptical (2 x 1.4 km) crater (Fig. 5.12). NAIRN (2002, p55) considers that these vents "provide the most convincing evidence for the existence of a ring structure at OVC". The crater is south of the major rotation of faults near OCC, and has a long-axis normal to local faults within the rift zone. The elongation of these features normal to regional structure is consistent with the overall geometry of intra-rift calderas in TVZ (chapter three).

The Okataina transfer zone

The dominant feature of OCC is the two structural lineaments which transect the caldera and extend beyond its margins to control the location of intra- and extra-caldera vents and major structural embayments in the caldera margin. These lineaments are the lateral extension of the axes of the overlapping rift segments at OCC, recording a major offset (~25 km) in the rift system coincident with OCC. Within the Okataina axial rift segment, these structures trend at a higher angle (>050°) than in the adjacent rift segments (~040°), which is concomitant with the rotation of faults on either side of OCC at the intersection of rift segments. The two vent lineaments are the only expression of these structures within the caldera, and are interpreted to reflect zones of intense fracturing controlling both magma pathways in the crust and zones of preferential tectonic subsidence. NAIRN (2002) previously suggested that the Haroharo linear vent zone may be a continuation of the Taupo Fault Belt to the south, and indicated that the equivalent Tarawera zone is not a direct continuation of structures to the south.

Thus, the Okataina axial rift segment: 1) connects the sub-parallel Kapenga and Whakatane rift segments; 2) exhibits fault and rift-axis rotation at the intersection with these segments; and 3) is characterised by a rotation of the extension direction relative to these segments (Fig. 2.19). These features suggest the Okataina domain represents a transfer zone in the axial rift (Appendix A, ACOCELLA *et al.*, 2003). Similar geometric and kinematic relationships are observed at transfer zones along other narrow rifts (e.g. GUDMUNDSSON *et al.*, 1993; ACOCELLA *et al.*, 2000) and in analogue models (ACOCELLA *et al.*, 1999; CORTI *et al.*, 2002, 2003, 2004).

5.5 DISCUSSION

5.5.1 Development of the Caldera Complex

Three caldera-forming events are recognised in the development of the caldera complex, each associated with the eruption of an ignimbrite. The 280 ka Matahina and 65 ka Rotoiti events constitute the main caldera forming events, while a newly identified event at 33 ka is associated with the Kawerau Ignimbrite (section 5.3.5; see also chapter six). Other caldera-forming events have previously been attributed to OCC, and the Kawerau Ignimbrite was considered to have been erupted much earlier at 240 ka by BERESFORD & COLE (2000b). It has been suggested that isolated outcrops of older pyroclastics on the periphery of OCC are the deposits of earlier caldera-forming events, but no earlier collapse structures are recognised. These deposits may relate to collapse structures that were subsequently destroyed, but owing to their restricted distribution and character, more likely relate to explosive phases from eruptive centres existing prior to the Matahina Caldera. Specifically, the 'quartz-biotite' ignimbrites, considered by NAIRN (1989, 2002) and BERESFORD & COLE (2000b) to represent an early phase of caldera-forming activity at Okataina, are considered here as an explosive phase in the development of a silicic dome complex on the east side of the caldera, without caldera collapse.

There has been a clear aspiration by some workers to divide the history into specific periods (WILSON *et al.*, 1984; BOWYER, 2001; SMITH *et al.*, 2002; NAIRN, 1989, 2002), as part of characterising the history of 'the volcano'. WILSON *et al* (1984) divide Okataina into early 'caldera-forming' (ending with the Rotoiti eruption) and later 'caldera-filling' episodes, while others have added a 'caldera modifying' phase prior to the eruption of the intra-caldera lavas (e.g. SMITH *et al.*, 2002). While these divisions have some basis in the documented eruptive history, they are highly simplified. For instance, the deposits of the 'caldera-filling' period are inherently better preserved than the deposits of similar previous

activity; the evidence for potential dome building and/or localised explosive deposits following the Matahina event would have been destroyed during subsequent collapse.

5.5.2 The Geometry and Mechanism of Collapse

In a summary of TVZ calderas, WILSON *et al* (1984, p8470) consider that (for Okataina) "in contrast to Taupo, regional faulting has not greatly controlled the caldera shape". New DEM and field data show that OCC is in fact strongly coupled with regional structure, firstly for its location at a major transfer zone in the axial rift system, and secondly in terms of its overall geometry and the conspicuous relationship between caldera-bounding scarps and regional faults. A significant factor in the three-dimensional collapse geometry of a caldera is the presence of pre-existing faults (Appendix C, COLE *et al.*, 2005). Faults provide lines of weakness along which caldera collapse will preferentially occur, and can break the caldera up into numerous blocks (e.g. Scafell, BRANNEY & KOKELAAR, 1994; Glencoe, MOORE & KOKELAAR, 1997, 1998; Snowden, KOKELAAR & BRANNEY, 1999; Valles, GOFF, 1983; NIELSON & HULEN, 1984; HEIKEN *et al.*, 1986; Silent Canyon, FERGUSON *et al.*, 1994). Faulting (more specifically fault zones) may also correspond to regions of magma accumulation, induce fault-normal (BOSWORTH *et al.*, 2003) or fault-parallel (ACOCELLA *et al.*, 2002) magma chamber and caldera elongation, promote along-strike magma migration (CORTI *et al.*, 2004), and can control the location of intra- and extra-caldera vents (e.g. Glencoe, MOORE & KOKELAAR, 1997, 1998; Tarawera linear vent zone, NAIRN, 1989, 2002; Taupo, SMITH & HOUGHTON, 1995; Long Valley, BAILEY *et al.*, 1976).

Many calderas have a complex morphology and structure that indicates they comprise multiple rather than single collapse features. Collapse structures may be clearly nested within an older structure (e.g. Campi Flegrei, ORSI *et al.*, 1996; ROSI *et al.*, 1983), or overlap with earlier structures (e.g. at Las Cañadas Caldera, MARTI & GUDMUNDSSON, 2000). At OCC, the main caldera structures overlap considerably, while a subsequent smaller caldera was nested within the older structures. While the caldera complex as a whole is coterminous with the transfer zone boundary faults, the Matahina and Rotoiti calderas are centred within the continuation of the Whakatane and Kapenga rift segments respectively. Both the Matahina and Rotoiti calderas are rectilinear structures with their geometries clearly dictated by their coincidence with faulting within the axial rift. Their individual eccentricity values (~0.7) are not entirely different from those of the Reporoa and Rotorua calderas (~0.8; Fig. 3.10); however they are both arranged clearly elongate to

the extension direction, consistent with the geometry of Taupo Caldera Complex (section 3.3.4; Fig. 3.10). Gravity depicts a single zone of basement collapse, with a geometry closely matching the combined outline of the mapped calderas. The gravity anomaly trends N15°W (Fig. 5.6d; 3.7c), consistent with both the extension direction in the Okataina rift segment (N19°W; Fig. 5.12b) and the trend of the caldera complex (N8°W; Fig 5.12a). Caldera ellipticity normal to the extension direction is interpreted as resulting from stress-induced stretching of the associated magma chamber (e.g. BOSWORTH et al., 2003), since the geometry of calderas and extension direction is consistent with that at Taupo Caldera Complex.

The structure of the caldera floor is obscured by caldera fill, thus the mechanisms of caldera collapse can only be inferred on the caldera architecture and the available sub-surface data. The gravity contours in figure 3.7c suggest the deepest collapse is within the southern caldera complex coincident with the centre of the Matahina caldera and southern Rotoiti caldera. The eastern margin is the steepest, while the caldera generally shallows to the north, indicating overall asymmetric subsidence within the caldera complex. While there is no clear distinction between multiple collapse structures in the gravity anomaly, the gravity data resolution is however poor, and further data points would likely depict a more structurally complex caldera floor.

The intense deformation intersecting OCC suggests that the pre-caldera area was similarly fractured and that basement collapse during caldera-forming eruptions occurred by subsidence of multiple blocks. Differential subsidence during the Matahina caldera-forming event occurred between overlapping normal faults within the Okataina transfer zone, forming a complicated zone of NE-trending blocks. Displacement appears to be positively correlated with deformation intensity, such that maximum subsidence occurred in the centre of the caldera complex, coincident with the trend of the Okataina rift segment. The steeply dipping eastern margin of the caldera, as shown by the gravity data, indicates that the location of basement collapse in this area was controlled by faults formed during caldera collapse. These are unrelated to regional structure, and thus likely represent faults propagating from the magma chamber; the east-west dimension therefore approximating the extent of the magma chambers prior to collapse. Areas of the caldera above shallow-dipping basement were expanded by subsidence on faults beyond the structural caldera margin, effectively extending the dimensions of collapse by simultaneous reactivation of regional faults.

All of the embayments are peripheral to the border of the caldera complex as defined by gravity (Fig. 5.6d; 3.7c) and characteristics of the caldera margin (section 5.4.2). The border faults for the large embayments are obscured at outcrop scale, and they are largely filled by later flat-lying deposits, but it is interesting to speculate that displacement may significantly increase with proximity to the caldera. The largest embayments relate largely to tectonic collapse, probably induced by or associated with caldera collapse during concomitant large-volume magma withdrawal and strain redistribution. MANVILLE & WILSON (2003) similarly consider that major faulted blocks adjacent to Taupo caldera foundered during caldera collapse, rather than reflecting accumulated slip on rift faults. Smaller embayments at OCC are interpreted as the result of localised eruption and collapse above major crustal defects but without widespread tectonic subsidence.

5.5.3 Relationship to Rift Architecture and Evolution

The linking and interaction between the offset Kapenga and Whakatane rift segments is accommodated by a structurally complex transfer zone coincident with the location of OCC (Fig. 5.12a). The coincidence of magmatic processes at transfer zones is highlighted in many other examples, including the East African Rift system (e.g. ROSENDAHL, 1987; HAYWARD & EBINGER, 1996) and the Rio Grande Rift (CHAPIN & CHATER, 1994). In addition, analogue models of transfer zones have shown that a feedback interaction between magma emplacement and strain localization may develop during their development, facilitating the accumulation of large volumes of magma in transfer zones (CORTI *et al.*, 2002, 2003).

The volcanic history of the Okataina transfer zone, including OCC, is considered as a function of the structural evolution of the transfer zone (figure 5.13). (1) Pre-caldera volcanism records the development of numerous local magma bodies scattered over a wide area of diffuse deformation, coupled strongly with the fault distribution. Scarce magma upwelling may have induced re-orientation of the extension direction and incipient fault rotation within the transfer zone. (2) Magma accumulation by amalgamation and hybridization of multiple magma bodies during increased dike-injection induces strain localization, enhancing further magma upwelling and causing stress-induced stretching of the chamber. Simultaneous lateral magma migration occurs toward the focus of caldera collapse, dictated by transfer zone boundary faults, with syn-eruptive fault reactivation outside the caldera as a consequence of magma drainage. (3) Curved faults at the edge of

the transfer zone adjacent to the caldera localize eruptive vent locations, while enhanced orthogonal extension in the centre of the zone is accommodated by magma migration and storage without significant volcanism. (4) Further rift-fault propagation and rotation localizes deformation and magmatism in the northern rift segment, similarly enhanced by lateral migration into the transfer zone and accompanied by chamber stretching parallel with the extension direction. Caldera collapse exploits pre-existing structures within the transfer zone. (5) Pre-existing structural weaknesses along each of the two propagating rift axes promotes multiple local chambers and venting coupled with fault distribution in the north and south of the caldera complex. (6) Complete rift-segment propagation and strongly localised deformation enhances development of multiple small, shallow magma chambers, and eruption at vents strongly coupled with the axes of the overlapping rift segments.

The development of volcanism at OCC therefore records the progressive interaction between offset rift segments and the propagation of overlapping rift segment axes. As rift propagation proceeded, a diffuse zone of volcanism progressively concentrated in the centre of the transfer zone then divided into two spatially restricted eruptive centres as through-going faults became established.

CHAPTER 6 The Kawerau Ignimbrite, a 33 ka Okataina eruptive

6.1 INTRODUCTION

A dark grey/black ignimbrite outcropping near the Kawerau township and in Puhipuhi Basin was mapped as the Kaingaroa Ignimbrite by NAIRN (1981; Fig. 6.1). Subsequent authors followed this interpretation (e.g. BAILEY & CARR, 1994; NAIRN *et al.*, 1994), largely since it was poorly exposed, and was supported by a fission-track age of 0.24 ± 0.05 Ma (B.P. KOHN, *pers. comm.*, in NAIRN, 1989), consistent with the Kaingaroa Ignimbrite's stratigraphic position. Detailed investigation of the Kaingaroa Ignimbrite *s.s.* by BERESFORD (1997) showed that the (at that time recently exposed) ignimbrite in this area differed in internal stratigraphy, mineralogy, and pumice chemistry, and it was subsequently renamed the Kawerau Ignimbrite (BERESFORD, 1997; BERESFORD & COLE, 2000b). BERESFORD & COLE (2000b) report general field characteristics, pumice petrology, and the presence of rare vapour-phase mineral manganoan fayalite in pumices. Attributing the ignimbrite to an Okataina source, they also discuss the implications for eruptive history and development of the caldera complex.

Further investigation of the Kawerau Ignimbrite was instigated as part of this study into the development of the Okataina Caldera Complex (OCC). A reassessment was justified by the short window of available exposure time of the ignimbrite (due to commercial forest replanting and growth), and since it gave an opportunity to constrain the early evolution of Okataina, particularly the origin of Puhipuhi Basin. During extensive fieldwork within Puhipuhi Basin and surrounding OCC, a much younger stratigraphic position was recognised for the Kawerau Ignimbrite. This was later supported by geochemical evidence linking it with the Mangaone Subgroup (MSg) eruptives. A much greater distribution than previously recognised, and its inclusion in a young sequence of eruptions from Okataina, has significant implications for the eruptive stratigraphy and development of OCC, and geologic hazards in the northern TVZ.

6.2 MANGAONE SUBGROUP PYROCLASTICS

The MSg tephras are a series of plinian and phreatoplinian deposits that were erupted from within the OCC (Fig. 6.2). Tephras of the MSg were first documented by VUCETICH & PULLAR (1964), who later defined five members of the 'Mangaoni (*sic*) Lapilli Formation' as "poorly shower-bedded pumice lapilli blocks, and minor ash beds, all lying between the

Oruanui Formation and the Rotoehu Ash" (VUCETICH & PULLAR, 1969). HOWORTH (1975) further subdivided these tephras into eight units and defined the Mangaone Subgroup as all eruptions from Okataina that are stratigraphically bracketed by the Kawakawa Tephra (the fall deposit associated with the Oruanui Formation, Taupo Caldera Complex) and the Rotoiti Breccia Formation (HOWORTH *et al.*, 1981). Detailed field examination of the Mangaone Subgroup by JURADO-CHICHAY & WALKER (2000, 2001) added four more units and further refined the stratigraphy and eruptive characteristics. SMITH *et al* (2002) add a further two poorly exposed units and report the geochemical characteristics of the Mangaone Subgroup tephras, identifying two compositional-stratigraphic groups, an older rhyodacite to low-SiO_2 rhyolite (71-75.5 wt%) group, and a younger high-SiO_2 (76-78%) group.

Two thin ignimbrites are reported from the Mangaone Subgroup, related to the final stage of two young Mangaone Subgroup eruptive phases, the Mangaone (Unit I) and Omataroa (Unit K) tephra units (Fig. 6.2). The larger of the two pyroclastic flow deposits formed during the final stage of the Mangaone eruption. Mangaone is the largest and coarsest fall deposit of the subgroup, and is >4 m thick over an area of ~30 km^2 (Fig. 6.2d; JURADO-CHICHAY & WALKER, 2000). The Mangaone Tephra is characterised by strong inverse grading, an abundance of lithics near the base, and a non-welded ignimbrite at or near the top in proximal areas (JURADO-CHICHAY & WALKER, 2000). Kawerau Ignimbrite is in this study considered a lateral correlative of the Mangaone flow unit and is overlain by Omataroa Tephra in a number of localities within Puhipuhi Basin. Lithic and pumice size distributions for the Mangaone fall unit give dispersal axes that indicate a source vent located within the eastern side of OCC (Fig. 6.2c; JURADO-CHICHAY & WALKER, 2000). The authors describe the overlying non-welded ignimbrite as "consisting of ash and a lesser proportion of pumice lapilli". They also note the presence of carbonised logs within the ignimbrite at this and other locations. The ignimbrite and ash are often not found together, which the authors suggest reflects wind dispersal of the ash to the east and north, with northeast directed topographically controlled pyroclastic flows. The ignimbrite exposures they observed were thin (0.20 m) but were widespread to the north and east of OCC (Fig. 6.3). Together with an observed lack of ponding, they attribute this to high emplacement energy. Around Kawerau they record some thicker sections of the ignimbrite, including a pumice rich facies. While recognising a significant thickness of non-welded ignimbrite forming a flat-topped terrace around Kawerau, they do not

positively correlate this with the Mangaone ignimbrite or any other Mangaone subgroup eruptive.

6.3 Lithology and Distribution

Mapping of the Kawerau Ignimbrite was undertaken during the summers of 1999/2000, 2000/2001, and in September/October 2001 when exposure levels were maximised between felling and replanting. During recent visits to Puhipuhi Basin (December 2004) most exposures were already overgrown and access to outcrops had been significantly reduced.

Kawerau Ignimbrite is exposed to the east and north of OCC (Fig. 6.3), and fills the Puhipuhi Basin on the eastern side of the caldera complex (Fig. 6.4). Within Puhipuhi Basin it is ~100 m thick, exposed on clear-felled knolls and locally forming steep bluffs adjacent to streams draining northward in the basin (Fig. 6.5). The ignimbrite thins considerably further away from the caldera but forms an area of partially dissected low hills around the Kawerau township (Fig. 6.1b). Kawerau Ignimbrite exhibits significant lateral and vertical variation between two end-member lithofacies that Beresford & Cole (2000b) associated with separate flow units. Internal variation is everywhere gradational, and no absolute separation is implied here by this division into lithofacies. The distinction is made here to enable discussion of the spatial variation within the ignimbrite. Both lithofacies are vitric throughout, with no signs of devitrification. They are typically silica case-hardened in outcrop, and commonly contain vapour phase manganoan fayalite in pumice described by Beresford & Cole (2000b).

Lithofacies 1 (L1) is a non-welded to partially welded dark-grey/black sandy (i.e. 1/16 mm fines poor) pumice rich ignimbrite. Two pumice types are represented in the deposit, consistent with the findings of Beresford & Cole (2000b). Type-A pumice are white/yellow-brown, highly vesicular crystal-poor rhyolites, while rare type-B pumice are dark brown, extremely crystal-poor poorly-vesicular dacites. At one location (V16/291323), large (M_P = 320 mm; where M_P = Maximum pumice = average of the 5 largest pumice clasts in a 9 m^2 area) conspicuously mingled pumice are found. The lithic fraction consists mostly of dark flow-banded or pale devitrified rhyolite, but with subordinate crystal-poor dacite fragments. Dacite fragments are typically found in distinct clusters, suggesting late stage fragmentation of larger lithic blocks. Rhyolites are commonly hornblende-phyric. Only one sample of Matahina Ignimbrite was identified.

No basalt lithics were found (*c.f.* BERESFORD, 1997). The pumice and lithic fraction of L1 is subtly normally graded, often with pumice-rich horizons and discontinuous lithic-rich lenses. M_P and M_L (Maximum lithic) are highly variable between outcrops but maximised in L1. L1 is largely restricted to Puhipuhi Basin and in low hills near Kawerau.

Lithofacies 2 (L2) is a non-welded sandy grey-yellow ignimbrite. Pumice abundance is variable with both pumice-poor and pumice-rich examples observed. Both type-A and -B pumices are present, but type B pumices are extremely rare. Both types are distinctly less abundant, smaller, and exhibit clearer normal grading than in L1. Type-A pumice rich horizons are common however. Lithic fragments are almost entirely rhyolite of the same type as in Lithofacies 1, with extremely rare dacite lapilli fragments. L2 is ubiquitous in exposures of Kawerau Ignimbrite, typically occurring by itself as a thin sheet or overlying L1 in exposures outside the caldera but also grading vertically downward and laterally into the thickest sections of L1 in Puhipuhi Basin. The relationship between L1 and L2 suggests significantly variable magmatic and eruptive characteristics during the emplacement of the ignimbrite.

A non-welded dark-grey sandy pumice-rich ignimbrite (L1) grades upwards into a yellow-brown pumice-poor ignimbrite (L2) with no distinct boundary at the type section in a large road-cut section on the main highway (Fig. 6.6; V15/343448; BERESFORD & COLE, 2000b). More than 40 m of the ignimbrite is exposed at this location, but the base is obscured beneath road level. The top is also obscured, but pumice lapilli of the Omataroa Tephra (Unit K) forms thick (2+ m) sections in an adjacent overlying outcrop. Several benches cut into the outcrop allow access to various levels of the section almost to the top. In contrast to BERESFORD & COLE (2000b), the graphic log this outcrop in figure 6.6 shows clear, if subtle, normal grading of pumice and lithic abundance and size. Type-A pumice are abundant throughout the section, and M_P reaches a maximum of 88 mm near the first bench. Type-B pumices are always smaller and reduce in size and abundance faster up-section from an apparent concentration in the lower third of the ignimbrite (Fig. 6.6). Lithic componentry shows dacite lithics decrease in abundance vertically through the section and become extremely rare in the upper parts. M_L is lowest in basal and uppermost sections, and greatest toward the middle of the ignimbrite. Several vague ~2 m thick lithic-rich horizons are present in the lower two-thirds of the outcrop. The ignimbrite is silica case-hardened; fresh pumices were extracted by spade and hammer for M_P calculations and geochemical analysis.

No other exposures of the ignimbrite exist (at the time of study) between the type section and Puhipuhi Basin, although partially dissected rounded hills typical of non-welded ignimbrite are continuous between these localities and form a 10-15 m high bench around the Kawerau area (FIG. 6.1b). JURADO-CHICHAY & WALKER (2000) refer to this as a likely Mangaone Subgroup deposit in their discussion of the Mangaone Tephra but assign no certain stratigraphic position. Here it is considered as a continuous landscape modifying facies of the Kawerau Ignimbrite which is a lateral equivalent of their Mangaone Tephra flow unit. Pumice geochemistry confirms this proposal, and is discussed in section 6.4.

6.3.1 Puhipuhi Basin

Within Puhipuhi Basin (Fig. 6.4), the Kawerau Ignimbrite is thick and landscape-forming (Figs. 6.5, 6.7a). The present day morphology and character of the ignimbrite in the basin is largely a function of continued stream erosion along pre-existing channels extending from the older ignimbrites forming the heavily incised plateau south of the basin (Fig. 6.4). Up to 50 % of the original extent of the ignimbrite in the basin may have been removed by fluvial erosion. Topographic control of ignimbrite emplacement is evidenced by the thickest sections of the ignimbrite lying adjacent to the modern stream channels; these channels acted as depocentres during ignimbrite emplacement, and once re-established have since eroded through the deposit to provide the largest exposures. In these locations the ignimbrite is partially welded and forms steep bluffs of mainly L1 ignimbrite with widely spaced vertical cooling joints (3-6 m; Fig. 6.7b).

Significant pre-emplacement relief and variable geology of the basin floor is implied by the basal contacts of the Kawerau Ignimbrite. It is locally in contact with the Matahina and Rotoiti Ignimbrites, and has a strongly erosive contact with underlying Mangaone Subgroup Tephras. Steep contacts between the Kawerau and Rotoiti ignimbrites and forest cover have clearly concealed their true relationship and Rotoiti was originally considered overlying and thus younger than the Kawerau Ignimbrite. Figure 6.7c illustrates the section adjacent to Homestead Road where isolated knolls of Rotoiti Ignimbrite extend above the juxtaposed Kawerau Ignimbrite. At V16/302337 pumice-rich sandy grey-black ignimbrite is exposed overlying an eroded surface on Rotoiti Ignimbrite. In this and several other sections in Puhipuhi Basin the Kawerau ignimbrite has filled a steep valley cut into Rotoiti Ignimbrite. Valleys previously developed on Rotoiti Ignimbrite and older Mangaone Subgroup Tephras in the basin are preferentially filled with L1 ignimbrite. At V16/286311 L2 ignimbrite has been incised into an almost vertical-sided box-canyon

infilled with Omataroa Tephra (Unit K, JURADO-CHICHAY & WALKER, 2000), indicating incision and infilling continued throughout the Mangaone Subgroup activity.

Kawerau Ignimbrite forms a dissected plateau at ~200 m a.s.l which has previously been referred to as 50 m higher than the basin rim (NAIRN, 1981, BERESFORD & COLE, 2000b). Figure 6.8 shows the distribution of Kawerau Ignimbrite in Puhipuhi Basin and the topographic expression of the basin in two cross-sections. The topographic extent of the basin is largely defined by the distribution of the ignimbrite but the basin margin is in fact nowhere lower than the upper surface of Kawerau Ignimbrite.

No complete sections are accessible in the centre of the basin, so a composite graphic log is presented in figure 6.9. At the lowest outcrop along Mangawhio Road (V16/291323), a sharp contact is observed between a sandy yellow-grey ignimbrite with few type-A pumice and overlying sandy-black pumice-rich L1 ignimbrite. No type-B pumices were observed in the lower unit, but large conspicuously (M_P = 380 mm) mingled type A and B pumice are found just above the contact. Large lithics (M_L = 110 mm) are characteristic at this basal level of L1 and contain a large proportion (38%) of dacite lithics. The lower unit is interpreted as an early flow that preceded the main eruption forming the Kawerau Ignimbrite. The absence of pumice type-B suggests emplacement prior to eruption of this magma. Above this exposure typical partially welded L1 ignimbrite forms vertically jointed bluffs. It contains smaller pumice and fewer dacite lithics. In lower parts of the bluffs type-A and -B pumice are similar in proportion, but the abundance of -B is reduced in upper parts of the ignimbrite.

L1 ignimbrite is similarly exposed at the section from which the fission-track age of 0.24 ± 0.05 Ma was obtained by B.P KOHN (reported in NAIRN, 1989; V16/292318). Pumices were extracted from this section to compare with other outcrops of the ignimbrite. In some locations along the main cliff face lithic-rich horizons are observed but these are not extensive and cannot be traced laterally more than 5 m due to poor exposure. L2 forms the poorly accessible upper 25 m of the ignimbrite in central Puhipuhi Basin, but is also found in limited exposures a small distance from the main bluffs in small erosion gullies. Over a distance of less than 50 m the L1 bluffs grade laterally into L2 ignimbrite. At V16/286323 (Fig. 6.10) L2 ignimbrite truncates several airfall units identified as young tephras of the Mangaone Subgroup (V. SMITH *pers. comm.* 2001). White pumice block beds with conspicuous inversely graded rhyolite lapilli alternate with thin ash horizons and pumice

lapilli beds. A soil horizon is exposed at the lowest accessible section some 40 m above the basin floor. The L2 ignimbrite was clearly erosive at this locality and contains large carbonised logs at the base. W. ESLER (*pers. comm.* 2004) has noted carbonised logs in the ignimbrite in the Microsilica quarry at Tikitere, and documented the pyroclastic erosion of the underlying Hauparu tephra at a nearby section.

On the eastern margin of Puhipuhi Basin, on a small road off Pokohu track (V16/311340), basal L1 Kawerau Ignimbrite overlies a ~3.5 m thick section of predominantly airfall tephra resting unconformably on eroded pinkish-coloured pumice-poor Matahina Ignimbrite (Fig. 6.11). The airfall sequence is considered equivalent to the section illustrated in figure 6.10. Thin lithic-rich pumice lapilli beds with well-developed normal grading alternate with coarse ash layers that may represent co-ignimbrite ash from early pyroclastic flows. A thin (0.25 m thick) pumice-poor sandy grey-brown ignimbrite with type-A pumice lapilli appears to be a small early flow deposit. Overlying is a ~1 m thick pumice block bed with inversely graded lithics that is correlated with the thick pumice-block bed exposed beneath the ignimbrite in figure 6.10. Further lapilli and coarse ash beds are overlain by 0.45 m of sandy yellow-grey pumice and lithic-poor ignimbrite. Above a pumice-rich gradational contact is sandy-black basal L1 ignimbrite with both pumice types (M_P = 65 mm). Proportions of rhyolite and dacite lithics are similar to basal L1 in figure 6.9, although clasts are considerably smaller (M_L = 30 mm). Large sections of the ignimbrite are obscured, but pumice-rich jointed bluffs of grey-black ignimbrite outcrop some 15+ m above the road. Similar bluffs are exposed sporadically along the eastern margin of the basin where they form a steep but largely obscured contact with Matahina Ignimbrite.

6.3.2 North of OCC

NAIRN (1989) notes the presence of Kaingaroa Ignimbrite 8 km to the north of Lake Rotoma. Reconnaissance field study in the vicinity of V15/233567 located an 8+ m thick road-cut section of L2 Kawerau Ignimbrite, and many thinner exposures. JURADO-CHICHAY & WALKER (2000) document Mangaone flow as widespread north of lakes Rotoiti and Rotoehu, and identify 5.3 m of the Mangaone flow at a similar location (Fig. 6.3a). In this area M_P and M_L are significantly reduced (Fig. 6.3b, c) and type-B pumice are extremely rare. The ignimbrite becomes light-grey/white in its upper parts and is overlain by younger members of the Mangaone Subgroup.

Many outcrops of the Mangaone flow unit have been identified to the northwest of OCC by W. ESLER (*pers. comm.* 2003) as part of an extensive and detailed study into the history of the Rotorua Basin. Within the Tikitere Graben the ignimbrite is commonly 10 m thick (*writ. comm.* W.ESLER, 2004). The most extensive outcrop of Mangaone flow is 1-3 km west of Ruahine Springs where it reaches 15 m in outcrop and >20 m in a borehole on the northern side of the microsilica quarry at U15/054434. Rare fine lapilli of type-B pumice are reported from the quarry exposure and in a highly silicified outcrop in the vicinity of U15/055450. Further deep exposures of the Mangaone flow *s.s* in the Lake Rotoiti area were interpreted as sediment by early workers (e.g. GRANGE, 1937; HEALY *et al.*, 1964). Work on the Mangaone flow in this area is ongoing and will be reported as part of a manuscript (SPINKS & ESLER, *in prep*) reinterpreting the Mangaone flow deposit to include the Kawerau Ignimbrite.

6.4 CORRELATION WITH THE MANGAONE SUBGROUP

Field work in the Puhipuhi Basin and surrounding OCC has established the Kawerau Ignimbrite as stratigraphically associated with the Mangaone Subgroup, and a likely equivalent of the Mangaone flow unit. Pumices from the Kawerau Ignimbrite were analysed for major and trace element chemistry by X-ray fluorescence spectrometry (XRF) at the University of Canterbury, using the general methods outlined in Weaver et al (1990), to which reference should be made for estimates of analytical precision. Twenty-seven new analyses were made in addition to the five presented by BERESFORD (1997) and discussed in BERESFORD & COLE (2000b).

Pumices of both types were collected from various locations within Puhipuhi Basin (including the outcrop from which the date was obtained), the type section at V15/343448, and from V15/233567 8 km north of Lake Rotoma. These were compared with available geochemistry data for the Mangaone Subgroup (SMITH, 2001; SMITH *et al.*, 2002). BERESFORD & COLE (2000b) have previously documented the distinct pumice chemistry of the Kawerau Ignimbrite relative to that of the Kaingaroa Ignimbrite with which it was originally correlated, and with other Okataina eruptives.

Whole pumice chemistry indicates significant compositional variation within the Kawerau magma system. Two types of magmatic component are recognised, consistent with the study of BERESFORD & COLE (2000b). Type-A pumice are high-silica rhyolites (<<10 wt% crystals); type-B are dacitic pumice (<2 wt% crystals). Rhyolitic pumice have the

phenocryst assemblage plagioclase + orthopyroxene + hornblende + Fe-Ti oxides. Dacitic pumice have the assemblage plagioclase + hornblende + orthopyroxene ± augite + Fe-Ti oxides. Detailed petrography of Kawerau Ignimbrite was discussed by BERESFORD (1997) and limited analysis during this study indicated such similar results such that no further detailed study was undertaken. Mineral chemistry and the composition of rare vapour-phase mineral manganoan fayalite are documented by BERESFORD & COLE (2000b) and are not considered further in this study.

6.4.1 Whole Rock Chemistry

Major element chemistry of the two pumice types in the Kawerau Ignimbrite is illustrated in figure 6.12. Yellow data points represent the data of BERESFORD (1997); red data are the analyses of this study. Also shown are the fields for 'young' and 'old' Mangaone Subgroup tephras (SMITH *et al.*, 2002). The data confirms the correlation between the ignimbrite exposed in three main areas, in Puhipuhi Basin, near Kawerau, and north of Lake Rotoma. Pumices from the Kawerau Ignimbrite exhibit significant variation in major and trace elements e.g. SiO_2: 66-76% (Fig. 6.12; appendix I); Rb: 60-90 ppm; Zr: 181-738 ppm (Fig. 6.13; appendix F). Two distinct pumice types are recognised based on vastly dissimilar major and trace element chemistry which correspond to the two pumice groups identified and described based on field and petrographic criteria.

Major element chemistry is clearly separated into two distinct compositional groups equivalent to the Mangaone Subgroup fields. Plots in figure 6.12 exhibit largely linear trends against SiO_2. Depletion trends are observed for TiO_2, CaO, Al_2O_3 and Fe_2O_3 against increasing SiO_2. K_2O shows an enrichment trend, while Na_2O shows no trend with increasing SiO_2. The dominant pumice type-A forms a distinct cluster within the young Mangaone field in all considered elements, while pumice type B correlates with the broader field of old Mangaone. No intermediate compositions are observed, suggesting the two magmas did not interact to a large degree before eruption. Mingled pumice observed in basal sections of the ignimbrite in Puhipuhi Basin suggests limited interaction may have occurred immediately prior to or during the eruption.

Trace element chemistry (Fig. 6.13) reveals the same two compositional groups distinguished in major-element data. Slight variations indicate weak compositional gradients in individual pumice types. Large-ion lithophile elements (LILE) Ba and Rb are enriched with respect to increasing SiO_2. The high field strength element (HFSE) Zr

shows a distinct correlation with SiO_2, and both groups decrease in Zr with increasing SiO_2. Kawerau pumice show anomalously high Zn and Zr with Zr abundance some ~400 ppm higher than for other TVZ rhyolites. In contrast to major element data, trace element data shows that type B pumice is distinct from the magma represented by 'old' Mangaone eruptives, suggesting it was a separate, additional magma.

6.4.2 Glass Chemistry

Glass shard analysis is commonly used to identify and fingerprint pyroclastic deposits (e.g. SMITH *et al.*, 2002; 2004a,b,c). Glass composition gives an accurate measure of the melt composition and is not influenced by crystal content, and thus not restricted to the large pumice samples required for precise XRF analysis. Preliminary analysis of Kawerau Ignimbrite matrix and pumice samples was undertaken at Auckland University by V. SMITH. Figure 6.13 presents selected results of these analyses. The data confirm (1) that type-A pumice in Kawerau Ignimbrite represent the same magma as Mangaone flow, thus confirming their correlation; (2) that type-B pumice are not related to 'old' Mangaone but represent a discrete magma batch; additionally they show (3) that matrix glass is predominantly the same composition as type-A pumice; (4) that one dacite pumice clast also contained glass of type-A composition suggesting late-stage mingling; (5) that the fall unit truncated by L2 ignimbrite at V16/286323 is the Mangaone fall deposit.

6.5 DISCUSSION

6.5.1 Age, Volume & Eruptive Source

Despite the existing fission-track age of 0.24 ± 0.05 Ma (B.P. KOHN, *pers. comm.* in NAIRN, 1989), the Kawerau Ignimbrite is convincingly shown to be an eruptive of the Mangaone Subgroup (43-31 ka, JURADO-CHICHAY & WALKER, 2000). Correlation with the Mangaone flow unit gives a conventional ^{14}C age of 28,060 a. and a recalculated calendar age of 33,000 b.p. (JURADO-CHICHAY & WALKER, 2000), an order of magnitude younger than the previous date. Zircon fission-tracks are annealed at magmatic temperatures so recycling of the dated zircon is highly unlikely. No further explanation can be given for the huge disparity in the two dates for the ignimbrite; the only speculative possibility is 'sample error' since fission-track dates on the 0.24 Kaingaroa Ignimbrite to the south of Okataina were carried out at the same time (i.e. when Kawerau Ignimbrite was considered part of the Kaingaroa Ignimbrite; I.A. NAIRN *pers. comm.* 2001). Kaingaroa Ignimbrite was later dated by fission-track at 0.22 ± 0.04 Ma (GRINDLEY *et al.*, 1994) and by the Ar/Ar method at 0.23 ± 0.03 Ma (HOUGHTON *et al.*, 1995). An attempt to date a

sample of Kawerau Ignimbrite during this study using the Ar/Ar method at the USGS Menlo park facilities by G. Leonard returned an erroneous result due to its young age, which is thus inferred to be younger than ~50 ka (G. LEONARD *writ. comm.* 2003).

JURADO-CHICHAY & WALKER (2000) give a volume estimate for the Mangaone tephra as 19.9 km^3 (6 km^3 DRE), which is ~25% of the total subgroup eruptions. The Mangaone flow itself is considered to have a volume of 3.6 km^3 (1.8 km^3 DRE). The addition of the Kawerau Ignimbrite significantly increases the volume, especially since much of the intra-caldera deposit may have been destroyed by later eruptions in OCC. Current outcrop of the combined ignimbrite likely totals <15 km^3, but the original volume may approach ~50 km^3 when intra-caldera volumes are considered. The Mangaone tephra must thus be >30 km^3, an estimated ~15 km^3 more than any other Mangaone Subgroup eruptive and closer to 35% of the total erupted magma. Significantly, it is therefore the largest eruption from Okataina since the Rotoiti caldera forming event at 65 ka.

The Mangaone Subgroup eruptives are attributed to a number of source locations within OCC based on lithic isopleths maps constructed for the fall deposits (JURADO-CHICHAY & WALKER, 2000; Fig 6.2). The source for Unit I (Mangaone) is located on the northwest margin of Puhipuhi basin on the eastern side of OCC. Distribution of the Kawerau Ignimbrite is consistent with a southern OCC source. Westward coarsening M_L and M_P data for the Kawerau Ignimbrite in Puhipuhi Basin indicate a southern OCC source west of the basin, consistent with the fall deposit. The thickness of the ignimbrite in Puhipuhi Basin could be claimed to suggest a basin source. A Puhipuhi vent for the Kawerau Ignimbrite should have destroyed the pre-ignimbrite geology of the basin, that is, the underlying ignimbrites and tephra sequences, during eruption and associated caldera collapse. The documented pre-ignimbrite surface in the basin thus largely precludes the basin as a source. JURADO-CHICHAY & WALKER (2000) also show the eruptive vents for units K and L within Puhipuhi Basin which here is considered highly unlikely. Extensive field examination within and around the basin during a period of abundant exposure failed to reveal any proximal ballistic exposures or features consistent with vents located within the basin. The Mangaone tephra, including the Kawerau Ignimbrite, and younger tephras of the Mangaone Subgroup, are therefore considered associated with source vents further to the west inside the caldera complex.

Puhipuhi Dacite

A poorly exposed dacitic cone and associated lavas in the western portion of Puhipuhi Basin is considered to be considerably older than the Rotoiti Pyroclastics by NAIRN (2002). Field work to elucidate the relationship with Kawerau Ignimbrite revealed that only young Mangaone Subgroup tephras are observed overlying the lavas, suggesting that they may be at least temporally related to the Mangaone eruptions, and possibly geochemically linked. The lavas are extensively altered, and no geochemical connection could be made between these and the dacitic magma of the Kawerau Ignimbrite. Regardless, their presence in the basin indicates that multiple magmas may have existed at depth.

6.5.2 Magma System associated with Kawerau Ignimbrite

The geochemical properties of the Kawerau magma system are discussed in BERESFORD (1997) and to a lesser extent in BERESFORD & COLE (2000b). Here the concern is only with how a model of the Kawerau magmatic system accounts for the following: (1) significant compositional variation, including the presence of subordinate dacitic magma; (2) mingling but no mixing of pumice types; (3) the relationship between the distribution of dacitic type-B pumice in the ignimbrite and eruptive processes.

Two magma types are identified (Figs. 6.12-14), and the large compositional gap between them and anomalous trace element chemistry of the type-B magma is interpreted to represent eruption of two distinct compositions. The lack of any intermediate compositions that would indicate magma mixing, and the large compositional gap, suggests the magma compositions represent separate distinct magma batches rather than a single zoned magma. Visibly mingled pumice in the basal L1 ignimbrite (Fig. 6.9) and bimodal glass populations in a single type-B pumice sample indicate that the two magmas were in contact during the eruption enabling limited mechanical mixing, most likely in the eruption conduit.

The interaction of a hot mafic magma with a cooler more silicic magma has been widely recognised as a potential trigger mechanism for explosive eruptions (e.g. SPARKS *et al.*, 1977; EICHELBERGER, 1995; EICHELBERGER *et al.*, 2000). The injection and interaction of mafic magmas has also been recognised to reactivate rhyolitic magmas in TVZ, e.g. the 3.3 ka Waimihia eruption from Taupo Caldera Complex (BLAKE *et al.*, 1992) and the 1305 A.D. Kaharoa eruption from the Tarawera Volcano (LEONARD *et al.*, 2002). SMITH *et al* (2004) document reactivation of a high-level rhyolite chamber by intrusion of a distinct

higher temperature rhyolite magma triggering the 15.8 ka Rotorua eruptive episode at Okataina. Limited hybridisation of the two homogenous magmas is thought to reflect their contrasting temperatures and viscosities (SMITH *et al.*, 2004). Limited interaction between the magmas represented in the Kawerau Ignimbrite may similarly be a function of the density, temperature and viscosity contrasts between the two magma types.

6.5.3 Eruption Model

The distribution of the two gradational lithofacies of the Kawerau Ignimbrite indicates that magmatic and eruptive process, and pre-emplacement topography, strongly contributed to the present character of the ignimbrite. Conspicuous differences in pumice and lithic populations are recorded between the two lithofacies. L1 is restricted to Puhipuhi Basin and in proximal areas near the margin of OCC. Further, L1 is concentrated in the thickest sections of Puhipuhi Basin and is thus considered a valley-ponded facies of the ignimbrite. The eruption and ignimbrite emplacement sequence is summarised here.

(1) The Mangaone eruptive episode initially records tapping of the dominant rhyolitic magma which comprises the fall unit preceding the ignimbrite. Thin ignimbrites within this sequence record pyroclastic flows from minor column collapse events. These are consistent with progressive widening of the vent represented by the inverse grading of lithics in the airfall tephras underlying the ignimbrite.

(2) Vent/magma migration, such as along a linear system, or the development of an additional vent(s), leads to tapping of a subordinate dacitic magma chamber with limited magma interaction in the eruptive conduit. Foundering of the vent leads to instability in the plinian column, subsequent partial column collapse, and directed pyroclastic flows. Pumice from the dacitic magma is preferentially concentrated in topographically controlled L1 pyroclastic flows that fill low-lying Puhipuhi Basin and much of the southern caldera complex. A much smaller volume of L1 escaped the caldera complex near Kawerau and to the northwest. Lithic concentrations near the base of L1 appear to represent the onset of caldera collapse.

(3) Waning supply of the dacite pumice in L2 records rapid depletion of the dacite magma. Eruption of further rhyolitic magma drives continued column collapse

and progressive emplacement of L2 pyroclastic flow(s) to the north and east of OCC. Limited ponding occurs in Tikitere Graben and on the partially dissected ignimbrite plateau north of OCC. Waning eruption thus develops widespread L2 (Mangaone flow *s.s*) sheet. Additional active vents may partly explain the paucity of dacite pumice in ignimbrite to the north of OCC.

6.5.4 Implications of Revised Stratigraphy

The Kawerau Ignimbrite has had a history of miscorrelation that further highlights the need for integrated field and petrographic studies in ignimbrite correlation (BERESFORD & COLE, 2000b). Additionally, it demonstrates the difficulties of field studies in forested areas of central TVZ. Originally considered part of the Kaingaroa Ignimbrite by NAIRN (1981), it was renamed Kawerau Ignimbrite by BERESFORD & COLE (2000b) based on a distinctive geochemistry. This study has further shown that it is in fact part of the Mangaone Subgroup, some ~200 ka younger than previously accepted. As such, the accepted history of OCC is revised in chapter five of this thesis.

In addition to the altered caldera history are implications for geologic hazards in northern TVZ. The recognition of a large partially welded ignimbrite with an emplacement age within the last 35 ka necessitates some assessment in terms of the potential hazards of a similar event. While two small ignimbrites were previously documented from the Mangaone Subgroup, recognition of a much larger deposit indicates a major departure from the largely monotonous and repetitive plinian-style activity documented from the Mangaone Subgroup. Pyroclastic flows should thus be considered alongside plinian fall dominated eruptions in hazard planning. The mechanism by which Kawerau Ignimbrite was formed (i.e. interaction of multiple magmas, and potentially multiple vents) suggests that 'stable' eruption columns may rapidly become dynamic features and lead to larger scale ignimbrite and caldera collapse events without the expected precursory activity of such larger events. Detailed hazard assessment based on a Kawerau Ignimbrite-style event is beyond the scope of this thesis.

7.1 CONCLUSIONS

The main outcome of this thesis is an understanding of rift architecture and kinematics in TVZ and their relationship with caldera volcanism. The following sections give the key points that arise from this thesis.

7.1.1 Rift Architecture & Kinematics in TVZ

- The structural characteristics of Modern TVZ define a segmented intra-arc rift system with offset and variably oriented rift segments.
- Fault striation and offset stream-channel structural data indicate there is a component of dextral strike-slip in four of the seven rift segments, which accounts for between 22% and 28% of the total displacement, and indicates that strain partitioning is not complete across the plate boundary zone.
- Kinematic and eruptive volume data show a correlation between the degree of pure extension and the volume of extruded magma along the length of Modern TVZ.
- Segments undergoing orthogonal extension correspond to the highly active silicic Taupo and Okataina Caldera Complexes; conversely, segments with a higher degree of dextral transtension correspond to volumetrically-less andesitic volcanism.
- Rift architecture has strongly influenced the characteristics of magma generation and emplacement, and volcanism at the surface.

7.1.2 Caldera volcanism in TVZ

- The four calderas in Modern TVZ are divided into two groups as a function of their proximity to (and influence of) active rift faulting.
- Extra-rift calderas are simple sub-circular monogenetic collapse structures without significant coupling to regional structure; intra-rift caldera complexes are rectilinear multiple-collapse structures with clear coupling to regional structure.
- At intra-rift calderas, caldera margins are coincident with and controlled by regional faults, and interaction with the axial rift zone extends their surface expression as major fault-bounded embayments in the caldera margins.

7.1.3 The evolution of Okataina Caldera Complex

- The OCC comprises two large overlapping calderas and a third nested caldera, and is significant in its location at a major transfer zone within the axial rift zone of Modern TVZ.
- The eruptive history at OCC is characterised by independent eruptive centres within and on the periphery of the caldera, punctuated by caldera forming eruptions at 280ka, 65 ka, and 33ka.
- The volcanic evolution within the Okataina transfer zone, including the OCC, follows the progressive interaction and propagation of offset rift segments, from large volume magma accumulation in the zone of orthogonal extension, to the development of two spatially distinct eruptive centres as deformation proceeds above overlapping rift axes.

7.1.4 The Kawerau Ignimbrite

- The Kawerau Ignimbrite has a revised age of 33 ka, ~220 ka younger than previously considered, based on stratigraphic relationships in Puhipuhi Basin and a geochemical correlation with the Mangaone tephra of the Mangaone Subgroup.
- The ignimbrite has a significantly greater distribution and volume than earlier studies have suggested, is the largest eruption at OCC since 65 ka and the youngest partially-welded ignimbrite in TVZ.

ACOCELLA, V., CIFELLI, F. & FUNICIELLO, R. (2000) Analogue models of collapse calderas and resurgent domes. *Journal of Volcanology and Geothermal Research* 104: 81-96

ACOCELLA, V., CIFELLI, F. & FUNICIELLO, R. (2001) The control of overburden thickness on resurgent domes: Insights from analogue models. *Journal of Volcanology and Geothermal Research* 111: 137-153

ACOCELLA, V., FACCENNA, C., FUNICIELLO, R. & ROSSETTI, F. (1999a) Sand-box modelling of basement controlled transfer zones in extensional domains, *Terra Nova* 11: 149-156

ACOCELLA, V. & FUNICIELLO, R. (1999) The interaction between regional and local tectonics during resurgent doming: the case of the island of Ischia, Italy. *Journal of Volcanology and Geothermal Research* 88: 109-123

ACOCELLA, V.A., FUNICIELLO, R., MAROTTA, E., ORSI, G. & DE VITA, S. (2004) The role of extensional structures on experimental calderas and resurgence. *Journal of Volcanology and Geothermal Research* 129: 199-217

ACOCELLA, V.A., GUDMUNDSSON, A. & FUNICIELLO, R. (2000) Interaction and linkage of extensional fractures: examples form the rift zone of Iceland, *Journal of Structural Geology* 22: 1233-1246

ACOCELLA, V. & KORME, T. (2002) Holocene extension direction in the axial zone of the main Ethiopian rift. *Terra Nova, in press.*

ACOCELLA, V., KORME, T., SALVINI, F. & FUNICIELLO, R. (2002) Elliptical calderas in the Ethiopian Rift: control of pre-existing structures. *Journal of Volcanology and Geothermal Research* 119: 189-203

ACOCELLA V. & ROSSETTI F. (2002) The role of extensional structures on pluton ascent and emplacement: the case of Southern Tuscany (Italy). *Tectonophysics* 354: 71-83

ACOCELLA, V., SALVINI, F., FUNICIELLO, R. & FACCENNA, C. (1999b) The role of transfer structures on volcanic activity at Campi Flegrei (Southern Italy). *Journal of Volcanology and Geothermal Research* 91: 123-139

ACOCELLA, V., SPINKS, K.D., COLE, J.W. & NICOL, A. (2003) Oblique back arc rifting of Taupo Volcanic Zone, New Zealand. *Tectonics* 22: 1045 doi: 0.1029/2002TC001447

BAILEY, R.A. (1965) Field and petrographic notes on the Matahina Ignimbrite. *In* THOMPSON, B.N., KERMODE, L.O. & EWART, A. (Eds): New Zealand volcanology – Central Volcanic region. *New Zealand Department of Scientific and Industrial Research Information Series* 50: 125-128

BAILEY, R.A & CARR, R.G. (1994) Physical geology and eruptive history of the Matahina Ignimbrite, Taupo Volcanic Zone, North Island, New Zealand. *New Zealand Journal of Geology and Geophysics* 37: 319-344

BAILEY, R.A. DALRYMPLE, G.B. & LANPHERE, M.A. (1976) Volcanism, structure, and geochronology of Long Valley Caldera, Mono County, California. *Journal of Geophysical Research* 81: 725-744

BALLANCE, P.F. (1976) Evolution of the upper Cenozoic magmatic arc and plate boundary in northern New Zealand. *Earth and Planetary Science Letters* 28: 356-370

BARBERI, F., INNOCENTI, F., LIRER, L. MUNNO, R. & PESCATORE, P. (1978) The Campanian Ignimbrite: a major prehistoric eruption in the Neapolitan area (Italy). *Bulletin of Volcanology* 41: 1-22

BARNARD, S, T. (2004) Potential physical effects of any future 1886 type eruption from Tarawera Volcano on the Bay of Plenty region. *Unpublished MSc thesis, University of Canterbury, New Zealand*

BEANLAND S., (1995) The North Island Dextral Fault Belt, *Ph.D. Thesis, Victoria University, Wellington, New Zealand*

BEANLAND S., & J. HAINES, (1998) The kinematics of active deformation in the North Island, New Zealand, determined from geologic strain rates, *New Zealand Journal of Geology and Geophysics* 41: 311-323

BEANLAND S., A. MELHUISH, A. NICOL, & J. RAVENS, (1998) Structure and deformational history of the inner forearc region, Hikurangi subduction margin, New Zealand, *New Zealand Journal of Geology and Geophysics* 41: 325-342

BEGGS, K.F. (2000) Magmatic processes associated with the Okareka and Rerewhakaiitu eruptive epidoes, Tarawera Volcanic complex, New Zealand. *Unpublished MSc. Thesis, University of Canterbury, New Zealand*

BELLAMY, S. (1991) Some studies of the Te Wairoa ignimbrites and the associated volcanic geology of the SW Okataina volcanic centre, Taupo Volcanic Zone. *MSc thesis, University of Waikato, New Zealand.*

BELLIER, O. & SEBRIER, M. (1994) Relationship between tectonism and volcanism along the Great Sumatran Fault Zone deduced by SPOT image analyses. *Tectonophysics*, 233: 215-231

BELLIER, O., BELLON, H., SEBRIER, M., SUTANTO, & MAURY, R.C. (1999) K-Ar age of the Ranau Tuffs: implications for the Ranau caldera emplacement and slip-partitioning in Sumatra (Indonesia). *Tectonophysics* 312: 347-359

BERESFORD, S.W. (1997) Volcanology and geochemistry of the Kaingaroa Ignimbrite, Taupo Volcanic Zone, New Zealand. *PhD thesis, University of Canterbury, New Zealand*

BERESFORD, S.W. & COLE, J.W. (2000a). Kaingaroa Ignimbrite, Taupo Volcanic Zone, New Zealand: evidence for asymmetric caldera subsidence of the Reporoa Caldera. *New Zealand Journal of Geology and Geophysics* 43: 471-481

BERESFORD, S.W. & COLE, J.W. (2000b) Kawerau Ignimbrite: a 0.24 Ma ignimbrite erupted from the Okataina caldera complex, Taupo Volcanic Zone, New Zealand. *New Zealand Journal of Geology and Geophysics* 43: 109-115

BERESFORD, S.W., COLE, J.W. & WEAVER, S.D. (2000) Weak chemical and mineralogical zonation in the Kaingaroa Ignimbrite, Taupo volcanic zone, New Zealand *New Zealand Journal of Geology and Geophysics* 43: 639-650

BERRYMAN, K.R. & VILLAMOR, P. (1999) Spatial and temporal zoning of faulting in the Taupo volcanic zone, New Zealand. Geological Society of New Zealand 1999 annual conference, programme and abstracts. *Geological Society of New Zealand Miscellaneous Publication* 107A: 15

BIBBY, H.M., CALDWELL, T.G., DAVEY, F.J. & WEBB, T.H. (1995) Geophysical evidence on the structure of the Taupo Volcanic Zone and its hydrothermal circulation. *Journal of Volcanology and Geothermal Research* 68: 29-58

BIBBY, H.M., CALDWELL, T.G. & RISK, G.F. (1998) Electrical resistivity image of the upper crust within the Taupo volcanic Zone, New Zealand. *Journal of Geophysical Research, B, Solid Earth and Planets* 103: 9665-9680

BLACK, T.M., SHANE, P.A.R., WESTGATE, J.A., & FROGGATT, P.C. (1996) Chronology and paleomagnetic constraints on widespread ignimbrites of the Taupo volcanic zone, New Zealand. *Bulletin of Volcanology* 58: 226-238

BLAKE, S., WILSON, C.J.N., SMITH, I.E.M & WALKER, G.P.L. (1992) Petrology and dynamics of the Waimihia mixed magma eruption, Taupo Volcanoc, New Zealand. *Journal of the Geological Society of London* 149: 193-207

BLANK, H.R. (1965) Ash flow deposits of the central King Country. *New Zealand Journal of Geology and Geophysics* 8: 588-607

BLUMENTHAL, E.C. (2004) Evacuation planning needed for any future rhyolite eruption from Tarawera Volcano. *Unpublished MSc thesis, University of Canterbury, New Zealand*

BODEN, D.R. (1986) Eruptive history and structural development of the Toquima caldera complex, central Nevada. *Geological Society of America Bulletin* 97: 61-74

BOSWORTH, W., BURKE, K. & STRECKER, M (2000) Magma chamber elongation as an indicator of intraplate stress field orientation: 'borehole break-out mechanism' and examples from the late Pleistocene to Recent Kenya rift Valley. *In*: Stress, Strain and Structure (Eds: M.W. JESSELL AND J.L. URAI) Volume 2, *Journal of the Virtual Explorer*

BOSWORTH, W., BURKE, K. & STRECKER, M. (2003) Effect of stress fields on magma chamber stability and the formation of collapse calderas. *Tectonics* 22: 1042 doi: 10.1029/2002TC001369

BOWER, S.M. & WOODS, A.W. (1998) On the influence of magma chambers in controlling the evolution of explosive volcanic eruptions. *Journal of Volcanology and Geothermal Research* 86: 67-78

BOWYER, D.A. (2001) Petrologic, geochemical, and isotopic evolution of rhyolite lavas from the Okataina, Rotorua, and Kapenga volcanic centres, Taupo Volcanic Zone, New Zealand. *PhD thesis, University of Waikato, Hamilton, New Zealand.*

BRANNEY, M.J. (1995) Downsag and extension at calderas: new perspectives on collapse geometries from ice-melt, mining, and volcanic subsidence. *Bulletin of Volcanology* 57: 303-318

BRANNEY, M.J. & KOKELAAR, B.P. (1994) Volcano-tectonic faulting, sof-state deformation and rheomorphism of tuffs during development of a piecemeal caldera, English Lake District. *Geological Society of America Bulletin* 106: 507-530

BRIGGS, N.D. (1973) Investigations of New Zealand pyroclastic flow deposits. *Unpublished PhD thesis, Victoria Univeristy of Wellington, New Zealand*

BRIGGS, R.M., GIFFORD, M.G., MOYLE, A.R., TAYLOR, S.R., NORMAN, M.D, HOUGHTON, B.F & WILSON, C.J.N. (1993) Geochemical zoning and eruptive mixing in ignimbrites from Mangakino volcano, Taupo Volcanic Zone, New Zealand. *Journal of Volcanology and Geothermal Research* 56: 175-203

BRIGGS, R.M., HALL, G.J., HARMSWORTH, G.R., HOLLIS, A.G., HOUGHTON, B.F., HUGHES, G.R., MORGAN, M.D. & WHITBREAD-EDWARDS, A.R. (1996) Geology of the Tauranga Area. Occasional Report, no. 22, *Department of Earth Sciences, University of Waikato, Hamilton, New Zealand.* 56

BROWN, S.J.A. (1994) Geology and geochemistry of the Whakamaru Group Ignimbrites, and associated rhyolite domes, Taupo Volcanic Centre, New Zealand. *Unpublished PhD thesis, University of Canterbury, New Zealand*

BROWN, S.J.A, BURT, R.M., COLE, J.W, KRIPPNER, S.J.P., PRICE, R.C. & CARTWRIGHT, I. (1998) Plutonic lithics in ignimbrites of Taupo Volcanic Zone, New Zealand: Sources and conditions of crystallisation. *Chemical Geology* 148: 21-41

BURT, R.M., BROWN, S.J.A., COLE, J.W., SHELLEY, D. & WAIGHT, T.E. (1998) Glass-bearing plutonic fragments from ignimbrites of the Okataina caldera complex, Taupo Volcanic Zone, New Zealand: remnants of a partially molten intrusion associated with preceding eruptions. *Journal of Volcanology and Geothermal Research* 84: 209-237

CAMBRAY, F.W., VOGEL, T.A. & MILLS J.G. JR. (1995) Origin of compositional heterogeneities in tuffs of the Timber Mountain Group: the relationship between magma batches and magma transfer and emplacement in an extensional environment. *Journal of Geophysical Research* 100: 15793-15805

CAMERON, E., GAMBLE, J., MCINTOSH, W. & SMITH, I. (2003) Establishing a valid radiometric age for Hauhungatahi, Tongariro National Park, North Island, New Zealand. *Geological Society of New Zealand Miscellaneous Publication 116A, Annual Conference Programme & Abstracts* 27

CAMPBELL, J.B. (1987) Introduction to remote sensing. *Guilford Press, New York.* 551

CAMPBELL, S.D.G., REEDMAN, A.J., HOWELLS, M.F. & MANN, A.C. (1987) The emplacement of geochemically distinct groups of rhyolites during the evolution of the Lower Rhyolitic Tuff Formation caldera (Ordovician), North Wales, U.K. *Geological Magazine*, 124: 501-511

CARR, R.G. (1984) The Matahina Ignimbrite: its evolution including its eruption and Post-depositional changes. *Unpublished PhD thesis, University of Auckland, New Zealand*

CARTER, L. (1980) NZ regional bathymetry 1: 6 000 000 (2nd ed). NZ Oceanographic Institute Chart. *New Zealand Department of Scientific and Industrial Research Miscellaneous Series* 15

CAS, R.A.F. & WRIGHT, J.V. (1997) Volcanic Successions: modern and ancient. *Chapman & Hall, London.* 528

CASHMAN, S.M., KELSEY, H.M., ERDMAN, C.F. CUTTEN, H.N.C. & K.R. BERRYMAN (1992) Strain partitioning between structural domains in the forearc of the Hikurangi subduction zone, New Zealand. *Tectonics* 11: 242-257

CHAPIN, C.E., & CHATER, S.M., (1994). Tectonic setting of the axial basins of the northern and central Rio Grande rift. *In:* KELLER, G.R., CHATER, S.M. (Eds.), Basins of the Rio Grande Rift: Structure, Stratigraphy, and Tectonic Setting. *Geological Society of America Special Paper* 291: 5– 25.

CHARLIER, B.L.A., PEATE, D.W., WILSON, C.J.N., LOWENSTERN, J.B., STOREY, M. & BROWN, S.J.A. (2003) Crystallisation ages in coeval silicic magma bodies: 238U-230Th disequilibrium evidence from the Rotoiti and Earth Flat eruption deposits, Taupo Volcanic Zone, New Zealand. *Earth and Planetary Science Letters* 206: 441-457

CHESNER, C.A., ROSE, W.I., DEINO, A., DRAKE, R & WESTGATE, J.A. (1991) Eruptive history of the Earth's largest Quaternary caldera (Toba, Indonesia). *Geology* 19: 200-203

CHRISTIANSEN, R.L., LIPMAN, P.W., CARR, W.J., BYERS, F.M., ORKILD, P.P. & SARGENT, K.A. (1977) Timber Mountain – Oasis Valley caldera complex of southern Nevada. *Geological Society of America Bulletin* 88: 943-959

CLOUGH, C.T.H., MAUFE, H.B., & BAILEY, E.B. (1909) The cauldron subsidence of Glencoe and the associated igneous phenomena: *Geological Society of London Quarterly Journal* 65: 611-678

COCHRANE, G.R. & TIANFENG, W. (1983) Interpretation of structural characteristics of the Taupo Volcanic Zone, New Zealand, from Landsat imagery. *International Journal of Remote Sensing* 4: 111-128

COLE, J.W. (1970a) Description and correlation of Holocene volcanic formations in the Tarawera-Rerewhakaiitu region. *Transactions of the Royal Society of New Zealand* (earth sciences) 8: 93-108

COLE, J.W. (1970b) Structure and eruptive history of the Tarawera Volcanic Complex. *New Zealand Journal of Geology and Geophysics* 13: 879-902

COLE, J.W. (1970c) Petrography of the rhyolite lavas of Tarawera Volcanic Complex. *New Zealand Journal of Geology and Geophysics* 13: 903-924

COLE, J.W. (1970d) Petrology of the basic rocks of Tarawera Volcanic Complex. *New Zealand Journal of Geology and Geophysics* 13: 925-936

COLE, J.W. (1978) Andesites of the Tongariro Volcanic Centre, North Island, New Zealand. *Journal of Volcanology and Geothermal Research* 3: 121-153

COLE, J.W. (1990) Structural control and origin of volcanism in the Taupo Volcanic Zone, New Zealand. *Bulletin of Volcanology* 52: 445-459

COLE, J.W., BROWN, S.J.A, BURT, R.M., BERESFORD, S.W. & WILSON, C.J.N. (1998) Lithic types in ignimbrites as a guide to the evolution of a caldera complex, Taupo volcanic centre, New Zealand. *Journal of Volcanology and Geothermal Research* 80: 217-237

COLE, J.W., GRAHAM, I.J., HACKETT, W.R. & HOUGHTON, B.F. (1986) Volcanology and Petrology of the Quaternary Composite Volcanoes of Tongariro Centre, Taupo Volcanic Zone. *In:* Late Cenozoic Volcanism in New Zealand (I.E.M. SMITH – ed) *Royal Society of New Zealand Bulletin* 23: 224-250

COLE, J.W. & LEWIS, K.B. (1981) Evolution of the Taupo-Hikurangi subduction system. *Tectonophysics* 72: 1-21

COLE, J.W., MILNER, D.M. & SPINKS, K.D. (2005) Calderas and caldera structures: a review. *Earth Science Reviews* 69: 1-26

CORTI, G., BONINI, M., MAZZARINI, M., BOCCALETTI, M., INNOCENTI, F., MANETTI, P., MULUGETA, G. & SOKOUTIS, D. (2002) Magma induced strain localisation in centrifuge moels of transfer zones. *Tectonophysics* 348: 205-218

CORTI, G., BONINI, M., SOKOUTIS, D., INNOCENTI, F., MANETTI, P., CLOETINGH, S. & MULUGETA, G. (2004) Continental rift architecture and patterns of magma migration: A dynamic analysis based on centrifuge models. *Tectonics* 23, TC2012, doi:10.1029/2003TC001561

CROSBY, N. (1998) Quaternary Geology and Tephrostratigraphy of the North-north-eastern Rotorua region. *Unpublished MSc thesis, University of Waikato, Hamilton, New Zealand*

DARBY D.J., K.M. HODGKINSON, & G.H BLICK, (2000) Geodetic measurement of deformation in the Taupo Volcanic Zone, New Zealand: the north Taupo network revisited, *New Zealand Journal of Geology and Geophysics* 43: 157-170

DARBY, D.J., & MEERTENS, C.M., (1995) Terrestrial and GPS measurements of deformation across the Taupo back arc and Hikurangi forearc regions in New Zealand. *Journal of Geophysical Research* 100: 8221-8232

DARRAGH, M.B. (2004) Eruption processes of the Okareka and Rerewhakaiitu eruption episodes, Tarawera Volcano, New Zealand. *Unpublished MSc thesis, University of Canterbury, New Zealand*

DAVEY, F.J., HENRYS, S.A. & LODOLO, E., (1995). Asymmetric rifting in a continental back-arc environment, North Island New Zealand. *Journal of Volcanology and Geothermal Research* 68: 209-238

DAVIS, W.J. (1985) Geochemistry and petrology of the Rotoiti and Earthquake Flat pyroclastic deposits. *Unpublished MSc thesis, Auckland University New Zealand*

DAVY, B.W. & CALDWELL, T.G. (1998) Gravity, magnetic and seismic surveys of the caldera complex, Lake Taupo, North Island, New Zealand. *Journal of Volcanology and Geothermal Research* 81: 69-89

DEMETS C., R.G. GORDON, D. ARGUS, & S. STEIN, (1994) Effect of recent revisions to the geomagnetic reversal time scale on estimates of current plate motions, *Geophysical Research Letters* 21: 2191-2194

DE SILVA, S.L. (1989) Altiplano-Puna volcanic complex of the central Andes. *Geology* 17: 1102-1106

DE SILVA, S.L. & FRANCIS, P.W. (1991) Volcanoes of the Central Andes. *Springer-Verlag* 216

DU BRAY, E.A. & PALLISTER, J.S. (1991) An ash flow caldera in cross-section: ongoing field and geochemical studies of the mid-Tertiary Turkey Creek Caldera, Chiricahua Mountains, SE Arizona. *Journal of Geophysical Research* 96: 13435-13457

EICHELBERGER, J.C. (1995) Silicic volcanism; ascent of viscous magmas from crustal reservoirs. *Annual Reviews of Earth and Planetary Science* 23: 41-63

EICHELBERGER, J.C., CHERTKOFF, D.G., DREHER, S.T. & NYE, C.J. (2000) Magmas in collision: rethinking chemical zonation in silicic magmas. *Geology* 28: 603-606

ESPANOLA, O.S. (1974) Geology and hot-springs of Tikitere and Tahake hydrothermal fields, Rotorua, New Zealand. *New Zealand Geological Survey Report* NZGS 68

EWART, A. (1967) The petrology of the central North Island rhyolitic lavas. Part 1 – Correlations between the phenocryst assemblages. *New Zealand Journal of Geology and Geophysics* 1: 182-197

EWART, A. (1968) The petrography of the central North Island rhyolitic lavas, Part 2 – regional petrography including notes on associated ash-flow pumice deposits. *New Zealand Journal of Geology and Geophysics* 11: 478-545

EWART, A., & HEALY, J. (1965) Rotorua volcanic geology. *In* THOMPSON, B.N., KERMODE, L.O. & EWART, A. (Eds) New Zealand Volcanology: Central Volcanic Region. *New Zealand Department of Scientific and Industrial Research Information Series* 50: 10-26

EWART, A., HILDRETH, W. & CARMICHAEL, I.S.E. (1975) Quaternary acid magma in New Zealand. *Contributions to mineralogy and petrology* 51: 1-27

EWART, A., TAYLOR, S.R. & CAPP, A.C. (1968) Trace and minor element geochemistry of rhyolitic volcanic rocks, Central North Island, New Zealand – total rock and residual liquid data. *Contributions to mineralogy and petrology* 18: 76-104

FERGUSON, J.F., COGBILL, A.H. & WARREN, R.G. (1994) A geophysical-geological transect of the Silent Canyon caldera complex, Pahute Mesa, Nevada. *Journal of Geophysical Research* 99: 4323-4339

FRANCIS, P.W. (1993) Volcanoes, a planetary perspective, *Oxford University Press*, New York 443

FRANCIS, P.W. & BAKER, M.C.W. (1978) Sources of two large ignimbrites in the central Andes: some Landsat evidence. *Journal of Volcanology and Geothermal Research* 4: 81-87

FRANCIS, P.W., BAKER, M.C.W. & HALLS, C. (1981) The Kari Kari Caldera, Bolivia, and the Cerro Rico Stock. *Journal of Volcanology and Geothermal Research* 10: 113-124

FRANCIS, P.W. & DE SILVA (1989) Application of the Landsat thematic mapper to the identification of potentially active volcanoes in the Central Andes. *Remote Sensing of the Environment* 28: 245-255

FROGGATT, P.C. & LOWE, D.J. (1990) A review of late quaternary silicic and some other tephra formations from New Zealand; their stratigraphy, nomenclature, distribution, volume, and age. *New Zealand Journal of Geology and Geophysics* 33: 89-109

GARDEWEG, M. & RAMIREZ, C.F. (1987) La Pacana caldera and the Atana Ignimbrite – A major ash flow tuff and resurgent caldera complex in the Andes of northern Chile. *Bulletin of Volcanology* 49: 547-566

GILLOT, P.Y., CHIESA, S., PASQUARE, G. & VEZZOLI, L., (1982) <33,000 yr K-Ar dating of the volcano-tectonic horst of the Isle of Ischia, Gulf of Naples. *Nature* 229: 242-244

GIONCADA, A., MAZZUOLI, R., BISSON, M. & PARESCHI, M.T. (2003) Petrology of volcanic products younger than 42 ka on the Lipari-Vulcano complex (Aeolian Islands, Italy): an example of volcanism controlled by tectonics. *Journal of Volcanology and Geothermal Research* 122: 191-220

GIONCADA, A. & SBRANA, A. (1991) 'La Fosse caldera', Vulcano: inferences form deep drillings. *Acta Vulcanol.* 1: 115-126

GLAZNER, A. (1991). Plutonism, oblique subduction and continental growth: an example from the Mesozoic of California. *Geology* 19: 784-786

GOFF, F. (1983) Subsurface structure of the Valles Caldera: a resurgent cauldron in northern New Mexico. *Geological Society of America Abstract Programs* 15: 381

GRAHAM, I.J., COLE, J.W., BRIGGS, R.M., GAMBLE, J.A. & SMITH, I.E.M. (1995) Petrology and petrogenesis of volcanic rocks from the Taupo Volcanic Zone: A review. *Journal of Volcanology and Geothermal Research* 68: 59-87

GRANGE, L.I. (1937) The geology of the Rotorua-Taupo Subdivision. *New Zealand Geological Survey Bulletin* 37. Wellington

GRAVLEY, D. M., WILSON, C.J.N., COLE, J.W. & LEONARD, G.S. (2003). Temporally and tectonically linked eruption and caldera collapse events in the central Taupo Volcanic Zone, New Zealand. Abstract, Geological Society of NZ Annual Conference, Dunedin 1-4 December 2003. *Geological Society of NZ Miscellaneous Publication* 116A: 63

GRINDLEY, G.W. (1959) Sheet N85 – Waiotapu. Geological map of New Zealand, 1:63 360. Wellington. *New Zealand Department of Scientific and Industrial Research*

GRINDLEY, G.W. (1960) Sheet 8 – Taupo. Geological map of New Zealand, 1:250 000. Wellington. *New Zealand Department of Scientific and Industrial Research.*

GRINDLEY, G.W., MUMME, T.C. & KOHN, B.P. (1994) Stratigraphy, paleomagnetism, geochronology and structure of silicic volcanic rocks, Waiotapu/Paeroa Range area, New Zealand. *Geothermics* 23: 473-499

GROCOTT J., BROWN M., DALLMEYER R.D., TAYLOR G.K. & TRELOAR P.J., (1994) Mechanisms of continental growth in extensional arcs: an example from the Andean plate-boundary zone. *Geology* 22: 391-394

GUDMUNDSSON, A. (1988) Formation of collapse calderas. *Geology* 16: 808-810

GUDMUNDSSON, A. (1990) emplacement of dikes, sills and crustal magma chambers at divergent plate boundaries. *Tectonphysics* 176: 257-275

GUDMUNDSSON, A. (1998) Magma chambers modelled as cavities explain the formation of rift zone central volcanoes and their eruption and intrusion statistics. *Journal of Geophysical Research* 103: 7401-7412

GUDMUNDSSON, A. (2002) Emplacement and arrest of sheets and dykes in central volcanoes. *Journal of Volcanology and Geothermal Research* 116: 279-298

GUDMUNDSSON, A., BRYNJOLFSSON, S., & JONNSSON, M.T. (1993) Structural analysis of a transform fault-rift zone junction in North Iceland, *Tectonophysics* 220: 205-221

HACKETT, W.R. & HOUGHTON, B.F., (1989) A facies model for a Quaternary andesitic composite volcano: Ruapehu, New Zealand. *Bulletin of Volcanology* 51: 51-68

HAMMOND, S.R. (1997) Offset caldera and crater collapse on Juan de Fuca ridge-flank volcanoes. *Bulletin of Volcanology* 58: 617-627

HAYWARD, N.J. & EBINGER, C.J. (1996) Variations in the along-axis segmentation of the Afar Rift system. *Tectonics* 15: 244-257

HEALY, J. (1962) Structure and volcanism in the Taupo Volcanic Zone, New Zealand. *In* Crust of the Pacific Basin. *Geophysical Monograph* 6: 151-157

HEALY, J. (1964) Volcanic Mechanisms in the Taupo Volcanic Zone, New Zealand. New Zealand *Journal of Geology and Geophysics* 7: 6-23

HEALY, J. (1992) Central Volcanic Region. In *Landforms of New Zealand.* J.M. SOONS AND M.J. SELBY (eds) 257-286

HEALY, J., SCHOFIELD, J.C. & THOMPSON, B.N. (1964) Sheet 5 Rotorua. Geological Map of New Zealand 1:250,000. *New Zealand Department of Scientific and Industrial Research*

HEGAN, B.D., JOHNSON, J.D. & SEVERNE, C.M. (2001) Landslide risk from the Hipaua geothermal area near Waihi Village at the southern end of Lake Taupo. *From* Hazardous Terrain Conference Proceedings, *New Zealand Geotechnical Society,* August 2001, Christchurch. 439-448

HEIKEN, G., GOFF, F., GARDNER, J.N., BALDRIDGE, W.S., HULEN, J.B., NEILSON, D.L. & VANIMAN, D. (1990) The Valles/Toledo Caldera Complex, Jemez volcanic Field, New Mexico. *Annual Reviews of Earth and Planetary Science* 18: 27-53

HEIKEN, G., GOFF, F., STIX, J., TAMANYU, S., SHAFIQULLAH, M., GARCIA, S. & HAGAN, R. (1986) Intracaldera volcanic activity, Toledo Caldera and Embayment, Jemez Mountains, New Mexico. *Journal of Geophysical Research* 91: 1799-1815

HEISS, J. (2004) The role of crustal processes on high alumina basalt of the Taupo Volcanic Zone. *Unpublished BSc (Hons) thesis, University of Canterbury, New Zealand*

HILDYARD, S.C. (1997) Volcanic geology and geochemistry of the Tikorangi Ignimbrite, Taupo Volcanic Zone, New Zealand. *Unpublished BSc(hons) thesis, University of Canterbury, New Zealand*

HILDYARD, S.C., COLE, J.W. & WEAVER, S.D. (2000) Tikorangi Ignimbrite: a 0.89 Ma mixed andesite-rhyolite ignimbrite, Matahana Basin, Taupo Volcanic Zone, New Zealand. *New Zealand Journal of Geology and Geophysics* 43: 95-107

HILL, D.P. (1976) Structure of Long Valley Caldera, California, from a seismic refraction experiment. *Journal of Geophysical Research* 81: 745-753

HOBDEN, B.J., HOUGHTON, B.F., LANPHERE, M.A & NAIRN, I.A. (1996) Growth of the Tongariro volcanic complex: new evidence from K-Ar age determinations. *New Zealand Journal of Geology and Geophysics* 39: 151-154

HOCHSTEIN, M.P. & HUNT, T.M. (1980) Guide to geophysics of the volcanic and geothermal areas of the North Island, New Zealand. *The Royal Society of New Zealand Miscellaneous Series* 3: 98

HOUGHTON, B.F., LATTER, J.H. & HACKETT, W.R. (1987) Volcanic hazard assessment for Ruapehu composite volcano, Taupo Volcanic Zone, New Zealand. *Bulletin of Volcanology* 49: 737-751

HOUGHTON, B.F., LLOYD, E.F., WILSON, C.J.N. & LANPHERE, M.A. (1991) K-Ar ages from the Western Dome Belt and associated rhyolitic lavas in the Maroa-Taupo area, Taupo Volcanic Zone, New Zealand. New Zealand *Journal of Geology and Geophysics* 34: 99-101

HOUGHTON, B.F., WILSON, C.J.N., MCWILLIAMS, M.O., LANPHERE, M.A., WEAVER, S.D., BRIGGS, R.M. & PRINGLE, M.S. (1995) Chronology and dynamics of a large silicic magmatic system: Central Taupo Volcanic Zone, New Zealand. *Geology* 23: 13-16

HOWELLS, M.F., CAMPBELL, S.D.G., REEDMAN A.J. & TUNNICLIFF, S.P. (1987) A fissure controlled acidic volcanic centre (Ordovician) at Yr Arddu, N Wales. *Geological Journal* 22: 133-149

HOWORTH, R. (1975) New formations of late Pleistocene tephras from the Okataina Volcanic Centre, New Zealand. *New Zealand Journal of Geology and Geophysics* 18: 683-712

HOWORTH, R., FROGGATT, C.G., VUCETICH, C.G. & COLLEN, I.D. (1981) Editorial. *In* Proceedings of Tephra Workshop, June 30 – July 1, 1980, Victoria University Wellington. Publication of the Geology Department, Victoria University Wellington 20: September 1981

HUNT, T.M. (1992) Gravity studies in the Rotorua area, New Zealand. *Geothermics* 21: 65-74

HUTTON, D.H.W. & REAVY, R.J. (1992) Strike slip tectonics and granite petrogenesis. *Tectonics* 11: 960-967

ITOH, Y., TAKEMURA, K. & KAMATA, H. (1998) History of basin formation and tectionic evolution at the termination of a large transcurrent fault system: deformation mode of central Kyushu, Japan. *Tectonophysics* 284: 135-150

JOHN, D.A. (1995) Tilted middle Tertiary ash-flow calderas and subjacent granitic plutons, southern Stillwater Range, Nevada; cross sections of an Oligocene igneous centre. *Geological Society of America Bulletin* 107: 180-200

JURADO-CHICHAY, Z. & WALKER, G.P.L. (2000) Stratigraphy and dispersal of the Mangaone Subgroup pyroclastic deposits, Okataina Volcanic Centre, New Zealand. *Journal of Volcanology and Geothermal Research* 104: 319-283

JURADO-CHICHAY Z, & WALKER, G.P.L. (2001) The intensity and magnitude of the Mangaone subgroup plinian eruptions from Okataina volcanic center, New Zealand, *Journal of Volcanology and Geothermal Research* 111: 219-237

KANE, M.F., MABEY, D.R. & BRACE, R.L. (1976) A gravity and magnetic investigation of the Long Valley Caldera, Mono County, California. *Journal of Geophysical Research* 81: 754-762

KARIG, D.E. (1970a) Ridges and Basins of the Tonga-Kermadec island arc system. *Journal of Geophysical Research* 75: 239-254

KARIG, D.E. (1970b) Kermadec Arc – New Zealand tectonic confluence. New Zealand *Journal of Geology and Geophysics* 13: 21-29

KEALL, J.M. (1988) Volcanology and ignimbrite stratigraphy along the Paeroa Fault, Taupo Volcanic Zone. Unpublished *M.Sc thesis, Victoria University, Wellington , New Zealand*

KENNEDY, B., STIX, J., LAVALLEE, Y. & VALLANCE, J. (1999) Controls on caldera structure and morphology: Results from experimental simulations. EOS *Transactions of the American Geophysical Union* 80: F1121

KILGOUR, G.N. (2002) The nature and dynamics of the Rotorua eruptive episode, Okataina Volcanic Centre, Taupo Volcanic Zone. *Unpublished MSc thesis, University of Waikato, New Zealand*

KOHN, B.P. (1973) Some studies of New Zealand Quaternary pyroclastic rocks. *Unpublished PhD thesis, Victoria University of Wellington, New Zealand*

KOKELAAR, P. (1988) Tectonic controls of Ordovician arc and marginal basin volcanism in Wales. *Journal of the Geological Society, London* 145: 759-775

KOKELAAR, B.P. & BRANNEY, M.J. (1999) 'Inside silicic calderas (Snowdon, Scafell, and Glencoe, UK): Interaction of caldera development, tectonism and hydrovolcanism'. *CEV Field Workshop*, Guidebook. 150

LAHSEN, A. (1982) Upper Cenozoic volcanism and tectonism in the Andes of northern Chile. *Earth Science Reviews* 18: 285-302

LEGROS, F., KELFOUN, K. & MARTI, J. (2000) The influence of conduit geometry on the dynamics of caldera-forming eruptions. *Earth and Planetary Science Letters* 179: 53-61

LEONARD, G.S. (1999) Magmatic processes associated with the c. 650 B.P. Kaharoa eruption, Tarawera Volcanic Complex, New Zealand. *Unpublished BSc (Hons.) thesis, University of Canterbury, Christchurch.*

LEONARD, G.S. (2003) The evolution of the Maroa Volcanic Centre, Taupo Volcanic Zone, New Zealand. *Unpublished PhD thesis. University of Canterbury, New Zealand*

LEONARD, G.S., COLE, J.W., NAIRN, I.A. & SELF, S (2002) Basalt triggering of the c. AD1305 Kaharoa rhyolite eruption, Tarawera Volcanic Complex, New Zealand. *Journal of Volcanology and Geothermal Research* 115: 461-486

LIPMAN, P.W. (1984) The roots of ash-flow calderas n North America: Windows into the tops of granitic batholiths. *Journal of Geophysical Research* 89: 8801-8841

LIPMAN, P.W. (1997) Subsidence of ash-flow calderas: relation to caldera size and magma chamber geometry. *Bulletin of Volcanology* 59: 198-218

LIPMAN, P.W. (2000a) Central San Juan caldera cluster: regional volcanic framework. *In:* Ancient Lake Creede, *Geological Society of America Special Paper* 346: 9-69

LIPMAN, P.W. (2000b) Calderas. *In* Encyclopedia of Volcanoes (H. SIGURDSSON, Ed)

LIPMAN, P.W., DUNGAN, M.A., BROWN, L.L. & DEINO, A. (1996) Recurrent eruption and subsidence at the Platoro caldera complex, southeastern San Juan volcanic field, Colorado: New tales form old tuffs. *Geological Society of America Bulletin* 108: 1039-1055

LOWTHER, K.J. (1997) Quaternary Geology and Tephrostratigraphy of the north-eastern Rotorua region. Unpublished *MSc thesis at the University of Waikato, Hamilton, New Zealand*

LYNCH, H.D. & MORGAN, P., (1987). The tensile strength of the lithosphere and the localization of extension. In: Coward, M.P., Dewey, J.F., Hancock, P.L (Eds.), Continental Extensional Tectonics. *Geological Society Special Publications.* 28: 53-65

LYNCH-BLOSSE, B.R. (1998) Ignimbrite stratigraphy of the southern Mamaku region, North Island, New Zealand. *Unpublished MSc thesis, University of Waikato, New Zealand*

MCCLAY, K.R. & WHITE, M.J. (1995) Analogue modelling of orthogonal and oblique rifting. *Marine and Petroleum Geology* 12: 137-151

MACDONALD, G.A. (1972) Volcanoes. Prentice-Hall, Englewood Cliffs, NJ. 510pp

MALINVERNO, A. & RYAN, W.B.F., (1986) Extension in the Tyrrhenian Sea and shortening in the Apennines as result of arc migration driven by sinking of the lithosphere. *Tectonics* 5: 227-245

MANNING, D.A. (1995) Late Pleistocene Tephrostratigraphy of the eastern Bay of Plenty region, New Zealand. Victoria University.

MANNING, D.A. (1996) Late Pleistocene Tephrostratigraphy of the eastern Bay of Plenty, New Zealand. *Quaternary International* 34-36: 3-12

MANVILLE, V. (2001) Sedimentology and history of Lake Reporoa: an ephemeral supra-ignimbrite lake, Taupo Volcanic Zone, New Zealand. *International Association of Sedimentology Special Publications* 30: 109-140

MANVILLE, V., WHITE, J.D.L., HOUGHTON, B.F. & WILSON, C.J.N. (1999) Paleohydrology and Sedimentology of a post-1.8 ka breakout flood from intracaldera Lake Taupo, North Island, New Zealand *Geological Society of America Bulletin* 111: 1435-1447

MANVILLE, V. & WILSON, C.J.N. (2003) Interactions between volcanism, rifting and subsidence: implications of intracaldera paleoshorelines at Taupo volcano, New Zealand. *Journal of the Geological Society, London,* 160: 3-6

MARRETT R., & ALLMENDINGER R.W. (1990) Kinematic analysis of fault-slip data, *Journal of Structural Geology* 12: 973-986

MARTI, J., ABLAY, G.J., REDSHAW, L.T. & SPARKS., R.S.J. (1994) Experimental studies of collapse calderas. *Journal of the Geological Society of London* 151: 919-929

MARTI, J. & GUDMUNDSSON, A. (2000) The Las Cañadas caldera (Tenerife, Canary Islands): an overlapping collapse caldera generated by magma-chamber migration. *Journal of Volcanology and Geothermal Research* 103: 161-173

MARTI, J., VILA, J. & REY, J. (1996) Deception Island (Bransfield Straight, Antarctica): an example of a volcanic caldera developed by extensional tectonics. *In:* McGuire, W.J., Jones, A.P. and Neuberg, J. (eds) Volcanic Instability on the Earth and Other Planets, *Geological Society Special Publication* 110: 253-265

MARTIN, R.C. (1961) Stratigraphy and structural outline of the Taupo Volcanic Zone. *New Zealand Journal Geology and Geophysics* 4: 449-478

MILNER, D.M. (2001) The structure and eruptive history of the Rotorua Caldera, Taupo Volcanic Zone, New Zealand. *Unpublished PhD thesis, University of Canterbury, New Zealand*

MILNER, D.M., COLE, J.W. & WOOD, C.P. (2002) Asymmetric, multiple-block collapse at Rotorua Caldera, Taupo Volcanic Zone, New Zealand. *Bulletin of Volcanology* 64: 134-149

MILNER, D.M., COLE, J.W. & WOOD, C.P. (2003) Mamaku Ignimbrite: a caldera-forming ignimbrite erupted from a compositionally zoned magma chamber in Taupo Volcanic Zone, New Zealand. *Journal of Volcanoloy and Geothermal Research* 122: 243-264

MODRINIAK, N. & STUDT, F.E. (1959) Geological structure and volcanism of the Taupo-Tarawera district. *New Zealand Journal of Geology and Geophysics* 2: 654-684

MOORE, I. & KOKELAAR, P. (1997) Tectonic influences in piecemeal caldera collapse at Glencoe Volcano, Scotland. *Journal of the Geological Society of London* 154: 765-768

MOORE, I. & KOKELAAR, P. (1998) Tectonically controlled piecemeal caldera collapse: A case study of Glencoe volcano, Scotland. *Geological Society of America Bulletin* 110: 1448-1466

MORLEY, C.K., (1999) Aspects of transfer zone geometry and evolution in East African Rifts. In: Morley, C.K. (Ed), Geoscience of rift Systems – Evolution of East Africa. *American Association of Petroleum Geologists Studies in Geology* 44: 479-492

MOUGINIS-MARK, P.J. & ROWLAND, S.K. (2001) The geomorphology of planetary calderas. *Geomorphology* 37: 201-223

NAIRN, I.A. (1971) Studies of the Earthquake Flat Breccia Formation and other unwelded pyroclastic flow deposits of the Central Volcanic region, New Zealand. Unpublished *MSc thesis, Victoria University of Wellington, New Zealand*

NAIRN, I.A. (1972) Rotoehu Ash and the Rotoiti Breccia Formation, Taupo Volcanic Zone, New Zealand. *New Zealand Journal of Geology and Geophysics* 15: 251-261

NAIRN, I.A. (1981) Some studies of the geology, volcanic history and geothermal resources of the Okataina volcanic centre, Taupo Volcanic Zone, New Zealand, *PhD thesis, Victoria University, Wellington, New Zealand*

NAIRN, I.A. (1989) Sheet V16AC – Mount Tarawera, geological map of New Zealand, 1:50,000. *New Zealand Department of Scientific and Industrial Research*

NAIRN, I.A. (2002) Geology of the Okataina Volcanic Centre. Institute of Geological & Nuclear Sciences geological map (25) & bulletin, 156p. *Institute of Geological & Nuclear Sciences Limited*

NAIRN I.A., & COLE, J.W. (1981) Basalt dikes in the 1886 Tarawera rift. New Zealand, *Journal of Geology and Geophysics* 24: 585-592

NAIRN, I.A., KOBAYASHI, T. & NAKAGAWA, M. (1998) The ~10 ka multiple vent pyroclastic eruption sequence at Tongariro Volcanic Centre, Taupo Volcanic Zone, New Zealand: Part 1. Eruptive processes during regional extension. *Journal of Volcanology and Geothermal Research* 86: 19-44

NAIRN, I.A. & KOHN, B.P. (1973) Relation of the Earthquake Flat Breccia to the Rotoiti Breccia, Central North Island, New Zealand. New Zealand *Journal of Geology and Geophysics* 16: 269-279

NAIRN, I.A., SHANE, P.R., COLE, J.W., LEONARD, G.J., SELF, S. & PEARSON, N. (2004) Rhyolite magma processes of the ~AD 1315 Kaharoa eruption episode, Tarawera volcano, New Zealand. *Journal of Volcanology and Geothermal Research* 131: 265-294

NAIRN, I.A. & WOOD, C.P. (1987) Active Volcanoes and Geothermal Systems, Taupo Volcanic Zone. *In:* Active volcanoes and geothermal systems, Taupo Volcanic Zone. *New Zealand Geological Survey Record* 22: 5-84

NAIRN, I.A, WOOD, C.P & BAILEY, R.A. (1994) The Reporoa Caldera, Taupo Volcanic Zone: source of the Kaingaroa Ignimbrites. *Bulletin of Volcanology* 56: 529-537

NAKAMURA, K., (1977) Volcanoes as possible indicators of tectonic stress orientation; principle and proposal. *Journal of Volcanology and Geothermal Research* 2: 1-16

NEWHALL, C.G. & DZURISIN, D. (1988) Historical unrest at large calderas of the world. *US Geological Survey Bulletin* 1855

NICOL, A. & BEAVAN, J. (2003) Shortening of an overriding plate and its implications for slip on a subduction thrust, central Hikurangi Margin, New Zealand. *Tectonics* 22 (6) 1070, doi:10.1029/2003TC001521

NIELSON, D.L. & HULEN, J.B. (1984) Internal geology and evolution of the Redondo Dome, Valles Caldera, New Mexico. *Journal of Geophysical Research* 89: 8695-8713

NOVAK, I.D. & SOULAKELLIS, N. (2000) Idenitifying geomorphic features using LANDSAT-5/TM data processing techniques on Lesvos, Greece. *Geomorphology* 34: 101-109

OLIVER, P.J. (1978) Seismotectonic, structural, volcanological, and geomorphic study of New Zealand. *In:* Landsat II over New Zealand, Monitoring our Resources from Space, edited by P.J. ELLIS ET AL., *Department of Scientific and Industrial Research Bulletin* 221: 298

ORSI, G., DE VITA, S. & DI VITO, M. (1996) The restless, resurgent Campi Flegrei nested caldera (Italy): constraints on its evolution and configuration. *Journal of Volcanology and Geothermal Research* 74: 179-214

ORSI, G., GALLO, G. & ZANCHI, A. (1991) Simple-shearing block resurgence in caldera depressions: A model from Pantelleria and Ischia. *Journal of Volcanology and Geothermal Research* 47: 1-11

PAIN, C.F. & PULLAR, W.A. (1975) Chronology of 'paleo surfaces' and present land surfaces in the Reporoa Basin, North Island, New Zealand. *New Zealand Journal of Science* 18: 313-322

PAKISER, L.C. (1961) Gravity, volcanism, and crustal deformation in Long Valley, California. *United States Geological Survey Professional Paper* 424B: 250-253

PATERSON S.R. & TOBSICH O.T., (1992) Rates of processes in magmatic arcs: implications for the timing and nature of pluton emplacement and wall rock deformation. *Journal of Structural geology* 14: 291-300

PETFORD, N., CRUDEN, A.R., MCCAFFREY, K.J.W. & VIGNERESSE, J.L., (2000) Granite magma formation, transport and emplacement in the Earth's crust. *Nature* 408, 669-673

PULLAR, W.A., BIRRELL, K.S. & HEINE, J.C. (1973) Named tephras and tephras formations occurring in the central North Island, with notes on derived soils and buried paleosols. *New Zealand Journal of Geology and Geophysics* 16: 497-518

PULLAR, W.A. & NAIRN, I.A. (1972) Matahi Basaltic Tephra Member, Rotoiti Breccia Formation. *New Zealand Journal of Geology and Geophysics* 15: 446-450

RAIT, G., CHANIER, F., WATERS, D.W. (1991) Landward- and seaward-directed thrusting accompanying the onset of subduction beneath New Zealand. *Geology* 19: 230-233

RILLER, U., PETRINOVIC, I., RAMELOW, J., STRECKER, M. & ONCKEN, O. (2001) Late Cenozoic tectonicsm, collapse caldera and plateau formation in the central Andes. *Earth and Planetary Science Letters* 188: 299-311

RISK, G.F., BIBBY, H.M. & CALDWELL, T.G. (1999) Resistivity structure of the central volcanic zone, New Zealand. *Journal of Volcanology and Geothermal Research* 90: 163-181

RITCHIE, A.B.H. (1996) Volcanic geology and geochemistry of the Waiotapu Ignimbirte, Taupo Volcanic Zone, New Zealand. *Unpublished MSc thesis, University of Canterbury, New Zealand*

ROCHE, O. & DRUITT, T.H. (2001) Onset of caldera collapse during ignimbrite eruptions. *Earth and Planetary Science Letters* 191: 191-202

ROCHE, O., DRUITT, T.H. & MERLE, O. (2000) Experimental study of caldera formation. *Journal of Geophysical Research* 105: 395-416

ROGAN, M. (1980) Geophysical studies of the Okataina Volcanic Centre. *Unpublished PhD thesis, University of Auckland, New Zealand*

ROGAN, M. (1982) A geophysical study of the Taupo Volcanic Zone, New Zealand. *Journal of Geophysical Research* 87: 4073-4088

ROSENDAHL, B.L. (1987) Architecture of continental rifts with special reference to east Africa. *Annual reviews of Earth and Planetary Science* 15: 445-503

ROSENDAHL, B.R., REYNOLDS, D., LORBER, P., BURGESS, C., MCGILL, J., SCOTT, D., LAMBAISE, J. & DERKSEN, S. (1986) Structural expressions of rifting: lessons from Lake Tanganyika. *In*: Frostick, L.E. *ed* Sedimentation in the East African Rifts. *Geological Society of London Special Publication* 25: 29-43

ROSI, M., SBRANA, A. & PRINCIPE, C. (1983) The Phlegraean Fields: structural evolution, volcanic history and eruptive mechanisms. *Journal of Volcanology and Geothermal Research* 17: 273-288

ROWLAND J.V. & SIBSON, R.H. (2001) Extensional fault kinematics within the Taupo Volcanic Zone, New Zealand: soft linked segmentation of a continental rift system, *New Zealand Journal of Geology and Geophysics* 44: 271-283

SATO H., (1994) The relationship between late Cenozoic tectonic events and stress field and basin development in northeast Japan. *Journal of Geophysical Research* 99: 22261-22274

SAWYER, D.A., FLECK, R.J., LANPHERE, M.A., WARREN, R.G., BROXTON, D.E. & HUDSON, M.R. (1994) Episodic caldera volcanism in the Miocene southwestern Nevada volcanic field: Revised stratigraphic framework, 40Ar/39Ar geochronology, and the implications for magmatism and extension. *Geological Society of America Bulletin* 106: 1304-1318

SCHMITZ, M.D. (1995) Geochemical studies of the Rotoiti Pyroclastic eruption, Okataina Volcanic Centre, Taupo Volcanic Zone, North Island, New Zealand. *Unpublished MSc thesis, University of Auckland, New Zealand*

SELF, S. (1983) Large scale silicic phreatomagmatic volcanism: a case study from New Zealand. *Journal of Volcanology and Geothermal Research* 17: 433-469

SELF, S., GOFF, F., GARDNER, J.N., WRIGHT, J.V. & KITE, W.M. (1986) Explosive rhyolitic volcanism in the Jemez mountains: vent locations, caldera development and relation to regional structure. *Journal of Geophysical Research* 91: 1779-1798

SHANE, P., BLACK, T. & WESTGATE, J. (1994) Isothermal plateau fission track age for the paleomagnetic excursion in the Mamaku Ignimbrite, New Zealand, and implications for late Quaternary stratigraphy. *Geophysical Research Letters* 21: 1695-1698

SHANE, P., NAIRN, I.A. & SMITH, V. (2005) Magma mingling in the ~50 ka Rotoiti eruption from Okataina Volcanic Centre: implications for geochemical diversity and chronology of large volume rhyolites. *Journal of Volcanology and Geothermal Research* 139: 295-313

SHERBURN, S., BANNISTER, S. & BIBBY, H. (2003) Seismic velocity structure of the central Taupo Volcanic Zone, New Zealand, from local earthquake tomography. *Journal of Volcanology and Geothermal Research* 122: 69-88

SISSONS, B.A. (1979) The horizontal kinematics of the North Island of New Zealand. *Unpublished PhD thesis, Victoria University of Wellington, New Zealand.*

SKINNER, D.N.B. (1986) Neogene volcanism of the Hauraki Volcanic region. In: Smith, I.E.M. (editor) Late Cenozoic volcanism in New Zealand. *Royal Society of New Zealand Bulletin* 23: 21-47

SMITH E.G.C. & T.H. WEBB, (1986) The seismicity and related deformation of the Central Volcanic Region, North Island, New Zealand, *Royal Society of New Zealand Bulletin* 23: 112-133

SMITH, R.C.M, SMITH, I.E.M., BROWNE, P.R.L. & HOCHSTEIN, M.P. (1993) Volcano-tectonic controls on sedimentation in the Taupo Volcanic Zone, New Zealand. *In* South Pacific Sedimentary Basins. *Sedimentary Basins of the World 2* (Ed. BALANCE, P.F.; series Ed. HSU, K.J.) 143-156

SMITH, R.L. & BAILEY, R.A. (1968) Resurgent cauldrons. *In*: COATS, R.R., HAY, R.L. AND ANDERSON, C.A. (eds) Studies in Volcanology. *Geological Society of America Memoir* 1116: 613-662

SMITH, R.T. & HOUGHTON, B.F. (1995) Vent migration and changing eruptive style during the 1800 ka Taupo eruption: new evidence from the Hatepe and Rotongaio phreatoplinian ashes. *Bulletin of Volcanology* 57: 432-439

SMITH, V.C. (2001) The stratigraphy and geochemistry of the Mangaone subgroup tephra beds, Okataina volcanic centre, New Zealand. *MSc thesis, Auckland University of Auckland, New Zealand*

SMITH, V.C., SHANE, P. & NAIRN, I.A. (2004a) Geochemical and mineralogical evolution of Okataina Volcanic Centre during the last 45 kyr, Taupo Volcanic Centre, New Zealand. In: IAVCEI General Assembly, Pucon. Conference Abstracts

SMITH, V.C., SHANE, P. & NAIRN, I.A. (2004b) Reactivation of a rhyolitic magma body by new rhyolitic intrusion before the 15.8 ka Rotorua eruptive episode: implications for magma storage in the Okataina Volcanic Centre, New Zealand. *Journal of the Geological Society, London* 161: 1-16

SMITH, V.C., SHANE, P. & NAIRN, I.A. (2004c) The contemporaneously active Okataina and Taupo rhyolitic volcanic centres: trend sin geochemistry, mineralogy, and magmatic properties during the last 50 kyr, Taupo Volcanic Zone, New Zealand. *In*: Manville, V. & Tilyard, D. (eds.) Programme and abstracts, *Geological Society of New Zealand Miscellaneous Publications* 117a: 98

SMITH, V.C., SHANE, P. & SMITH, I.E.M (2002) Tephrostratigraphy and geochemical fingerprinting of the Mangaone Subgroup tephra beds, Okataina Volcanic Centre, New Zealand. *New Zealand Journal of Geology and Geophysics* 45: 207-219

SOENGKONO, S. (1999) Te Kopia geothermal system (New Zealand): the relationship between its structure and extent. *Geothermics* 28: 767-784

SOENGKONO, S. (2000) Assessment of faults and fractures at the Mokai Geothermal Field, Taupo Volcanic Zone, New Zealand. *Proceedings World Geothermal Congress* 1771-1776

SOENGKONO, S. & HOCHSTEIN, M.P. (1996) Interpretation of magnetic anomalies over the Reporoa geothermal field, Taupo Volcanic Zone, New Zealand. *Proceedings 18th N.Z. Geothermal workshop*: 243-248

SOENGKONO, S., HOCHSTEIN, M.P., SMITH, I.E.M. & ITAYA, T. (1992) Geophysical evidence for widespread reversely magnetised pyroclastics in the western Taupo Volcanic Zone (New Zealand). New Zealand Journal of Geology and Geophysics 35: 47-55

SPARKS, R.S.J., FRANCIS, P.W., HAMER, R.D., PANKHURST, R.J., O'CALLAGHAN, L.O., THORPE, R.S. & PAGE, R. (1985) Ignimbrites of the Cerro Galan Caldera, NW Argentina. *Journal of Volcanology and Geothermal Research* 24: 205-248

SPARKS, R.S.J., SIGURDSSON, H. & WILSON, L. (1977) Magma mixing: a mechanism for triggering acid explosive eruptions. *Nature* 267: 315-318

SPEED, J.A. (2001) The 11.9 ka Waihau eruptive episode, Okataina Volcanic Centre. *Unpublished MSc thesis, University of Auckland, New Zealand*

SPEED, J., SHANE, P. & NAIRN, I. (2002) Volcanic stratigraphy and phase chemistry of the 11,900 yr BP Waihau eruptive episode, Tarawera Volcanic Complex, New Zealand. *New Zealand Journal of Geology and Geophysics* 45: 395-410

SPINKS, K.D. (1998) The Rahopaka Ignimbrite and associated volcaniclastics. *Unpublished BSc(hons) thesis. University of Canterbury, New Zealand.*

SPINKS, K.D. (2001) Block and ash flows of the Waiohau eruptive Episode, Tarawera Volcanic Centre. *Unpublished report prepared for Geological Investigations Ltd*

SPINKS, K.D., ACOCELLA, V.A., COLE, J.W. & BASSETT, K.N. (*in press*) Structural control of volcanism and caldera development in the transtensional Taupo Volcanic Zone, New Zealand. *Journal of Volcanology and Geothermal Research special volume: Tectonics and physics of volcanoes*

SPINKS, K.D., COLE, J.W. & LEONARD, G.S. (2004) Caldera Volcanism in the Taupo Volcanic Zone *In*: MANVILLE, V. (ed.) Field Trip Guides, *Geological Society of New Zealand Miscellaneous Publication* 117B: 111-135

SPINKS, K.D. & ESLER, W. (*in prep*) A 33 ka caldera-forming ignimbrite eruption: a revised distribution and stratigraphy for the Kawerau Ignimbrite, Okataina caldera complex

STAGPOOLE, V.M. (1994) Interpretation of refraction seismic and gravity data across the eastern margin of the Taupo Volcanic Zone, New Zealand. *Geothermics* 23: 501-510

STAGPOOLE, V. M. & BIBBY, H. M. (1999). Residual gravity anomaly map of the Taupo Volcanic Zone, New Zealand, 1:250 000, version 1.0. Institute of Geological & Nuclear Sciences Geophysical Map 13. *Institute of Geological & Nuclear Sciences Limited, Lower Hutt, New Zealand.*

STERN, T.A. & DAVEY, F.J. (1987) A seismic investigation of the crustal and upper mantle structure within the central volcanic region of New Zealand. New Zealand *Journal of Geology and Geophysics* 30: 217-231

STEVENS, N. (2002) Emplacement of the large andesite lava flow in the Oturere Stream valley, Tongariro Volcano, from airborne interferometric radar. *New Zealand Journal of Geology and Geophysics* 45: 387-394

SUTTON, A.N., BLAKE, S., & WILSON, C.J.N. (1995) An outline geochemistry of rhyolite eruptives from Taupo volcanic centre, New Zealand. *Journal of Volcanology and Geothermal Research* 68: 153-175

SUTTON, A. N., BLAKE, S., WILSON, C.J.N. & CHARLIER, B.L.A. (2000). Late Quaternary evolution of a hyperactive rhyolite magmatic system: Taupo volcanic centre, New Zealand. *Journal of the Geological Society, London* 157: 537-552

TAYLOR B., CROOK, K. & SINTON, J. (1994) Extensional transform zones and oblique spreading centers, *Journal of Geophysical Research* 99: 19707 19718

THOMPSON, B.N. (1974) Geology of the Rotorua Geothermal District. *In* Geothermal resources Survey, Rotorua Geothermal District. *New Zealand Department of Scientific and Industrial Research* 10-36

THOURET, J.C. (1999) Volcanic Geomorphology – an overview. *Earth-Science Reviews* 47: 95-131

TIBALDI, A., (1992) The role of transcurrent intra-arc tectonics in the configuration of a volcanic arc. *Terra Nova* 4: 567-577

TIKOFF, B. & DE SAINT BLANQUAT, M., (1997) Transpressional shearing and strike-slip partitioning in the Late Cretaceous Sierra Nevada magmatic arc, California. *Tectonics* 16: 442-459

TROLL, V.R., WALTER, T.R. & SCHMINCKE, H.U. (2002) Cyclic caldera collapse: Piston or piecemeal subsidence? Field and experimental evidence. *Geology* 30: 135-138

UPTON, P., KOONS, P.O. & EBERHART-PHILLIPS, D. (2003) Extension and partitioning in an oblique subduction zone, New Zealand: Constraints from three-dimensional numerical modelling, *Tectonics* 22: 1068 doi:10.1029/2002TC001431

VENTURA, G. (1994) Tectonics, structural evolution and caldera formation on Vulcano Island (Aeolian Archipelago, southern Tyrrhenian Sea). *Journal of Volcanology and Geothermal Research* 60: 207-224

VIGNERESSE, J.L., TIKOFF, B. & AMEGLIO, L. (1999) Modification of the regional stress field by magma intrusion and formation of tabular granitic plutons. *Tectonophysics* 302: 203-224

VILLAMOR, P., & BERRYMAN, K., (2001) A late Quaternary extension rate in the Taupo Volcanic Zone, New Zealand, derived from fault slip data. *New Zealand Journal of Geology and Geophysics* 44: 243-269

VUCETICH, C.G. & PULLAR, W.A. (1964) Stratigraphy of Holocene ash in the Rotorua and Gisbourne districts. *In* Stratigraphy and chronology of late Quaternary volcanic ash in Taupo, Rotorua, and Gisbourne districts. *New Zealand Geological Survey bulletin* 73: 43-88

VUCETICH, C.G. & PULLAR, W.A. (1969) Stratigraphy and chronology of Late Pleistocene volcanic ash beds in central North Island, New Zealand. *New Zealand Journal of Geology and Geophysics* 12: 784-837

WALCOTT, R.I. (1978) Geodetic strains and large earthquakes in the axial tectonic belt of North Island, New Zealand. *Journal of Geophysical Research A, Space Physics* 83: 4419-4429

WALCOTT R.I., (1984) The kinematics of the plate boundary zone through New Zealand: a comparison of short and long-term deformation. *Geophysical Journal of the Royal Astronomical Society* 79: 613-633

WALKER, G.P.L. (1984) Downsag calderas, ring faults, caldera sizes, and incremental caldera growth. *Journal of Geophysical Research* 89B: 8407-8416

WALTER, T.R. & TROLL, V.R. (2001) Formation of caldera periphery faults: An experimental study. *Bulletin of Volcanology* 63: 191-203

WEAVER, S.D., GIBSON, I.L., HOUGHTON, B.F. & WILSON, C.J.N. (1990) Mobility of rare earth and other elements during crystallisation of peralkaline silicic lavas. *Journal of Volcanology and geothermal Research* 43: 57-70

WEBB T.H., & H. ANDERSON, (1998) Focal mechanisms of large earthquakes in the North Island of New Zealand: slip partitioning at an oblique active margin, *Geophysics Journal International* 134: 40-86

WILLIAMS, H. (1941) Calderas and their origin. University of California publications. *Bulletin of the Department of Geological Sciences* 25: 239-346

WILLIAMS, H. & MCBIRNEY, A.R. (1979) 'Volcanology'. Freeman, Cooper and Co., San Francisco (publ.) 397

WILSON, C.J.N. (1991) Ignimbrite morphology and the effects of erosion: a New Zealand case study. *Bulletin of Volcanology*, 53: 635-644

WILSON, C.J.N. (1993). Stratigraphy, chronology, styles and dynamics of late Quaternary eruptions from Taupo volcano, New Zealand. *Philosophical Transactions of the Royal Society of London* A: 205-306

WILSON, C.J.N., (1996) Taupo's atypical arc. *Nature* 379: 27-28

WILSON, C.J.N., HOUGHTON, B.F., LANPHERE, M.A. & WEAVER, S.D. (1992) A new radiometric age estimate for the Rotoehu Ash from Mayor Island volcano, New Zealand. New Zealand *Journal of Geology and Geophysics* 35: 371-374

WILSON, C.J.N, HOUGHTON, B.F. & LLOYD, E.F. (1986) Volcanic history and evolution of the Maroa – Taupo area, Central North Island. In: I.E.M Smith (Editor), Late Cenozoic volcanism in New Zealand. *Royal Society of New Zealand Bulletin* 23: 194-223

WILSON, C.J.N, HOUGHTON, B.F., MCWILLIAMS, M.O., LANPHERE, M.A., WEAVER, S.D. & BRIGGS, R.M. (1995) Volcanic and structural evolution of Taupo Volcanic Zone: a review. *Journal of Volcanology and Geothermal Research* 68: 1-28

WILSON, C.J.N., ROGAN, A.M., SMITH, I.E.M., NORTHEY, D.J., NAIRN, I.A. & HOUGHTON, B.F. (1984) Caldera Volcanoes of the Taupo Volcanic Zone, New Zealand. *Journal of Geophysical Research* 89: 8463-8484

WILSON, C.J.N., SWITSUR, V.R. & WARD, A.P., (1998) A new ^{14}C age for the Oruanui (Wairakei) eruption, New Zealand. *Geology Magazine* 125: 287-300

WILSON, C.J.N, & WALKER, G.P.L. (1985). The Taupo eruption, New Zealand. *Philosophical Transactions of the Royal Society of London* Series A 314: 199-228

WISE, D. (1982) Linesmanship and the practise of Linear Geo-art. *Geological Society of America Bulletin* 93: 886-888

WOOD, C.P. (1992). Geology of the Rotorua Geothermal System. *Geothermics* 21: 25-41

WOOD, C.P. (1994) Aspects of the geology of the Waimangu, Waiotapu, Waikite and Reporoa geothermal areas, Taupo Volcanic Zone, New Zealand. *Geothermics* 23: 401-421

WRIGHT, I.C., (1992) Shallow structure and active tectonism of an offshore continental back-arc spreading system: the Taupo Volcanic Zone. *New Zealand Journal of Marine Geology* 103: 287-309

WRIGHT, I.C. (1996) Volcaniclastic processes on modern submarine arc volcanoes: sidescan and photographic evidence from the Rumble IV and V volcanoes, Southern Kermadec Arc (SW Pacific). *Marine Geology* 136: 21-39

WRIGHT, I.C. (1997) Morphology and evolution of the remnant Colville and active Kermadec arc ridges south of 33°30'S. *Marine Geophysical Research* 19: 177-193

WRIGHT, I.C., GAMBLE, J.A. & SHANE, P.A.R. (2003) Submarine silicic volcanism of the Healy caldera, southern Kermadec arc (SW Pacific): 1 – volcanology and eruption mechanisms. *Bulletin of Volcanology* 65: 15-29

WRIGHT, I.C., PARSON, L.M. & GAMBLE, J.A. (1996) evolution and interaction of migrating cross-arc volcanism and backarc rifting: an example from the southern Havre Trough (35°20'-37°S). *Journal of Geophysical Research* 101: 22071-22086

Acknowledgements

During the last six years a huge number of people have provided scientific, financial, motivational and emotional support, and without their support this project would certainly never have been successful nor would likely have approached completion. These last pages give me an opportunity then to acknowledge all those people and organisations that have supported me throughout this research.

My supervisor Professor Jim Cole has been an outstanding role model, teacher, coach and friend over the last ten years, and it is his eternal encouragement and support that has got me through my university career. He instilled in me a terrific desire to achieve academic success, inspiring me to look outside the square and question long-held assumptions. Many times he coaxed me from the murky depths of research and personal despondency, bolstering my confidence and getting me back on track with wise words and friendly advice. Jim always encouraged me to hone my teaching skills throughout my postgraduate career and it was a great privilege to be entrusted with his teaching when he was away on academic leave. Many thanks also to Christine Cole – for many great dinners, for her genuine concern for my well-being, and for keeping Jim off my back (if only briefly).

Valerio Acocella has been a huge academic influence and good friend over the last six years, as an enthusiastic tour guide in Italy, a field partner in TVZ, a challenging but intensely-motivating co-author and a prolific scientist who inspired me to be confident and proud of my work.

The staff of the Department of Geological Sciences have been great teachers and colleagues, and several deserve specific mention. Jarg Pettinga was a great source of encouragement and advice, especially with DEM imagery and structural analysis, and instilled in me the importance of good graphics. Kari Bassett is thanked for her support and genuine interest in the subject, getting me back on track when needed, and being a sounding board for my many unconstrained ideas. Steve Weaver, again for continued encouragement, for advice on geochemical matters and crustal process issues, and for his general TVZ knowledge and expertise. The technical staff in the department were critical to the progress of my research, and were terrific sources of support – Cathy Knight, Rob Spiers, Arthur Nicholas, Kerry Swanson, John Southward, Joyce Seale, and Jane Guise – thank you. John Southward in particular was a savior on the frequent occasions that my computer would resist efforts to power up or would endeavour to corrupt several years of data. Thanks to all others who stopped by the office to see how I was getting on, especially those I often shared late nights in the department with - Dave Bell, David Nobes and Richard Holdaway. Dave Bell was a great help during my time teaching at CPIT, and was always willing to debate the proficiency of the NZ cricket side. Anekant Wandres was a great PhD colleague, friend and squash competitor, with an inspiring attitude to life and work. Many thanks also go to Alison Johnston, our enthusiastic librarian, for finding obscure journal articles, taking my pleas for certain books seriously, and actually getting them in our library.

Many thanks must also go to the numerous visitors to the department that were interested in my research and gave me valuable feedback – particularly Basil Tikoff who showed great interest and gave superb advice during a brief visit. Andy Nicol provided terrific advice on all matters structural and was encouraging in the field and as a co-author on the Tectonics paper.

Ian Nairn – the oracle of Okataina, a great and continual source of advice, support, encouragement, and help in the field.

Will Esler – for being a terrific friend and motivator during my time in TVZ, for providing somewhere to pour over maps and discuss ignimbrites for hour after hour, for his genuine interest in my research, and his general scientific acumen which rejuvenated a somewhat weary research student when things got tough.

Many people at IGNS – particularly Colin Wilson, Bruce Houghton, and Peter Wood – for help with access to GNS files, for advice, constructive criticism, and above all their shared desire and emanating enthusiasm to understand the complexities of TVZ.

Environment BOP kindly granted me access to their aerial photo collections; Fletcher Forests gave uninhibited access to their forests, aerial photos and digital topographic data; DOC let me stay for free at their Tarawera lake-side campsite.

I should also like to thank the University of Canterbury for my PhD scholarship, and the Mason Trust for field expenses and funding my attendance at the IUGG 'Inside Calderas' trip through the UK in July 1999. The Royal Society awarded me a student travel grant to attend the IAVCEI Chile meeting in November 2004, and the Geological Society of New Zealand funded travel to various annual GSNZ conferences.

Thanks to the many other PhD researchers who set the pace in TVZ research: Steve Beresford who originally inspired me to get into research; Vicki Smith for helping out in the field and with geochemical data, and for being an understanding friend; Darren Gravley and Graham Leonard for sharing a house during summer field work in TVZ, and especially Darren for genuine interest in my research and being a terrific colleague and friend since we started this PhD debacle that infamous summer of '99.

I was exceedingly fortunate to share an office with two great friends whom with I shared the best and worst of the PhD game: Dave Milner during the early days of my project, and later with Tim McConnico. Dave was a great scientific advisor, co-author, and flat-mate, and really set the standard. Tim has been a fantastic mate, office-mate, and advisor on all things, who put up with my continual ranting on TVZ, always took up my offer to escape the office to hit golf balls or visit the girls at the local French bakery, and was absolutely vital to my continued sanity in the department.

Thanks also to the many other good mates within and outside the department who suffered my absence and presence, always knew when I needed a beer and have waited forever for me to finish and– it's certainly my shout.

Most importantly, thanks to Dad, Mum, and my sister Andrea – for continued and unrelenting financial, emotional, and motivational support, and for eventually understanding that I didn't know when I would finish. You know now.

....and finally in the words of another Canterbury graduate – Groundhog Day IS finally over!

Rift Architecture and Caldera Volcanism in the Taupo Volcanic Zone, New Zealand

A thesis submitted in fulfilment of
the requirements for the degree of

Doctor of Philosophy in Geology

at the
University of Canterbury
By

Karl D. Spinks

2. Figures

University of Canterbury
2005

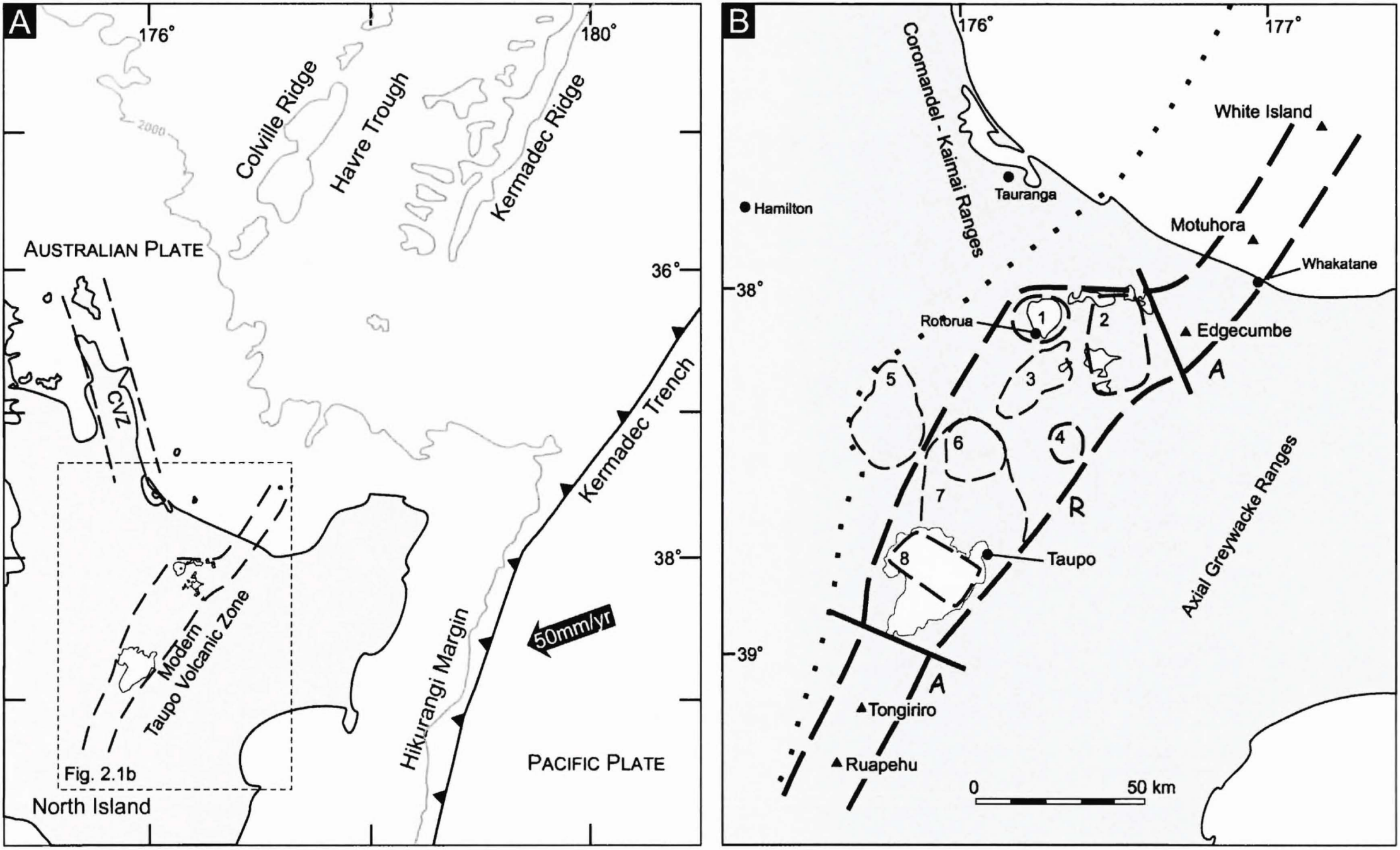

FIGURE 2.1 (A) Setting of TVZ in the North Island of New Zealand, with respect to the Kermadec Trench and Ridge, and to Havre Trough (outlined by the 2000 m isobath). The boundary of modern TVZ (<300 ka) is shown by dashed lines. Modified from DAVEY *et al* (1995); (B) Map of TVZ showing calderas and compositional segmentation into A = Andesite and R = Rhyolite segments. Calderas: 1) Rotorua; 2) Okataina; 3) Kapenga; 4) Reporoa; 5) Mangakino; 6) Maroa; 7) Whakamaru; 8) Taupo.

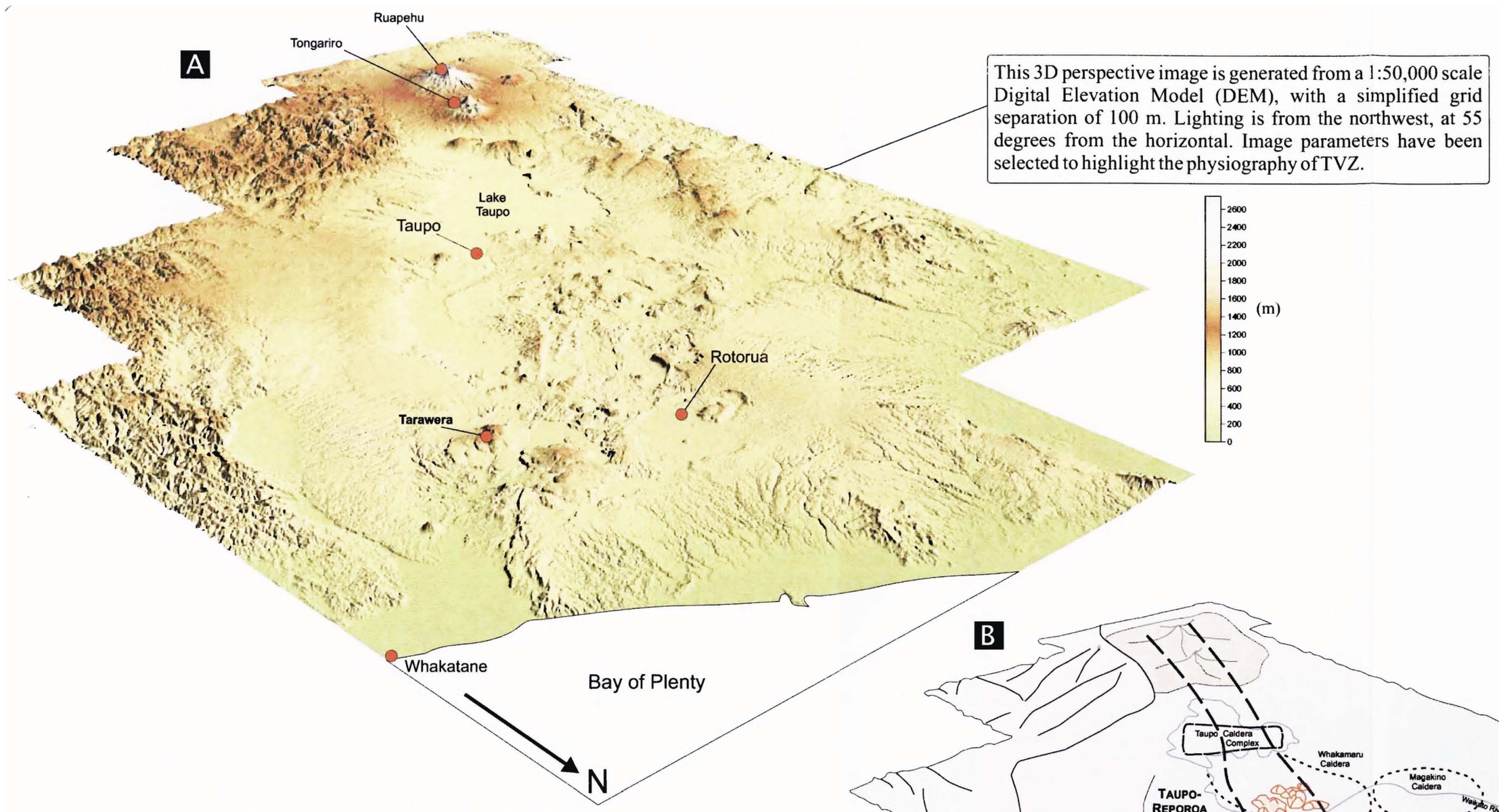

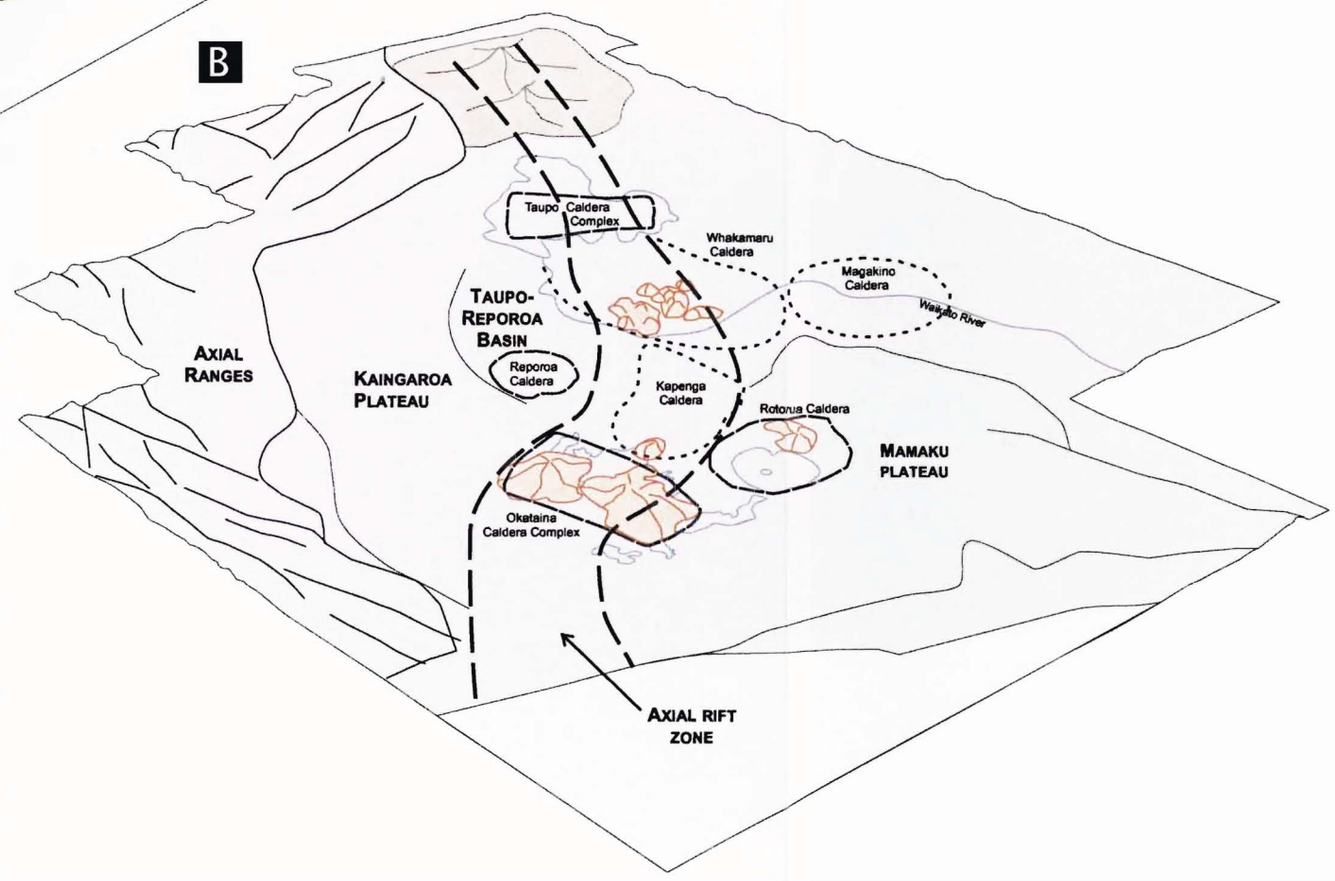

FIGURE 2.2 General Physiography of Taupo Volcanic Zone. (A) 3D perspective image of onshore TVZ looking down the axis of TVZ from the Bay of Plenty toward Ruapehu in the south. (B) Schematic Sketch based on (A) showing the main structural features of TVZ, in particular the large ignimbrite plateaus on each flank of TVZ, the Taupo-Reporoa Basin, and the axial rift zone extending the length of TVZ. A significant feature is the major bend in the axial rift zone at Okataina Caldera Complex. The locations of calderas in TVZ are outlined; the margins of modern TVZ calderas (refer text) are shown with a heavier dashed line compared to other TVZ calderas according to their clear surface expression; the location of older calderas is much less certain (see chapter 5). Modern TVZ caldera are notably located both within, and to either side of, the axial rift zone. Major dome complexes and the volcanic massifs of Ruapehu and Tongariro are also highlighted (red and brown respectively), as are lakes (blue).

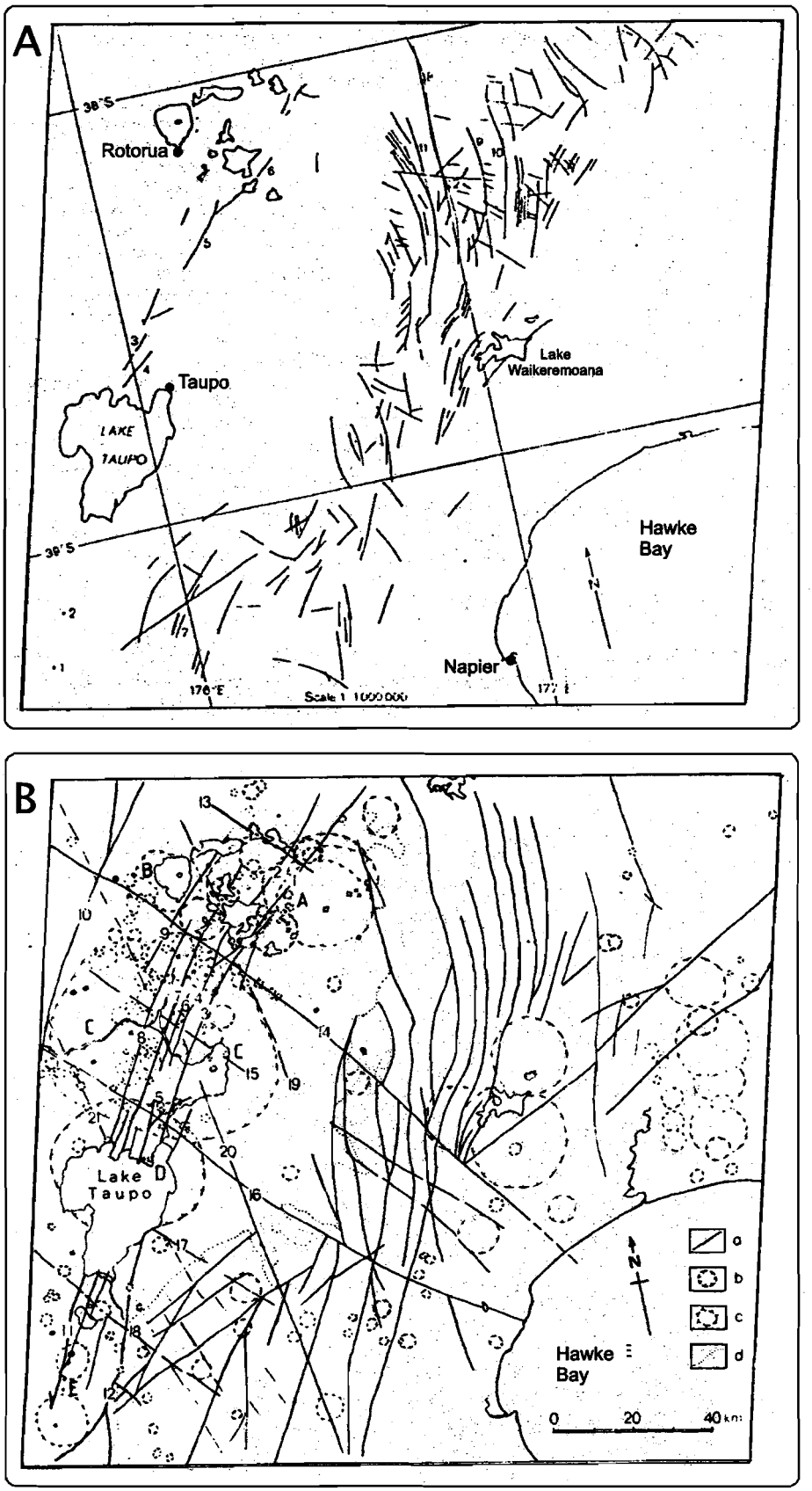

FIGURE 2.3: Early analyses of TVZ structure using Satellite imagery. (A) Lineament map from OLIVER (1978); (B) Satellite interpretation from COCHRANE & WAN TIANFENG (1983); a: lineament or fault; b: ring structure, crater or caldera; c: volcanic cone or dome; d: boundary of volcanic rock.

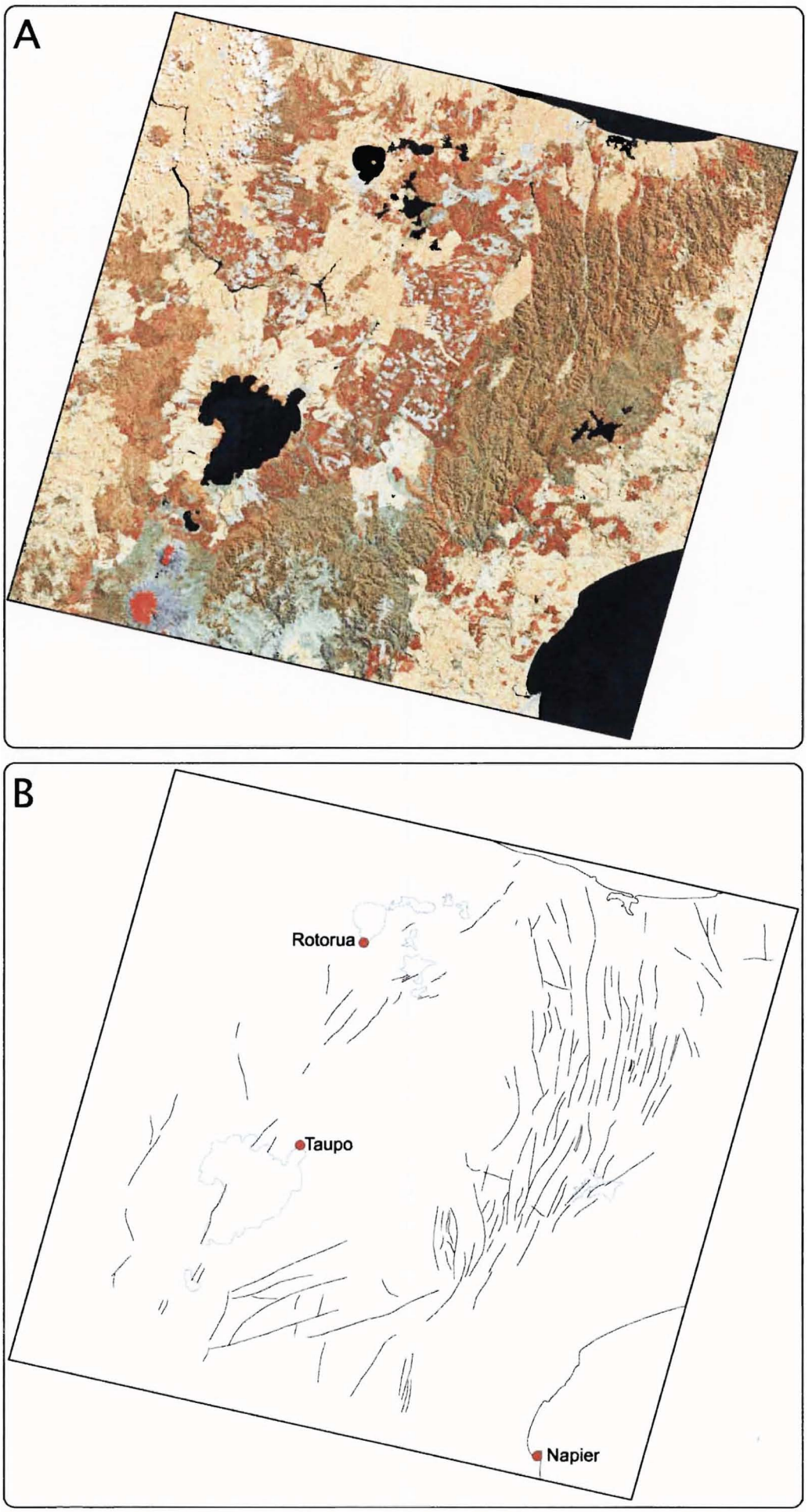

FIGURE 2.4: (A) LANDSAT image (ETM3, path 72, row 86/87, 29 Sept 1999) of central North Island, New Zealand, bands 4, 5, and 7 (RGB respectively). (B) Lineament analysis of image in (A). Lakes are outlined in blue.

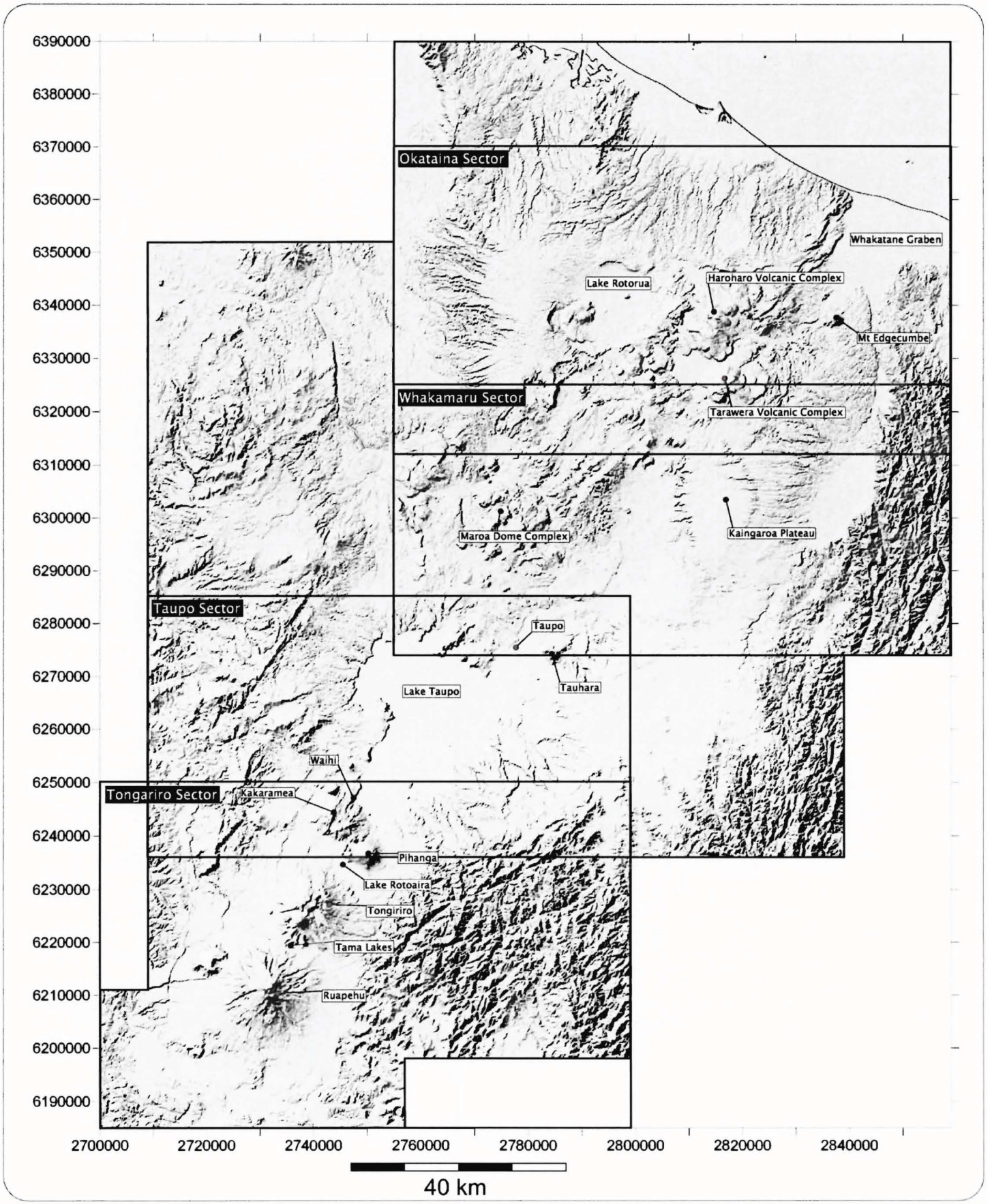

FIGURE 2.5: Shaded Relief Image of Taupo Volcanic Zone and outline of the 4 sectors used for physiographic analysis of TVZ. Main towns and features are located.

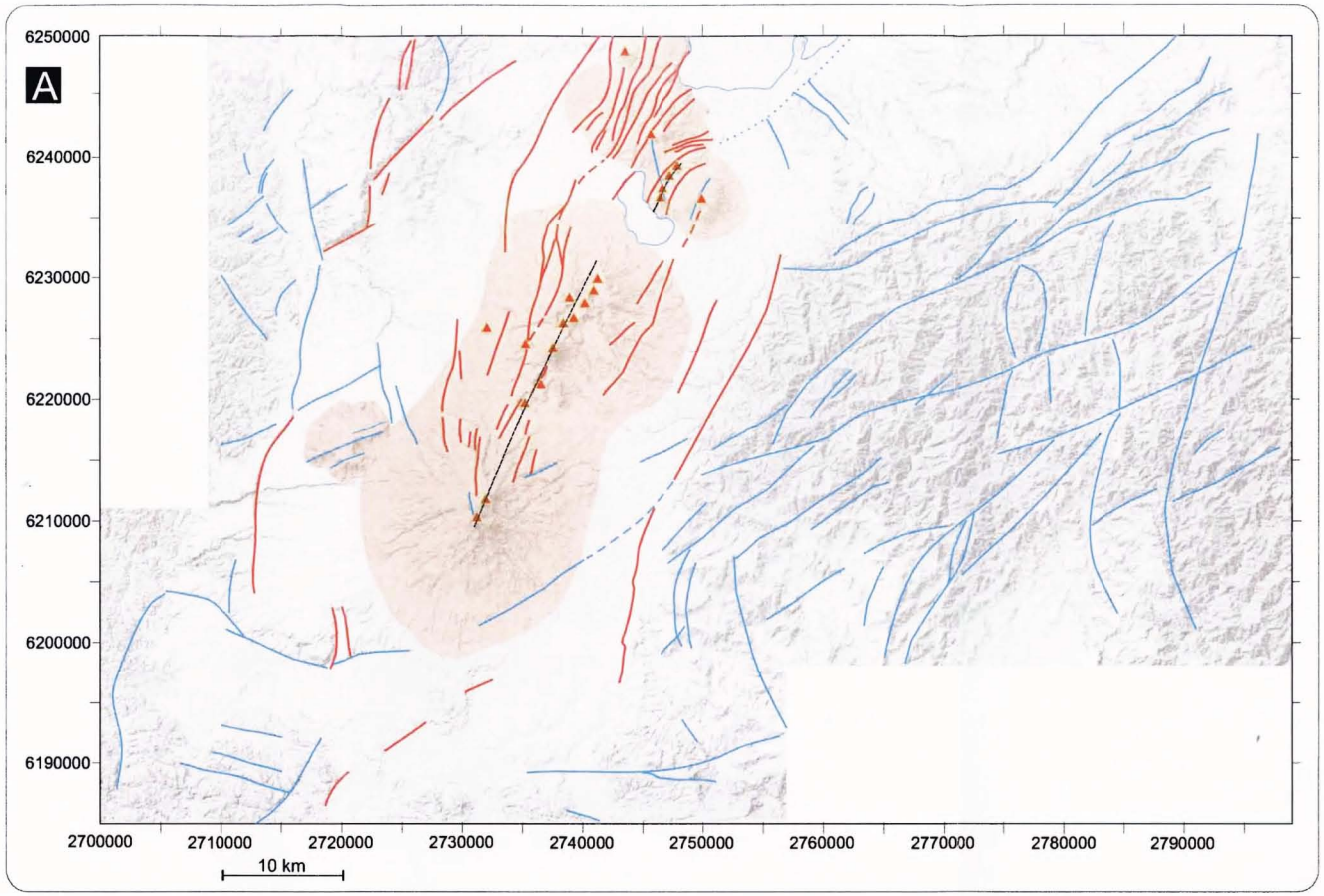

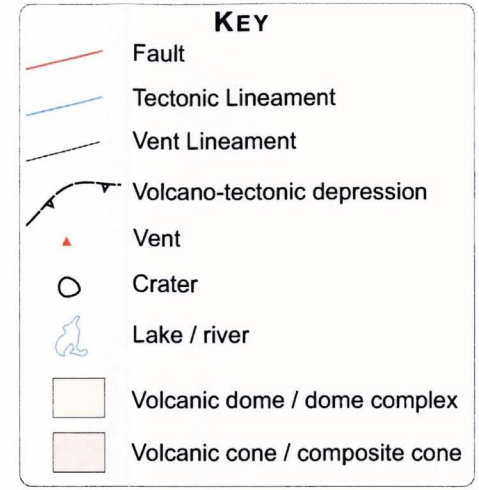

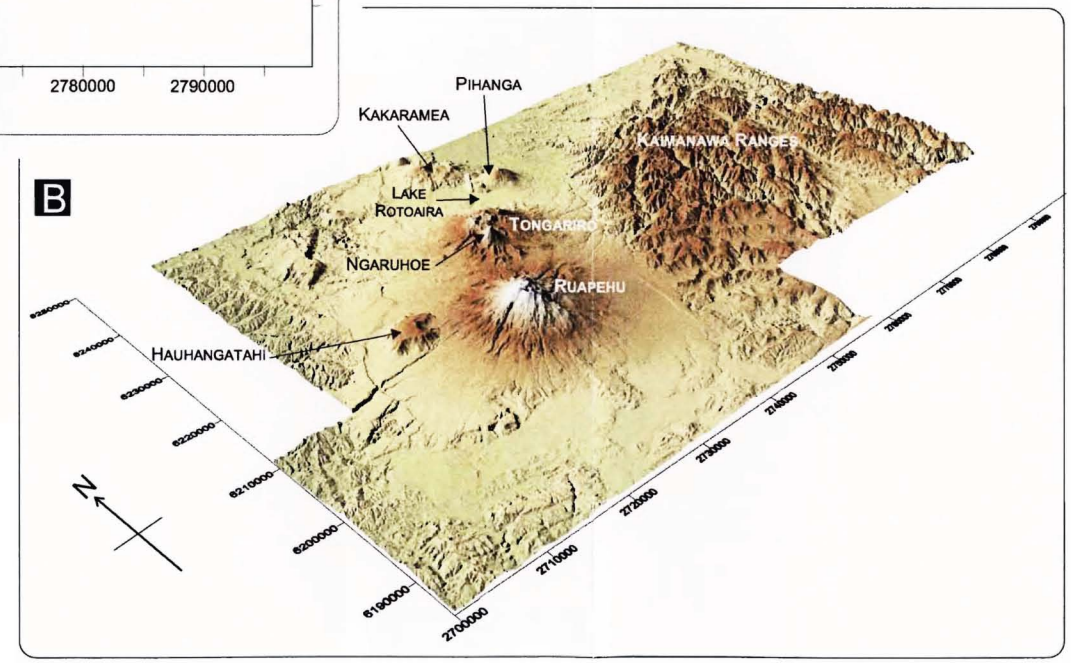

FIGURE 2.6: Structure and physiography of the Tongariro sector. (A) Lineament map shows the contrasting NNE-trending faults dominating the southern part of TVZ with ENE-trending tectonic lineaments in the Kaimanawa Ranges to the east of Tongariro and Ruapehu volcanoes. Vents are strongly aligned in a zone parallel to faulting in this southermost part of the axial rift zone. This part of the zone forms a rectilinear boundary with basement rocks to the west, south and east. (B) 3D perspective surface image of the same area as (A) highlighting the locations mentioned in text. NB key is also for figures 2.7-2.10

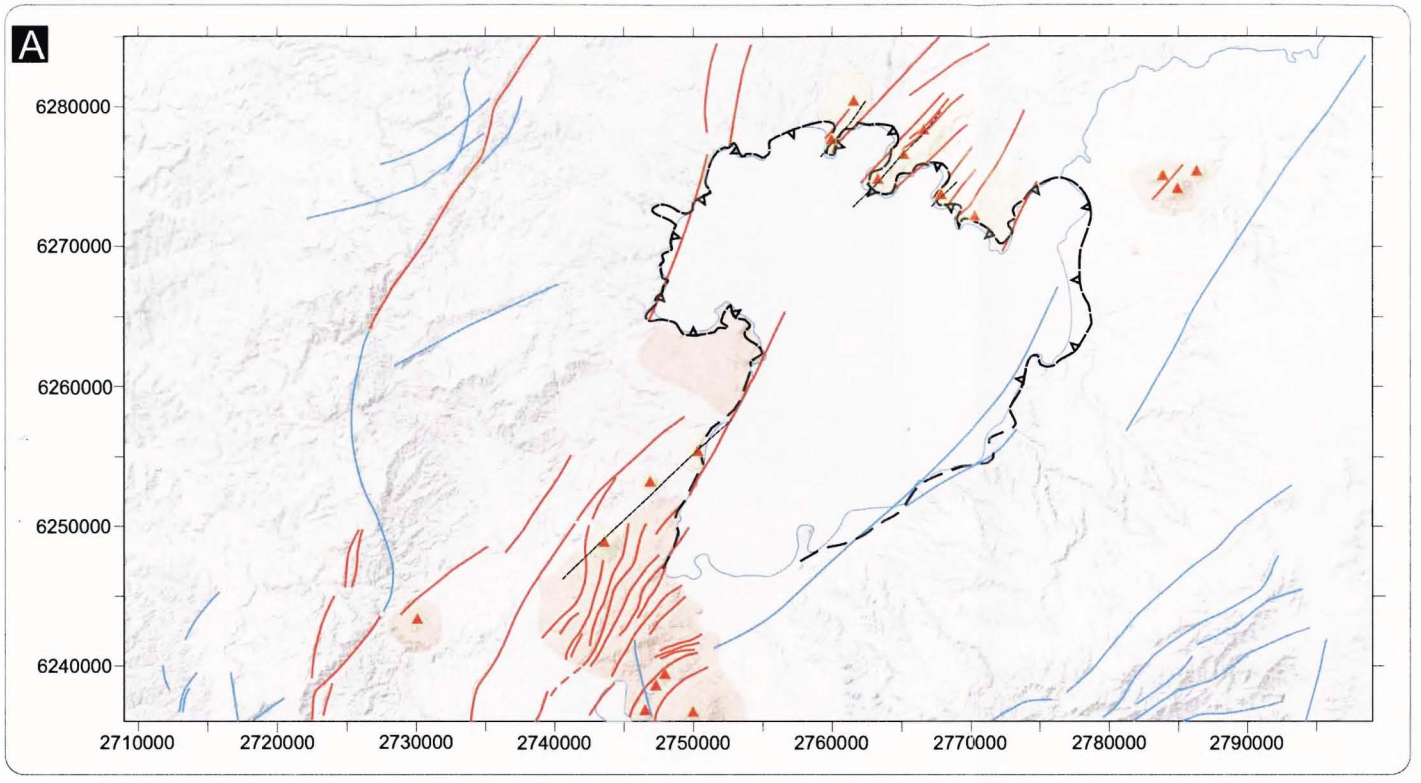

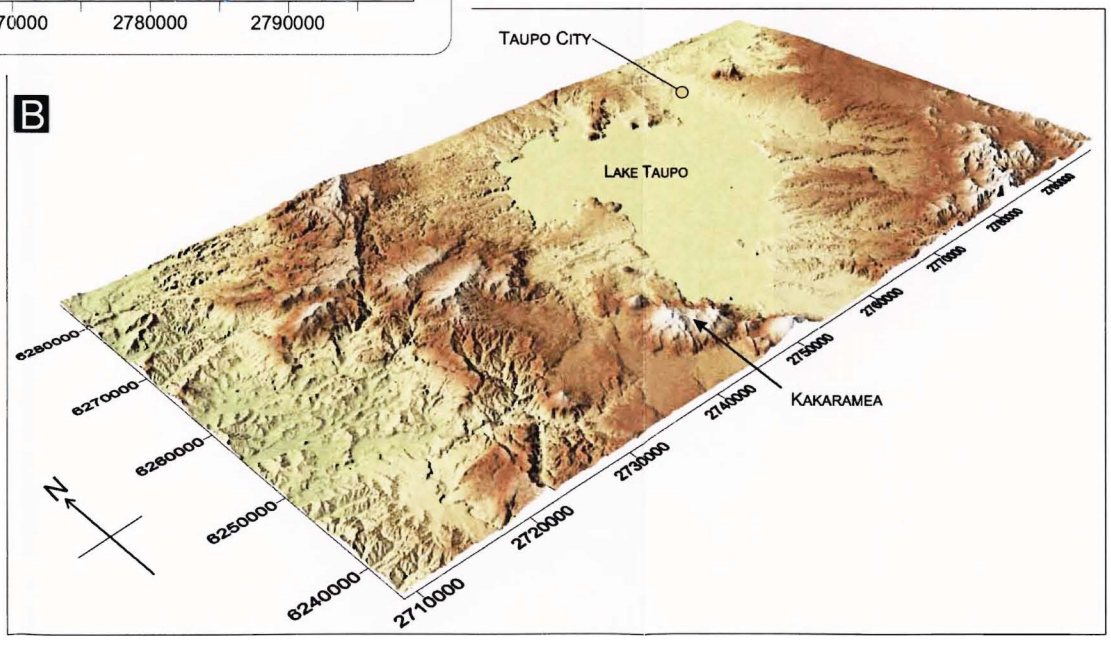

FIGURE 2.7: Structure and physiography of the Taupo sector. (A) Lineament map is dominated by NNE-trending faults and tectonic lineaments which bound Lake Taupo and the Taupo Caldera Complex. Faults clearly intersect and are semi-continuous with the caldera complex suggesting a more rectilinear margin than the topographic outline. The axial rift zone defined by the narrow band of closely-spaced faults in the Tongariro sector noticeably widens at Lake Taupo. Fault trends on the northern and southern shores of the lake are offset by at least 10 degrees. (B) 3D perspective surface image of (A) highlighting locations mentioned in text. The widening of TVZ and the change in dominant style of volcanism from composite cones to large volcano-tectonic depressions and rhyolite dome complexes are conspicuous in this sector.

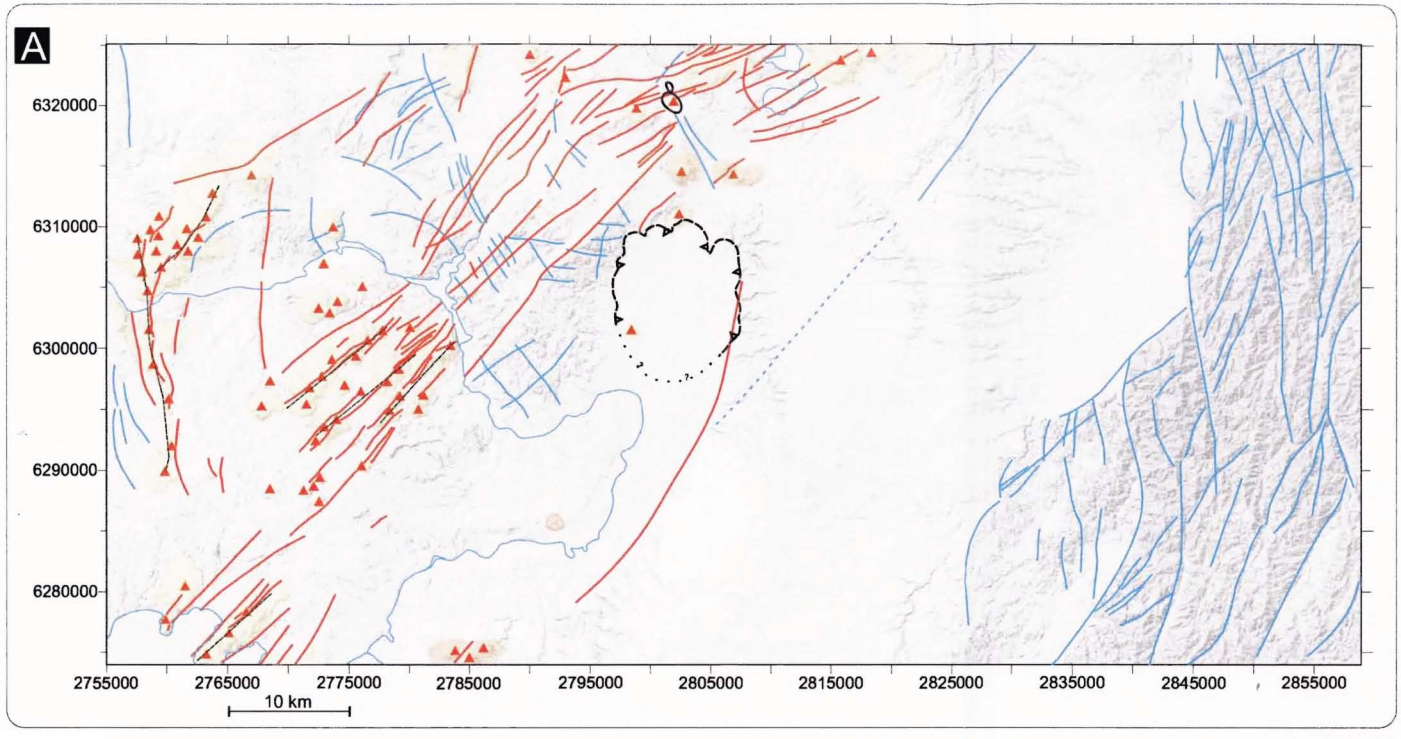

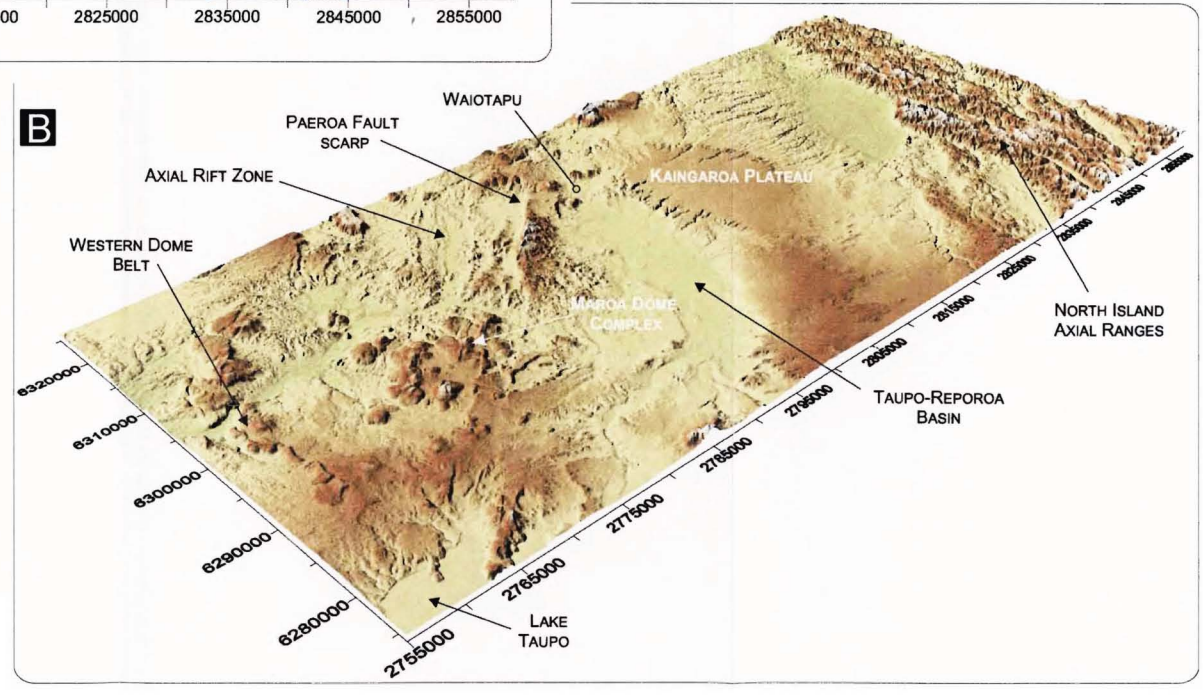

FIGURE 2.8: Structure and physiography of Whakamaru sector. (A) Lineaments in this sector are scattered over a wider area than in the Taupo sector to the south but faults are concentrated in the 15-20 km wide axial rift zone, where opposite verging fault scarps define a graben morphology. Faulting in this zone is semi-continuous in this sector with a conspicuous offset north of lake Taupo where the axis of faulting dissecting the Maroa dome complex is ~10 km to the NW. Reporoa caldera is located away from the axial rift zone but the eastern caldera margin is semi-continuous with a large fault bordering the Taupo-Reporoa Basin. Faulting in the north of this sector conspicuouly rotates to trend NE near the southern margin of Okataina Caldera Complex. The axial rift zone is also dissected by a number of small NNE-trending tectonic lineaments. Dome complexes and eruptive vents are clearly parallel with regional faults. Western Dome Belt lies on a trend significantly different than that defined by the closely spaced faulting in the axial rift zone. (B) 3D perspective surface image of (A) highlighting the locations and features mentioned in the text. The main tectonic units of TVZ, the axial rift zone and the flanking ignimbrite plateau, are conspicuous in their distinct morphologies.

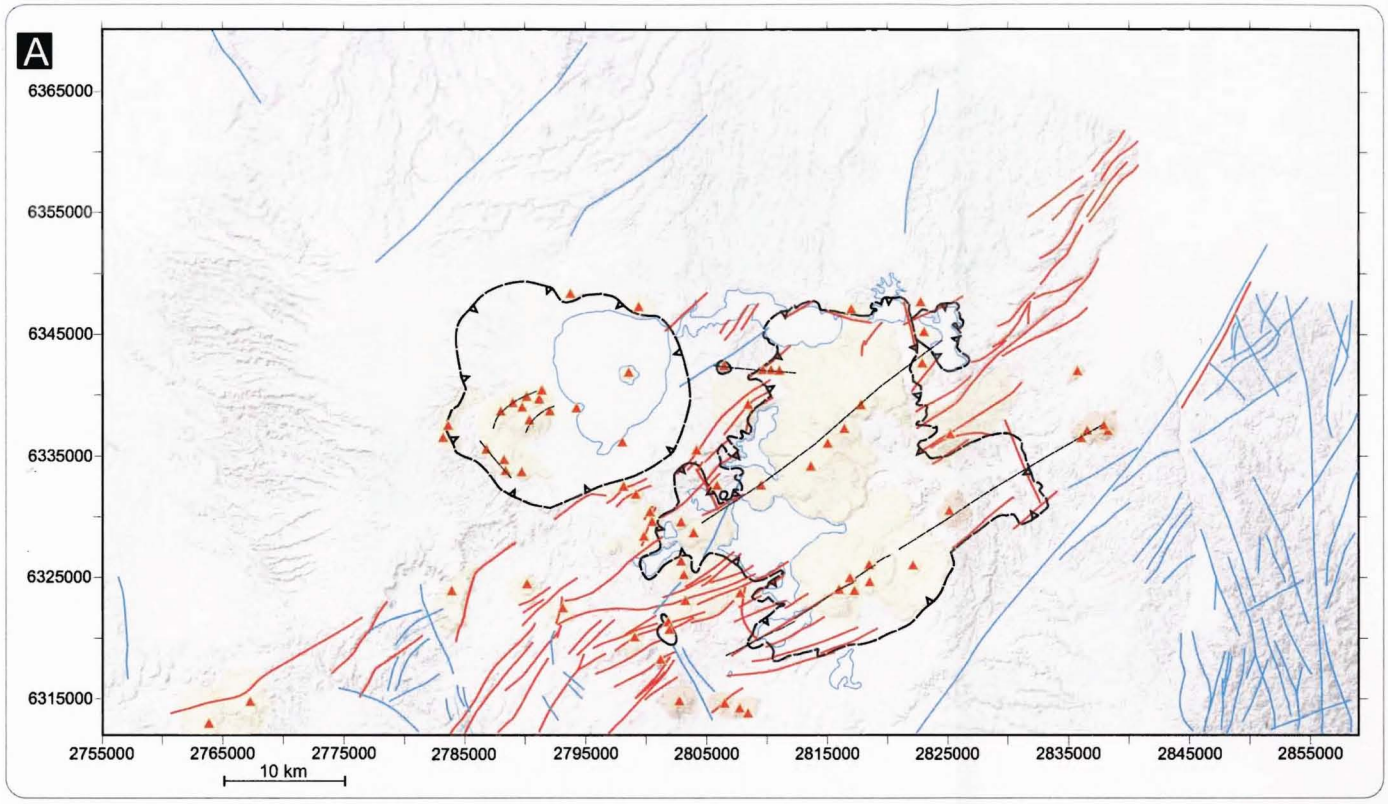

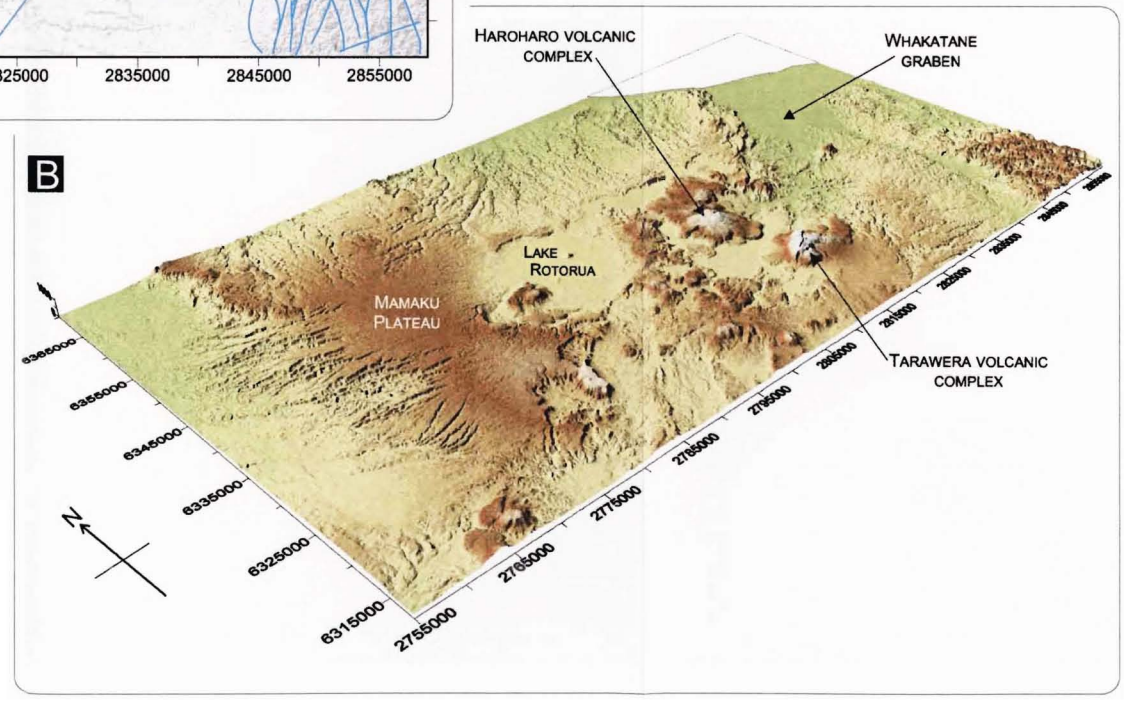

FIGURE 2.9: Structure and Physiography of the Okataina sector. (A) Lineament map shows that deformation is largely restricted to the axial rift zone, which shows a distinct bend at Okataina Caldera Complex (OCC). Rotorua caldera is located away from the axial rift zone and its margins are not dissected by regional faulting. Major vent lineaments crossing the OCC are subparallel and semicontinuous with the central part of the axial rift zone to the north and south of the caldera complex. Tectonic lineaments are scarce and occur predominantly within the NISB to the east of TVZ, where they appear to intersect the Whakatane graben. Major dome complexes occur both within and outside of the large caldera structures in this sector of TVZ. (B) 3D perspective surface image of (A), viewed from the southwest, highlighting the locations mentioned in the text.

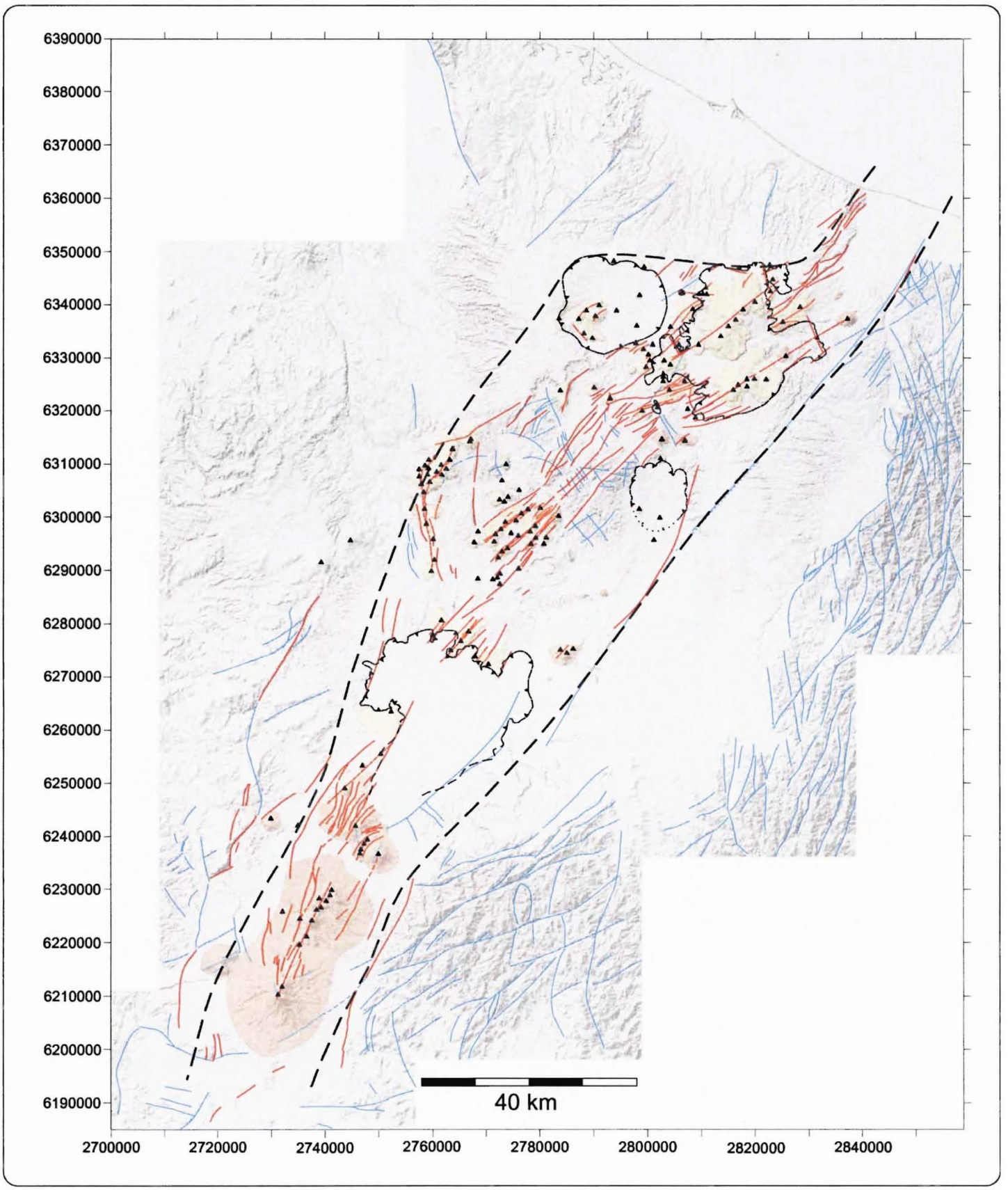

FIGURE 2.10 Shaded relief image of onshore TVZ compiling data from detailed analysis of four TVZ sectors (figures 2.6 through 2.9). Also shown is the outline of modern TVZ (<300 ka).

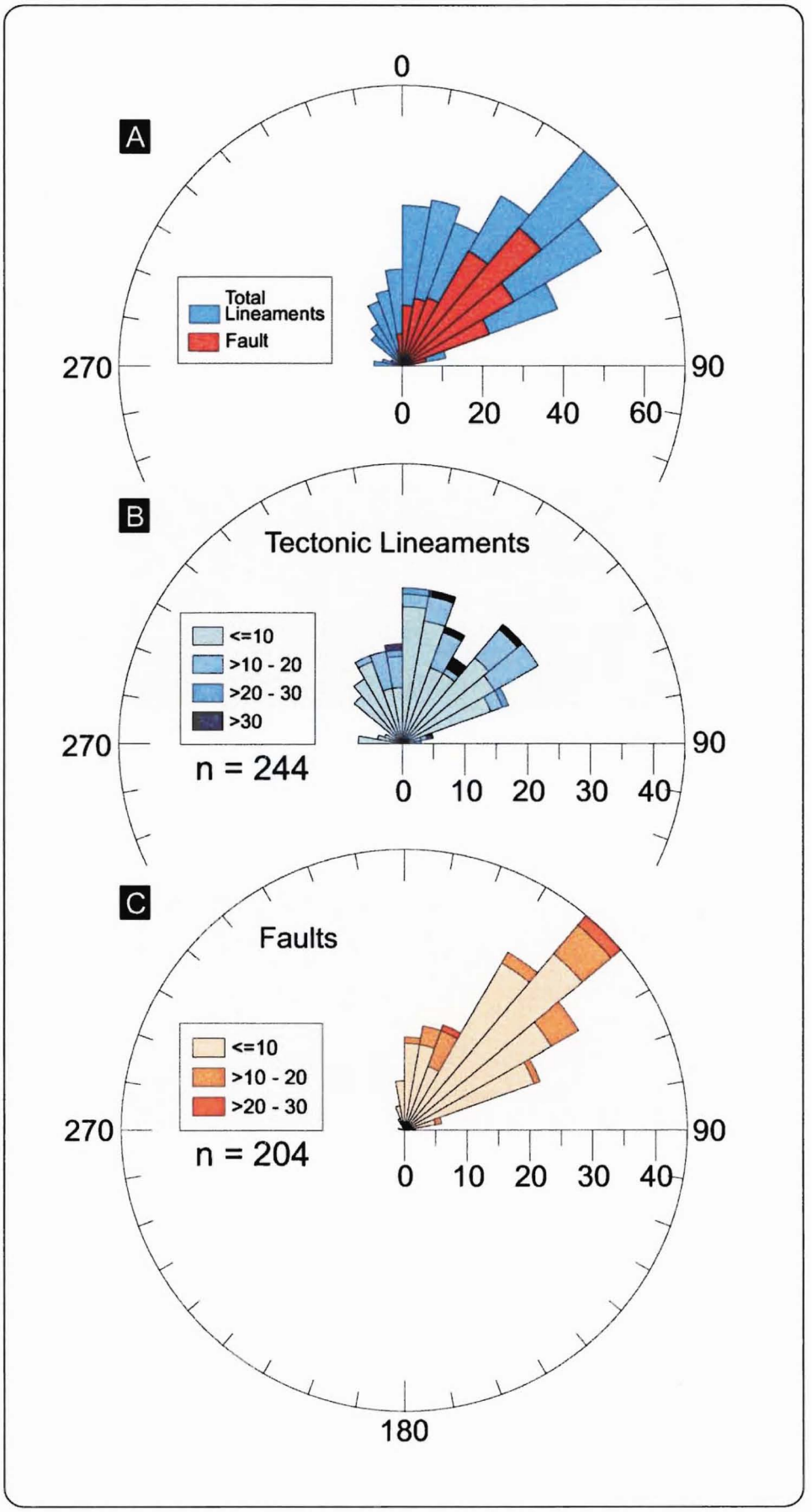

FIGURE 2.11: Rose diagrams illustrating orientation and magnitude of lineaments in Fig 2.10: (a) orientation of all lineaments (faults highlighted in red); (b) orientation and length (km) of tectonic lineaments; (c) orientation and length (km) of faults.

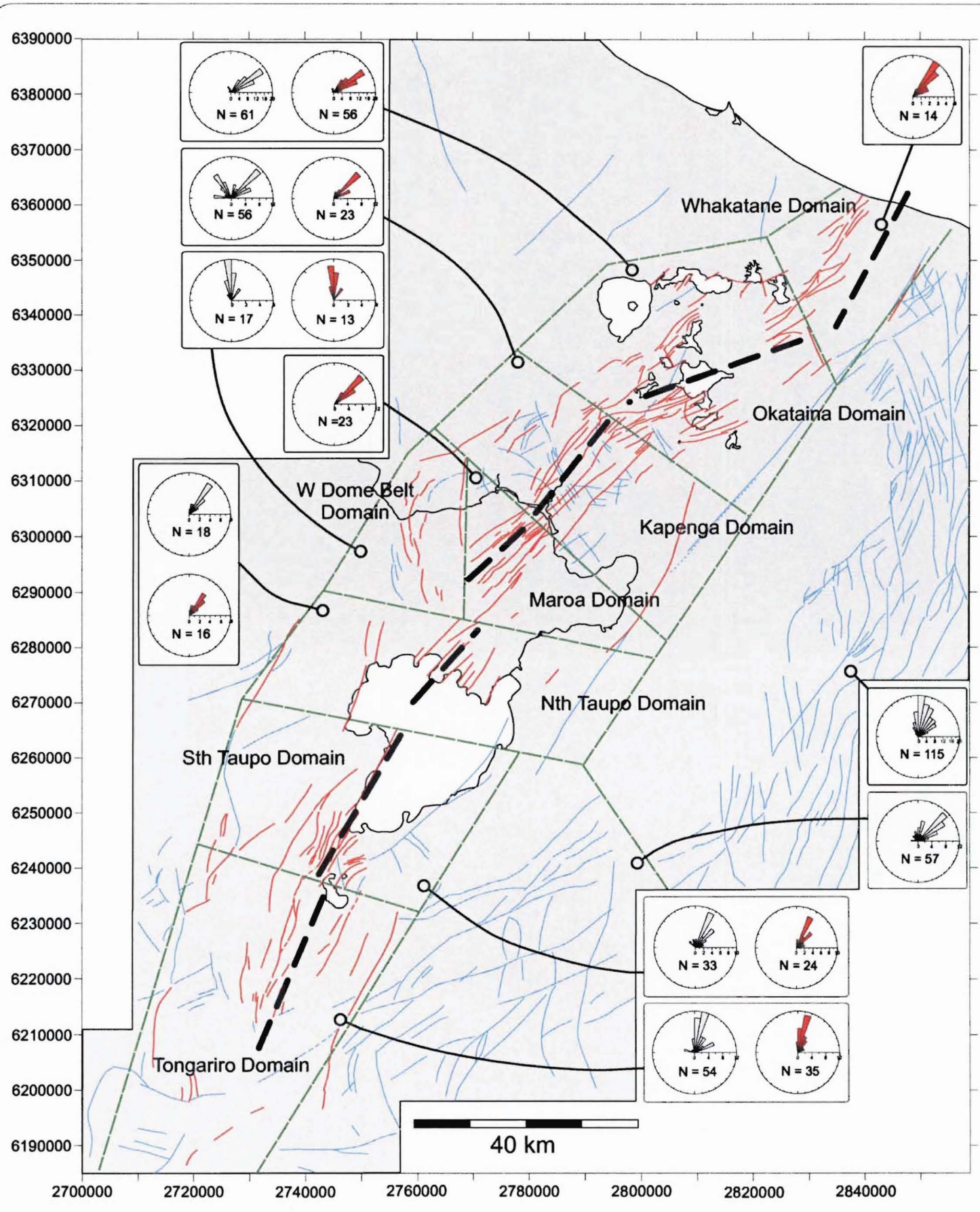

FIGURE 2.12: Lineaments divided into structural domains. Rose diagrams give an indication of the general lineament orientations in each domain; faults (in red) are more tightly constrained within the total lineament population (grey).

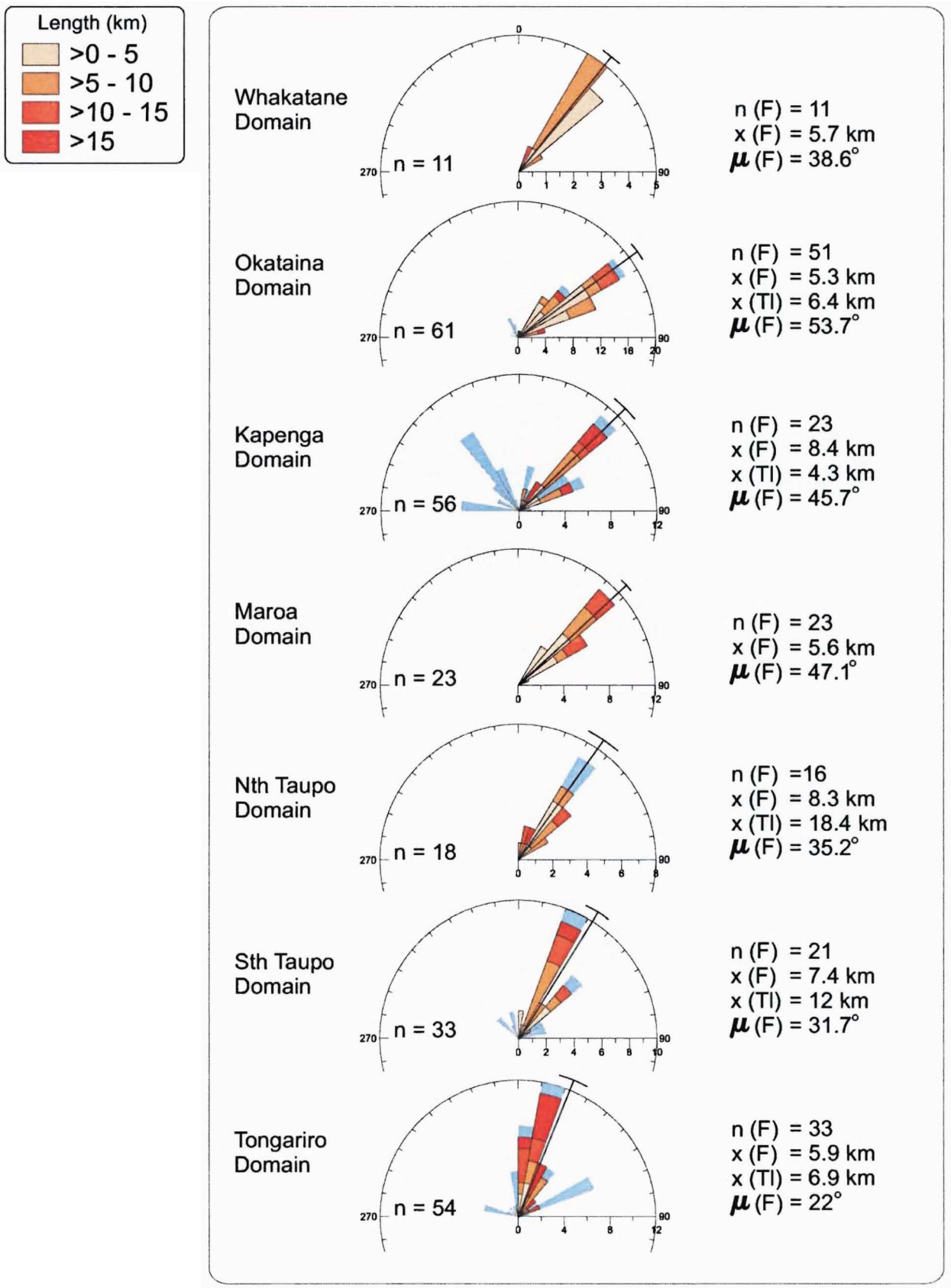

FIGURE 2.13: Detailed Rose diagrams of the main TVZ domains in Fig. 2.12. Mean and std. dev. shown by line and error bar.

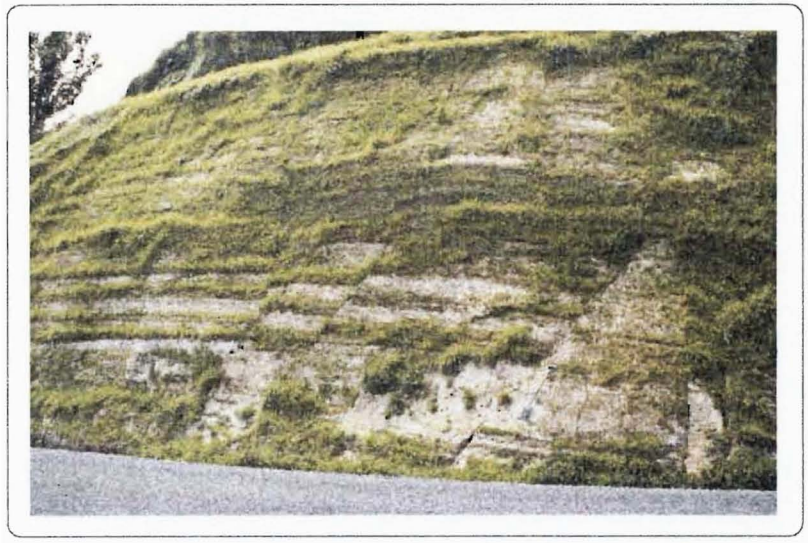

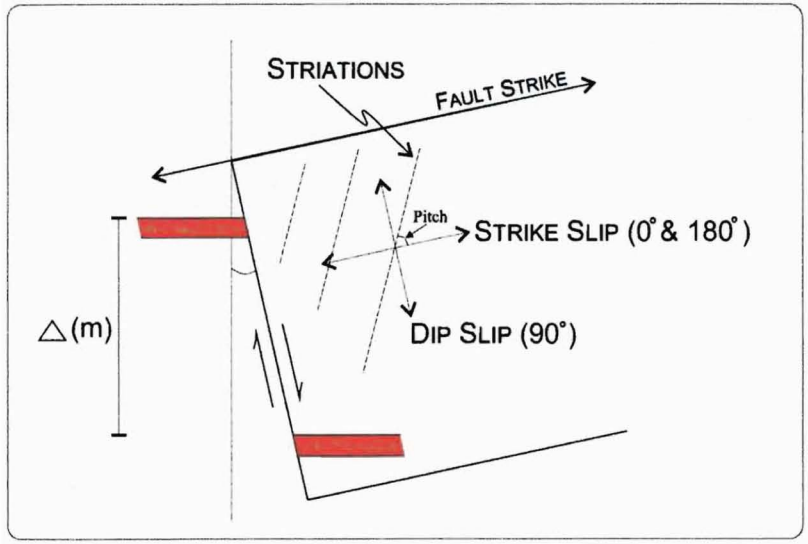

FIGURE 2.14: (A) A typical fault exposure in the Kapenga domain, V16/936181. Exposure is obscured by hydroseeding but vegetation highlights displacements along various faults. (B) Schematic diagram showing how slip directions for faults were calculated by measuring the pitch of striations on a fault plane.

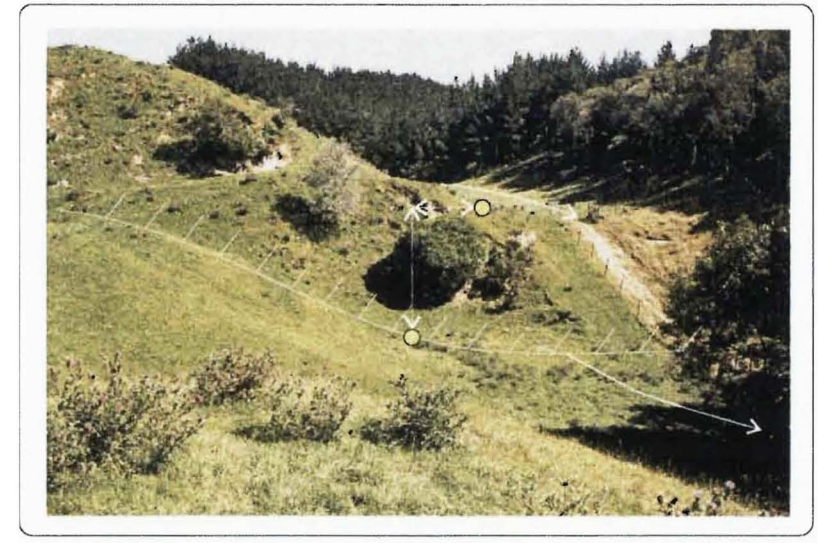

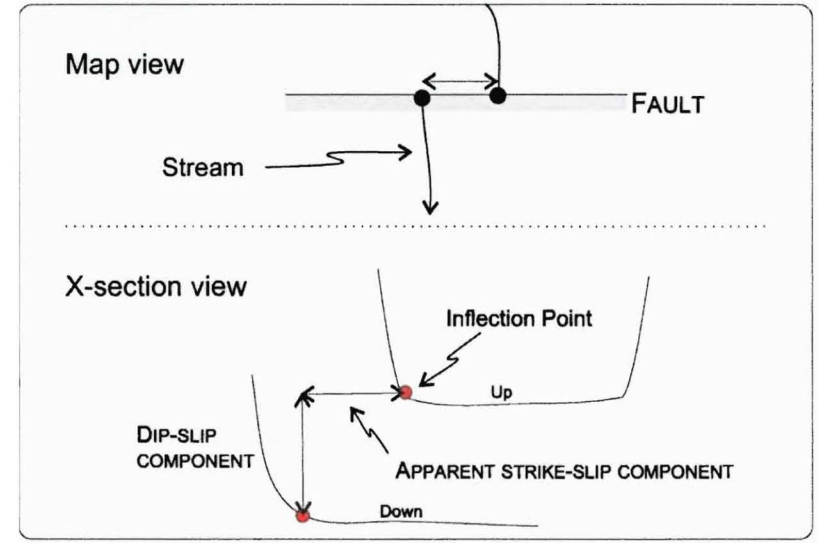

FIGURE 2.15: (A) Example of an abandoned stream channel offset by a fault near Highlands Loop Rd (V16/019238). View is slightly oblique to fault plane. (B) Slip directions at offset stream channels were calculated using estimates of horizontal and vertical displacement of channel axes. Some error is involved in locating the inflection points and projecting them onto the fault plane.

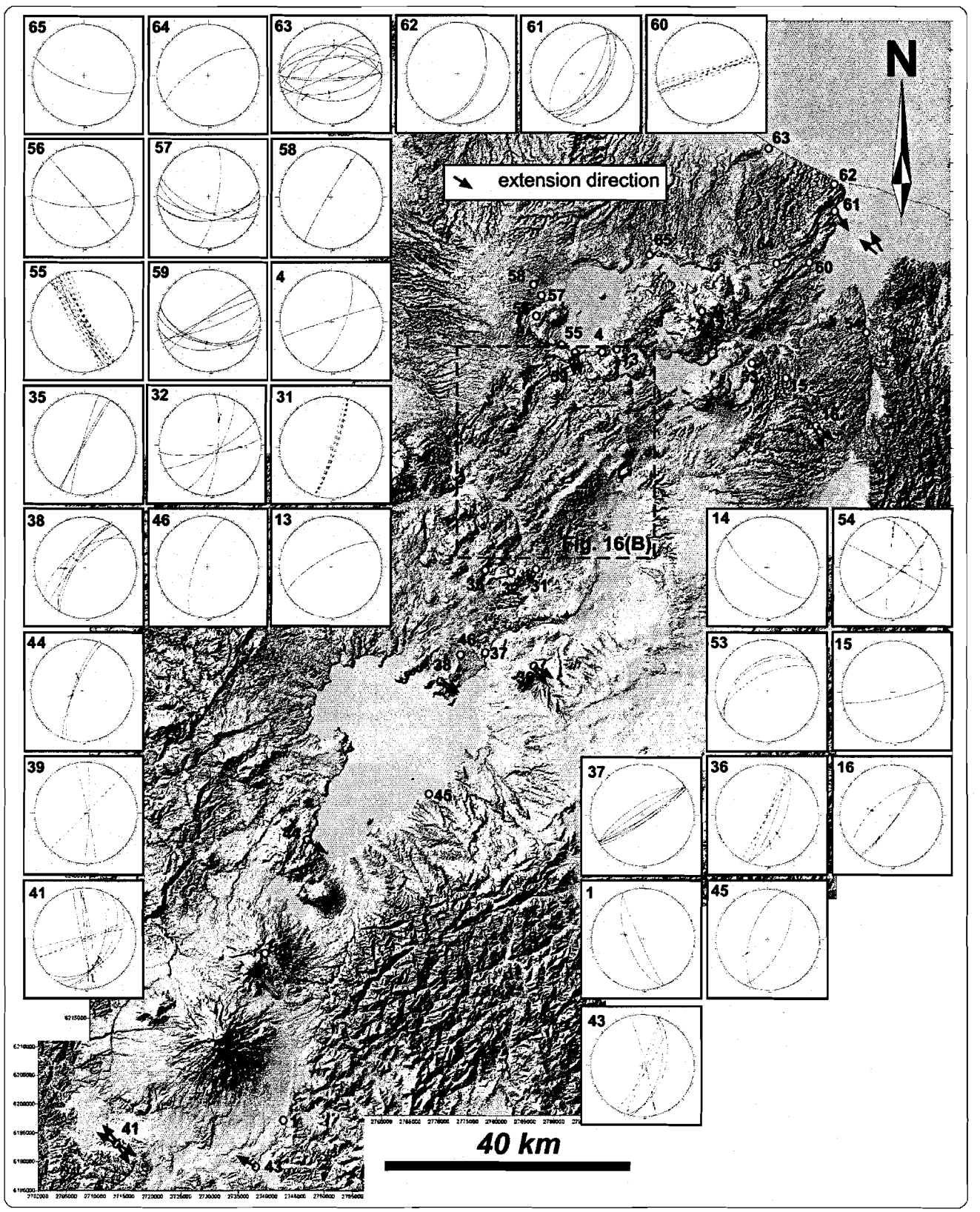

FIGURE 2.16: Structural data collected for (A)Modern TVZ and (B) for the Kapenga segment. The data are plotted on individual lower hemisphere stereonets for each sample site; solid lines = faults; dashed lines = joints; arrows show sense of movement as inferred form pitch of striations; black arrows on image are extension directions of faults with displacement >1 m, determined using the procedure of MARRITT & ALLMENDINGER (1990).

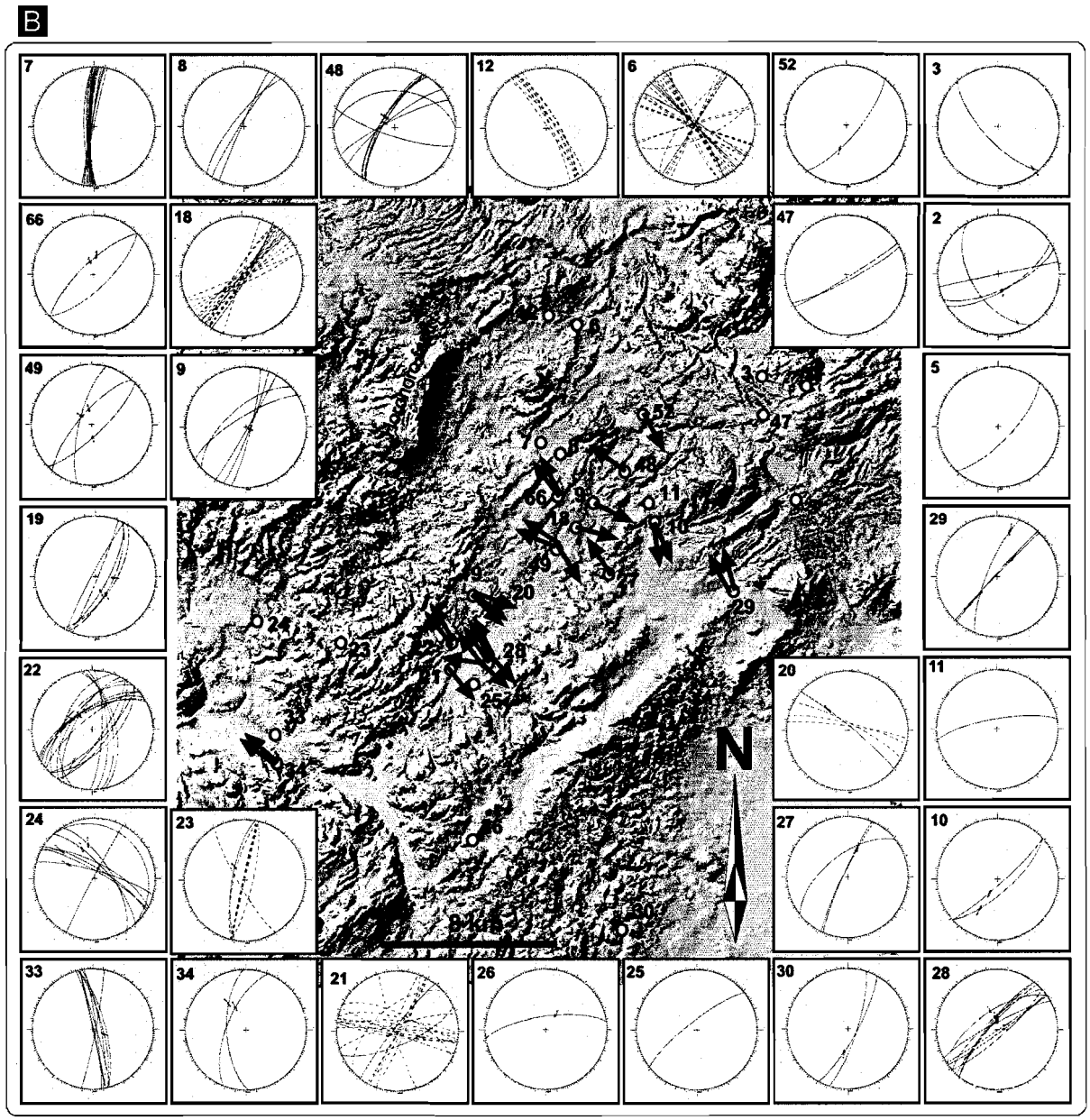

FIGURE 2.16 (Continued)

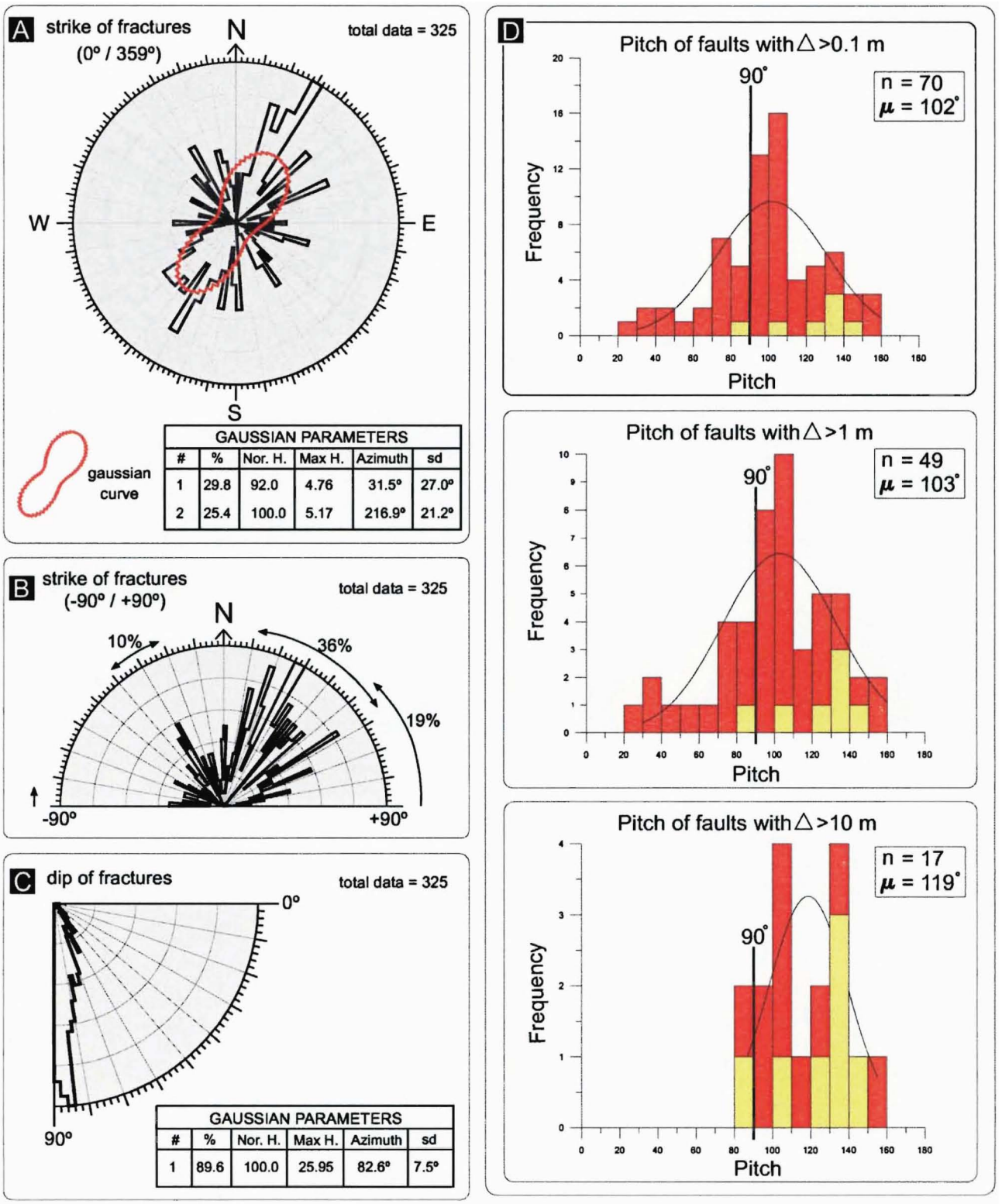

FIGURE 2.17: Geometry and kinematics of fractures measured in the field. A) Strike 0/360) of the fractures; B) strike (-90/+90) of the fractures; C) dip of fractures; D) pitch of faults as a function of their displacement ; contribution of offset stream channel data is highlighted in yellow. NB 'pitch of faults' refers to the pitch of the fault plane striations.

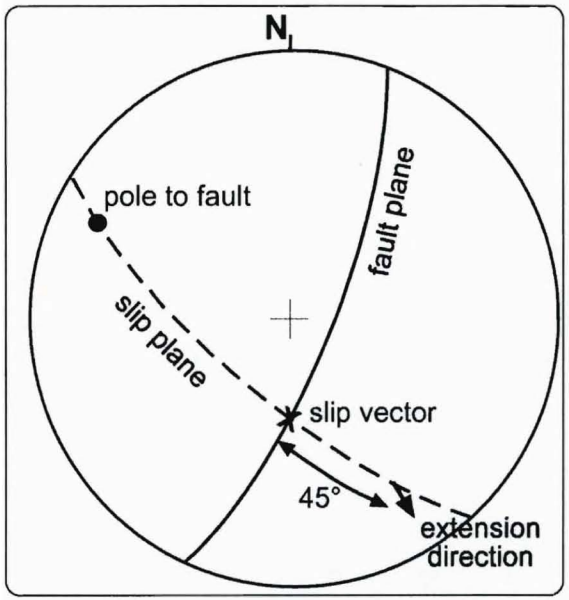

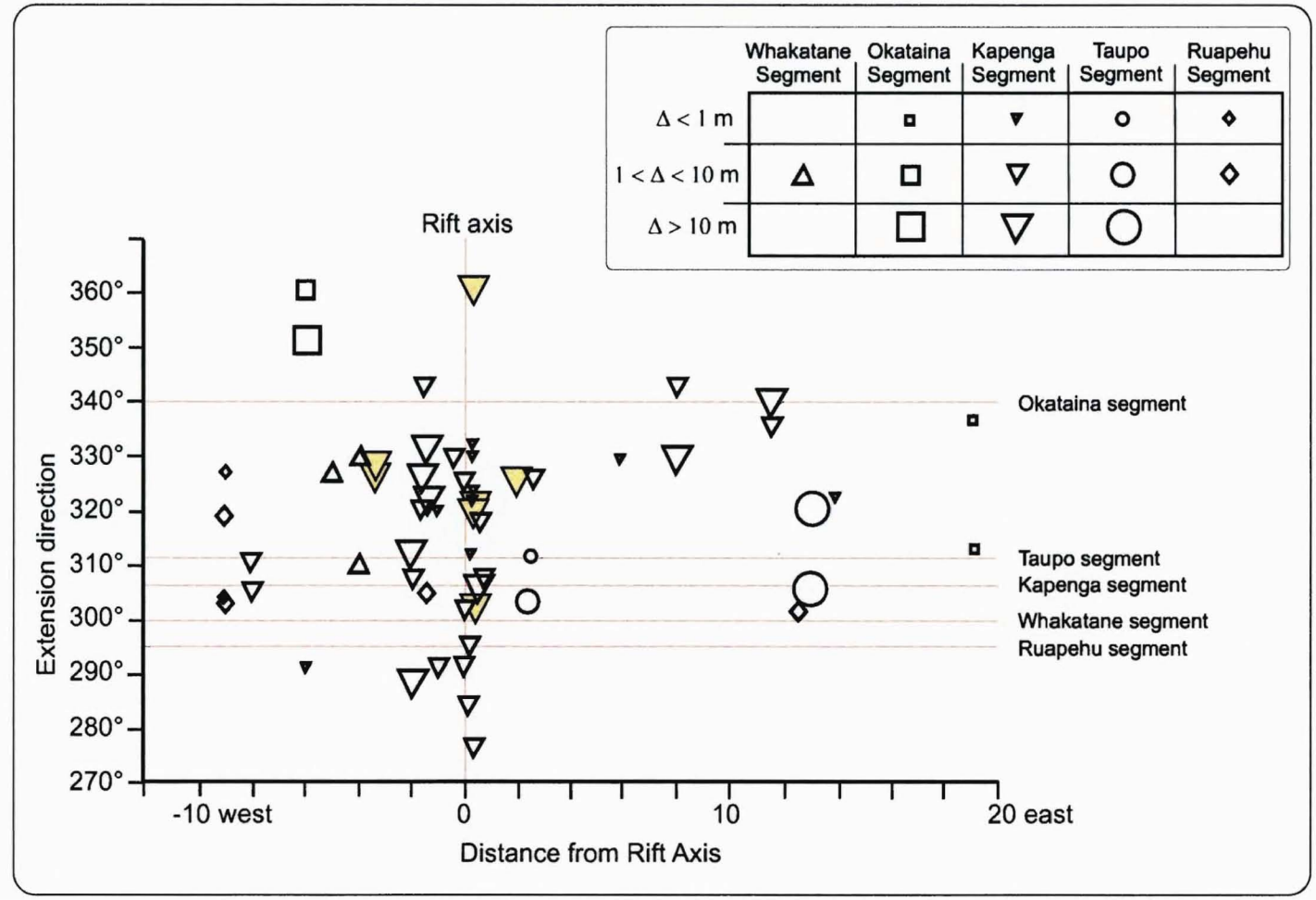

FIGURE 2.18: (A) Stereographic procedure used to evaluate the extension direction from the strike, dip, and pitch of a fault (modified after MARRETT & ALLMENDINGER (1990). (B) Extension directions of the faults plotted as a function of their segment, distance form segment axis, and their displacement. Red horizontal lines represent the trend orthogonal to each segment. Yellow shaded data symbols indicate data from offset stream channels. Modified from ACOCELLA, SPINKS *et al* (2003).

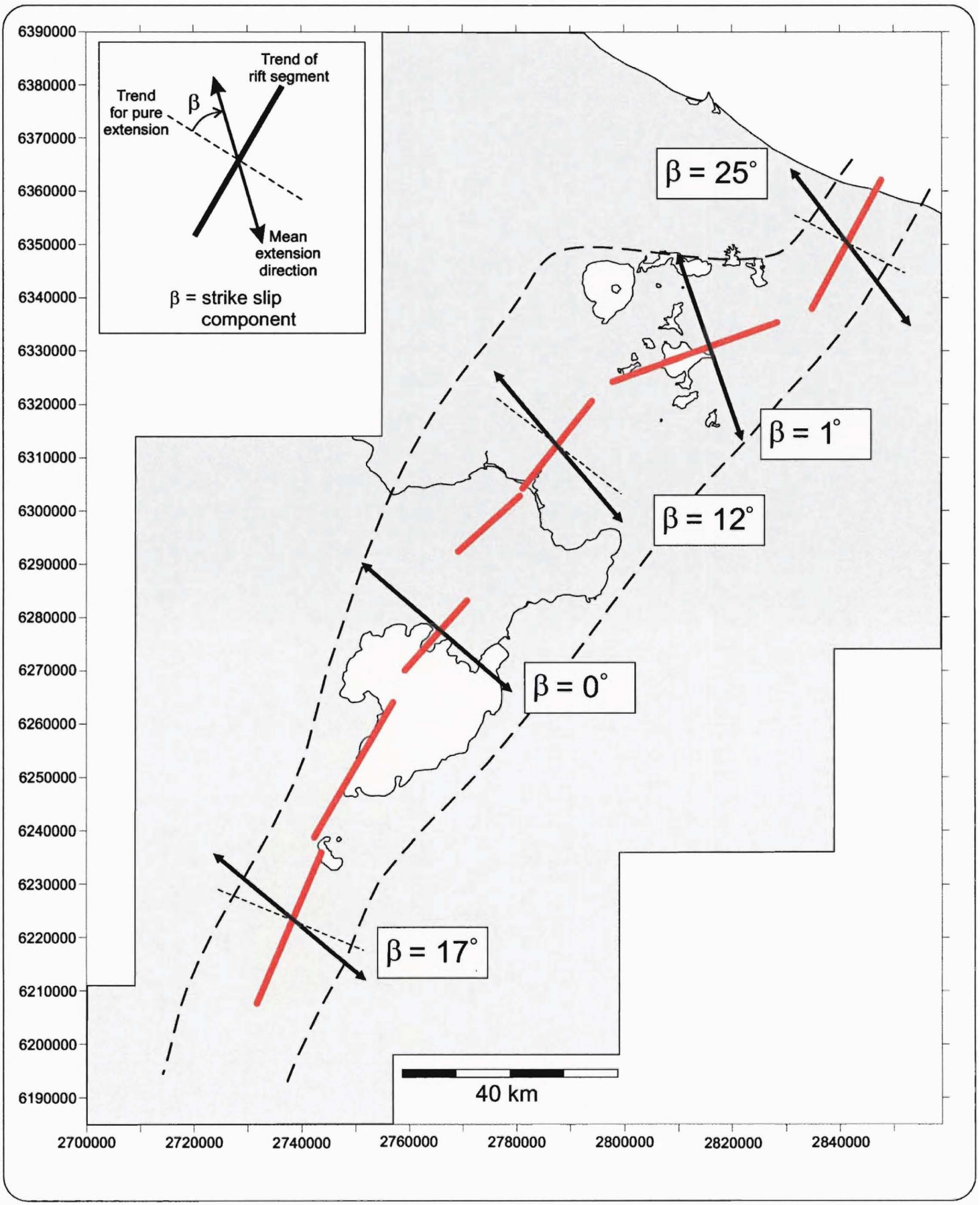

FIGURE 2.19: Rift segments of TVZ and their mean extension directions. Extension directions could not be calculated for the Taupo Sth and Maroa rift segments, due to insufficient structural data in these domains. Extension directions after Acocella et al (2003). β (see inset) is the angle between the direction perpendicular to the trend of the rift segment and the extension direction.

	Tongariro / Sth Taupo	Nth Taupo	Maroa / Kapenga	Okataina	Whakatane
length (km)	60	25	30	35	50
Erupted volume (km^3)	200±50	480±120	200±50	430±108	80±20
Erupted volume / km	3.3±0.8	19.2±4.8	6.7±1.7	12.3±3.1	1.7±0.4
β	17°±	0°±	12°±	1°±	25°±

TABLE 2.1: Table reporting the length of axial rift segments, their erupted volume, erupted volume per km, and β values. Some segments have been combined due to a lack of structural data. Erupted volumes are compiled from FROGATT & LOWE (1990); JURADO-CHICHAY & WALKER (2001); NAIRN (1989, 2002); BELLAMY (1991); WILSON *et al* (1984; 1986); SUTTON *et al* (1995); BAILEY & CARR, (1994); HOBDEN *et al* (1999); HACKETT & HOUGHTON (1989); D. GRAVLEY (2005); LEONARD (2003).

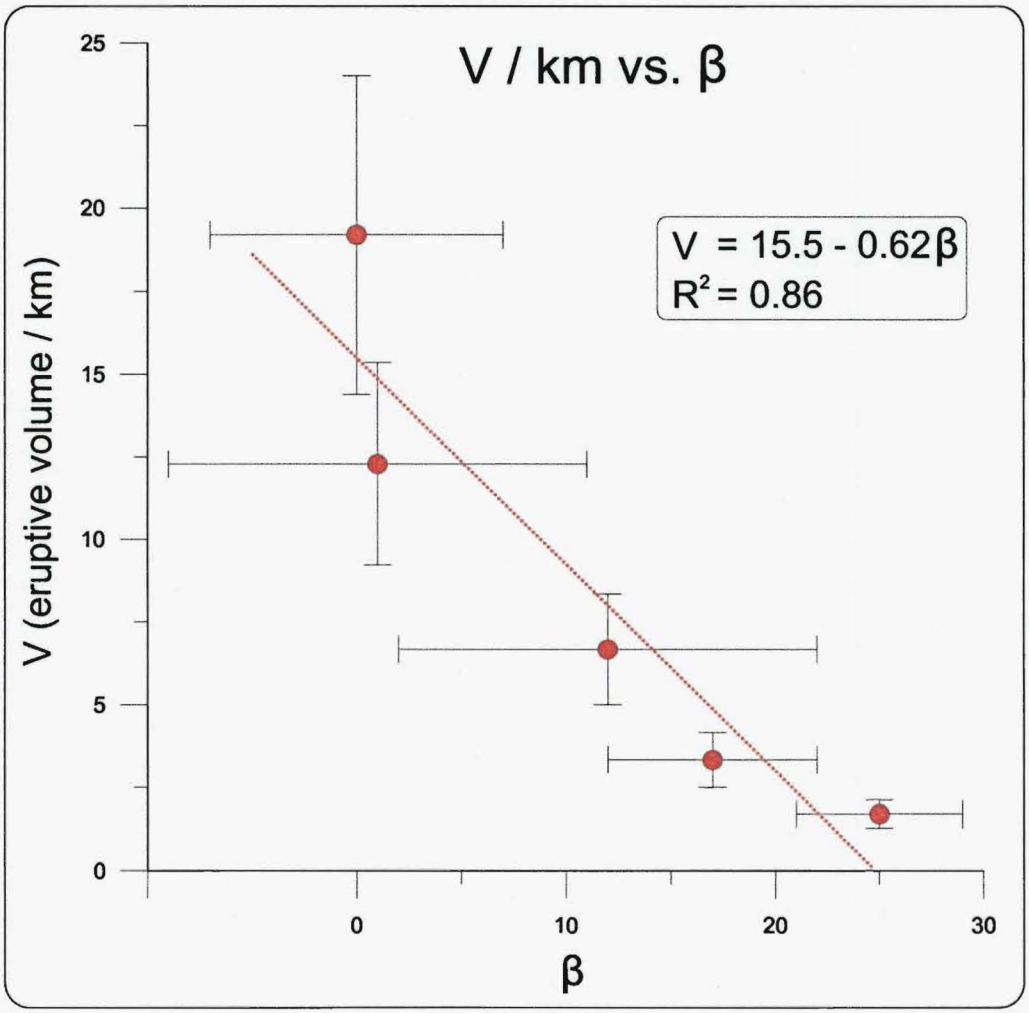

FIGURE 2.20: Diagram showing the relationship between the amount of dextral shear (β) calculated for segments of TVZ and the erupted volume per km of segment length relative to the last 300 ka. Segments with pure extension (Nth Taupo and Okataina) are associated with the largest eruptive volumes, while segments with dextral shear exhibit lower eruptive volumes.

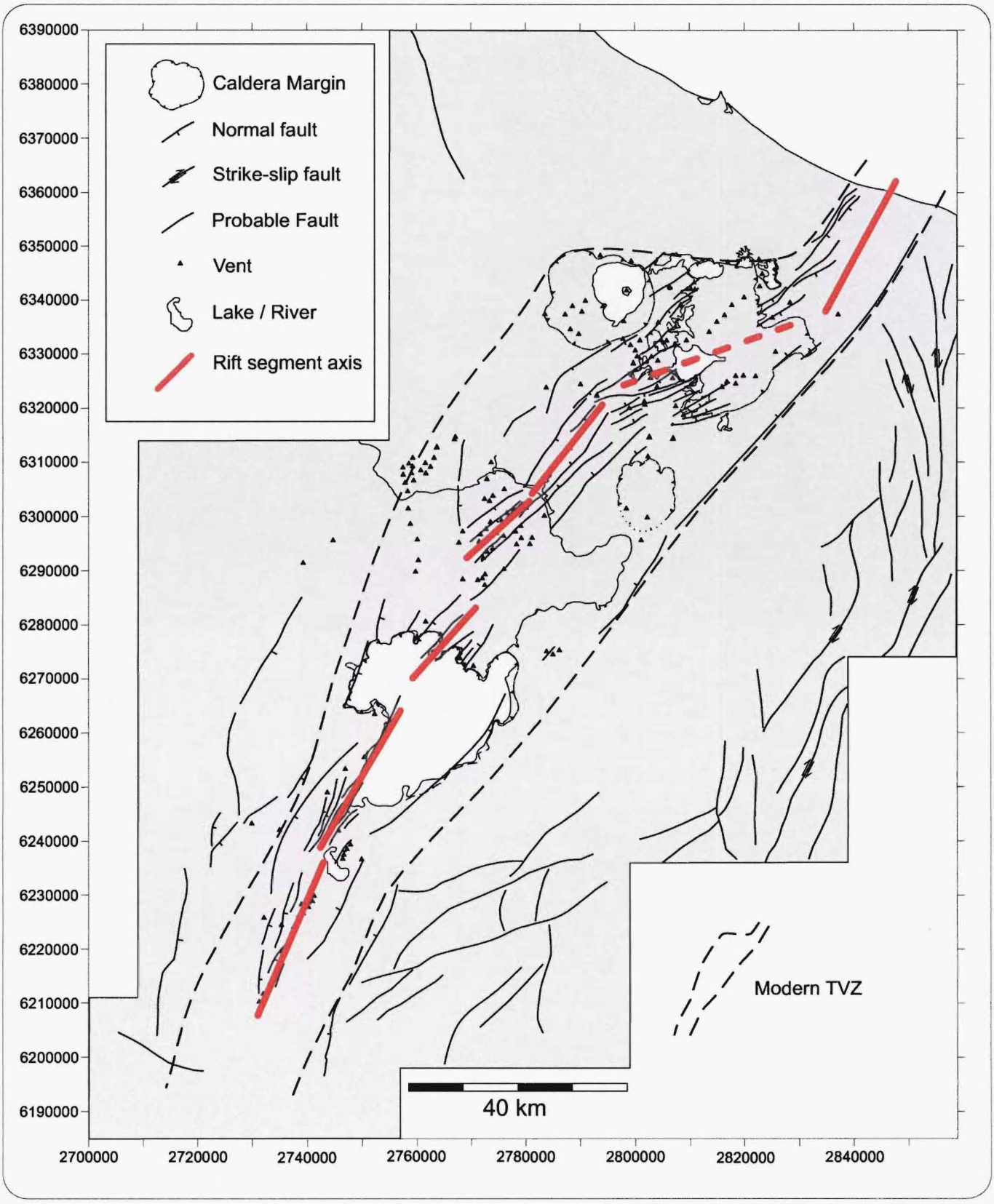

FIGURE 2.21: Summary map of TVZ based on analysis of shaded relief imagery and field work. See text for further discussion.

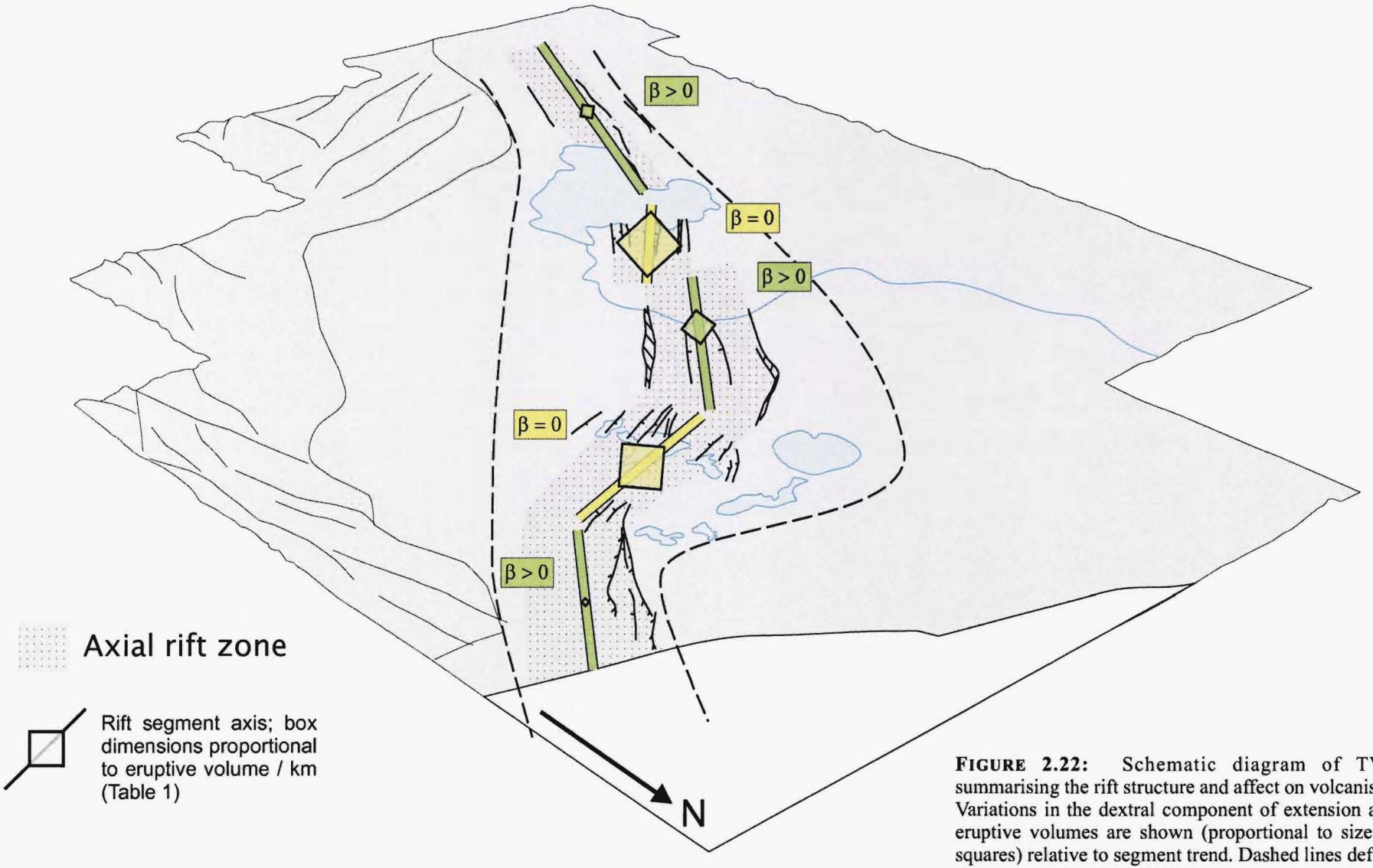

FIGURE 2.22: Schematic diagram of TVZ summarising the rift structure and affect on volcanism. Variations in the dextral component of extension and eruptive volumes are shown (proportional to size of squares) relative to segment trend. Dashed lines define the margins of modern TVZ.

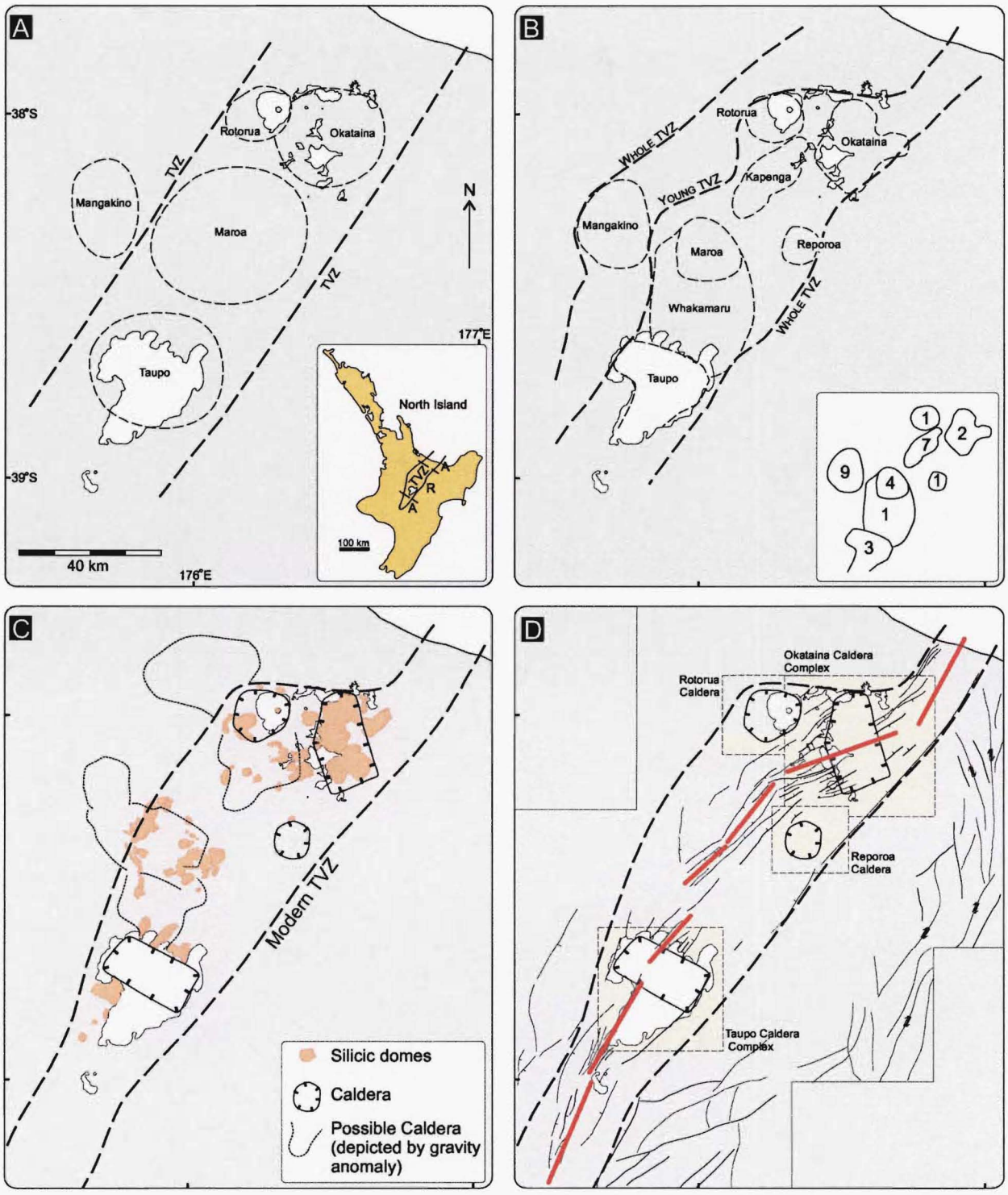

FIGURE 3.1: Maps showing the outlines of silicic centres in central TVZ. (A) the 4 centres proposed by COLE (1990); inset shows location of TVZ and division into andesite and rhyolite portions. (B) the 8 calderas proposed by WILSON *et al* (1984, 1986), NAIRN *et al* (1994), and HOUGHTON *et al* (1995); inset: number of caldera forming events (HOUGHTON *et al*., 1995). (C) calderas and caldera complexes as identified in this study. Calderas of Modern TVZ (<300 ka) defined by analysis of new DEM data; dashed outlines define the margins of potential caldera structures proposed based on existing geophysical data. Some of these are coterminous with calderas in (B). (D) New structural map of TVZ highlighting the location of modern TVZ calderas described in this chapter. Their structure and evolution is largely a function of their proximity to the axial rift zone (rift segment axes in red).

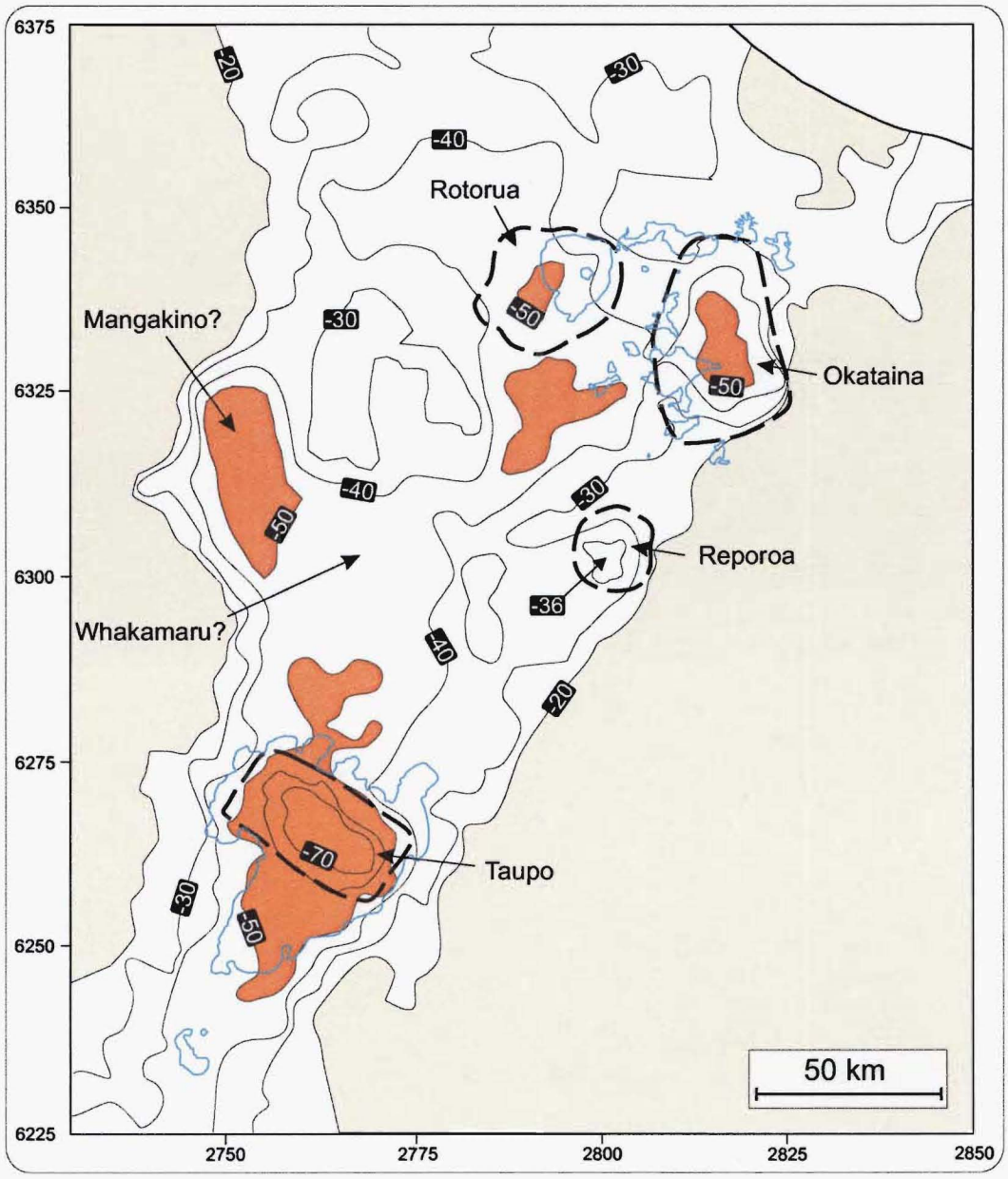

FIGURE 3.2: Residual Bouguer gravity anomaly of TVZ with outlines of modern calderas. Areas less than -50 mgal and greater than -20 mgal are highlighted in red and yellow respectively. Lakes are outlined in blue. Grid coordinates are in the New Zealand map grid (NZMG). Note that Okataina and Taupo are associated with much larger (size and intensity) negative gravity anomalies than Rotorua and Reporoa. Gravity contours from DAVY & CALDWELL (1988) and NAIRN *et al* (1994).

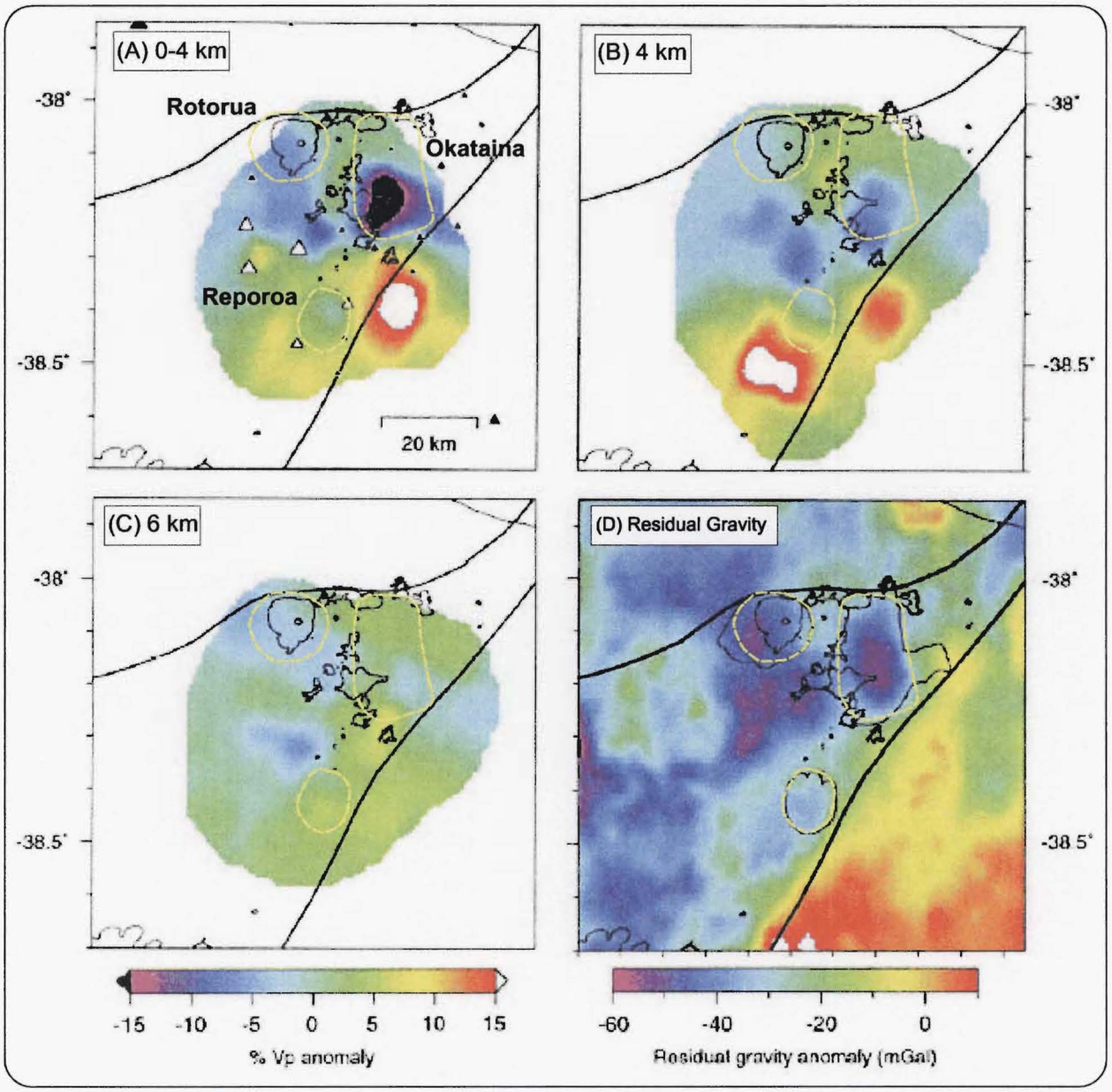

FIGURE 3.3: (A-C) Vp anomaly for depths of 0-4, 4, and 6 km. (D) Residual Gravity for TVZ (after STAGPOOLE & BIBBY, 1999). Calderas are overlain in yellow. Note consistent large and more intense Vp and gravity anomaly for Okataina compared with Rotorua and Reporoa. Modified from SHERBURN *et al* (2003).

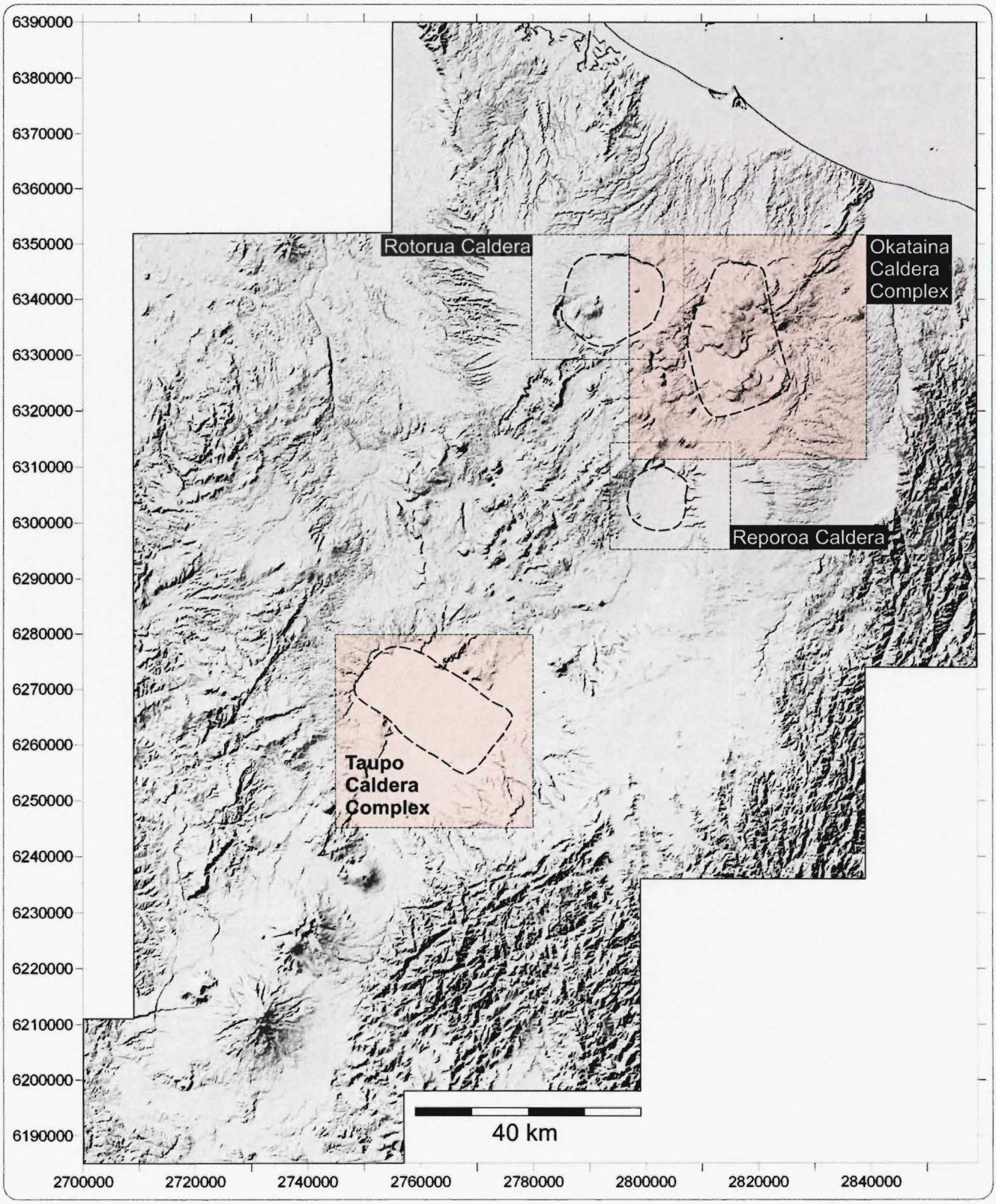

FIGURE 3.4: Shaded relief Image of TVZ highlighting the locations of the axial rift caldera complexes (red) and off-axis calderas (yellow) of the Modern TVZ calderas.

FIGURE 3.5: Rotorua Caldera

A 3D surface image illustrating physiography of Rotorua Caldera

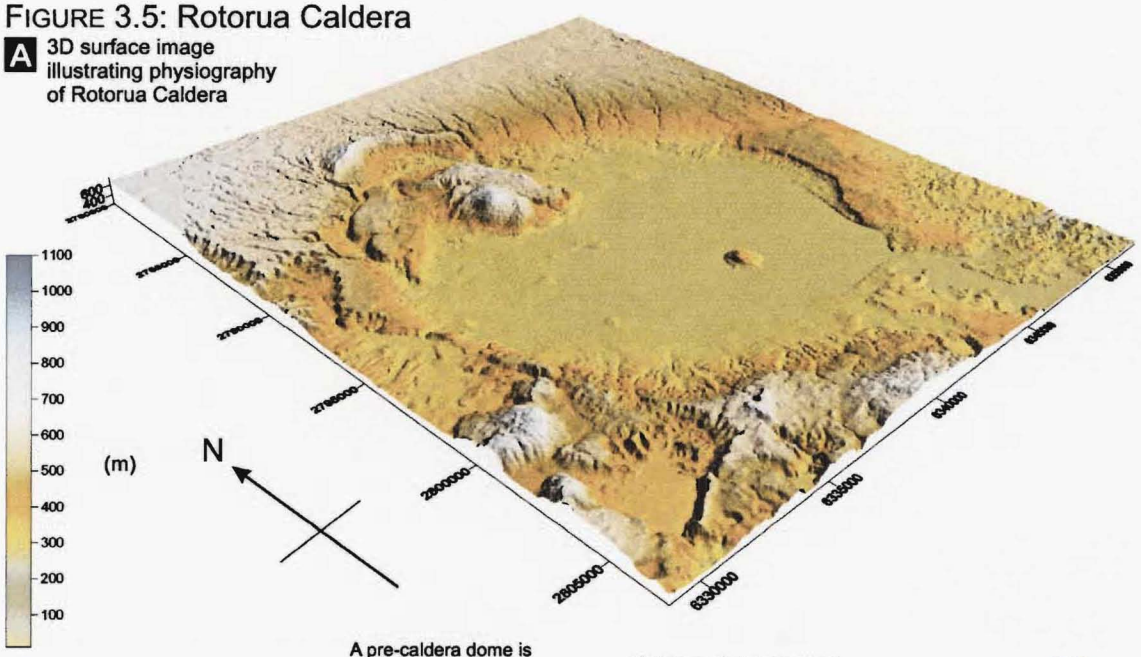

B Schematic image showing the main surface features of the caldera

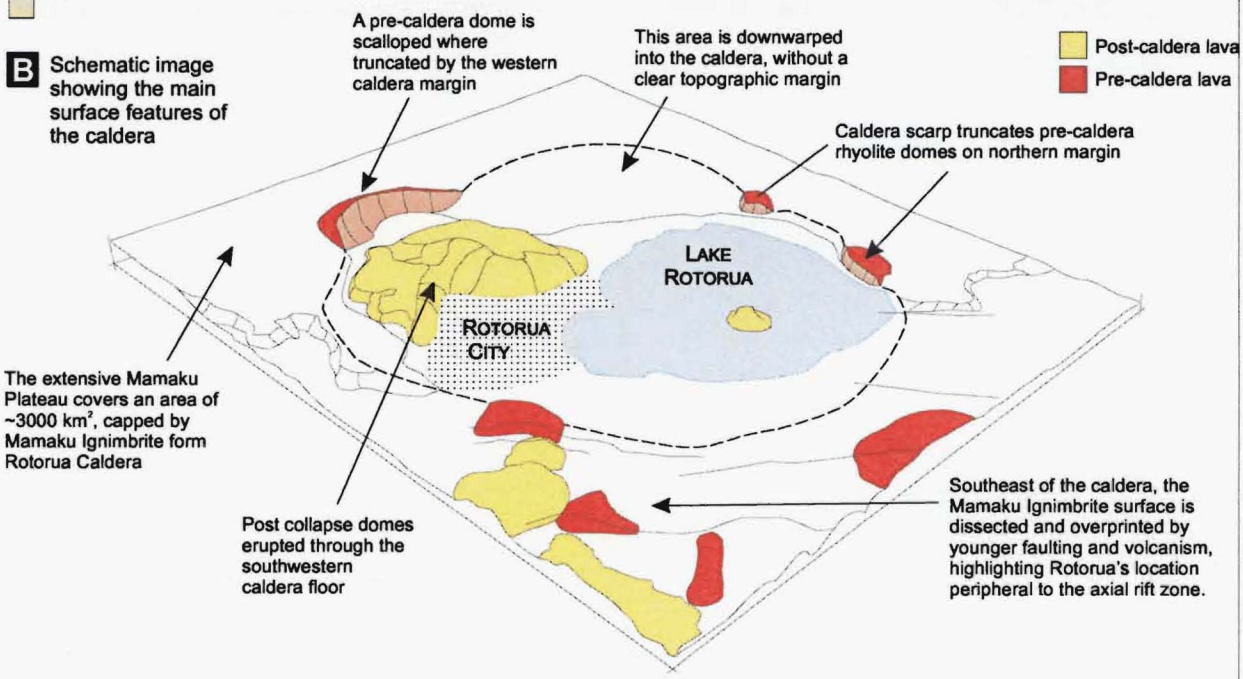

C Gravity contours from HUNT (1994)

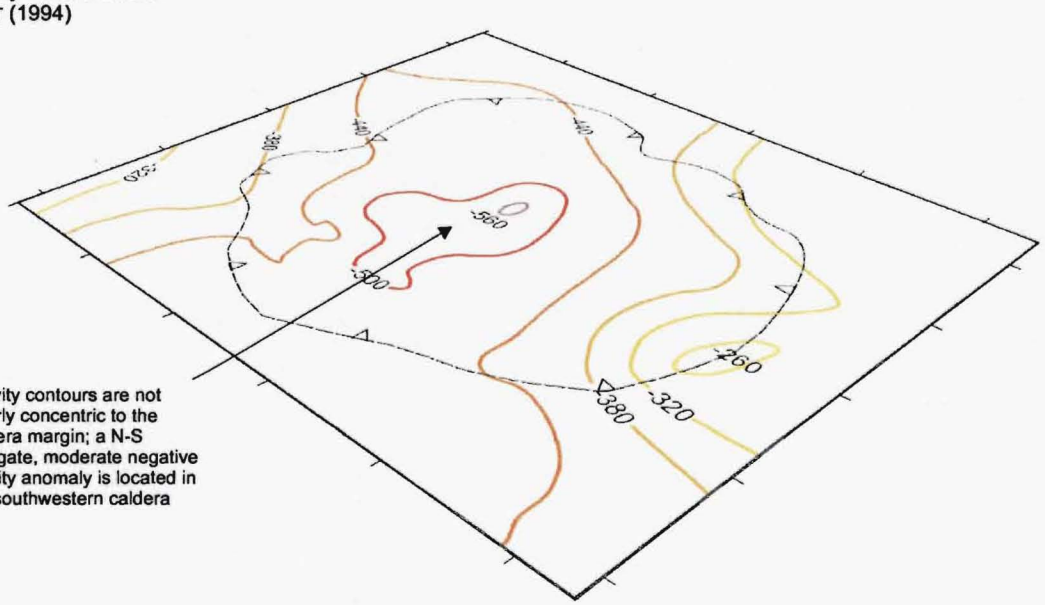

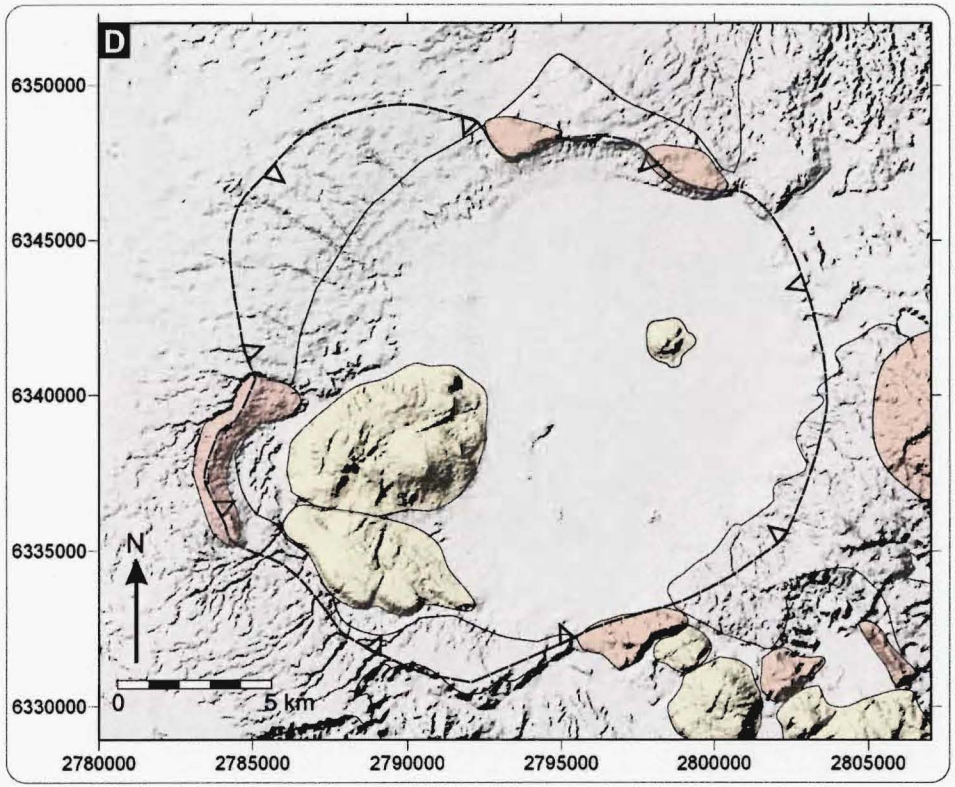

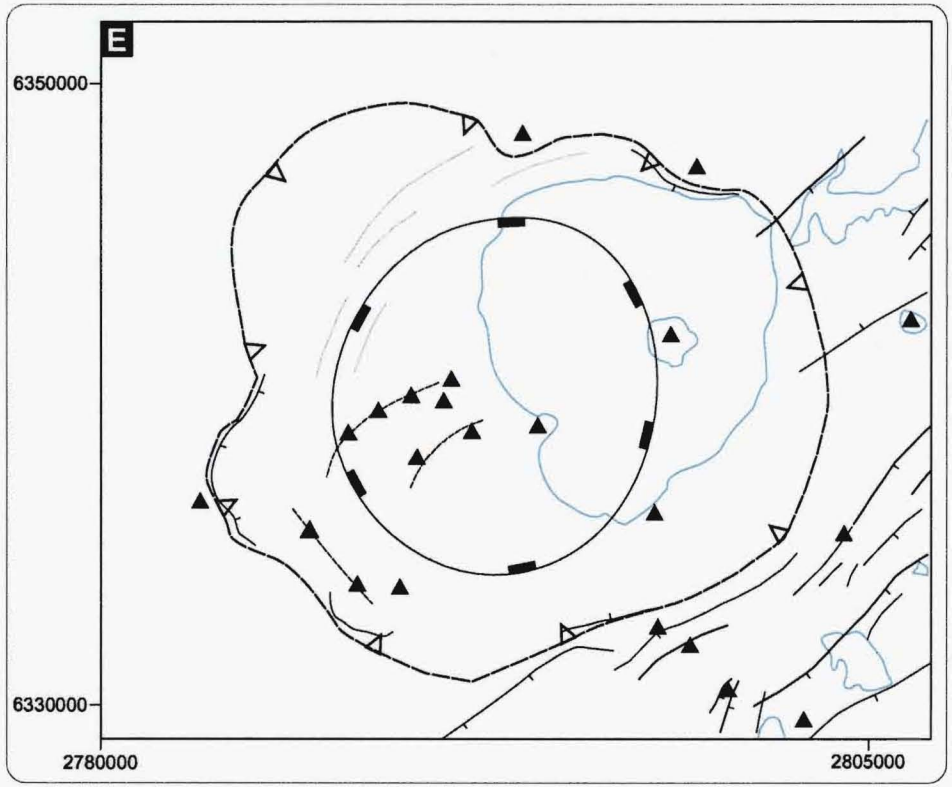

FIGURE 3.5 (cont): (D) Shaded Relief Image of Rotorua Caldera and geology. Shown are pre- and post- caldera lavas and the ignimbrite related to caldera formation. (E) Structure map of Rotorua Caldera generated from analysis of DEM data.

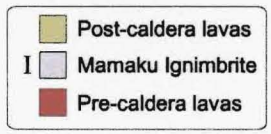

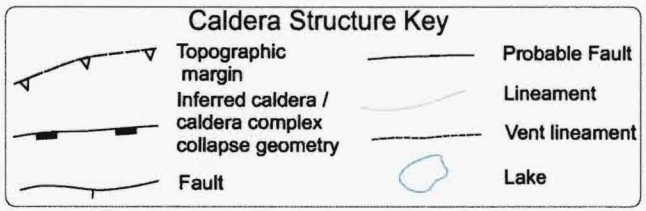

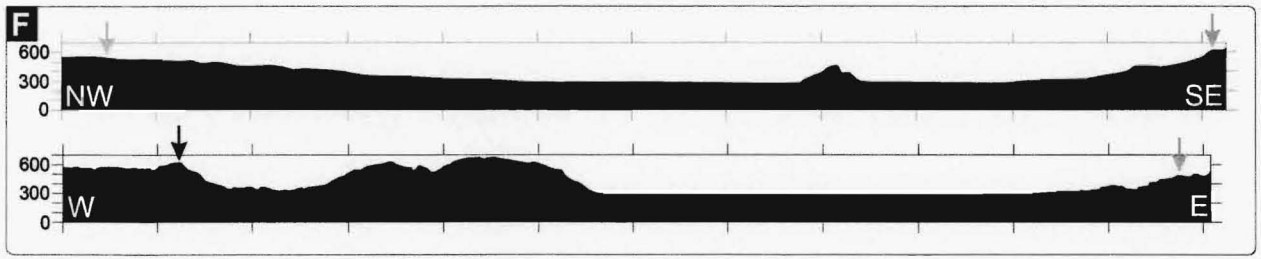

FIGURE 3.5 (cont): (F) Topographic cross-sections of Rotorua Caldera. Arrows mark caldera margin; grey arrows are shown where margin is less certain. 2x vertical exaggeration.

FIGURE 3.6: Reporoa Caldera

A 3D surface image illustrating physiography of Reporoa Caldera

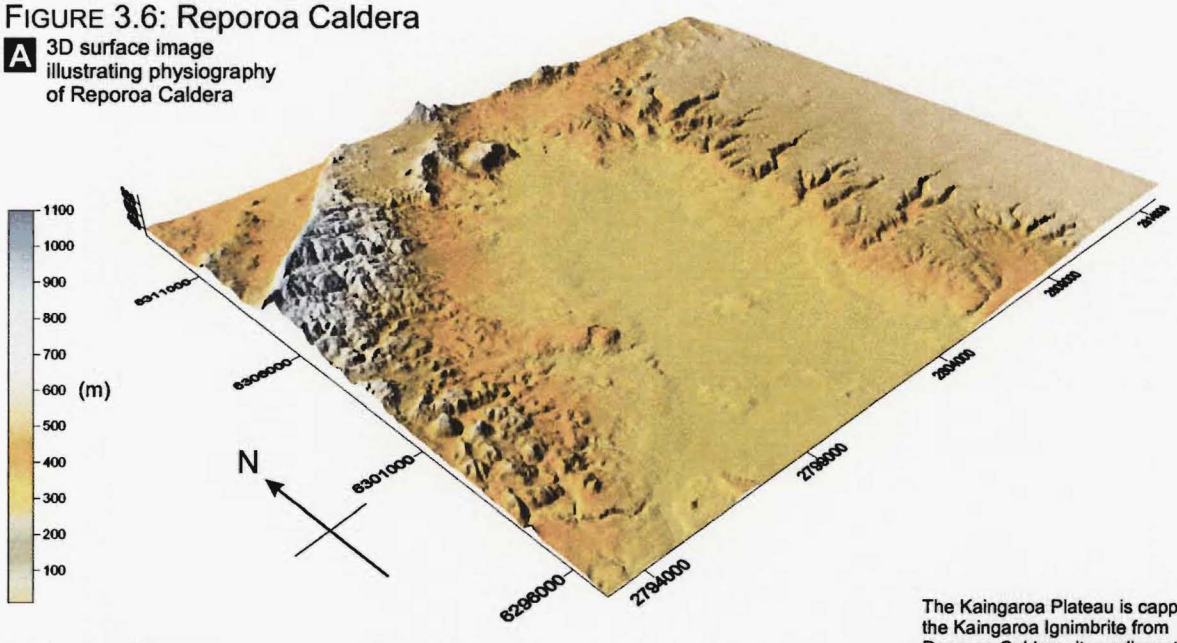

B Schematic image showing the main surface features of the caldera

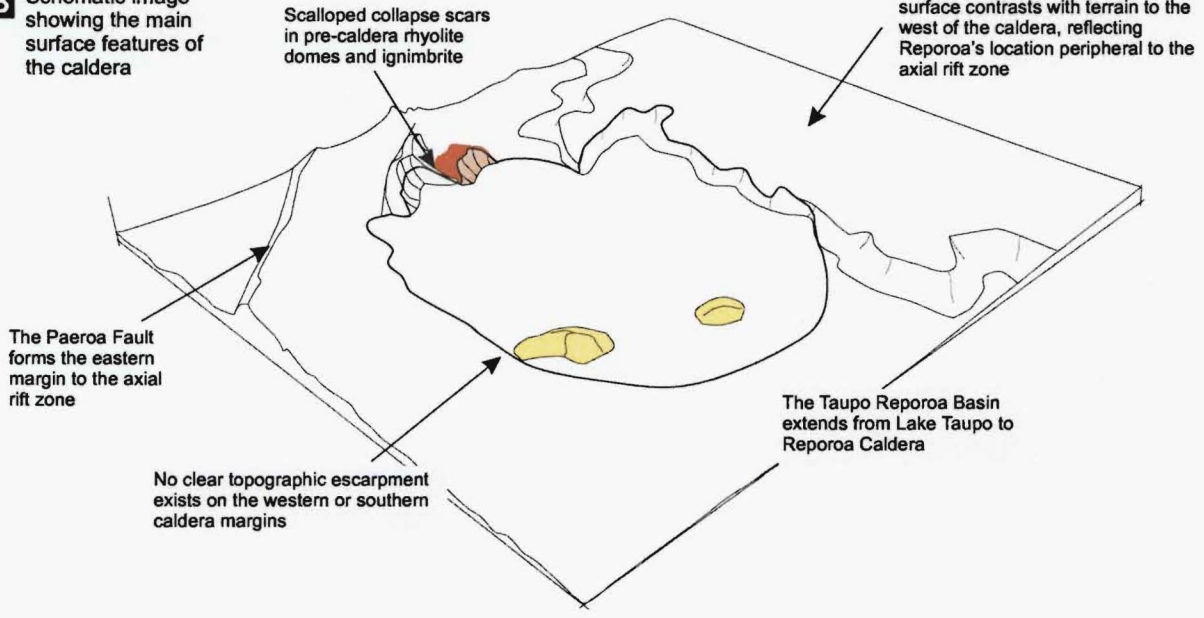

C Gravity contours from NAIRN (1994).

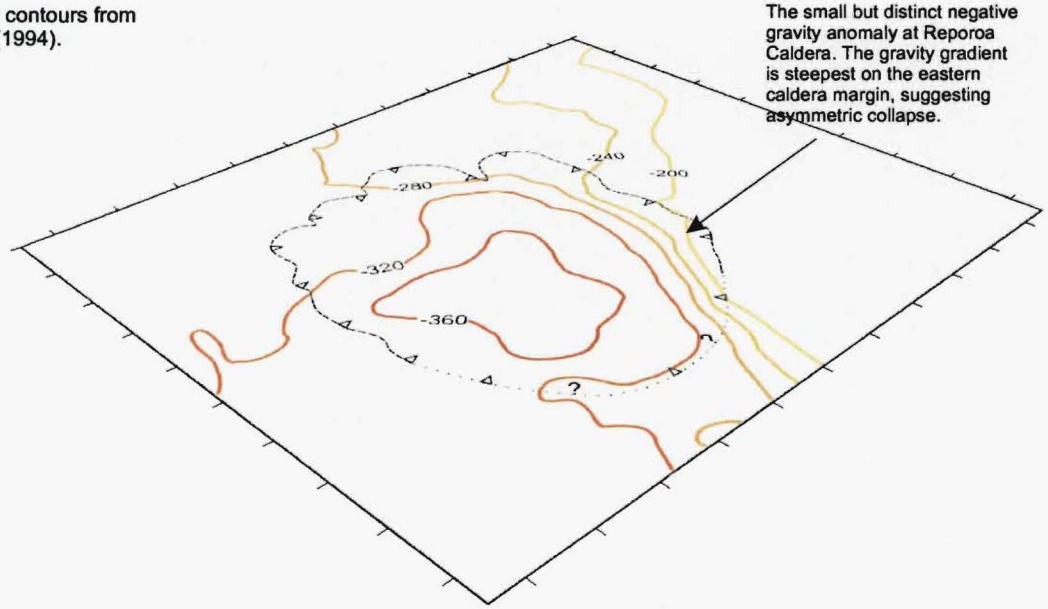

FIGURE 3.7: Okataina Caldera Complex

A 3D surface image illustrating physiography of Okataina Caldera Complex

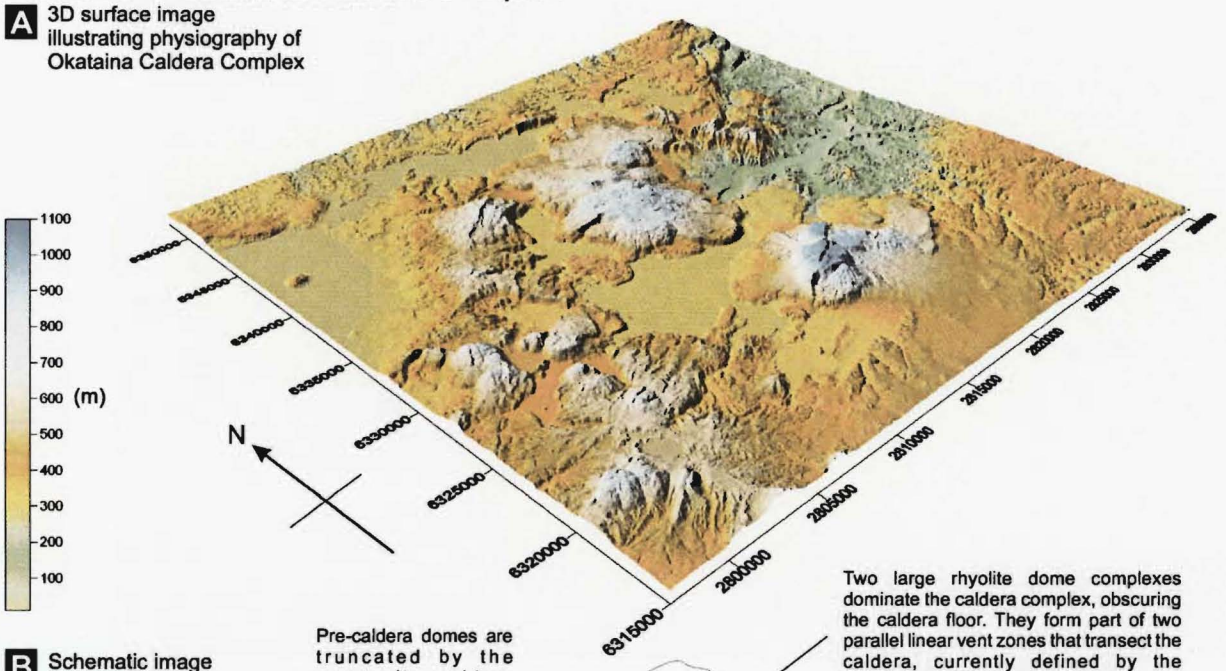

B Schematic image showing the main surface features of the caldera

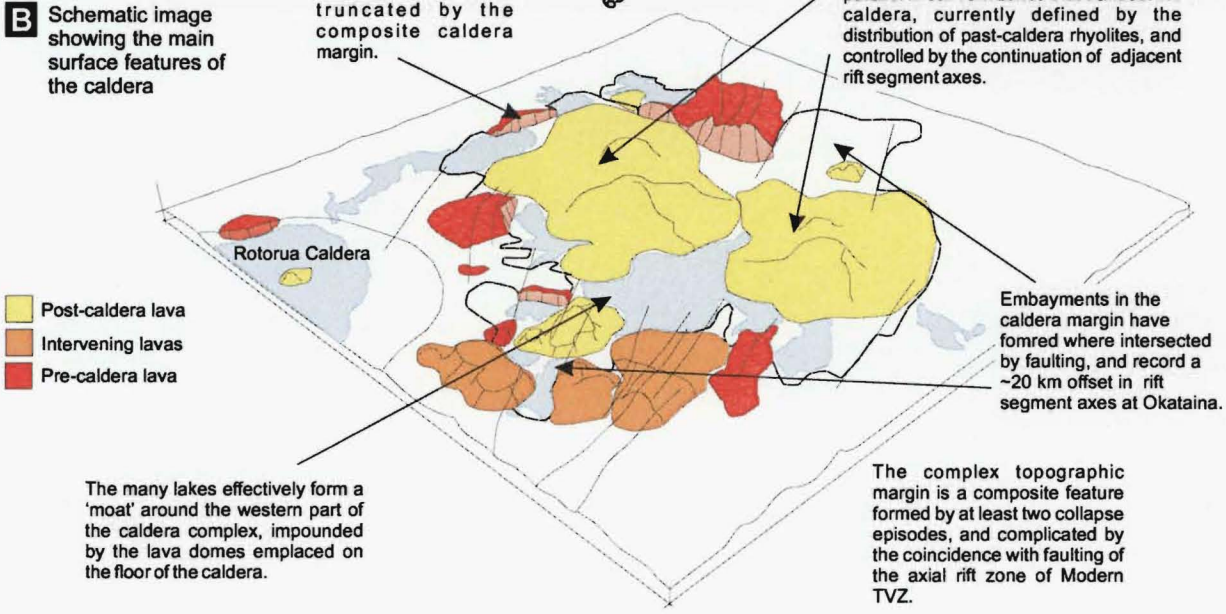

C Gravity contours from NAIRN (2002)

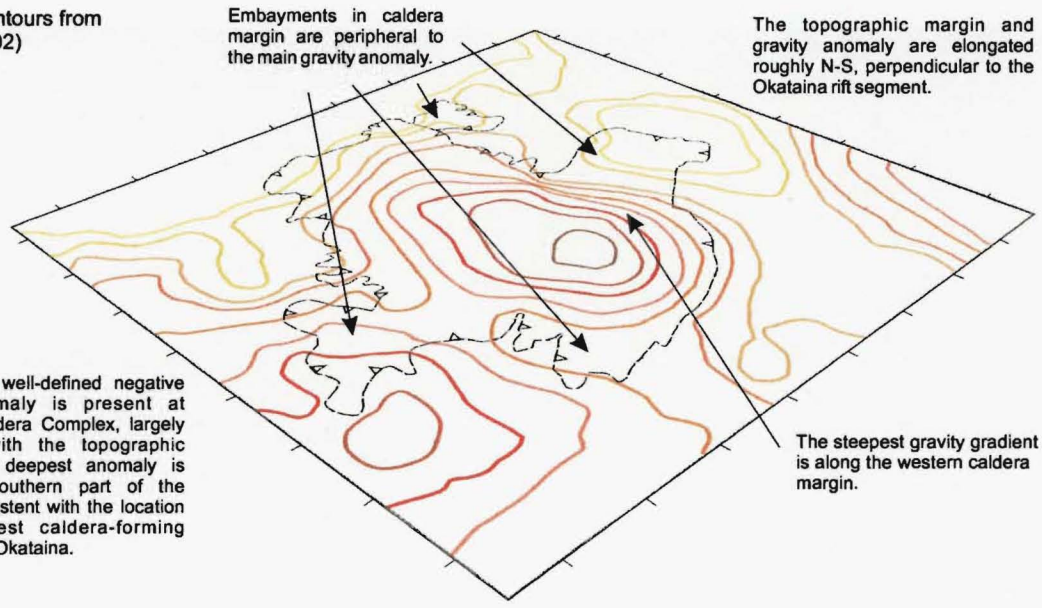

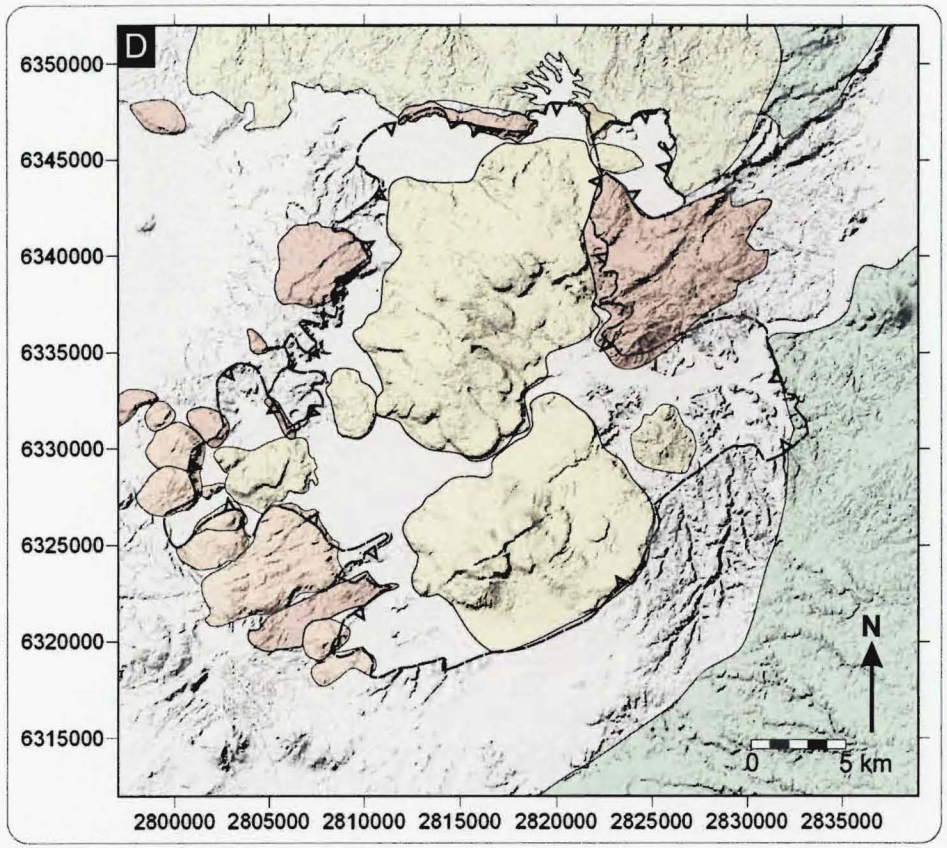

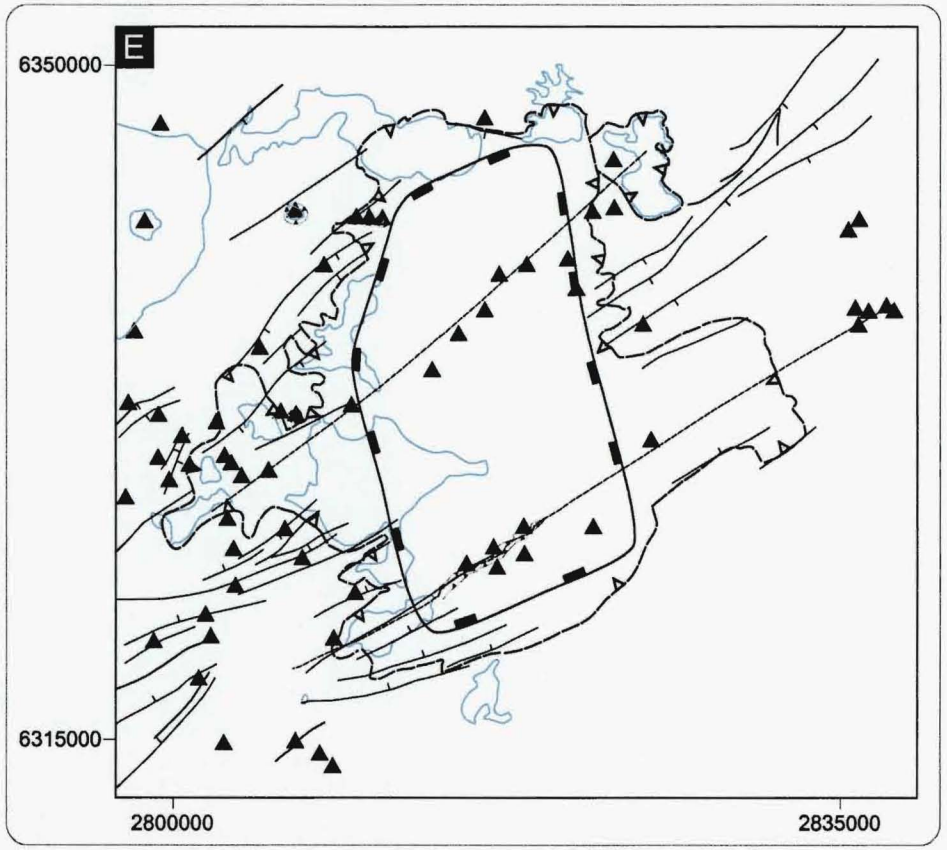

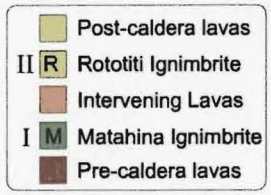

FIGURE 3.7(cont): (D) Shaded relief image of Okataina Caldera Complex (OCC) with key geology. Shown are rhyolite lavas erupted before, between and after the 2 main caldera-forming events. Geology from this study and after Nairn (1989). (E) Structure map of OCC generated from DEM data. Key is the same as for Figure 3.5(E).

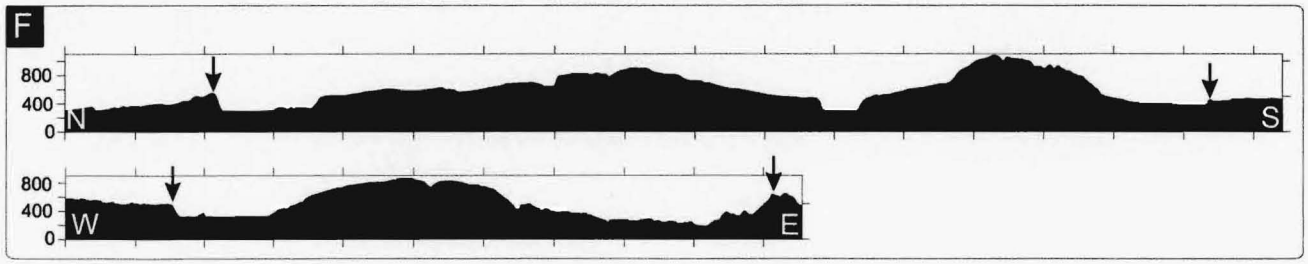

FIGURE 3.7(Cont): (F) Topographic cross-sections of OCC. Arrows mark caldera margin. 2x vertical exaggeration. Ticks along x-axis are 2 km apart.

FIGURE 3.8: Taupo Caldera Complex

A 3D surface image illustrating physiography of Taupo Caldera Complex

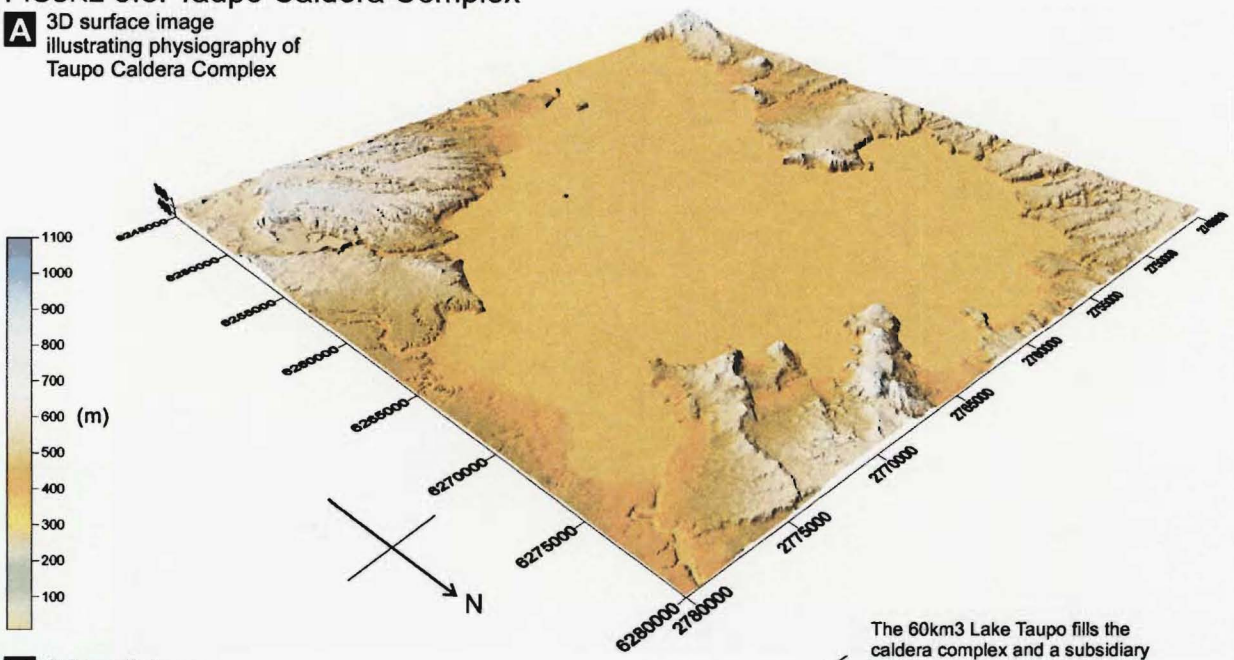

B Schematic image showing the main surface features of the caldera

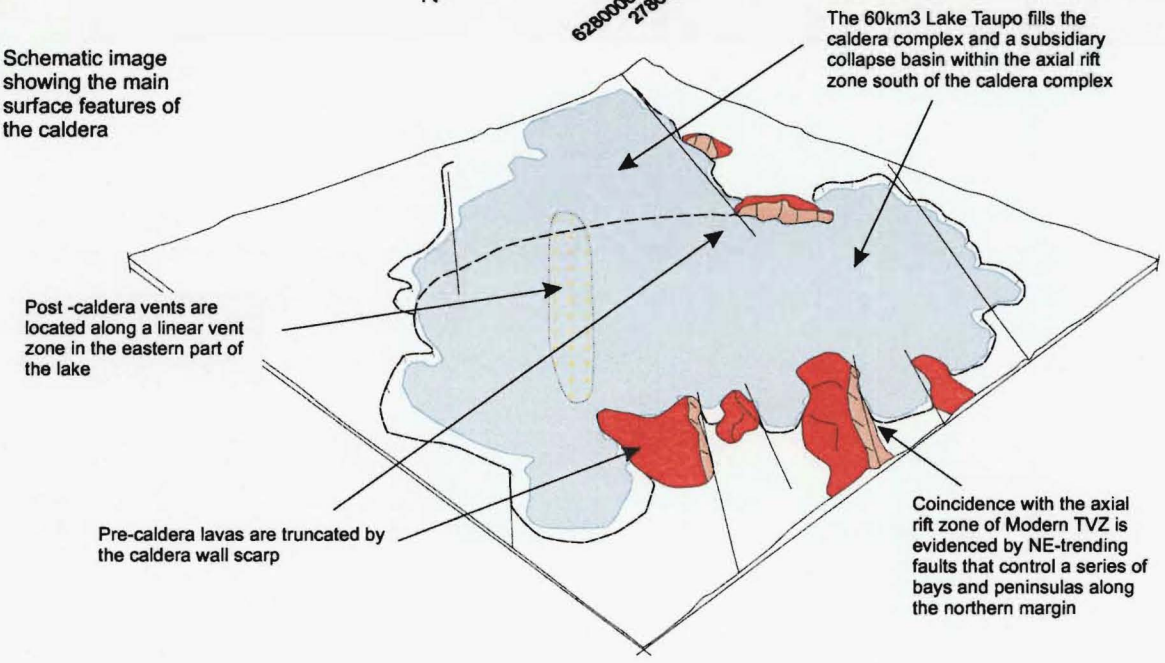

C Gravity contours from DAVY & CALDWELL (1998)

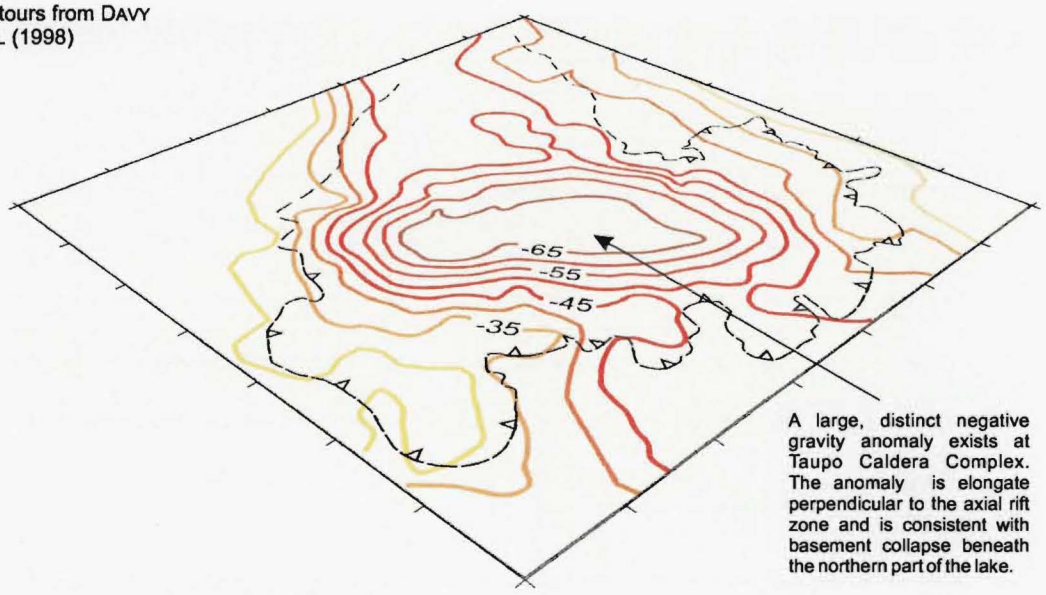

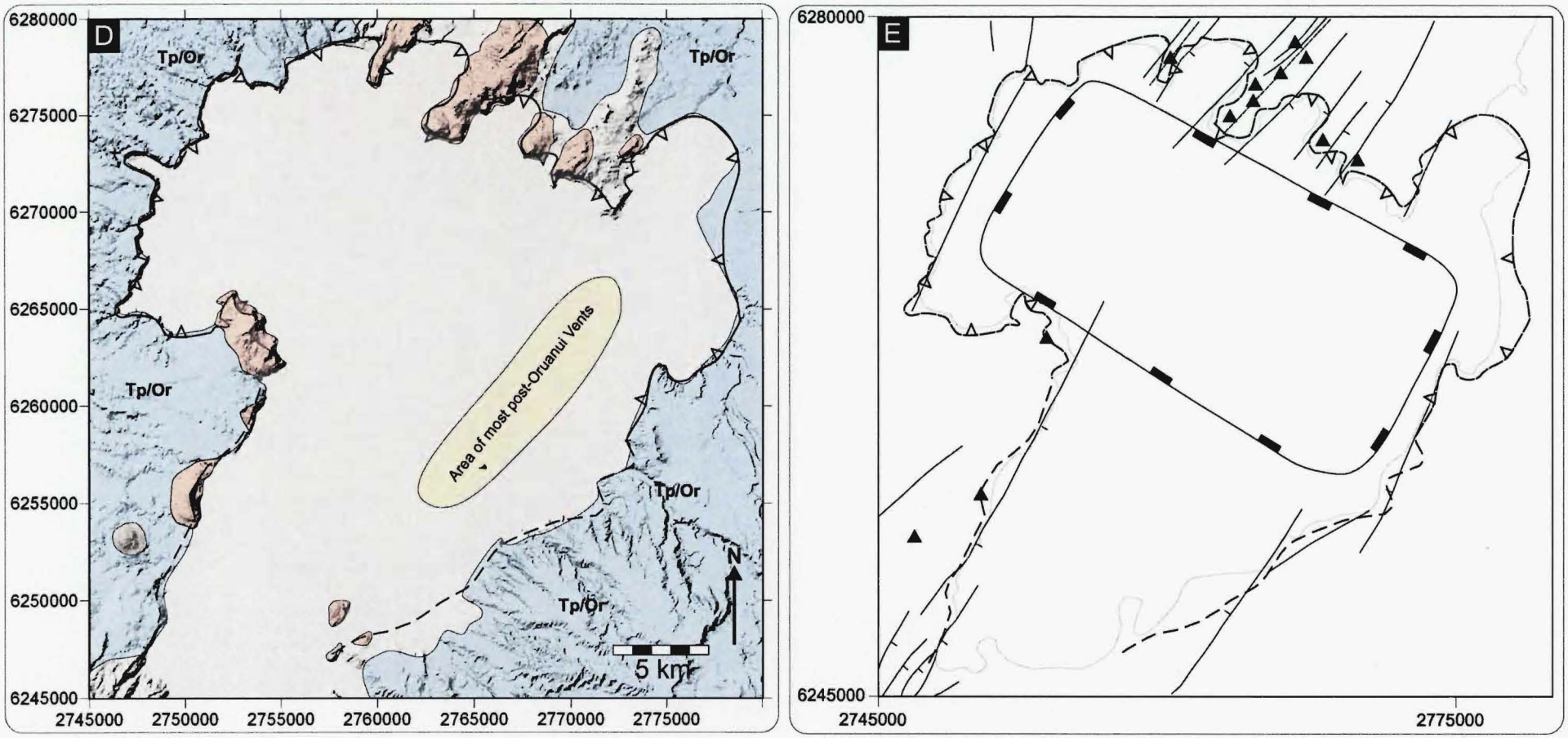

FIGURE 3.8 (cont): (D) Shaded relief image of Taupo Caldera Complex with key Geology. Shown are the pre-caldera lavas, caldera-forming ignimbrites, and the location of post-oruanui (collapse I) vents. Geology from this study and after COLE *et al* (1998). (E) Structure map of Taupo generated from analysis of DEM data. Key is the same as for Figure 2.5 (E).

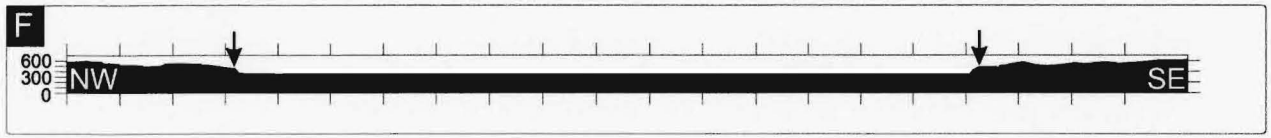

FIGURE 3.8 (cont): Topographic cross-section of Taupo Caldera Complex. Arrows mark caldera margin. 2x vertical exaggeration. Ticks along x-axis are 2 km apart.

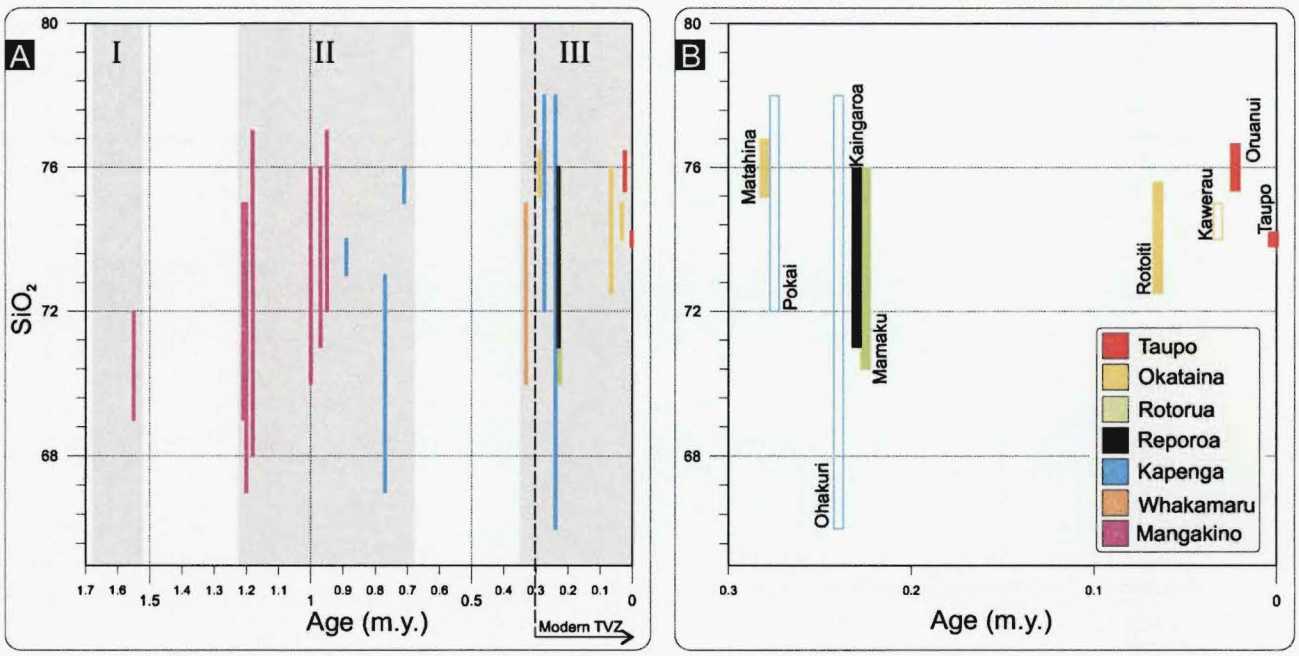

FIGURE 3.9: (A) SiO_2 variation in caldera-forming ignimbrites, shown as a function of erupted age and caldera source. (B) Expanded period of Modern TVZ (< 300 ka).

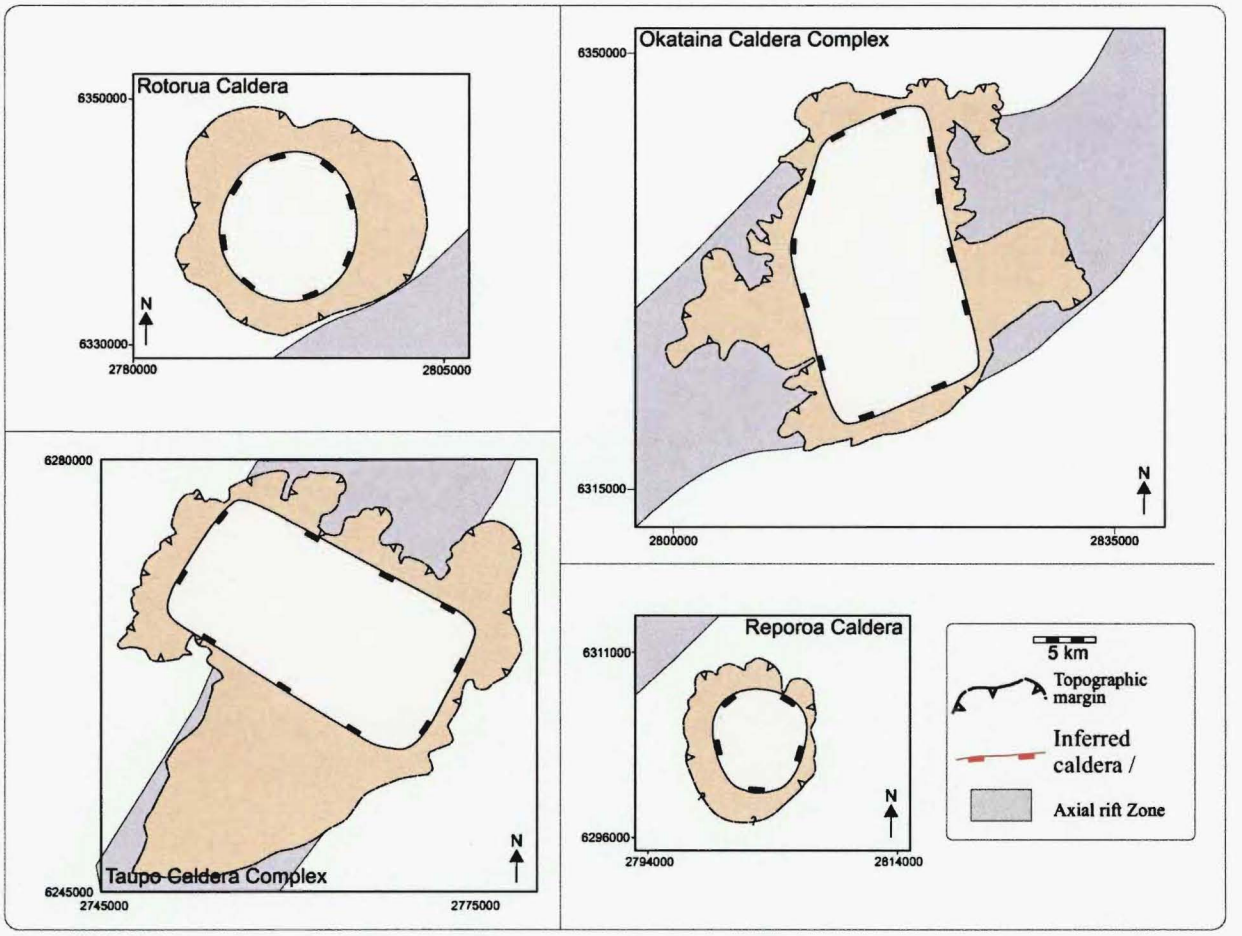

FIGURE 3.10 Calderas of Modern TVZ at the same scale for comparison, and the location of each caldera with respect to the axial rift zone (grey shading). The two single event calderas, Rotorua and Reporoa, are peripheral to the rift, while the two active caldera complexes, Okataina and Taupo, are located within the rift. Note the significant step between adjacent rift segments at Okataina, and relationship to embayments in the topographic margin at Okataina and Taupo. Inset (above) shows location of each caldera within TVZ.

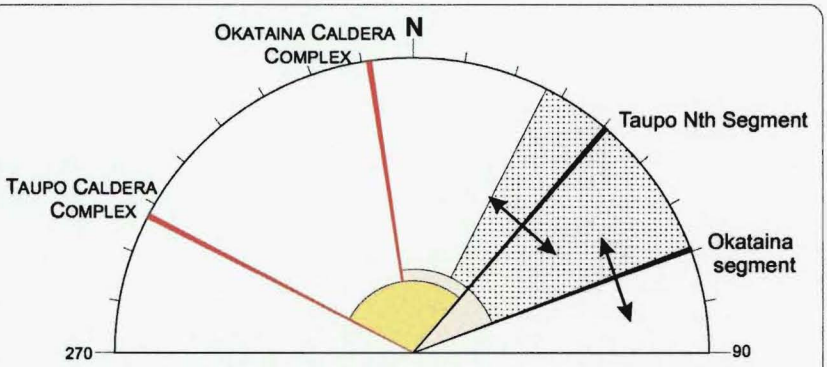

Caldera	Eccentricity $E = L_{min}/L_{max}$	Caldera Trend	Rift Segment trend
Okataina	0.55	352°	70°
Taupo	0.55	297°	41°
Rotorua	0.78	65°	
Reporoa	0.81	0°	

FIGURE 3.11: A summary of the main features (eccentricity and trend) of the studied calderas, and their relationship to the trend of rift segment axes and their extension direction (arrows). Extension directions from ACOCELLA, SPINKS et al (2003). Dotted sector represents the range in trend of rift segments in the central rhyolitic portion of TVZ for comparison.

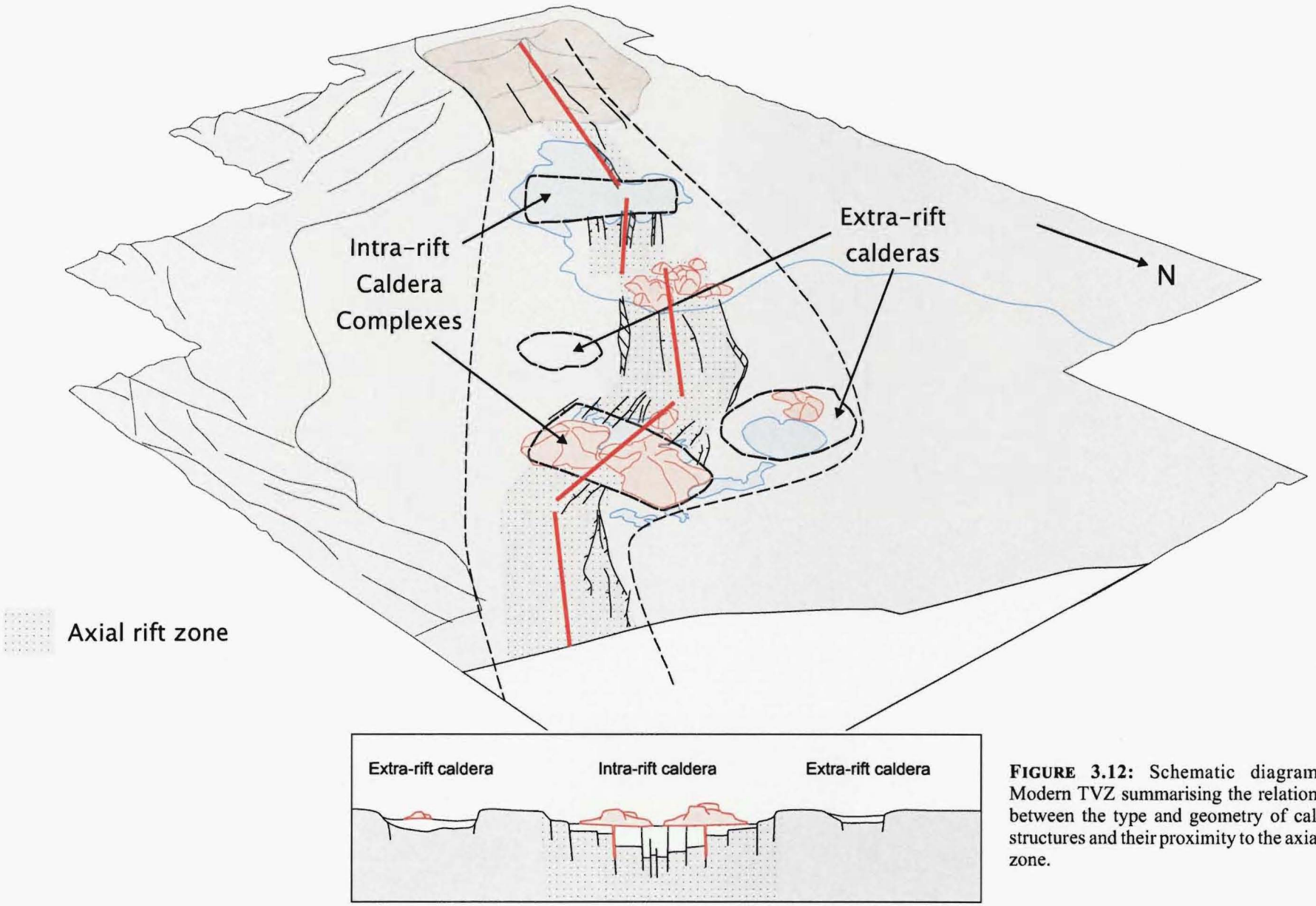

FIGURE 3.12: Schematic diagram of Modern TVZ summarising the relationship between the type and geometry of caldera structures and their proximity to the axial rift zone.

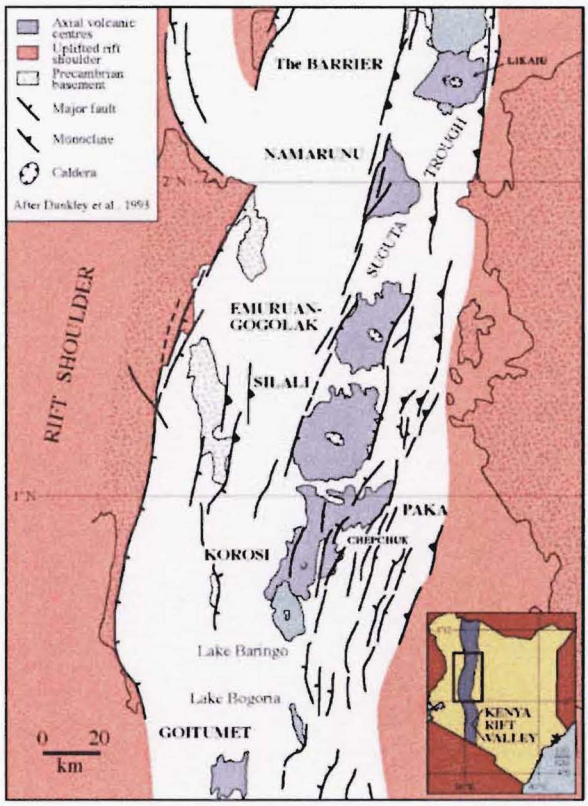

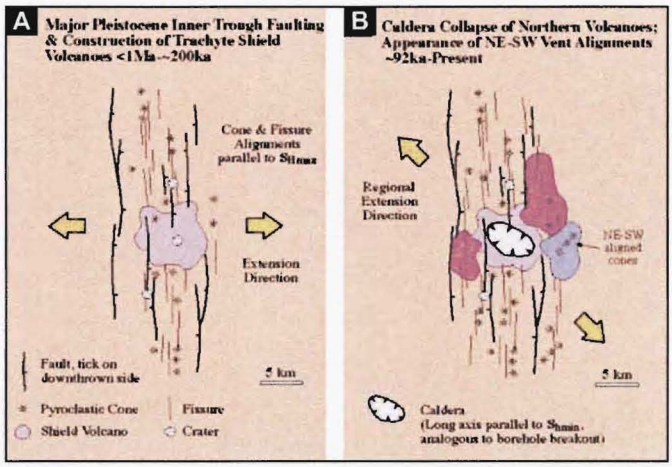

▲ **FIGURE 4.2:** Proposed interaction between Pleistocene regional stress fields and the evolution of axial shield volcanoes in the northern Kenyan rift valley. Caldera collapse (elongate NW-SE) and development of NE-SW volcanic lineaments were caused by ~45° rotation of the regional stress field sometime at about 200-100 ka. From BOSWORTH *et al* (2000).

◀ **FIGURE 4.1:** Major faulting and location of axial volcanoes in the northern Kenya rift. From BOSWORTH *et al* (2000).

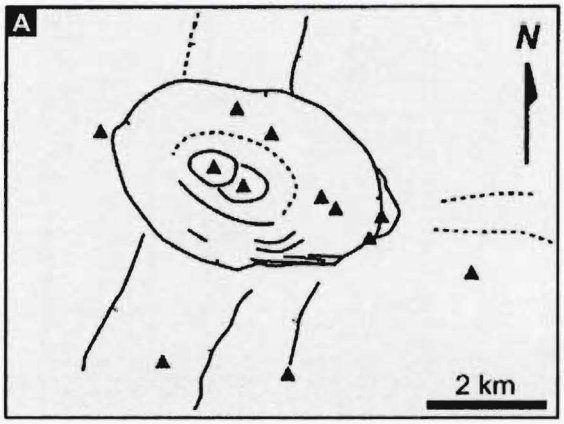

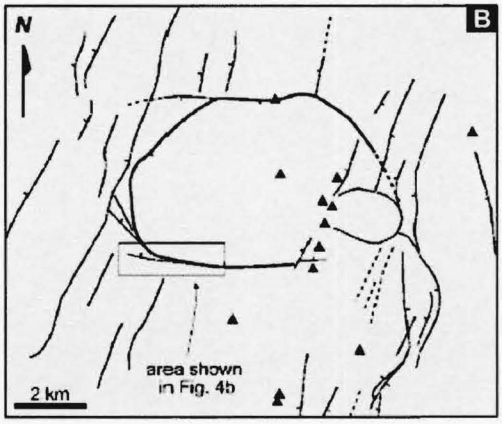

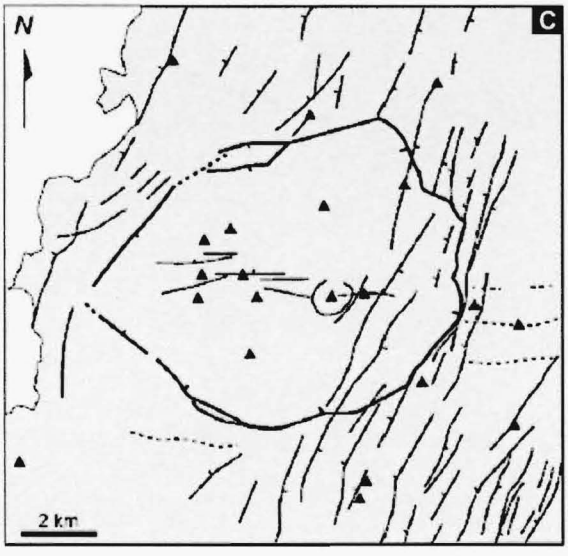

FIGURE 4.3: Structural maps of three Quaternary calderas in the Ethiopian Rift (a) Fantale; (b) Gariboldi; (c) Gedemsa. E-W elongate calderas are oblique to NW-SE extension and thought to relate to pre-rift E-W trending structures (ACOCELLA *et al.*, 2002).

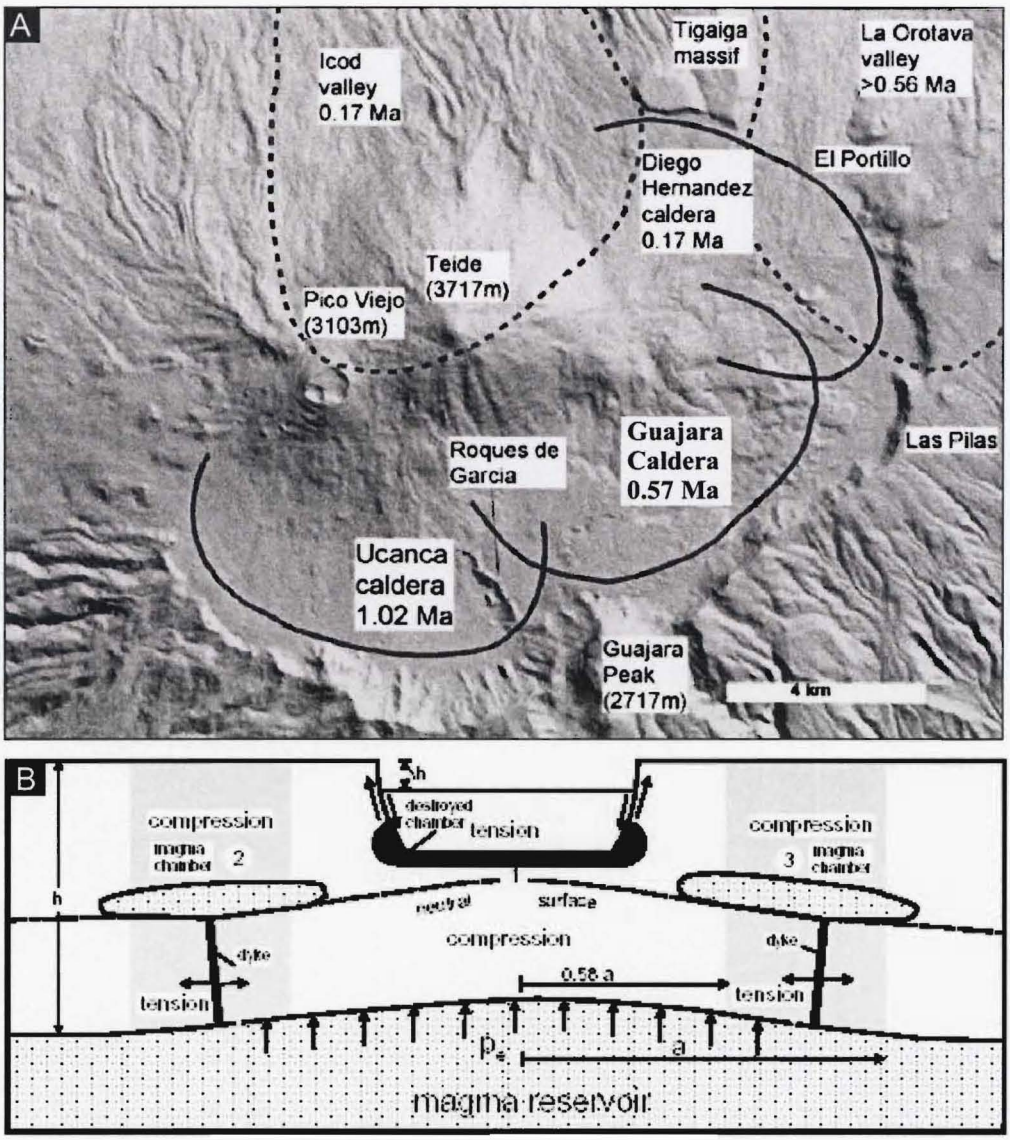

▲ **FIGURE 4.4:** (A) Shaded relief image of the three overlapping calderas (solid lines) at Las Canadas in Tenerife; (B) Formation of overlapping calderas due to migration of magma chambers following caldera collapse. Reduction in crustal thickness and changes in local stress field encourage dike injection wither side of old chamber. From MARTI & GUDMUNDSSON (2000).

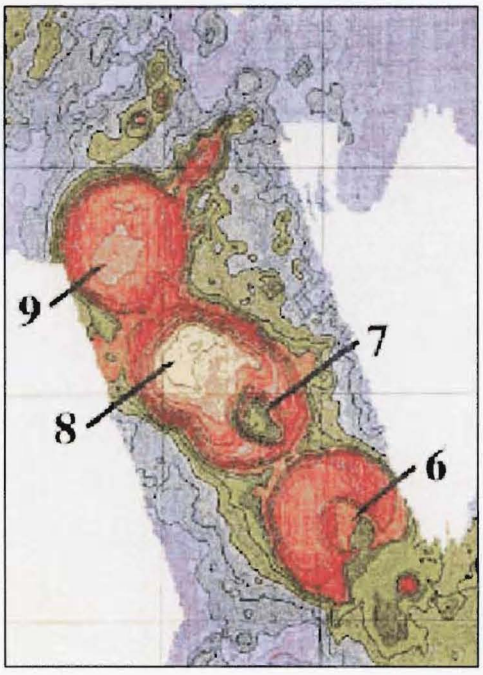

▶ **FIGURE 4.5:** Enlargement of part of the Juan de Fuca ridge showing offset craters and calderas on the Vance seamount chain. Note the distinct caldera on volcano No. 7. Craters and calderas are on the ridge-facing side of the volcano and interpreted as forming when the youngest conduits are abandoned. Bathymetric contour interval is 50m. From HAMMOND (1997)

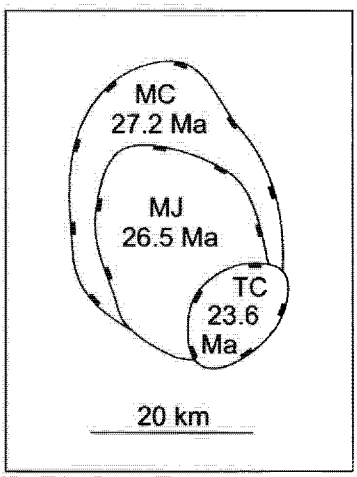

◀ **FIGURE 4.6:** The inferred configuration of the overlapping to nested Moores Creek (MC), Mount Jefferson (MJ), and Trail Canyon (TC) calderas at Toquima caldera complex, Nevada Caldera. Southeastward migration of caldera volcanism parallels regional NW-Striking faults suggesting fundamental structural control of the rise and eruption of magma. Redrawn after BODEN (1986).

▶ **FIGURE 4.7:** Rectilinear structural caldera margins and major structural features at the Silent Canyon caldera complex (SCC). Redrawn after FERGUSON *et al* (1994).

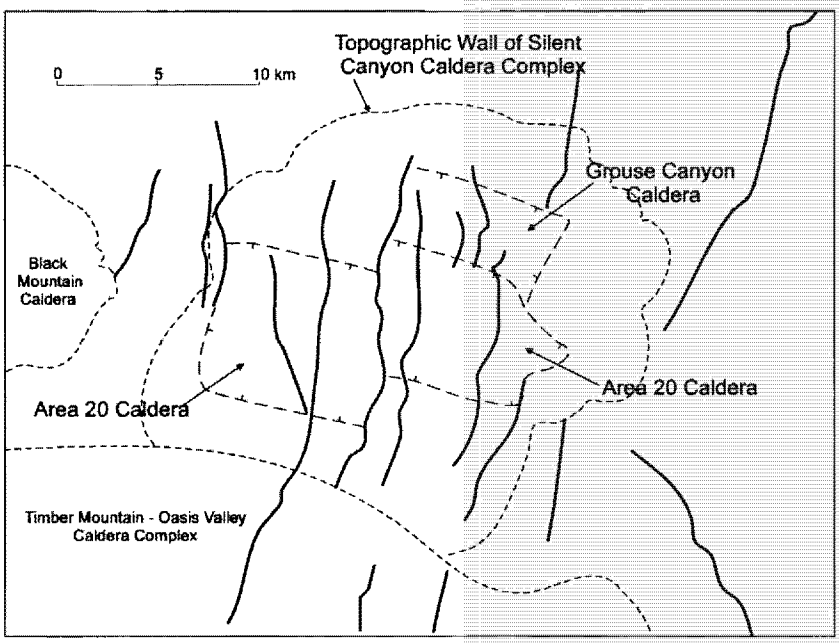

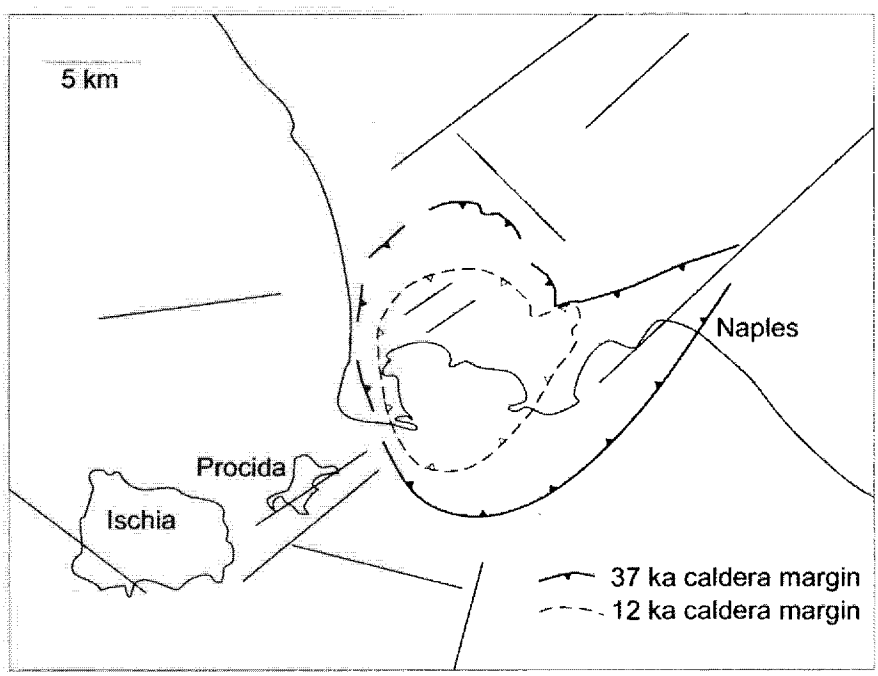

◀ **FIGURE 4.8:** Structural map of the Campi Flegrei district after ACOCELLA *et al* (1999) and ORSI *et al* (1996). Conspicuous rectilinear margins for part of the Campi Flegrei caldera are related to NE-trending regional faults in a NE-SW trending transfer zone.

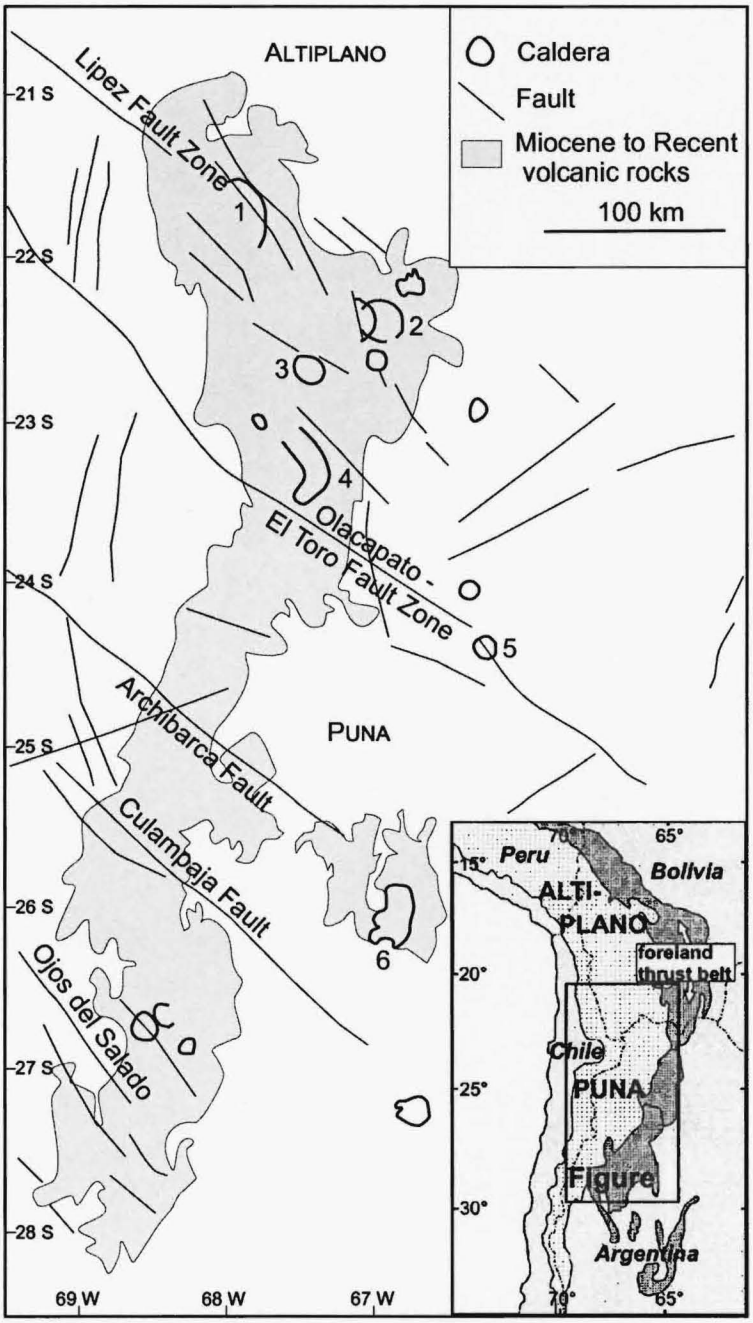

FIGURE 4.9: Simplified structural map of the southern central Andes showing dominant faults and calderas. Numbers indicate calderas: 1, Cerro Pastos Grandes; 2, Vilama; 3, Cerro Guacha; 4, La Pacana; 5, Negra Muerta; 6, Cerro Galan. Redrawn an adapted after RILLER *et al* (2001).

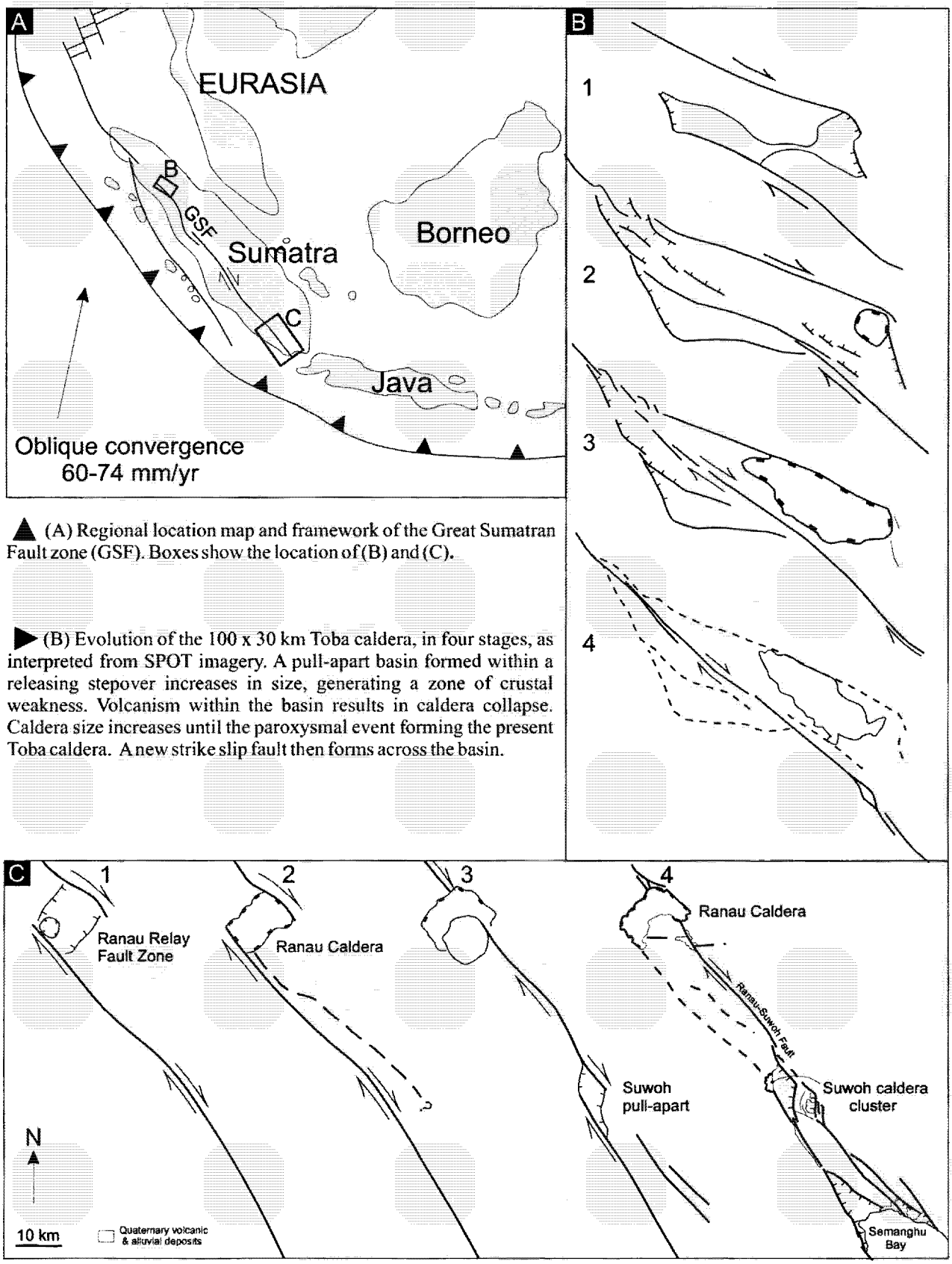

▲ (A) Regional location map and framework of the Great Sumatran Fault zone (GSF). Boxes show the location of (B) and (C).

▶ (B) Evolution of the 100 x 30 km Toba caldera, in four stages, as interpreted from SPOT imagery. A pull-apart basin formed within a releasing stepover increases in size, generating a zone of crustal weakness. Volcanism within the basin results in caldera collapse. Caldera size increases until the paroxysmal event forming the present Toba caldera. A new strike slip fault then forms across the basin.

▲ (C) Development of the Ranau and Suwoh stepovers, and associated calderas. (1) A pull-apart basin forms within a releasing stepover, with normal faults bounding the future Ranau caldera. (2) Increasing volcanism causes incremental caldera growth until a paroxysmal eruption results in collapse margins coincident with stepover boundary faults. (3) Extinction of the Ranau stepover is marked by a new strike slip fault forming across the basin. (4) Calderas presently forming within Suwoh pull-apart equivalent to early development of the Ranau stepover.

FIGURE 4.10: Development of the Ranau and Toba calderas within releasing pull-apart structures along the Great Sumatran Fault zone. Modified from BELLIER & SEBRIER (1994), and BELLIER *et al.*, (1999).

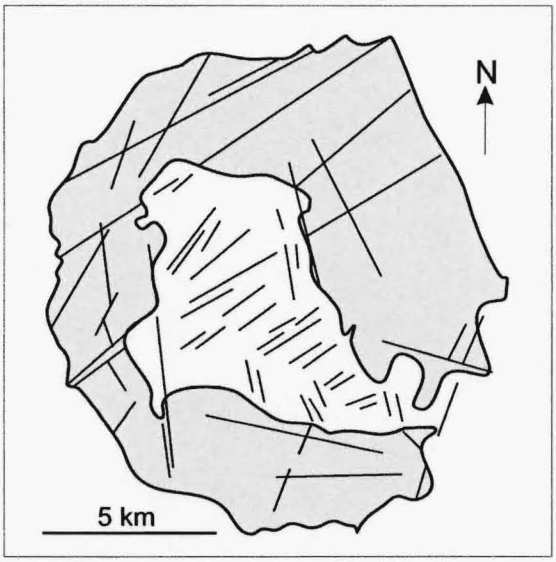

◀ **FIGURE 4.11:** Simplified tectonic map of Deception Island highlighting the dense network of structural lineations crossing the island. The caldera margin appears to reflect the intersection of orthogonal linear faults rather than by an arcuate 'ring-fault'. After MARTI *et al* (1996).

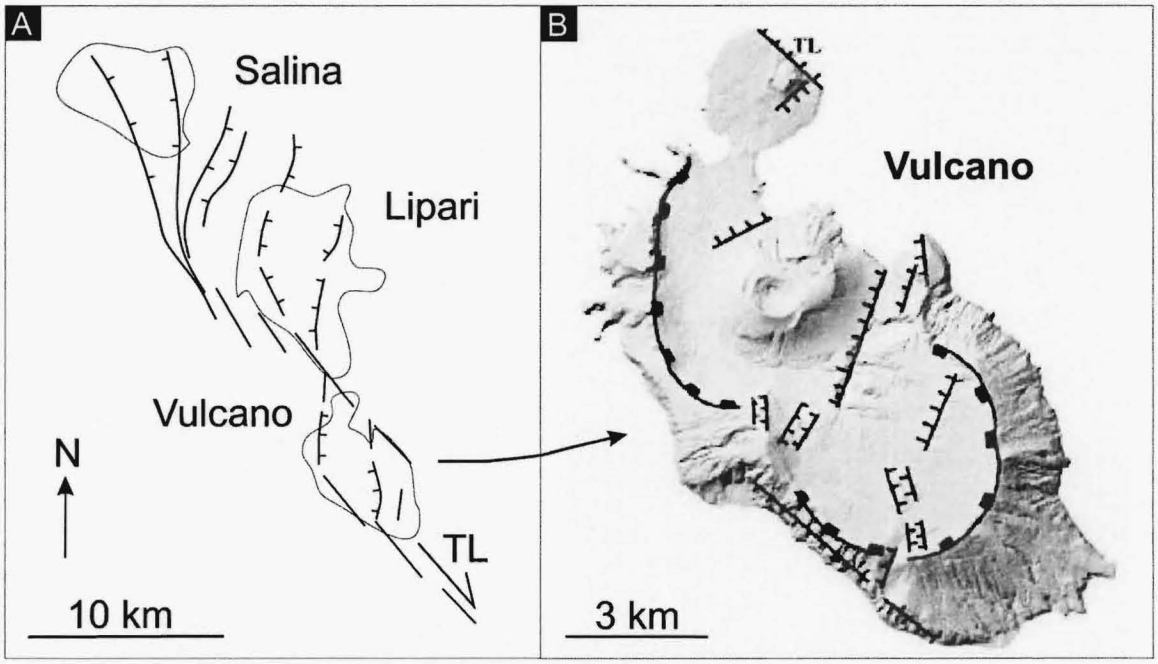

▲ **FIGURE 4.12** (A) Interpretation of the fault systems in the Vulcano-Lipari-Salina region; (B) Shaded relief and simplified structural map of Vulcano. From GIONCADA *et al* (2003).

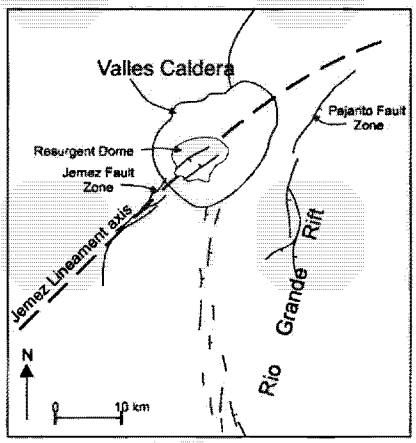

FIGURE 4.13 (A) Tectonic sketch map of the major structural features in the Jemez Mountains showing the Rio Grande Rift, Jemez Lineament and the Valles Caldera. Redrawn from SELF *et al* (1986).

(B) Schematic NW-SE cross-section of the Valles Caldera, based on deep drill hole and geophysical data. Redrawn from HEIKEN *et al* (1990).

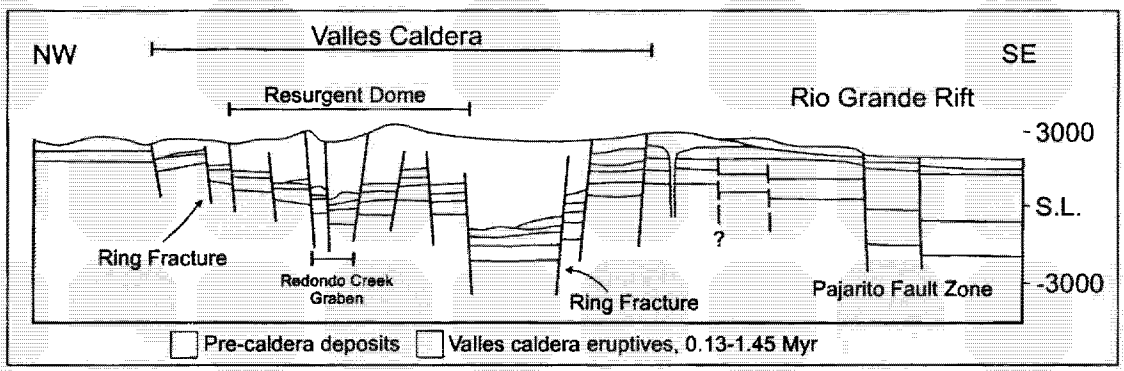

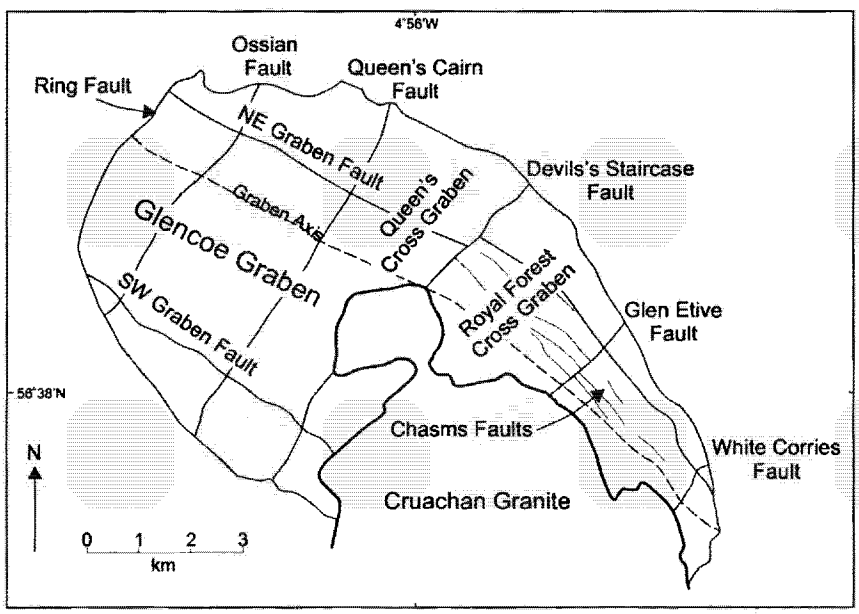

FIGURE 4.14 (A) Map showing the main structural features of Glencoe Caldera volcano. Redrawn from MOORE & KOKELAAR (1998).

(B) Simplified block showing the model presented by MOORE & KOKELAAR (1997) for piecemeal caldera collapse at Glencoe. Redrawn from MOORE & KOKELAAR (1997).

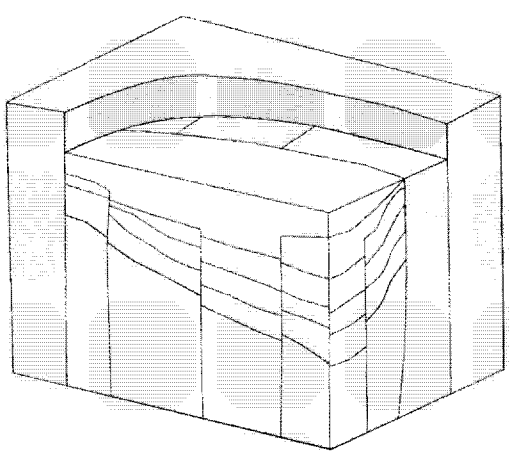

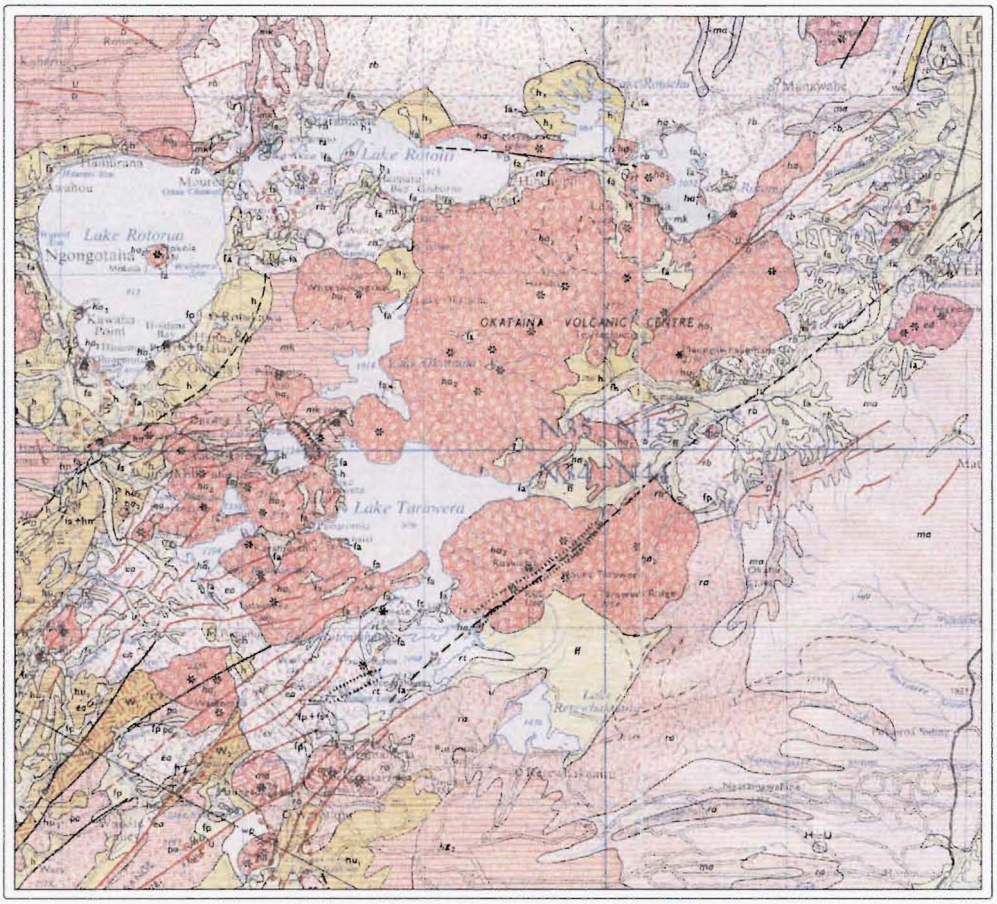

FIGURE 5.1: Healy et al (1964) map of the Okataina area

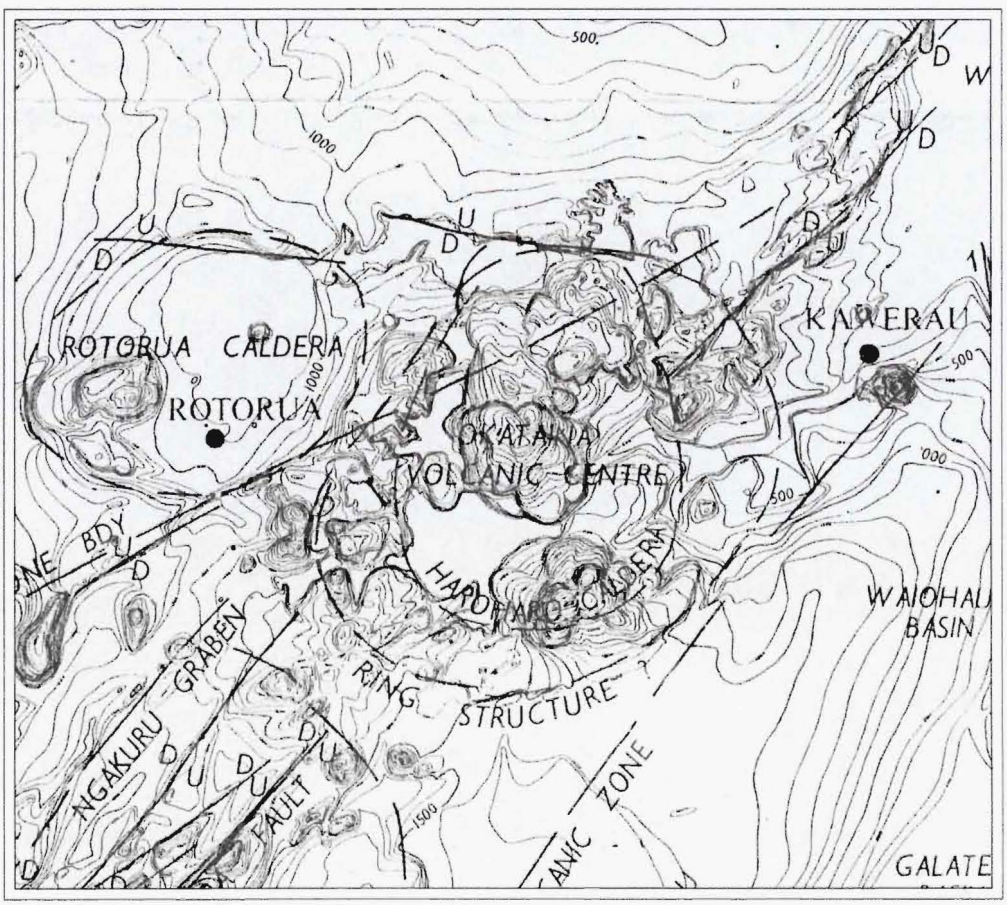

FIGURE 5.2: HEALY'S (1964) caldera and ring structure based on smoothed topographic contours.

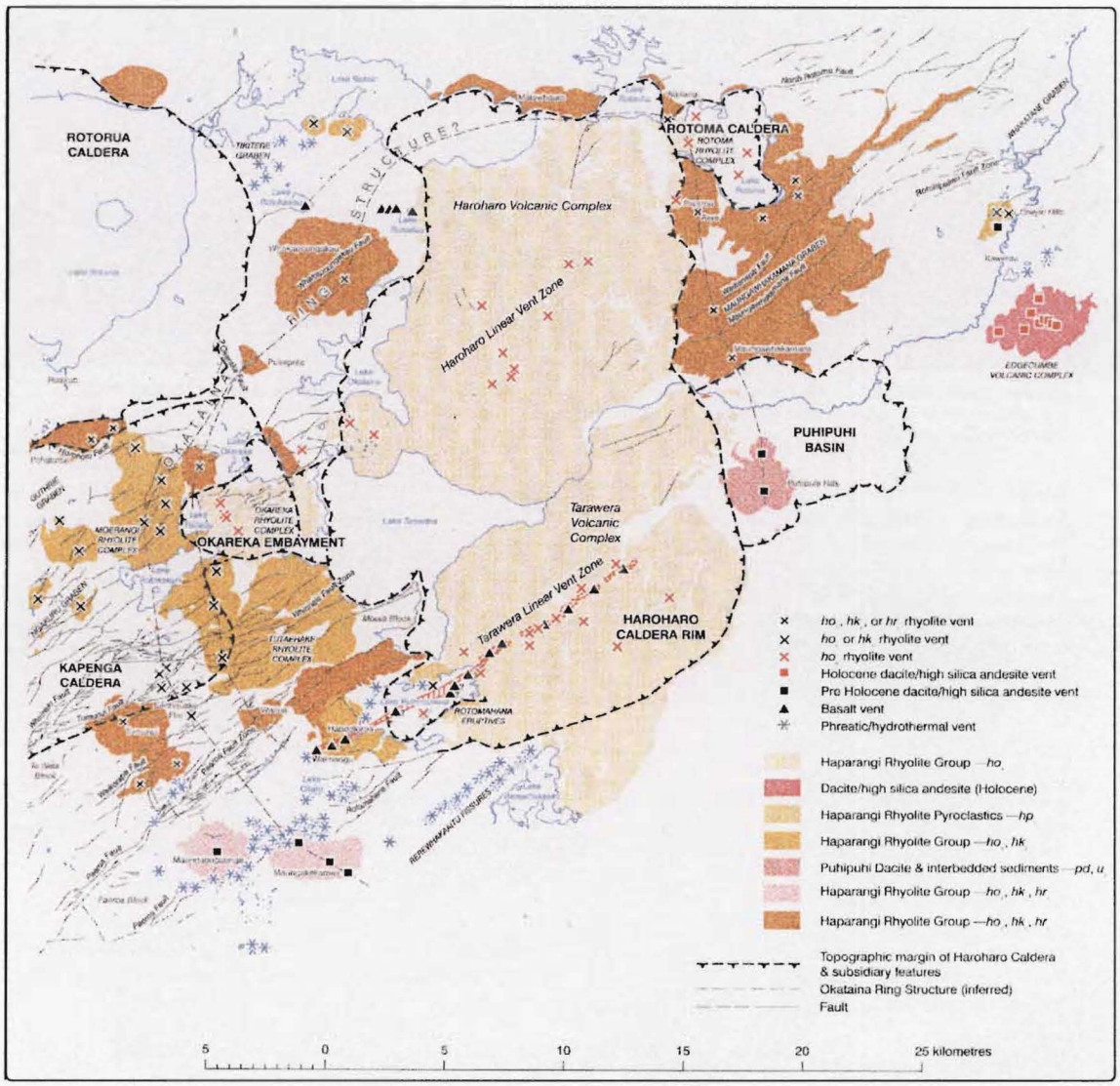

FIGURE 5.3: NAIRN'S (2002) 'Regional tectonic map of the Okataina Volcanic Centre'.

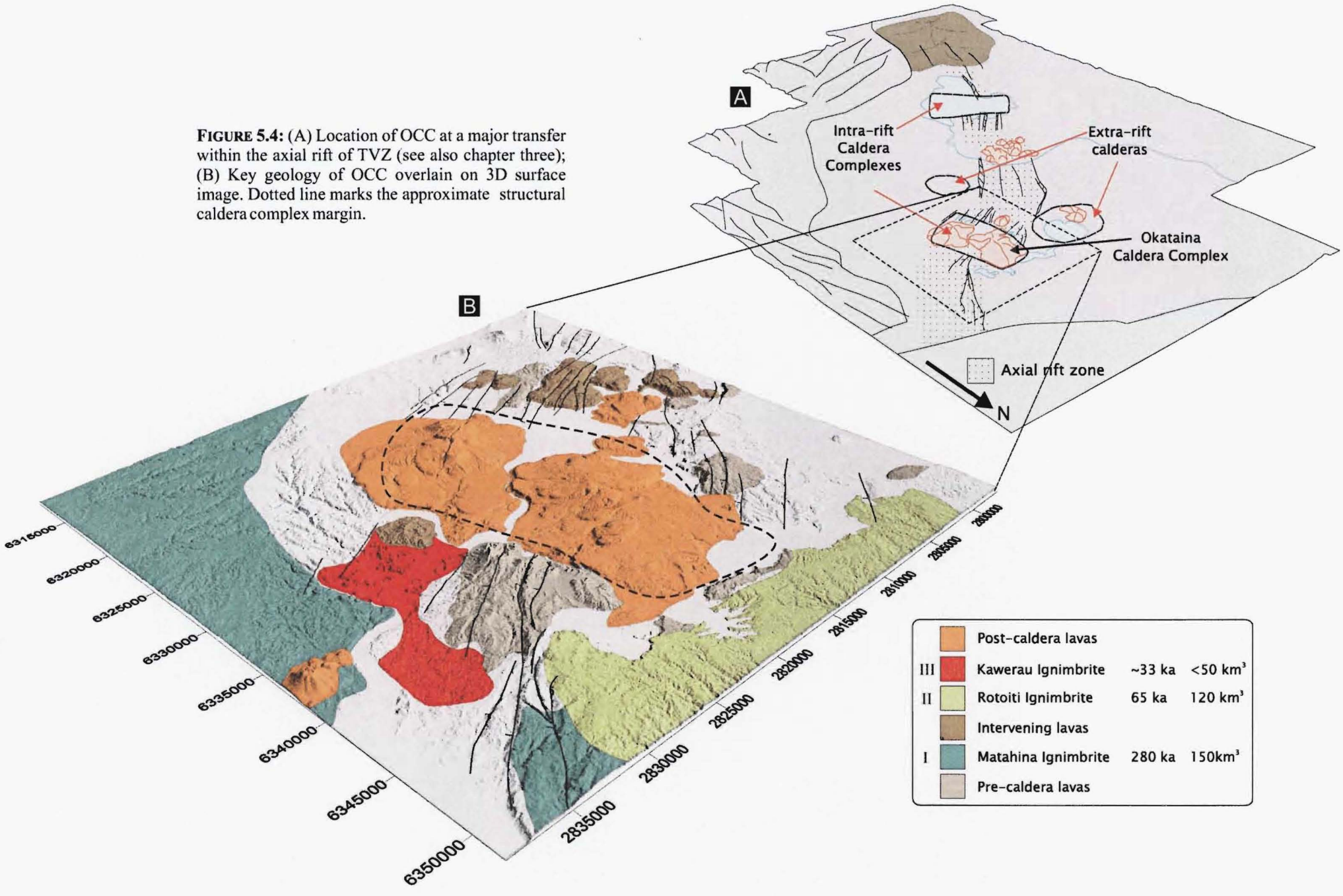

FIGURE 5.4: (A) Location of OCC at a major transfer within the axial rift of TVZ (see also chapter three); (B) Key geology of OCC overlain on 3D surface image. Dotted line marks the approximate structural caldera complex margin.

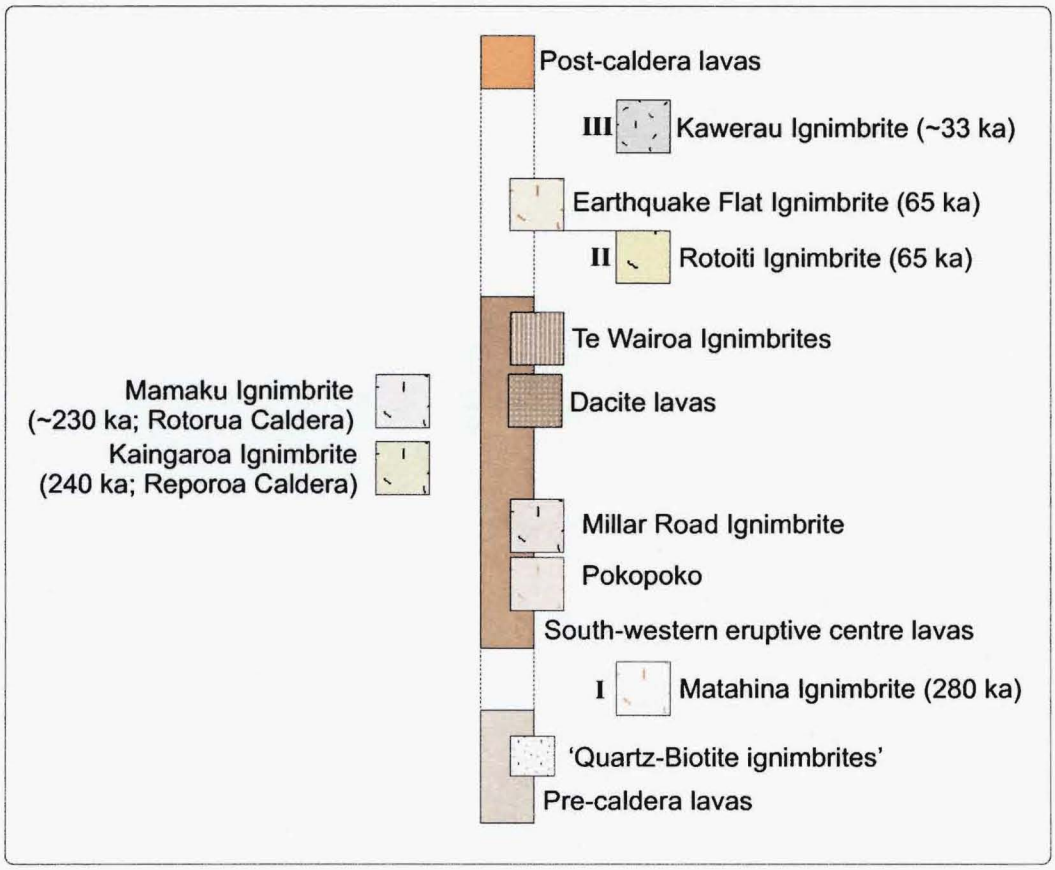

FIGURE 5.5: Stratigraphic column for the key eruptive units at OCC. The column relates to the model of eruptive history on the following two pages. Central column of lavas is shown as semi-continuous since time breaks are only apparent and most lavas are not dated. Pyroclastic deposits on the periphery of the caldera are shown overlapping with lavas since most relate to dome-building episodes, predominantly in the south-western eruptive centre (see text for discussion). Successive caldera-forming eruptions at OCC are marked as I, II and III respectively. Units on far left are major deposits from caldera sources adjacent to OCC. No vertical time scale is assumed.

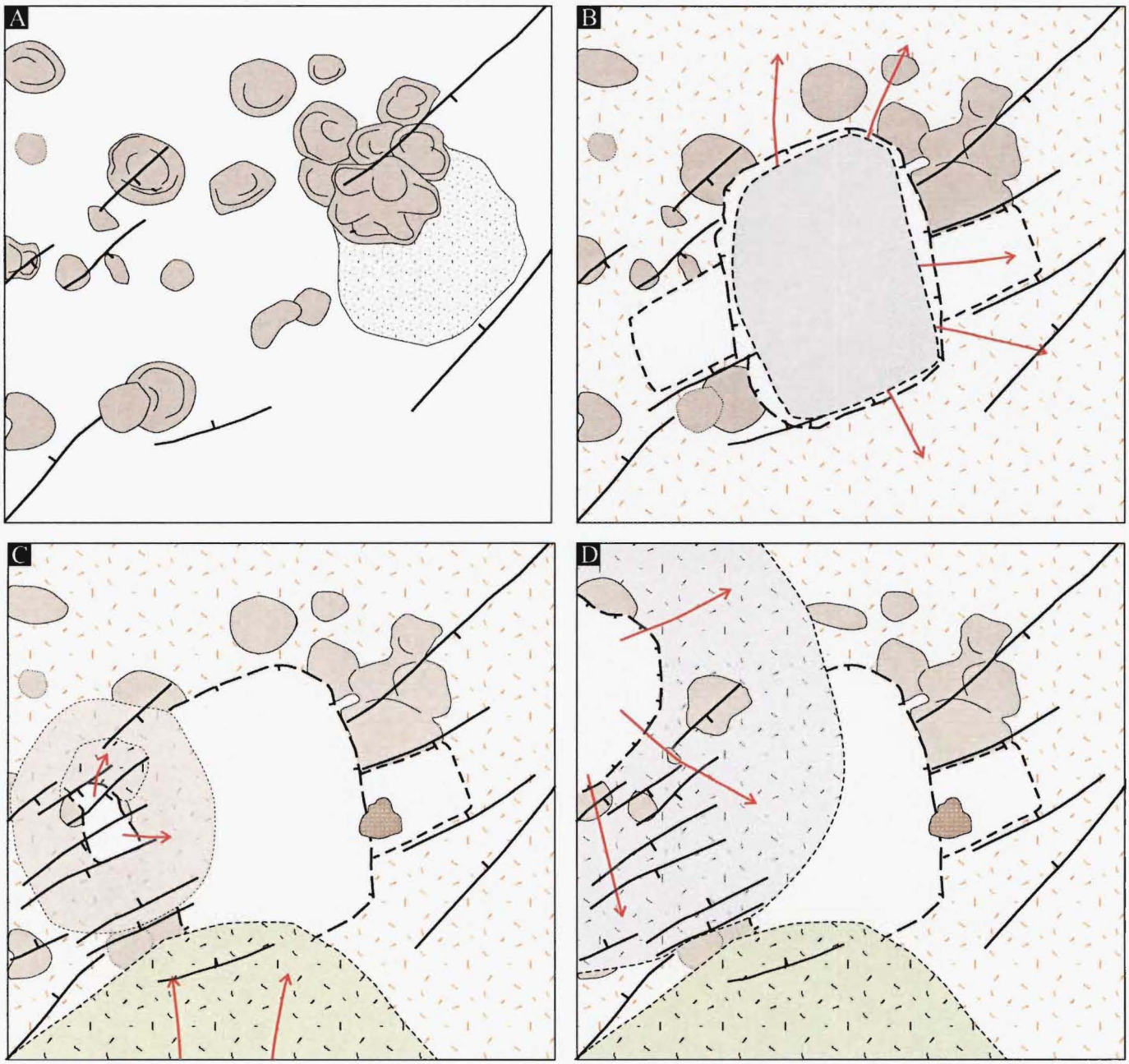

FIGURE 5.5 (cont): Model of the eruptive history of OCC. Arrows show primary flow directions. See text for discussion

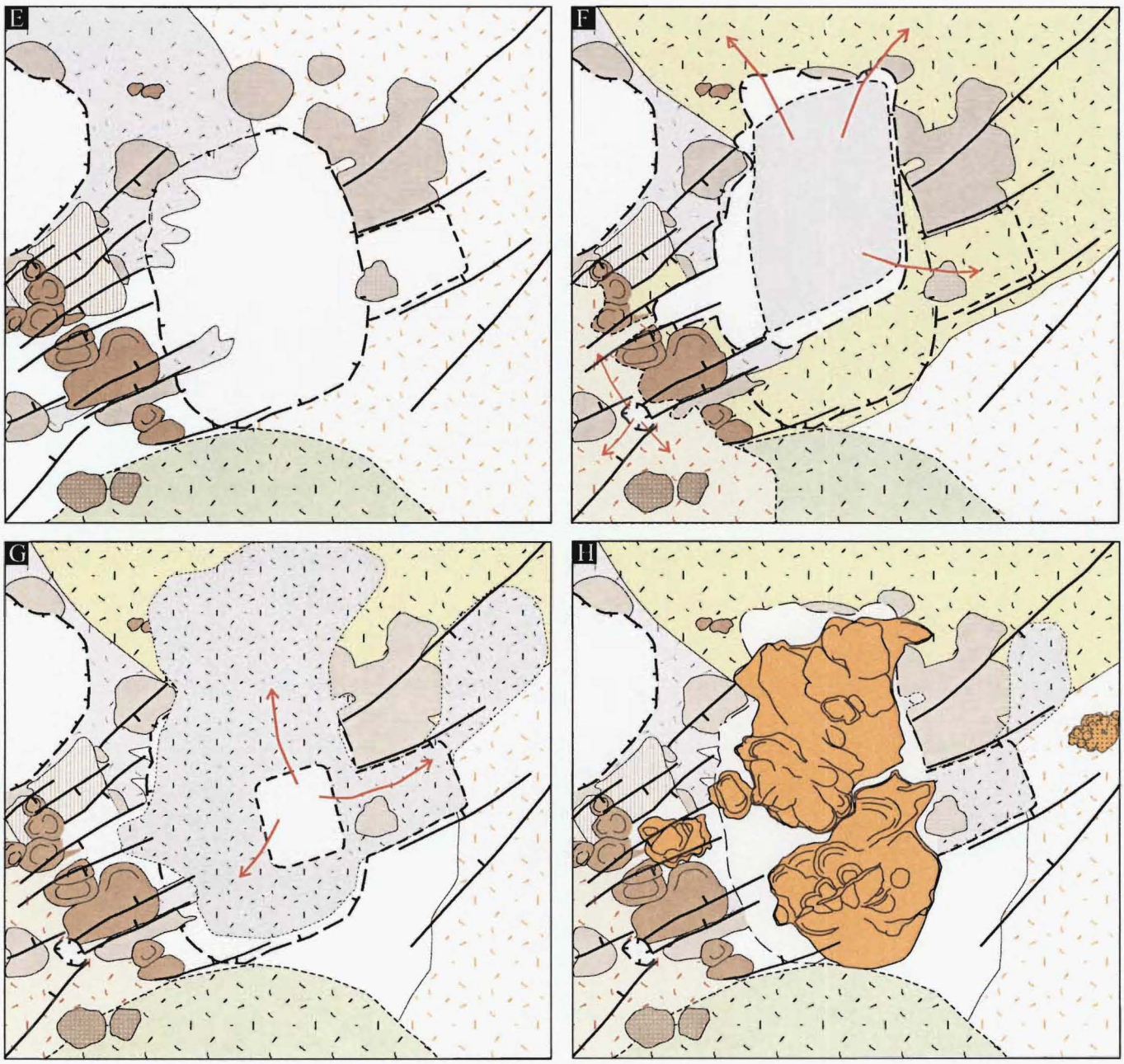

FIGURE 5.5 (cont)

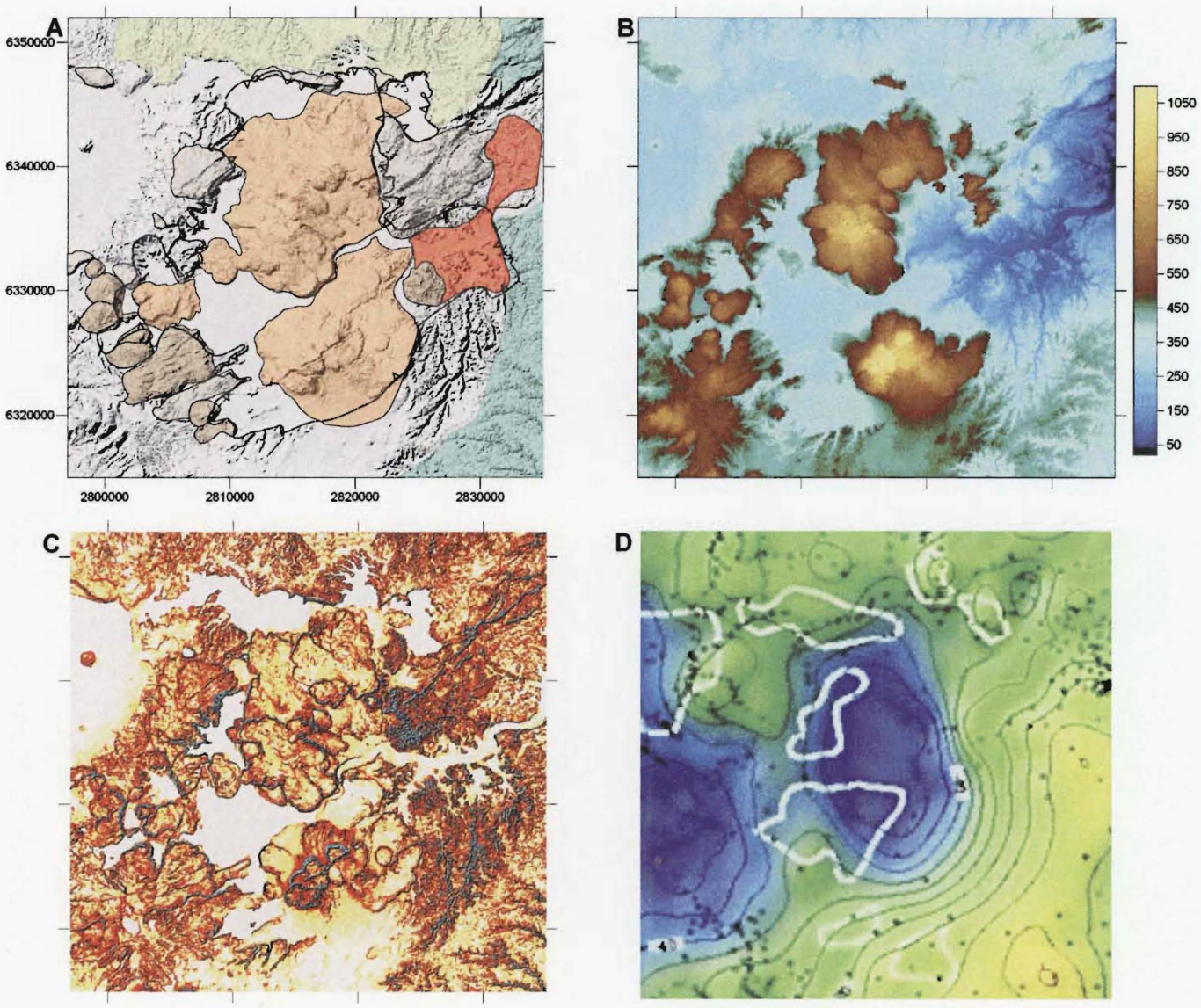

FIGURE 5.6: Okataina Caldera Complex illustrated with various geomorphic and geologic parameters. (A) Shaded relief image with key geology (key is the same as for Fig. 5.4); (B) Elevation image highlighting the location of constructional volcanism; (C) Surface 'roughness' image (calculated at each point as a function of statistical variance with respect to the eight surrounding nodes) highlighting the variation in incision of ignimbrite plateau and the youthful morphology of intra-caldera lavas with respect to surrounding older lavas; (D) residual gravity (after STAGPOOLE & BIBBY, 1999), showing geometry and extent of basement collapse feature. Subsidiary embayments in the caldera margin (A) are outside the margins of the collapse feature, which is rectilinear and elongate normal to the axial rift zone.

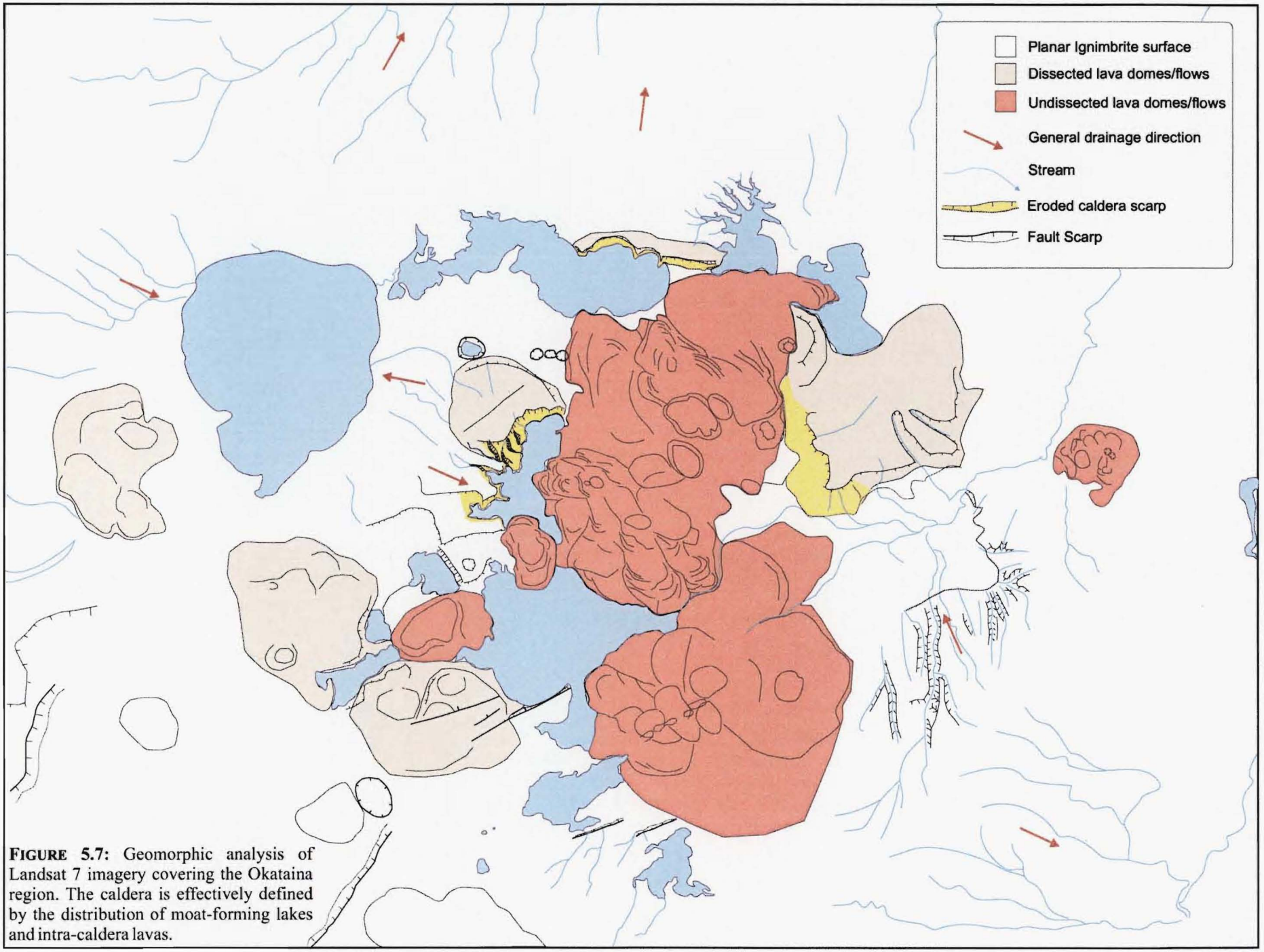

FIGURE 5.7: Geomorphic analysis of Landsat 7 imagery covering the Okataina region. The caldera is effectively defined by the distribution of moat-forming lakes and intra-caldera lavas.

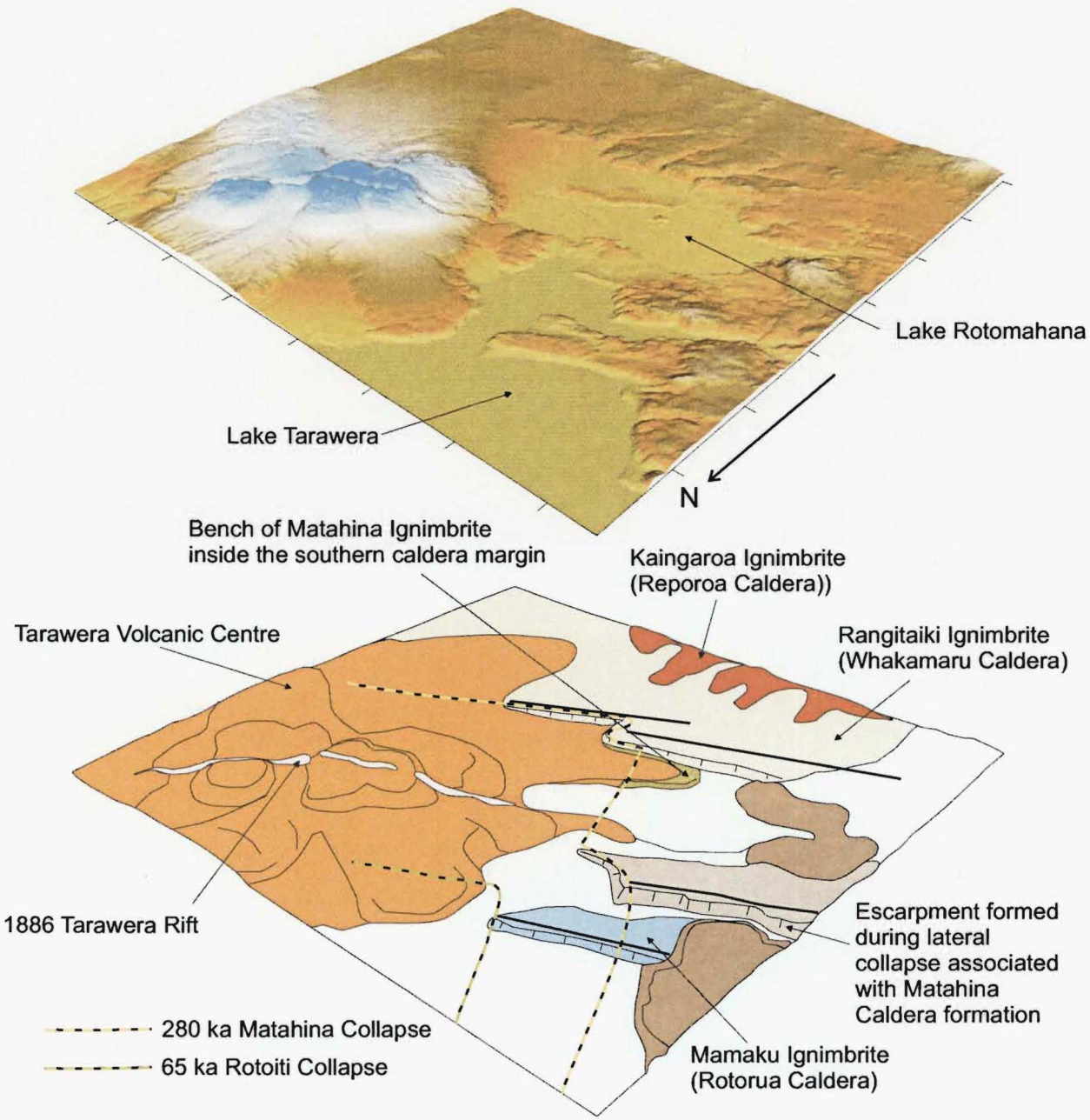

FIGURE 5.8: (A) Surface image of the complex south-western margin of OCC. Ticks on border are 2 km apart. (B) Schematic sketch showing the main features of the area and location of the margins for individual collapse events. Solid black lines are major faults that controlled the margins of caldera and lateral collapse embayments.

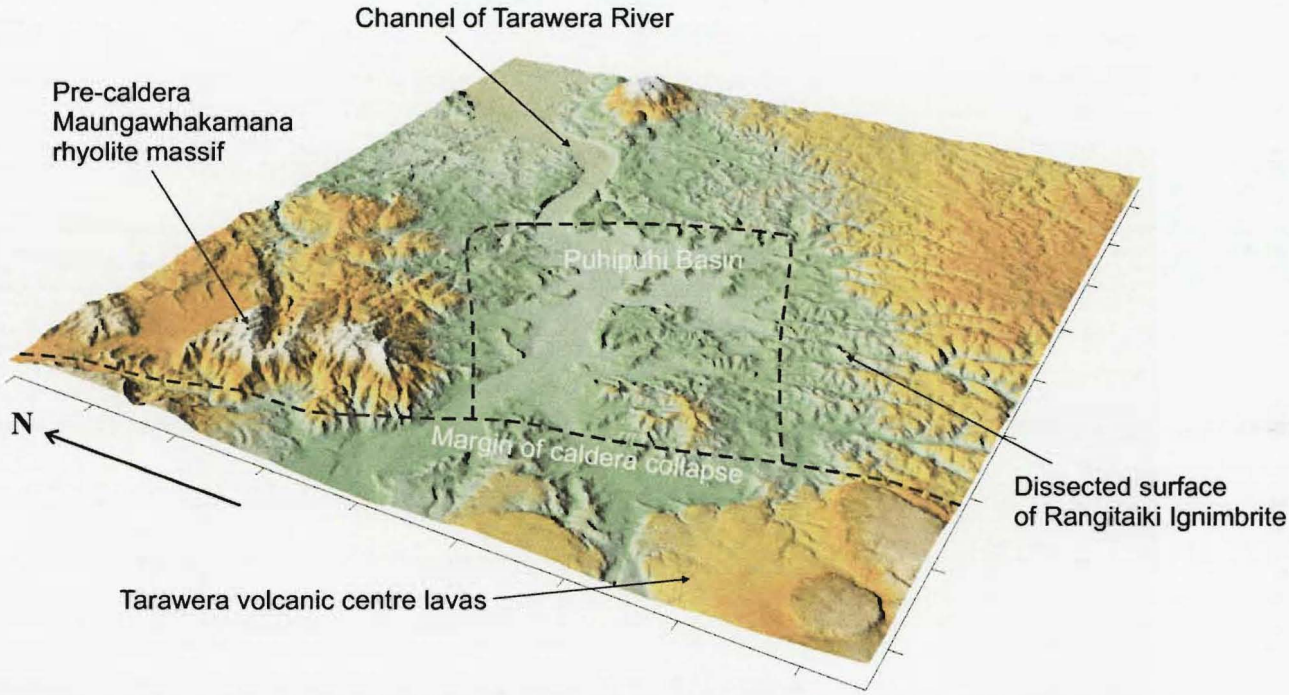

FIGURE 5.9: Surface image of the eastern margin of OCC. Ticks on border are 2km apart.

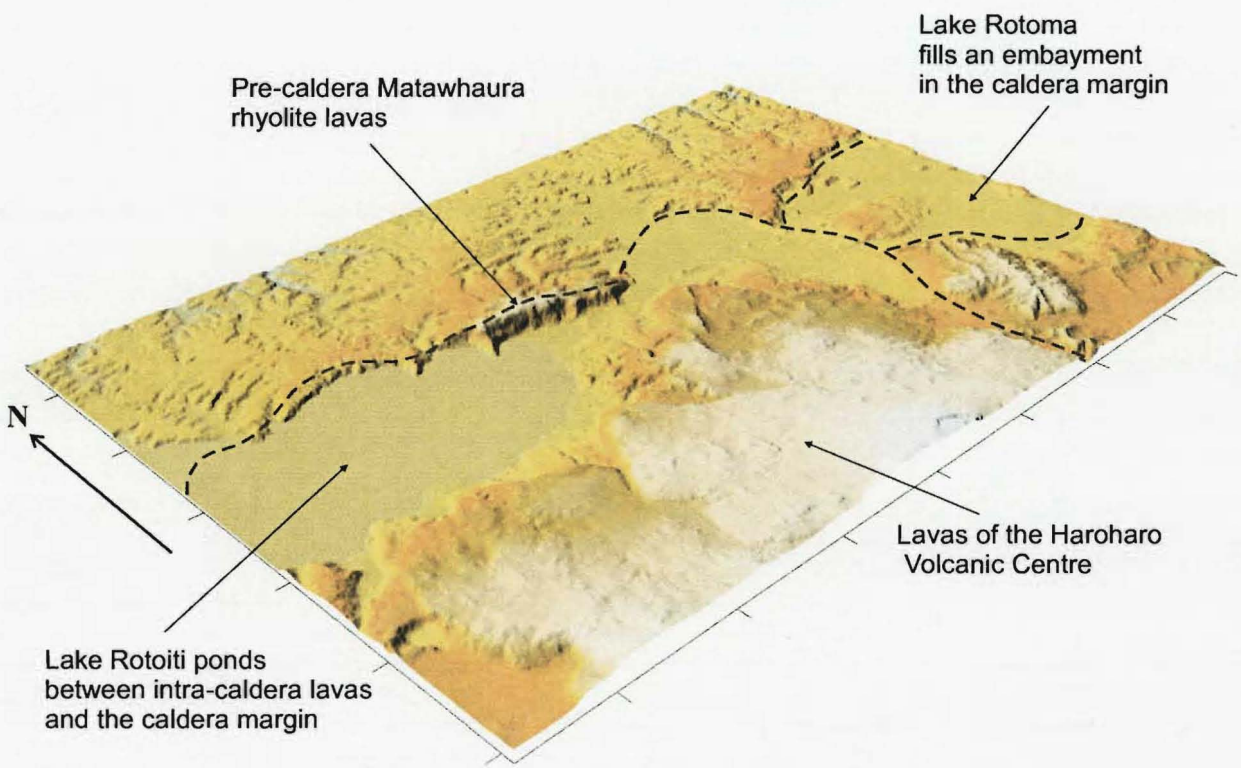

FIGURE 5.10: Surface image of the northern margin of OCC. Ticks on border are 2 km apart.

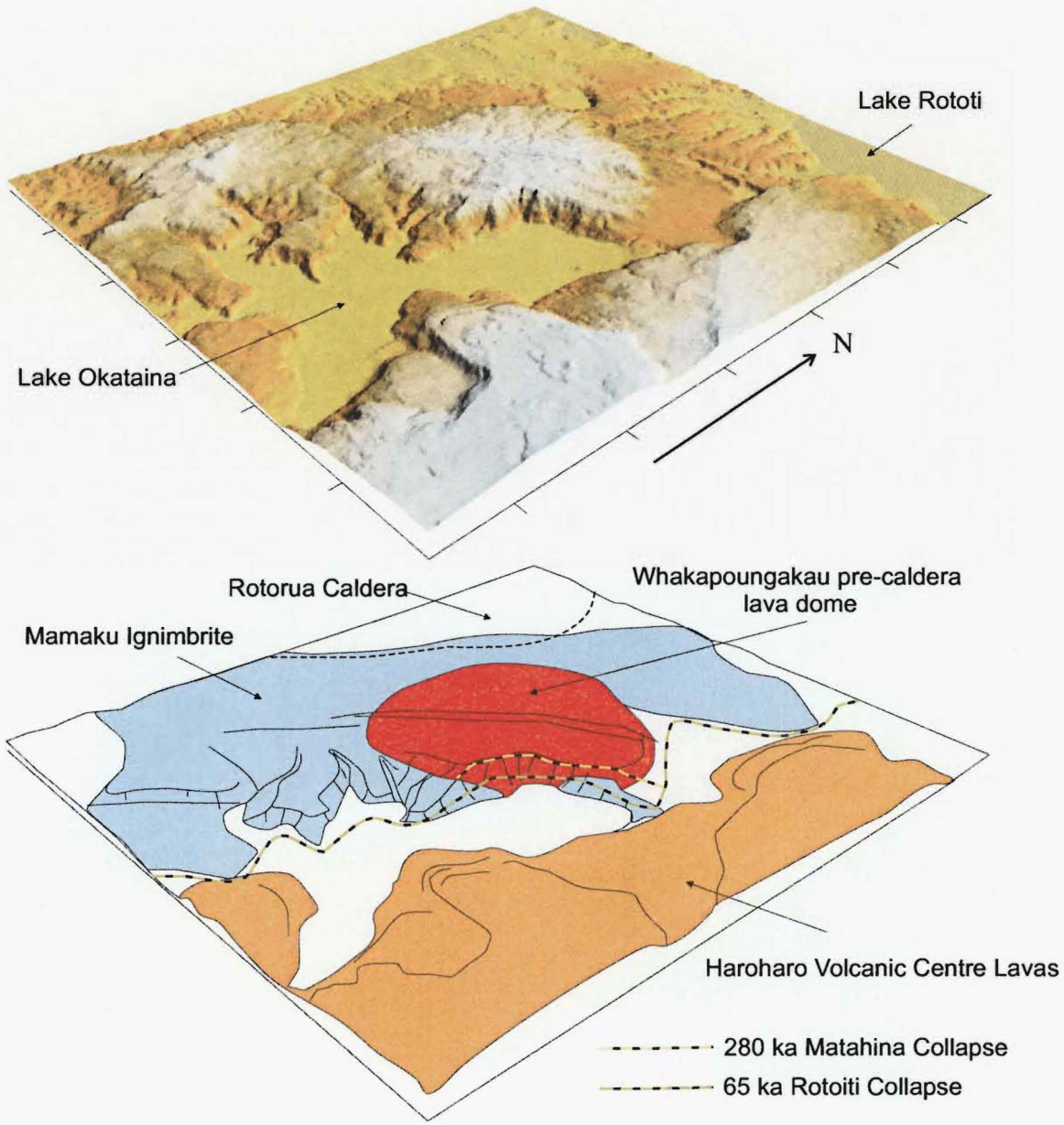

FIGURE 5.11: (A) Surface image of the western OCC margin. Ticks on border are 2 km apart. (B) Schematic sketch showing the main features. An initial scarp produced by the 280 ka Matahina Caldera collapse was later inundated by 220 ka Mamaku Ignimbrite from Rotorua Caldera. Collapse during the 65 ka Rotoiti event resulted in a scalloped escarpment in Mamaku Ignimbrite, leaving a small bench against the Whakapoungakau lava dome. Haroharo lavas ponded on the caldera floor to damn lakes against the caldera margin.

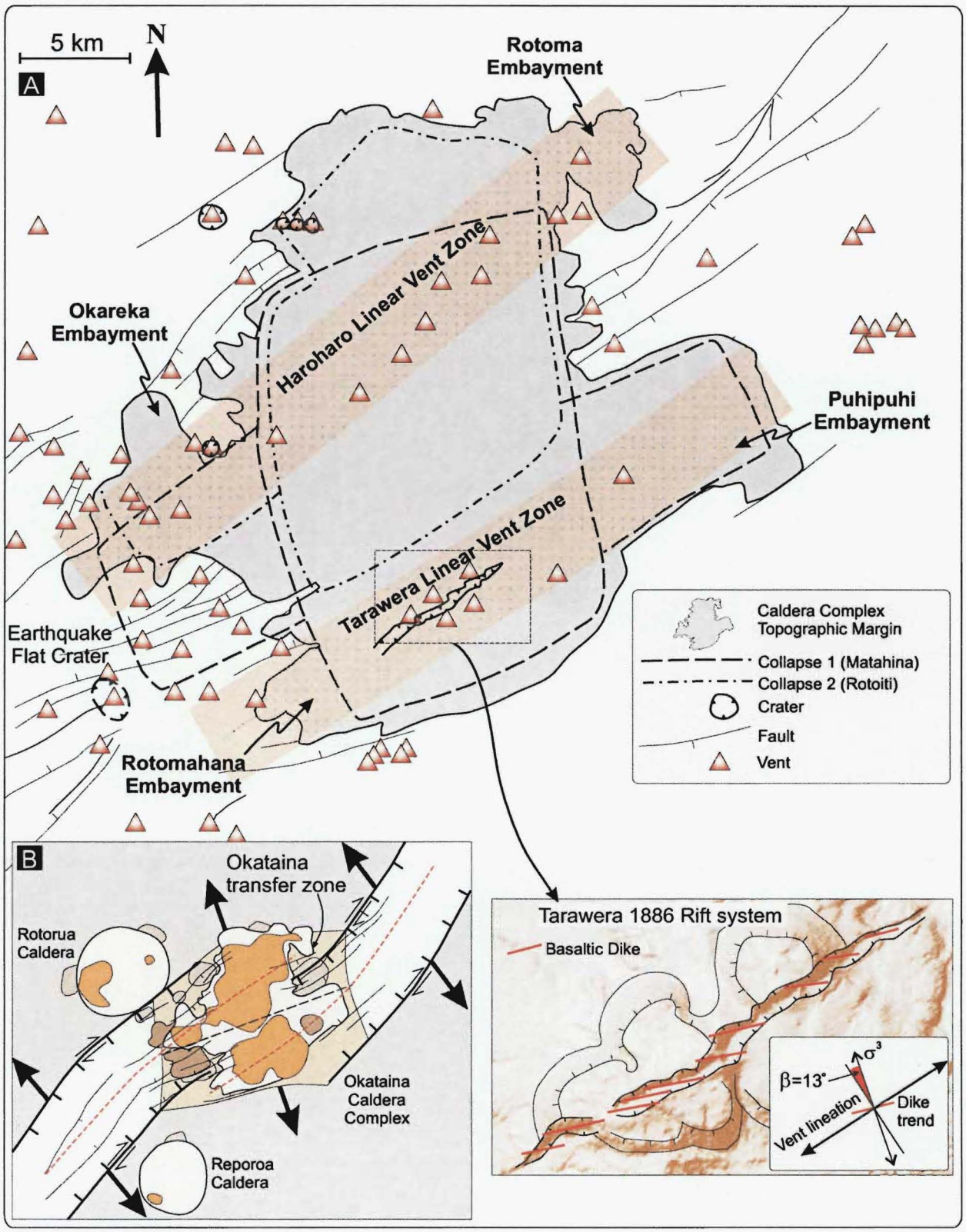

FIGURE 5.12: (A) The structural characteristics of OCC. Inset shows the orientation of en echelon basaltic dikes in the Tarawera Rift relates to the extension direction and trend of the Tarawera linear vent zone resulting in a zone of dextral shear. (B) Shows the relationship between the location and geometry of the OCC and major vent lineations to its location in a major transfer zone of the axial rift zone. Dashed red lines are the Kapenga and Whakatane rift segment axes (chapter two), which transect OCC. Dashed black line is the trend of the Okataina rift segment, which with a local rotation of the extension direction (Large arrows) results in a zone of orthogonal extension at OCC.

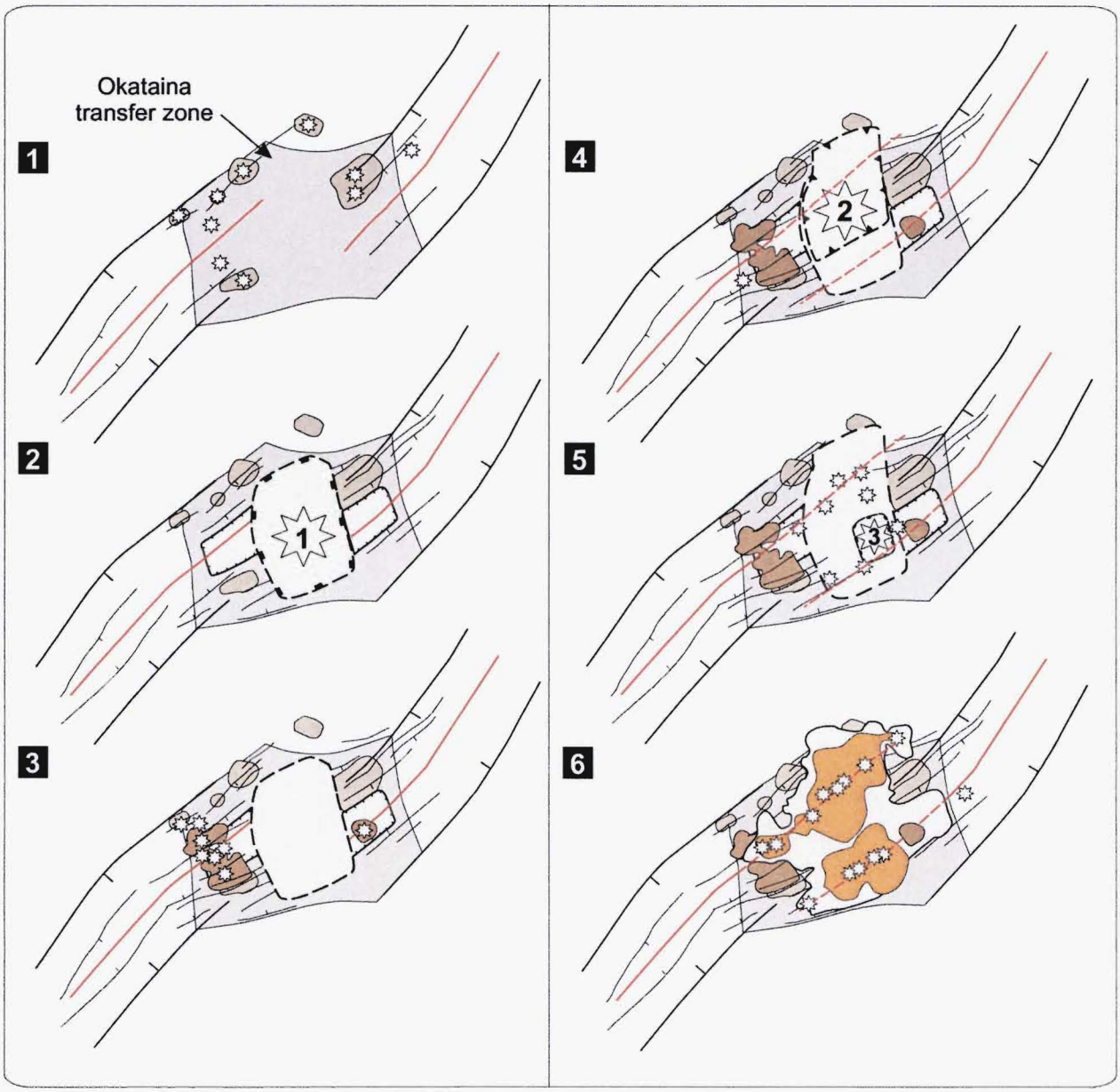

FIGURE 5.13: Volcanic and structural evolution of the Okataina transfer zone. See text for detailed discussion. (1) Transfer zone forms between offset rift segments, volcanism coupled with regional fault distribution in each segment; (2) Caldera collapse coincident with transfer zone boundary faults, subsidiary embayments form in axial rift on either caldera margin; (3) Incipient interaction of rift segments promotes volcanism on either side of caldera; (4) Second major caldera collapse coincident with transfer zone faults, preferential collapse in centre of transfer zone; (5) Propagation of rift axes into transfer zone induces magma rise and controls the location of vents within the caldera, including further caldera collapse; (6) Localised deformation along pre-existing rift axes controls volcanism within and outside the caldera complex.

FIGURE 6.1: Typical landscapes formed by the Kawerau Ignimbrite. (A) Forested knolls and low hills in northern Puhipuhi Basin taken from near V16/302337 (B) Looking northwest from near the top of Mt Edgecumbe toward Kawerau Township. Kawerau Ignimbrite forms the series of dissected low hills in the middle distance.

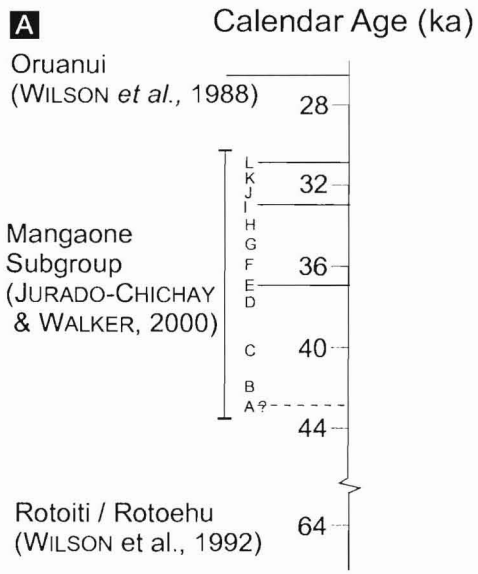

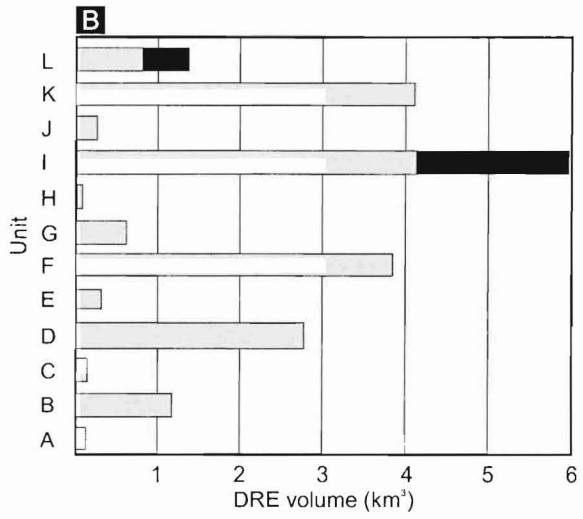

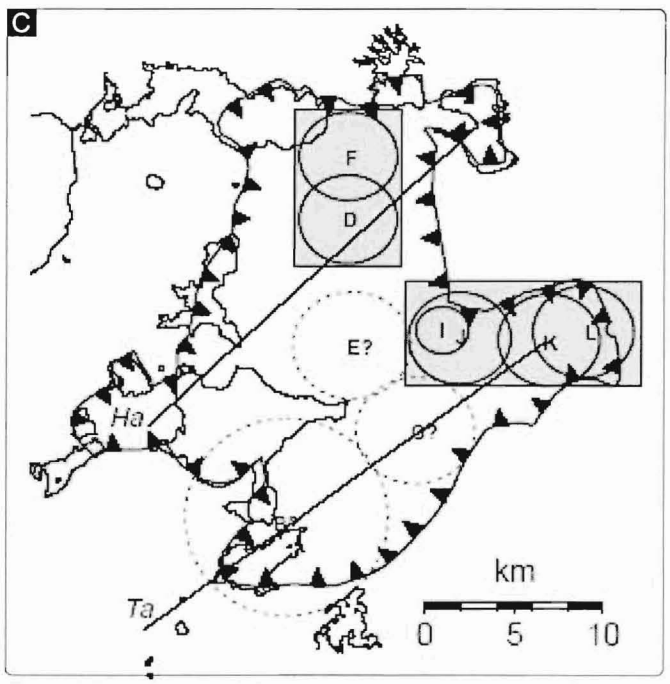

FIGURE 6.2: Summary of time-space-volume relationships of the Mangaone Subgroup redrawn from JURADO-CHICHAY & WALKER (2000, 2001a). **(A)** Calculated ^{14}C Calender ages for the Mangaone Subgroup. **(B)** Bulk volumes of the Mangaone Subgroup eruptions in stratigraphic order. Grey bars indicate fall DRE volumes and black bars pyroclastic flow DRE volumes. Inclusion of Kawerau Ignimbrite extends unit I flow volume considerably. **(C)** Vent locations estimated from lithic isopleth maps. Circles reflect approximate error, and shaded areas are thought to indicate migrating vents. Vents within Puhipuhi Basin are thought highly unlikely in this study.

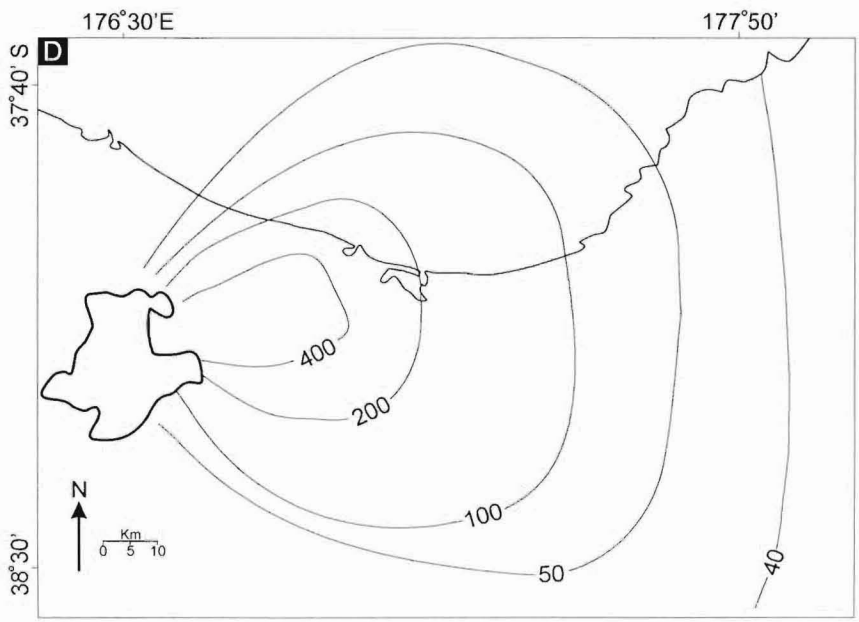

FIGURE 6.2 (D): Dispersal map for Unit I (fall thickness in cm), which preceded deposition of the Kawerau Ignimbrite.

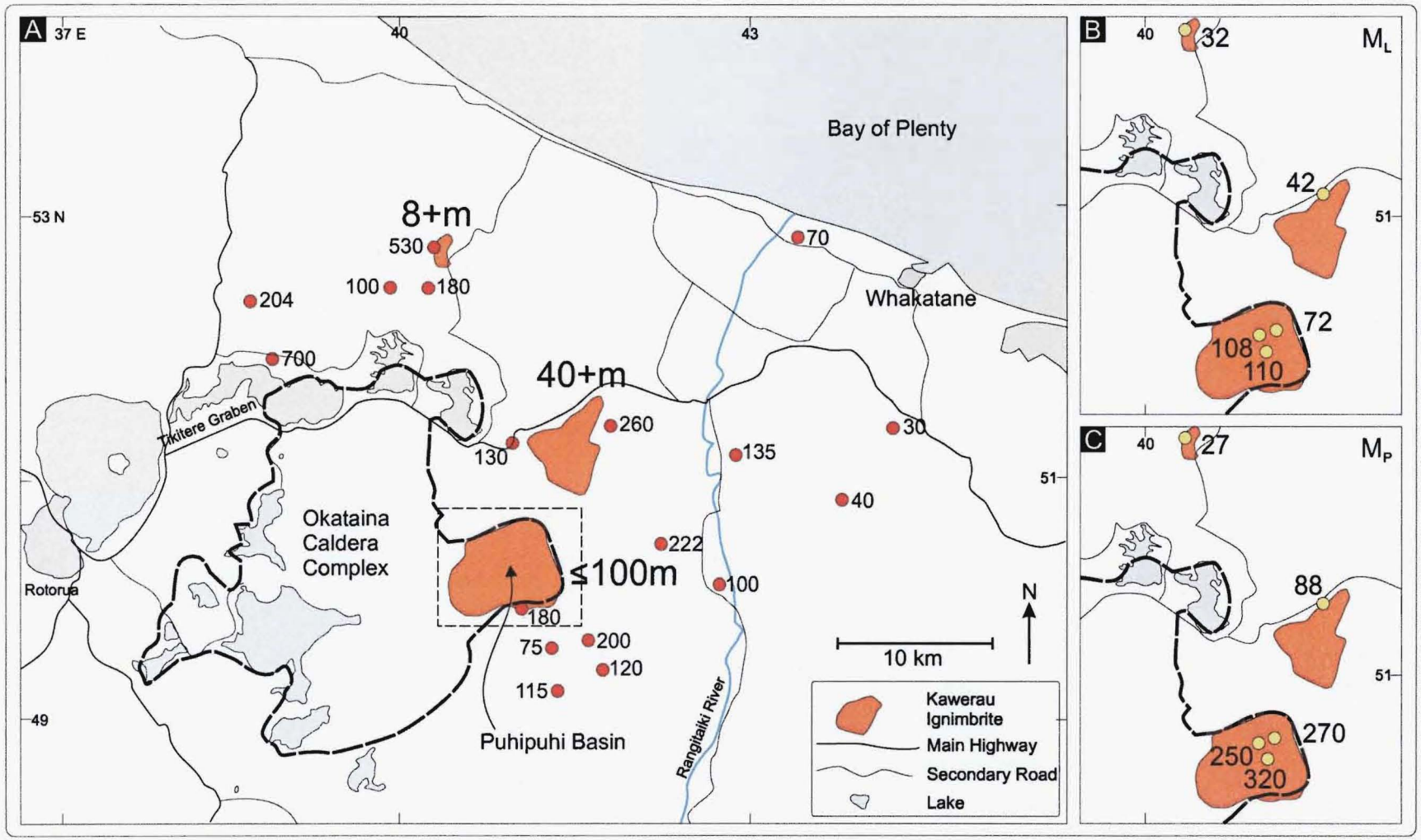

FIGURE 6.3: Map of the Kawerau Ignimbrite in the Bay of Plenty region. (A) Approximate thickness of the ignimbrite in the three main areas of exposure. Also shown (red data points) are thickness measurements for the Mangaone flow unit of JURADO-CHICHAY & WALKER (2000) and the margin of Okataina Caldera Complex (OCC). (B) & (C): M_L & M_P data respectively for Kawerau Ignimbrite. The data suggests an OCC source west of Puhipuhi Basin.

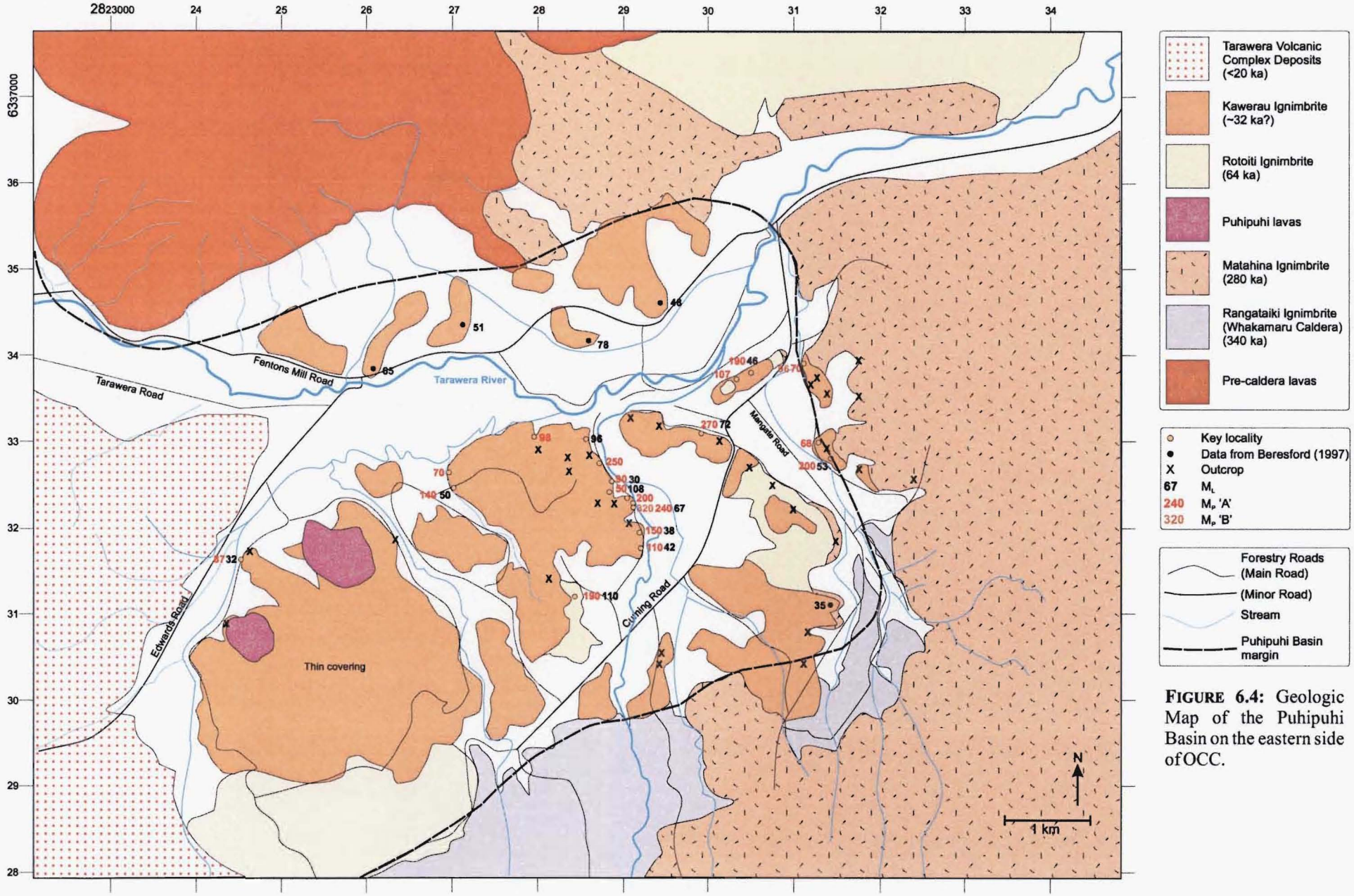

FIGURE 6.4: Geologic Map of the Puhipuhi Basin on the eastern side of OCC.

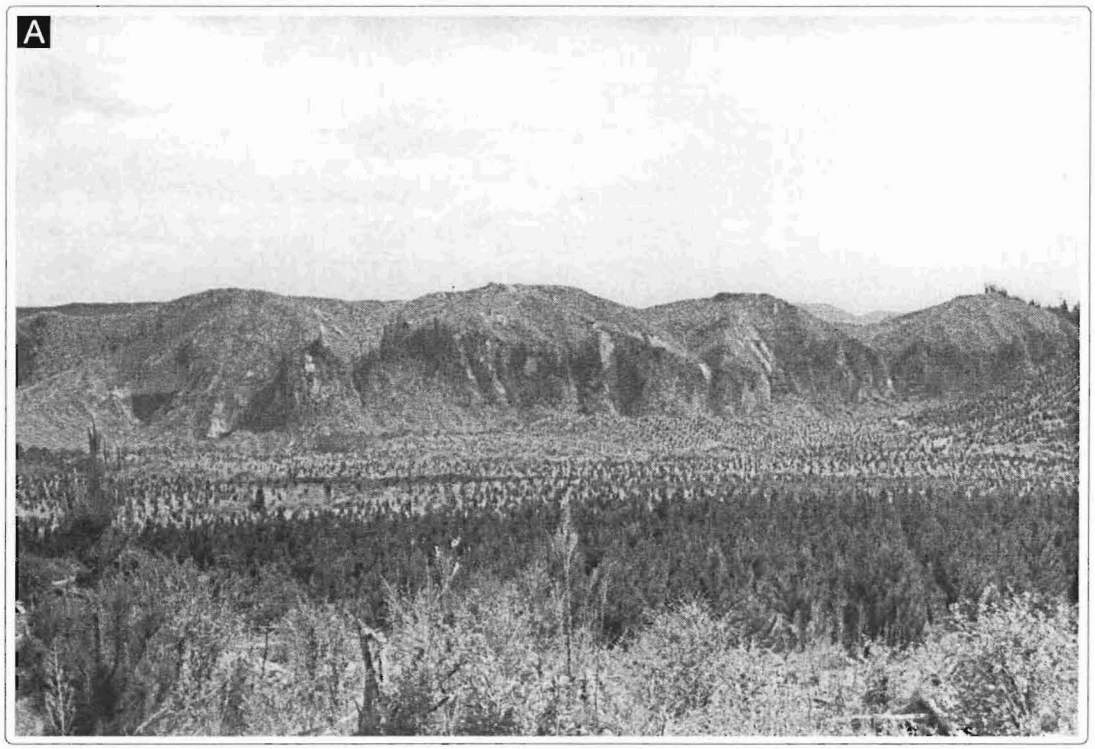

FIGURE 6.5: Typical views of the Kawerau Ignimbrite in Puhipuhi Basin. (A) Looking west from V16/301323 toward the main bluffs adjacent to Mangawhio Stream (and the ephemeral Mangawhio forestry road). Incised plateau is 100 m above basin floor and is largely comprised by the ignimbrite. (B) Partially welded bluffs at V16/291333. Jointed bluffs of L1 are seen to the left along the hillside.

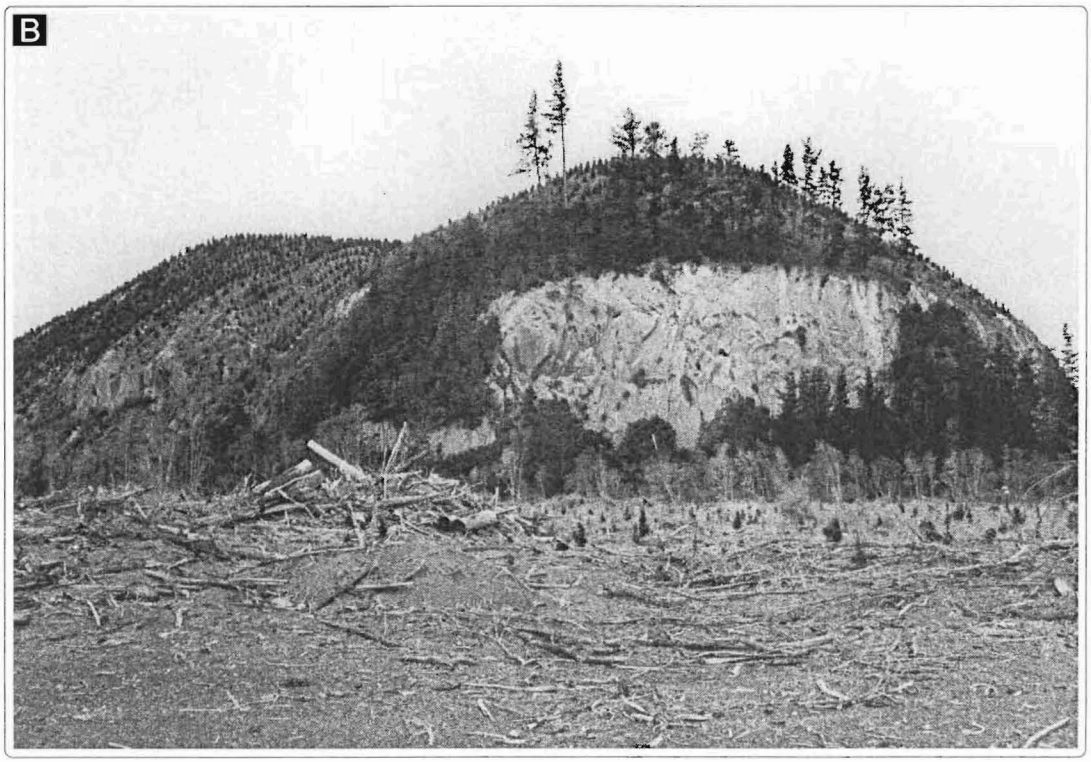

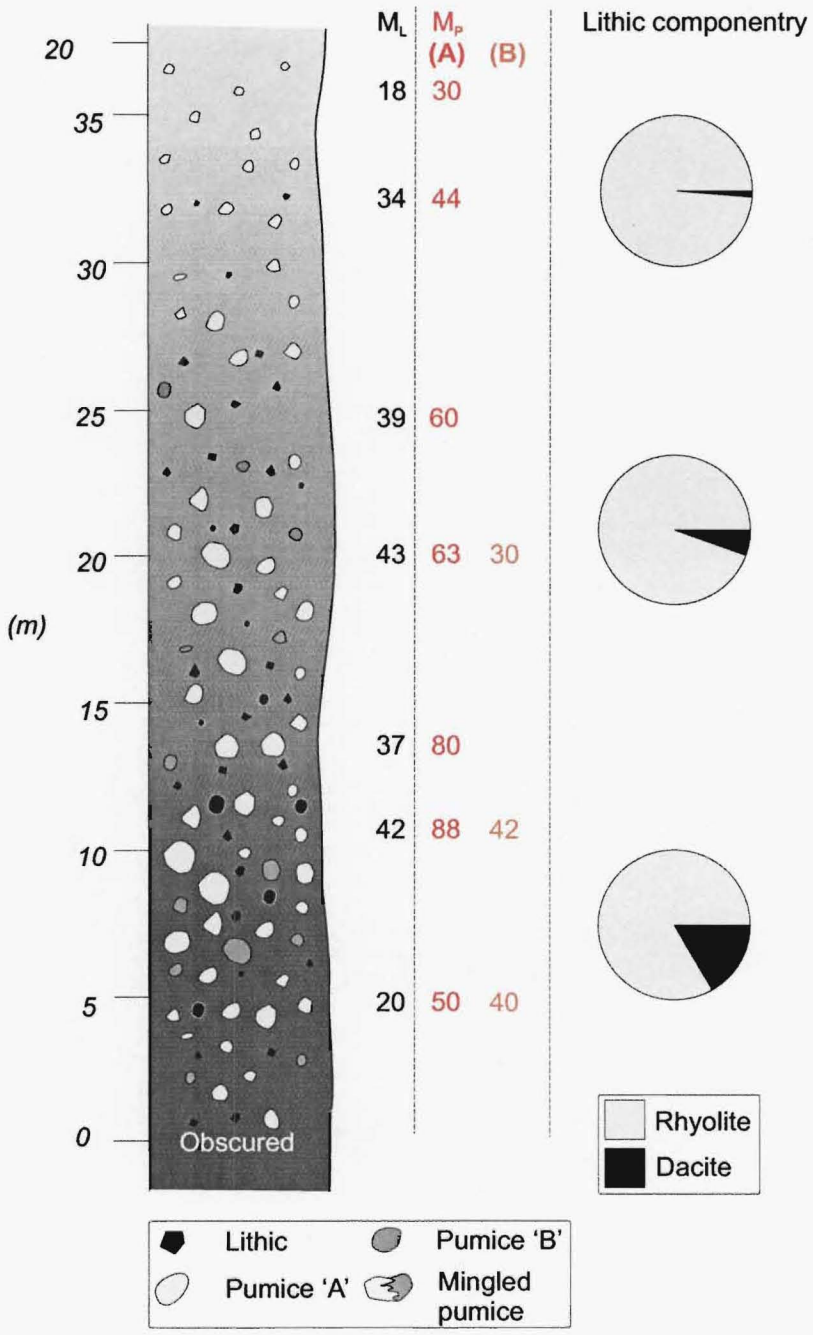

FIGURE 6.6: Kawerau Ignimbrite at the type section (V15/343448). See text for discussion. Up-section dark to light shading in this and the following stratigraphic logs represents progressive change from L1 to L2; no distinct boundary exists to divide the ignimbrite into flow units.

FIGURE 6.7: Kawerau Ignimbrite in Puhipuhi Basin. **(A)** Looking southeast from V16/305337 down Mangate Rd. On the left Kawerau Ignimbrite abuts against welded cliffs of Matahina Ignimbrite fomring the eastern margin of the basin. On the right it overlies Rotoiti Ignimbrite. The horizon is formed on Matahina Ignimbrite and Rangitaiki Ignimbrite southeast fo the basin.

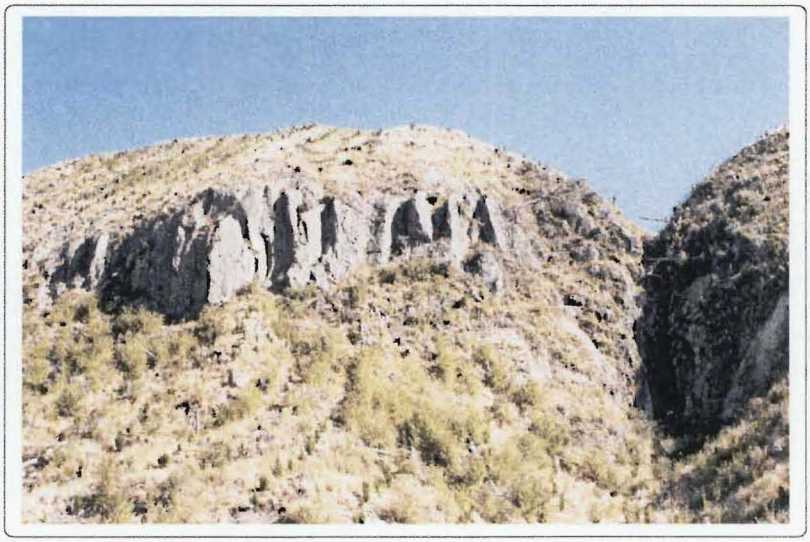

FIGURE 6.7: (B) Partially welded L1 Kawerau Ignimbrite commonly forms vertical bluffs with widely spaced, irregular cooling joints around the basin. This is at V16/295/331. Upper and lower parts of the ignimbrite are often obscured.

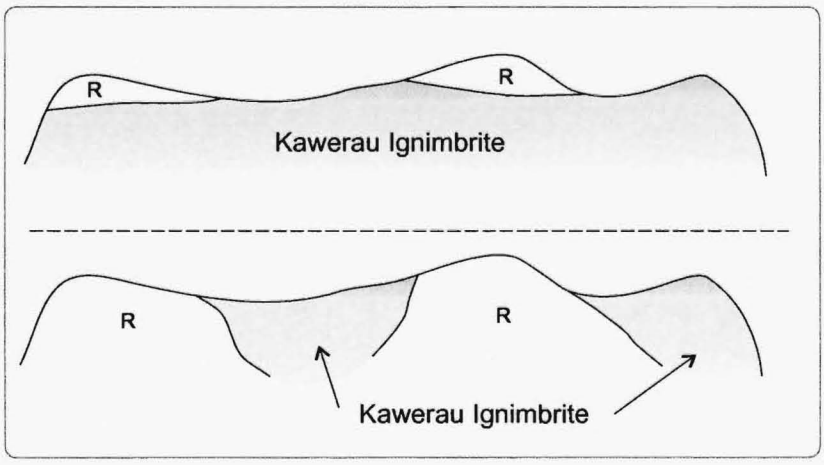

FIGURE 6.7: (C) Kawerau and Rotoiti ignimbrites adjacent to Homestead Rd (vicinity of V16/305337). Upper sketch shows relationship as originally perceived, with higher elevation Rotoiti overlying an older Kawerau Ignimbrite. Lower sketch shows actual relationship, with Kawerau filling localised channels incised into the older Rotoiti Ignimbrite.

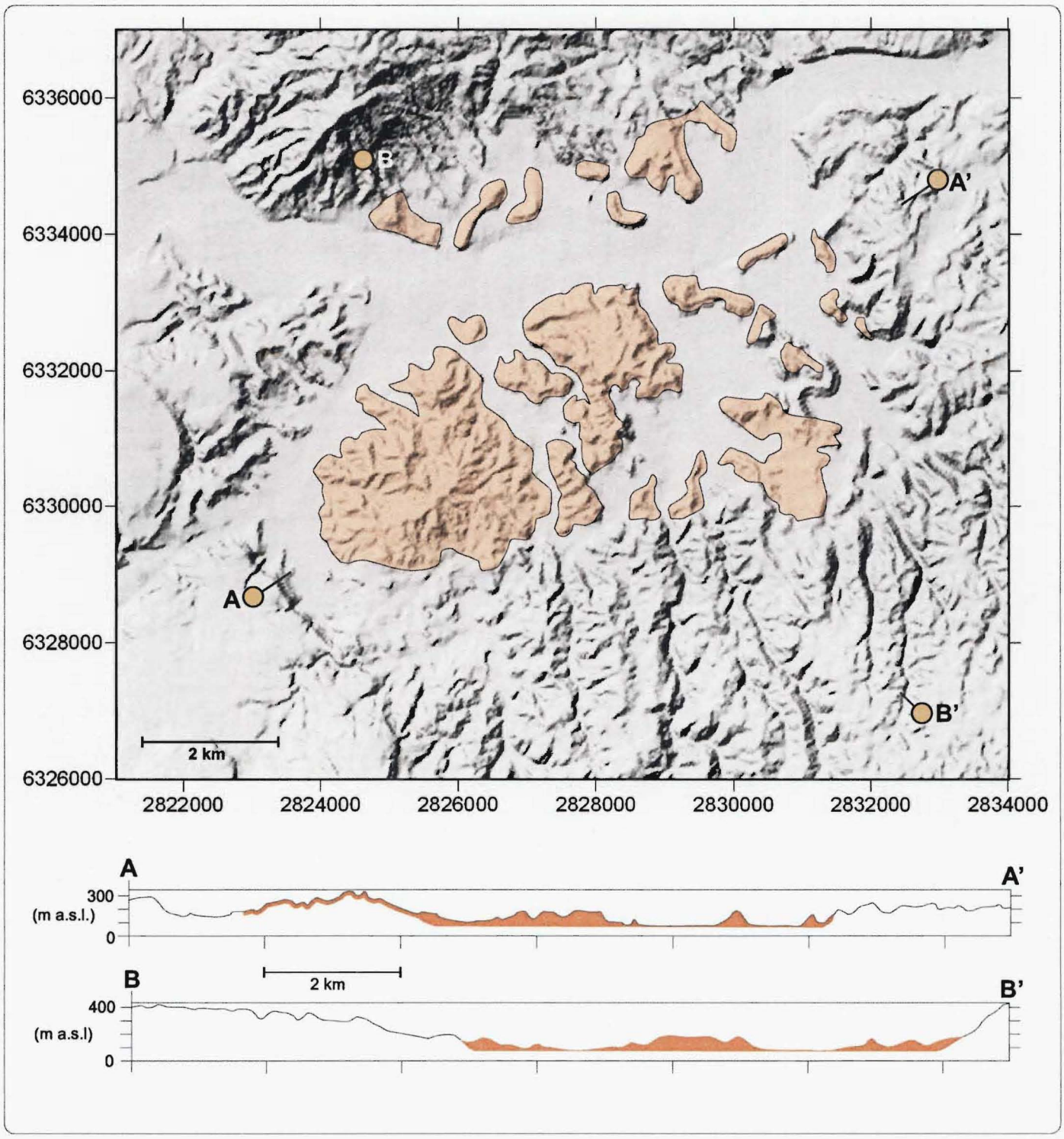

FIGURE 6.8: Shaded relief map and cross-sections showing the distribution of Kawerau Ignimbrite in Puhipuhi Basin. Ignimbrite plateau within the basin sits below the edge of the basin rim formed in older ignimbrites and lavas, in contrast to the ascertion of NAIRN (1981) and subsequent workers that it was 50 m higher then the basin rim. Up to 50% of the original volume of ignimbrit within the basin has been removed by subsequent erosion, mostly along established drainage systems.

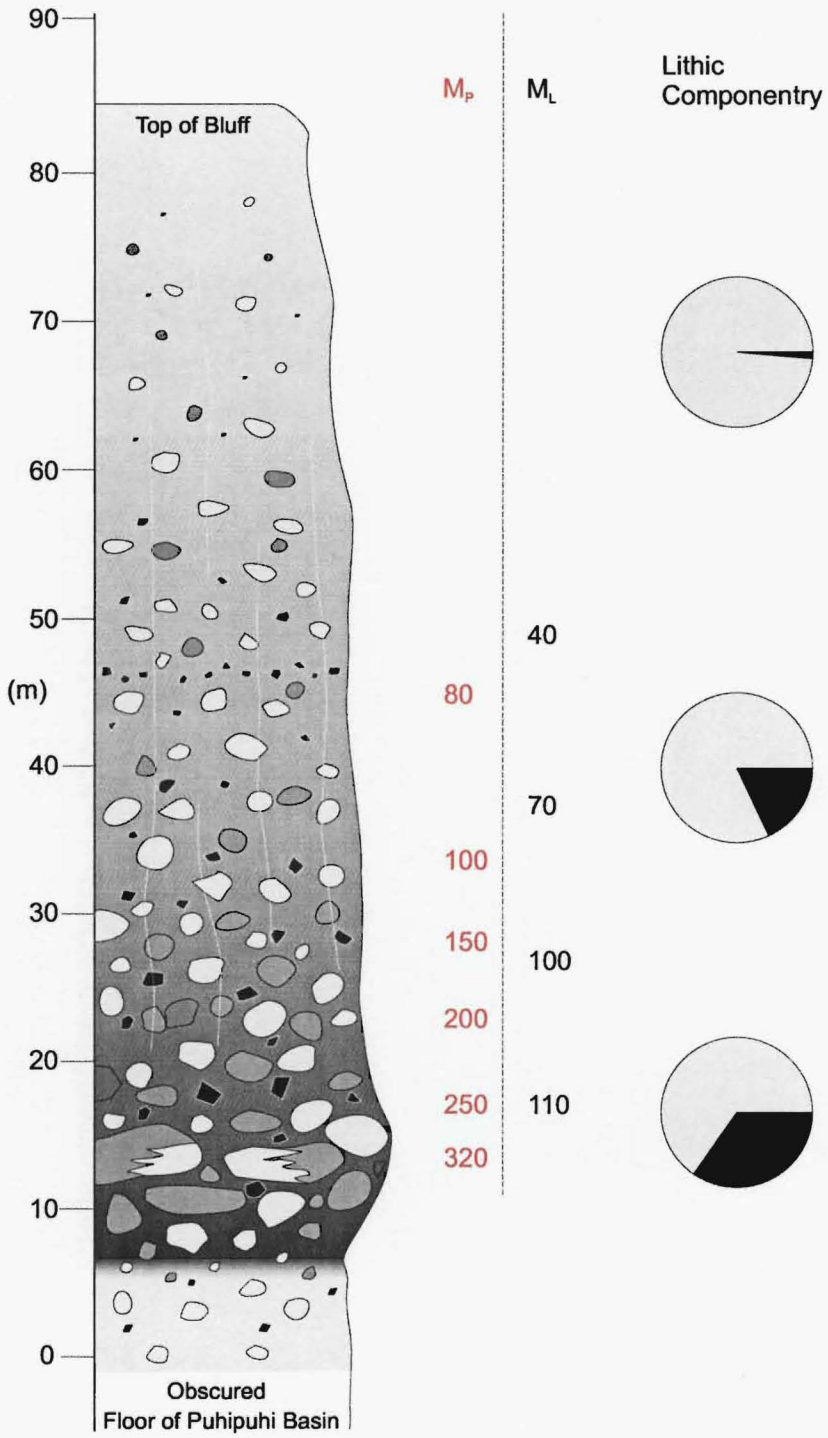

FIGURE 6.9: Composite graphic log of Kawerau Ignimbrite in Puhipuhi Basin. Key is same for Figure 6.6.

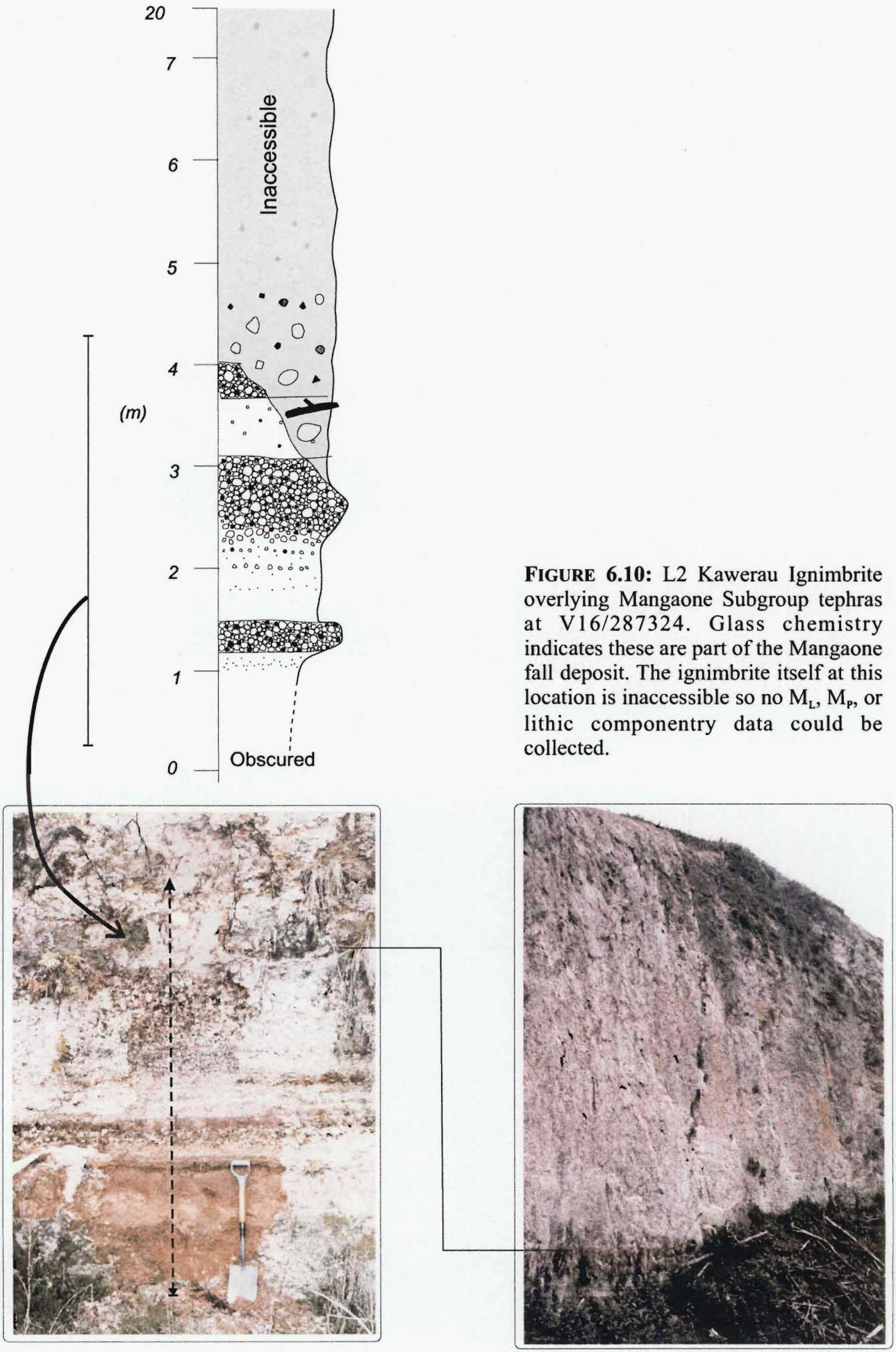

FIGURE 6.10: L2 Kawerau Ignimbrite overlying Mangaone Subgroup tephras at V16/287324. Glass chemistry indicates these are part of the Mangaone fall deposit. The ignimbrite itself at this location is inaccessible so no M_L, M_P, or lithic componentry data could be collected.

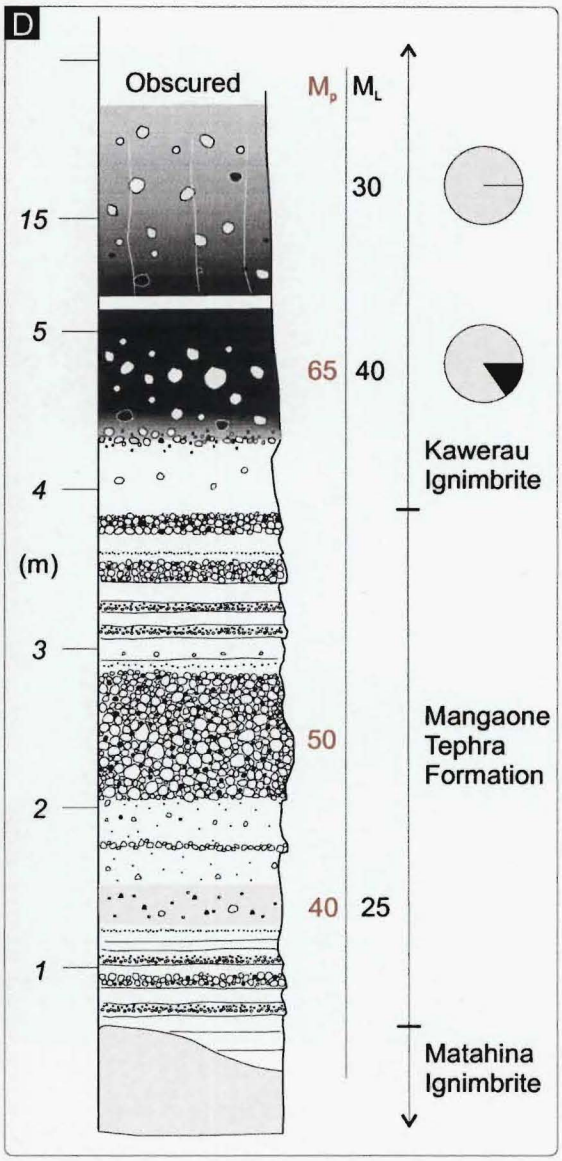

FIGURE 6.11: Mangaone tephra beds and L1 Kawerau Ignimbrite overlying the eroded surface of Matahina Ignimbrite at V16/311340. Spade in (a) and (b) sits between 3 and 4 m in the stratigraphic log, the hammer in (c) is similarly at 3.5 m. See text for further discussion.

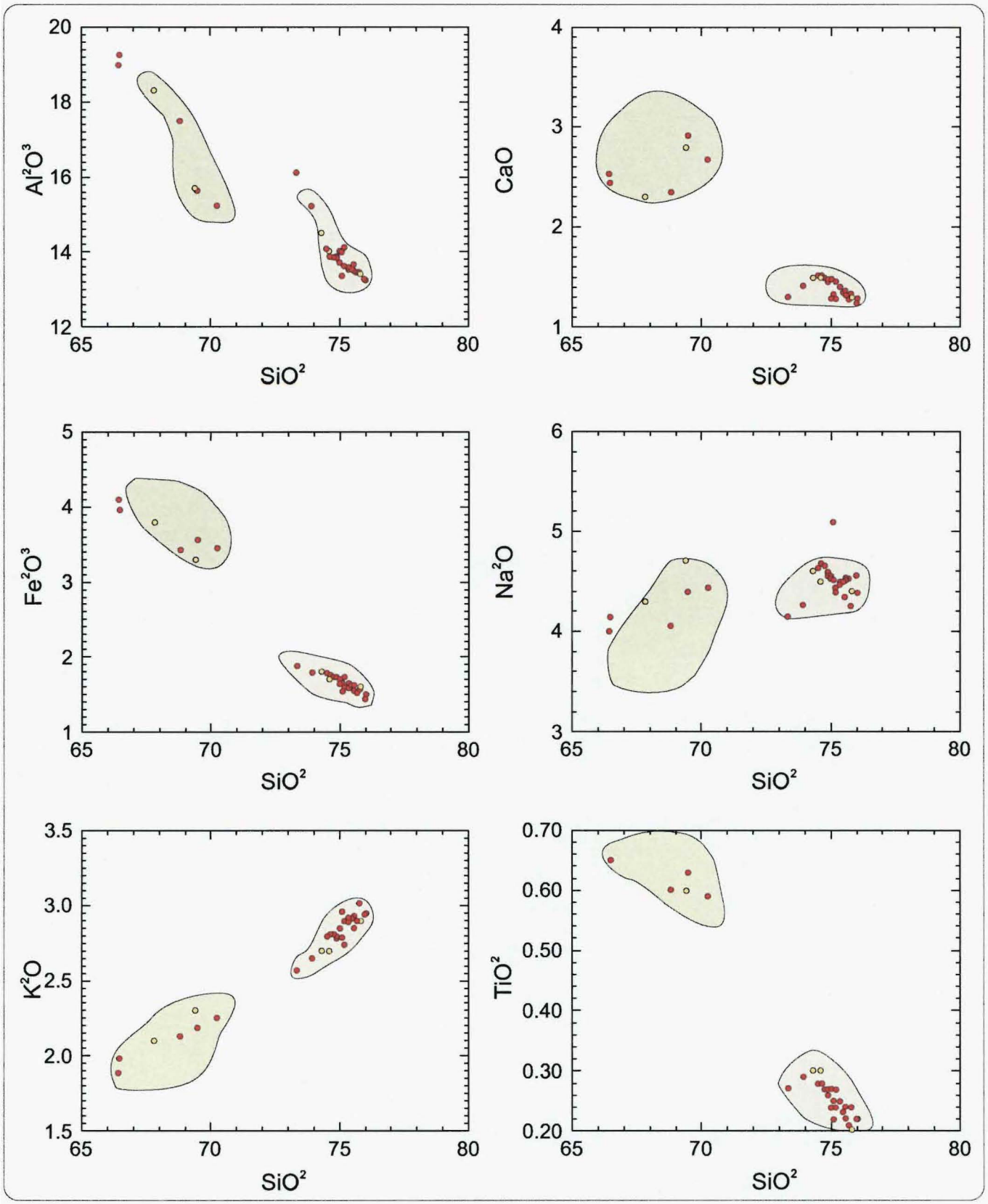

FIGURE 6.12: Major element compositions of pumice clasts in the Kawerau Ignimbrite. Also shown are the fields for *old* (green) and *young (yellow)* Mangaone Subgroup eruptives from Smith (2001).Yellow data points are data from BERESFORD (1997); red data points are analyses of this study. Values are wt. %.

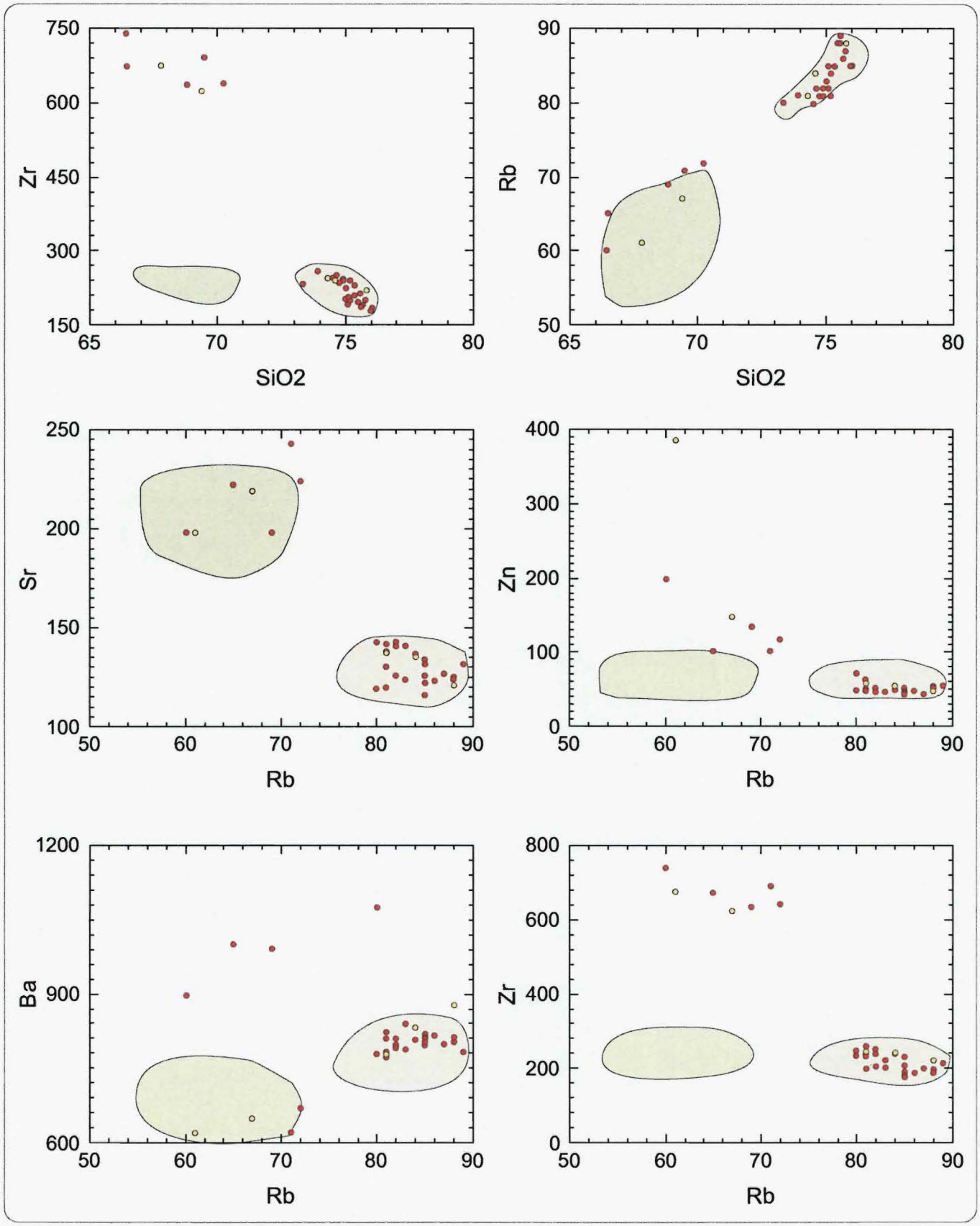

FIGURE 6.13: Trace element compositions of pumice clasts in the Kawerau Ignimbrite. Also shown are the fields for *old* (green) and *young (yellow)* Mangaone Subgroup eruptives from SMITH (2001). All values are ppm.

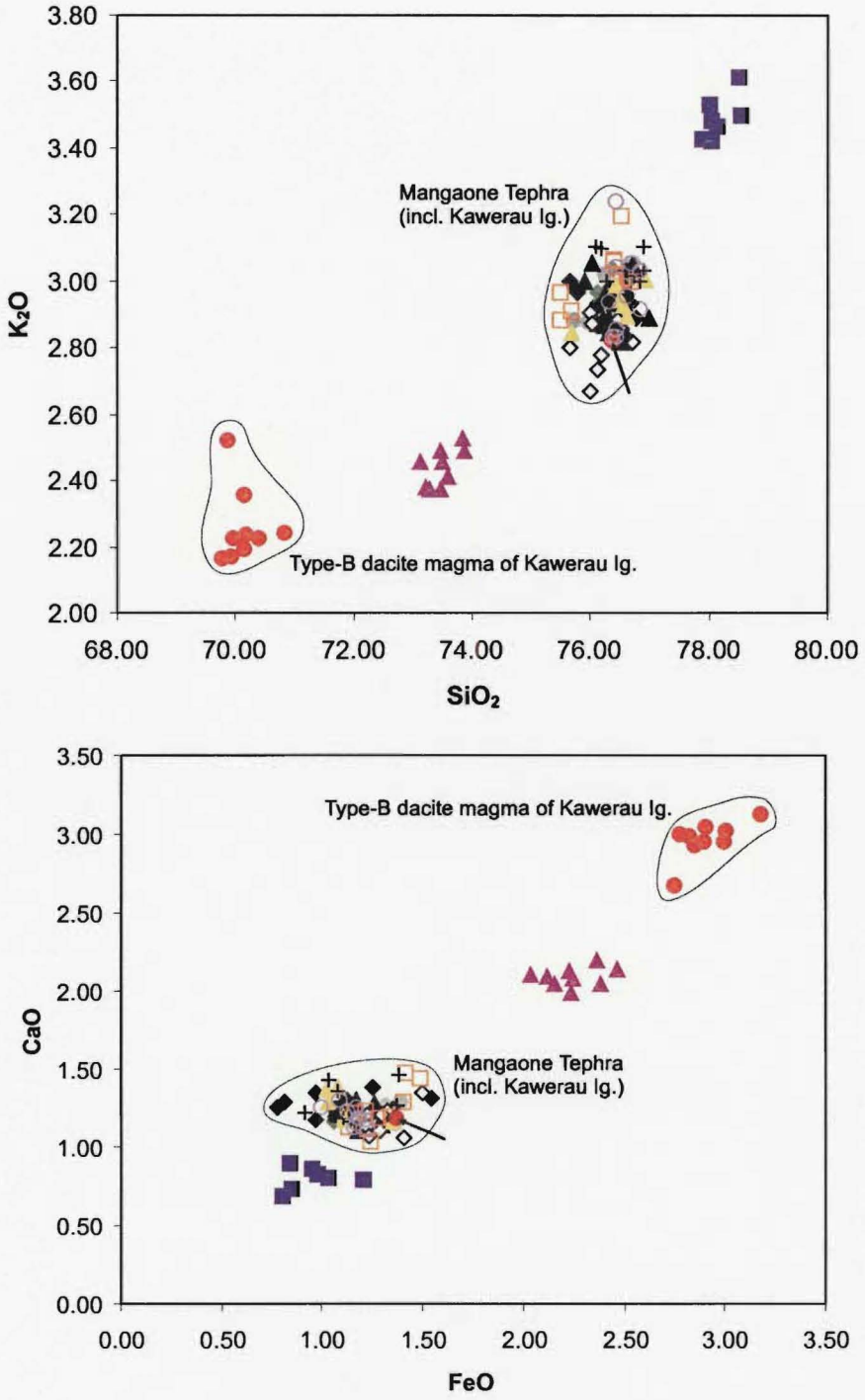

FIGURE 6.14: Representative plots of glass chemistry data for pumice and matrix of the Kawerau Ignimbrite, illustrating clear correlation between the predominant rhyolitic magma and that of the Mangaone tephra. Dacitic magma is distinct from 'old' Mangaone Subgroup tephras. Arrows show rhyolitic glass shard in mingled 'B' pumice.

Rift Architecture and Caldera Volcanism in the Taupo Volcanic Zone, New Zealand

A thesis submitted in fulfilment of
the requirements for the degree of

Doctor of Philosophy
in Geology

at the
University of Canterbury
By

Karl D. Spinks

3. Appendices

University of Canterbury
2005

Appendix A

'ACOCELLA, V., **SPINKS, K.**, COLE, J. & NICOL, A. (2003) Oblique back-arc rifting of Taupo Volcanic Zone, New Zealand. *Tectonics*, vol. 22, no. 4, 1045, doi:10.1029/2002TC001447'

Contribution: field structural analysis & data collection (with V. Acocella; offset stream data also with A. Nicol); data compilation & analysis (with V. Acocella); literature review, lineament analysis, DEM production, image manipulation, partial contribution to write-up.

UNIVERSITÀ DEGLI STUDI ROMA TRE

DIPARTIMENTO DI SCIENZE GEOLOGICHE

Largo S. L. Murialdo, 1, 00146
Roma, Italy
tel. 39+6+54888.043 -fax
39+6+54888.201

Roma, 14 – 9 - 04

To whom it may concern,

As corresponding author of the paper "Oblique back-arc rifting of Taupo Volcanic Zone, New Zealand" published on Tectonics (2003, 22, 4, 1045, doi:10.1029/2002TC001447") by Acocella V., Spinks K., Cole J., Nicol, A., I declare that co-author Karl Spinks had a crucial role in the development of such paper.

In fact he was: 1) actively planning and coordinating the research, constantly providing expert and enthusiastic advice; 2) actively getting all the data on the field, providing stimulating and mature discussions; 3) responsible for the development of the remote sensing section, including the building of the DEM for TVZ; 4) actively participating, with stimulating, critical and pertinent discussions, at the elaboration and interpretation of the structural data and the related model proposed in the paper.

Without his contributes, this paper would never have been not only published, but also conceived.

Sincerely,

Valerio Acocella

TECTONICS, VOL. 22, NO. 4, 1045, doi:10.1029/2002TC001447, 2003

Oblique back arc rifting of Taupo Volcanic Zone, New Zealand

V. Acocella

Dipartimento di Scienze Geologiche, Università Roma Tre, Rome, Italy

K. Spinks and J. Cole

Department of Geological Sciences, University of Canterbury, Christchurch, New Zealand

A. Nicol

Institute of Geological and Nuclear Sciences, Lower Hutt, New Zealand

Received 8 August 2002; revised 5 February 2003; accepted 4 April 2003; published 28 August 2003.

[1] Taupo Volcanic Zone (TVZ) is a back arc rift in North Island, New Zealand. Its geometry and kinematics are investigated using shaded relief images, field examination of faults and offset stream channels. The results show that TVZ trends NNE, is ~250 km long by ~20 km wide and consists of five segments. Extension is principally manifest as steeply dipping (60°–90°) normal faults parallel to TVZ; these, in the last 300 kyr, have experienced a component of dextral shear. TVZ is therefore an oblique back arc rift. The dextral shear is ~37% of the total displacement, which, for previously estimated spreading rates ~7 mm/yr, corresponds to ~2.6 mm/yr. This value is similar to previous estimates of the dextral shear from the back arc to the forearc domains in the North Island. Distributed dextral shear across TVZ thus suggests that strain partitioning across the plate boundary at latitudes of TVZ is less significant than previously thought. *INDEX TERMS:* 8150 Tectonophysics: Plate boundary—general (3040); 8109 Tectonophysics: Continental tectonics—extensional (0905); 8010 Structural Geology: Fractures and faults; *KEYWORDS:* strain partitioning, back arc, oblique rifting, active faults, Taupo Volcanic Zone. **Citation:** Acocella, V., K. Spinks, J. Cole, and A. Nicol, Oblique back arc rifting of Taupo Volcanic Zone, New Zealand, *Tectonics*, *22*(4), 1045, doi:10.1029/2002TC001447, 2003.

1. Introduction

[2] Analysis of the geometry and kinematics of faults within rift systems allows a greater understanding of the relationships between the formation and evolution of rifts, magmatic activity and regional plate tectonics. In back arc settings, for example, an improved understanding of the structure and kinematics of rift zones may contribute to a greater comprehension of the dynamics of plate convergence [*Taylor and Karner*, 1983]. This becomes particularly relevant in conditions of oblique convergence, where a strike-slip component of relative plate motion may contribute to the evolution of a back arc [*Taylor et al.*, 1994].

[3] Taupo Volcanic Zone (TVZ) is a back arc rift developed in association with oblique convergence along the Hikurangi margin in the North Island of New Zealand [*Cole*, 1990, and references therein]. Here oblique convergence is commonly believed to be partitioned, in the overriding Australian plate, into contractional and strike-slip components (Figure 1) [*Cashman et al.*, 1992; *Beanland*, 1995; *Webb and Anderson*, 1998]. Precisely how the kinematics of the back arc of the North Island relates to such partitioning has not been resolved by widespread field investigations.

[4] A component of dextral shear along TVZ has been inferred from the en echelon configuration of fractures and eruptive fissures [*Nairn and Cole*, 1981], the presence of dextral faults in the basement [*Cole*, 1990] and focal mechanisms from microearthquakes [*Smith and Webb*, 1986]. Recent results from geological mapping [*Rowland and Sibson*, 2001] and GPS measurements [*Darby and Meertens*, 1995; *Darby et al.*, 2000] suggest, however, orthogonal rifting of TVZ; in particular, *Darby and Meertens* [1995] report a mean extension direction, along the whole TVZ, of 124°–304° (±13°), which trends at 94° to the mean trend of the rift (030°).

[5] At the scale of TVZ, a consensus has not been reached regarding the structure (e.g., rift symmetry and segmentation). For example, most of the onshore TVZ rift is considered symmetric [*Rowland and Sibson*, 2001], while seismic reflection profiles from the northern end of the rift show it to be asymmetric [*Davey et al.*, 1995]. Moreover, even though TVZ has been considered as a continuous structure, with a uniform widening [*Grapes et al.*, 1987], it has been recently divided into segments separated by accommodation zones [*Bryan et al.*, 1999; *Rowland and Sibson*, 2001].

[6] Within this framework, we aim to address three principal questions. First, was the TVZ formed in association with orthogonal rifting and, if not, what is the angle of obliquity of rifting. Second, are there any relationships between fault geometry and kinematics, and volcanism

0278-7407/03/2002TC001447$12.00

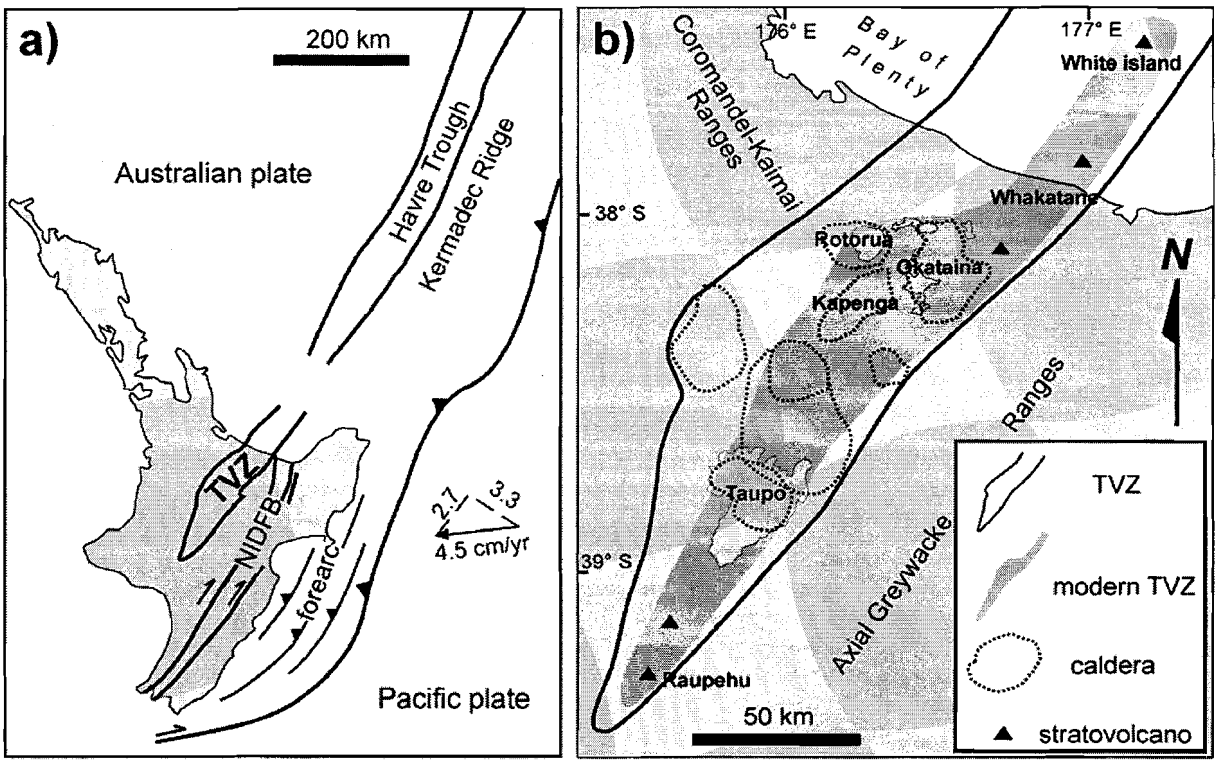

Figure 1. (a) Schematic relationship of TVZ to the boundary between the Pacific and Australian plates and forearc structures (oblique convergence vectors are shown in cm/yr) from *DeMets et al.* [1994]. (b) Schematic map of the Taupo Volcanic Zone (TVZ), showing the major caldera complexes [after *Wilson et al.*, 1995].

along the rift. Third, can the kinematics of the rift be reconciled with the kinematics of the plate boundary in the North Island of New Zealand. The structure and kinematics of TVZ are examined using a shaded relief image and fieldwork throughout TVZ. The data show that TVZ is an oblique back arc rift, with a component of dextral shear. The implications of this conclusion are discussed with reference to slip partitioning across the obliquely convergent plate boundary in the North Island of New Zealand.

2. TVZ and Its Tectonic Framework

[7] The NNE-SSW trending Taupo Volcanic Zone is the southernmost part of the Havre-Lau volcanic rift zone and results from convergence between the Australian plate and the westward subducting Pacific plate (Figure 1a) [*Kamp*, 1984; *Stern*, 1985; *Benes and Scott*, 1996; *Parson and Wright*, 1996]. The plate interface is offshore and to the east of the North Island of New Zealand, along the Hikurangi trough. The mean convergence vector at the latitude of TVZ is oriented at ~263°, with a velocity ~4.5 cm/yr [*DeMets et al.*, 1994] (Figure 1a). Strain partitioning has been inferred to occur across the plate boundary zone in the North Island [*Cashman et al.*, 1992; *Beanland and Haines*, 1998; *Webb and Anderson*, 1998]. Contraction could mainly occur in the forearc, whereas strike-slip motion may be largely restricted to the North Island Dextral Fault Belt (NIDFB), which partly defines the eastern margin of the North Island Axial Ranges [*Cashman et al.*, 1992; *Beanland*, 1995; *Beanland and Haines*, 1998; *Beanland et al.*, 1998; *Webb and Anderson*, 1998]. Strain partitioning may not be complete, as strike-slip faults have been observed in the forearc, while reverse faults and folds occur within the NIDFB [*Cashman et al.*, 1992; *Beanland*, 1995; *Davey et al.*, 1997; *Beanland et al.*, 1998].

[8] The eastward shift of the subduction thrust may have been responsible for an eastward migration of the NIDFB (at least in the last 6 Ma) [*Lamb*, 1988] and of the back arc rift and associated volcanism [*Cole and Lewis*, 1981; *Brothers*, 1984]. Extension and volcanic activity are an expression of back arc spreading within continental lithosphere [*Stern*, 1985; *Cole and Nairn*, 1986; *Tatsumi and Tsunakawa*, 1992; *Cole et al.*, 1995; *Davey et al.*, 1995].

[9] TVZ marks the present location of back arc spreading within the North Island and produces a crustal thinning of up to 15 km [*Bibby et al.*, 1995] (Figure 1). Recent GPS measurements from throughout the TVZ [*Darby and Meertens*, 1995] and fault slip data [*Villamor and Berryman*, 2001] suggest that the present spreading rate across TVZ onshore and north of Lake Taupo is 6–8 mm/yr.

[10] Volcanic activity accompanied the development of TVZ in the last 1.5 Ma [*Houghton et al.*, 1995]. The present

site of active volcanism and extension is focused in a NNE-SSW trending narrow zone (20–30 km wide), which is referred to here as the modern TVZ (Figure 1b) and mainly formed in the last 300 kyr [*Houghton et al.*, 1995; *Wilson et al.*, 1995]. The modern TVZ is divided into three parts along its length: (1) a central part (from Okataina to Taupo; Figure 1b), with several calderas associated with rhyolite volcanism at the surface [*Rogan*, 1982; *Wilson et al.*, 1984; *Graham et al.*, 1995] and plutons at depth [*Soengkono*, 1995; *Brown et al.*, 1998]; (2) two lateral parts (Ruapehu to the south and Whakatane-White island to the north; Figure 1b), with andesite-dacite strato-volcanoes [*Wilson et al.*, 1995; *Wilson*, 1996]. The central section is an extraordinarily productive region of rhyolitic volcanism ($\sim$0.28 m^3s^{-1}) and geothermal fluxes ($\sim$4200 MW), which are unparalleled on the planet [*Wilson*, 1996]. The two largest magmatic systems, associated with the Taupo and Okataina caldera complexes, located at the boundaries of the central part (Figure 1b), are responsible for the extrusion of thousands of cubic kilometers of ignimbrites in the last 300 kyr [*Nairn*, 1981, 1986, 1989; *Sutton et al.*, 2000; *Jurado-Chichay and Walker*, 2001; *Wilson*, 2001]. Seismic activity has been accompanying extension along TVZ [*Smith and Webb*, 1986, and references therein]. The most recent and well-studied earthquake occurred at Edgecumbe, in the Whakatane graben (north TVZ) in 1987. This earthquake was characterized by the development of NE-SW trending faults and extensional fractures at the ground surface, with almost pure extension, consistent with focal mechanisms [*Grapes et al.*, 1987; *Beanland et al.*, 1989; *Crook and Hannah*, 1989; *Anderson et al.*, 1990]. This study focuses on the definition of the geometry and kinematics of modern TVZ (<300 ka).

3. DEM Analysis

[11] Analysis of a shaded relief image was undertaken to determine the location and strike of normal faults that define the structure of the modern TVZ. The shaded relief image was generated from a Digital Elevation Model (DEM), produced by Landcare Research New Zealand Ltd. The DEM was generated from the Land Information New Zealand 1:50,000-scale topographic database (20 m contours) and has a grid separation of 25 m.

[12] The shaded relief image enabled the recognition of lineaments, possibly of a tectonic origin, both within and outside the modern TVZ. Within the modern TVZ, these lineaments are frequently coincident with fault scarps mapped within rhyolitic volcanic rocks < circa 300 ka [*Rowland and Sibson*, 2001, and references therein; *Villamor and Berryman*, 2001, and references therein]. These faults are generally active, at least toward the axis of TVZ, and thus we infer that most lineaments within the modern TVZ are the morphological expression of active faults.

[13] The shaded relief image indicates that the modern TVZ is mainly characterized by an array of NNE-SSW trending lineaments, with a mean resolvable length of 10–15 km (Figure 2). The lineaments on the image are quite scattered over a broad area (40–70 km wide), with the axial region of TVZ (<30 km wide) characterized by the highest densities in the array. These high densities occur within the youngest rocks, consistent with the view that this axial region is the focus of strain accumulation. Here, within the high strain zone, fault scarps verge toward the rift axis. This scarp geometry is well developed in the Kapenga area, where the central portion divides mainly opposite-verging subparallel scarps, resembling a graben.

[14] The overall trend of the lineaments along the modern TVZ is NNE-SSW; nevertheless, faults and vent lineaments in the Okataina area have a mean NE-SW to ENE-WSW strike, suggesting a bend in TVZ (inset Figure 2). Moreover, the analysis of the shaded relief image suggests that the modern TVZ is not a continuous structure. On the basis of the presence, trend and lateral continuity of lineaments, five segments have been identified. These are here referred to as the Ruapehu, Taupo, Kapenga, Okataina and Whakatane segments (dotted lines in Figure 2). These segments may be soft or hard linked and partly correspond with segments identified by *Rowland and Sibson* [2001]. The Whakatane and Kapenga segments are hard linked (in structural continuity) by the Okataina segment, while the Taupo segment is soft linked (without evident structural continuity) to the Kapenga segment (Figure 2).

4. Structural Data

[15] Structural field data consist of measurements of the fractures along TVZ and of the evaluation of the displacement of offset stream channels. Fault orientation and slip directions, together with joint and dike orientations, were collected during fieldwork in TVZ, from the Whakatane graben in the north to Ruapehu volcano in the south, over a distance of 200 km. These data were mainly ($\sim$90%) sampled from layered pyroclastic deposits (younger than 300 ka) [*Houghton et al.*, 1995; *Wilson et al.*, 1995] along TVZ and subordinately from lake sediments (younger than 200 ka) [*Villamor and Berryman*, 2001] within parts of the Kapenga graben and Rotorua caldera. The majority of faults are from within the modern TVZ and reflect deformation younger than 300 ka.

[16] Data consist of faults (68%), joints (31%) and dikes (1%). All of the data are plotted on Schmidt lower hemisphere nets in Figure 3a (whole TVZ) and 3b (inset of Kapenga area), where measurements from 30 sites are differentiated. In these plots, faults are represented with solid curves and joints by dashed curves (except for sites 36 and 39, where dashed lines refer to feeder dikes with thickness $\sim$5 m). In this paper we use the general term fracture for all types of mechanical discontinuities or breaks in the host rock, including faults (i.e., shear fractures with movement parallel to the failure surface) and joints (i.e., extension normal to the failure surface). Figure 4 shows two examples of large (displacement $\Delta > 10$ m) normal faults in the Taupo (a) and Kapenga (b) segments.

4.1. Geometry of Fractures

[17] Joints are subvertical and characterized by small (<5 cm) dilations. Their dominant strikes are roughly NE-

TVZ segments	data (lineaments)	mean trend	standard deviation
WS	21	N37°E	7.2°
OS	31	N69°E	13.1°
KS	32	N37°E	8.3°
TS	13	N40°E	4.4°
RS	25	N28°E	9.4°

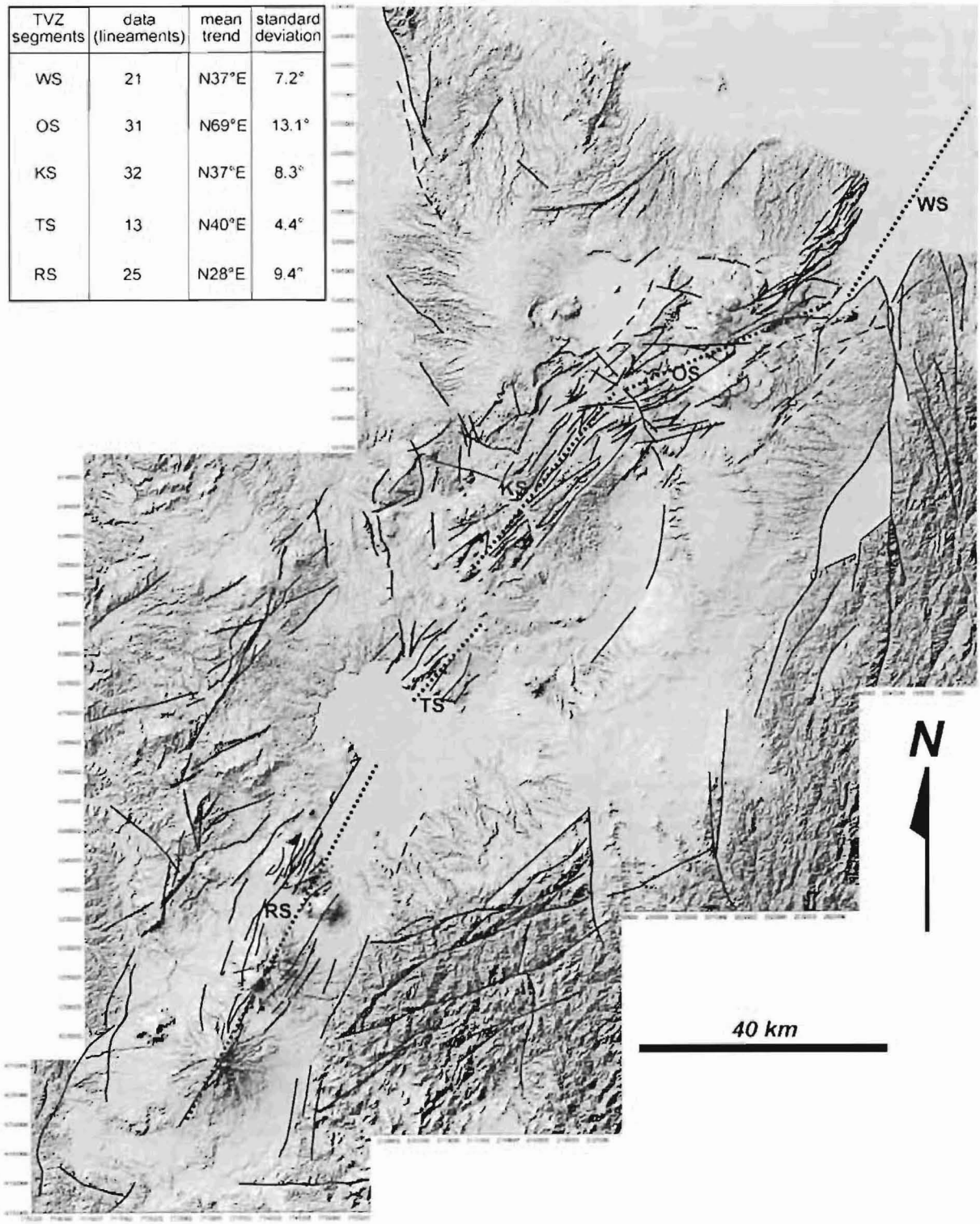

SW (throughout TVZ, sites 6, 18, 31, 41, 43, 60 in Figure 3) and NW-SE (in the northern part of the Kapenga area, sites 6, 12, 55 in Figure 3). Faults typically have high angle (~60°) to subvertical (80°–90°) dips and displacements (typically a few centimeters to a few hundred meters) with predominantly extensional motion. The strike (0°–359°) of fractures is shown in Figure 5a. Preferred values of fracture strike are ~N31° (for fractures dipping to the east) and ~N217° (for fractures dipping to the west), with approximately equal numbers in each dip direction. This NNE-SSW direction is parallel to TVZ. The strike of the fractures from −90° to +90° are shown in Figure 5b: 36% of the fractures cluster around N33°E ± 23° (TVZ trend), whereas 19% cluster around N70°E ± 26° (mostly in the Okataina area; Figure 3) and 10% around N31°W ± 23° (mostly in the Kapenga-Rotorua area; Figure 3). The mean strike of fractures for each of the segments identified using the shaded relief image is reported in the inset in Figure 3a. The measured fractures are mainly subvertical, with a mean dip of 83° (Figure 5c).

[18] The comparison of Figures 2 and 3 shows that, for a given area, the density of the lineaments found on the image is consistent with the density of the fractures found in the field. Moreover, the strike of the fractures measured in the field is parallel to the strike of nearby lineaments shown on the image. This is evident comparing the insets in Figures 2 and 3, which report the mean trend of the lineaments and strike of fractures for each segment. Here we are attempting to delineate the orientation of fractures and lineaments that are associated with the principal trend of TVZ; therefore only lineaments and fractures within ±30° of the trends of the corresponding TVZ segment have been considered. The trends of the lineaments and fractures are very similar, given the considered error ranges. This confirms the widespread tectonic control on the formation of the lineaments observed along TVZ and supports the interpretation that most lineament forming scarps result from tectonic activity.

4.2. Kinematics of Faults

[19] The motion of all of the TVZ faults observed was consistent with extensional components of displacements. Prior to the present study, however, few fault slip vector data had been collected and a component of strike-slip displacement on many of the faults could not be discounted. In order to constrain better the kinematics of faults within TVZ, we have measured the orientations of striations or grooves on fault planes and derived slip vectors from offset abandoned stream channels. The slip sense for striations and grooves on fault surfaces was often determined from displacement of the ground surface above the measurement site.

[20] Displaced streams, abandoned between 15 and 25 ka BP (see data from *Villamor and Berryman* [2001]), provided piercing points with which to estimate slip vectors on seven faults with throws >10 m. Displacements were derived by locating the stream channel axis on each side of the fault (Figure 6). In most cases, the channels trend at high angles (>70°) to the faults and are typically eroded at each fault. Therefore, the channel axes were projected up to 5–10 m to the fault and piercing points located in both walls of the fault using GPS and tape measure. Slip vectors were calculated using these points together with the orientation of the fault surface. The trends of these slip vectors have uncertainties of up to ±28° (table in Figure 6) and are considered to be less precise than slip data measured from fault surfaces.

[21] The pitch of slip vectors from faults and offset stream channels is presented in Figure 5d. Pitch values range from 0° to 180°; 0° and 180° correspond to pure strike-slip motions, whereas pitches = 90° correspond to pure dip-slip motions. The pitch of slip vectors on faults subparallel to TVZ trend are reported as a function of the evaluated displacement (Δ in meters) in Figure 5d; since the stream offsets are all on faults with displacements larger than 10 m, these have been added (in lighter gray) to the faults with $\Delta >$ 10 m. The whole fault population ($\Delta > 0.1$ m) clusters around a mean pitch = 99°. The mean pitch becomes progressively more oblique with increase in fault throw, changing from 103° for the selected faults with $\Delta > 1$ m displacement to 119° for the selected faults with large, $\Delta >$ 10 m, displacement. The range of variation (standard deviation in Figure 5d) of these values decreases with increasing displacement. Figure 5d thus shows that the mean values for the pitch of the normal faults are >90°, from which we suggest a component of dextral shear.

[22] Not all the faults have the same reliability to assess the kinematics of an area; faults with larger displacements (tens of meters) are in fact probably more reliable than faults with smaller displacements (few centimeters), which may be more easily influenced by external processes (gravity, compaction, emplacement of dikes, etc.). Therefore, we calculate the mean pitch of the whole fault population by weighting the faults according to the order of magnitude of their throw. Small faults ($\Delta < 1$ m) = weight 1, medium faults ($1 < \Delta < 10$ m) = weight 10, large faults ($\Delta > 10$ m) = weight 100. The mean pitch derived from such weighting = 118°.

[23] The range between 99° (mean pitch related to the unweighted data) and 118° (mean pitch related to the weighted data), with a mean value of 109° ± 10°, represents the possible variation in the evaluation of the dextral shear along TVZ. If we take into account the displacement of the measured faults, given this mean pitch of 109°, the dextral (D) and the extensional (E) (i.e., dip slip) components can

Figure 2. (opposite) Shaded relief image of TVZ. The major lineaments, corresponding to scarps possibly related to tectonic activity, have been overprinted; dashed lines correspond to probable lineaments. The figure also shows the proposed division in segments (dotted lines) of the portions of modern TVZ, where lineaments with similar trends cluster (RS = Ruapehu segment, TS = Taupo segment, KS = Kapenga segment, OS = Okataina segment, WS, Whakatane segment). The inset shows the mean trend of the lineaments for each of the defined segments.

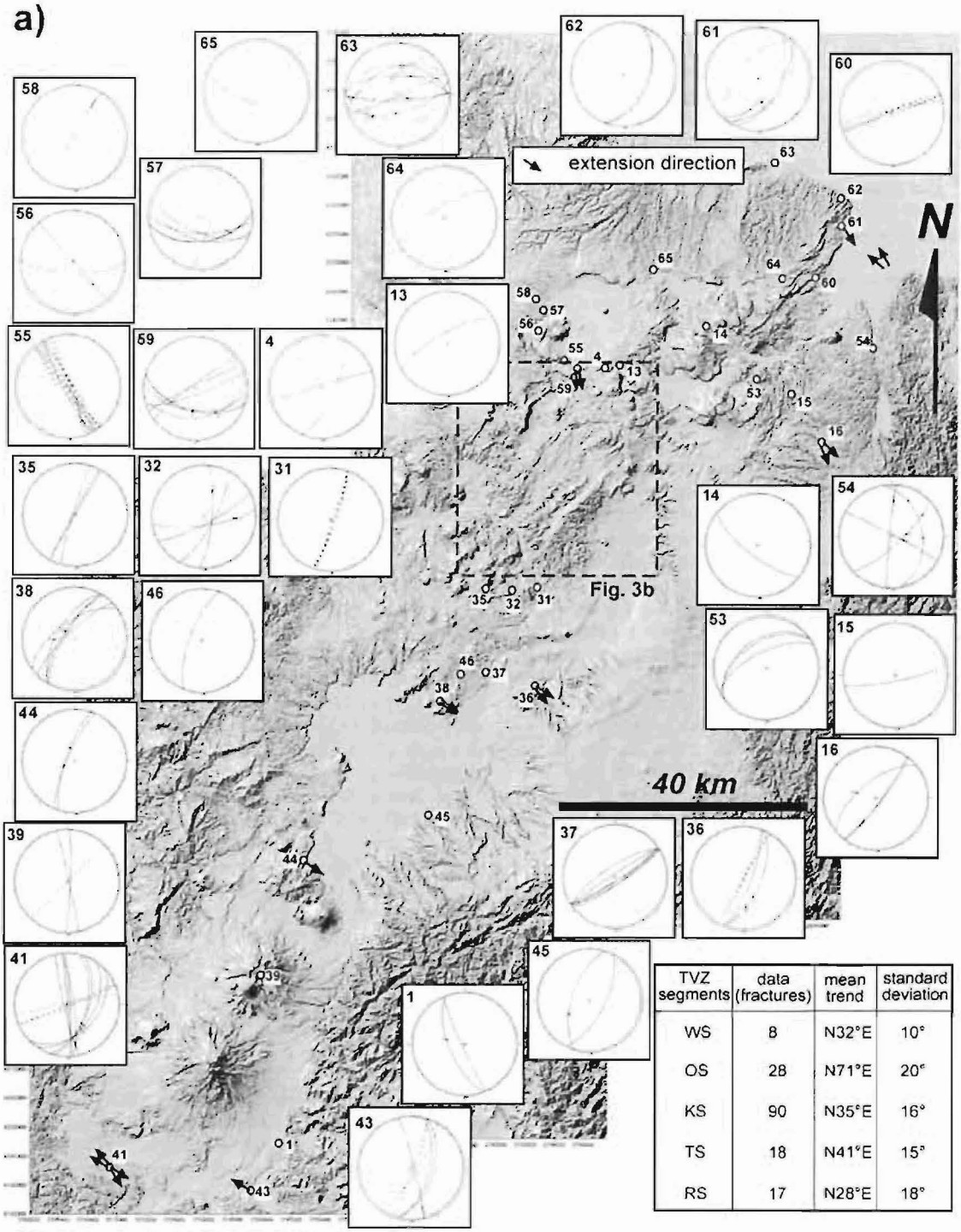

Figure 3. Structural data relative to (a) modern TVZ and (b) an inset of the Kapenga segment. The data are plotted on individual lower hemisphere stereonets for each sample site; solid lines = faults; dashed lines = joints; arrows within the plots represent sense of movement, as inferred from striations; black arrows on the shaded relief image represent extension directions of faults with $\Delta > 1$ m, determined using the procedure of *Marrett and Allmendinger* [1990]. The inset in Figure 3a shows the mean trend of the measured fractures for each segment of TVZ, as defined in Figure 2.

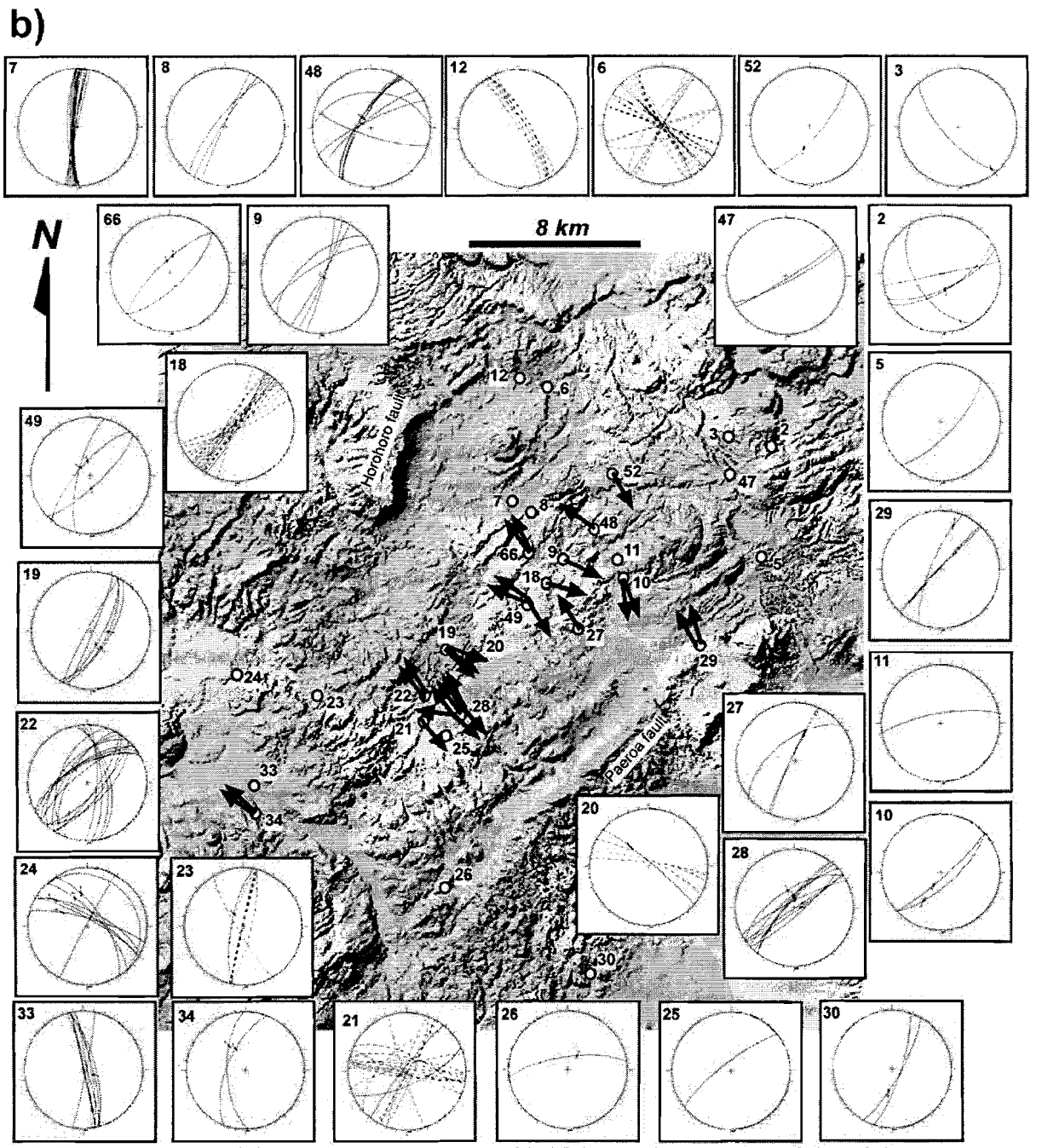

Figure 3. (continued)

be evaluated. The ratio D/E between the dextral and extensional shear is:

$$D/E = \sin(109° - 90°)/\cos(109° - 90°) = 0.34 \quad (1)$$

This shows that the strike slip component D = 34% of the vertical displacement E or D = sin19° = 33% of the total displacement.

[24] Even though the pitch data in Figure 5d are for steep or subvertical faults subparallel (±30°) to TVZ trend, they

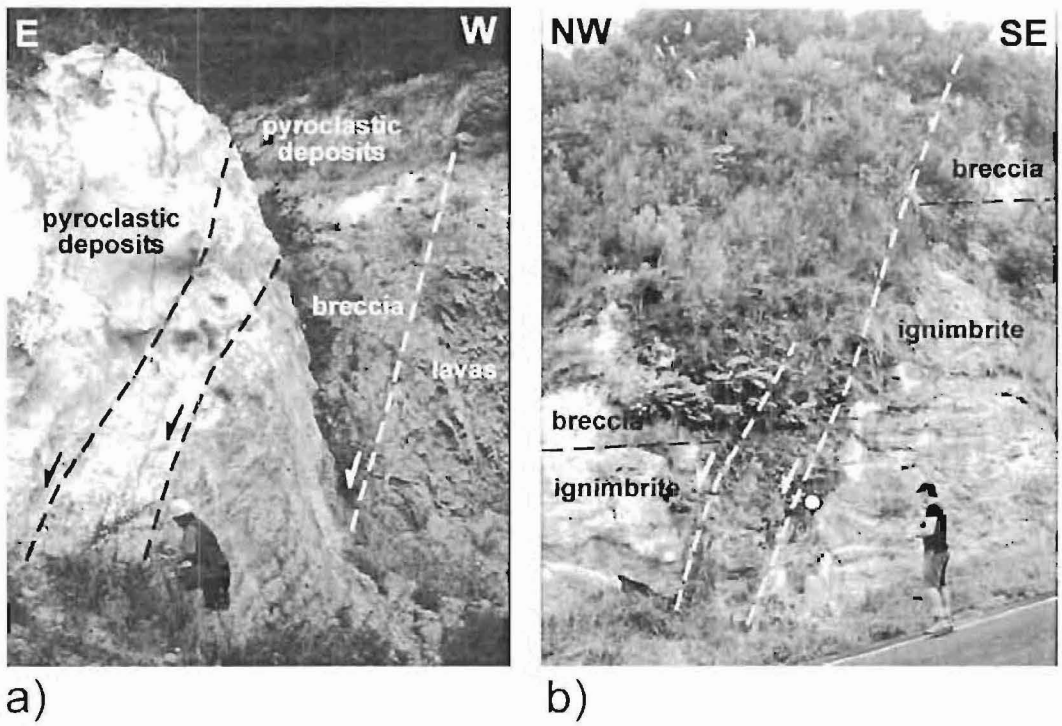

Figure 4. Pictures of faults with large (>10 m) displacements found along TVZ. a) NNE-SSW trending fault on the northeastern portion of Lake Taupo (site 36 in Figure 3a). (b) NNE-SSW trending Paeroa fault on the eastern border of the Kapenga graben; this fault shows marked dextral motion; the white circle shows where the oblique slickensides were observed (site 29 in Figure 3b).

could be affected by local variations in fault strike and dip. To reduce the impact of fault orientation on the results, we derive the fault extension directions using the procedure of *Marrett and Allmendinger* [1990]. Their stereographic technique permits the determination of the orientations of the maximum, minimum and intermediate strain axes. The extension direction is at 45° from the slip vector along the plane which passes through the pole to the fault and the slip vector (Figure 7a). The arrows at the measurement sites in Figure 3 represent the estimated extension directions of the faults with $\Delta > 1$ m.

[25] The extension directions obtained from faults subparallel (±30°) to the trend of TVZ are shown in Figure 7b, where they are plotted as a function of their distance from the rift axis (in km) and their displacement. Faults from each segment (see Figure 2) are distinguished using different symbols. The rift axis is located where the main dip direction of faults switches from east to west dipping, consistently with the results from *Rowland and Sibson* [2001]. The displacement of the faults (small: $\Delta < 1$ m; medium: $1 < \Delta < 10$ m; large: $\Delta > 10$ m) is indicated by the size of the symbol. Finally, the directions orthogonal to the trend of each segment in TVZ, which correspond to a pure extension direction, are indicated in Figure 7b.

[26] Most of the faults have an extension direction between 300° and 340° (Figure 7b). In particular, all the data within the Ruapehu and Whakatane segments and most (especially for larger displacements) of the data from the Kapenga segment are above the line of orthogonal extension. This suggests that the faults in these segments have a dextral component of motion. Conversely, the data within the Taupo and Okataina segments show predominately an orthogonal extension. The eastern portion of the Kapenga graben indicates a weak increase in the obliquity of the extension direction from the axis of the graben.

[27] The data shown in Figure 7b are summarized in the map (and the underlying table) in Figure 8, which documents the mean fault strike and the mean trend of extension for TVZ segments (only for faults with $\Delta > 1$ m). The data show slight variation in extension directions of different segments; however, given the uncertainties and the number of data points, these differences are within the resolution of the data. Unlike the other segments, the mean trends of the Whakatane and Ruapehu segments in the insets of Figures 2 and 3, obtained through lineaments and fractures, are slightly different (<7°) from the general trend of the Whakatane graben and the alignment of volcanoes along the Ruapehu segment (Figure 2). Nevertheless, we consider these large-scale morphological features as more representative for the overall trend of the related segments. Thus, the general trends of the Whakatane and Ruapehu segments in Figure 8 are slightly different from those in the insets of Figures 2 and 3.

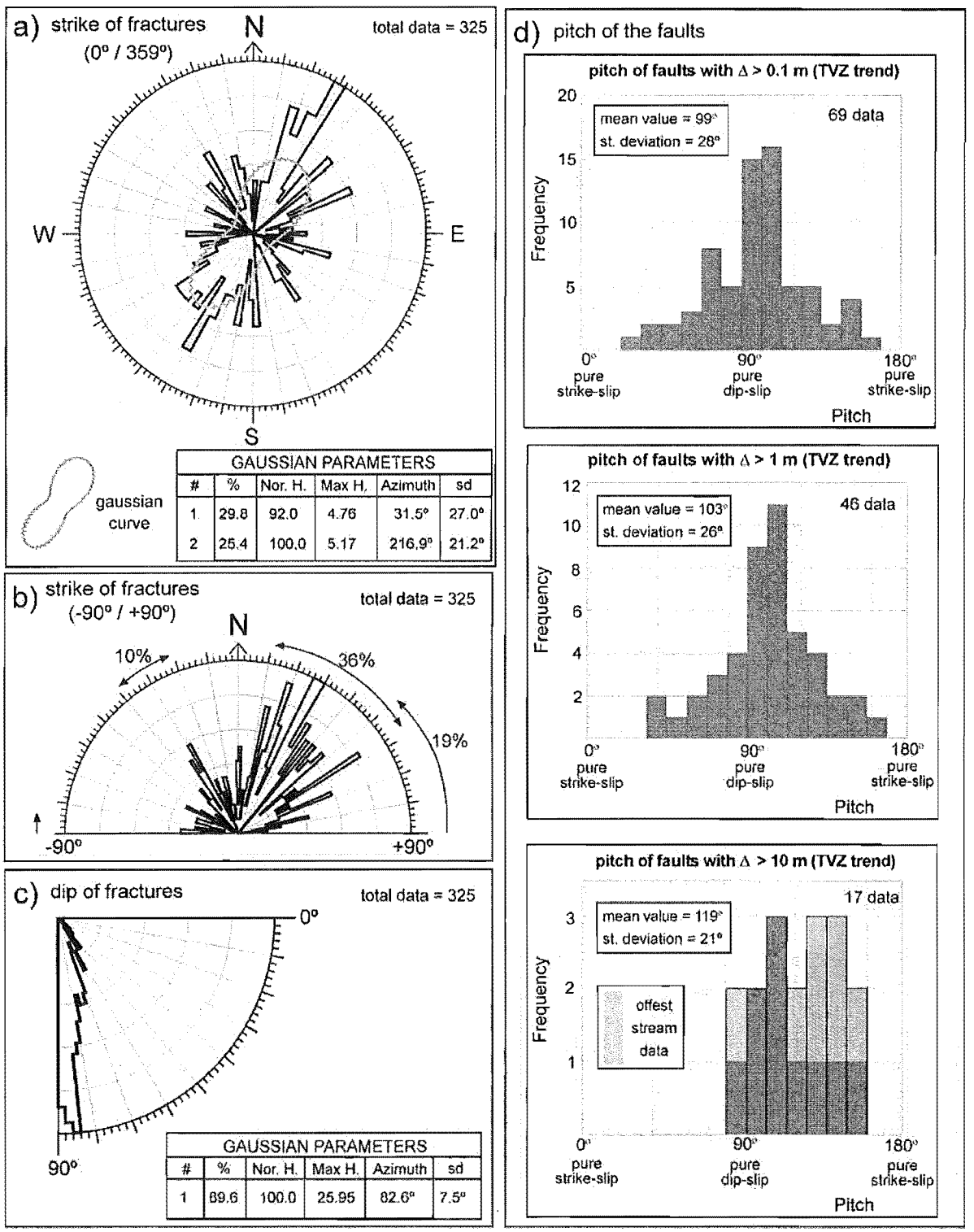

Figure 5. Geometry and kinematics of the fractures measured in the field. (a) Strike (0°/360°) of the fractures; b) strike (−90°/+90°) of the fractures; (c) dip of the fractures; (d) pitch of the faults as a function of their displacement Δ; upper diagram includes faults with Δ > 0.1 m (whole fault population), central diagram includes faults with Δ > 1 m and lower diagram includes only faults with Δ > 10 m.

Location	Grid ref	Fault orientation		Slip direction		Slip direction errors			Principal strain axes		Pitch
		strike	dip	trend	plunge	trend (+/-)		plunge	extension	shortening	
Highlands Rd	019 238	75°	67°	207°	58°	+21°	-5°	15°	180°/18°	317°/62°	133°
Tumunui Rd	981 247	230°	70°	340°	68°	+28°	-2°	7°	327°/19°	128°/65°	110°
North Barber Rd	959 233	220°	70°	359°	60°	+25°	-8°	22°	326°/22°	096°/60°	139°
North Barber Rd	961 233	220°	74°	10°	60°	+13°	-7°	16°	330°/25°	100°/52°	150°
Rotohauhau Flt	949 206	215°	65°	304°	65°	+7°	-2°	2°	304°/20°	126°/67°	89°
Rotohauhau Flt	951 208	217°	65°	346°	58°	+15°	-2°	8°	321°/15°	091°/65°	129°
Rotohauhau Flt	951 208	217°	65°	354°	58°	+14°	-4°	10°	323°/15°	90°/61°	137°

a)

b)

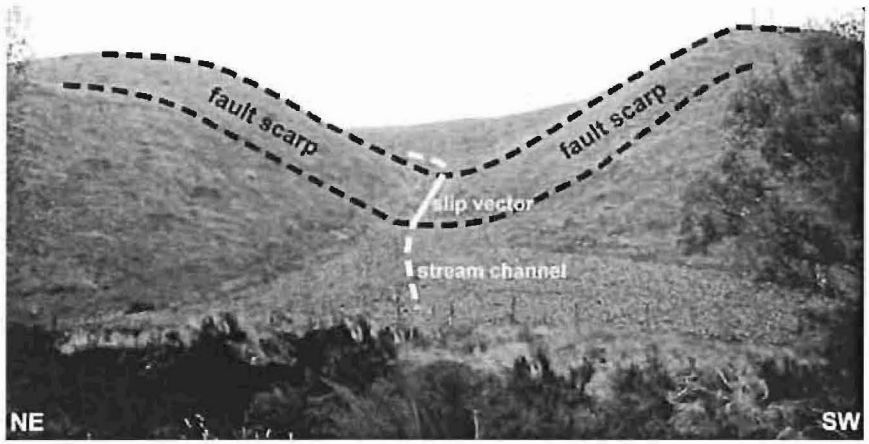

Figure 6. (a) Data from 7 offset abandoned stream channels, Kapenga area. Their locations are given as a grid reference from NZMS 260, sheet U16. Fault dips were estimated from nearby fault exposures or from structure contours on the fault surface. Slip directions were calculated using estimates of horizontal and vertical displacement of channel axes. Measurement errors mainly reflect uncertainty in the position of the channel axis and projection of the channel to the fault surface. The principal strain axis orientations were estimated from the fault orientation, slip direction and slip sense using the method of *Marrett and Allmendinger* [1990]. (b) Example of an abandoned stream channel offset by a fault from Tumunui Rd (see Figure 6a table details). Photo shows view approximately normal to the fault scarp. Offset of the stream channel requires 9 ± 2 m of vertical and 3.5 ± 1.5 m of horizontal displacement.

[28] We define the angle β between the direction perpendicular to the trend of the rift segment and the extension direction (Figure 8, inset); this angle is proportional to the component of horizontal shear along the segment: $\beta = 0°$ corresponds to a pure orthogonal extension; $\beta > 0°$ (clockwise direction) corresponds to a component of dextral shear and $\beta < 0°$ (anti-clockwise direction) corresponds to a component of sinistral shear. The data obtained from TVZ show that different segments are characterized by different components of dextral shear, ranging from 0° (Okataina and Taupo segments) to 23° (Whakatane segment). Except for the Okataina segment, the extension direction along each of the segments is consistent (130°–143°), with a mean value of 137°. For a mean trend of 030° for TVZ and a trend of 137° for the extension direction, the mean $\beta = 17°$ for the whole TVZ. For a hypothetical fault with a strike of 030° and a dip of 83°, this β corresponds with slip vector that pitches at 113° and has a dextral component that is ~43% of the vertical displacement, or 39% of the total displacement.

5. Discussion

5.1. Architecture of the TVZ

[29] The good match in the trend of the lineaments and strike of the fractures suggests that most of the scarps identified as lineaments on the shaded relief image are tectonic. Recognition that most lineaments are tectonic has allowed us to evaluate the strikes, locations and densities of faults within the modern TVZ. In addition, fieldwork has provided details of the geometry (strike, dip) and kinematics of the fractures along TVZ. Collation of the shaded relief image and field data produced the structural map in Figure 9.

[30] Modern TVZ is a NNE-SSW trending rift zone, 20–30 km wide, with a major bend (toward an ENE-WSW

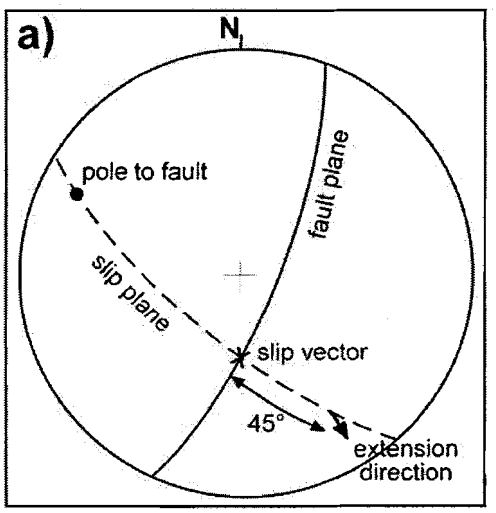

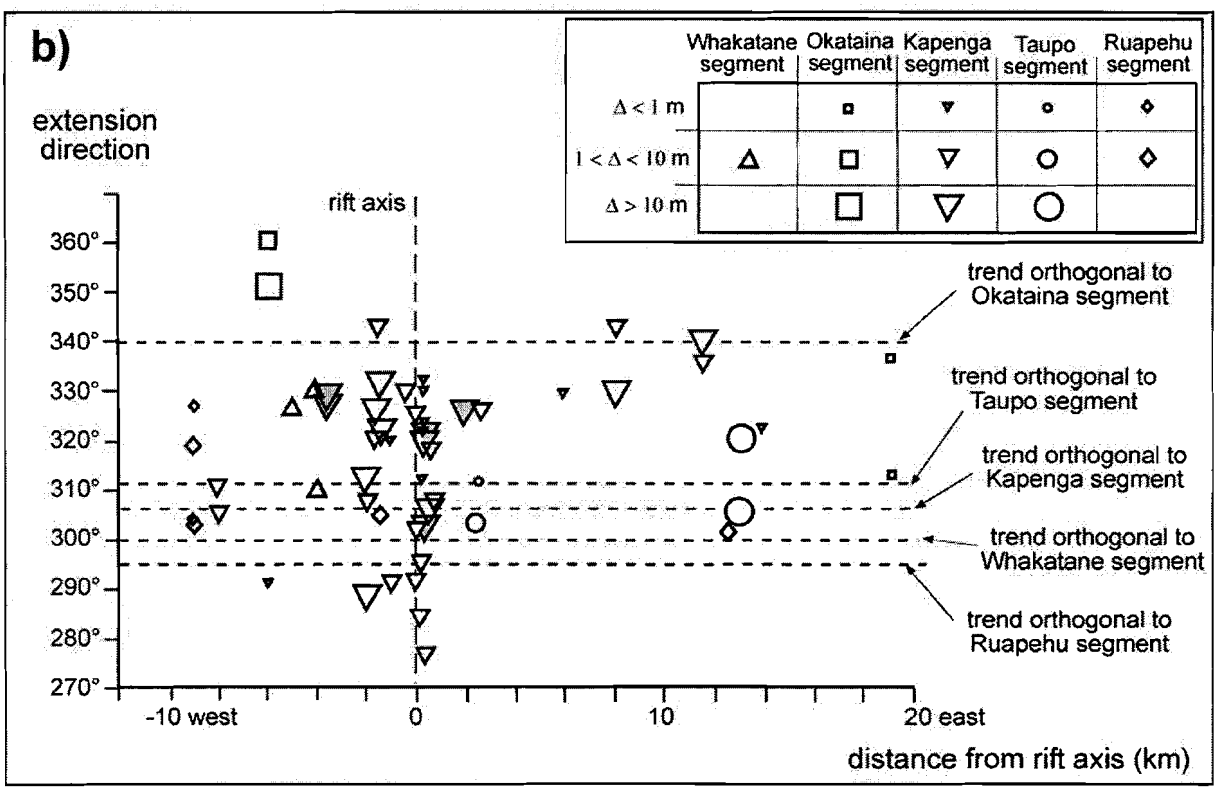

Figure 7. (a) Stereographic procedure used to evaluate the extension direction from the strike, dip and pitch of a fault (modified after *Marrett and Allmendinger* [1990]). (b) Extension directions of the faults as a function of their location within TVZ, their distance from the axis and their displacement. Gray triangles indicate data from offset stream channels.

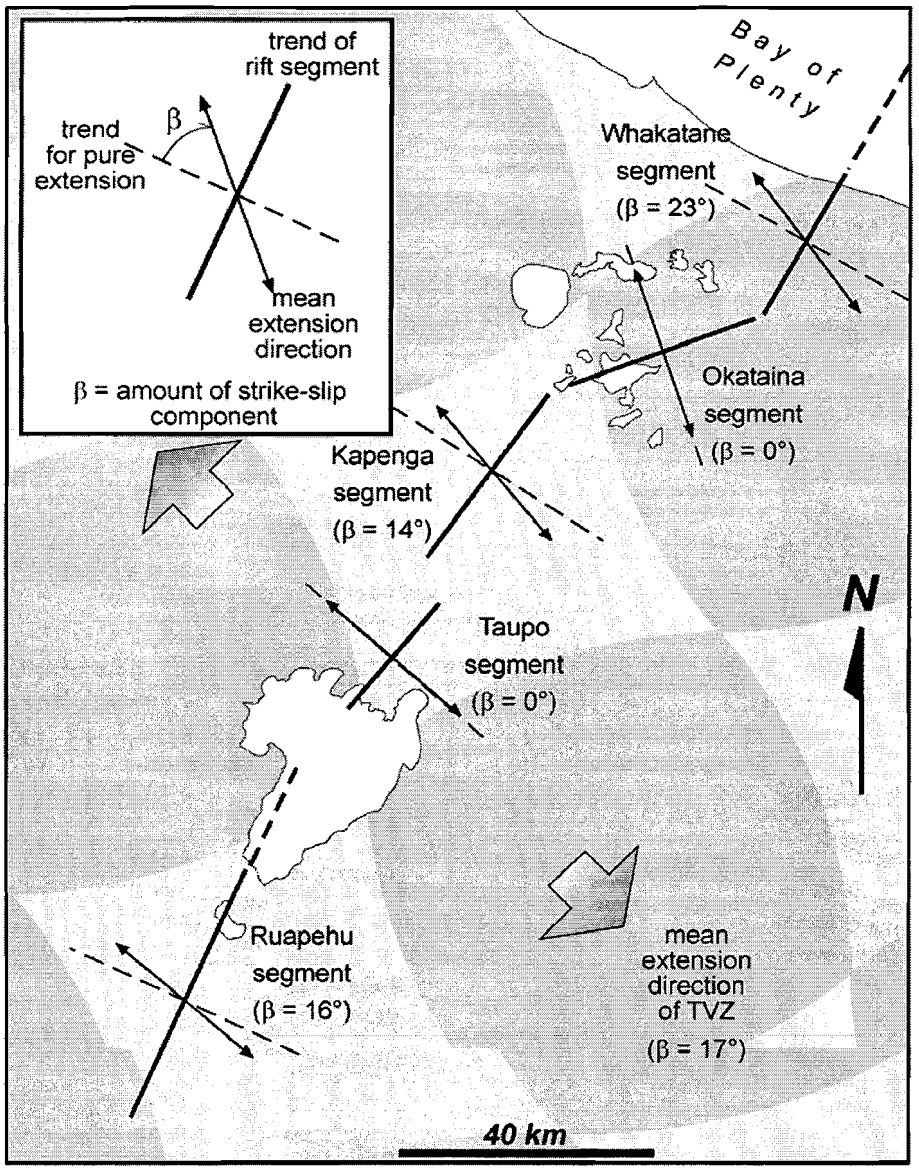

rift zone	trend	extension direction	β
Whakatane	N30°E ± 8°	N37°W ± 3° (3 data)	23°± 4° (dx shear)
Okataina	N70°E ± 17°	N19°W ± 15° (4 data)	1°± 10° (no shear)
Kapenga	N36°E ± 12°	N40°W ± 16° (43 data)	14°± 10° (dx shear)
Taupo	N41°E ± 9°	N49°W ± 8° (4 data)	0° ± 7° (no shear)
Ruapehu	N25°E ± 13°	N50°W ± 7° (6 data)	16° ± 5° (dx shear)
TVZ	N30°E ± 6°	N43°W ± 16° (56 data)	17° ± 11° (dx shear)

direction) in the Okataina area (Figure 9). TVZ appears to be a symmetric rift, with a central graben axis (Figure 9). This conclusion is supported by the similar number of opposite-verging scarps (Figure 2) and fractures (Figure 5a) parallel to the TVZ.

[31] In detail, the Okataina segment (1) connects, through obliquely trending fault and vent lineations, the parallel Whakatane and Kapenga grabens; (2) has curved faults accommodating such connection (and partly controlling the subsequent development of the Okataina caldera structures); and (3) is characterized by a slight (~20°) variation in the extension direction (orthogonal to the Okataina structures) with respect to the Whakatane and Kapenga areas (Figure 8), consistent with their en echelon dextral configuration. These features suggest that the Okataina segment is a transfer zone within TVZ. Similar geometric and kinematic features have been observed along other transfer zones in narrow rifts [*Gudmundsson et al.*, 1993; *Acocella et al.*, 2000] and in analogue models [*Acocella et al.*, 1999]. The inset in Figure 9 shows a map view of a sandbox experiment simulating the interaction between two parallel offset segments; the extension direction (pulling direction) is orthogonal to the trend of the interacting segments [*Acocella et al.*, 1999]. As a result, a transfer zone, oblique to the two segments and characterized by internal rotations of the extension direction, is developed, similar to that observed in the Okataina area. Analogue models of narrow rifts are consistent with rift architecture being inherited from pre-existing structures, which may also be the case for the Okataina segment [*Cole*, 1990].

[32] The structural map in Figure 9 shows widespread N-S faults outside the modern TVZ. North striking faults east of the modern TVZ are active and may carry some dextral motion [*Beanland*, 1995]. North striking faults west of the modern TVZ may be inactive and could reflect extension during the early Pliocene (circa 4–5 Ma), associated with volcanism at this time in the Coromandel region [*Cole and Lewis*, 1981; *Brothers*, 1984].

5.2. Kinematics of the TVZ

[33] The predominant displacement of TVZ faults is extensional; nevertheless, a component of dextral motion occurs on the Whakatane, Kapenga and Ruapehu segments (Figure 8). By contrast, the Taupo and Okataina segments show, on average, an orthogonal direction of extension, with no dextral shear. The lesser component of dextral shear on the Okataina and Taupo segments in part reflects the more easterly strike of these segments of the rift (070° and 041°, respectively). With a uniform regional extension direction, these changes in segment trend would increase the proportion of segment-normal extension. The change in segment orientation is not, however, sufficient to account for all of the observed rotation in the extension direction. Therefore, we propose that within the Okataina segment the orthogonal nature of extension also reflects of a local rotation in the extension direction. Similar rotations in extension direction in bends of narrow rifts are observed in analogue models (Figure 9a) and are due to a local readjustment of the strain within interacting offset segments [*Pollard and Aydin*, 1984; *Gudmundsson et al.*, 1993]. These areas of pure extension typically also exhibit slightly lower fault dips (Figure 10). For example, the mean dip value of the fractures in Okataina is 76° (Figure 10), whereas the mean dip of the fractures along TVZ is 83° (Figure 5c). The slight decrease in dip may be related to the pure extensional (rather than oblique) stress field in the Taupo and Okataina areas, which, according to the Andersonian model of faulting, enhances high angle (rather than subvertical) faulting.

[34] The dextral shear, with the exception of the Taupo and Okataina areas, is widespread along TVZ. The mean dextral shear has been estimated as (1) 34% of the total displacement (mean value of the pitches from the weighted and unweighted fault populations); (2) 39% of the total displacement (using extension directions of the faults with $\Delta > 1$ m; Figures 7 and 8). The adopted methodologies are thus consistent with similar values (34%–39%) of the dextral component of the faults within TVZ.

[35] In synthesis, different evidence points to a dextral component of shear along TVZ, corresponding to a mean ~37% of the total displacement; this shows that TVZ is an oblique back arc rift. Assuming a mean spreading rate ~7 mm/yr on the Taupo and Kapenga segments of TVZ [*Darby and Meertens*, 1995; *Villamor and Berryman*, 2001], pure extension and dextral shear account for ~6.5 and ~2.6 mm/yr of deformation, respectively.

5.3. Implications for Volcanic Activity

[36] Volcanic activity along modern TVZ has been mainly focused (in volumetric terms) within the magmatic systems responsible for the Taupo and Okataina caldera complexes. These are the largest volcanic complexes (diameter ~30 km) in modern TVZ, and have erupted several thousands of km^3 of ignimbrites in the last 300 kyr [*Jurado-Chichay and Walker*, 2001; *Wilson*, 2001]. The Okataina caldera complex has a subcircular shape, with a slight NE-SW elongation [*Nairn*, 1981, 1989]. Volcanic activity occurred in two subparallel NE-SW trending zones crosscutting the caldera complex [*Wilson et al.*, 1984], subparallel to TVZ. The Taupo caldera complex is characterized by two elliptical

Figure 8. (opposite) Schematic view of TVZ segments, their mean extension direction and mean trend. β (see inset) is the angle between the direction perpendicular to the trend of the rift segment and the extension direction. The table reports the measured trends, extension directions and β values for each segment and for the whole TVZ. Two data for the Whakatane graben are taken from *Beanland et al.* [1989], *Crook and Hannah* [1989]. These two data refer to the focal mechanisms and the surface fractures occurred during the Edgecumbe earthquake (1987). These were both consistent with a NE-SW trending fault plane with almost pure extension, indicating active NW-SE extension in the NNE trending Whakatane graben.

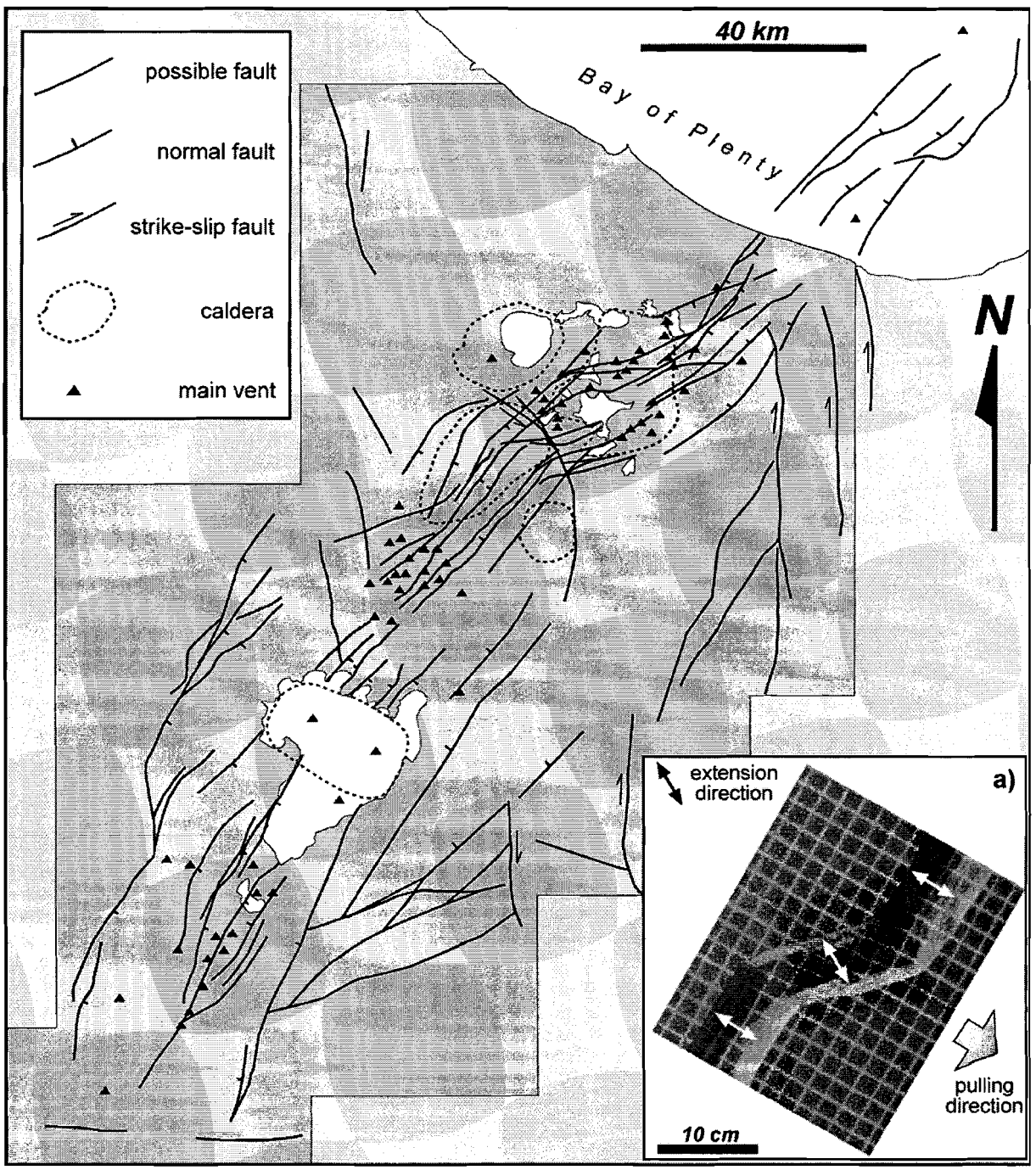

Figure 9. Structural map of TVZ, using data from the shaded relief image and the field. The NNE-SSW trending TVZ shows a major transfer zone at the Okataina segment. Inset shows an analogue model of a transfer zone, characterized by similar geometry and kinematics as the Okataina segment (modified after *Acocella et al.* [1999]).

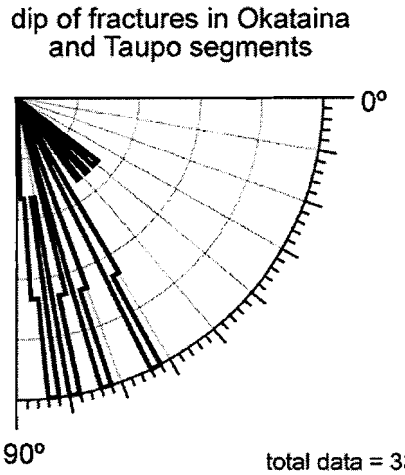

GAUSSIAN PARAMETERS					
#	%	Nor. H.	Max H.	Azimuth	sd
1	95.1	100.0	1.68	76.4°	9.8°

Figure 10. Dip values of the fractures in the Okataina and Taupo segments. The mean dip of both centers (76°) is lower than the overall mean dip (83°) of the fractures in TVZ.

nested calderas [*Cole et al.*, 1998], elongate perpendicular to the trend of the Taupo segment [*Davy and Caldwell*, 1998]. Nevertheless, in a similar fashion to Okataina, the most recent and largest vents cluster along two subparallel NNE-SSW trending zones at the margins of Lake Taupo [*Wilson et al.*, 1984].

[37] The structural data outlined in this paper indicate that Taupo and Okataina are the only TVZ segments characterized by orthogonal extension direction and no dextral shear. Therefore, in these areas, the total strain budget was accommodated by pure extension, which is expected to locally elevate the rates of extrusion. Given the obliquity of rifting, we interpret the higher frequency extrusion of the Taupo and Okataina volcanic complexes to reflect the higher rates of extension in these segments (Figure 11). The Okataina segment is a hard linked transfer zone between Whakatane and Kapenga segments. This transfer zone forms a right stepping jog which, given the dextral component of shear, results in a slight releasing bend in the rift that would be expected to enhance extension in this region (Figure 11). The Taupo segment, conversely, does not show any apparent connection with the Kapenga segment to the north, which is shifted to the west, while connection with the Ruapehu segment to the south is partly masked by the presence of the Lake Taupo. The Taupo segment is thus considered to be the northernmost, curved termination of the Ruapehu segment. The more easterly trend of the Taupo segment, compared to the Ruapehu segment to the south, together with the bulk extension direction, will locally increase the extension rate on the Taupo segment (Figure 11). A similar mechanism, at a smaller scale, has been invoked to explain volcanic activity at the curved tips of oblique faults along the Ethiopian rift [*Korme et al.*, 1997].

5.4. Implications for Plate Boundary Deformation

[38] Contraction along the Hikurangi margin in the North Island may be accommodated principally in the forearc basin and accretionary wedge and strike-slip in the dextral shear zone of the NIDFB (Figure 1) [*Cole*, 1990; *Cashman et al.*, 1992; *Beanland*, 1995; *Webb and Anderson*, 1998]. A number of workers have inferred strike-slip faulting both east of the NIDFB in the forearc and also to the west in TVZ, which would suggest that partitioning is incomplete [*Cole and Lewis*, 1981; *Walcott*, 1984; *Smith et al.*, 1989; *Cashman et al.*, 1992; *Davey et al.*, 1997; *Beanland et al.*, 1998].

[39] Our data indicate a rate of dextral shear of ~2.6 mm/yr within the central portion of the modern TVZ (i.e., mainly on the Kapenga segment) and confirm that dextral shear is not confined to the NIDFB. The data therefore support previous inferences that strain partitioning within the Australian plate

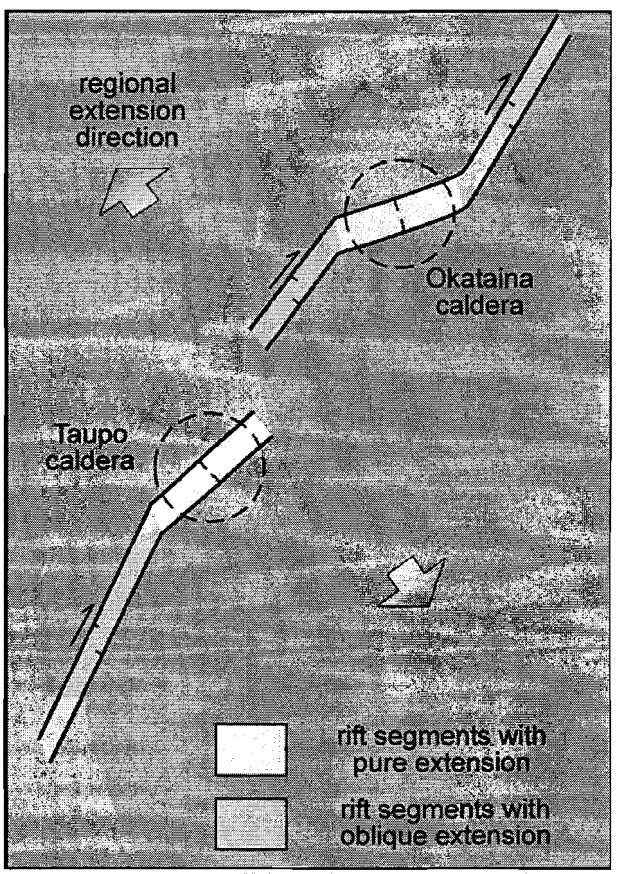

Figure 11. Schematic cartoon showing the possible structural control of the Okataina and Taupo caldera complexes. These areas are characterized, in the frame of the oblique rifting of TVZ, by pure extension. These favored conditions enhance the melting, rise and extrusion of magmas, suggesting an explanation for the observed anomalous extrusion rates within TVZ.

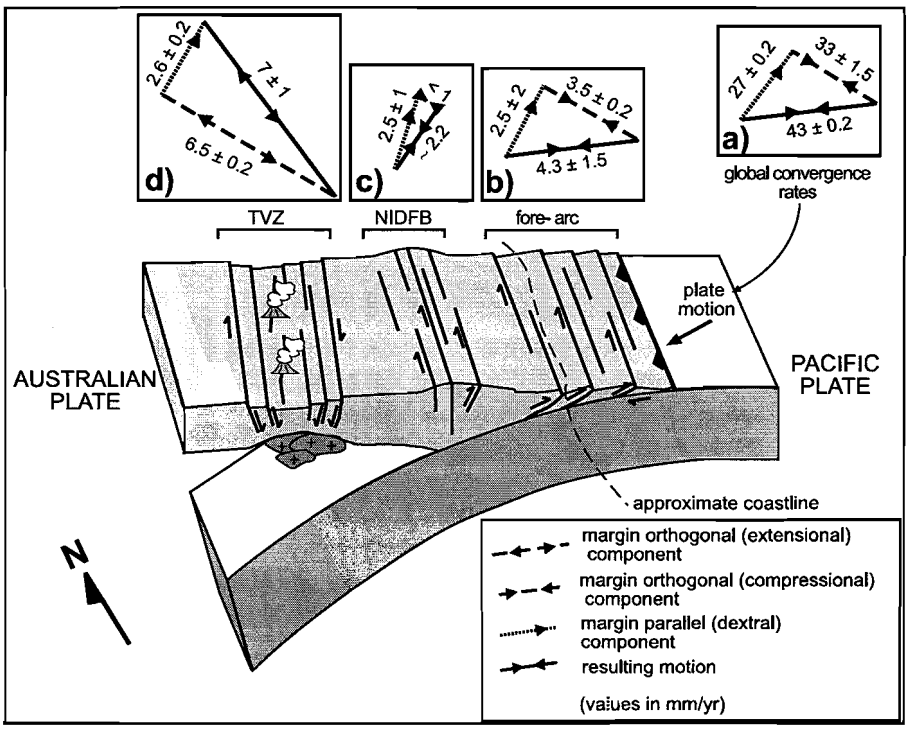

Figure 12. Schematic cartoon showing the tectonic setting of TVZ, divided into back arc (TVZ), NIDFB and forearc domains. The convergence rates and their partitioning (margin-parallel and margin-orthogonal) are reported for the Australian and Pacific plates (inset a) and for the onshore portion of the three domains (insets b, c, d). The data collected in TVZ, consistent with a dextral shear ~2.6 mm/yr, show that the strike-slip component is quite constant throughout the whole convergence system.

is not complete. Within the modern TVZ, dextral shear appears to be distributed across the zone, with no indications that strike-slip is confined to discrete zones or faults; rather, mainly oblique-slip pitches were measured (Figure 5d).

[40] Convergence in the eastern North Island is schematically shown, with the Pacific plate subducting toward the west beneath the Australian plate, in Figure 12. The plate convergence rates from *DeMets et al.* [1994] are shown in inset "a," along with the inferred bulk margin-normal and margin-parallel slip vectors for the onshore forearc region and the NIDFB (see discussion below for sources of data). The total convergence rate of the plates (45 ± 0.2 mm/yr) and its overall partitioning into contractional (35 ± 0.2 mm/yr) and dextral (27 ± 0.2 mm/yr) component at TVZ latitude is derived from *DeMets et al.* [1994], and references therein (Figure 12, inset "a").

[41] Uncertainties affect the estimates of the dextral shear in the NIDFB and the forearc region in Figure 12. The NIDFB comprises several strands and cumulative dextral shear along this fault zone may be underestimated. Also, there is no data for the offshore portion of the forearc, where a possible additional strike-slip component may play an important role. Therefore, the rates of dextral shear in the NIDFB and the forearc reported in Figure 12 may be underestimated. Considering these possible limitations, we take into account the available published work to evaluate the possible implications of our data for plate boundary deformation in the North Island.

[42] The estimated rate (~2.6 mm/yr) of dextral shear along TVZ is comparable to the 1–3 mm/yr suggested for the NIDFB east of the central (i.e.. Taupo and Kapenga segments) TVZ [*Beanland*, 1995] and to the ~2.5 mm/yr proposed by *Cashman et al.* [1992] (Figure 12, inset "c"). The rate of dextral shear in TVZ and the northern NIDFB are of a similar order, suggesting that strike-slip is distributed across this region. Therefore, in this part of the plate boundary, slip partitioning of strike-slip and dip-slip motion may not be significant.

[43] Whether these observations also apply further to the east in the forearc is uncertain. However, to the south and east within the forearc region, GPS data (J. Beavan, personal communication, 2001) suggest a component of dextral shear. This is supported by the estimates of *Cashman et al.* [1992] and *Beanland et al.* [1998] and references therein, which are schematically reported in the inset "b" of Figure 12.

[44] Such observations do not provide unequivocal evidence for oblique-slip on faults within the forearc, but, when considered in conjunction with our results from TVZ, raise questions about the significance of strain partitioning across the terrestrial portion of the plate boundary in the North Island. We believe, therefore, that, in the North Island, strain partitioning between different parallel faults

may not be as significant as previously thought. While it seems unlikely that slip is completely partitioned across the plate boundary, the importance of such partitioning remains a point of debate. In light of these new data, further investigation is required to test the validity of the strain partitioning model along the Hikurangi margin. Finally, the obliquity of fault slip in the modern TVZ highlights the possibility that oblique relative plate motions can be transferred to the back arc environment of the overriding plate.

6. Conclusions

[45] The main results of this study suggest the following points.

[46] 1. TVZ comprises five rift segments; the overall trend of TVZ is NNE-SSW, with a major transfer zone in the ENE-WSW trending Okataina segment.

[47] 2. The normal faults along TVZ show a dextral component of shear, which on average corresponds to 37% of the total displacement, and, for spreading rates of ~7 mm/yr, to a rate of dextral shear ~2.6 mm/yr. This indicates that TVZ is an oblique rift.

[48] 3. The Taupo and Okataina caldera complexes are located in segments of the rift characterized by pure extension. The higher proportion of extension in these segments is partly due to their more NE-SW trend rather than NNE-SSW (mean direction of TVZ). High rates of extension in these segments may locally enhance upward flow of magma and could be partly responsible for the high rates of extrusion in the Taupo and Okataina caldera complexes.

[49] 4. Dextral shear is not confined to individual structures and appears to be distributed across TVZ. The rates of dextral shear within TVZ are similar to those of the NIDFB and the forearc east of TVZ. At the latitudes of TVZ, dextral shear is therefore spread across a region in excess of 200 km wide and appears not to be partitioned onto discrete faults.

[50] **Acknowledgments.** V. A. wishes to thank R. Funiciello for encouragement, support and helpful discussions and the Department of Geological Sciences of Roma Tre and the Head of Department, A. Praturlon, for financial support. F. Salvini kindly provided the DAISY software program. The authors thank Will Esler, D. Gravley, G. Leonard, D. Milner, and I. A. Nairn for helpful discussions and field assistance. Two anonymous reviewers helped improve the paper.

References

Acocella, V., C. Faccenna, R. Funiciello, and F. Rossetti, Sand-box modelling of basement controlled transfer zones in extensional domains, *Terra Nova*, *11*, 149–156, 1999.

Acocella, V., A. Gudmundsson, and R. Funiciello, Interaction and linkage of extensional fractures: Examples from the rift zone of Iceland, *J. Struct. Geol.*, *22*, 1233–1246, 2000.

Anderson, H., E. Smith, and R. Robinson, Normal faulting in a back arc basin: Seismological characteristics of the March 2, 1987, Edgecumbe, New Zealand, earthquake, *J. Geophys. Res.*, *95*, 4709–4723, 1990.

Beanland, S., The North Island Dextral Fault Belt, Ph.D. thesis, Victoria Univ., Wellington, New Zealand, 1995.

Beanland, S., and J. Haines, The kinematics of active deformation in the North Island, New Zealand, determined from geologic strain rates, *N. Z. J. Geol. Geophys.*, *41*, 311–323, 1998.

Beanland, S., K. R. Berryman, and G. H. Blick, Geological investigations of the 1987 Edgecumbe earthquake, New Zealand, *N. Z. J. Geol. Geophys.*, *32*, 73–91, 1989.

Beanland, S., A. Melhuish, A. Nicol, and J. Ravens, Structure and deformational history of the inner forearc region, Hikurangi subduction margin, New Zealand, *N. Z. J. Geol. Geophys.*, *41*, 325–342, 1998.

Benes, V., and S. D. Scott, Oblique rifting in the Havre Trough and its propagation into the continental margin of New Zealand: Comparison with analogue experiments, *Mar. Geophys. Res.*, *18*, 189–201, 1996.

Bibby, H. M., T. G. Caldwell, F. J. Davey, and T. H. Webb, Geophysical evidence on the structure of the Taupo Volcanic Zone and its hydrothermal circulation, *J. Volcanol. Geotherm. Res.*, *68*, 29–58, 1995.

Brothers, R. N., Subduction regression and oceanward migration of volcanism, North Island, New Zealand, *Nature*, *309*, 698–700, 1984.

Brown, S. J. A., R. M. Burt, J. W. Cole, S. J. P. Krippner, R. C. Price, and I. Cartwright, Plutonic lithics in ignimbrites of Taupo Volcanic Zone, New Zealand: Sources and conditions of crystallization, *Chem. Geol.*, *148*, 21–41, 1998.

Bryan, C. J., S. Sherburn, H. M. Bibby, S. C. Bannister, and A. W. Hurst, Shallow seismicity of the central Taupo Volcanic Zone, New Zealand: Its distribution and nature, *N. Z. J. Geol. Geophys.*, *42*, 533–542, 1999.

Cashman, S. M., H. M. Kelsey, C. F. Erdman, H. N. C. Cutten, and K. R. Berryman, Strain partitioning between structural domains in the forearc of the Hikurangi subduction zone, New Zealand, *Tectonics*, *11*, 242–257, 1992.

Cole, J. W., Structural control and origin of volcanism in the Taupo volcanic zone, New Zealand, *Bull. Volcanol.*, *52*, 445–459, 1990.

Cole, J. W., and K. B. Lewis, Evolution of the Taupo-Hikurangi subduction system, *Tectonophysics*, *72*, 1–21, 1981.

Cole, J. W., and I. A. Nairn, Volcanism in the Taupo Volcanic Zone, in *Monogr. Ser. Miner. Deposits*, vol. 26, pp. 23–29, Gebruder Borntraeger, Berlin-Stuttgart, 1986.

Cole, J. W., D. J. Darby, and T. A. Stern, Taupo Volcanic Zone and central volcanic region back arc structures of North Island, New Zealand, in *Back Arc Basins: Tectonics and* Magmatism, edited by B. Taylor, pp. 1–28, Plenum Press, New York, 1995.

Cole, J. W., S. J. A. Brown, R. M. Burt, S. W. Beresford, and C. J. N. Wilson, Lithic types in ignimbrites as a guide to the evolution of a caldera complex, Taupo volcanic center, New Zealand, *J. Volcanol. Geotherm. Res.*, *80*, 217–237, 1998.

Crook, C. N., and J. Hannah, Regional horizontal deformation associated with the 1987 Edgecumbe earthquake, Bay of Plenty, New Zealand—An introduction, *N. Z. J. Geol. Geophys.*, *32*, 93–98, 1989.

Darby, D. J., and C. M. Meertens, Terrestrial and GPS measurements of deformation across the Taupo back arc and Hikurangi forearc regions in New Zealand, *J. Geophys. Res.*, *100*, 8221–8232, 1995.

Darby, D. J., K. M. Hodgkinson, and G. H. Blick, Geodetic measurement of deformation in the Taupo Volcanic Zone, New Zealand: The north Taupo network revisited, *N. Z. J. Geol. Geophys.*, *43*, 157–170, 2000.

Davey, F. J., S. A. Henrys, and E. Lodolo, Asymmetric rifting in a continental back arc environment, North Island, New Zealand, *J. Volcanol. Geotherm. Res.*, *68*, 209–238, 1995.

Davey, F. J., S. Henrys, and E. Lodolo, A seismic crustal section across the East Cape convergent margin, New Zealand, *Tectonophysics*, *269*, 199–215, 1997.

Davy, B. W., and T. G. Caldwell, Gravity, magnetic and seismic surveys of the caldera complex, Lake Taupo, North Island, New Zealand, *J. Volcanol. Geotherm. Res.*, *81*, 69–89, 1998.

DeMets, C., R. G. Gordon, D. Argus, and S. Stein, Effect of recent revisions to the geomagnetic reversal time scale on estimates of current plate motions, *Geophys. Res. Lett.*, *21*, 2191–2194, 1994.

Graham, I. J., J. W. Cole, R. M. Briggs, J. A. Gamble, and I. E. M. Smith, Petrology and petrogenesis of volcanic rocks from the Taupo Volcanic Zone: A review, *J. Volcanol. Geotherm. Res.*, *68*, 59–87, 1995.

Grapes, R. H., B. A. Sissons, and H. W. Wellman, Widening of the Taupo volcanic zone, New Zealand, and the Edgecumbe earthquake of March 1987, *Geology*, *15*, 1123–1125, 1987.

Gudmundsson, A., S. Brynjolfsson, and M. T. Jonnsson, Structural analysis of a transform fault-rift zone junction in North Iceland, *Tectonophysics*, *220*, 205–221, 1993.

Houghton, B. F., C. J. N. Wilson, M. O. McWilliams, M. A. Lanphere, S. D. Weaver, R. M. Briggs, and M. S. Pringle, Chronology and dynamics of a large silicic magmatic system: Central Taupo Volcanic Zone, New Zealand, *Geology*, *23*, 13–16, 1995.

Jurado-Chichay, Z., and G. P. L. Walker, The intensity and magnitude of the Mangaone subgroup plinian eruptions from Okataina volcanic center, New Zealand, *J. Volcanol. Geotherm. Res.*, *111*, 219–237, 2001.

Kamp, P. J. J., Neogene and Quaternary extent and geometry of the subducted Pacific plate beneath North Island, New Zealand: Implications for Kaikoura Tectonics, *Tectonophysics*, *108*, 241–266, 1984.

Korme, T., J. Chorowicz, B. Collet, and F. F. Bonavia, Volcanic vents rooted on extension fractures and their geodynamic implications in the Ethiopian Rift, *J. Volcanol. Geotherm. Res.*, *79*, 205–222, 1997.

Lamb, S. H., Tectonic rotations about vertical axes during the last 4 Ma in part of the New Zealand plate-boundary zone, *J. Struct. Geol.*, *10*, 875–893, 1988.

Marrett, R., and R. W. Allmendinger, Kinematic analysis of fault-slip data, *J. Struct. Geol.*, *12*, 973–986, 1990.

Nairn, I. A., Some studies of the geology, volcanic history and geothermal resources of the Okataina volcanic center, Taupo Volcanic zone, New Zealand, Ph.D. thesis, Victoria Univ., Wellington, New Zealand, 1981.

Nairn, I. A., Okataina volcanic centre, in *Monogr. Ser. Miner. Deposits*, vol. 26, pp. 29–35, Gebruder Borntraeger, Berlin-Stuttgart, 1986.

Nairn, I. A., Sheet V16AC–Mount Tarawera, geological map of New Zealand, 1:50,000, Dep. of Sci. and Ind. Res., Wellington, 1989.

Nairn, I. A., and J. W. Cole, Basalt dikes in the 1886 Tarawera rift, New Zealand, *J. Geol. Geophys.*, *24*, 585–592, 1981.

Parson, L. M., and I. C. Wright, The Lau-Havre-Taupo back arc basin: A southward-propagating, multistage evolution from rifting to spreading, *Tectonophysics*, *263*, 1–22, 1996.

Pollard, D. D., and A. Aydin, Propagation and linkage of oceanic ridge segments, *J. Geophys. Res.*, *89*, 10,017–10,028, 1984.

Rogan, M., A geophysical study of the Taupo Volcanic Zone, New Zealand, *J. Geophys. Res.*, *87*, 4073–4088, 1982.

Rowland, J. V., and R. H. Sibson, Extensional fault kinematics within the Taupo Volcanic Zone, New Zealand: Soft linked segmentation of a continental rift system, *N. Z. J. Geol. Geophys.*, *44*, 271–283, 2001.

Smith, E. G. C., and T. H. Webb, The seismicity and related deformation of the Central Volcanic Region, North Island, New Zealand, *Bull. R. Soc. N. Z.*, *23*, 112–133, 1986.

Smith, E. G. C., T. Stern, and M. Reyners, Subduction and back arc activity at the Hikurangi convergent margin, New Zealand, *Pure Appl. Geophys.*, *129*, 203–231, 1989.

Soengkono, S., A magnetic model for deep plutonic bodies beneath the central Taupo Volcanic Zone, North Island, New Zealand, *J. Volcanol. Geotherm. Res.*, *68*, 193–207, 1995.

Stern, T. A., A back arc basin formed within continental lithosphere: The central volcanic region of New Zealand, *Tectonophysics*, *112*, 385–409, 1985.

Sutton, A. N., S. Blake, C. J. N. Wilson, and B. L. A. Charlier, Late Quaternary evolution of a hyperactive rhyolite magmatic system: Taupo volcanic centre, New Zealand, *J. Geol. Soc. London*, *157*, 537–552, 2000.

Tatsumi, Y., and H. Tsunakawa, Cenozoic volcanism, stress gradient and back arc opening in the North Island, New Zealand: Origin of Taupo-Rotorua depression, *Island Arc*, *1*, 40–50, 1992.

Taylor, B., and G. D. Karner, On the evolution of marginal basins, *Rev. Geophys.*, *21*, 1727–1741, 1983.

Taylor, B., K. Crook, and J. Sinton, Extensional transform zones and oblique spreading centers, *J. Geophys. Res.*, *99*, 19,707–19,718, 1994.

Villamor, P., and K. Berryman, A late Quaternary extension rate in the Taupo Volcanic Zone, New Zealand, derived from fault slip data, *N. Z. J. Geol. Geophys.*, *44*, 243–269, 2001.

Walcott, R. I., The kinematics of the plate boundary zone through New Zealand: A comparison of short and long-term deformation, *Geophys. J. R. Astron. Soc.*, *79*, 613–633, 1984.

Webb, T. H., and H. Anderson, Focal mechanisms of large earthquakes in the North Island of New Zealand: Slip partitioning at an oblique active margin, *Geophys. J. Int.*, *134*, 40–86, 1998.

Wilson, C. J. N., Taupo's atypical arc, *Nature*, *379*, 27–28, 1996.

Wilson, C. J. N., The 26.5 ka Oruanui eruption, New Zealand: And introduction and overview, *J. Volcanol. Geotherm. Res.*, *112*, 133–174, 2001.

Wilson, C. J. N., M. A. Rogan, I. E. M. Smith, D. J. Northey, I. A. Nairn, and B. F. Houghton, Caldera volcanoes of the Taupo Volcanic Zone, New Zealand, *J. Geophys. Res.*, *89*, 8463–8484, 1984.

Wilson, C. J. N., B. F. Houghton, M. O. McWilliams, M. A. Lanphere, S. D. Weaver, and R. M. Briggs, Volcanic and structural evolution of Taupo Volcanic Zone, New Zealand: A review, *J. Volcanol. Geotherm. Res.*, *68*, 1–28, 1995.

V. Acocella, Dipartimento di Scienze Geologiche, Università Roma Tre, Largo S.L. Murialdo, 1, I-00146 Rome, Italy. (acocella@uniroma3.it)

J. Cole and K. Spinks, Department of Geological Sciences, University of Canterbury, Private Bag 4800, Christchurch, New Zealand.

A. Nicol, Institute of Geological and Nuclear Sciences, P.O. Box 30368, Lower Hutt, New Zealand.

Appendix B

'**Spinks, K.D.**, Acocella, V.A., Cole, J.W. & Bassett, K.N (in press) Structural control of volcanism and caldera development in the transtensional Taupo Volcanic Zone, New Zealand. *Journal of Volcanology and Geothermal Research* Special Volume: Tectonics and Physics of Volcanoes.'

Contribution: All caldera research, all literature review, all compiling of data, all drawing of figures, 95% of manuscript based on data contained within chapters two & three of this thesis.

Available online at www.sciencedirect.com

SCIENCE DIRECT®

Journal of Volcanology and Geothermal Research xx (2005) xxx–xxx

Journal of volcanology and geothermal research

www.elsevier.com/locate/jvolgeores

Structural control of volcanism and caldera development in the transtensional Taupo Volcanic Zone, New Zealand

Karl D. Spinks[a,*], Valerio Acocella[b], Jim W. Cole[a], Kari N. Bassett[a]

[a]*Dept. Geological Sciences, University of Canterbury, Private Bag 4800, Christchurch, New Zealand*
[b]*Dip. Scienze Geologiche Roma TRE. Largo S.L. Murialdo, 1, 00146 Roma, Italy*

Accepted 16 November 2004

Abstract

The Taupo Volcanic Zone (TVZ), New Zealand, comprises several segments with variable components of extension, and is characterised by longitudinal segmentation into a central zone dominated by rhyolitic calderas and extremities with only andesitic composite volcanoes. Modern (<300 ka) TVZ was investigated to define (a) the overall relationship between regional structures and volcanism and (b) the structural control on the evolution of calderas. New remote sensing and field structural data have been combined with previously published data for TVZ. The results show a general correlation between the amount of extension and the volume and style of eruption in each segment. The segments with the greatest extension coincide with the highly active Taupo and Okataina caldera complexes; conversely, the segments with the greatest dextral transtension correspond to volumetrically less active andesitic stratovolcanoes. Within Modern TVZ, two types of caldera are distinguished based on their structure and development. Calderas within the main zone of rifting (Taupo, Okataina) are multiple (two or more major eruptions) collapse structures with rectilinear margins, overprinted by younger volcanism and faulting. Their complexity is related to the proximity (and influence) of active faulting within TVZ. In contrast, calderas peripheral to the main rift (Rotorua, Reporoa) are sub-circular monogenetic collapse structures, with minor post-collapse volcanism. Their simpler evolution and structure is a attributable to their location away from the main rift zone. Thus, TVZ exemplifies the situation where firstly, magma is erupted as a function of the extension rate along the axial rift zone, and secondly, volcanism is manifest as distinctive caldera structures according to their proximity to the axial rift zone.

Keywords: transtension; erupted volume; caldera; rift zone; Taupo Volcanic Zone

1. Introduction

Understanding how regional structure may affect or control volcanism is a major task in defining the evolution of rift zones and magmatic provinces. Such

* Corresponding author. Tel.: +64 3 3642700; fax +64 3 3642769.
E-mail address: k.spinks@geol.canterbury.ac.nz (K.D. Spinks).

0377-0273/$ - see front matter © 2004 Elsevier B.V. All rights reserved.
doi:10.1016/j.jvolgeores.2004.11.014

an understanding requires a sufficient knowledge of the overall structural and volcanic features of a region as well as their mutual relationships. Of particular importance are the geometry (general architecture and segmentation) and kinematics (direction and magnitude of extension) of a rift zone. Primary volcanic parameters to consider include the volume, composition, and age of eruptive products, and the types of volcanoes (stratovolcanoes, calderas, vents, and fissures).

Of principle interest is the effect of tectonics on the rise, emplacement, and eruption of magmas under conditions of pure and oblique convergence (Nakamura, 1977; Glazner, 1991; Tikoff and de Saint Blanquat, 1997; Acocella and Rossetti, 2002). In these settings, the rise of magmas forming a volcanic arc is typically controlled by strike-slip structures, such as observed in the central Andes (De Silva, 1989), NE Japan (Sato, 1994), and Mexico (Tibaldi, 1992). Nevertheless, localised areas of rifting may also form within convergent settings, as observed along the Taupo Volcanic Zone of New Zealand (Cole, 1990) or the Tyrrhenian margin of Italy (Malinverno and Ryan, 1986). To study these situations, specific consideration must be given to the interaction between strain rates and magmatism (e.g. Paterson and Tobsich, 1992; Petford et al., 2000), and how tectonics influences magma composition and eruption styles (e.g. Grocott et al., 1994; Riller et al., 2001).

In this study, we address some of these issues, investigating the structural control on volcanism in the transtensional intra-arc rift of the Taupo Volcanic Zone (TVZ) in the North Island of New Zealand (Fig. 1). We focus on the structural and volcanic aspects of the activity in the last 300 ka. Aspects of the rift geometry and caldera structure acquired through an original detailed analysis of Digital Elevation Model (DEM) imagery (Fig. 2A) and field work are constrained by recently acquired structural data (Acocella et al., 2003; Fig. 2B). These new data are combined with previously pub-

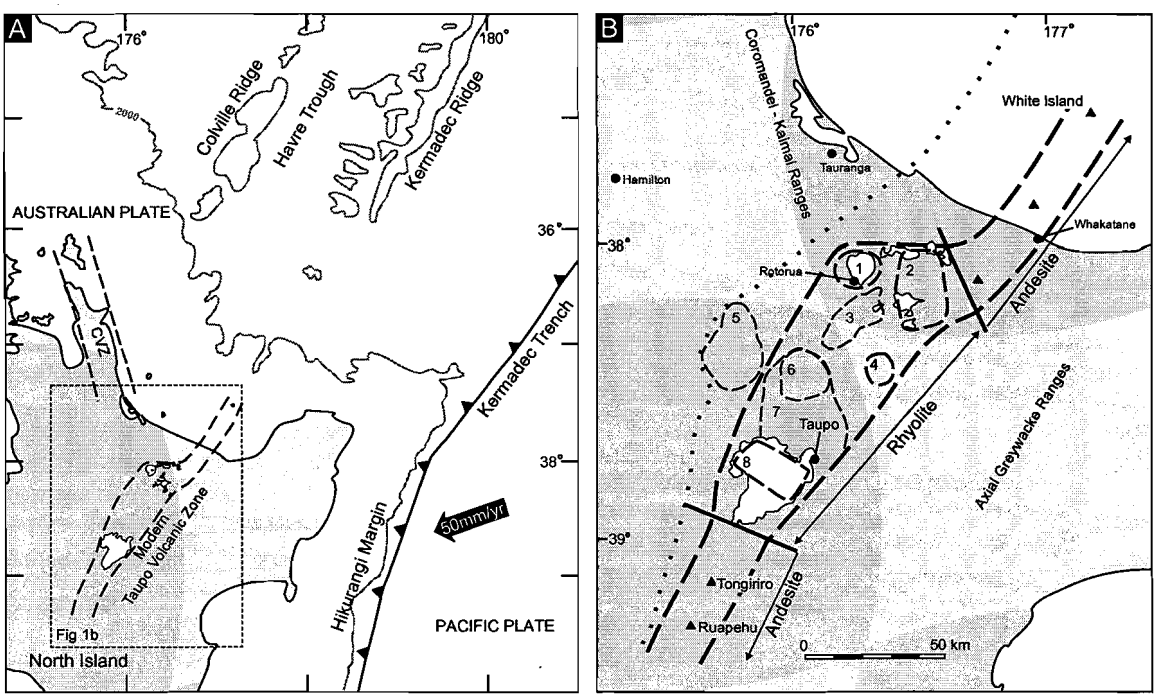

Fig. 1. (A) Setting of the Taupo Volcanic Zone (TVZ) in the North Island of New Zealand, with respect to the Kermadec Trench and Ridge, and to the Havre Trough (outlined by the 2000 m isobath). The boundary of modern TVZ (<300 ka) is shown by dashed lines. Modified from Davey et al. (1995). (B) Map of TVZ showing calderas and compositional segmentation into andesitic and rhyolitic segments. Calderas: (1) Rotorua; (2) Okataina; (3) Kapenga; (4) Reporoa; (5) Mangakino; (6) Maroa; (7) Whakamaru; (8) Taupo.

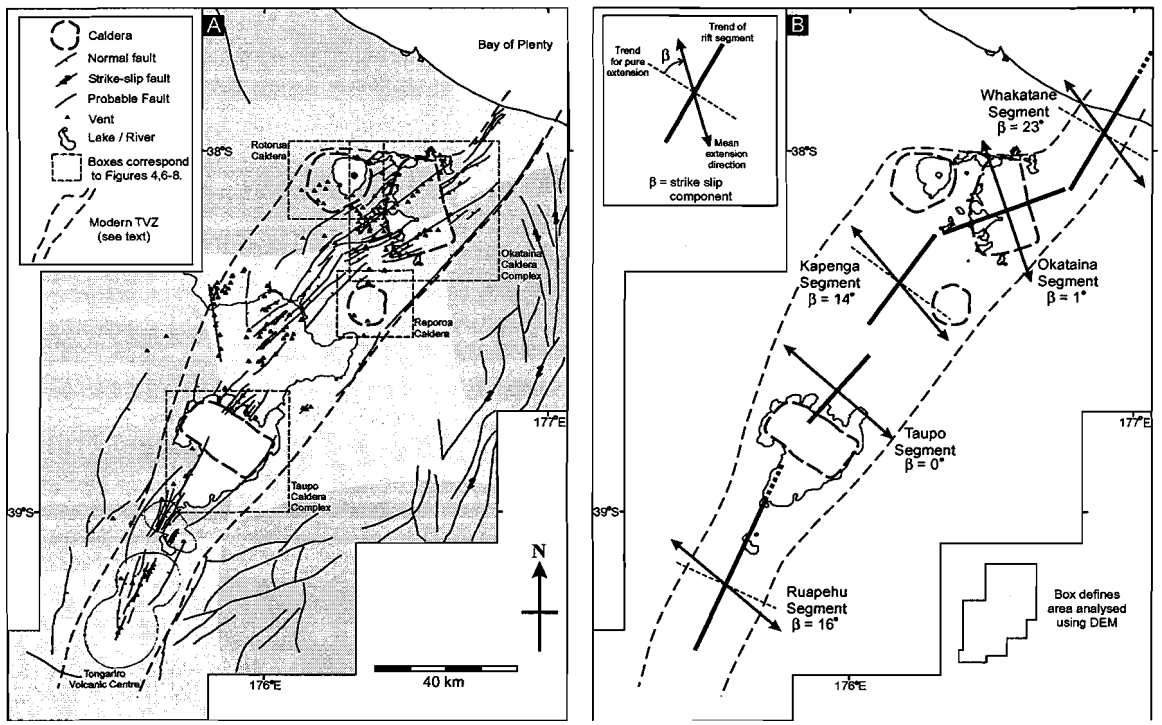

Fig. 2. (A) Summary of regional structure of TVZ showing the location of the 4 modern calderas and their relationship to rift structures. (B) Rift segments of TVZ showing their extension direction and the amount of dextral shear (β) in each segment, after Acocella et al. (2003).

lished volcanological, geochemical, and geophysical data.

2. TVZ and its tectonic setting

TVZ is a zone of Quaternary calc–alkaline volcanism and intra-arc rifting in the North Island of New Zealand (Fig. 1A). Westward subduction of the Pacific plate beneath the Australian plate has formed the Taupo–Hikurangi arc-trench system (Cole and Lewis, 1981), contiguous with the Kermadec Ridge–Havre Trough system to the north; the boundary between active intra-arc extension in TVZ and that of the Havre trough however is offset in an en echelon style (Carter, 1980; Wright, 1992; Fig. 1A). TVZ therefore marks the present location of intra-arc rifting, related to an overall convergent setting within the North Island, and associated with a highly thinned crust of 15 km (Bibby et al., 1995).

Volcanic activity in TVZ began at ~2 Ma (Houghton et al., 1995). The present site of active volcanism and extension is focused in a NNE–SSW-trending zone, 250 km long, from Ruapehu to White Island (Fig. 1B). This zone encompasses all activity in the last 300 ka (Houghton et al., 1995; Wilson et al., 1995) and is referred to here as Modern TVZ (Fig. 1B). Modern TVZ is divided into three parts along its length (Fig. 1B): (a) a central part (from Okataina to Taupo) with several calderas associated with rhyolite volcanism at the surface (Wilson et al., 1984, 1995; Graham et al., 1995) and plutons at depth (Soengkono, 1995; Brown et al., 1998) and (b) two lateral parts (Ruapehu to the south and Whakatane–White Island to the north) with andesite–dacite stratovolcanoes (Wilson et al., 1995; Wilson, 1996; Houghton et al., 1995). The central section is an extraordinarily productive region of rhyolitic volcanism (~0.28 m^3 s^{-1}) and geothermal fluxes (~4200 MW), unparalleled on the planet (Wilson, 1996).

This study focuses on defining the structural control on volcanism within Modern TVZ (<300 ka). Eight calderas or caldera complexes have been described from the central part of TVZ spanning 1.6 Ma (Wilson

et al., 1995; Fig. 1B); four of these (Okataina, Taupo, Rotorua, and Reporoa) have formed in the last 300 ka. These comprise both multiple event caldera complexes (Okataina and Taupo) and single event calderas (Reporoa and Rotorua; Fig. 2A). In particular, the Okataina and Taupo caldera complexes, located at the boundaries of the central part are the most productive rhyolitic volcanoes on earth, with eruption rates of c. 0.1 $m^3 s^{-1}$ and c. 0.2 $m^3 s^{-1}$, respectively, averaged over the last 65 ka (Wilson, 1993).

Remote sensing and ground-based structural analysis of Modern TVZ show that it consists of five segments (Fig. 2B), with a variable amount of dextral shear. The overall dextral shear component along TVZ is ~37% of the total displacement (Acocella et al., 2003); considering the estimated extension of ~7 mm/year (Darby and Meertens, 1995; Villamor and Berryman, 2001), the dextral shear component corresponds to ~2.6 mm/year. The segments with the highest dextral component are at the extremities (Whakatane and Ruapehu) and in the middle of the central part (Kapenga) of TVZ, whereas pure extension is restricted to those segments containing the Okataina and Taupo caldera complexes (Acocella et al., 2003).

3. Results

3.1. The relationship between extension and eruptive volumes

Recent structural data (Acocella et al., 2003) suggest that the five segments of TVZ have different amounts of dextral shear, expressed by an angle β: the higher the β, the higher the dextral component; if β=0°, then the segment undergoes pure extension (Fig. 2B). For each of these segments, we have attempted to constrain the volume of eruptives based on published volumetric data (Table 1). Volumes are Dense Rock Equivalent (DRE) taken from a large number of sources; the calculation of such volumes from both lavas and pyroclastics, therefore, involves some significant errors. In all cases, we used a standard 25% error. The quoted volumes are considered to be underestimates of the true volumes, particularly where they include largely unknown volumes of caldera fill.

We considered only the volumes erupted in the last 300 ka, for consistency with the structural data collected by Acocella et al. (2003). We did not consider the volumes erupted in the last 300 ka by the Rotorua and Reporoa Calderas as these are located outside the axis of TVZ and cannot be specifically related to any of the identified segments.

Table 1
Table reporting the eruptive volumes, segment length, erupted volume per km of segment, and previously calculated (Acocella et al., 2003) β values

	Ruapehu	Taupo	Kapenga	Okataina	Whakatane
Erupted volumes (km^3)	200±50	480±120	200±50	430±108	80±120
Length of segment (km)	60	40	30	35	85
Erupted volumes/km	3.3±0.8	12±3	6.7±1.7	12±3	0.9±0.22
β	16°±5°	0°±7°	14°±10°	1°±10°	23°±4°

Erupted volumes and ages were compiled from: Froggatt and Lowe, 1990; Jurado-Chichay and Walker, 2001; Nairn, 1989; Bellamy, 1991; Wilson et al., 1984, 1986; Sutton et al., 1995; Bailey and Carr, 1994; Hobden et al., 1999; Hackett and Houghton, 1989; Gravley, 2005; Leonard, 2003.

In order to compare volumes in different segments, we divide the total eruptive volume of a segment by its length, obtaining a volume per km. The values of β (Fig. 2B) and the related volume estimates for each segment are reported in Table 1.

Fig. 3 shows the relationship between the obliquity of extension (β), as evaluated by Acocella et al. (2003), and the erupted volumes per km for each segment. Despite the relatively significant errors associated with estimating eruptive volumes and evaluating β, the inverse correlation shows that segments with the larger extensional components (β~0°) are associated with larger eruptive volumes; in contrast, segments with the larger components of dextral shear (β>0°) are associated with lower eruptive volumes. Fig. 3 thus shows the focusing of eruptive activity at the purely extensional Okataina and Taupo segments.

In general, the segments with higher β values are also associated with stratovolcanoes (Whakatane and Ruapehu), whereas the segments with smaller β are associated with calderas, indicating that, within the axial zone of TVZ, calderas are related to the highest extension or tensile conditions.

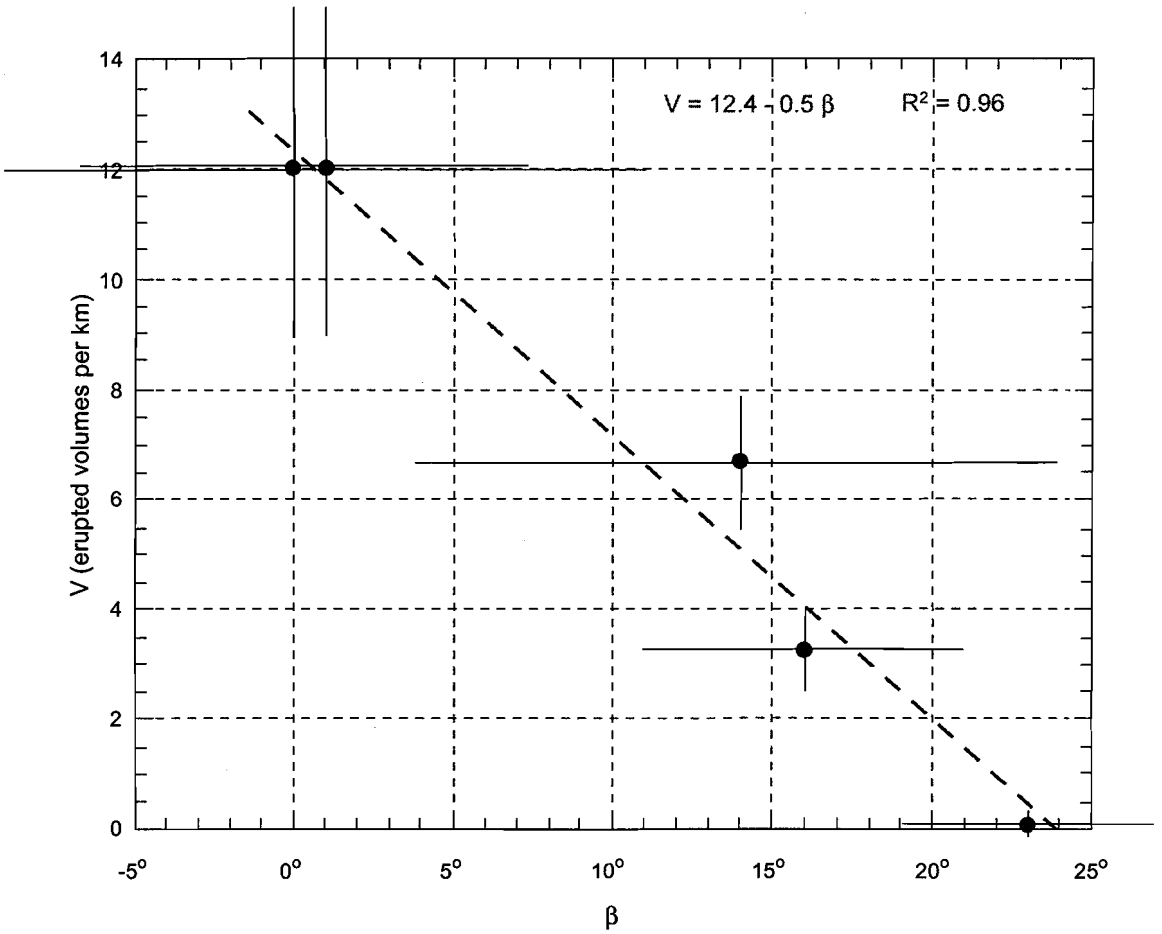

Fig. 3. Diagram showing the relationship between the amount of dextral shear (β)? within each segment of TVZ (for location see Fig. 2B) and the erupted volumes per km of segment length relative to the last 300 ka. Segments with pure extension (Taupo and Okataina) are associated with the largest erupted volumes.

3.2. Calderas in modern TVZ

In the following sections, we consider the calderas in Modern TVZ (Reporoa, Rotorua, Okataina, Taupo) in light of existing volcanological, geochemical, and geophysical data, and new morphotectonic and structural data, derived from DEM analysis and field studies (Figs. 4, 6–8).

3.2.1. Reporoa caldera

Reporoa Caldera (Nairn et al., 1994) is located at the northern end of the Taupo–Reporoa depression ~15 km E of the Kapenga segment axis (Fig. 2). It formed during the eruption of the 0.23±0.01 Ma (Houghton et al., 1995) Kaingaroa Ignimbrite, with a total eruptive volume of 100 km^3 (Nairn et al., 1994; Beresford and Cole, 2000; Fig. 4).

Lithic componentry data suggest that Reporoa formed during asymmetric collapse, accompanied by radial emplacement of pyroclastic flows (Beresford and Cole, 2000). The resulting elliptical caldera (Nairn et al., 1994) is well expressed along the northern and eastern margins, but largely open to the west and south. Older deposits along the caldera rim are unrelated to the Kaingaroa magma system or to the development of Reporoa Caldera (Beresford and Cole, 2000); minor (<2 km^3) post-caldera rhyolite domes are geochemically distinct from the Kaingaroa magma system (Beresford, 1997).

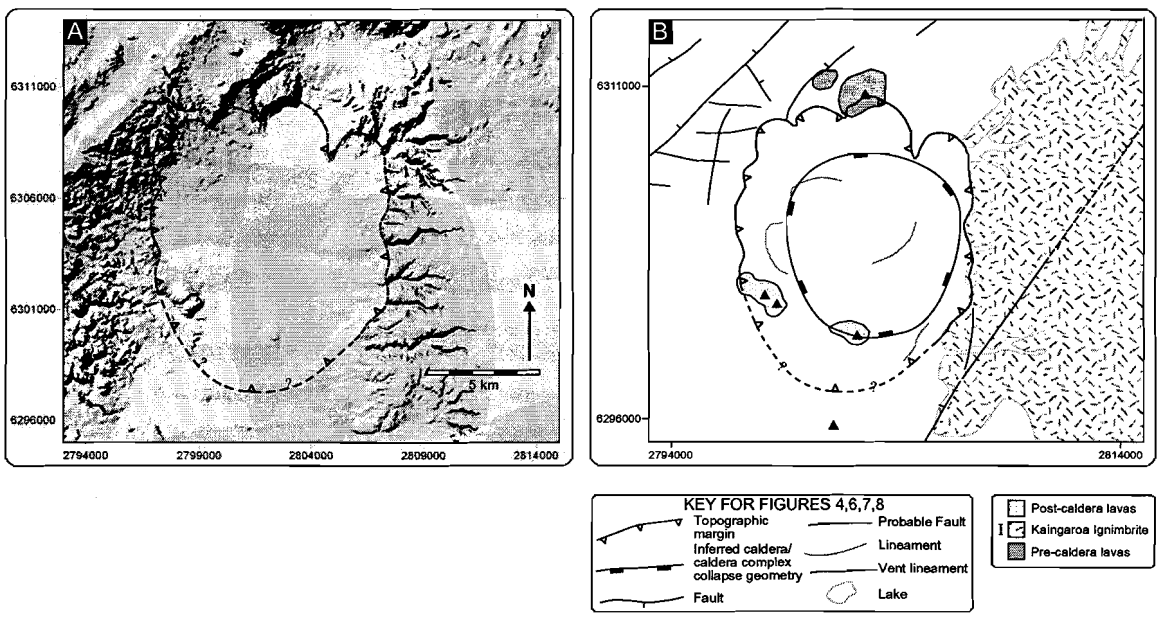

Fig. 4. Reporoa Caldera. (A) Shaded relief image of Reporoa caldera. Shaded relief images for this figure and Figs. 6–8 are generated from a 1:50,000 scale DEM; Grid coordinates are shown in the New Zealand map grid (NZMG). (B) Structure map of the Reporoa Caldera derived from analysis of DEM data. Also shown are pre- and post-caldera lavas, and the ignimbrite related to caldera formation. Geology after Beresford and Cole (2000).

The caldera has a small but clear negative gravity anomaly (Nairn et al., 1994; Stagpoole, 1994; Stagpoole and Bibby, 1999; Fig. 5) and a low P-wave velocity (Vp) anomaly consistent with low density, low Vp caldera fill (Sherburn et al., 2003). The gravity anomaly corresponds well with the topographic expression of the caldera, with a gentle western margin and a steep eastern margin (Nairn et al., 1994), consistent with asymmetric collapse (Beresford and Cole, 2000). The location and morphology of post-caldera rhyolite domes and a buried dome complex inferred to exist by magnetic studies (Soengkono and Hochstein, 1996) exhibit no clear vent lineation; however, Nairn et al. (1994) consider these erupted along fractures related to the caldera rim and a supposed inner caldera ring fault.

New DEM and field data (Figs. 2A and 4B) show that Reporoa caldera is located several km eastwards from the eastern boundary of the area of active tectonism within TVZ, most of the active faults being restricted to the Kapenga graben (Fig. 2). Reporoa Caldera is sub-circular, with approximate dimensions 11×13 km and well-preserved 250-m-high collapse scarps along the northern boundary. The N–S long axis of the caldera (Eccentricity $E=L_{min}/L_{max}=0.85$, where L_{min} and L_{max} are the shorter and longer caldera axes, respectively) is oblique to the regional trend of faults to the west; in the east a NE-trending fault scarp (Fig. 4B) merges with the N–S-trending eastern caldera margin. The caldera is neither dissected by younger faults nor does its margin truncate older structures. Although regional structures may have played a limited role in controlling the asymmetric collapse of Reporoa Caldera (Beresford and Cole, 2000), the overall morphology of the caldera has remained largely unaffected by regional fault geometry.

3.2.2. Rotorua caldera

Rotorua Caldera is located 15–20 km NW of the junction between Okataina and Kapenga rift axes (Fig. 2). The caldera formed during the eruption of the 220–230 ka Mamaku Ignimbrite (Shane et al., 1994; Houghton et al., 1995; Black et al., 1996; Milner et al., 2002), with a minimum eruption volume (including the intra-caldera ignimbrite) of 145 km^3 DRE (Milner et al., 2003). Although earlier events have been proposed (e.g. Wood, 1992), recent works

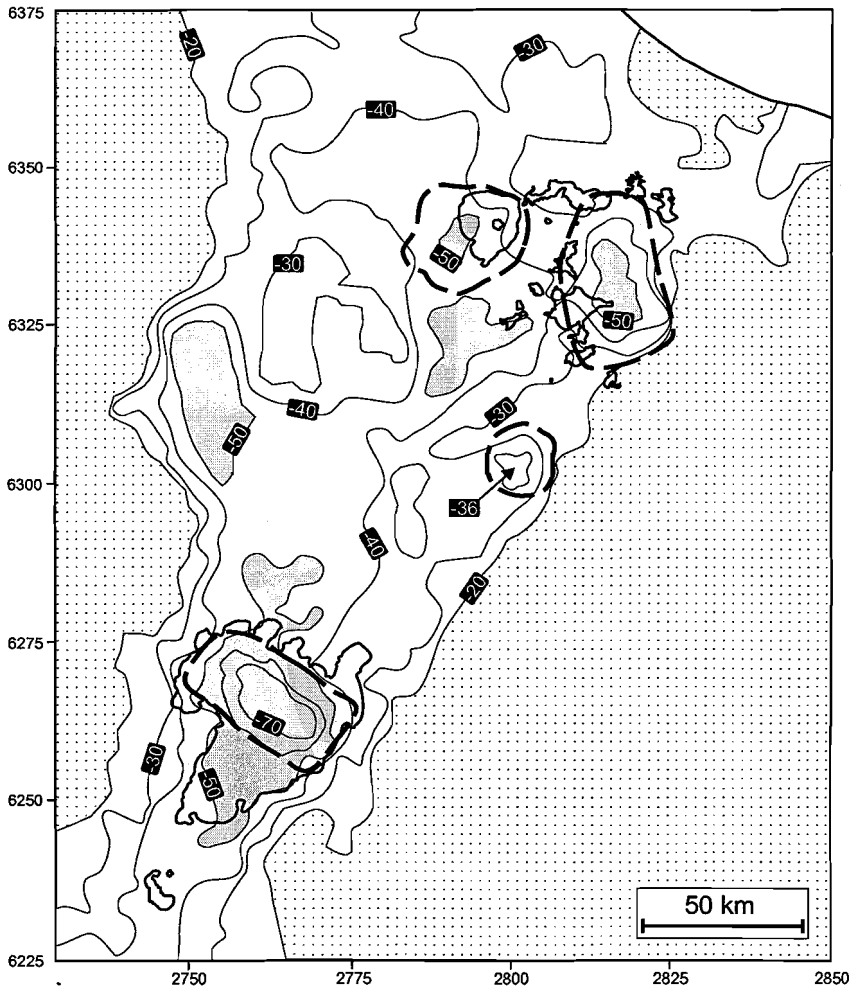

Fig. 5. Residual Bouguer gravity anomaly of TVZ with outlines of modern calderas. Areas less than −50 mgal and greater than −20 mgal are highlighted with shading and hatching respectively. Grid coordinates are in the New Zealand map grid (NZMG). Note that Okataina and Taupo are associated with much larger (size and intensity) negative gravity anomalies than Rotorua and Reporoa. Gravity contours from Davy and Caldwell (1988) and Nairn et al. (1994).

(Milner et al., 2002, 2003) indicate that Rotorua is a single-event caldera.

Pre-caldera rhyolite domes scattered around the rim of the 21×22 km structure (Milner et al., 2002; Fig. 6B) are geochemically distinct from each other and from the Mamaku magma system. By contrast, most of the post-caldera dome-forming volcanism (~4 km^3, Wilson et al., 1984) is geochemically similar to the Mamaku magma system (Milner et al., 2002).

Rotorua Caldera is characterised by a N–S elongate negative residual gravity anomaly to the west and southwest of Lake Rotorua (Rogan, 1982; Hunt, 1992; Fig. 5); surrounding gravity contours are not concentric to the caldera margin (Fig. 5), defining an asymmetric rise towards NE and NW. A low Vp anomaly is consistent with the negative gravity anomaly and a collapse structure filled with volcaniclastic material (Sherburn et al., 2003).

New DEM and field data (Figs. 2A and 6B) show that Rotorua is located several kilometres west of the present area of active tectonism within TVZ, most of the active faults being restricted to the junction between the Kapenga and Okataina segments

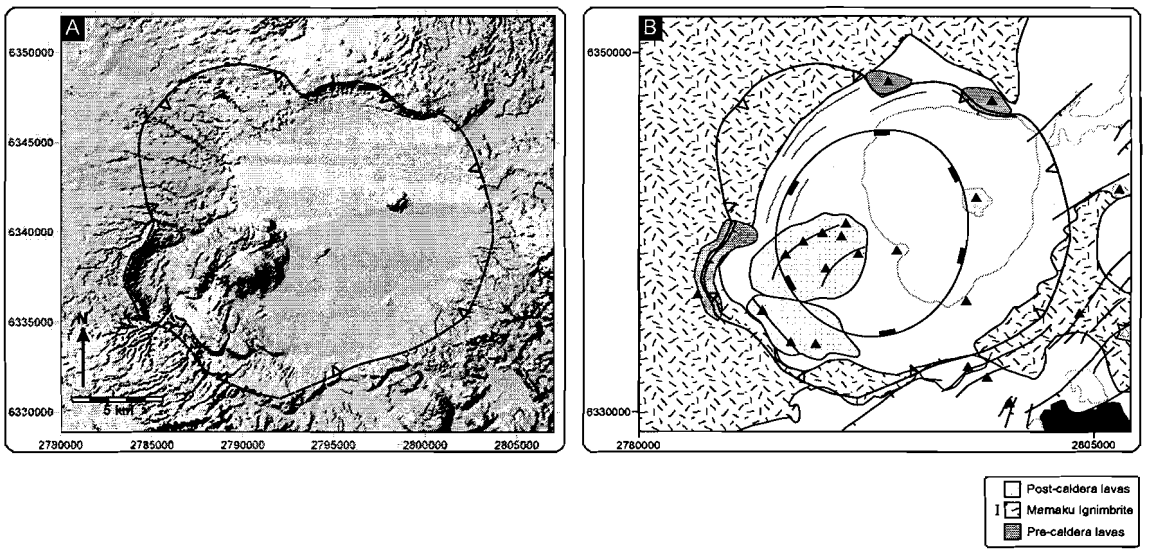

Fig. 6. Rotorua Caldera. (A) Shaded relief image of Rotorua caldera. (B) Structure map of Rotorua Caldera generated from analysis of DEM data. Also shown are pre- and post-caldera lavas and the ignimbrite related to caldera formation. Geology after Milner et al. (2002).

(Fig. 2). Rotorua Caldera is expressed on DEM imagery as a sub-circular, approximately 20×16 km collapse structure with an eccentricity E=0.8. The caldera floor is dominated by the ~9 km diameter lake and the youthful morphologies of post-caldera dome complexes. The topographic margin is semi-continuous around the caldera and best expressed where formed by scarps in pre-caldera rhyolite domes or Mamaku Ignimbrite (Fig. 6A); elsewhere the margin is marked by the limit of the inwards dipping Mamaku Ignimbrite, referred to as the limit of deformation by Milner et al. (2002). The southeast margin of the caldera roughly parallels NE-trending regional faults in the adjacent Okataina segment. Other lineaments in the caldera are arcuate and relate to caldera bounding scarps and associated deformation, rather than to regional structures.

3.2.3. Okataina caldera complex

The Okataina Caldera Complex (OCC) is a complex of overlapping and nested collapse structures, largely filled with post-caldera rhyolites (Fig. 7). The caldera complex is the result of two main collapse events associated with the 0.28±0.01 Ma Matahina Ignimbrite (Bailey and Carr, 1994; date from Houghton et al., 1995) and 65 ka Rotoiti eruption (Nairn, 1981, 1989; age from Houghton et al., 1995), and modified by substantial intra-caldera rhyolite volcanism (e.g. Jurado-Chichay and Walker, 2000; Nairn, 1989). Magmatic volume estimates for the Matahina and Rotoiti events are 150 km^3 (Bailey and Carr, 1994) and 120 km^3 (Froggatt and Lowe, 1990), respectively; other eruptives from OVC account for at least 150 km^3 (e.g. Froggatt and Lowe, 1990; Jurado-Chichay and Walker, 2001; Bellamy, 1991). The Matahina and Rotoiti ignimbrites extend predominantly to the east and north, and appear to be related to sources in the southern and northern parts of the caldera complex respectively (Nairn, 1989; Fig. 7B).

The pre-caldera lavas are petrogenetically distinct; lavas and pyroclastics erupted between the major caldera-forming events also relate to at least two separate magma types (Bowyer, 2001). Considerable studies of eruptive activity since the Rotoiti event (e.g. Leonard et al., 2002; Bowyer, 2001; Smith, 2001; Jurado-Chichay and Walker, 2000) indicate that these eruptions involved multiple small magma batches.

A distinct large negative residual gravity anomaly (Rogan, 1982; Davy and Caldwell, 1988; Fig. 5) and low Vp anomaly (Sherburn et al., 2003) define an N–S elongated depression consistent with the mapped caldera margin and filled with a large volume of low Vp, low density, volcaniclastic sediment. Modelling of gravity and magnetic data gives different depths to

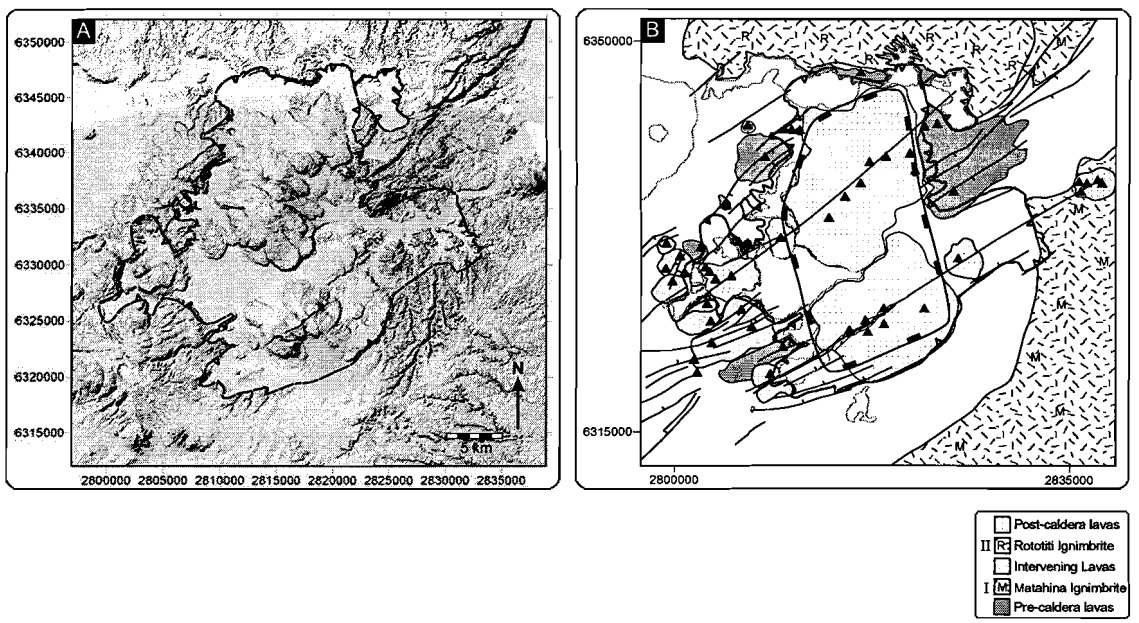

Fig. 7. Okataina Caldera Complex. (A) Shaded relief image of Okataina Caldera Complex. (B) Structure map of Okataina Caldera Complex generated from analysis of DEM data. Also shown are pre- and post-caldera lavas and caldera-forming ignimbrites. I and II relate to the first and second caldera forming events respectively. Geology from Nairn (1989).

the basement of 5 km and 1–2 km, respectively (Rogan, 1982). However, a clear low Vp anomaly at 4 km effectively corresponds to a minimum depth extent of the collapse structure (Sherburn et al., 2003).

New DEM and field data show that Okataina is located along the major ENE–WSW trending bend of the axial rift zone of TVZ (Figs. 2A and 7B). The OCC is a complex structure delineated by morphologically youthful intra-caldera volcanic features in juxtaposition with the older and more dissected terrain of pre-caldera lavas and ignimbrites forming the caldera margin (Fig. 7A). The caldera-bounding scarps are eroded and many parts are obscured by post-caldera eruptives. The 28×15 km caldera complex is strongly rectangular with an eccentricity E=0.54 (Fig. 7B) and a long axis trending N8°W, roughly perpendicular to the Okataina rift axis (Fig. 2B). The structure of the caldera floor is obscured by intra-caldera rhyolite massifs and the current margin is thus a composite feature.

Distinct embayments in the topographic margin extend where zones of intense ESE–WSW-trending regional faulting within the Okataina segment intersect the caldera. The caldera-bounding scarps in the south and southwest are parallel to and often continuous with these regional faults and to NE-trending faults along the western caldera margin (Fig. 7B). The embayments form subsidiary basins to the main N–S trending structure, and are continuous with the conspicuous linear vent zones transecting the caldera, formed by the post-caldera rhyolite dome complexes. The two linear zones are roughly axial to the adjacent Kapenga and Whakatane rift segments. As such they mark their continuation in the Okataina area, herein recording a ~20 km offset of the rift axis (Fig. 2).

3.2.4. Taupo caldera complex

Taupo caldera complex (Cole et al., 1998; Fig. 8) has been frequently active in the past ca. 65 ka (Wilson et al., 1986; Houghton et al., 1995), while its poorly constrained early eruptive history indicates activity over ca. 300 ka (Wilson et al., 1986). The caldera-forming Oruanui eruption at 26.5 ka (calibrated; Wilson, 1993) erupted ~400 km^3 of magma (Self, 1993; Wilson, 1991; Sutton et al., 1995).

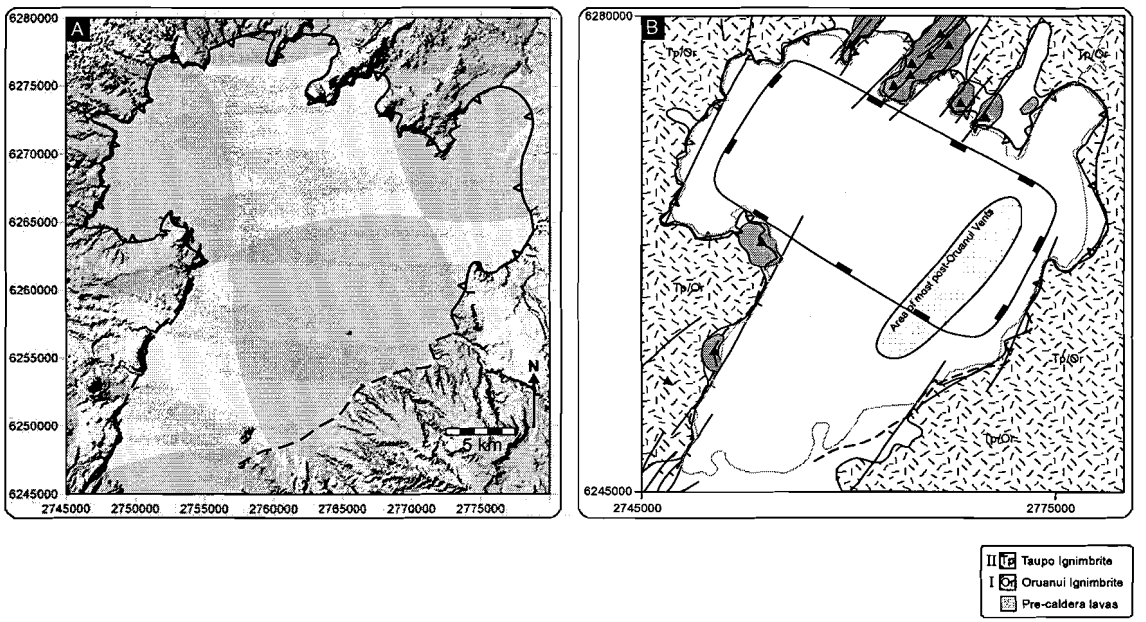

Fig. 8. Taupo caldera complex. (A) Shaded relief image of Taupo Caldera Complex. (B) Structure map of Taupo Caldera Complex identifying pre- caldera lavas, caldera forming ignimbrites, and the location of post Oruanui vents. Geology after Wilson (1993) and Sutton et al. (1995).

Wilson (1993) has identified 28 separate eruptions since the Oruanui eruption, the largest of these, the 35 km^3 Taupo eruption, occurred about 1800 years ago in the eastern part of the lake (Wilson and Walker, 1985; Smith and Houghton, 1995; Fig. 8B).

Petrological studies (e.g. Sutton et al., 1995, 2000) show a complex magmatic system, involving distinct magma types with short crustal-residence times. Eruptive activity prior to and following the main caldera-forming events reflect multiple distinct magma batches, while larger homogeneous magma bodies were generated prior to the Oruanui and Taupo caldera-forming eruptions (Sutton et al., 1995). Lithic componentry analysis of the Oruanui and Taupo ignimbrites identifies different lithic suites between the two ignimbrites, interpreted as reflecting mutually exclusive collapse structures (Cole et al., 1998).

A clear trapezoidal-shaped negative gravity anomaly is documented over the northern part of the lake, with northern and southern sides aligned perpendicular to the eastern TVZ margin (Davy and Caldwell, 1988; Fig. 5). It is the most intense negative gravity anomaly in TVZ (Davy and Caldwell, 1988), and is consistent with a NW–SE-trending caldera collapse structure filled with volcaniclastics of relatively low density. Geophysical data also demonstrate differential subsidence towards the caldera in the southern part of the lake, and a NW–SE-trending structural boundary marking the southern caldera margin (Davy and Caldwell, 1988).

New DEM and field data (Figs. 2A and 8B) show that Taupo is located within the axial rift zone of TVZ. The 28×16 km caldera complex is strongly rectangular, with an eccentricity E=0.57 and a long axis trending N63°W, roughly perpendicular to the Taupo rift segment (Fig. 2B). NE-trending regional faults controlling a series of peninsulas and embayments are cut by the northern caldera margin, while the eastern and western margins are partially scalloped but generally linear features (Fig. 8B). The southern part of Lake Taupo occupies a NE-trending fault-bounded depression intersecting the southern caldera margin; the western margin of this structure is a continuation of fault systems dissecting the Tongariro Volcanic Centre to the south. A prominent structural feature is the divergence in fault trend (~20°) to the south and north of the caldera complex (Fig. 8B). This bend effectively forms the boundary between the Ruapehu and Taupo rift segments (Acocella et al., 2003). Vents

for pre-caldera lavas to the south and north of the caldera complex lie along NE-trending lineaments (Fig. 8B); the vents for post-Oruanui eruptions mostly occur along the eastern edge of the caldera complex (Wilson, 1993; Fig. 8B).

4. Discussion

4.1. Along-axis relationships between tectonics and volcanism

Fig. 3 shows an inverse correlation between the dextral component of transtension and the volume of erupted magma along the transtensional segmented Modern TVZ. The largest eruptive volumes from the caldera complexes in the Okataina and Taupo segments are associated with the highest degree of extension; conversely, the lower erupted volumes from the andesitic volcanoes in the Ruapehu and Whakatane segments are associated with the highest degree of dextral shear.

The major implication of this correlation is a genetic link between the degree of extension and the eruptive volume and style. As a first approximation, we can consider two main possibilities to account for this relationship. (1) Upper-crustal tectonic processes have controlled the location of magma storage and extrusion. Crustal extension in fact relaxes the least horizontal compressive stress ó3, enhancing the rise of magmas through the crust mainly by dike propagation (e.g. Gudmundsson, 1998, 2003). (2) The presence of large volumes of magma at specific locations in the upper crust has controlled the structural evolution of the rift system. Magmatism may have an important role in influencing the structural style and evolution of rifts (e.g. Vigneresse et al., 1999; Lynch and Morgan, 1987; Morley, 1999).

Four points suggest that the first model is more likely. (1) Enhanced dike propagation within crust subject to regional extension is the simplest way in which to accommodate the rise and storage of magma at shallow crustal levels; greater extension at specific localities will lead to accumulation of larger magma volumes. (2) Eruptive vents for all styles of volcanism in TVZ, including Taupo and Okataina, are typically aligned parallel to regional structure. (3) The geometry of Taupo and Okataina calderas indicates strong tectonic influence on caldera formation and evolution. (4) The extension axes for the Taupo and Okataina segments are consistent with the evaluated overall N46°W extension direction for TVZ (Acocella et al., 2003).

4.2. Across-axis relationships between tectonics and volcanism

The collected data have shown how modern TVZ is characterised by 4 calderas, located outside (Reporoa, Rotorua) and within (Okataina and Taupo) the axial rift zone.

Reporoa and Rotorua are monogenetic calderas, related to the eruption of a single ignimbrite. Both have been the sites of only minor post-caldera volcanism and are associated with a relatively simple magmatic system: only at Rotorua caldera are some post-caldera eruptives associated with the magma related to caldera formation. Smaller (both in intensity and extent) negative gravity anomalies and DEM and field data suggest simple, sub-circular collapse structures, with a series of arcuate scarps. At both calderas regional tectonic structures are scarce or absent.

Conversely, Okataina and Taupo are multiple collapse structures, responsible for at least 2 ignimbrites and characterised by voluminous post-caldera volcanism. Here, the spatially associated pre- and post-caldera-forming eruptives reflect magma bodies independent of the caldera-forming magma system. Larger (both in intensity and extent) negative gravity and Vp anomalies, in addition to DEM and field data, suggest larger and more complex collapse structures, depicted by generally linear margins, defining a rectangular geometry perpendicular to regional structures. The roughly perpendicular nature of caldera long axes and local rift structure is consistent with similar relationships documented elsewhere (Bosworth et al., 2003) as a function of chamber expansion parallel to the minimum horizontal stress. Both Okataina and Taupo are characterized by the widespread presence of significant regional tectonic structures. Here, the intersection of regional faults with the caldera margin has formed subsidiary collapse structures extending beyond the structural depression outlined by geophysical data, forming an oversized, complex topographic margin.

These data show that caldera structures of modern TVZ can be divided into two groups. (1) Extra-rift

calderas are simple, relatively small, sub-circular, monogenetic structures, without significant coupling to active regional structure (Reporoa and Rotorua). (2) Intra-rift caldera complexes are large, multiple collapse structures, with rectangular margins and clear coupling to active regional structure (Okataina and Taupo; Fig. 9). This distinction demonstrates the role of active regional tectonics in controlling the location, structure, and development of caldera systems within a rift zone.

The presence of a major caldera within an active axis of a rift zone is a common situation worldwide. In a model of caldera volcanism in TVZ, however, we also have to accommodate the presence of calderas outside the axial rift zone. Among the possible explanations, we must consider the alignment of Rotorua and Reporoa Calderas with the southern continuation of the Miocene–Pleistocene Coromandel Volcanic Zone (CVZ; Skinner, 1986; Fig. 1). Pre-existing structures related to the NNW–SSE trending CVZ likely extend beneath the central portion of TVZ, and may constitute preferred pathways for the rise of magmas both inside and outside the axial rift zone. This hypothesis is supported by, firstly, the common appearance of minor ~NW–SE fractures in the Kapenga and Rotorua area (Acocella et al., 2003).

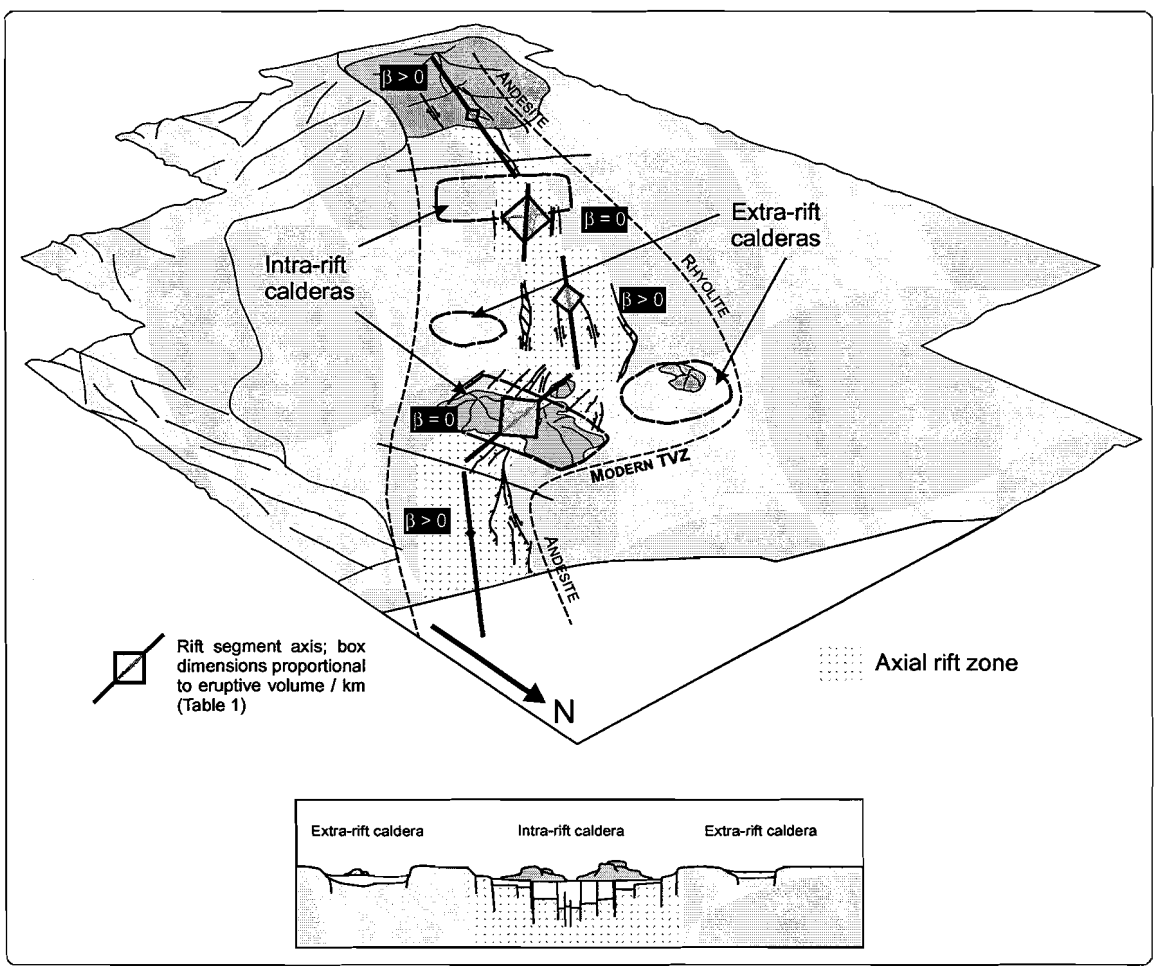

Fig. 9. Schematic figure of TVZ (oblique map and section view) summarizing the overall structural control on volcanism. The variations in the dextral component of extension (β), the erupted volumes (proportional to squares), and the caldera structures in modern TVZ are reported as a function of segment trend (along axis) and the distance from axis (across axis).

These fractures may be a weak surface expression of an inherited structure, reactivated during the evolution of modern TVZ. Secondly, the hypothesis is supported by the conspicuous relationship between the major bend in the rift axis at Okataina and the suggested presence and orientation of pre-existing CVZ structures.

This relationship can be investigated in a semi-quantitative way, considering the angles ϕ=53° (between the rift trend and the pre-existing structures) and α=40° (between the rift trend and the trend of the Okataina transfer zone) and the overall aspect ratio A=2.35 (length/width) of the Okataina transfer zone. Previous work (Acocella et al., 1999) showed a correlation between the trend of basement discontinuities (ϕ) and the orientation (α) and shape (A) of transfer zones, both on narrow rifts worldwide and in analogue experiments. The fact that the ϕ, α, and A values obtained for the TVZ are consistent with those obtained experimentally and from other transfer zones (Fig. 7 in Acocella et al., 1999) suggests that the presence of the pre-existing CVZ structures may play an important role in controlling the architecture of TVZ in the Okataina area.

4.3. General considerations

The presented data have provided some insight into the structural control on volcanic activity both within and across the axial zone of TVZ. However, a classical issue in TVZ studies is the conspicuous segmentation into andesitic extremities and a central zone dominated by rhyolitic calderas (e.g. Cole, 1990; Wilson et al., 1995).

The presented data allow us to consider this broad compositional segmentation in TVZ, at least in the last 300 ka, as reflecting upper crustal processes rather than deeper dynamics. The dominance of rhyolite in the central zone has been attributed to partial melting of basement CVZ lavas (Cole, 1990). However, chemical data suggest a more complex petrogenetic model involving some combination of fractionation of basaltic parent magmas with crustal assimilation (e.g. Graham et al., 1995). No petrogenetic model has been able to sufficiently account for the anomalously high thermal flux in central TVZ. We speculate that the increased component of crustal extension in the central zone may account for the restricted distribution of rhyolitic volcanism by inducing extreme thinning, a decrease in pressure, and partial melting of mantle asthenosphere, generating an anomalous heat source for (1) partial melting of suitable crustal materials (e.g. Cole, 1990) or (2) high rates of mafic magma production below the crust (leading to fractionation). Regardless of the precise petrogenetic model, the selective presence of voluminous rhyolitic volcanism in the central part of TVZ in the last 300 ka can be explained as a function of rift zone architecture, by (1) creating an area of preferred rhyolite generation at depth, where CVZ lavas are likely to form part of the basement; (2) focusing the rise and accumulation of magma at high levels in the crust.

The proposed model therefore shows how TVZ constitutes an example of rift architecture influencing the characteristics of magma generation and emplacement, and the type of volcanism observed at the surface.

5. Conclusions

New remote sensing and field-based structural data have been combined with previously published data on Modern TVZ. The results show a correlation between the amount of extension and the volumes of extruded magma, as well as the style of eruption in each segment. Segments with the highest degree of extension correspond to the highly active rhyolitic Taupo and Okataina Caldera Complexes; conversely, segments with a higher degree of dextral transtension correspond to volumetrically more moderate andesite stratovolcanoes. As far as the calderas are concerned, these exhibit different features as a function of their proximity to (and influence of) active rift faulting within TVZ. Intra-rift calderas (Taupo, Okataina) are multiple collapse structures with rectilinear margins, overprinted by younger volcanism and faulting, associated with multiple major eruptions. Extra-rift calderas (Rotorua, Reporoa) are sub-circular monogenetic collapse structures, associated with one major ignimbrite, with minor post-collapse volcanism. Therefore, TVZ exemplifies the situation where (1) along the axial rift zone, magma may be erupted as a function of the extension rate, and (2) volcanism is manifest as different caldera structures according to their proximity to the axial zone.

Acknowledgements

This work is partly the result of a PhD study by KDS, funded through a University of Canterbury Doctoral Scholarship and the Mason Trust, both of which are gratefully acknowledged. KDS is indebted to W Esler, Dr DM Milner, and Profs. JR Pettinga, SD Weaver, and B Tikoff for helpful ideas and discussions. We thank DM Milner and TS McConnico for early reviews which greatly improved the manuscript. VA would like to thank IGCP project 455 for the opportunity for discussions on these issues at different international meetings, and R Funiciello for his very useful comments and encouragement. The authors are grateful to SL Brenner and A Gudmundsson for helpful reviews which improved the manuscript.

References

Acocella, V., Rossetti, F., 2002. The role of extensional structures on pluton ascent and emplacement: the case of Southern Tuscany (Italy). Tectonophysics 354, 71–83.

Acocella, V., Faccenna, C., Funiciello, R., Rossetti, F., 1999. Sandbox modelling of basement controlled transfer zones in extensional domains. Terra Nova 11, 149–156.

Acocella, V., Spinks, K.D., Cole, J.W., Nicol, A., 2003. Oblique back arc rifting of Taupo Volcanic Zone, New Zealand. Tectonics 22 (4), 1045.

Bailey, R.A., Carr, R.G., 1994. Physical geology and eruptive history of the Matahina Ignimbrite, Taupo Volcanic Zone, North Island, New Zealand. N.Z. J. Geol. Geophys. 37, 319–344.

Bellamy, S., 1991. Some studies of the Te Wairoa ignimbrites and the associated volcanic geology of the SW Okataina volcanic centre, Taupo Volcanic Zone. MSc thesis, Univ. Waikato, New Zealand.

Beresford, S.W., 1997. Volcanology and geochemistry of the Kaingaroa Ignimbrite, Taupo Volcanic Zone, New Zealand. PhD thesis, Univ. Canterbury, New Zealand.

Beresford, S.W., Cole, J.W., 2000. Kaingaroa Ignimbrite, Taupo Volcanic Zone, New Zealand: evidence for asymmetric caldera subsidence of the Reporoa Caldera. N.Z. J. Geol. Geophys. 43, 471–481.

Bibby, H.M., Caldwell, T.G., Davey, F.J., Webb, T.H., 1995. Geophysical evidence on the structure of the Taupo Volcanic Zone and its hydrothermal circulation. J. Volcanol. Geotherm. Res. 68, 29–58.

Black, T.M., Shane, P.A.R., Westgate, J.A., Froggatt, P.C., 1996. Chronology and paleomagnetic constraints on widespread ignimbrites of the Taupo volcanic zone, New Zealand. Bull. Volcanol. 58, 226–238.

Bosworth, W., Burke, K., Strecker, M., 2003. Effect of stress fields on magma chamber stability and the formation of collapse calderas. Tectonics 22 (4), 1042.

Bowyer, D.A., 2001. Petrologic, geochemical, and isotopic evolution of rhyolite lavas from the Okataina, Rotorua, and Kapenga volcanic centres, Taupo Volcanic Zone, New Zealand. PhD thesis, Univ. Waikato, New Zealand.

Brown, S.J.A., Burt, R.M., Cole, J.W., Krippner, S.J.P., Price, R.C., Cartwright, I., 1998. Plutonic lithics in ignimbrites of Taupo Volcanic Zone, New Zealand: sources and conditions of crystallisation. Chem. Geol. 148, 21–41.

Carter, L., 1980. NZ regional bathymetry 1: 6000000 (2nd ed). NZ Oceanographic Institute Chart. Misc. Ser. 15. Dept. Sci. Ind. Res., Wellington, NZ.

Cole, J.W., 1990. Structural control and origin of volcanism in the Taupo volcanic zone, New Zealand. Bull. Volcanol. 52, 445–459.

Cole, J.W., Lewis, K.B., 1981. Evolution of the Taupo–Hikurangi subduction system. Tectonophysics 72, 1–21.

Cole, J.W., Brown, S.J.W., Burt, R.M., Beresford, S.W., Wilson, C.J.N., 1998. Lithic types in ignimbrites as a guide to the evolution of a caldera complex, Taupo volcanic centre, New Zealand. J. Volcanol. Geotherm. Res. 80, 217–237.

Darby, D.J., Meertens, C.M., 1995. Terrestrial and GPS measurements of deformation across the Taupo back arc and Hikurangi forearc regions in New Zealand. J. Geophys. Res. 100, 8221–8232.

Davey, F.J., Henrys, S.A., Lodolo, E., 1995. Asymmetric rifting in a continental back-arc environment, North Island New Zealand. J. Volcanol. Geotherm. Res. 68, 209–238.

Davy, B.W., Caldwell, T.G., 1988. Gravity, magnetic and seismic surveys of the caldera complex, Lake Taupo, North Island New Zealand. J. Volcanol. Geotherm. Res. 81, 69–89.

De Silva, S.L., 1989. Altiplano–Puna volcanic complex of the central Andes. Geology 17, 1102–1106.

Froggatt, P.C., Lowe, D.J., 1990. A review of late quaternary silicic and some other tephra formations from New Zealand; their stratigraphy, nomenclature, distribution, volume, and age. N.Z. J. Geol. Geophys. 33, 89–109.

Glazner, A., 1991. Plutonism, oblique subduction and continental growth: an example from the Mesozoic of California. Geology 19, 784–786.

Graham, I.J., Cole, J.W., Briggs, R.M., Gamble, J.A., Smith, I.E.M., 1995. Petrology and petrogenesis of volcanic rocks from the Taupo Volcanic Zone: a review. J. Volcanol. Geotherm. Res. 68, 59–87.

Gravley, D.M., 2005. The Ohakuri Pyroclastic Deposits and the Evolution of the Rotorua-Ohakuri Volcanotectonic Depression. Unpubl. PhD. thesis, University of Canterbury, Christchurch, New Zealand.

Grocott, J., Brown, M., Dallmeyer, R.D., Taylor, G.K., Treloar, P.J., 1994. Mechanisms of continental growth in extensional arcs: an example from the Andean plate-boundary zone. Geology 22, 391–394.

Gudmundsson, A., 1998. Magma chambers modelled as cavities explain the formation of rift zone central volcanoes and their eruption and intrusion statistics. J. Geophys. Res. 103 (B4), 7401–7412.

Gudmundsson, A., 2003. Surface stresses associated with arrested dikes in rift zones. Bull. Volcanol. 65, 606–619.

Hackett, W.R., Houghton, B.F., 1989. A facies model for a Quaternary andesitic composite volcano: Ruapehu, New Zealand. Bull. Volcanol. 51, 51–68.

Hobden, B.J., Houghton, B.F., Davidson, J.P., Weaver, S.D., 1999. Small and short-lived magma batches at composite volcanoes: time windows at Tongariro volcano, New Zealand. J. Geol. Soc. (Lond.) 156, 865–868.

Houghton, B.F., Wilson, C.J.N., McWilliams, M.O., Lanphere, M.A., Weaver, S.D., Briggs, R.M., Pringle, M.S., 1995. Chronology and dynamics of a large silicic magmatic system: central Taupo Volcanic Zone, New Zealand. Geology 23, 13–16.

Hunt, T.M., 1992. Gravity studies in the Rotorua area, New Zealand. Geothermics 21, 65–74.

Jurado-Chichay, Z., Walker, G.P.L., 2000. Stratigraphy and dispersal of the Mangaone Subgroup pyroclastic deposits, Okataina Volcanic Centre, New Zealand. J. Volcanol. Geotherm. Res. 104, 283–319.

Jurado-Chichay, Z., Walker, G.P.L., 2001. The intensity and magnitude of the Mangaone subgroup plinian eruptions from Okataina Volcanic Centre, New Zealand. J. Volcanol. Geotherm. Res. 111, 219–237.

Leonard, G.S., 2003. The Evolution of Maroa Volcanic Centre, Taupo Volcanic Zone, New Zealand. Unpubl. PhD. thesis, University of Canterbury, Christchurch, New Zealand.

Leonard, G.S., Cole, J.W., Nairn, I.A., Self, S., 2002. Basalt triggering of the c. AD 1305 Kaharoa rhyolite eruption, Tarawera Volcanic Complex, New Zealand. J. Volcanol. Geotherm. Res. 115, 461–486.

Lynch, H.D., Morgan, P., 1987. The tensile strength of the lithosphere and the localization of extension. In: Coward, M.P., Dewey, J.F., Hancock, P.L. (Eds.), Continental Extensional Tectonics, Geol. Soc. Spec. Pub., vol. 28, pp. 53–65.

Malinverno, A., Ryan, W.B.F., 1986. Extension in the Tyrrhenian Sea and shortening in the Apennines as result of arc migration driven by sinking of the lithosphere. Tectonics 5, 227–245.

Milner, D.M., Cole, J.W., Wood, C.P., 2002. Asymmetric, multiple-block collapse at Rotorua Caldera, Taupo Volcanic Zone, New Zealand. Bull. Volcanol. 64, 134–149.

Milner, D.M., Cole, J.W., Wood, C.P., 2003. Mamaku Ignimbrite: a caldera-forming ignimbrite erupted from a compositionally zoned magma chamber in Taupo Volcanic Zone, New Zealand. J. Volcanol. Geotherm. Res. 122, 243–264.

Morley, C.K., 1999. Aspects of transfer zone geometry and evolution in East African Rifts. In: Morley, C.K. (Ed.), Geoscience of Rift Systems—Evolution of East Africa, American Association of Petroleum Geologists Studies in Geology, vol. 44, pp. 479–492.

Nairn, I.A., 1981. Some studies of the geology, volcanic history and geothermal resources of the Okataina volcanic centre, Taupo Volcanic Zone, New Zealand. PhD thesis, Victoria Univ., Wellington, New Zealand.

Nairn, I.A., 1989. Sheet V16AC-Mount Tarawera, geological map of New Zealand, 1:50,000, Dep. of Sci. and Ind. Res., Wellington.

Nairn, I.A., Wood, C.P., Bailey, R.A., 1994. The Reporoa Caldera, Taupo Volcanic Zone: source of the Kaingaroa Ignimbrites. Bull. Volcanol. 56, 529–537.

Nakamura, K., 1977. Volcanoes as possible indicators of tectonic stress orientation: principle and proposal. J. Volcanol. Geotherm. Res. 2, 1–16.

Paterson, S.R., Tobsich, O.T., 1992. Rates of processes in magmatic arcs: implications for the timing and nature of pluton emplacement and wall rock deformation. J. Struct. Geol. 14, 291–300.

Petford, N., Cruden, A.R., McCaffrey, K.J.W., Vigneresse, J.L., 2000. Granite magma formation, transport and emplacement in the Earth's crust. Nature 408, 669–673.

Riller, U., Petrinovic, I., Ramelow, J., Strecker, M., Oncken, O., 2001. Late Cenozoic tectonism, collapse caldera and plateau formation in the central Andes. Earth Planet. Sci. Lett. 188, 299–311.

Rogan, M., 1982. A geophysical study of the Taupo Volcanic Zone. New Zealand. J. Geophys. Res. 87, 4073–4088.

Sato, H., 1994. The relationship between late Cenozoic tectonic events and stress field and basin development in northeast Japan. J. Geophys. Res. 99, 22261–22274.

Self, S., 1993. Large scale silicic phreatomagmatic volcanism: a case study from New Zealand. J. Volcanol. Geotherm. Res. 17, 433–469.

Shane, P., Black, T., Westgate, J., 1994. Isothermal plateau fission track age for the paleomagnetic excursion in the Mamaku Ignimbrite, New Zealand, and implications for late Quaternary stratigraphy. Geophys. Res. Lett. 21, 1695–1698.

Sherburn, S., Bannister, S., Bibby, H., 2003. Seismic velocity structure of the central Taupo Volcanic Zone, New Zealand, from local earthquake tomography. J. Volcanol. Geotherm. Res. 122, 69–88.

Skinner, D.N.B., 1986. Neogene volcanism of the Hauraki Volcanic region. In: Smith, I.E.M. (Ed.), Late Cenozoic Volcanism in New Zealand, R. Soc. N.Z. Bull., vol. 23, pp. 21–47.

Smith, V., 2001. The stratigraphy and geochemistry of the Mangaone subgroup tephra beds, Okataina volcanic centre, New Zealand. MSc thesis, Auckland Univ. Auckland, New Zealand.

Smith, R.T., Houghton, B.F., 1995. Vent migration and changing eruptive style during the 1800 ka Taupo eruption: new evidence from the Hatepe and Rotongaio phreatoplinian ashes. Bull. Volcanol. 57, 432–439.

Soengkono, S., 1995. A magnetic model for deep plutonic bodies beneath the central Taupo Volcanic Zone, North Island, New Zealand. J. Volcanol. Geotherm. Res. 68, 193–207.

Soengkono, S., Hochstein, M.P., 1996. Interpretation of magnetic anomalies over the Reporoa geothermal field, Taupo Volcanic Zone, New Zealand. Proceedings 18th N.Z. Geothermal Workshop, pp. 243–248.

Stagpoole, V.M., 1994. Interpretation of refraction seismic and gravity data across the eastern margin of the Taupo Volcanic Zone. Geothermics 23, 501–510.

Stagpoole, V.M., Bibby, H.M., 1999. Residual gravity anomaly map of the Taupo Volcanic Zone, New Zealand, 1:250 000, version 1.0. Institute of Geological & Nuclear Sciences Geophysical Map 13. Institute of Geological & Nuclear Sciences Limited, Lower Hutt, New Zealand.

Sutton, A.N., Blake, S., Wilson, C.J.N., 1995. An outline geochemistry of rhyolite eruptives from Taupo volcanic centre, New Zealand. J. Volcanol. Geotherm. Res. 68, 153–175.

Sutton, A.N., Blake, S., Wilson, C.J.N., Charlier, B.L.A., 2000. Late Quaternary evolution of a hyperactive rhyolite magmatic system: Taupo volcanic centre, New Zealand. J. Geol. Soc. (Lond.) 157, 537–552.

Tibaldi, A., 1992. The role of transcurrent intra-arc tectonics in the configuration of a volcanic arc. Terra Nova 4, 567–577.

Tikoff, B., de Saint Blanquat, M., 1997. Transpressional shearing and strike-slip partitioning in the Late Cretaceous Sierra Nevada magmatic arc, California. Tectonics 16, 442–459.

Vigneresse, J.L., Tikoff, B., Ameglio, L., 1999. Modification of the regional stress field by magma intrusion and formation of tabular granitic plutons. Tectonophysics 302, 203–224.

Villamor, P., Berryman, K., 2001. A late Quaternary extension rate in the Taupo Volcanic Zone, New Zealand, derived from fault slip data. N.Z. J. Geol. Geophys. 44, 243–269.

Wilson, C.J.N., 1991. Ignimbrite morphology and the effects of erosion: a New Zealand case study. Bull. Volcanol. 53, 635–644.

Wilson, C.J.N., 1993. Stratigraphy, chronology, styles and dynamics of late Quaternary eruptions from Taupo volcano, New Zealand. Philos. Trans. R. Soc. Lond., A, 205–306.

Wilson, C.J.N., 1996. Taupo's atypical arc. Nature 379, 27–28.

Wilson, C.J.N., Walker, G.P.L., 1985. The Taupo eruption, New Zealand. Philos. Trans. R. Soc. Lond. Ser. A: Math. Phys. Sci. 314, 199–228.

Wilson, C.J.N., Rogan, M.A., Smith, I.E.M., Northey, D.J., Nairn, I.E., Houghton, B.F., 1984. Caldera volcanoes of the Taupo Volcanic Zone, New Zealand. J. Geophys. Res. 89, 8463–8484.

Wilson, C.J.N., Houghton, B.F., Lloyd, E.F., 1986. Volcanic history and evolution of the Maroa–Taupo area, Central North Island. In: Smith, I.E.M. (Ed.), Late Cenozoic Volcanism in New Zealand, R. Soc. N.Z. Bull., vol. 23, pp. 194–223.

Wilson, C.J.N., Houghton, B.F., McWilliams, M.O., Lanphere, M.A., Weaver, S.D., Briggs, R.M., 1995. Volcanic and structural evolution of Taupo Volcanic Zone, New Zealand: a review. J. Volcanol. Geotherm. Res. 68, 1–28.

Wood, C.P., 1992. Geology of the Rotorua geothermal system. Geothermics 21, 25–41.

Wright, I.C., 1992. Shallow structure and active tectonism of an offshore continental back-arc spreading system: the Taupo Volcanic Zone, New Zealand. Mar. Geol. 103, 287–309.

Appendix C

'Cole, J.W., Milner, D.M. & **Spinks, K.D.** (2005) Calderas and caldera structures: a review. *Earth-Science Reviews* 69: 1-26'

Contribution: Generation and compilation of ideas regarding caldera structure and terminology with other authors; Complete manuscript review and partial re-write, particularly of section's 8 and 9.

Available online at www.sciencedirect.com
SCIENCE DIRECT
Earth-Science Reviews 69 (2005) 1–26
EARTH-SCIENCE REVIEWS
www.elsevier.com/locate/earscirev

Calderas and caldera structures: a review

J.W. Cole*, D.M. Milner, K.D. Spinks

Department of Geological Sciences, University of Canterbury, PO Box 4800, Private Bag 4800, Christchurch, New Zealand

Received 17 April 2002; accepted 22 June 2004

Abstract

Calderas are important features in all volcanic environments and are commonly the sites of geothermal activity and mineralisation. Yet, it is only in the last 25 years that a thorough three-dimensional study of calderas has been carried out, utilising studies of eroded calderas, geophysical analysis of their structures and analogue modelling of caldera formation. As more data has become available on calderas, their individuality has become apparent. A distinction between 'caldera', 'caldera complex', 'cauldron', and 'ring structure' is necessary, and new definitions are given in this paper. Descriptions of calderas, based on dominant composition of eruptives (basaltic, peralkaline, andesitic–dacitic, rhyolitic) can be used, and characteristics of each broad group are given. Styles of eruption may be effusive or explosive, with the former dominant in basaltic calderas, and the latter dominant in andesitic–dacitic, rhyolitic and peralkaline calderas.

Four 'end-member' collapse styles occur—plate or piston, piecemeal, trapdoor, and downsag—but many calderas have multiple styles. Features of so-called 'funnel' and 'chaotic' calderas proposed in the literature can be explained by other collapse styles and the terms are considered unnecessary.

Ground deformation comprises subsidence or collapse (essential characteristics of a caldera) and uplifting/doming and fracturing due to tumescence and/or resurgence (frequent, but not essential). Collapse may occur on pre-existing structures, such as regional faults or on faults created during the caldera formation, and the shape of the collapse area will be influenced by depth, size and shape of the magma chamber. The final morphology of a caldera will depend on how the caldera floor breaks up; whether collapse takes place in one event or multiple events, whether vertical movement is spasmodic or continuous throughout the eruptive sequence, and whether blocks subside uniformly or chaotically at one or more collapse centres.

A meaningful description of any caldera should therefore include; number of collapse events, presence or absence of resurgence, caldera-floor coherency, caldera-floor collapse geometry, and dominant composition of eruptives.

Keywords: Caldera; Terminology; Structure; Tumescence/resurgence; Morphology

1. Introduction

Calderas and caldera complexes are depressions that have been recognised in all volcanic environments on Earth and in the Solar System. The largest

* Corresponding author. Tel.: +64 3 364 2766; fax: +64 3 364 2769.
E-mail address: jim.cole@canterbury.ac.nz (J.W. Cole).

0012-8252/$ - see front matter © 2004 Elsevier B.V. All rights reserved.
doi:10.1016/j.earscirev.2004.06.004

caldera known is that of Olympus Mons on Mars, a nested structure containing six collapse centres that together measure 80×65 km (Mouginis-Mark and Robinson, 1992). On Earth, calderas and caldera complexes range in size from <1 km diameter up to 40×75 km (La Garita Caldera; Lipman, 2000a), and are formed during the eruption of between 1 and 5000+ km^3 of ejecta, mainly of ignimbrite. Historic eruptions associated with caldera collapse have lead to huge fatalities in Indonesia (Krakatau; Simkin and Fiske, 1983), and are considered to have caused the destruction of the Minoan civilisation at Santorini (Druitt et al., 1999). Larger eruptions are generally less frequent than smaller ones (once every 100 years for 1 to 10 km^3 eruptions; once every 100,000 years for >1000 km^3 eruptions; Fisher et al., 1997).

Calderas are also frequently the sites of vigorous geothermal activity, making them potential sites for electricity generation, e.g., in Taupo Volcanic Zone, New Zealand (Bibby et al., 1995), and the sites of mineralisation, e.g., in Arizona (Lipman and Sawyer, 1985, Lipman, 1992); New Mexico (Goff and Gardner, 1994); Nevada (Mills et al., 1988) and Fiji (Eaton and Setterfield, 1993).

The word 'caldera' is derived originally from the Latin word 'caldaria'—meaning 'boiling pot'. It was used in the Canary Islands for any large 'bowl-shaped' or 'cauldron-shaped' topographic depression, and the term is applied in that sense to the amphi-theatre-shaped heads of many valleys. von Buch (1820) described the 'Caldera of Palma' (now known as Taburiente), which he considered to be formed by forces in the crust pushing up strata, like a huge blister, until the rocks cracked radially and volcanic material was emitted, to form an elevation crater or 'erhebungskratere'. In the mid-19th century many authors (e.g., Prevost, 1843; Lyell, 1858; Scrope, 1859 and Hartung, 1860) discussed calderas. However, it is only in the last 25 years that a combination of careful mapping of eroded calderas (e.g., Lipman, 1984, 1995, 2000a; Branney and Kokelaar, 1994), descriptions of modern (restless) calderas (e.g., Newhall and Dzurisin, 1988), geodetic work (e.g., Dvorak and Dzurisin, 1997) and experimental analogue modelling of caldera structures (e.g., Komuro et al., 1984; Komuro, 1987; Marti et al., 1994; Roche et al., 2000; Acocella et al., 1999, 2000, 2001) has provided a better understanding of the three-dimensional form, and probable collapse dynamics, of calderas.

Lipman (2000b) has provided an excellent review of calderas, largely based on his work on calderas in the US and overseas, including comments on societal implications, a table of important caldera eruptions, and a bibliography of key papers. The present review paper concentrates on caldera terminology and further evaluates caldera structure and process of formation. It uses a broad grouping, based on dominant composition of the major eruptives associated with caldera collapse, to describe the range of calderas. It is not intended as a classification. A format for clear, accurate descriptions of calderas is given in Section 10 of this paper.

2. Distribution of calderas

Calderas occur in all volcanic environments. Basaltic calderas are characteristic of oceanic intra-plate hot spot locations (e.g., Hawaii; Walker, 1988), but also occur at some divergent plate boundaries in a mid-ocean ridge situation (e.g., East Pacific Rise; Fornari et al., 1984, and Iceland; Gudmundsson, 1995, although calderas in Iceland are commonly associated with central volcanoes that include more silicic volcanism). Andesitic–dacitic calderas are typically associated with convergent plate boundaries where they occur on volcanoes in island arcs (e.g., Tofua, Tonga Islands; Baker et al., 1971) and continental margin arcs (e.g., Crater Lake, Oregon; Bacon, 1983). Peralkaline calderas are associated with areas of high extension. They are common in the East African Rift (e.g., Ethiopia; Acocella et al., 2002), but also occur in areas of unusually high rates of localised extension in convergent margin (e.g., Mayor Island, New Zealand; Houghton et al., 1992) or intra-plate oceanic islands (e.g., Canary Islands; Schmincke, 1967; Marti and Gudmundsson, 2000). Rhyolitic calderas occur mostly in continental or continental-margin areas where mild extension occurs, either associated with a convergent plate boundary (e.g., Taupo Volcanic Zone, New Zealand; Wilson et al., 1995) or with rifting in continental crust (e.g., Rio Grande Rift, south central USA; Elston, 1984). Rhyolitic calderas have also been observed associated with continental hotspots (e.g., Yellowstone, Wyom-

ing, USA; Hildreth et al., 1984), and have recently been found in some submarine arc–back-arc systems (e.g., Kermadec arc; Wright and Gamble, 1999; Wright et al., 2003). Descriptions of representative calderas of each composition are given in Section 6.

3. Terminology

In his classic publication on 'Calderas and their Origin', Williams (1941) noted that "Few terms in the volcanologist's vocabulary have suffered more vicissitudes than the term 'caldera'", and this problem has continued to the present day. Reck (1936) summarised early usage and Williams (1941) summarised classifications used during the first part of the 20th century. William's classification (Table 1) was broad, and included many different types of volcanic events. Later, Williams and McBirney (1979) redefined 'calderas' as "large collapse depressions, more or less circular or cirque-like in form, the diameter of which is many times greater than any included vent", and all but collapse calderas in Williams' (1941) scheme were excluded. In the 1980s, process was regarded as more important, and Walker (1984) noted the significance of 'downsag' in many calderas. Lipman (1995, 2000b) followed this up with an 'end-member' classification of dominant collapse processes (Table 1).

Table 1
Comparison of classifications by Williams (1941), Williams and McBirney (1979) and Lipman (1995)

Williams (1941)	Williams and McBirney (1979)	Lipman (1995)
Explosion		
Collapse		
Krakatau	Krakatoan	Plate (piston)
Kilauea	Hawaiian	Piecemeal
Katmai	Katmai	Downsag
	Valles	Trapdoor
	Galapagos	Funnel
	Masaya	
	Atitlan	
Cryptovolcanic		
Glen Coe		
Miscellaneous		
Erosion		
Volcanic graben		
Summit		
Sector		
Volcanic vents or fissure troughs		
Major volcano-tectonic depressions		

As more data has become available on calderas it is increasingly clear that 'calderas' of all compositions show a wide range of features as a response to the collapse process. It is therefore impossible to 'pigeonhole' or classify them into well-defined types, as attempted by Williams (1941) and earlier authors. The approach of Lipman (1995, 2000b), in establishing 'end-member' types, is much more realistic and recognises the wide range of features associated with the structures. But even this classification is restrictive in that many calderas have morphologies that can be attributed to more than one collapse process and/or structural style. Perhaps the simplest method of grouping calderas is on dominant composition of the main eruptive magma, recognising, however, that many calderas may contain more than one eruptive type (e.g., many rhyolitic calderas frequently contain some intermediate or mafic volcanism). This is in no way intended as a classification.

We also suggest that it is important to distinguish between well-defined calderas and older, eroded structures, and suggest the following terminology that will indicate preservation and complexity (Fig. 1), and will be used in this review:

- *Caldera*—A volcanic structure, generally large, which is principally the result of collapse or subsidence into the top of a magma chamber during or immediately following eruptive activity.
- *Caldera complex*—Spatially and structurally associated nested or overlapping calderas of different ages. As structures are generally poorly or incompletely preserved, ignimbrites should be assigned only on the basis of volcanological criteria.
- *Cauldron*—A eroded caldera in which most of the eruptives accompanying caldera collapse have been removed by erosion, and older volcanic or sedimentary units below the caldera floor are now exposed.
- *Ring structure*—A magma chamber or chambers, exposed by deep erosion (generally >2 km), beneath an inferred caldera structure.

The definition of a caldera given in this paper precludes the use of the term 'caldera' for a purely

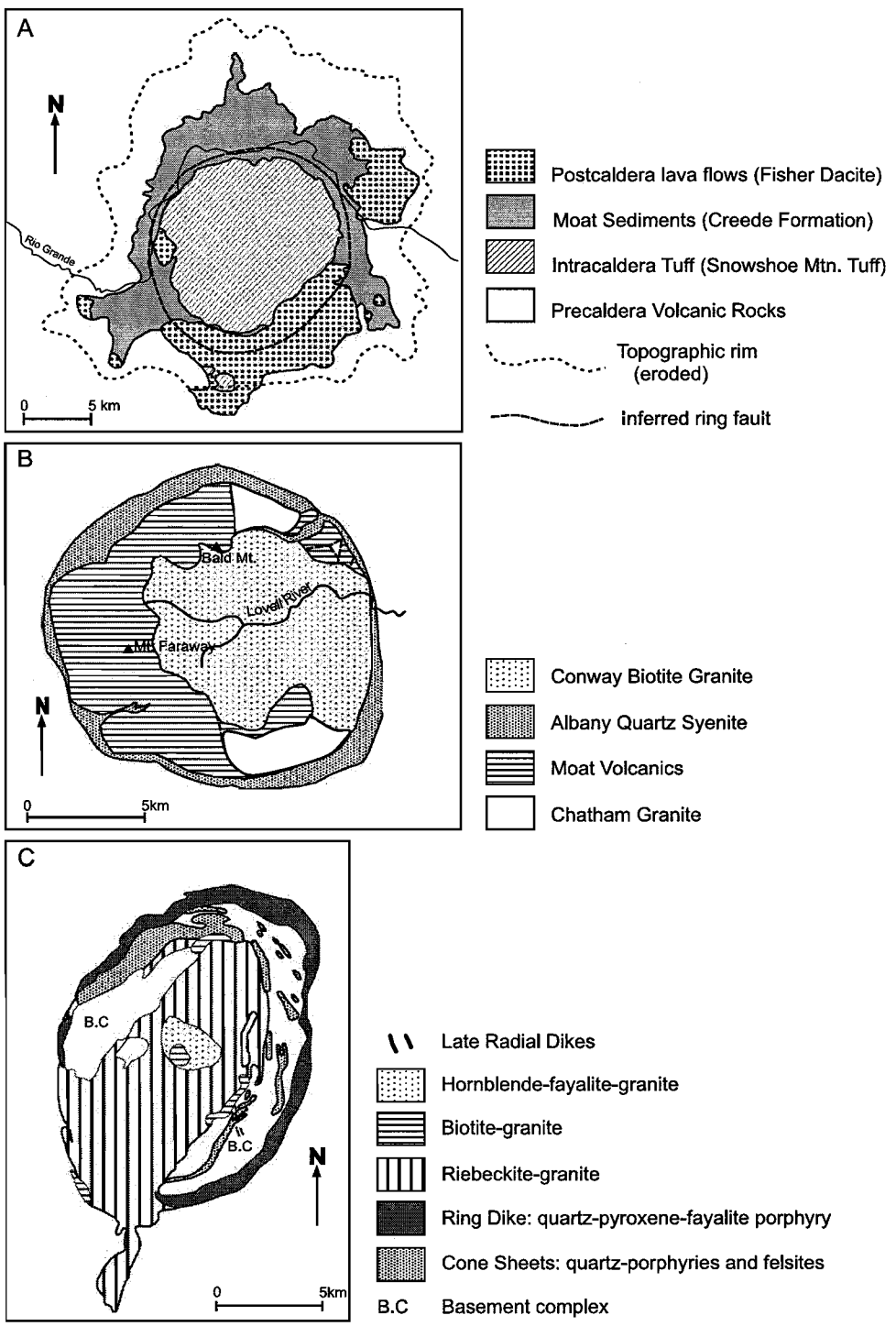

Fig. 1. Differences between (A) caldera, (B) cauldron and (C) ring structure. The examples used are: (A) Creede Caldera, Colorado (Bethke and Hay, 2000); (B) Ossipee Cauldron, Carroll County, NH (Kingsley, 1931); (C) Kudaru Ring Structure, Northern Nigeria (Bain, 1934).

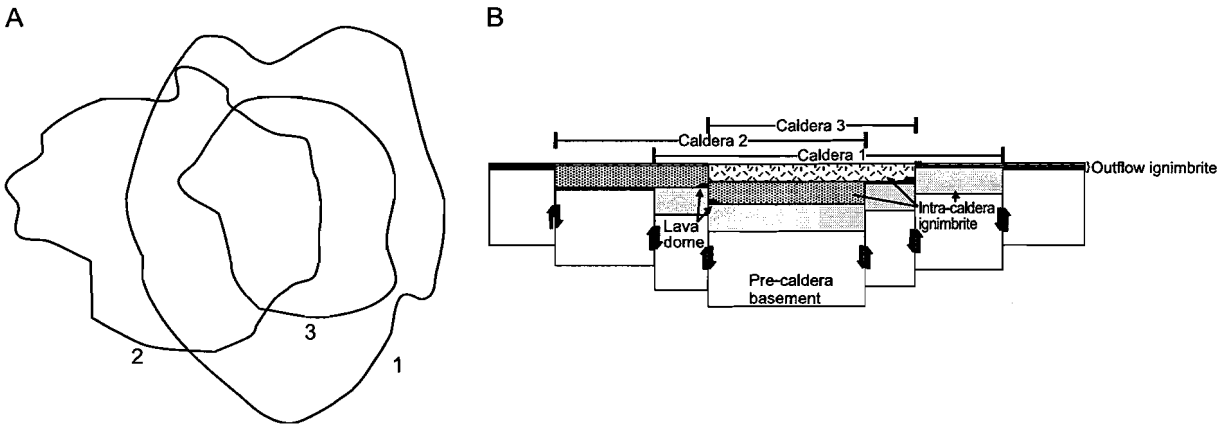

Fig. 2. (A) Collapse associated with three spatially overlapping calderas. If all three areas of collapse occur during one eruptive episode, the resultant caldera is said to be piecemeal (see Section 7). If each collapse occurs after a period of time the result is a caldera complex. (B) Faults utilised by early collapse events may be reactivated in successive events. The fault–caldera relationship can only be interpreted from thickness relationships of ignimbrites that were deposited during the caldera forming events (e.g., Branney and Kokelaar, 1994).

erosional structure, as originally suggested by Williams (1941), and more recently used by Karátson et al. (1999).

The distinction between a caldera and a caldera complex may not be clear from structure alone (Fig. 2). There may be collapse at a number of loci during a single eruptive episode, which will create a piecemeal caldera (see Section 7). If however the overlapping calderas form during eruptions of different ignimbrites the result is a caldera complex (e.g., Taupo caldera complex, New Zealand; Cole et al., 1998). Faults utilised by early collapse events may be reactivated in successive events. The fault–caldera relationship can only be interpreted from thickness relationships of ignimbrites (Fig. 2B) that were deposited during the caldera forming events (i.e., if there is a great change in thickness of one ignimbrite across a fault then it is likely that the fault was reactivated during caldera collapse; e.g., Branney and Kokelaar, 1994).

Collapse is not always immediately beneath the erupting vent. In 1912, magma travelled over 10 km from a magma source under Mt Katmai, Alaska, and erupted as an ignimbrite from Novarupta (Hildreth, 1991), but the present 4 km^3 caldera collapsed at Mt Katmai. The caldera formed by magma draw down as it migrated to Novarupta, in a situation more akin to the lateral movement that occurs in Hawaiian volcanoes than classic explosive-style calderas.

The distinction between 'caldera' and 'cauldron' is not clear cut, and an argument could be put forward to abandon the term 'cauldron'. However, the term is well established in the literature, and we feel should only be used in future for examples where erosion has removed most of the surface volcanics associated with the caldera collapse event or events.

4. Anatomy of a caldera

The shape and size of calderas is variable. Some calderas are near circular and have a simple history of collapse (e.g., Reporoa, New Zealand; Nairn et al., 1994, Beresford and Cole, 2000; Creede, CO, USA; Bethke and Hay, 2000), while others are more rectilinear (e.g., Taupo, New Zealand; Cole et al., 1998; Silent Canyon, USA; Ferguson et al., 1994). Size can also vary from small 'pit-craters' (e.g., Halemaumau, Hawaii; Decker, 1987) to very large collapse structures (e.g., La Garita, Colorado, USA; Lipman, 2000a) and many form part of caldera complexes.

An individual caldera may be considered in terms of topographic and structural elements (Fig. 3A, B), as identified by Lipman (1984, 1997, 2000b), including (Fig. 3C): a collapse collar, inner topographic wall, caldera floor, ring fault, landslide breccia and intracaldera ignimbrite. These features are described in more detail in Lipman (2000b). The structural boundary comprises that part of the caldera that has collapsed by movement along faults, and topographic boundary joins the high points that surround the

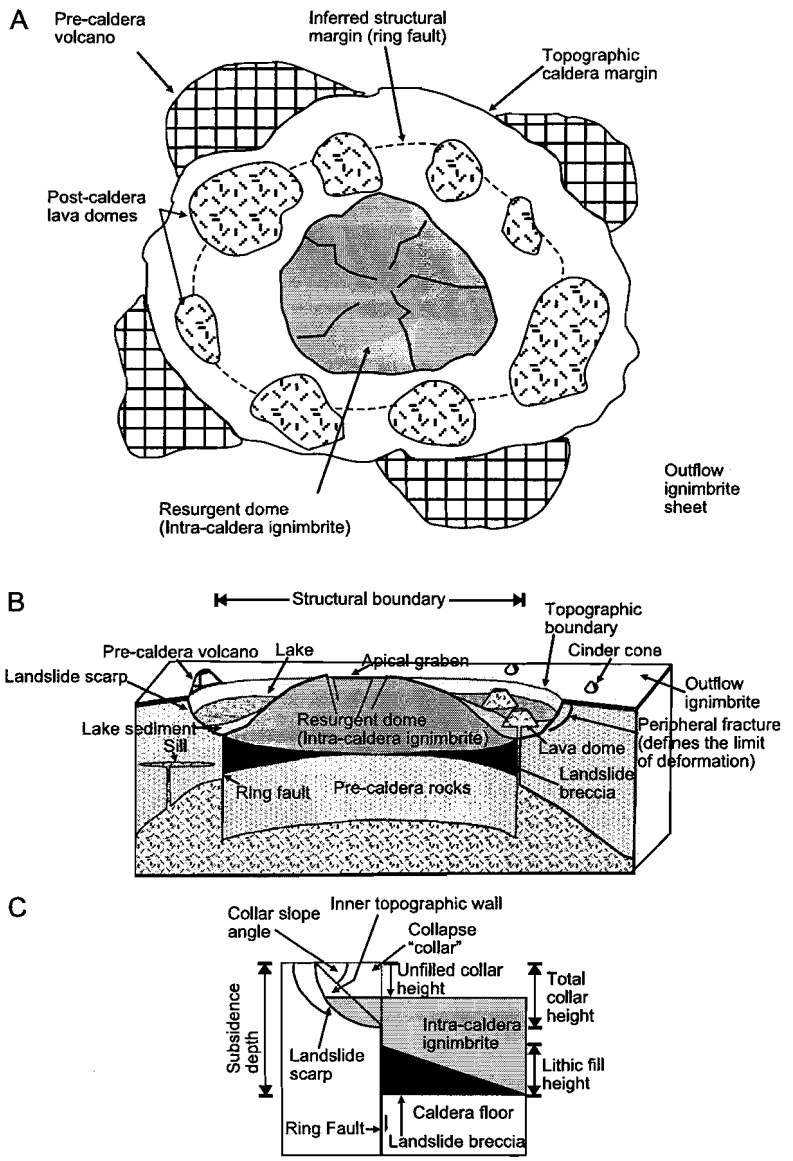

Fig. 3. (A) Schematic map of a typical resurgent piston-type caldera. (B) Block diagram of a typical resurgent piston-type caldera. (C) Terminology of a classic piston collapse structure after Lipman (1997). A caldera may or may not have all of the labelled features.

caldera. The topographic boundary is normally wider than the structural rim and forms by mass wasting, erosion and "scalloping" after caldera formation (Lipman, 1984; Nairn et al., 1994). Collapse of a caldera often leads to deformation outside the topographic rim, particularly where downsag has occurred (see Section 7), but a limit of deformation can usually be defined, which encompasses all areas that have been visibly affected by formation of a particular caldera.

5. Caldera development

Lipman (1984, 2000b) identifies a number of stages in the development of a caldera:

(1) Pre-collapse volcanism—Surface volcanism, frequently accompanied by tumescence, but this tumescence is not easily preserved and formation of pre-caldera lava domes and small

explosive eruptions are often the only record of magma accumulation and migration to shallow crustal levels.

(2) Caldera subsidence—Collapse associated with large-scale magma withdrawal (eruption). Eruptions often begin with a central vent phase and proceed to a ring vent phase coincident with caldera collapse (e.g., Kaingaroa Ignimbrite; Beresford and Cole, 2000, and others). This change from central to ring vent phases of a caldera forming eruption was well described for the dacitic–andesitic 6800 yr BP Mt Mazama eruption that lead to the formation of the caldera that now contains Crater Lake (Bacon, 1983).

(3) Post-collapse magmatism and resurgence—Volcanism after caldera formation can be randomly scattered within the caldera or localised along regional structural trends. Renewed rise of magma may uplift the central portion of the caldera either by doming or block uplift. This uplift may also be caused by intrusion of sill complexes.

(4) Hydrothermal activity and mineralisation—This may occur throughout the life of the caldera, but begins to dominate activity late in the cycle creating geothermal systems, and may or may not lead to ore deposition.

This is a general cycle based on rhyolitic calderas of North America, but is applicable to many other calderas. The evolution of a caldera may or may not include all of the stages outlined or may involve only part of the activity described for any one stage. Pre- and post-collapse volcanism, and resurgence or tumescence, may or may not occur and hydrothermal activity probably occurs throughout the caldera cycle. Multiple phases of volcanism and collapse may also occur (e.g., Okataina and Taupo caldera complexes, New Zealand; Nairn, 1989, Cole et al., 1998).

6. Examples of calderas

Although there is not a direct relationship between composition of the eruptives and 'types' of caldera, it is a useful way of indicating variation. Features of calderas associated with basaltic, peralkaline, andesitic–dacitic and rhyolitic eruptions are given below:

6.1. 'Basaltic' calderas

Basaltic calderas may be dominantly effusive or dominantly explosive. Dominantly effusive basaltic calderas are associated with shield volcanoes at hotspots such as Hawaii and the Galapagos Islands and calderas created by tumescence and magma drawdown, sometimes with minor, associated explosive eruptions (Simkin and Howard, 1970; Decker, 1987; Walker, 1988). Tumescence is regarded in Hawaii as due to intrusion of sills (Fig. 4), which expand and inflate the top of the shield creating radial or concentric fractures at the ground surface (Walker, 1988). This inflation leads to expansion at the surface creating normal faults. Flank eruptions may cause magma from the central reservoir to drain leading to accentuation of the surficial caldera or development of an ephemeral pit crater (Williams and McBirney, 1968; Decker, 1987). Calderas form in a similar way at Galapagos, the only difference being the absence of linear rift zones at the surface that occur in Hawaiian examples (Walker, 1988; Munro and Rowland, 1996). The 1968 collapse event in Fernandina (Galapagos) created a caldera with a volume that was 10 times greater than the erupted products (Simkin and Howard, 1970), perhaps because faults created by expansion/tumescence were already unstable and a small amount of magma withdrawal thereby allowed the formation of a comparatively large volume caldera (Simkin and Howard, 1970; Munro and Rowland, 1996).

A good example of a dominantly explosive basaltic caldera is Masaya Volcano in Nicaragua. Masaya is a nested structure in a low basaltic shield (Rymer et al., 1998) that was originally thought to have formed dominantly by magma drawdown and collapse into the magma chamber (Williams and McBirney, 1979). More recent work shows this not to be the case and that collapse was concurrent with explosive eruptions that produced basaltic ignimbrites and widespread basaltic plinian fall deposits up to 8.9 and 12 km^3, respectively (Williams and Stoiber, 1983). Masaya volcano goes through periods of intense degassing when lavas are extruded from the degassed magma (Walker et al., 1993). Explosive eruptions may occur after periods when the magma is unable to degas and become supersaturated with volatiles. This leads to explosive eruptions and caldera collapse (Williams

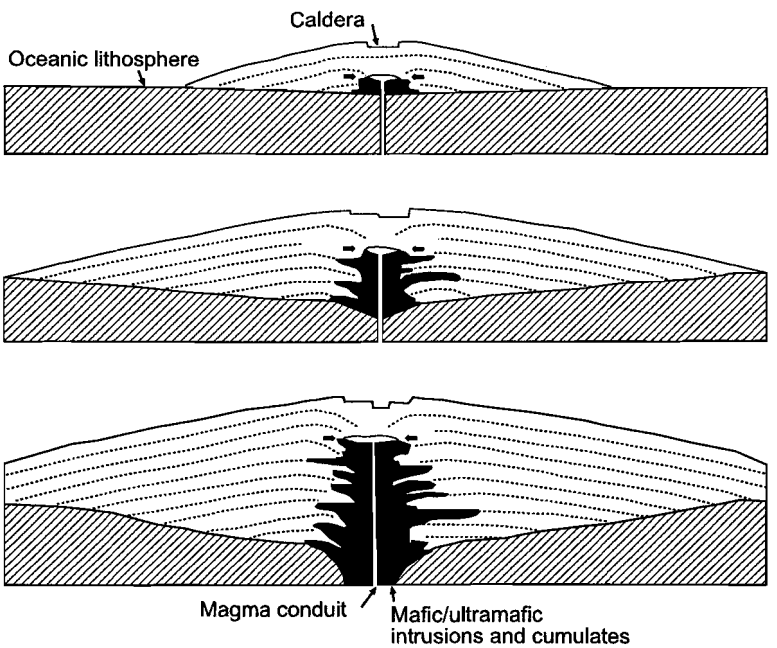

Fig. 4. Cross-section of shield and caldera evolution at Hawaiian volcanoes (from Walker, 1988). The intruding magma and sills can expand the shield thereby causing extension and collapse at the surface. These models assume the magma chamber (between the arrows) remains at a constant depth beneath the edifice. Caldera formation may also be due to magma withdrawal. Extension due to magma intrusion may lead to an unstable situation which, along with magma withdrawal, leads to caldera formation.

and Stoiber, 1983; Walker et al., 1993). Collapse is interpreted (based on gravity data and small observed pit crater collapses) to have occurred on outward-dipping faults (Rymer et al., 1998).

6.2. '*Peralkaline*' *calderas*

Peralkaline calderas are typically associated with zones of rifting, not necessarily related to a subduction system; e.g., Pantelleria, associated with a submerged continental rift (Mahood, 1983, 1984; Mahood and Hildreth, 1986; Orsi et al., 1991), Mayor Island, New Zealand, associated with NNE striking Ngatoro Basin and normal faults of the Mayor Island fault belt (Cole, 1990; Houghton et al., 1992), and calderas of the K'one (Gariboldi) volcanic complex, Ethiopia, associated with the Main Ethiopian Rift (Cole, 1969; Acocella, et al., 2002).

Peralkaline volcanic edifices are usually shield-like (Mahood, 1984; Houghton et al., 1992) and go through stages of caldera collapse and caldera filling (similar to explosive basaltic calderas). Peralkaline calderas tend to be moderate diameter (most are <12 km in diameter), circular, and collapse is usually <300 m, in response to small volume pyroclastic eruptions (e.g., Mayor Island, caldera wall height ~350 m, with pyroclastic units of one collapse episode 1–10 km^3; Houghton et al., 1992). At Pantelleria, the wall height is ~90 m (youngest episode; Hildreth and Mahood, 1986), estimated eruption volume 7 km^3 (Green Tuff; Wolff and Wright, 1981). An exception is Gran Canaria that has a caldera wall up to 1 km high, and has erupted pyroclastic material in the order of 100 km^3 (Schmincke, 1967) but probably represents numerous collapse events (as have occurred at nearby Las Canadas; Marti et al., 2000).

Caldera formation is usually in response to explosive eruptions that lead to deposition of tuffaceous material (e.g., Schmincke, 1967; Mahood and Hildreth, 1983; Houghton et al., 1992; Marti and Gudmundsson, 2000), and is often followed by extrusion of lavas from a central vent, which may eventually fill the caldera (Mahood, 1984). At some peralkaline calderas, post-caldera lava extrusion is associated with magma intrusion into the root zone of the caldera that leads to uplift (resurgence) of the

central portion of the caldera floor (e.g., Suswa, Johnson, 1969; Pantelleria, Mahood and Hildreth, 1983; Mahood, 1984; Orsi et al., 1991).

6.3. *'Andesite–dacite' calderas*

Calderas associated with andesitic–dacitic volcanism usually involve the destruction of stratocones. The collapse of Mt Mazama to form Crater Lake, USA (studied by Williams, 1942; Bacon, 1983); Krakatau, Indonesia (Self and Rampino, 1981; Simkin and Fiske, 1983), and Santorini, Greece (Druitt et al., 1999) are the best studied examples of this 'type' of caldera.

Crater Lake Caldera formed ~6800 yr BP with the eruption of the spectacularly compositionally zoned Mazama Ash (51–59 km^3), described by Bacon (1983). The eruption cycle began with the extrusion of dacite domes on the flanks of Mt Mazama. The climactic eruption started with eruption of the Wineglass Welded Tuff (~4–12 km^3) that was followed by a ring vent phase (ejection of Mazama Ash) during caldera collapse (Fig. 5). During this eruption 40–52 km^3 of the stratocone of Mt Mazama collapsed into the caldera.

The eruptions of Krakatau, Mt Mazama, Batur, and Santorini volcanoes all resulted in the collapse of a volcanic cone of basalt/basaltic andesite/andesite composition to form a caldera (Self and Rampino, 1981; Bacon, 1983; Wheller and Varne, 1986; Druitt et al., 1999). An important point is that the material erupted in the climactic phases was either totally dacitic, or was from a zoned magma chamber in which there was a significant amount of dacitic material. This suggests that the magma resided in the magma chamber for long enough to evolve and

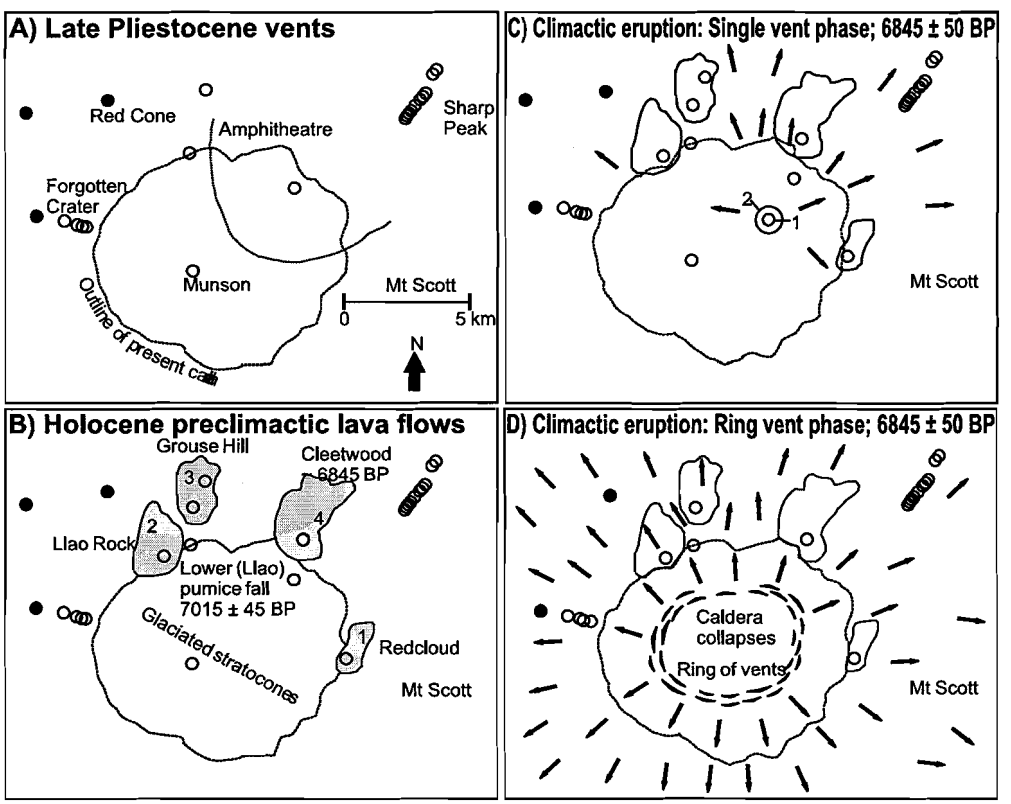

Fig. 5. The 6845 yr BP eruption of Mt Mazama and formation of Crater Lake. Eruption began with the extrusion of lava flows and domes on the flanks of the cone. The climactic phase started with eruption of pyroclastic material (Wineglass Tuff) from a central vent. Caldera collapse occurred coherently and in a piston-like manner and eruption took place from a ring of vents at the margins of the collapsing block. (From Bacon, 1983).

become more silicic than the magma usually erupted. The climactic eruptions are also usually of much higher volume then usual. This may mean that a stage was reached that was favourable for magma accumulation, perhaps the overlying structure had caused lithostatic pressure to be high enough that eruption was prevented until the condition of the magma became critical and eruption proceeded.

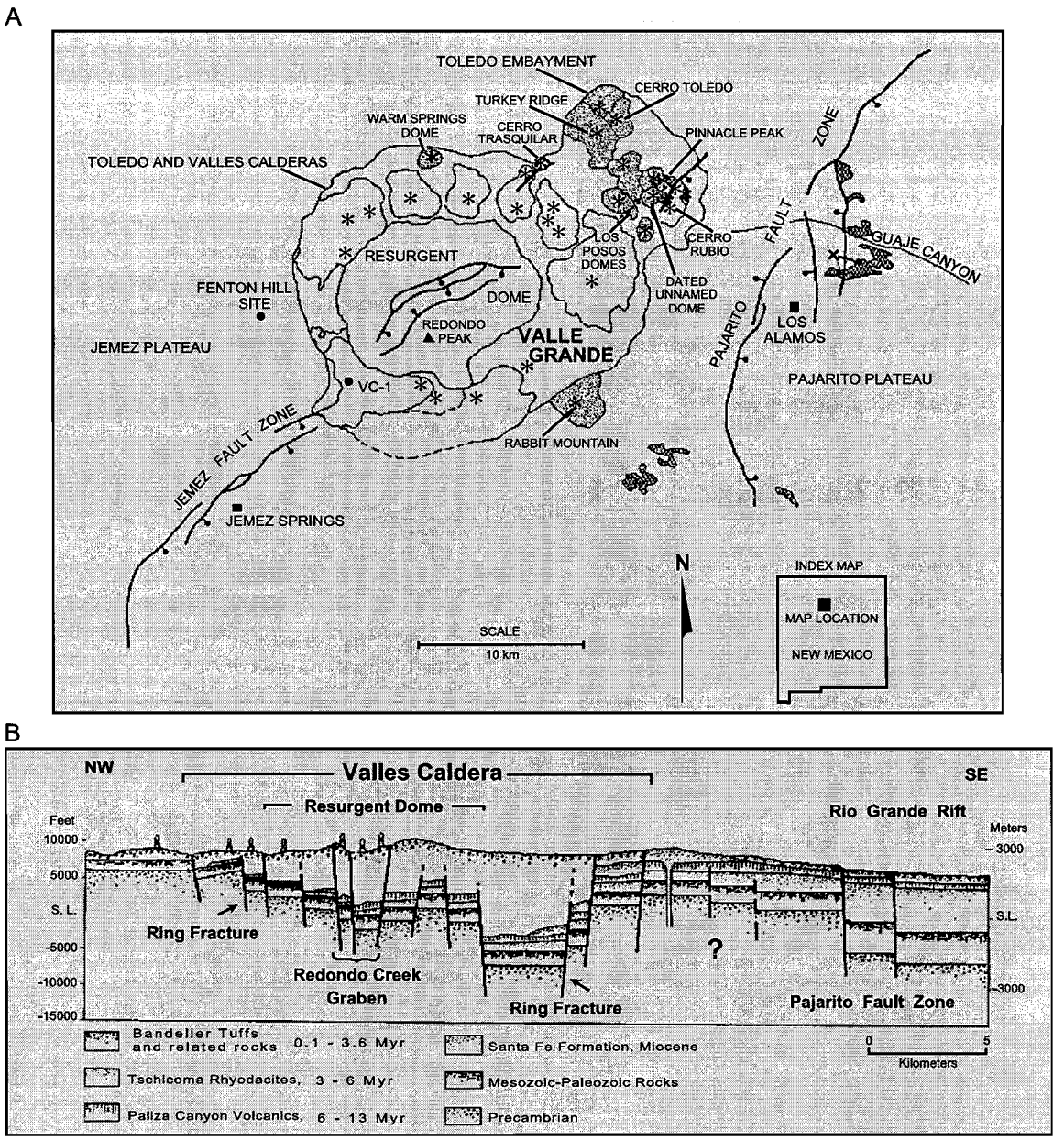

Fig. 6. (A) Generalised map of the Valles and Toledo calderas, New Mexico. Asterisks are vent locations for intra-caldera domes and flows. Stippled pattern indicates rhyolite domes associated with the Toledo caldera (from Heiken et al., 1986). (B) Schematic cross-section of the Valles caldera and Pajarito Fault Zone, based on deep drill holes and gravity data (from Self et al., 1986).

6.4. 'Rhyolitic' calderas

Rhyolitic calderas are associated with the largest volume pyroclastic deposits recorded and are usually huge collapse depressions. The calderas that form are usually >10 km in diameter and subsidence of the caldera floor is regularly >1 km. The structures are usually, but not always, in areas that have experienced extensive volcanic activity over a considerable time period before the caldera-forming episode (e.g., Conejos Formation prior to formation of the Platoro Caldera Complex, Colorado; Dungan et al., 1989). This activity may have formed lava flows, low shields, cones, domes and explosion craters, but have not developed a single large stratovolcano. The composition of these pre-caldera volcanics may range from basaltic to rhyolitic. Accompanying caldera collapse is the deposition of voluminous silicic ignimbrites (dacitic to high-silica rhyolite), which may be very widespread in their distribution. After collapse, resurgence may occur, in which the central part of the caldera becomes uplifted as a structural dome. This may be due to the upward resurgence of magma in the underlying magma chamber or post-

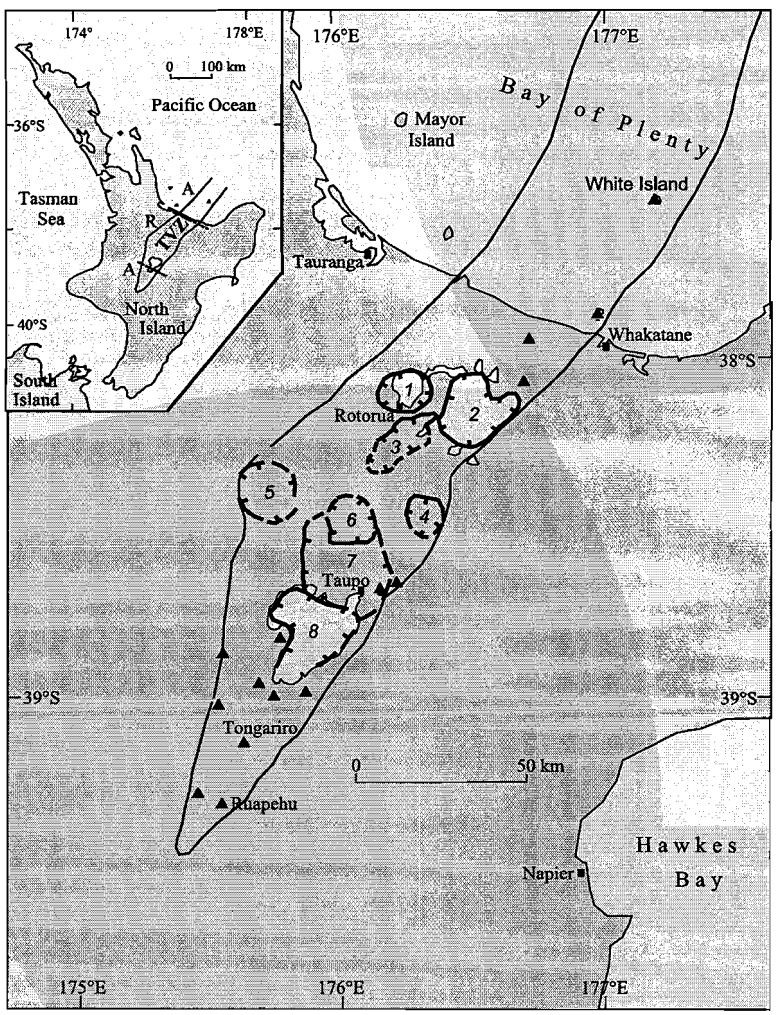

Fig. 7. Schematic map of the Taupo Volcanic Zone (TVZ), New Zealand, showing location of the rhyolitic calderas and caldera complexes. 1=Rotorua, 2=Okataina, 3=Kapenga, 4=Reporoa, 5=Mangakino, 6=Maroa, 7=Whakamaru, 8=Taupo. After Wilson et al. (1995). Triangles represent andesite–dacite volcanoes. Inset: A=Andesite dominated part of TVZ; R=Rhyolite dominated part of TVZ.

caldera sill emplacement and often leads to further lava extrusion.

One of the best studied of this type of caldera, and the first one where resurgence was fully discussed, is the Valles caldera, New Mexico, USA (Fig. 6; Smith et al., 1961; Smith and Bailey, 1968; Heiken et al., 1986, 1990) where the eruption and deposition of two major high-silica rhyolitic ignimbrites accompanied the collapse. The first (lower member, Bandelier Tuff; Heiken et al., 1986; Self et al., 1986) occurred at 1.47 Ma, from ring fractures around the Valles caldera (Heiken et al., 1990), and the second (upper member, Bandelier Tuff) at 1.12 Ma, during which most collapse occurred. The ignimbrite is now exposed on all sides of the caldera with thicknesses ranging from 15 to 270 m, and within the caldera with 400–1100 m of densely welded ignimbrite (Fig. 6B). Geophysical evidence suggests the collapse was asymmetric (Fig. 6B; Neilson and Hulen, 1984; Heiken et al., 1986), producing two calderas (Toledo and Valles; Fig. 6A) with nearly coincident 'trapdoor' form to the caldera floor. Resurgence of more than 1

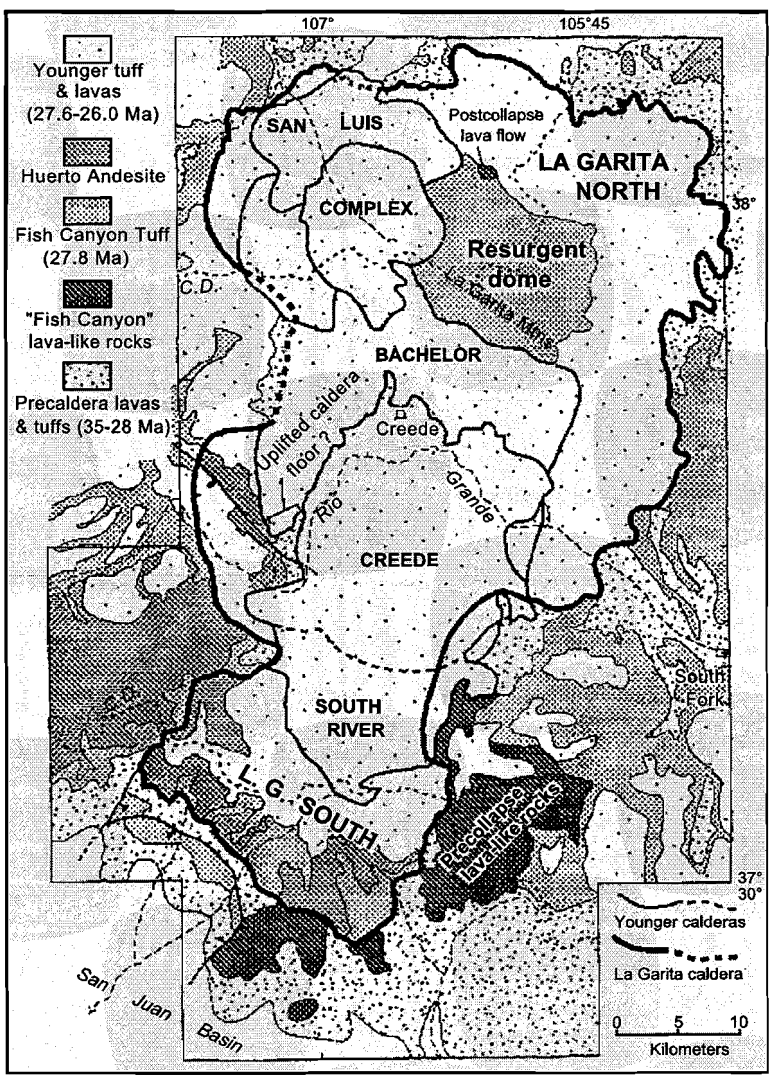

Fig. 8. Generalised map of the Central San Juan caldera complex, showing caldera topographic margins, resurgent domes and caldera related granitic intrusions (from Lipman et al., 1997).

km occurred during the next 100 ka (Self et al., 1986), accompanied by radial fracturing, to form Redondo Dome (Fig. 6A). At the same time a caldera lake formed depositing sediments in the 'moat' surrounding the resurgent dome. Between 1 and 0.13 Ma rhyolite domes and lava flows, and some airfall deposits and small ignimbrites, were erupted around the ring fracture system (Fig. 6A). Other large rhyolitic calderas include: Long Valley, California, USA (Bailey et al., 1976), erupting the Bishop Tuff (Wilson and Hildreth, 1997); Cerro Galan, Argentina (Francis et al., 1978, 1983, 1989), erupting the Cerro Galan ignimbrite (Sparks et al., 1985); and Campi Flegrei (Barberi et al., 1991), a dominantly trachytic caldera complex that initially (35 ka) erupted the Campanian Ignimbrite (Rosi et al., 1983), followed by the eruption (12 ka) of the Neapolitan Yellow Tuff (Orsi et al., 1992; Scarpati et al., 1993). Continued collapse (<4 ka) means that Campi Flegrei must be regarded as a caldera which is still active.

Frequently multiple calderas or caldera complexes occur within broadly extensional areas. The Taupo Volcanic Zone, New Zealand (<1.6 Ma), for example, includes eight calderas (Wilson et al., 1995) or caldera complexes (Fig. 7), of which the Taupo (Cole et al., 1998) and Okataina (Nairn, 1989) caldera complexes are the youngest. In the central USA, the Central San Juan caldera complex (Fig. 8; Central San Juan caldera cluster; Lipman, 2000a) was active between 28.3 and 26.5 Ma, with multiple collapse associated with the eruption of nine major ignimbrites. The largest (La Garita caldera) formed during the eruption of the ca. 5000 km^3 Fish Canyon Tuff (Lipman, 2000a; Bachmann et al., 2002). Multiple collapse has resulted in subsidence of up to 17 km and erosion has been sufficient to reach sub-volcanic batholiths (Fig. 8). The youngest caldera in the complex is the Creede Caldera (source of the Snowshoe Mountain tuff, 26.7 Ma) which has a well-developed resurgent dome, surrounded by moat sediments (Creede Formation; Bethke and Hay, 2000; Lipman, 2000a).

7. End-member styles of caldera collapse

Numerous processes of caldera collapse have been suggested in the literature. Lipman (1995) suggested calderas could be categorised according to four end-member collapse styles: Plate or piston, piecemeal, trapdoor and downsag collapse (Fig. 9). He also noted the 'funnel' geometry of many small calderas. In Lipman (1997, 2000b) the terms 'chaotic subsidence' and 'funnel calderas' were also discussed, but it was noted that 'chaotic subsidence' has not been documented for any well-exposed large caldera, and the features thought to have resulted from such chaotic subsidence may be explained by alternative collapse processes. We agree with this observation. The term 'funnel caldera' is discussed in Section 7.5.

7.1. Plate/piston collapse

Plate/piston collapse involves the subsidence of a coherent block of rock into an evacuating chamber along a ring fault (Figs. 1 and 9A). The caldera floor may be variably faulted but the displacement along intra-caldera floor faults is at least an order of magnitude less than that of the ring fault (Lipman, 2000b). Syn-collapse intra-caldera eruptive units should be planar within the caldera without significant thickness variation anywhere across the caldera floor. Numerous North American calderas are interpreted to be of this type, e.g., Creede (Steven and Lipman, 1976; Bethke and Hay, 2000), Crater Lake (Williams, 1941; Bacon, 1983), and Valles (Smith et al., 1961; Heiken et al., 1986; Self et al., 1986).

7.2. Piecemeal

Piecemeal refers to a caldera with numerous floor blocks and/or multiple collapse centres (Lipman, 1997, 2000b; Fig. 9B). Branney and Kokelaar (1994) have defined piecemeal calderas as ranging from those with block faulted floors to those that lack coherent caldera floors because the entire collapsing block has been reduced to a mega-breccia (they provide Aira Caldera as an example where this has occurred). Collapse may be due to (1) multiple magma chambers with overlapping eruption times in which eruption of one may trigger eruption of the other (e.g., Scafell Caldera; Branney and Kokelaar, 1994; Kokelaar and Branney, 1999); (2) where tectonically controlled faults break the caldera floor into numerous blocks prior to eruption and control collapse location (e.g., Glencoe Caldera; Moore and Kokelaar, 1997, 1998), or (3) where the entire caldera

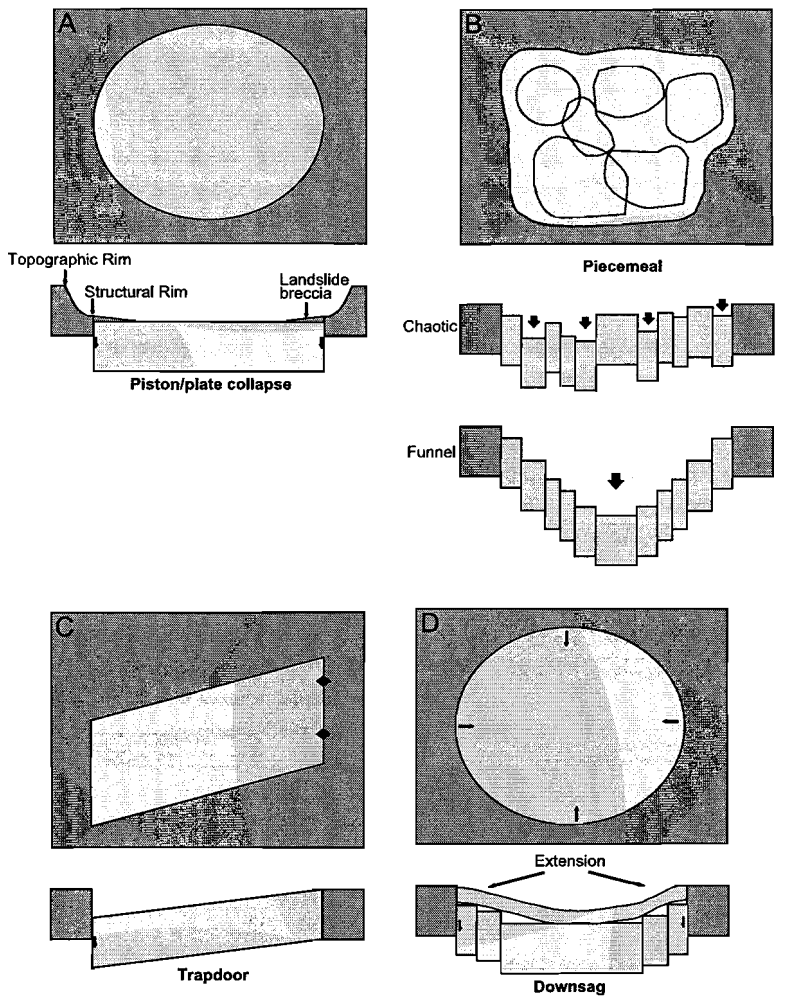

Fig. 9. Four end member mechanisms of caldera collapse: (A) piston/plate, (B) piecemeal, (C) trapdoor, (D) downsag. The origin of the so-called 'chaotic' and 'funnel' calderas is discussed in the text.

floor has been rendered a megabreccia (Branney and Kokelaar, 1994), this is chaotic subsidence in some schemes. Syn-eruptive caldera fill shows marked and rapid thickness increase in the corresponding collapse centre (Moore and Kokelaar, 1998; Kokelaar and Branney, 1999).

Nearly all calderas are piecemeal by Branney and Kokelaar's (1994) definition, and, in its strictest sense it would include Crater Lake caldera, which is one of the type examples of piston collapse. Lipman (1997) noted that most piston-like caldera floors contain faults that break them up; he suggests that where displacement down the bounding (ring) fault is greater than the subsidence from faults within the subsiding block by at least an order of magnitude the features should still be termed a piston or plate caldera. We agree with this constraint.

7.3. Trapdoor

Trapdoor collapse is envisaged to occur where formation of a ring fault is incomplete. Collapse is hinged on one side where downsag occurs, and is deepest towards the other side (Fig. 9C). It will also occur when a block subsides asymmetrically in a complete ring fault, leading to a feature similar to 'trapdoor-like' structures (e.g., Valles caldera; Heiken et al., 1986).

7.4. Downsag

This type of collapse occurs where ring faults either do not form or do not penetrate the ground surface (Figs. 9D and 10). Instead some or all of the rocks overlying the magma chamber deform by bending without fracture (Walker, 1984; Milner et al., 2002). There are no distinct caldera walls and the ground surface dips gently towards the caldera collapse centre (Walker, 1984). Features of downsag often occur in association with other collapse processes including mild flexuring and fracturing (Fig. 10) immediately prior to formation of a well defined faulted caldera boundary, processes that accompany inception of faulting in brittle upper crustal rocks, incomplete ring fault subsidence, (e.g., hinge of trapdoor collapse), and late inward dipping tilting and fracturing of the topographic wall after collapse (Branney, 1995; Lipman, 2000b). Other methods that can lead to a downsag morphology are forced folding where flat-lying strata deform over a rigid, brittly deforming caldera floor (Milner et al., 2002) and the formation of a tilted block towards the margin of deformation (Roche et al., 2000; see Section 8.2). Bolsena Caldera (Italy) and Taupo and Rotorua calderas (New Zealand) have all been used as examples of downsag collapse (Walker, 1984; Milner et al., 2002).

7.5. Funnel calderas

Funnel calderas are often identified by a geophysical response that are broadly 'V'-or 'funnel'-shaped. Such anomalies can, however, be due to a number of things, including: piecemeal collapse where the entire caldera floor is broken up (chaotic collapse of Scandone, 1990) and consists of numerous blocks (megabreccia) that can subside and rotate independently but deeper towards a single collapse centre; non-chaotic collapse where coherent blocks are displaced by sequentially greater amounts towards the collapse centre with or without ring faults. Halinan (1993), for example, showed that collapse occurred along concentric ring faults, "telescoping" towards the area of deepest collapse, at Guayabo Caldera, Costa Rica; collapse into a small or deep magma chamber, where a tilted marginal block dominates the caldera (Roche et al., 2000); or by explosive coring of the

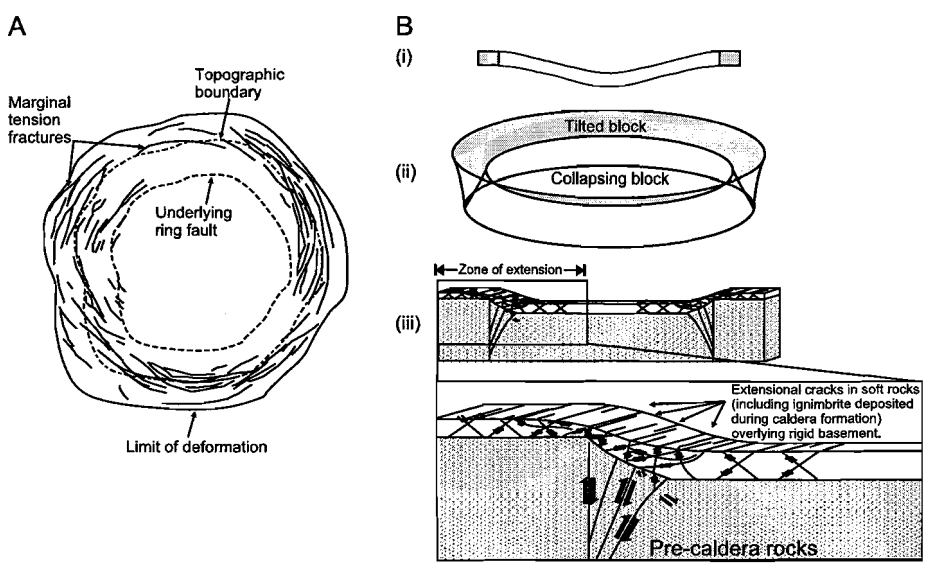

Fig. 10. During downsag the ground surface may warp downwards to generate a downsag caldera (A). Downsag must be accompanied by extension and flexure towards the margins of collapse that may lead to the development of tension fractures. (B) Downsag may be generated by (i) downwarping of the entire thickness of crust overlying a magma chamber, (ii) just at the margins of a brittly fracturing collapse structure (from Roche et al., 2000), or (iii) by the force folding of soft rocks overlying a rigid faulted basement (after Ameen, 1990). Downwarping of the entire crust above a magma chamber is unlikely to occur particularly in the short time that a caldera takes to form. Downsag is much more likely to occur by methods (ii) and (iii).

conduit (Aramaki, 1984). We agree with Lipman (2000b) that 'funnel calderas' should not be regarded as a separate end-member type, but that the shape may result from a variety of processes.

8. Collapse and uplift at calderas, including information from analogue modelling

8.1. Caldera collapse

Collapse or subsidence is essential to form a caldera and analogue models help constrain the subsurface features formed beneath them. Caldera collapse has previously been considered as occurring on steeply inward-dipping faults (e.g., Gudmundsson, 1998), and this was supported by studies of some eroded calderas (e.g., Grizzly Peak; Fridrich et al., 1991). However, experimental studies suggest that faults associated with collapse can be vertical, inward dipping, or outward dipping near the surface, and may vary in dip direction with depth (Fig. 11A; Marti et al., 1994; Odonne et al., 1999; Roche et al., 2000). Collapse principally occurs on steeply outward-dipping reverse faults accompanied by an outer set of inward-dipping normal faults and an intervening tilted block (Fig. 11B; Acocella et al., 2000, 2001; Roche et al., 2000). Outward-dipping reverse faults have been observed at many eroded calderas (e.g., Yoshida, 1984; John, 1995), are indicated by geophysical analysis (Mori and McKee, 1987; Rymer et al., 1998), and from experimental data.

Roche et al. (2000) suggest from their experiments that the geometry of the collapse structure depends strongly on the depth, size, and shape of the magma chamber. Shallow magma chambers with large diameters (low caldera–roof aspect ratio) lead to coherent single-block collapse structures while deep chambers with small diameters (high caldera–roof aspect ratio) lead to a series of multiple nested blocks. The width of the extensional tilted block around the rim of the collapse structure is largely independent of the caldera–roof aspect ratio; a narrow marginal zone of flexure forms where the ratio is low (Figs. 10B and 11B), but where the ratio is high this zone may account for up to 80% of the caldera surface morphology. The tilted block may extend beyond the margin of the subsiding caldera floor, and the annular zone of flexure produced may relate to areas of downsag around calderas (e.g., Walker, 1984).

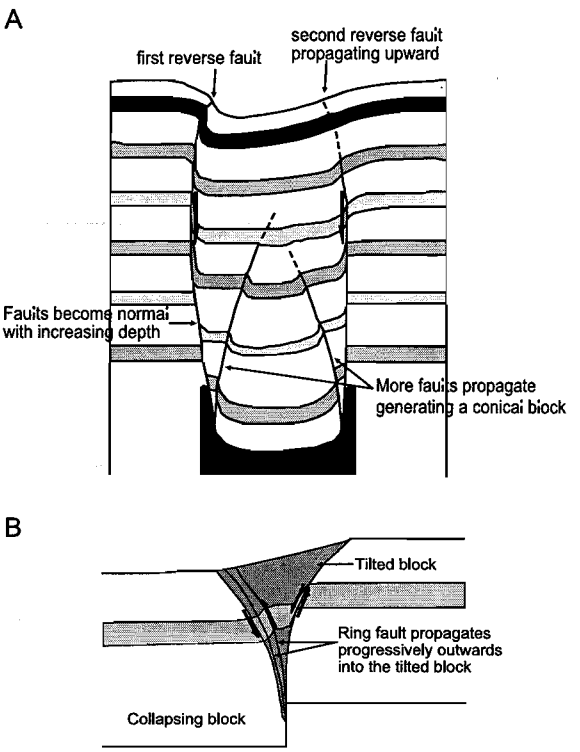

Fig. 11. (A) The result of one of Roche et al.'s (2000) laboratory experiments. Note the caldera block bounding fault is outward dipping and reverse at the surface steepening to vertical at depth and the conical block forming in the subsiding caldera floor block. With increasing depth to the "magma chamber" more conical blocks are created during caldera formation. Note also that faults bounding the collapsing block dip outwards at shallow depths. (B) A sketch of the tilted block found in Roche et al. (2000) analogue experiments. The caldera "ring fault" propagates progressively into the tilted block as subsidence proceeds. The tilted block may account for downsag structures seen towards the margins of caldera collapse. Funnel shaped calderas result with small or deep chambers as the tilted block takes up a greater proportion of the surface.

The shape of the magma chamber also has a substantial influence on the stress regime around the chamber and on the initiation and shape of collapse (e.g., Gudmundsson, 1988, 1998; Marti et al., 1994). Collapse was consistently asymmetric in the experiments of Roche et al. (2000), with collapse initiating on the side of the caldera with the greatest roof thickness. For elliptical shaped calderas with low roof aspect ratio, fault propagation from the middle of one side often significantly progressed prior to nucleation of a second fault on the opposite side of the chamber.

Where chamber shapes have sharp corners (square and rectangular chambers), faults propagate from the middle of one side until arrested by a corner, leading to asymmetric collapse along that side until further fault propagation occurs along the other side and the process is repeated. The surface expression of the ring fault in some analogue models is seen to propagate parallel to the caldera margin, from a single point (e.g., Kennedy and Stix, 2003), 'unzipping' in a fashion that has also been inferred from stratigraphic variations in some ignimbrites (e.g., Valles Caldera, Self et al., 1986; Long Valley Caldera, Hildreth and Mahood, 1986; Wilson and Hildreth, 1997; Reporoa Caldera, Beresford and Cole, 2000).

Scandone (1990) considered caldera formation occurs in the same way that mining subsidence collapse pits proceed (Fig. 12A, B); by chaotic collapse of successively higher blocks of rock beneath a zone of relaxation into the magma chamber The 'peeling' of successively higher blocks continues until stability is reached. If this does not happen before the collapse reaches the surface, or if the zone of relaxation penetrates the surface, a depression results. If the magma chamber is wide enough, and ring fractures do not form, sagging can occur at the surface above the area of detaching subsurface blocks (e.g., Fig. 12A). The surface depression formed in such a way will always be of smaller volume than that of the initial cavity beneath, due to the chaotic or broken nature of the collapsing block. Collapse associated with ice melt pits (Fig. 12C; Branney, 1995), and associated with withdrawal of oil from a reservoir (Odonne et al., 1999), are also analogous to caldera collapse.

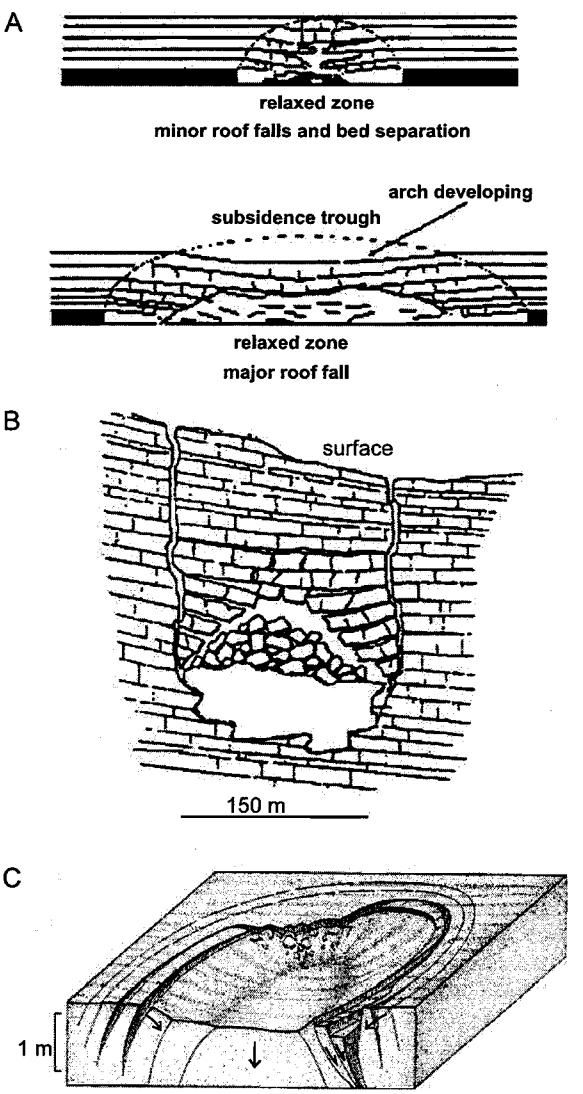

Fig. 12. Comparisons between mining (A and B), and ice (C) collapse pits and calderas. If the relaxation zone reaches the surface, a depression will form akin to a downsag caldera (A), if it doesn't the ground surface remains unchanged unless the cavity is large enough and deep in which case a central fault bounded block forms (B) and can collapse like a piston. (A) and (B) are from Scandone (1990) and (C) is from Branney (1995).

8.2. Tumescence and resurgence

Tumescence and resurgence are episodes of uplift that may occur before and after caldera collapse, respectively, and are associated mainly with subsurface magmatic pressure (Lipman, 2000a).

Tumescence is the doming of overlying strata as magma intrudes and accumulates within the crust. Simple analytical equations of surface displacement caused by uplift from a point source are well known (e.g., Mogi, 1958; Okada, 1985), and produce a simple bell-shaped curve, dependent on the depth of source and the extent of uplift. Analogue models simulating the emplacement of a large volume magma chamber show that the shape of the tumescent dome also depends on boundary conditions between the chamber and the crust (e.g., Withjack and Scheiner, 1982; Komuro et al., 1984; Davison et al., 1993; Schultz-Ela et al., 1993; Acocella and Mulugeta, 2002). Concentric and radial fracturing of the sur-

rounding strata occurs as the deformation proceeds (Komuro et al., 1984; Marti et al., 1994), while at the ground surface, extension associated with doming leads to the formation of a circular collapse pit at the apex of the uplift (Marti et al., 1994; Roman-Berdiel et al., 1995; Acocella and Mulugeta, 2002). Radial dikes and cone sheets have been associated with various plutons and calderas such as Gran Canaria (Schirnick et al., 1999) and the Zarza Intrusive Complex (Johnson et al., 1999), and relate to uplift associated with magma intrusion.

Analogue modelling also indicates that faults generated by inflation are reactivated during subsidence with the opposite kinematics (Fig. 13; Marti et al., 1994; Acocella et al., 2000). Reverse faults form during both inflation and collapse, followed by extensional structures due to gravitational instability on the margins of the uplifted and collapsed portions, respectively (Acocella et al., 2000).

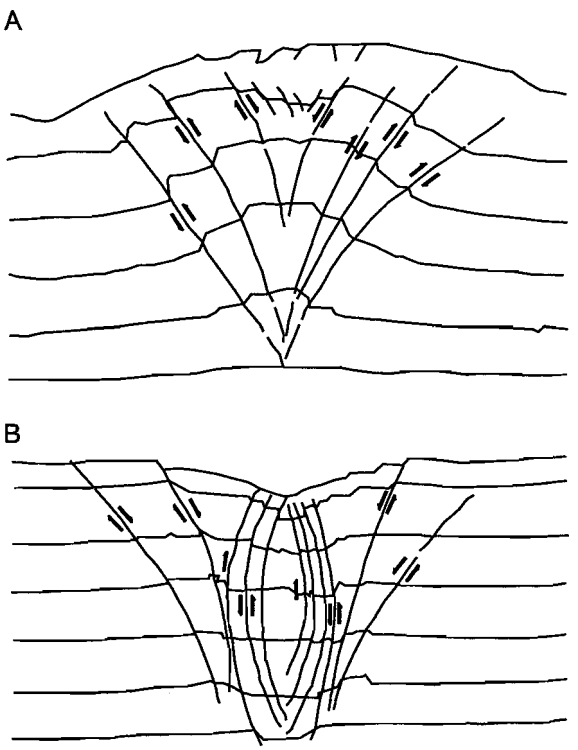

Fig. 13. (A) Cross-section through an experimental tumescent dome showing reverse faults accommodating the uplift and with the beginnings of apical collapse. (B) Faults that were active during tumescence can reverse their sense of movement during caldera collapse (from Marti et al., 1994).

Resurgence is common at many large silicic calderas and is caused by renewed magmatic pressure as a magma chamber(s) is recharged. Faults created during collapse may be reactivated in the opposite sense as part of the caldera is forced upwards (e.g., Ischia; Acocella and Funiciello, 1999). New faults may be created and are usually exposed in the resurgent dome (e.g., Valles, Smith and Bailey, 1968; Fig. 6). Intracaldera deposits are uplifted and post-caldera sediments can provide a record of the resurgence process (Smith and Bailey, 1968). De Natale and Pingue (1993) and De Natale et al. (1997) found that uplift occurred predominantly along existing fracture systems within the four calderas they studied.

Acocella et al. (2001) find that the geometry of resurgence is also strongly dependent on chamber roof aspect ratio. For low roof aspect ratios (T/O~0.4) a resurgent dome with a crestal depression is produced, while higher aspect ratios (T/O~1) develop a resurgent block with uniformly dipping layers.

8.3. Comment

Although analogue models have significantly advanced the understanding of processes by which caldera formation proceeds, most early models were carried out without consideration of pre-existing discontinuities or allowing for the influence of regional stress fields during collapse. External forces that modify stress regimes around a magma chamber, and cause disruption to overlying strata, are missing in many analogue models. Acocella et al. (2004), however, have incorporated an extensional tectonic regime into their analogue modelling and show that pre-caldera extension produces elliptical collapse structures with long axes parallel to the extension direction; resurgence also has a long axis perpendicular to this extension direction. They also suggest that the elliptical collapse and resurgent structures form by reactivation of pre-existing structures such that elliptical calderas may form even from circular magma chambers in areas undergoing extension.

Another limitation of analogue models is the constraints of the mediums in which the collapse is studied. Usually the models use sand or sometimes flour, neither of which has significant cohesion, and the properties of the collapsing block are uniform from the top to the base of the experimental pile.

Caldera floor rocks are usually heterogeneous and are often lithified, complicating both the formation and propagation of structures involved in caldera collapse. The structures formed during analogue models thus far are ideal structures and further experimentation is required to resolve the types of structure that form when external stresses are applied to non-uniform strata with pre-existing defects during caldera collapse. They need to be looked at in conjunction with caldera geology, geodetic measurements (e.g., Dvorak and Dzurisin, 1997) and numerical finite element models (e.g., Trasatti et al., 2003), to better understand the processes.

9. Role of pre-existing structures on calderas and their sub-surface magma chambers

A significant factor in caldera collapse and morphology is the presence of pre-existing faults. These faults will provide lines of weakness along which caldera collapse will preferentially occur and can break up the caldera floor into numerous blocks (e.g., Scarfell, Branney and Kokelaar, 1994; Glencoe, Moore and Kokelaar, 1997, 1998; Rotorua, Milner et al., 2002). Faults also create potential sites of magma accumulation, and have been shown to sometimes control the location of erupting vents (e.g., Glencoe, Moore and Kokelaar, 1997, 1998; Tarawera vent alignment, Nairn, 1989; Taupo, Smith and Houghton, 1995).

9.1. Calderas

Regional and local structures have a profound affect on the morphology of calderas. Marti et al. (1994) showed that faults created during tumescence are reactivated during magma withdrawal in the early stages of caldera collapse (Fig. 13), but that these structures become less important as collapse proceeds. Reverse fault movement may dominate during this early stage of caldera formation, but as collapse proceeds, fault movements are dominantly along the ring fault and normal faults that break up the caldera floor (Komuro et al., 1984; Marti et al., 1994; Acocella et al., 2002).

Moore and Kokelaar (1997, 1998) show how cross-cutting grabens at Glencoe have controlled the location of erupting vents and the margins of the collapsing caldera floor. Tectonic structures have controlled the collapse geometry of Snowdon Caldera generating a number of rectangular prismatic blocks that subsided by different amounts asymmetrically during caldera formation (Kokelaar and Branney, 1999). Ferguson et al. (1994) studying the Silent Canyon Complex in Nevada, identified rectilinear structural caldera boundaries, strongly influenced by, and sometimes coincident with, regional tectonic faults (Fig. 14A), and Acocella et al. (2002) have shown that pre-existing structure in the Ethiopian rift has controlled caldera elongation in that region. John (1995) found that faults created during the formation of the Job Canyon Caldera, Stillwater Range, Nevada, were reactivated with the same sense during the formation of the Poco Canyon Caldera; Beresford and Cole (2000) found that the eastern margin of the Reporoa Caldera was coincident with the regional Kaingaroa Fault, and Milner et al. (2002) have illustrated the effect that pre-existing structures had on the form of Rotorua Caldera (Fig. 14B).

Regional structure may also affect uplift. Acocella and Funiciello (1999) show the effect of existing faults on the resurgent dome of Ischia, Italy. Regional faults at Ischia, as well as those created during caldera collapse, have been reactivated in a reversed sense due to resurgence and have created a dome with a polygonal morphology (Fig. 14C). Pre-existing structures have also been shown to affect the morphology of resurgence at Pantelleria (Orsi et al., 1991; Tibaldi and Vezzoli, 2000), Campi Flegrei, and Rabaul calderas (De Natale et al., 1997).

9.2. Geometry of the magma chamber beneath calderas

Because the shape of the magma chamber is one of the main controls on the final shape of the collapsed area (Roche et al., 2000), it is important to know what controls the location and geometry of the magma chamber. Extension allows accumulation and emplacement of large magma bodies (Hutton and Reavy, 1992) and may or may not trigger their final eruption. Cambray et al. (1995) illustrate the possibility that extension can create the space into which a large rhyolitic body (or bodies) can be emplaced, but that it may be during the tectonically quiescent times

that the eruption actually takes place (i.e., when pressure instabilities cannot be accommodated by further extension). Alternatively, extension can reduce the lithostatic pressure, thereby promoting eruption from a chamber already residing in the crust. Jellinek and DePaolo (2003) consider that large magma chambers (>10^2 km^3), with warm surrounding wall rocks that have a low effective viscosity, are needed to get catastrophic caldera-forming eruptions. Pre-existing structures may also control the geometry of magma chambers. McNulty et al. (2000) show that the margins of the Mt Givens Pluton were controlled by tectonic fractures and that space for the pluton to accumulate was created by down-faulting of a series of elongate fault-bound blocks. Fault movement and pre-existing structures thereby governed the overall shape of the pluton. Bosworth et al. (2003) consider that magma chambers will become elongate parallel to the minimum horizontal stress (i.e., direction of extension) and during eruption will form elliptical calderas.

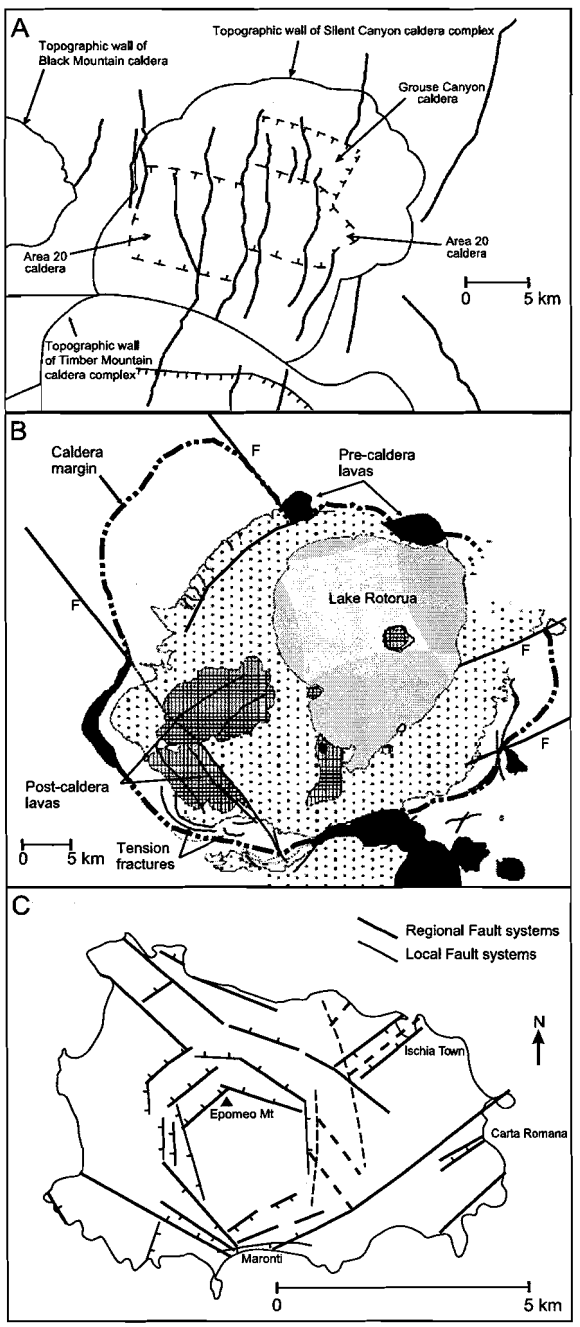

10. Caldera descriptions

From this review, it is evident that many processes affect the form of calderas and it is difficult to categorise calderas as of any one 'type'. In many ways each caldera is unique. Variables that will affect caldera structure include: tectonic setting, pre-existing structure, composition of magma, magma chamber geometry and depth, size of the eruption, number and symmetry of collapse events, and whether or not tumescence or resurgence has taken place. When describing a caldera it is better to use descriptive terms rather than interpretations of the process that created the structure, so that it is probably better to use 'symmetric collapse' rather than 'piston' or 'asymmetric collapse' rather than 'trapdoor'. Equally, it is better to use 'single block

Fig. 14. (A) Line map of the Silent Canyon caldera complex (from Ferguson et al., 1994). Caldera boundaries are sub-parallel to regional tectonic structures (heavy black lines) and, in some cases, are coincident with them. Regional tectonics can affect the sites of magma accumulation and can also affect the shape of the collapsing block of the caldera. (B) Schematic map of Rotorua Caldera (from Milner et al., 2002). The regional NE–SW and NW–SE faults have influenced the break-up of the caldera floor into a number of blocks that each subsided more or less independently of one another. (C) Ischia, Italy, where pre-existing structures have influenced the morphology of the resurgent block (from Acocella and Funiciello, 1999).

collapse' or 'multiple block collapse', rather than 'piston' or 'piecemeal'. The shape of the caldera is also important. These terms should be used irrespective of the level of erosion.

Good surface expression does not necessarily equate with a clear understanding of caldera structure. Some features of the caldera, such as symmetry, will be easier to determine when much of the surface expression has been removed by erosion (e.g., Scarfell). At young calderas, collapse geometry and structure below the caldera floor are likely to be based largely on geophysical observation and interpretation from surface morphology.

11. Summary

- The key element for caldera formation is the removal of magmatic support from the crust overlying the chamber, but the process of caldera collapse, final caldera morphology and type of associated eruption depend on many factors.
- It is suggested here that the key feature of 'calderas' is collapse or subsidence into the top of a magma chamber, while eroded caldera structures can be called 'cauldrons' or 'ring structures', depending on how much erosion has occurred. There is complete gradation between 'calderas' and 'cauldrons' and it must be remembered that they simply reflect different parts of a caldera structure. It should also be recognised that erosion will reveal more information on the internal structure of calderas, in contrast to young, uneroded structures, where internal structure may be obscured by the eruptive morphology. In 'ring structures' evidence of caldera structure has largely been removed by erosion, exposing a magma chamber or chambers, which are the plutonic equivalent of the caldera volcanics.
- Composition of erupting magma at a caldera-forming volcano is a useful criteria for subdividing calderas for descriptive purposes. These eruptions can be effusive or explosive. Effusive eruptions are mainly associated with basaltic calderas such as those of Hawaii and the Galapagos. Effusive lavas build the original edifice (shield) and erupt from central vents or fissures. Lateral migration of magma may be associated with eruption of lavas from vents towards the flanks of the volcanoes resulting in depletion of the magma reservoir and caldera collapse. Effusion is also associated with the more silicic andesitic, rhyolitic and peralkaline volcanoes, but does not usually lead to caldera formation. Lava flows and small volume explosive eruptions build the stratocone of andesitic volcanoes and peralkaline shields. Small domes and lava flows often precede and follow the main caldera-forming event at rhyolitic calderas. Large explosive andesitic–dacitic and rhyolitic eruptions generally lead to the emplacement of high volume ignimbrites and creation of large collapse depressions. The removal of such a large volume leads to the collapse of the ignimbrite source area and the formation of a caldera.
- Faults involved in the caldera collapse process may be primary and initiated during caldera collapse or reactivated older tectonic or volcanic structures. The primary faults may be steeply inward or outward dipping or vertical and dip may vary with depth. Depth to the magma chamber will affect the way collapse occurs. Pre-existing structures can break up the caldera floor into a number of blocks that can collapse independently from one another depending on the withdrawal dynamics and depth to the underlying magma chamber.
- Tumescence causes doming of the overlying strata, and in analogue models there is commonly a circular collapse pit formed at the apex of the dome. Resurgence is due to recharge of the magma chamber and/or possibly isostatic rebound as the crust returns to equilibrium. Resurgence may occur just inside the caldera or may be regional and the processes of tumescence and resurgence may generate pathways for the emplacement of radial dikes and cone sheets.
- The shape and growth of the underlying magma chamber plays a crucial role in the collapse process. Caldera collapse may be initiated if the chamber is shallow enough and has reached a critical width, and the dimensions of the chamber play an important role in the collapse geometry.
- The final morphology of a caldera will vary according to the way the caldera floor breaks up, how collapse proceeds during the eruption—in particular the symmetry and coherency of the

caldera floor, and the presence of post-caldera deformation.

- Calderas are formed by a variety of processes, and many contain eruptives of more than one composition. Current terminology and classification can therefore be confusing. Any description of calderas should take into account the number of collapse events, collapse geometry, the presence or absence of resurgence or other deformation, and the dominant composition of the erupting magma. The inclusion of all the above leads to a much clearer picture of the caldera being described. A typical description of a caldera, using these criteria, would be 'a single event, non-resurgent, multiple-block, asymmetric collapse, elliptical rhyolitic caldera'.

Acknowledgements

Many people have contributed to ideas in this review paper. Particular thanks go to Dr. Michael Branney and Dr. Peter Lipman, with whom the authors have had many useful discussions. D.M.M. and K.D.S. were funded by a University of Canterbury Doctoral Scholarship and the Mason Trust and D.M.M. by a Claude McCarthy Fellowship. J.W.C. received a University of Canterbury Research Grant (U6314) towards the cost of the study. The paper was reviewed by Valerio Acocella and an anonymous reviewer, to whom the authors are most grateful.

References

Acocella, V., Funiciello, R., 1999. The interaction between regional and local tectonics during resurgent doming: the case of the island of Ischia, Italy. J. Volcanol. Geotherm. Res. 88, 109–123.

Acocella, V., Mulugeta, G., 2002. Experiments on surface deformation induced by pluton emplacement. Tectonophysics 352, 275–293.

Acocella, V., Salvini, F., Funiciello, R., Faccenna, C., 1999. The role of transfer structures on volcanic activity at Campi Flegrei (Southern Italy). J. Volcanol. Geotherm. Res. 91, 123–139.

Acocella, V., Cifelli, F., Funiciello, R., 2000. Analogue models of collapse calderas and resurgent domes. J. Volcanol. Geotherm. Res. 104, 81–96.

Acocella, V., Cifelli, F., Funiciello, R., 2001. The control of overburden thickness on resurgent domes: insights from analogue models. J. Volcanol. Geotherm. Res. 111, 137–153.

Acocella, V., Korme, T., Salvini, F., Funiciello, R., 2002. Elliptic calderas in the Ethiopian Rift: the control of pre-existing structures. J. Volcanol. Geotherm. Res. 119, 189–203.

Acocella, V., Funiciello, R., Marotta, E., Orsi, G., de Vita, S., 2004. The role of extensional structures on experimental calderas and resurgence. J. Volcanol. Geotherm. Res. 129, 199–217.

Ameen, M.S., 1990. Macrofaulting in the Purbeck–Isle of Wight monocline. Proc. Geol. Assoc. 101, 31–46.

Aramaki, S., 1984. Formation of Aira Caldera, Southern Kyushu, ~22,000 years ago. J. Geophys. Res. 89B, 8485–8501.

Bachmann, O., Dungan, M., Lipman, P., 2002. The Fish Canyon magma body, Colorado: rejuvenation and eruption of an upper crustal near-solidus batholithic magma chamber upon voluminous mafic underplating. J. Petrol. 43 (8), 1469–1503.

Bacon, C.R., 1983. Eruptive history of Mount Mazama and Crater Lake Caldera, Cascade Range, USA. J. Volcanol. Geotherm. Res. 18, 57–115.

Bailey, R.A., Dalrymple, G.B., Lanphere, M.A., 1976. Volcanism, structure and geochemistry of Long Valley Caldera, Mono County, California. J. Geophys. Res. 81, 725–744.

Bain, A.D.N., 1934. The younger intrusive rocks of the Kudaru Hills, Nigeria. Q. J. Geol. Soc. Lond. 90, 201–223.

Baker, P.E., Harris, P.G., Reay, A., 1971. The geology of Tofua Island, Tonga. Bull.-R. Soc. N. Z. 8, 67–79.

Barberi, F., Cassano, E., La Torre, P., Sbrana, A., 1991. Structural evolution of Campi Flegrei caldera in light of volcanological and geophysical data. J. Volcanol. Geotherm. Res. 48, 33–49.

Beresford, S.W., Cole, J.W., 2000. Kaingaroa Ignimbrite, Taupo Volcanic Zone, New Zealand: evidence for asymmetric caldera subsidence of the Reporoa Caldera. N.Z. J. Geol. Geophys 43, 471–481.

Bethke, P.M., Hay, R.L., 2000. Overview: ancient Lake Creede. Spec. Pap.-Geol. Soc. Am. 346, 1–8.

Bibby, H.M., Caldwell, T.G., Davey, F.J., Webb, T.H., 1995. Geophysical evidence on the structure of the Taupo Volcanic Zone and its hydrothermal circulation. J. Volcanol. Geotherm. Res. 68, 29–58.

Bosworth, W., Burke, K., Strecker, M., 2003. Effect of stress fields on magma chamber stability and the formation of collapse calderas. Tectonics 22, 21. Article 1042.

Branney, M.J., 1995. Downsag and extension at calderas: new perspectives on collapse geometries from ice-melt, mining, and volcanic subsidence. Bull. Volcanol. 57, 303–318.

Branney, M.J., Kokelaar, B.P., 1994. Volcanotectonic faulting, soft-state deformation and rheomorphism of tuffs during development of a piecemeal caldera, English Lake District. Geol. Soc. Am. Bull. 106, 507–530.

Cambray, F.W., Vogel, T.A., Mills Jr., J.G., 1995. Origin of compositional heterogeneities in tuffs of the Timber Mountain Group: the relationship between magma batches and magma transfer and emplacement in an extensional environment. J. Geophys. Res. 100, 15793–15805.

Cole, J.W., 1969. Gariboldi Volcanic Complex, Ethiopia. Bull. Volcanol. 33, 566–578.

Cole, J.W., 1990. Structural control and origin of volcanism in the Taupo volcanic zone, New Zealand. Bull. Volcanol. 52, 445–459.

Cole, J.W., Brown, S.J.A., Burt, R.M., Beresford, S.W., Wilson, C.J.N., 1998. Lithic types in ignimbrites as a guide to the evolution of a caldera complex, Taupo volcanic centre, New Zealand. J. Volcanol. Geotherm. Res. 80, 217–237.

Davison, I., Insley, M., Harper, M., Weston, P., Blundell, D., McClay, K., Quallington, A., 1993. Physical modeling of overburden deformation around salt diapirs. Tectonophysics 228, 255–274.

Decker, R.W., 1987. Dynamics of Hawaiian volcanoes: an overview. Volcanism in Hawaii. US Geol. Surv. Prof. Paper, 1350, 997–1018.

De Natale, G., Pingue, F., 1993. Ground deformation modeling in volcanic areas. In: Scarpa, R., Tilling, R. (Eds.), Monitoring and Mitigation of Volcano Hazards. Springer-Verlag, Berlin, pp. 365–388.

De Natale, G., Petrazzuoli, S.M., Pingue, F., 1997. The effect of collapse structures on ground deformations in calderas. Geophys. Res. Lett. 24, 1555–1558.

Druitt, T.H., Edwards, L., Mellors, R.M., Pyle, D.M., Sparks, R.S.J., Lanphere, M., Davies, M., Barriero, B., 1999. Santorini volcano. Mem.-Geol. Soc. Lond. 19.

Dungan, M.A., Lipman, P.W., Colucci, M., Ferguson, K., Balsey, S., 1989. Southeastern (Platoro) Caldera Complex. In: Chapin, C.E., Zidek, J. (Eds.), Field Excursion to Volcanic Terranes in the Western United States. Volume 1 Southern Rocky Mountains Region. Mem.-N. M. Bur. Mines Miner. Resour., vol. 46, pp. 305–329.

Dvorak, J.J., Dzurisin, D., 1997. Volcano geodesy: the search for magma reservoirs and the formation of eruptive vents. Rev. Geophys. 35, 343–384.

Eaton, P.C., Setterfield, T.N., 1993. The relationship between epithermal and porphyry hydrothermal systems within the Tavua Caldera, Fiji. Econ. Geol. 88, 1053–1083.

Elston, W.E., 1984. Mid-Tertiary ash-flow cauldrons, southwestern New Mexico. J. Geophys. Res. 89B, 8733–8750.

Ferguson, J.F., Cogbill, A.H., Warren, R.G., 1994. A geophysical–geological transect of the Silent Canyon complex, Pahute Mesa, Nevada. J. Geophys. Res. 99B, 4323–4339.

Fisher, R.V., Heiken, G., Hulen, J.B., 1997. Volcanoes: Crucibles of Change. Princeton Univ. Press, Princeton, NJ, USA, 317 pp.

Fornari, D.J., Ryan, W.B.F., Fox, P.J., 1984. The evolution of craters and calderas on young seamounts: insights from sea MARC 1 and SEABEAM sonar surveys of a small seamount group near the axis of the East Pacific Rise at 10°N. J. Geophys. Res. 89, 11069–11083.

Francis, P.W., Hammill, M., Kretzschmar, G., Thorpe, R.S., 1978. The Cerro Galan Caldera, north-west Argentina and its tectonic setting. Nature 274, 749–751.

Francis, P.W., O'Callaghan, L., Kretzschmar, G.A., Thorpe, R.S., Sparks, R.S.J., Page, R.N., 1983. The Cerro Galan ignimbrite. Nature 301, 51–53.

Francis, P.W., Sparks, R.S.J., Hawkesworth, C.J., Thorpe, R.S., Pyle, D.M., Tait, S.R., Mantovani, M.S.M., McDermott, F., 1989. Petrology and geochemistry of volcanic rocks of the Cerro Galan caldera, north-west Argentina. Geol. Mag. 126, 515–547.

Fridrich, C.J., Smith, R.P., DeWitt, E., McKee, E.H., 1991. Structural, eruptive and intrusive evolution of the Grizzly Peak caldera, Sawatch Range, Colorado. Geol. Soc. Am. Bull. 103, 1160–1177.

Goff, F., Gardner, J.N., 1994. Evolution of a mineralized geothermal system, Valles Caldera, New Mexico. Econ. Geol. 89, 1803–1832.

Gudmundsson, A., 1988. Formation of collapse calderas. Geology 16, 808–810.

Gudmundsson, A., 1995. Infrastructure and mechanics of volcanic systems in Iceland. J. Volcanol. Geotherm. Res. 64, 1–22.

Gudmundsson, A., 1998. Formation and development of normal-fault calderas and the initiation of large explosive eruptions. Bull. Volcanol. 60, 160–170.

Halinan, S., 1993. Non-chaotic collapse at funnel calderas: gravity study of the ring fractures at Guayabo Caldera, Costa Rica. Geology 21, 367–370.

Hartung, G., 1860. Die Azoren in ihrer ausseren erscheinung und nach ihrer geognostischen, Natur. W. Engelmann, Leipzig.

Heiken, G., Goff, F., Stix, J., Tamanyu, S., Shafiqullah, M., Garcia, S., 1986. Intracaldera volcanic activity, Toledo Caldera and embayment, Jemez Mountains, New Mexico. J. Geophys. Res. 91B, 1799–1815.

Heiken, G., Goff, F., Gardner, J.N., Baldridge, W.S., 1990. The Valles/Toledo Caldera Complex, Jemez Volcanic Field, New Mexico. Annu. Rev. Earth Planet. Sci. 18, 27–53.

Hildreth, W., 1991. The timing of caldera collapse at Mount Katmai in response to magma withdrawal toward Novarupta. Geophys. Res. Lett. 18, 1541–1544.

Hildreth, W., Mahood, G.A., 1986. Ring fracture eruption of the Bishop Tuff. Geol. Soc. Am. Bull. 97, 396–403.

Hildreth, W., Christiansen, R.L., O'Neil, J.R., 1984. Catastrophic isotopic modification of rhyolitic magma at times of caldera subsidence, Yellowstone plateau volcanic field. J. Geophys. Res. 89B, 8339–8369.

Houghton, B.F., Weaver, S.D., Wilson, C.J.N., Lanphere, M.A., 1992. Evolution of a Quaternary peralkaline volcano: Mayor Island, New Zealand. J. Volcanol. Geotherm. Res. 51, 217–236.

Hutton, D.H.W., Reavy, R.J., 1992. Strike slip tectonics and granite petrogenesis. Tectonics 11, 960–967.

Jellinek, A.M., DePaolo, D.J., 2003. A model for the origin of large silicic magma chambers: precursors of caldera-forming eruptions. Bull. Volcanol. 65, 363–381.

John, D.A., 1995. Tilted middle Tertiary ash-flow calderas and subjacent granitic plutons, southern Stillwater Range, Nevada: cross section of and Oligocene igneous center. Geol. Soc. Am. Bull. 107, 180–200.

Johnson, R.W., 1969. Volcanic geology of Mt Suswa, Kenya. Philos. Trans. R. Soc. Lond. Ser. A: Math. Phys. Sci. 265, 383–412.

Johnson, S.E., Paterson, S.R., Tate, M.C., 1999. Structure and emplacement history of a multiple centre, cone-sheet-bearing

ring complex: the Zarza Intrusive Complex, Baja California, Mexico. Geol. Soc. Am. Bull. 111 (4), 607–619.

Karátson, D., Thouret, J.-C., Moriya, I., Lomoschitz, A., 1999. Erosion calderas: origins, processes, structural and climatic control. Bull. Volcanol. 61, 174–193.

Kennedy, B., Stix, J., 2003. Igneous Rock Associations: 1. Styles and mechanisms of collapse. Geosci. Can. 30, 59–72.

Kingsley, L., 1931. Cauldron subsidence in the Ossipee Mountains. Am. J. Sci. 22, 139–168.

Kokelaar, B.P., Branney, M.J., 1999. Inside silicic calderas (Snowdon, Scafell, and Glencoe, UK): interaction of caldera development, tectonism and hydrovolcanism. CEV Field Workshop, Guidebook. 150 pp.

Komuro, H., 1987. Experiments on cauldron formation: a polygonal cauldron and ring fractures. J. Volcanol. Geotherm. Res. 31, 139–149.

Komuro, H., Fujita, Y., Kodama, K., 1984. Numerical and experimental models on the formation mechanism of collapse basins during the Green Tuff orogenesis of Japan. Bull. Volcanol. 47, 649–666.

Lipman, P.W., 1984. The roots of ash flow calderas in western North America: windows into the tops of granitic batholiths. J. Geophys. Res. 89B, 8801–8841.

Lipman, P.W., 1992. Ash-flow calderas as structural controls of ore deposits—recent work and future problems. U.S. Geol. Surv. Bull. 2012, L1–L12.

Lipman, P.W., 1995. Subsidence of ash-flow calderas; role of magma chamber geometry. IUGG Gen. Assem. 21 (Week A), 452.

Lipman, P.W., 1997. Subsidence of ash-flow calderas: relation to caldera size and magma chamber geometry. Bull. Volcanol. 59, 198–218.

Lipman, P.W., 2000a. The central San Juan caldera cluster: regional volcanic framework. Spec. Pap.-Geol. Soc. Am. 346, 9–71.

Lipman, P.W., 2000b. Calderas. In: Sigurdsson, H. (Ed.), Encyclopedia of Volcanoes. Academic Press, San Francisco, pp. 643–662.

Lipman, P.W., Sawyer, D.A., 1985. Mesozoic ash-flow caldera fragments in southeastern Arizona and their relation to porphyry copper deposits. Geology 13, 652–656.

Lipman, P., Dungan, M., Bachmann, O., 1997. Comagmatic granophyric granite in the Fish Canyon Tuff, Colorado: implications for magma-chamber processes during a large ash-flow eruption. Geology 25, 915–918.

Lyell, Sir C., 1858. On the structure of lavas which have consolidated on steep slopes; with remarks on the mode of origin of Mount Etna, and on the theory of 'Craters of Elevation'. Philos. Trans. R. Soc. Lond. 148, 703–786.

McNulty, B.A., Tobisch, O.T., Cruden, A.R., 2000. Multistage emplacement of the Mt Givens pluton, central Sierra Nevada batholith, California. Geol. Soc. Am. Bull. 112, 119–135.

Mahood, G.A., 1983. Calderas in strongly peralkaline systems. Eos, Trans. Am. Geophys. Union 64 (45), 883.

Mahood, G.A., 1984. Pyroclastic rocks and calderas associated with strongly peralkaline magmatism. J. Geophys. Res. 89B, 8540–8552.

Mahood, G., Hildreth, W., 1983. Nested calderas and trapdoor uplift at Pantelleria, Strait of Sicily. Geology 11, 722–726.

Mahood, G.A., Hildreth, W., 1986. Geology of the peralkaline volcano at Pantelleria, Strait of Sicily. Bull. Volcanol. 48, 143–172.

Marti, J., Gudmundsson, A., 2000. The Las Canadas caldera (Tenerife, Canary Islands): an overlapping collapse caldera generated by magma-chamber migration. J. Volcanol. Geotherm. Res. 103, 161–173.

Marti, J., Ablay, G.J., Redshaw, L.T., Sparks, R.S.J., 1994. Experimental studies of caldera collapse. J. Geol. Soc. (Lond) 151, 919–929.

Marti, J., Folch, A., Neri, A., Macedonio, G., 2000. Pressure evolution during explosive caldera-forming eruptions. Earth Planet. Sci. Lett. 175, 275–287.

Mills, B.A., Boden, D.R., Sander, M.V., 1988. Alteration and precious metal mineralization associated with the Toquima caldera complex, Nye County, Nevada. In: Schafer, R.W., Cooper, J.J., Vikre, P.G. (Eds.), Bulk-Mineable Precious Metals Deposits of the Western United States. Symposium Proceedings. Geol. Soc, Nevada, pp. 303–332.

Milner, D.M., Cole, J.W., Wood, C.P., 2002. Asymmetric, multiple-block collapse at Rotorua Caldera, Taupo Volcanic Zone, New Zealand. Bull. Volcanol. 64, 134–149.

Mogi, K., 1958. Relations between the eruptions of various volcanoes and the deformation of the ground surface around them. Bull. Earthq. Res. Inst. Univ. Tokyo 36, 99–134.

Moore, I., Kokelaar, P., 1997. Tectonic influences in piecemeal caldera collapse and Glencoe volcano, Scotland. J. Geol. Soc. (Lond) 154, 765–768.

Moore, I., Kokelaar, P., 1998. Tectonically controlled piecemeal caldera collapse: a case study of Glencoe volcano, Scotland. Geol. Soc. Am. Bull. 110, 1446–1466.

Mori, J., McKee, C., 1987. Outward-dipping ring-fault structure at Rabaul Caldera as shown by earthquake locations. Science 235, 193–195.

Mouginis-Mark, P.J., Robinson, M.S., 1992. Evolution of Olympus Mons Caldera, Mars. Bull. Volcanol. 54, 347–360.

Munro, D.C., Rowland, S.K., 1996. Caldera morphology in the western Galapagos and implications for volcano eruptive behaviour and mechanisms of caldera formation. J. Volcanol. Geotherm. Res. 72, 85–100.

Nairn, I.A., 1989. Sheet V16 AC, Mount Tarawera. Geological Map of New Zealand 1:50,000. Dep. Sci. Ind. Res., Wellington.

Nairn, I.A., Wood, C.P., Bailey, R.A., 1994. The Reporoa caldera, Taupo volcanic zone: source of the Kaingaroa Ignimbrites. Bull. Volcanol. 56, 529–537.

Neilson, D.L., Hulen, J.B., 1984. Internal geology and evolution of the Redondo Dome, Valles Caldera, New Mexico. J. Geophys. Res. 89B, 8695–8711.

Newhall, C.G., Dzurisin, D., 1988. Historical unrest at large calderas of the world. U.S. Geol. Surv. Bull. 1855 (2 vols., 1108 pp).

Odonne, F., Menard, I., Messonnat, G.J., Rolando, J.P., 1999. Abnormal reverse faulting above a depleting reservoir. Geology 27, 111–114.

Okada, Y., 1985. Surface deformation due to shear and tensile faults in a half-space. Bull. Seismol. Soc. Am. 75, 1135–1154.

Orsi, G., Gallo, G., Zanchi, A., 1991. Simple-shearing block resurgence in caldera depressions. A model from Pantelleria and Ischia. J. Volcanol. Geotherm. Res. 47, 1–11.

Orsi, G., Antonio, M., De Vita, S., Gallo, G., 1992. The Neapolitan Yellow Tuff, a large-magnitude trachytic phreatoplinian eruption; eruptive dynamics, magma withdrawal and caldera collapse. J. Volcanol. Geotherm. Res. 53, 275–287.

Prevost, M.C., 1843. Soc. Geol. France 2, 105.

Reck, H., 1936. Santorin, der Werdegang eines Inselvulkans und sein Ausbruch 192–1928. D. Reimer, Andrews and Steiner, Berlin. 3 vols.

Roche, O., Druitt, T.H., Merle, O., 2000. Experimental study of caldera formation. J. Geophys. Res. 105B, 395–416.

Roman-Berdiel, T., Gapais, D., Bruin, J.P., 1995. Analogue models of laccolith formation. J. Struct. Geol. 17, 1337–1346.

Rosi, M., Sbrana, A., Principe, C., 1983. The Phlegrean Fields structural evolution, volcanic history and eruptive mechanisms. J. Volcanol. Geotherm. Res. 17, 273–288.

Rymer, H., van Wyk de Vries, B., Stix, J., Williams-Jones, G., 1998. Pit crater structure and processes governing persistent activity at Masaya Volcano, Nicaragua. Bull. Volcanol. 59, 345–355.

Scandone, R., 1990. Chaotic collapse caldeas. J. Volcanol. Geotherm. Res. 42, 285–308.

Scarpati, C., Cole, P., Perrotta, A., 1993. The Neapolitan Yellow Tuff—a large volume mutiphase eruption from Campei Flegrei, southern Italy. Bull. Volcanol. 55, 343–356.

Schirnick, C., van den Bogard, P., Schmincke, H.-U., 1999. Cone sheet formation and intrusive growth of an oceanic island—the Miocene Tejeda complex on Gran Canaria (Canary Islands). Geology 27, 207–210.

Schmincke, H.-U., 1967. Cone sheet warm, resurgence of Tejeda caldera, and early geologic history of Gran Canaria. Bull. Volcanol. 31, 153–162.

Schultz-Ela, D.D., Jackson, M.P.A., Vendeville, B.C., 1993. Mechanism of active salt diapirism. Tectonophysics 228, 275–312.

Scrope, G.P., 1859. Extinct Volcanoes of Central France. John Murray, London.

Self, S., Rampino, M.R., 1981. The 1883 eruption of Krakatau. Nature 294, 699–704.

Self, S., Goff, G., Gardner, J.N., Wright, J.V., Kite, W.M., 1986. Explosive rhyolitic volcanism in the Jemez Mountains: vent locations, caldera development and relation to regional structure. J. Geophys. Res. 91B, 1779–1798.

Simkin, T., Fiske, R.S., 1983. Krakatau 1883: The Volcanic Eruption and its Effects. Smithsonian Inst. Press, Washington, DC, 464 pp.

Simkin, T., Howard, K.A., 1970. Caldera collapse in the Galapagos Islands, 1968. Science 169, 429–437.

Smith, R.L., Bailey, R.A., 1968. Resurgent caldrons. Mem. Geol. Soc. Am. 116, 613–662.

Smith, R.T., Houghton, B.F., 1995. Vent migration and changing eruptive style during the 1800a Taupo eruption: new evidence from the Hatepe and Rotongaio phreatoplinian ashes. Bull. Volcanol. 57, 432–439.

Smith, R.L., Bailey, R.A., Ross, C.S., 1961. Structural evolution of the Valles Caldera, New Mexico, and its bearing on the emplacement of ring dikes. U.S. Geol. Surv. Prof. Paper 424, 145–149.

Sparks, R.S.J., Francis, P.W., Hamer, R.D., Pankhurst, R.J., O'Callaghan, L.O., Thorpe, R.S., Page, R., 1985. Ignimbrite of the Cerro Galan Caldera, NW Argentina. J. Volcanol. Geotherm. Res. 24, 205–248.

Steven, T.A., Lipman, P.W., 1976. Calderas of the San Juan volcanic field, southwestern Colorado. U.S. Geol. Surv. Prof. Paper 95 (35 pp).

Tibaldi, A., Vezzoli, L., 2000. Late Quaternary monoclinal folding induced by caldera resurgence at Ischia, Italy. Forced Folds and Fractures, Special Publication-Geol. Soc. London vol. 169, pp. 103–113.

Trasatti, E., Giunchi, C., Bonafede, M., 2003. Effects of topography and rheological layering on ground deformation in volcanic regions. J. Volcanol. Geotherm. Res. 122, 89–110.

von Buch, L. 1820. Uber die Zusammensetzung der Basaltischen Inseln und über Erhebungs Kratere. A lecture delivered before the Prussian Academy on Sciences in May 1818, Berlin.

Walker, G.P.L., 1984. Downsag calderas, ring faults, caldera sizes, and incremental caldera growth. J. Geophys. Res. 89B, 8407–8416.

Walker, G.P.L., 1988. Three Hawaiian calderas: an origin through loading by shallow intrusions? J. Geophys. Res. 93B, 14773–14784.

Walker, J.A., Williams, S.N., Kalamarides, R.I., Feigenson, M.D., 1993. Shallow open-system evolution of basaltic magma beneath a subduction zone volcano: the Masaya Caldera Complex, Nicaragua. J. Volcanol. Geotherm. Res. 56, 379–400.

Wheller, G.E., Varne, R., 1986. Genesis of dacitic magmatism at Batur Volcano, Bali Indonesia: implications for the origins of stratovolcano calderas. J. Volcanol. Geotherm. Res. 28, 363–378.

Williams, H., 1941. Calderas and their origin. Bull. Dep. Geol. Sci., vol. 25. University of California publications, pp. 239–346.

Williams, H., 1942. Geology of the Crater Lake National Park, Oregon. Carnegie Inst. Publication, Washington, p. 540.

Williams, H., McBirney, A.R., 1968. Geological and geophysical features of calderas. NASA Progress Report. Manned Spacecraft Centre, Houston, TX, USA, 87 pp.

Williams, H., McBirney, A.R., 1979. Volcanology. Freeman, Cooper and Co, San Francisco Publ., Berkeley, CA, 397 pp.

Williams, S.N., Stoiber, R.E., 1983. "Masaya-type caldera"—redefined as the mafic analogue of "Krakatau-type caldera". Eos, Trans. Am. Geophys. Union 64 (45), 877.

Wilson, C.J.N., Hildreth, W., 1997. The Bishop Tuff: new insights from eruptive stratigraphy. J. Geol. 105, 407–439.

Wilson, C.J.N., Houghton, B.F., McWilliams, M.O., Lanphere, M.A., Weaver, S.D., Briggs, R.M., 1995. Volcanic and structural evolution of Taupo Volcanic Zone, New Zealand: a review. J. Volcanol. Geotherm. Res. 68, 1–28.

Withjack, M.O., Scheiner, C., 1982. Fault patterns associated with domes—an experimental and analytical study. Am. Assoc. Pet. Geol. Bull. 66, 302–316.

Wolff, J.A., Wright, J.V., 1981. Formation of the Green Tuff, Pantelleria. Bull. Volcanol. 44, 681–690.

Wright, I.C., Gamble, J.A., 1999. Southern Kermadec submarine caldera arc volcanoes (SW Pacific): caldera formation by effusive and pyroclastic eruption. Mar. Geol. 161, 207–227.

Wright, I.C., Gamble, J.A., Shane, P.A.R., 2003. Submarine silicic volcanism of the Healy caldera, southern Kermadec arc (SW Pacific): 1—Volcanology and eruption mechanisms. Bull. Volcanol. 65, 15–29.

Yoshida, T., 1984. Tertiary Ishizuki cauldron, southwestern Japan arc: formation by ring fracture subsidence. J. Geophys. Res. 89B, 8502–8510.

Appendix D

'**Spinks, K.D.**, Cole, J.W. & Leonard, G.S. (2004) Caldera volcanism in the Taupo Volcanic Zone. In: Manville, V. (ed) Field Trip Guides: Geological Society of New Zealand Miscellaneous Publication 117B: 111-135'

Contribution: Sole authorship for introductory material (field trip itinerary not included here was written in conjunction with other authors).

Field Trip 7

CALDERA VOLCANISM IN THE TAUPO VOLCANIC ZONE

Field Trip Guide
Friday 9 December-Sunday 12 December 2004

K.D. SPINKS[1], J.W. COLE[1], G.S. LEONARD[2]

[1] Department of Geological Sciences, University of Canterbury, Private Bag 4800, Christchurch, New Zealand

[2] Institute of Geological and Nuclear Sciences, P.O. Box 30368, Lower Hutt, New Zealand

INTRODUCTION

Central TVZ is the most frequently active and productive Quaternary silicic system on Earth (HOUGHTON *et al.*, 1995) characterised by intense and volumetrically dominant rhyolitic volcanism that is expressed largely as major calderas and caldera complexes. Caldera-forming silicic volcanism in TVZ began at c. 1.6 Ma, and at least thirty-four caldera-forming eruptions have occurred since then during three main periods: 1.68-1.53 Ma, 1.21-0.68 Ma, and 0.34-present (HOUGHTON *et al.*, 1995). Six of the calderas identified in central TVZ (Okataina, Taupo, Rotorua, Reporoa, Ohakuri and Whakamaru) have formed in the last 350 ka. These comprise both multiple event caldera complexes (Okataina, Taupo and Whakamaru) and single event calderas (Reporoa, Ohakuri and Rotorua). The Okataina and Taupo caldera complexes, located at the boundaries of the central part are the most productive rhyolitic volcanoes on earth, with eruption rates of c. 0.1 m^3s^{-1} and c. 0.2 m^3s^{-1} respectively, averaged over the last 65 ka (WILSON, 1993). Remote sensing and structural data obtained on deposits younger than 300 ka along TVZ show that it comprises a number of segments with variable dextral components of shear, and significantly that pure extension is restricted to those segments containing the Okataina and Taupo caldera complexes (ACOCELLA, *et al.*, 2003). The diversity of calderas within modern TVZ thus provides an opportunity to examine the role of rift architecture in controlling the location and development of caldera volcanism (SPINKS *et al.*, in press),

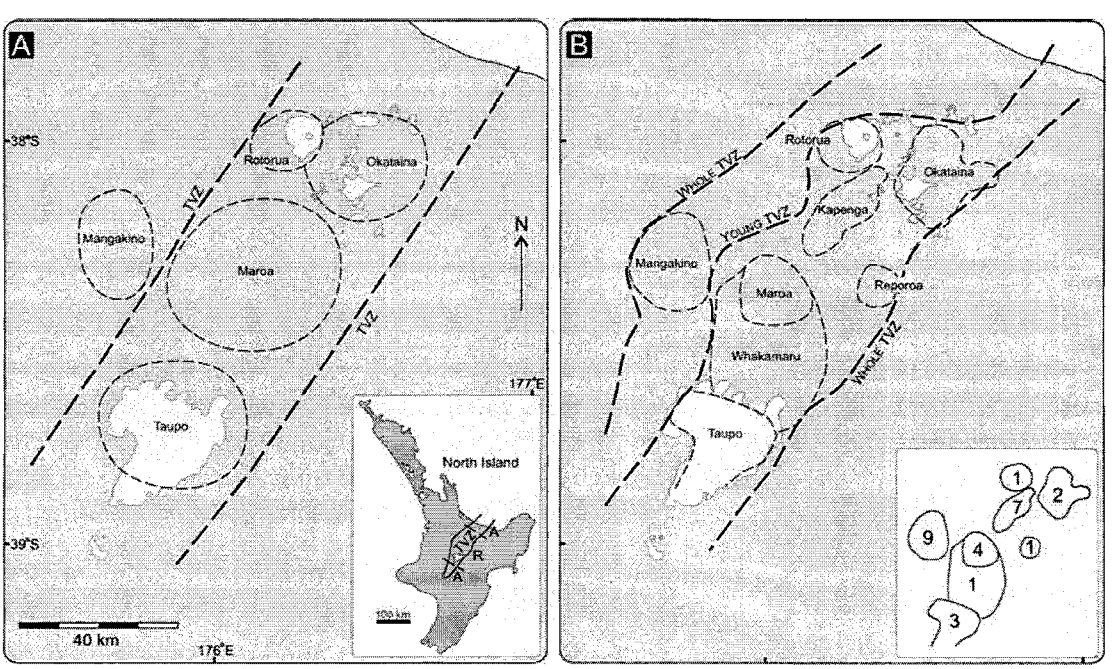

Figure 1 A: Rhyolitic centres of the Taupo Volcanic Zone (from Cole, 1990); **B:** Calderas of the Taupo Volcanic Zone (from Wilson et al., 1995). Numbers in inset represent known ignimbrites or ignimbrite groups erupted from each caldera.

Terminology

Rhyolitic volcanism in central TVZ is traditionally divided into 'volcanic centres' or 'calderas' and their associated vents. COLE (1990) described four composite rhyolitic volcanic centres in TVZ), while more recently (e.g. HOUGHTON *et al.*, 1995; WILSON *et al.*, 1995) recognised eight caldera centres (FIG.1). These terms are used interchangeably in the literature while none are suitably defined. In particular, a 'volcanic centre' is a rather subjective concept based on some arbitrary spatial association of vents and adjacent caldera structures. In some situations (as in COLE, 1990) the term is used for broad areal groups of associated extrusive and explosive volcanics, and are thus larger than calderas. In other situations the term is used for a constrained group of volcanics associated with one volcano and is usually within a caldera (e.g. Maroa Volcanic Centre). In this field guide, the terms 'caldera' or 'caldera-complex' are used only to define the collapse structure, and volcanic centre is used in the latter sense for a specific space-time association, usually within a caldera or caldera complex.

CALDERA RECOGNITION IN TVZ

The eight documented calderas in TVZ are expressed at the surface by clustering of known or inferred vent locations and/or at depth by geophysically defined basement depressions. High production rates in TVZ and concomitant rapid burial makes caldera delineation in TVZ difficult, and only four of the currently recognised calderas (Taupo, Okataina, Rotorua and Reporoa; those corresponding to modern TVZ) are sufficiently exposed to enable analysis of surface morphology. Other collapse structures have been buried and/or destroyed by subsequent activity. Specifically, 'Kapenga volcanic centre' was first postulated entirely on geophysical evidence (ROGAN, 1982; WILSON *et al.*, 1984), and while at least seven ignimbrites are attributed to it (HOUGHTON *et al.*, 1995), no deposits are unequivocally related to any proposed caldera-forming events or documented collapse structures. The Mangakino and Whakamaru calderas also have effectively no surface expression, and recent work within the proposed Maroa Caldera does not indicate any separate caldera-forming event or caldera structure associated with the Maroa Dome Complex (LEONARD, 2003). Further calderas may be implied by extensive ignimbrite deposits exposed at the surface (e.g. Ohakuri Ignimbrite; GRAVLEY, 2005), and in drillhole samples (e.g. Rautawhiri Breccia; BROWN, 1994) but source areas do not provide evidence of caldera structure at the surface. Even where calderas are exposed at the surface, caldera structure is often obscured by caldera infill, including both intra-caldera ignimbrite and post-caldera volcanism. In addition, coincidence with intense regional faulting at some calderas forms complex structures where the relative contributions of volcanism and tectonism in landscape development are intimately associated and potentially difficult to resolve. Our current recognition of calderas is shown diagrammatically in FIG. 2.

Geophysical Analysis

Geophysical techniques, particularly gravity analysis, help elucidate the geometry and extent of caldera structures at depth. Gravity response is a function of density contrasts between lithologies, and for calderas, where dense basement rocks are deeper within the caldera than outside the caldera margins, burial by a potentially thick succession of intra-caldera, low-density pyroclastic material leads to a negative gravity anomaly. A caldera is therefore expected to have a negative gravity anomaly that will reflect the shape of the collapse structure at depth.

TVZ is characterised by a broad gravity low, and superimposed on this are several large negative residual gravity anomalies up to 75 mGal which indicate the presence of thick sequences of low-density volcaniclastic sediments and effectively mark the location of the rhyolitic calderas (ROGAN, 1982; DAVY & CALDWELL, 1998). Major well-defined negative gravity anomalies are coincident with the Okataina and Taupo caldera complexes, and an extensive region of gravity lows extends between these structures. These partly coincide with documented calderas and as

such may provide a more accurate depiction of the buried caldera structures such as Whakamaru and Mangakino. While it is somewhat justifiable to consider much of the basement depression in the central TVZ (inside the -40 mGal contour for example) representative of caldera collapse, the gravity signal records zones of relatively low-density material, and these could similarly be accounted for by progressive filling of tectonic structures from various adjacent sources.

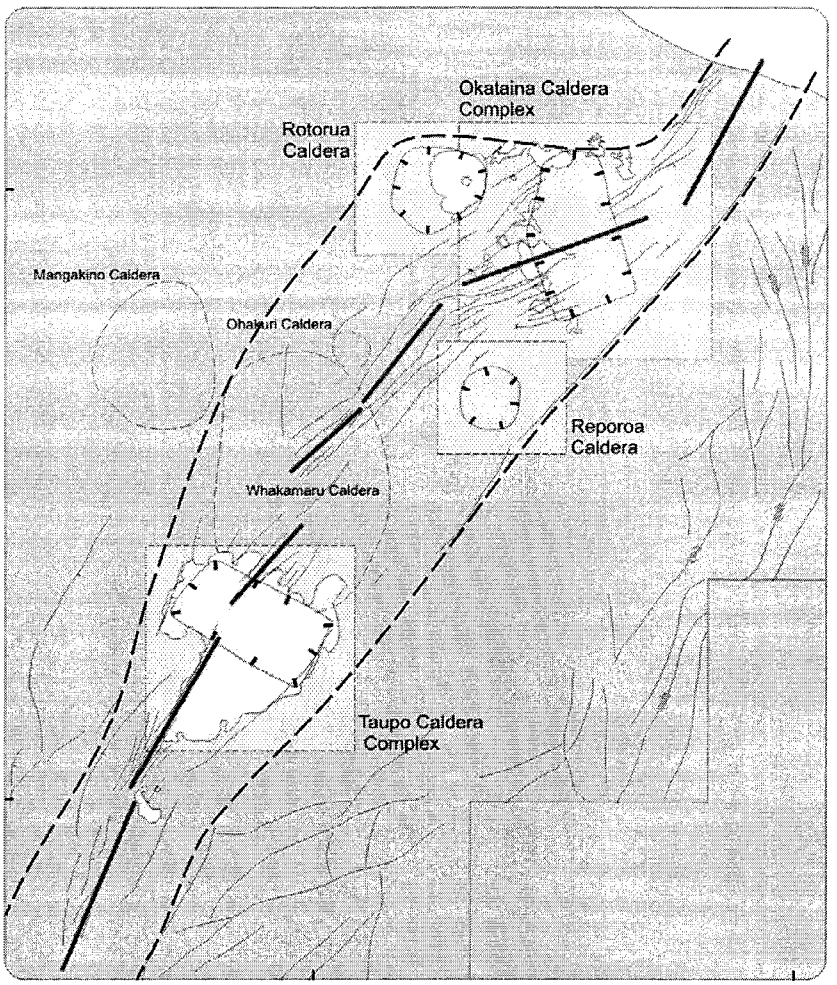

Figure 2 Summary of regional structure of TVZ and the location of currently recognised calderas. The highlighted calderas are the four 'modern' calderas (<300 ka) of Spinks et al (in press). The solid lines indicate rift segments of Acocella et al (2003).

POST 350KA CALDERAS IN TVZ

In the following sections the post 350ka TVZ calderas (Whakamaru, Reporoa, Ohakuri, Rotorua, Okataina, Taupo) are considered in light of existing volcanological, geochemical and geophysical data, and new morphological and structural data, derived from DEM analysis and field studies, to assess the influence of the structural framework on caldera shape and development.

Whakamaru Caldera and Maroa Dome Complex

The proposed Whakamaru Caldera has no clear topographic margin and was proposed by WILSON *et al.* (1986) on the basis of the thickness and distribution of the Whakamaru-group ignimbrites, exposed east and west of central TVZ (FIG. 3). Whakamaru group ignimbrites constitute the largest eruptive episode in TVZ history, with a exposed volume of at least 1000 km^3. These ignimbrites extend north to the southern margin of OVC, east and west to the boundaries of TVZ and south to partially form the eastern walls of Taupo Caldera. Several

episodes of collapse occurred at Whakamaru Caldera, with dome emplacement between collapse events. Other caldera boundaries are defined based on drillhole thickness of Whakamaru ignimbrite and are thick inside the structure (Wairakei, Mokai, Tauhara, Rotokawa) and thin (outflow sheets) outside the structure (Broadlands, Waiotapu) (BROWN 1994).

The proposed Whakamaru caldera is defined to the west by the Western Dome Belt, a 32 km long curvilinear chain of simple and compound silicic domes inferred from field evidence to post-date the Whakamaru eruptions (WILSON *et al.*, 1986). WILSON *et al.* (1986) divided the Western Dome Belt into 1) the Western Dome Complex (WDC), comprising the domes south of the Waikato River, and 2) the North-western Dome Complex (NWDC), north of the Waikato River, They are regarded as the result of post-collapse volcanism localised along the western caldera margin. Eruption of the domes has clearly been controlled by an N-S-trending fault system which has subsequently ruptured to displace the domes. Domes immediately east of the faults are probably younger features. Given that the domes and faults are aligned along a lineation oblique to the regional trend, if the lavas of the WDC are post-collapse features, then faulting likely relates to continued movement along the margins of the Whakamaru Caldera.

Domes of the NWDC curve around from an N-S orientation associated with the WDC, to trend NE at the northern end of the complex. The semi-continuous fault pattern suggests these faults too may reflect the caldera margin, but could equally reflect the northwestern margin of TVZ.

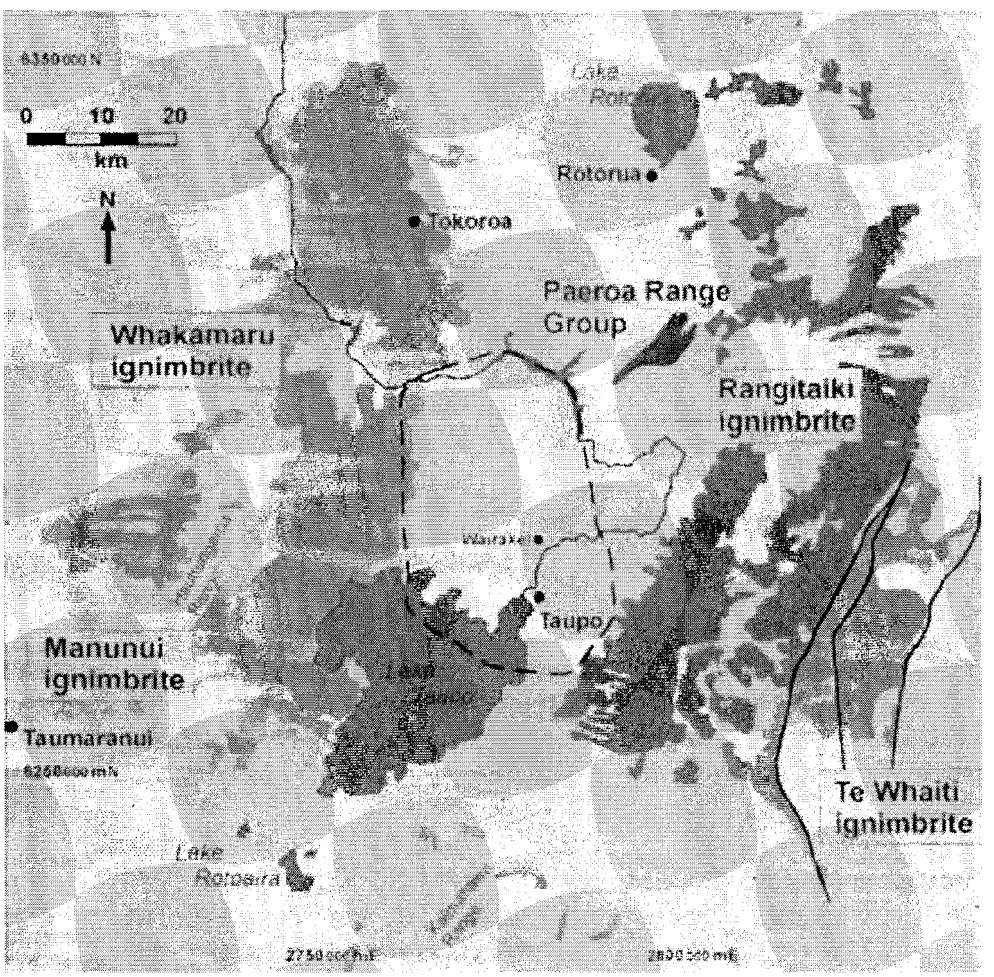

Figure 3 Map showing the distribution of outcrop of the Whakamaru group ignimbrites (from Brown, et al., 1998). The dashed line represents the outline of the Whakamaru caldera as proposed by Wilson et al (1986).

Maroa Dome Complex is an accumulation of youthful simple and composite silicic domes. Dome are strongly aligned along NNE trends and extensively faulted along the same lineation, indicating the same regional structure is responsible for controlling vent locations and subsequent deformation. Vent and fault lineations are sub-parallel with faulting in the Kapenga graben to the NE.

Reporoa Caldera

Reporoa Caldera (NAIRN *et al.*, 1994) is located at the northern end of the Taupo-Reporoa depression ~15 km E of the Kapenga segment axis (FIG 2), originally interpreted as part of a large fault angle depression between the Taupo and Kaingaroa fault belts (MODRINIAK & STUDT, 1959). It was redefined by NAIRN *et al.* (1994) as a caldera and the source of the 0.23 +/- 0.01 Ma (HOUGHTON *et al.*, 1995) Kaingaroa Ignimbrite, with a total eruptive volume of 100 km^3 (NAIRN *et al.*, 1994; BERESFORD & COLE, 2000a). Kaingaroa Ignimbrite extends radially for 20-30 km beyond the caldera, mostly to the east of Reporoa Caldera where it caps the Kaingaroa Plateau (FIG. 4).

Pre-caldera volcanism in the Reporoa area comprises rhyolite lavas unrelated to the Kaingaroa magma system or the formation of Reporoa caldera (BERESFORD & COLE, 2000a) and older ignimbrites from caldera sources to the west (RITCHIE, 1996; WILSON *et al.*, 1986; BERESFORD *et al.*, 2000a). Minor (<2 km^3) post-caldera rhyolite domes are geochemically and isotopically distinct from the Kaingaroa magma system (BERESFORD, *et al.*, 2000). Lithic componentry data for the Kaingaroa Ignimbrite presented by BERESFORD & COLE (2000a) identify multiple stages in the eruption event: 1) an initial single vent phase; 2) a multiple vent or ring fracture phase on the eastern side with asymmetric caldera collapse leading to eastward-directed pyroclastic flows; 3) piston collapse accompanied by radially directed pyroclastic flows.

The caldera has a small but clear negative gravity anomaly (NAIRN *et al.*, 1994; STAGPOOLE, 1994; STAGPOOLE & BIBBY, 1999) and a low Vp anomaly consistent with low density, low Vp caldera fill (SHERBURN *et al.*, 2003). The gravity anomaly corresponds well with the topographic expression of the caldera, with a gentle and largely open western margin and a steep eastern margin, consistent with asymmetric collapse (BERESFORD & COLE, 2000a). Gravity data partly define the buried southern margin, which NAIRN *et al.* (1994) consider to coincide with a small rhyolite dome. NAIRN *et al.* (1994) also interpret post-caldera rhyolite domes and a buried dome complex inferred to exist by magnetic studies (SOENGKONO & HOCHSTEIN, 1996) to have erupted along fractures related to the caldera rim and a supposed inner caldera ring fault.

New DEM and field data (SPINKS *et al.*, in press) show that Reporoa caldera is located several km eastwards from the eastern boundary of the area of active tectonism within TVZ, most of the active faults being restricted to the Kapenga graben. Kaingaroa Ignimbrite extends eastward from the caldera, capping the Kaingaroa Plateau and forming a clear geomorphic fan on a sequence of older ignimbrites extending to the axial ranges. The asymmetry of Kaingaroa Ignimbrite distribution is partially an artefact of the heavily faulted terrain to the west of the caldera. Distribution of the Kaingaroa Ignimbrite in this area is strongly controlled by normal faulting (BERESFORD, 1997) and the situation is analogous to that for the Mamaku Ignimbrite from Rotorua Caldera, which is poorly exposed within the adjacent active rifting zone.

Reporoa is a morphologically simple sub-circular caldera (FIG. 4), with approximate dimensions of 11 x 13 km and well-preserved 250 m high collapse scarps along the northern boundary. The N-S long axis of the caldera (eccentricity E = 0.81) is oblique to the regional trend of faults to the west; in the east a NE-trending fault scarp merges with the N-S trending eastern caldera margin. The flat-floored caldera has a well defined topographic margin in the north and east, but is open to the west and south. The caldera margin is neither dissected by younger faults nor does

it truncate older structures. Reporoa has contained lakes at various stages in its history, evidenced by lacustrine sediments and terraces above the current basin floor (MANVILLE, 2001 *and refs within*). Minor lineaments within the caldera may record modern subsidence or reflect the lacustrine history of the basin.

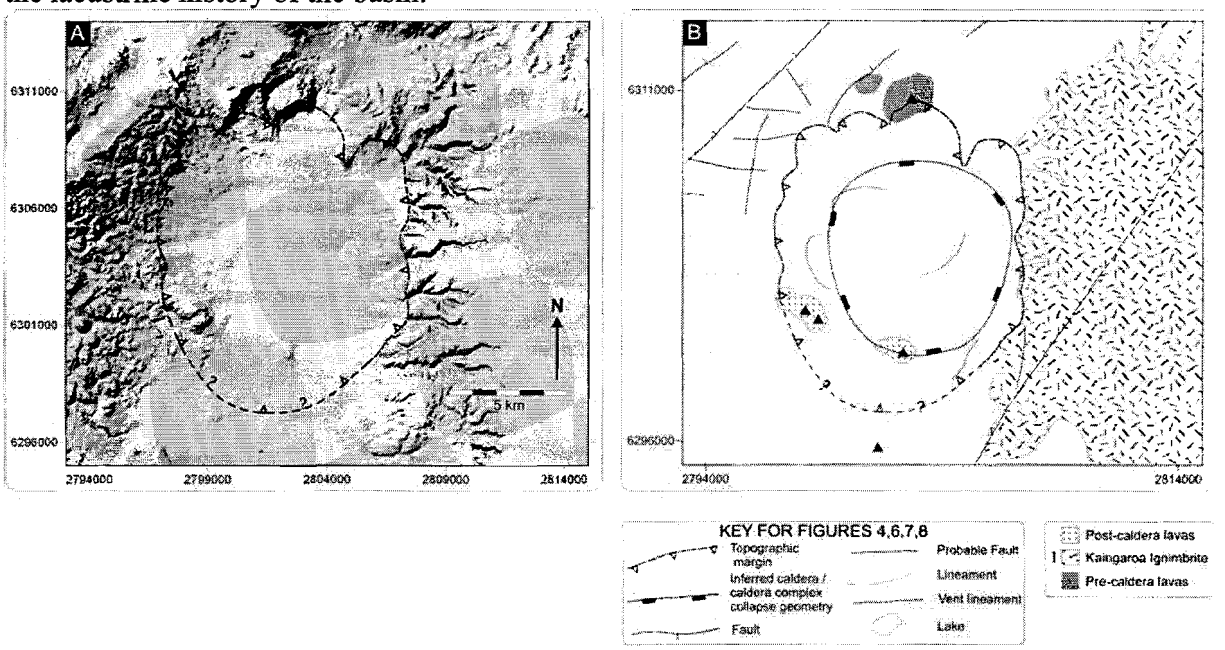

Figure 4 Reporoa Caldera. **A:** Shaded relief image generated from a 1:50,000 scale DEM; Grid coordinates are shown in the New Zealand map grid (NZMG). **B:** Structure map of the Reporoa Caldera derived from analysis of DEM data. Also shown are pre- and post-caldera lavas and the Kaingaroa ignimbrite related to caldera formation. (from Spinks et al, in press)

BERESFORD & COLE (2000a) interpret the eastern margin of Reporoa Caldera as coinciding with the Kaingaroa fault forming the eastern margin of the Taupo-Reporoa Basin. In fact, this fault is much more likely to continue sub-parallel to regional structure and pass obliquely beneath the Kaingaroa Plateau. BERESFORD (1997) inferred a 'hole' in the pre-caldera stratigraphy where proximal flows of the Kaingaroa Ignimbrite were restricted; middle and upper units of the ignimbrite maintain a near uniform thickness across the plateau. This 'hole' likely represents the down-faulted area west of the NE-trending Kaingaroa Fault, restricting early flows, and explaining the lack of early flow units of the Kaingaroa Ignimbrite. A NE-trending structure is visible northeast of Kaingaroa plateau, dividing two opposing drainage networks, and may be reflected in a subtle elevation change (west side downthrown) across the plateau.

Rotorua Caldera

Rotorua caldera is perhaps the most conspicuous caldera in TVZ, accentuated by its large, sub-circular caldera lake, Lake Rotorua (FIG. 5). The caldera is located 15-20 km NW of the junction between Okataina and Kapenga rift axes (FIG. 2), and formed during and immediately following the eruption of the c.240 ka Mamaku Ignimbrite (SHANE *et al.*, 1994; HOUGHTON *et al.*, 1995; BLACK *et al.*, 1996; MILNER *et al.*, 2002; WILSON *et al.*, 1984), with a minimum eruption volume (including intra-caldera ignimbrite) of 145 km^3 DRE (MILNER *et al.*, 2003). Some authors have proposed earlier events at Rotorua caldera to account for older ignimbrites in the area (WOOD, 1992), or that Rotorua is not a caldera at all (HUNT, 1992), but a detailed study by MILNER *et al.* (2002, 2003) confirm Rotorua as a single-event caldera, and the source of the Mamaku Ignimbrite.

A number of pre-caldera rhyolite domes are exposed in the vicinity of Rotorua Caldera. MILNER *et al.* (2002) showed that those on the rim of the caldera are geochemically distinct from each

other and from the Mamaku magma system. The post-caldera Ngongotaha and Pukehangi rhyolite dome complexes, and lavas exposed at Kawaha Point are geochemically similar to the Mamaku Ignimbrite system and may reflect a final eruptive phase from the Mamaku magma system (MILNER *et al.*, 2002). Smaller rhyolite domes are geochemically distinct and thought to be much younger.

Stratigraphic evidence outlined by MILNER *et al.* (2002) indicates caldera collapse occurred throughout the eruption and emplacement of the Mamaku Ignimbrite during a single eruptive episode. MILNER *et al.* (2002) describe asymmetric caldera collapse deepest in the southwest of the caldera, with a component of downsag expressed in the overlying Mamaku Ignimbrite. Mamaku Ignimbrite geochemistry indicates the eruption of a single, compositionally zoned magma reservoir, represented by three petrogenetically related pumice types. An andesitic juvenile component in upper parts of the Mamaku Ignimbrite are thought to reflect a discrete magma injected into the residual silicic chamber and tapped during later phases of the eruption during advanced stages of caldera collapse (MILNER *et al.*, 2003).

Rotorua Caldera is characterised by an N-S elongate negative residual gravity anomaly to the west and southwest of Lake Rotorua, including Rotorua city and the post-caldera rhyolite dome of Ngongotaha (ROGAN, 1982; DAVY & CALDWELL, 1998; HUNT, 1992). The surrounding gravity contours are not specifically concentric to the caldera margin, defining an asymmetric rise in basement towards the northeast and northwest caldera margins. The basement gradient is shallowest towards the east and steepest around the south-western margin.

DEM and field data show that Rotorua Caldera is located several km westwards from the present area of active tectonism within TVZ, with most of the active faults restricted to the junction between the Kapenga and Okataina segments (FIG. 2). To the south and east of the caldera, the Mamaku Ignimbrite surface is downfaulted and has been largely overprinted by volcanism and faulting. This is in contrast with the extensive ignimbrite surface to the north and west of the caldera reflecting the location of Rotorua Caldera west of the actively rifting portion of TVZ.

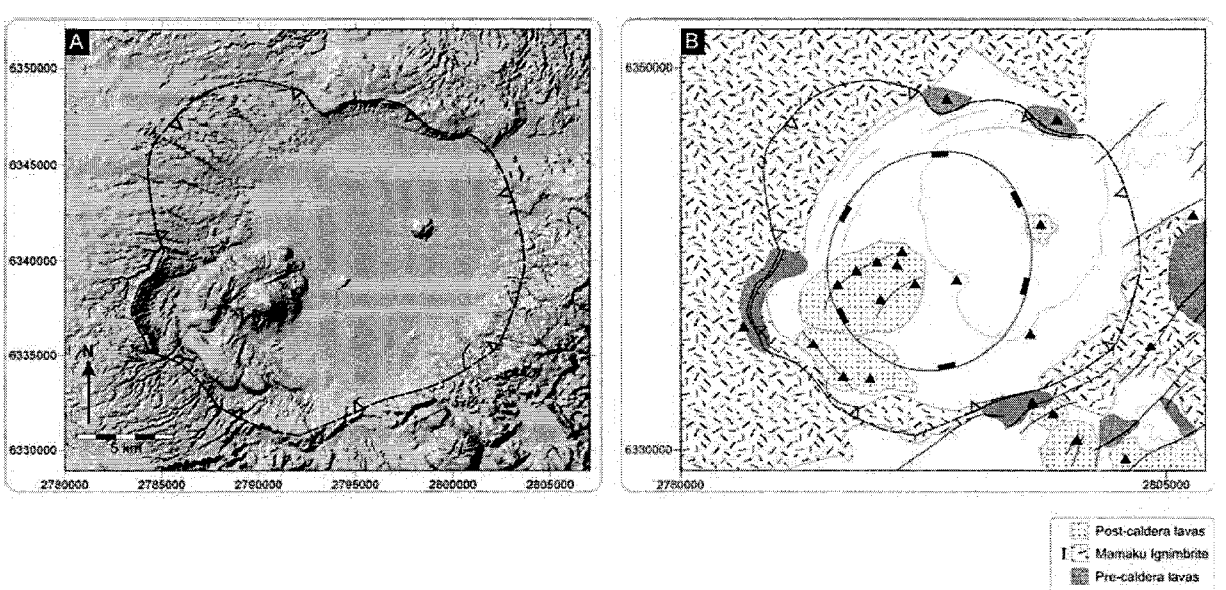

Figure 5 Rotorua Caldera. **A:** Shaded relief image of Rotorua Caldera. **B:** Structure map of Rotorua Caldera generated from analysis of DEM data. Also shown are pre- and post-caldera lavas and the Mamaku ignimbrite related to caldera formation (from Spinks et al., in press)

Rotorua is a simple sub-circular caldera with dimensions of approximately 20 x 16 km (FIG. 5). The caldera floor is dominated by the ~9 km diameter caldera lake and the youthful

morphologies of post-caldera rhyolite dome complexes. Pre- and post-caldera rhyolite domes form prominent topographic features against the flat-lying ignimbrite plateau to the west of the caldera. The topographic margin is semi-continuous around the caldera and best expressed where formed by arcuate scarps in pre-caldera rhyolite domes or Mamaku Ignimbrite; elsewhere the margin is marked by the limit of the inwards dipping Mamaku Ignimbrite, referred to as the limit of deformation by MILNER *et al.* (2002). The southeast margin of the caldera roughly parallels NE-trending regional faults in the adjacent Okataina segment. The caldera margin does not truncate any regional structures and only in the NE is dissected by younger faulting. Other lineaments in the caldera are arcuate and relate to caldera bounding scarps and associated deformation, rather than to regional structure. In the northwest of the caldera several low scarps sub-parallel to the caldera margin are located within the area defined by MILNER *et al.* (2002) as having deformed by downsag into the caldera during collapse. The vents of the Ngongotaha and Pukehangi post-caldera rhyolite domes define several lineations within the caldera, interpreted by MILNER *et al.* (2002) as reflecting eruption along major dislocations bounding the area of deepest basement collapse.

Ohakuri Caldera

The Ohakuri caldera is a newly recognised structure in the Whangapoa basin, 25kms SSW of Rotorua (FIG. 6), which is considered the source of the c. 240 ka Ohakuri pyroclastic deposits (GRAVLEY, 2005). It overlies the northern margin of the older Whakamaru caldera and lies adjacent to the axis of the modern Taupo Fault Belt. It is difficult to define either the topographic or structural caldera margins precisely because of subsequent deposition of volcaniclastic sediments, but its presence is inferred from distribution of air fall deposits, distribution of and transport directions within the Ohakuri ignimbrite, and from geophysical data.

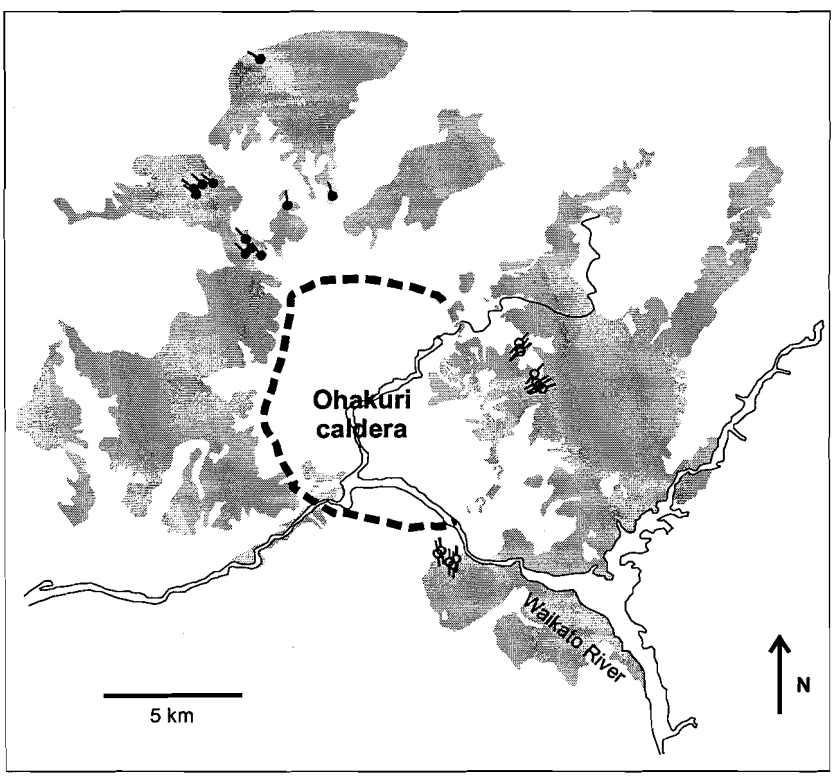

Figure 6 Ohakuri caldera and pyroclastic deposits (from Gravley, 2005). Filled circles represent uni-directional indicators from dune structures (with bar pointing in direct of flow). Open circles represent bi-directional indicators measured from channel structures.

Stratigraphic evidence presented by GRAVLEY *et al.* (2003) suggests that the Mamaku ignimbrite and the Ohakuri pyroclastic deposits were erupted in rapid succession, from the Rotorua and Ohakuri calderas respectively. They suggest that the most feasible way of achieving this linkage is through volcano-tectonic processes, in which contemporaneous faulting triggered almost concurrent events 25km apart.

Okataina Caldera Complex

Okataina Caldera Complex (OCC) is a complex of overlapping and nested collapse structures (FIG. 7), largely filled by the products of post-caldera rhyolite volcanism. The composite structure is the result of two main collapse events associated with the 0.28 ± 0.01 Ma Matahina Ignimbrite (BAILEY & CARR, 1994; date from HOUGHTON *et al.*, 1995) and 65 ka Rotoiti eruption (NAIRN, 1981, 1989; date from HOUGHTON *et al.*, 1995), and modified by substantial intra-caldera rhyolite volcanism (e.g. JURADO-CHICHAY & WALKER, 2000; NAIRN, 1989, 2002). Further older (>300 ka) and younger (>65 ka) collapse events are likely, but potential deposits and precise collapse margins are obscured and/or overprinted by subsequent activity. Magmatic volume estimates for the Matahina and Rotoiti events (including intra-caldera estimates) are 150 km^3 (BAILEY & CARR, 1994) and 120 km^3 (FROGGATT & LOWE, 1990) respectively; other eruptives from within and adjacent to OCC account for at least 150 km^3 (e.g. NAIRN, 1989; FROGGATT & LOWE, 1990; BELLAMY, 1991; JURADO-CHICHAY & WALKER, 2001). The Matahina and Rotoiti ignimbrites extend predominantly to the east and north, and appear related to overlapping but distinct sources in the southern and northern parts of the caldera complex respectively (NAIRN, 1989).

A number of rhyolite dome lavas scattered around the rim of the caldera-complex record volcanism in the Okataina area predating the first collapse event (NAIRN, 1989, 2002). No precise dates exist for these lavas, but BOWYER (2001) showed that they are chemically distinct and relate to discrete magma batches. Geochemical variation is small however, and no significant variability exists between pre-caldera lavas adjacent to the Okataina and Rotorua calderas; this would imply that these lavas are not related specifically to a Rotorua or Okataina 'volcanic centre'. Only one pre-caldera magma batch has a similar chemistry with the Matahina magma system (e.g. NAIRN, 1981; BOWYER, 2001).

Lavas and associated pyroclastics erupted between the major caldera-forming events are predominantly exposed to the southwest of the caldera where it intersects the Kapenga axial rift segment (FIG. 2) and relate to multiple magma batches (BELLAMY, 1991; BOWYER, 2001). Following the second caldera collapse event during the eruption of the Rotoiti Pyroclastics, a major phase of explosive volcanism ensued from sources within the caldera complex prior to the development of the two large rhyolite lava massifs that currently fill the caldera. Two main magma types were erupted during the explosive phase, generating 14 eruptive episodes (SMITH *et al.*, 2002); during more recent effusive activity multiple magmas were often involved with a single eruptive episode. The two documented caldera-forming events at Okataina are spatially overlapping but are significantly temporally separated (> 200 ka) and reflect geochemically distinct magma systems (BURT *et al.*, 1998). Both the Matahina and Rotoiti ignimbrites exhibit minor geochemical variation (BURT *et al.*, 1998) as likely by-products of weakly zoned magma chambers. Volcanism in the Okataina area from the earliest to the most recent eruptives, including the caldera forming events, therefore records the eruption of multiple discrete magma chambers rather than the progressive tapping of a single large chamber.

A distinct large negative residual gravity anomaly (ROGAN, 1982; DAVY & CALDWELL, 1998) and low Vp anomaly (SHERBURN *et al.*, 2003) define an N-S elongated depression consistent with the mapped caldera margin and filled with a large volume of low Vp, low density, volcaniclastic sediment. A clear low Vp anomaly at 4km effectively corresponds to a minimum

depth extent of the collapse structure (SHERBURN *et al.*, 2003). Gravity data presented by NAIRN (2002) indicates a N-S elongate negative gravity anomaly roughly concentric to the topographic margin, and centered beneath Tarawera Volcanic Complex and the southern part of Haroharo Volcanic Complex. The contours open on the west side of the structure but gravity high's separate the structure from basement highs to the east and Rotorua Caldera to the west. Topographic embayments in the caldera complex margin are also peripheral to the main basement depression indicated by gravity and Vp data.

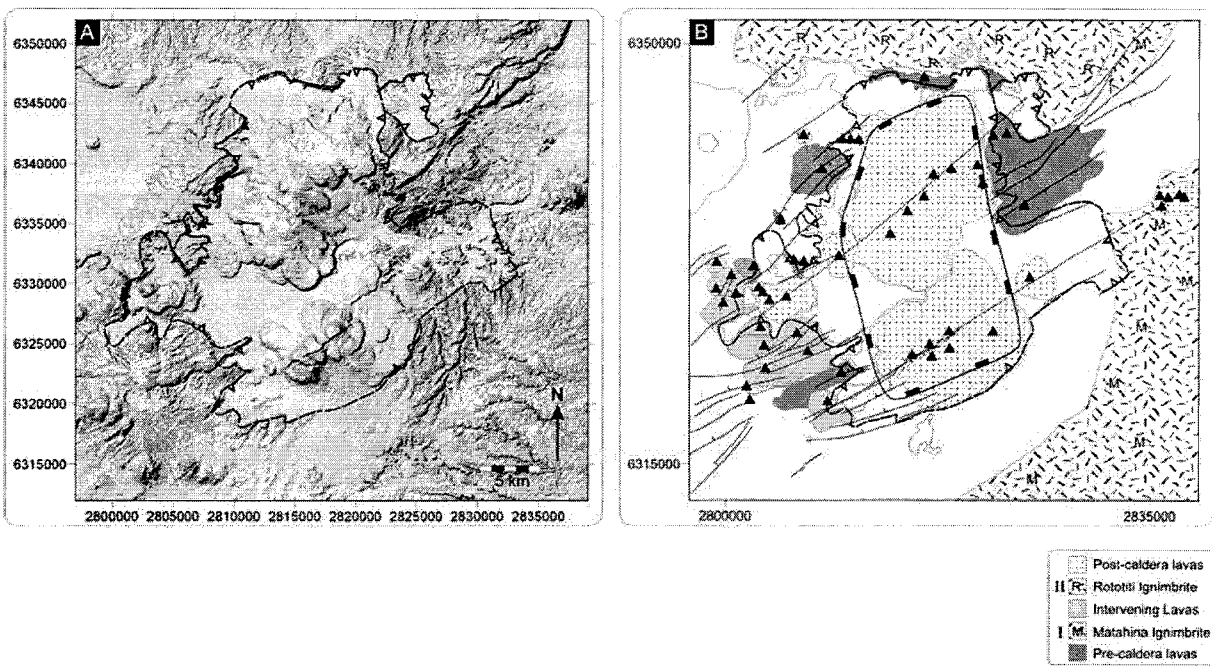

Figure 7 Okataina caldera complex. **A:** Shaded relief image of Okataina Caldera Complex; **B:** Structure map of Okataina Caldera Complex from analysis of DEM data. Also shown are pre- and post-caldera lavas and caldera-forming ignimbrites. I and II relate to the first and second caldera-forming events respectively (from Spinks et al., in press).

Morphotectonic analysis of the caldera using DEM and Remote Sensing data reveals that Okataina is significant in its location at a structurally complex transfer zone in the axial rift where the axes of adjacent segments are offset by more than 20 km. This major ENE-trending bend in the transtensional rift accompanies local rotation of the extension direction resulting in a zone of orthogonal extension. The OCC is a complex structure delineated by morphologically youthful intra-caldera volcanic features in juxtaposition with the older and more dissected terrain of pre-caldera lavas and ignimbrites forming the caldera margin. The 28 x 15 km caldera complex is strongly rectangular with a long axis trending N8°W, roughly perpendicular to the Okataina rift axis.

The topographic margin at Okataina is variably manifest as scalloped slump scars in pre-caldera rhyolite domes and ignimbrites, eroded caldera walls, rectilinear fault scarps coincident with regional faulting, and in the SW by the steep margins of post-caldera constructional rhyolite domes. As such, the composite topographic margin defines a depression considerably modified from the original multiple collapse structure. Distinct embayments occur on each side of OCC where it is intersected by regional faulting of the axial rift within the Okataina transfer zone. These are contiguous with two intra-caldera dome complexes forming two overlapping linear vent zones, which transect the caldera complex as the lateral continuation of the adjacent rift segment axes. The boundaries of individual collapse events are complex and largely overprinted by subsequent volcanism and tectonism, but caldera reconstructions suggest the major collapses are centered on the axes of the intersecting rift segments. Lakes at Okataina exhibit a moat

pattern where they have ponded between the topographic rim of the caldera and caldera-filling post-caldera constructional volcanism; lakes filling earlier manifestations of the structure may have been much larger.

Taupo Caldera Complex

Taupo Caldera Complex (COLE *et al.*, 1998) has been frequently active in the past ca. 65 ka (WILSON *et al.*, 1986; HOUGHTON *et al.*, 1995), while its poorly constrained early eruptive history indicates activity over ca. 300 ka (WILSON *et al.*, 1986; COLE *et al.*, 1998). The caldera-forming Oruanui eruption at 26.5 ka (calibrated; WILSON, 1993) generated a c.430 km^3 fall deposit, a 320 km^3 bulk volume non-welded density current deposits (mostly ignimbrite) and ~420 km^3 of caldera-fill material erupted, equivalent to ~530 km^3 of magma (WILSON, 2001). The Oruanui event is thus largely responsible for the modern caldera morphology (Fig. 8). WILSON (1993) has identified 28 separate eruptions since the Oruanui eruption, the most recent and largest of these, the caldera forming 35 km^3 Taupo ignimbrite eruption, occurred about 1800 years ago from vents near the Horomatangi Reefs in the eastern part of the lake (WILSON & WALKER, 1985; SMITH & HOUGHTON, 1995).

The early history (>65 ka) of volcanism in the vicinity of modern Lake Taupo is represented mainly by domes and limited pyroclastics scattered around the lake (SUTTON *et al.*, 1995). Two ignimbrites exposed on the margin of the caldera are commonly attributed to a Taupo source (SUTTON *et al.*, 1995; COLE *et al.*, 1998), although their limited extent means their relationship to the current caldera complex is ambiguous. Pre-caldera rhyolite lavas form a series of headlands along the northern caldera margin and to the southwest of the caldera, while the large caldera-filling domes and flows characteristic of OCC are noticeably absent. Post-Oruanui activity has been studied in detail, and a sequence of 28 eruptions is now recognized (WILSON, 1993; SUTTON *et al.*, 1995). Vents for the post-Oruanui explosive eruptions are inferred by isopach data to be concentrated along a NE-trending lineation in the eastern part of modern Lake Taupo (WILSON, 1993). Construction of a dome complex in this area during the post-Oruanui phase is suggested by lithic componentry data for the Taupo Ignimbrite (COLE *et al.*, 1998) with its likely destruction during the Taupo eruption. Lithic componentry analysis of both the Oruanui and Taupo ignimbrites identifies different lithic suites, interpreted by COLE *et al.* (1998) as reflecting dissimilar sub-caldera geology beneath mutually exclusive collapse structures.

Petrological studies (e.g. SUTTON *et al.*, 1995; 2000) show a complex magmatic system, involving the stepwise appearance of compositionally distinct magma batches with short crustal-residence times. Eruptives prior to the Oruanui eruption form distinct compositional and spatial groups, while a large isotopically homogeneous magma body was generated prior to the Oruanui caldera-forming eruption (SUTTON *et al.*, 1995). Some of the pre-Oruanui domes exposed on the northern caldera margin, and widespread tephras erupted between 65ka and the Oruanui eruption, are the same composition as the Oruanui magma, and thus record the coalescence of a large magma chamber. SUTTON *et al.* (1995) also point out that compositionally distinct magmas were erupted during the same period from different areas around Taupo, and that ignimbrite pumice chemistry indicates additional magma batches may have been eviscerated during the Oruanui eruption. Eruptives of the post-Oruanui sequence form four temporally grouped magma types and are compositionally distinct from the Oruanui magma. The youngest magma, associated with the Taupo eruption, represents the largest homogeneous magma accumulation in the post-Oruanui sequence (SUTTON *et al.*, 1995).

A large trapezoidal-shaped negative Bouguer gravity anomaly is documented over the northern part of the lake (DAVY & CALDWELL, 1998) consistent with earlier onshore investigations (ROGAN, 1982). It is the most intense negative gravity anomaly in TVZ (DAVY & CALDWELL, 1998), and indicates a collapse structure filled with volcaniclastics of relatively low-density. The

gravity anomaly is consistent with a caldera collapse structure elongate NW-SE, perpendicular to the axial rift zone in this segment. The gravity data do not facilitate identification of individual collapse structures, and DAVY & CALDWELL (1998) consider the structures are nested, with the Taupo eruption producing additional subsidence in the northeast part of the modern lake. Geophysical data also demonstrate differential subsidence towards the caldera in the southern part of the lake, and a NW-SE-trending structural boundary marking the southern caldera margin (DAVY & CALDWELL, 1998). Seismic reflection, gravity and magnetic data presented by DAVY & CALDWELL (1998) all suggest that a line between Karangahape Cliffs and Motutere Point marks a major structural boundary perpendicular to the trend of TVZ.

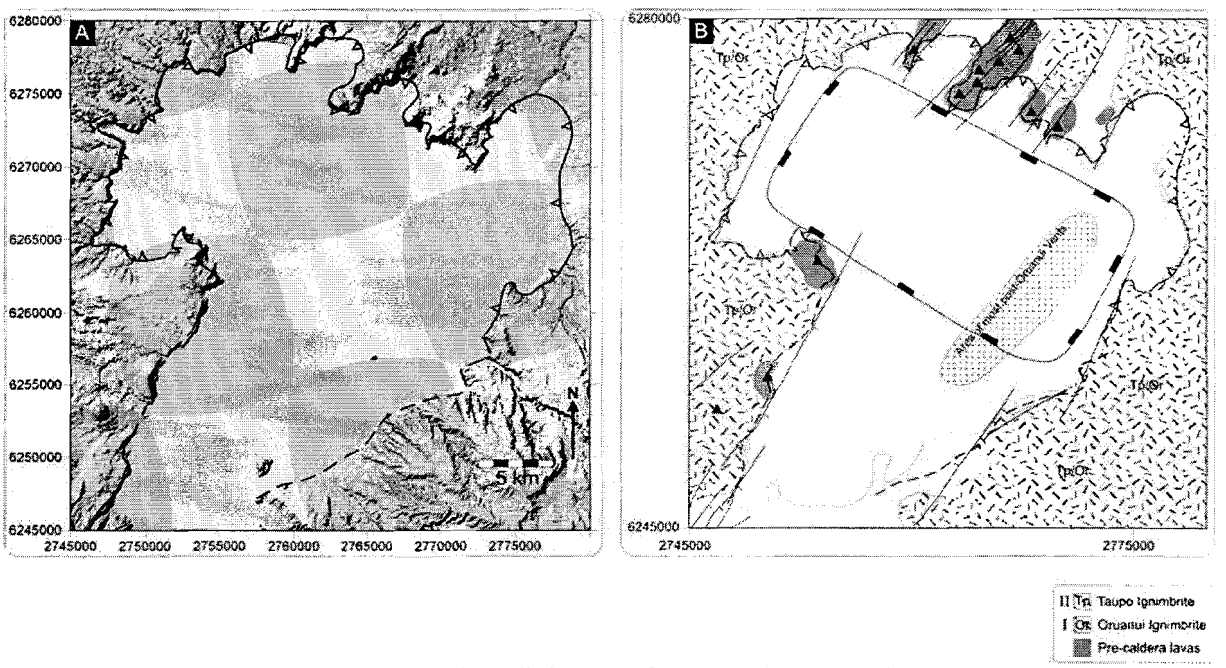

Figure 8 Taupo Caldera Complex. **A:** Shaded relief image of Taupo Caldera Complex; **B:** Structure map of Taupo Caldera Complex from analysis of DEM data. Also shown are pre-caldera lavas and caldera-forming ignimbrites and the location of the post-Oruanui vents (from Spinks et al., in press).

New DEM and field data show that Taupo is located within the axial rift zone of TVZ. The 28 x 16 km caldera complex is rectangular and a long axis trending N63°W, roughly perpendicular to the Taupo North rift segment (FIG. 8). The northern caldera margin intersects NE-trending regional faults controlling a series of peninsulas and embayments in the topographic margin. Pre-caldera lavas to the southwest and north of the modern lake are aligned along regional trends. To the east and west of the caldera, the planar ignimbrite surface is gently tilted toward the lake where the eastern and western margins are partially eroded but generally NE-trending linear features .

The southern part of Lake Taupo occupies a NE-trending fault-bounded depression intersecting the southern caldera margin; the western margin of this structure is a continuation of fault systems dissecting the Tongariro Volcanic Centre to the south. A prominent structural feature is the divergence in fault trend (~20°) to the south and north of the caldera complex. This bend effectively forms the boundary between the Tongariro and Taupo South rift segments. Vents for pre-caldera lavas to the south and north of the caldera complex lie along NE-trending lineaments; the vents for post-Oruanui eruptions mostly occur along the eastern edge of the caldera complex (WILSON, 1993).

Across-axis relationship between tectonism and magmatism

The characteristics of Modern TVZ calderas (i.e. <300 ka; Taupo, Okataina, Rotorua and Reporoa) clearly elucidate the complex eruptive and structural history of Okataina and Taupo in relation to Rotorua and Reporoa. These data therefore show that caldera structures of Modern TVZ can be divided into two groups (1) extra-rift calderas (Reporoa and Rotorua) are simple, relatively small, sub-circular, monogenetic structures, without significant coupling to active regional structure, and where caldera-forming ignimbrites are associated with zoned magma chambers, and (2) intra-rift caldera complexes (Okataina and Taupo) are large, multiple collapse structures, with rectangular geometries and clear coupling to regional structure; here homogeneous magmas are erupted during caldera-forming events (FIG 9). This distinction demonstrates the role of active regional tectonics in influencing the location, structure and development of caldera systems within a rift zone.

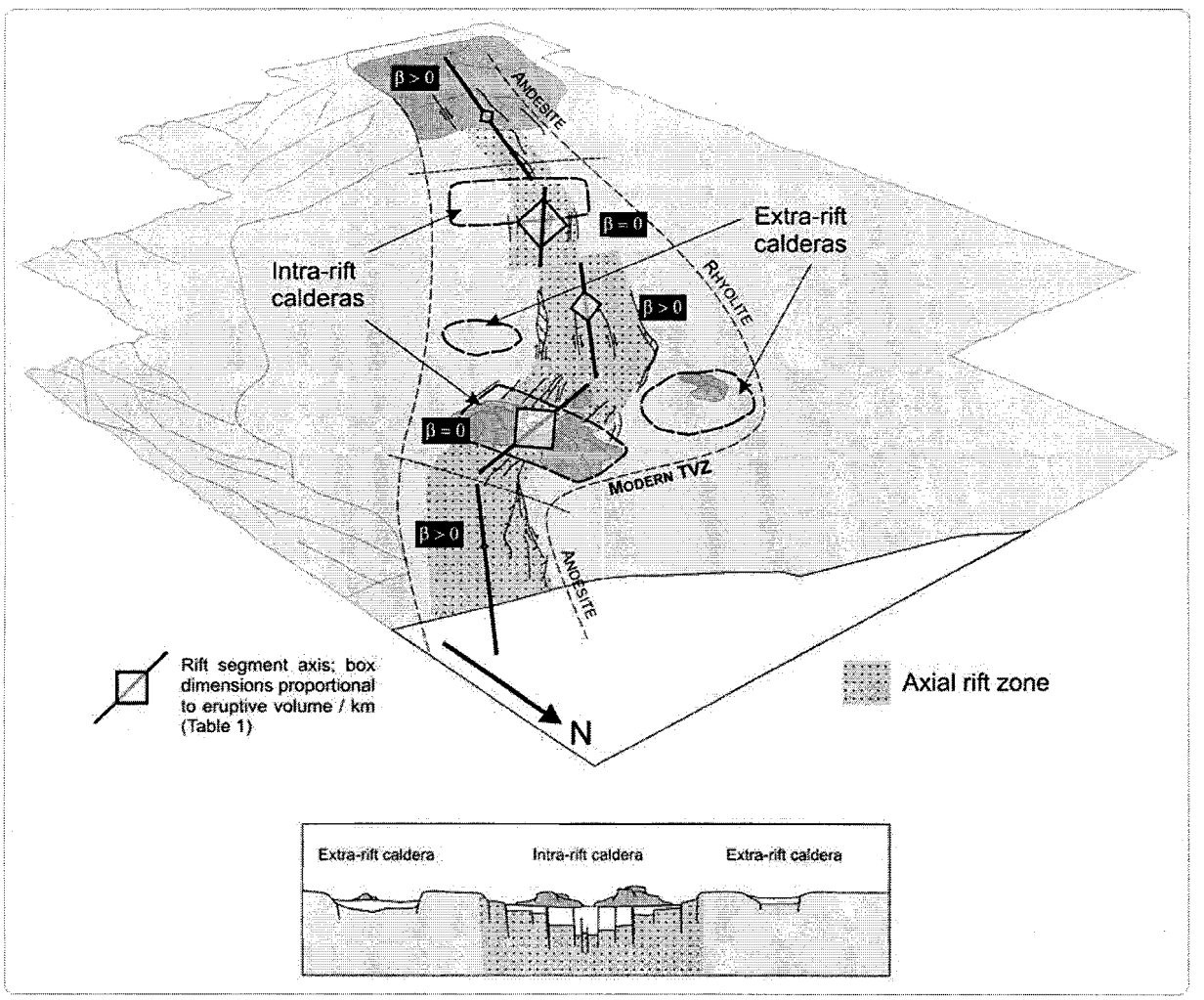

Figure 9 Schematic figure of TVZ (oblique map and section view) summarising the overall structural control on volcanism. The variation in the dextral component of extension (ß), the erupted volumes (proportional to squares), and the caldera structures in 'modern' TVZ, are reported as a function of segment trend (along axis) and the distance from axis (across axis). (from Spinks et al., in press)

REFERENCES

Acocella, V., Spinks, K.D., Cole, J.W. and Nicol, A. 2003. Oblique back arc rifting of Taupo Volcanic Zone, New Zealand. Tectonics, 22(4):1045 doi: 0.1029/2002TC001447

Bailey, R.A and Carr, R.G. 1994. Physical geology and eruptive history of the Matahina Ignimbrite, Taupo Volcanic Zone, North Island, New Zealand. N.Z. Jour. Geol. Geophys., 37: 319-344

Bellamy, S. 1991. Some studies of the Te Wairoa ignimbrites and the associated volcanic geology of the SW Okataina volcanic centre, Taupo Volcanic Zone. Unpublished MSc thesis, University of Waikato, Hamilton, New Zealand.

Beresford, S.W. 1997. Volcanology and geochemistry of the Kaingaroa Ignimbrite, Taupo Volcanic Zone, New Zealand. Unpublished PhD thesis, University of Canterbury, Christchurch, New Zealand.

Beresford, S.W. and Cole, J.W. 2000a. Kaingaroa Ignimbrite, Taupo Volcanic Zone, New Zealand: evidence for asymmetric caldera subsidence of the Reporoa Caldera. N.Z. J. Geol. Geophys., 43: 471-481.

Beresford, S.W. and Cole, J.W. 2000b. Kawerau Ignimbrite: a 0.24 Ma ignimbrite erupted from the Okataina caldera complex, Taupo Volcanic Zone, New Zealand. N.Z. J Geol. Geophys. 43 (1): 109-115.

Beresford, S.W., Cole, J.W., and Weaver, S.D. (2000). Weak chemical and mineralogical zonation in the Kaingaroa Ignimbrite, Taupo Volcanic Zone, New Zealand. N.Z. Jour. Geol. Geophys. 43(4): 639-680.

Black, T.M., Shane, P.A.R., Westgate, J.A. and Froggatt, P.C. 1996. Chronology and paleomagnetic constraints on widespread ignimbrites of the Taupo volcanic zone, New Zealand. Bull. Volcanol. 58, 226-238

Blank, H.R. 1965. Ash-flow deposits of the Central King Country, New Zealand. N.Z. J Geol. Geophys. 8: 588-607.

Bowyer, D.A. 2001. Petrologic, geochemical, and isotopic evolution of rhyolite lavas from the Okataina, Rotorua, and Kapenga volcanic centres, Taupo Volcanic Zone, New Zealand. Unpublished PhD thesis, University of Waikato, Hamilton, New Zealand.

Briggs, N.D. 1973. Investigations of New Zealand pyroclastic flow deposits. Unpublished PhD thesis, Victoria University of Wellington, New Zealand. 433p.

Briggs, N.D. 1976. Welding and crystallization zonation in Whakamaru Ignimbrite, Central North Island, New Zealand. N.Z. J Geol. Geophys. 19 (2): 189-212.

Brooker, M.R., Houghton, B.F., Wilson, C.J.N. and Gamble, J.A. 1993. Pyroclastic phases of a rhyolitic dome-building eruption; Puketarata tuff ring, Taupo volcanic zone, New Zealand. Bull. Volcanol. 55: 395-406.

Brown, S.J.A. 1994. Geology and geochemistry of the Whakamaru Group Ignimbrites and associated rhyolite domes, Taupo Volcanic Zone, New Zealand. Unpublished PhD thesis, University of Canterbury, Christchurch, New Zealand.

Brown, S.J.A., Smith, R.T. and Cole, J.W. 1994. Compositional and textural characteristics of the strombolian and surtseyan K-Trig basalts, Taupo Volcanic Centre, New Zealand: implications for eruption dynamics. N.Z. J Geol. Geophys. 37: 113-126.

Brown, S.J.A, Burt, R.M., Cole, J.W, Krippner, S.J.P., Price, R.C. and Cartwright, I., 1998. Plutonic lithics in ignimbrites of Taupo Volcanic Zone, New Zealand: Sources and conditions of crystallisation. Chem. Geol., 148: 21-41.

Burt, R.M., Brown, S.J.A., Cole, J.W., Shelley, D. and Waight, T.E. (1998). Glass-bearing plutonic fragments from ignimbrites of the Okataina volcanic complex, Taupo Volcanic Zone, New Zealand; remnants of a partially molten intrusion associated with preceding eruptions. J. Volcanol. Geotherm. Res. 84: 209-337.

Cole, J.W. 1990. Structural control and origin of volcanism in the Taupo volcanic zone, New Zealand. Bull. Volcanol., 52: 445-459

Cole, J.W., Brown, S.J.W., Burt, R.M., Beresford, S.W. and Wilson, C.J.N. 1998. Lithic types in ignimbrites as a guide to the evolution of a caldera complex, Taupo volcanic centre, New Zealand. J. Volcanol. Geotherm. Res. 80, 217-237.

Dade, W.B. and Huppert, H.E. 1996. Emplacement of the Taupo Ignimbrite by a dilute turbulent flow. Nature, 381: 509-512.

Davy, B.W. and Caldwell, T.G. 1998. Gravity, magnetic and seismic surveys of the caldera complex, Lake Taupo, North Island, New Zealand. J. Volcanol. Geotherm. Res., 81, 69-89.

Ewart, A. 1965. Mineralogy and petrogenesis of the Whakamaru Ignimbrite in the Maraetai area of the Taupo Volcanic Zone, New Zealand. N.Z. J Geol. Geophys. 8 (4): 611-677.

Froggatt, P.C., Wilson, C.J.N. and Walker, G.P.L. 1981. Orientation of logs in the Taupo Ignimbrite as an indicator of flow direction and vent position. Geology 9: 109-111.

Froggatt, P.C. and Lowe, D.J. 1990. A review of late quaternary silicic and some other tephra formations from New Zealand; their stratigraphy, nomenclature, distribution, volume, and age. N.Z. J. Geol. Geophys., 33: 89-109.

Gravley, D.M. 2005. The Ohakuri pyroclastic deposits and the evolution of the Rotorua-Ohakuri volcanotectonic depression. Unpublished PhD thesis, University of Canterbury, Christchurch, New Zealand.

Gravley, D. M., Wilson, C.J.N., Cole, J.W. and Leonard, G.S. 2003. Temporally and tectonically linked eruption and caldera collapse events in the central Taupo Volcanic Zone, New Zealand. Abstract, Geological Society of NZ Annual Conference, Dunedin 1-4 December 2003. Geological Society of NZ Miscellaneous Publication 116A: 63

Grindley, G.W. 1960. Sheet 8 – Taupo. Geological map of New Zealand 1:250:000. New Zealand Department of Scientific and Industrial Research, Wellington.

Grindley, G.W. 1965. The Geology, structure and exploitation of the Wairakei Geothermal Field, Taupo, New Zealand. New Zealand Geological Survey Bulletin 75. 131p.

Hatherton, T. 1954. The magnetic properties of the Whakamaru Ignimbrites. N.Z. J. Sci Tech.,358: 421-432.

Henneberger, H.C. 1983. Petrology and evolution of the Ohakuri hydro-thermal system, Taupo Volcanic Zone, New Zealand. Unpublished MSc (Hons) thesis, University of Auckland, New Zealand.

Houghton, B.F., Lloyd, E.F., Wilson, C.J.N. and Lanphere, M.A. 1991. K/Ar ages of obsidians from some rhyolite lavas in the Maroa-Taupo area, Taupo Volcanic Centre, New Zealand. N.Z. J Geol. Geophys. 34: 99-101.

Houghton, B.F., Wilson, C.J.N., McWilliams, M.O., Lanphere, M.A., Weaver, S.D., Briggs, R.M. and Pringle, M.S. 1995. Chronology and dynamics of a large silicic magmatic system: Central Taupo Volcanic Zone, New Zealand. Geology 23, 13-16

Hunt, T.M. (1992) Gravity studies in the Rotorua area, New Zealand. Geothermics 21: 65-74.

Kohn, B.P. 1973. Some studies of New Zealand Quaternary pyroclastic rocks. Unpublished PhD thesis, Victoria University of Wellington, New Zealand.

Jackson, R.S. 2004. The Rautawiri Breccia, Taupo Volcanic Zone, New Zealand. Unpublished BSc (Hons) project, University of Canterbury, Christchurch, New Zealand.

Jurado-Chichay, Z. and Walker, G.P.L. 2000. Stratigraphy and dispersal of the Mangaone Subgroup pyroclastic deposits, Okataina Volcanic Centre, New Zealand. J. Volcanol. Geotherm. Res., 104: 319-283.

Lamarche, G. 1992. Seismic reflection survey in the geothermal field of the Rotorua Caldera, New Zealand. Geothermics, 21: 109-120.

Leonard, G.S. 2003. The evolution of Maroa Volcanic Centre, Taupo Volcanic Zone, New Zealand. Unpublished PhD thesis, University of Canterbury, Christchurch, New Zealand.

Leonard, G.S., Cole, J.W, Nairn, I.A and Self, S. 2002. Basalt triggering of the c. AD 1305 Kaharoa rhyolite eruption, Tarawera Volcanic Complex, New Zealand. J. Volcanol. Geotherm. Res., 115: 461-486.

Lewis, J.F. 1968. Tauhara Volcano, Taupo Zone, Part 1 – Geology and structure. N.Z. J Geol. Geophys. 11 (1): 212-224.

Manville, V. 2001. Sedimentology and history of Lake Reporoa: an ephemeral supra-ignimbrite lake, Taupo Volcanic Zone, New Zealand. Spec. Pub. Int. Ass. Sediment. 30: 109-140.

Martin, R.C. 1961. Stratigraphy and structural outline of the Taupo Volcanic Zone. N.Z. J Geol. Geophys. 4: 449-478.

Martin, R.C. 1965. Lithology and eruptive history of the Whakamaru Ignimbrite in the Maraetai area of the Taupo Volcanic Zone, New Zealand. N.Z. J Geol. Geophys. 8: 680-702.

Milner, D.M., Cole, J.W. and Wood, C.P. 2002. Asymmetric, multiple-block collapse at Rotorua Caldera, Taupo Volcanic Zone, New Zealand. Bull. Volcanol. 64, 134-149

Milner, D.M., Cole, J.W. and Wood, C.P. 2003. Mamaku Ignimbrite: a caldera-forming ignimbrite erupted from a compositionally zoned magma chamber in Taupo Volcanic Zone, New Zealand. J. Volcanol. Geotherm. Res. 122, 243-264.

Modriniak, N and Studt, F.E. 1959. The geological structure and volcanism of the Taupo-Tarawera District. N.Z. J Geol. Geophys. 2 (4): 654-684.

Nairn, I.A. 1981. Some studies of the geology, volcanic history and geothermal resources of the Okataina volcanic centre, Taupo Volcanic Zone, New Zealand, Unpublished PhD thesis, Victoria University, Wellington, New Zealand.

Nairn, I.A. 1989. Sheet V16AC – Mount Tarawera, geological map of New Zealand, 1:50,000, Department of Scientific and Industrial Research, Wellington.

Nairn, I.A. 2002. Geology of the Okataina Volcanic Centre, Institute of Geological and Nuclear Sciences Geological Map 25: 156p + map.

Nairn, I.A, Wood, C.P. and Bailey, R.A. 1994. The Reporoa Caldera, Taupo Volcanic Zone: source of the Kaingaroa Ignimbrites. Bull. Volcanol. 56, 529-537

Newnham, R.M., Eden, D.N., Lowe, D.J. and Hendy, C.H. 2003. Rerewhakaaitu Tephra, a land-sea marker for the last termination in New Zealand, with implications for global climate change. Quaternary Science Reviews, 22: 289-308.

Northey, D.J. 1983. Seismic studies of the structure beneath Lake Taupo. Unpublished PhD thesis, Victoria University of Wellington, New Zealand.

Ritchie, A. 1996. Volcanic geology of the Waiotapu and related ignimbrites, Taupo Volcanic Zone. Unpublished MSc. thesis, University of Canterbury, Christchurch, New Zealand.

Rogan, M., 1982. A geophysical study of the Taupo Volcanic Zone, New Zealand. J. Geophys. Res., 87: 4073-4088.

Self, S. and Sparks, R.S.J. 1978. Characteristics of widespread pyroclastic deposits formed by the interaction of silicic magma and water. Bull. Volcanol. 41: 196-212.

Shane, P., Black, T. and Westgate, J. 1994. Isothermal plateau fission track age for the paleomagnetic excursion in the Mamaku Ignimbrite, New Zealand, and implications for late Quaternary stratigraphy. Geophys. Res. Lett. 21, 1695-1698.

Sherburn, S., Bannister, S. and Bibby, H. 2003. Seismic velocity structure of the central Taupo Volcanic Zone, New Zealand, from local earthquake tomography. J. Volcanol. Geotherm. Res., 122: 69-88.

Smith, R.T. 1998. Eruptive and depositional models for units 3 and 4 of the 1.85 Ka Taupo eruption. Unpublished Ph.D. thesis, University of Canterbury, Christchurch, New Zealand.

Smith, R.T. and Houghton, B.F. 1995. Vent migration and changing eruptive style during the 1800 ka Taupo eruption: new evidence from the Hatepe and Rotongaio phreatoplinian ashes. Bull. Volcanol., 57: 432-439.

Smith, V.C., Shane, P. and Smith, I.E.M. 2002. Tephrostratigraphy and geochemical fingerprinting of the Mangaone Subgroup tephra beds, Okataina Volcanic Centre, New Zealand. N.Z. J Geol. Geophys., 45: 207-219.

Soengkono, S. and Hochstein, M.P. 1996. Interpretation of magnetic anomalies over the Reporoa geothermal field, Taupo Volcanic Zone, New Zealand. Proceedings 18th N.Z. Geothermal workshop: 243-248.

Spinks, K.D. 2005. Rift Architecture and Caldera Geometry of the Taupo Volcanic Zone, New Zealand. Unpublished Ph.D. thesis, University of Canterbury, Christchurch, New Zealand.

Spinks, K.D., Acocella, V., Cole, J.W. and Bassett, K.N. in press. Structural control on volcanism and caldera development in the transtentional Taupo Volcanic Zone, New Zealand. J. Volcanol. Geotherm. Res..

Stagpoole, V.M. 1994. Interpretation of refraction seismic and gravity data across the eastern margin of the Taupo Volcanic Zone. Geothermics, 23: 501-510.

Stagpoole, V. M. and Bibby, H. M. 1999. Residual gravity anomaly map of the Taupo Volcanic Zone, New Zealand, 1:250 000, version 1.0. Institute of Geological & Nuclear Sciences Geophysical Map 13. Institute of Geological & Nuclear Sciences Limited, Lower Hutt, New Zealand.

Sutton, A.N., Blake, S. and Wilson, C.J.N. 1995. An outline geochemistry of rhyolite eruptives from Taupo volcanic centre, New Zealand. J. Volcanol. Geotherm. Res., 68: 153-175.

Sutton, A. N., Blake, S., Wilson, C.J.N. and Charlier, B.L.A. 2000. Late Quaternary evolution of a hyperactive rhyolite magmatic system: Taupo volcanic centre, New Zealand. J. Geol. Soc. London, 157: 537-552.

Sutton, R. 1990. The geology, petrography and geochemistry of the area surrounding Rangatira Point, northeast Lake Taupo, New Zealand. Unpublished B.Sc. (hons) thesis, Victoria University of Wellington, Wellington, New Zealand.

Talbot, J.P., Self, S., and Wilson, C.J.N. 1994. Dilute gravity current and rain-flushed ash deposits in the 1.8 ka Hatepe Plinian deposit, Taupo, New Zealand. Bull. Volcanol., 56: 538-551.

Walker, G.P.L. 1980. The Taupo Pumice: product of the most powerful known (ultraplinian) eruption? J. Volcanol. Geotherm. Res. 8: 69-94.

Walker, G.P.L. 1981. An ignimbrite veneer deposit: the trail maker of a pyroclastic flow. J. Volcanol. Geotherm. Res. 9: 409-421.

Wilson, C.J.N. 1985. The Taupo eruption, New Zealand. II. The Taupo ignimbrite. Phil. Trans. Roy. Soc., Lond. A314: 229-310.

Wilson, C.J.N. 1993. Stratigraphy, chronology, styles and dynamics of late Quaternary eruptions from Taupo volcano, New Zealand. Phil. Trans. R. Soc. Lond., A 205-306.

Wilson, C.J.N. 2001. The 26.5 ka Oruanui eruption, New Zealand: an introduction and overview. J. Volcanol. Geotherm. Res. 112: 133-174.

Wilson, C.J.N., Rogan, M.A., Smith, I.E.M., Northey, D.J., Nairn, I.A. and Houghton, B.F. 1984. Caldera volcanoes of the Taupo Volcanic Zone, New Zealand. J. Geophys. Res., 89: 8463-8484.

Wilson, C.J.N, and Walker, G.P.L. 1985. The Taupo eruption, New Zealand. Phil. Trans. R. Soc. London, Ser. A, 314: 199-228.

Wilson, C.J.N, Houghton, B.F. and Lloyd, E.F. 1986. Volcanic history and evolution of the Maroa – Taupo area, Central North Island. In: I.E.M Smith (Editor), Late Cenozoic volcanism in New Zealand. R. Soc. N.Z. Bull., 23: 194-223.

Wilson, C.J.N., Houghton, B.F., McWilliams, M.O., Lanphere, M.A., Weaver, S.D. and Briggs, R.M. 1995. Volcanic and structural evolution of Taupo Volcanic Zone, New Zealand: A review. J. Volcanol. Geotherm. Res., 68: 1-28.

Wood, C.P. 1992. Geology of the Rotorua Geothermal System. Geothermics 21: 25-41

Block and Ash Flows of the Waiohau Eruptive Episode

KARL SPINKS, 2001

INTRODUCTION

Objectives and Method

The heavily dissected plateau south of the Tarawera River to the edge of the Pokohu Lava flow is volcanic breccia of the "northern pyroclastics" NAIRN (1981). These deposits are thought to be block and ash flows generated by dome collapse during the construction of the Tarawera massif (NAIRN, *pers comm.* 2000). This conclusion is speculative however, and the nature and extent of these deposits is poorly understood. The prime objective of this study is therefore to investigate these deposits, with particular regard to their physical volcanology, in order to establish their genesis. Clear felling by Fletcher Forests of the area northeast of Mt Tarawera to the Tarawera River during 1998 enabled access into difficult terrain and created new exposures. A limited time window was available to investigate these deposits and hence the instigation of this study.

Basic field investigations were used to determine the nature and extent of the deposits in order to understand their genesis and relationship to the growth of the Tarawera Volcanic Complex. Lithological classifications concentrated on grainsize distributions, component analysis and the degree and type of welding. The nature of the study did not enable detailed petrographic or geochemical analysis.

Terminology

Block and ash flows have been widely described in the literature as resulting from the collapse of lava domes and flows, but the exact mechanism by which block and ash flows are generated is debated. Since the 1902 eruption of Mt Pelee, two models have been used: one attributes block and ash flows to gravitational collapse of lava flows or domes (Merapi-type); the other to explosive dome collapse (Pelean-type) (FISHER *et al.*, 1980). Most historic examples of block and ash flows, such as at Mt Unzen during 1990-1995 (UI *et al.*, 1999), Mt Merapi in 1930 (NEUMANN VAN PADANG, 1933), and Montserrat during 1996-1998, have been caused by gravitational collapse of the oversteepened front of lava domes or flows. Block and Ash flows of explosive dome collapse origin have been described from Mt Pelee in 1902 (LE CROIX, 1904), Merapi in 1942-1943 (VAN BEMMELEN, 1949) and Mt St Helens in 1986 (MELLORS *et al*, 1988).

Where the excess pore pressure of lava is less than the tensile strength (SATO *et al.* ,1992), the explosive collapse of a dome and fragmentation into fine particles are unlikely. However, SATO *et al* (1992) suggests that at Mt Unzen, variable degrees of degassing of the dacite magma produced a wide range of excess pore pressures, allowing lateral explosions where pore pressure locally exceeded the tensile strength of the lava. It is therefore likely that block and ash flows can be generated from either gravitational or explosive dome collapse, or both, and that the source mechanism may vary within an eruptive episode.

UI *et al* (1999) describe gravitational collapse resulting from both exogenous and endogenous dome growth at Mt Unzen. Block and Ash flows produced from the exogenous growth phase resulted from crack propagation in lava lobes leading to collapse of the lobe front and subsequent fragmentation. Endogenous dome growth during 1994 generated local bulge of the dome leading to collapse of unstable lava blocks and further fragmentation.

TAKAHASHI & TSUJIMOTO (2000) suggest that transport of particles in Merapi-type block and ash flows begins as granular flow, where coarse particles are suspended in flow by repeated collision (dispersive grain pressure) causing further fragmentation. A semi-fluidised zone is thought to develop on top when fragmentation has proceeded to the extent such that the upwards flow of gas is strong enough to suspend particles. Granular flow is essentially driven by gravity, and a lessening of gradient can therefore lead to relatively sudden deposition. According to TAKAHASHI & TSUJIMOTO (2000) deposition from Merapi-type block and ash flows occurs by progressive transfer of material from the fluidised zone to a basal layer as a consequence of a reduction in upwards gas streaming.

Waiohau Eruptive Sequence

Pyroclastic fall, flow, and surge deposits have been documented as part of the Waiohau pyroclastic sequence, and record phases of explosive volcanism before, during, and after the emplacement of lava domes and flows within the Waiohau eruptive episode. Based on the stratigraphy established by COLE (1970) and NAIRN (1981, 1989) and

recently defined in greater detail by SPEED (2001), the Waiohau Pyroclastics are thought to represent the early and intermediate stages of the Waiohau eruptive episode.

While a detailed assessment of the eruptive sequence is beyond the scope of this report, a simplified synopsis is given here. Plinian eruptive events dominated the early and intermediate stages of the eruptive episode. Eastern Dome (Figure 1) was also thought to have extruded early, and was the vent site of early explosive eruptions (SPEED, 2001). Any further dome growth at this time may have been destroyed by subsequent explosive eruptions or dome collapse.

The exact timing of the 'Debris Avalanche' of SPEED (2001; and the subject of this report) is uncertain but was followed by the emplacement of the Waikakareao Lavas and the deposits of further explosive eruptions. In the final phase of the eruptive episode, the Pokohu Lavas were extruded, and Kanakana Dome formed at the main vent site for the Plinian eruptives and lavas.

WAIOHAU BLOCK AND ASH FLOWS

BAF1 - Description

A previously undescribed sequence of pyroclastic breccia, lapilli and ash is exposed in isolated outcrops along a short section south of Waterfall Road. Figure 2 is a graphic log of the section at V16/203332. The base of the sequence is obscured however it is thought that these deposits represent the first of the units deposited in the northern pyroclastics as part of the Waiohau sequence. The basal 6m is poorly sorted pyroclastic breccia dominated by blocks up to 800mm (longest dimension). The unit is not bedded but shows vague normal grading until the upper 500mm, which is conspicuously finer grained. The deposit is well indurated, and vertical jointing is well developed with 1m spacing and joint surfaces cleanly cut through large crystalline rhyolite blocks. The joint-bounded columns have fallen away from the exposure, creating a pseudo-3-dimensional view. Many of the clasts appear aligned and there is some evidence for imbrication. Gas escape structures are present towards the top of the unit, their lapilli contents preferentially picked out by erosion. Besides the large lithic clasts the most conspicuous feature is the smoothness of the outcrop surface. Jointing has left almost

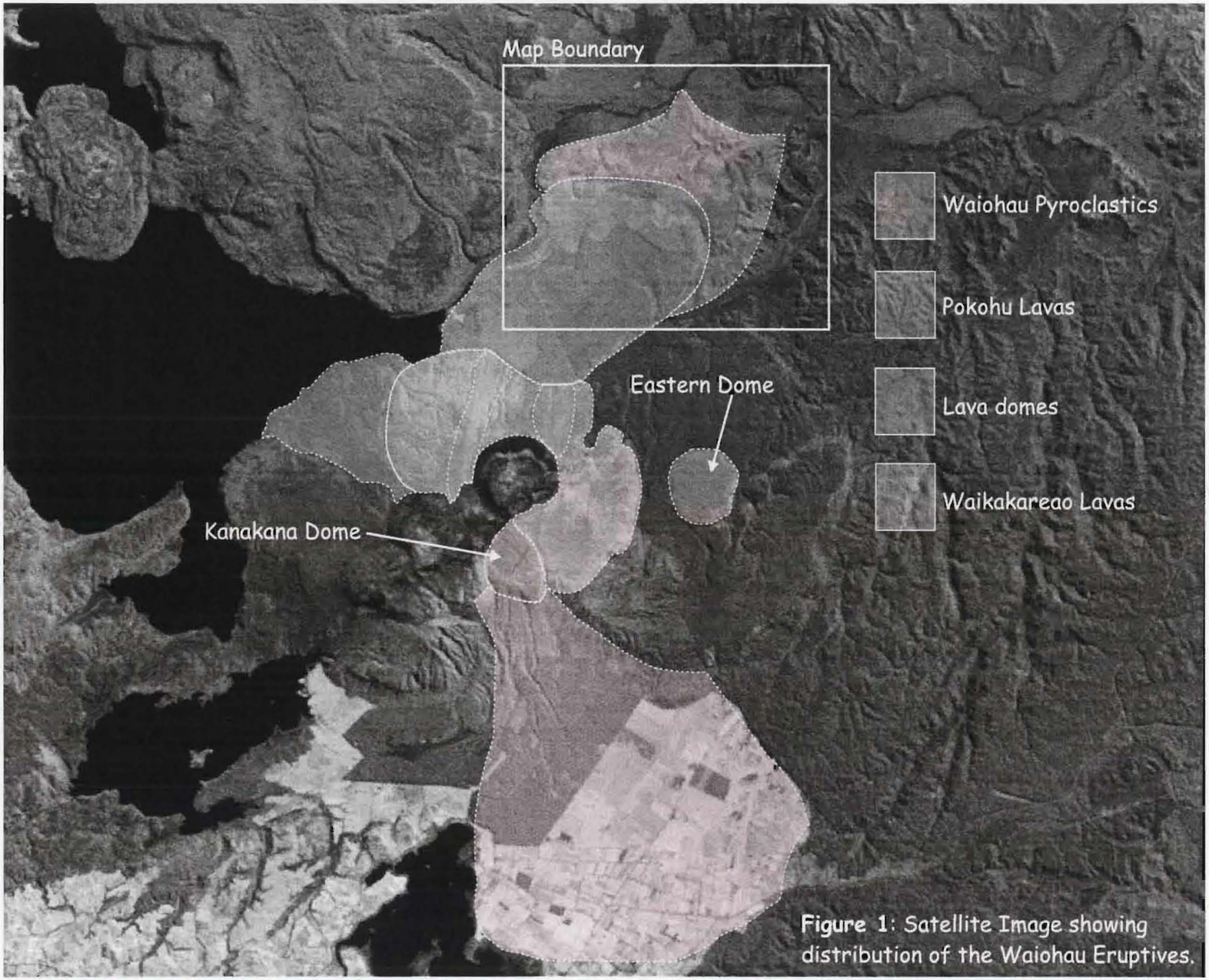

Figure 1: Satellite Image showing distribution of the Waiohau Eruptives.

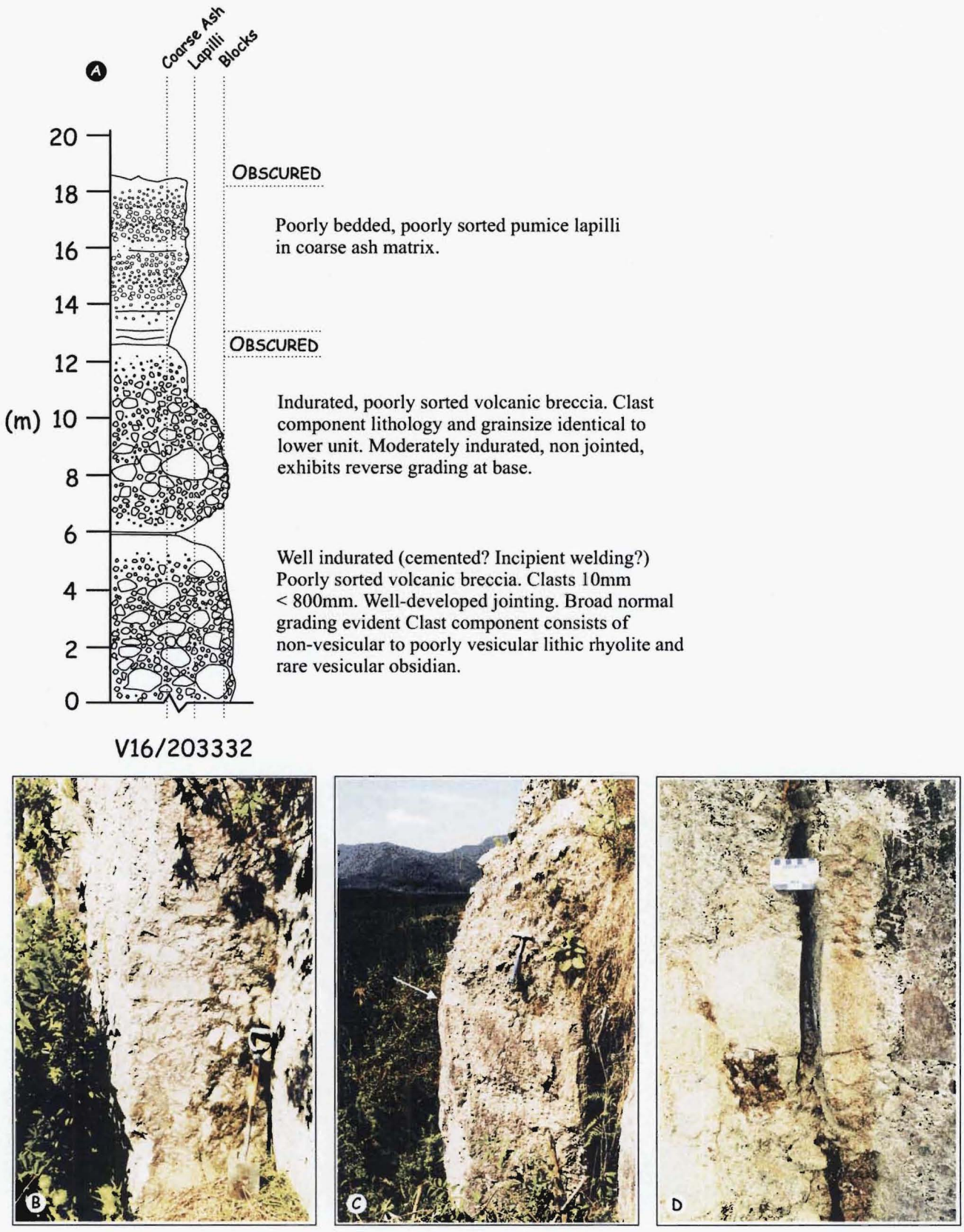

Figure 2: BAF1 outcrop at V16/203332. A) Graphic Log; B) Clean joint surfaces in the lower flow unit; C) The contact (arrow) between lower and upper flow units; D) a crack developed along a joint surface, cutting through a lithic rhyolite clast.

perfectly flat surfaces giving cross-sections through even the largest clasts. The clasts are predominantly angular flow-banded non-vesicular and poorly-vesicular rhyolite blocks and lapilli and rare vesicular obsidian lapilli. It appears from field inspection that almost all size ranges from coarse ash to block are present in the deposit.

A sharp contact separates this unit from the overlying pyroclastic breccia. A 30mm thick fine ash layer separates the two and appears to mantle the upper surface of the lower unit. The upper unit is not bedded but reverse grading can be picked out by a rapid increase in the size of the largest clasts upwards from the base to a maximum about 2m above the base. Normal grading is then observed towards the top, where the maximum size drops from 600mm to 100mm over half a metre. Less indurated than the first, this unit also lacks jointing and clean surfaces, its blocky nature more easily picked out by an irregular profile. The clast population and grainsize distribution is essentially identical to the lower unit.

Overlying an obscured contact is a further 6 metres of poorly bedded pyroclastics dominated by pumice lapilli in a coarse ash matrix. Pumice size and concentration varies but all changes appear gradational. Exposure is obscured by vegetation but a soil horizon above appears to be overlain by the Rotoma Ash (9 ka) which caps the plateau south of Waterfall Road.

Interpretation

The block-rich breccias exposed south of Waterfall Road probably represent the first block and ash flows to descend from the Tarawera massif during the Waiohau eruptive episode. Several lines of evidence suggest that deposition occurred from hot, gas-solid particulate dispersions: (1) Jointing in rocks this young can only be a function of cooling from an originally hot deposit; (2) the presence of gas escape pipes; (3) incipient welding (essentially hot cementation?) of clasts and matrix. Many other features are consistent with a block and ash flow origin: (1) reverse grading, attributed to particle collision during granular flow; (2) monolithologic clast component, attributed to sampling of a single magma at source. Minor variation in lithology may reflect sampling of different dome facies or the incorporation of accidental lithics during transport.

The two breccias are considered as individual flow units, deposited from different collapse events, however the nature of the contact between them suggests only a minor temporal separation. Fine-grained fall deposits are often associated with block and ash flows, derived from the main flow and dispersed far more widely than the flow deposits. The thin fine-grained layer between the two flow units may represent the ash-cloud associated with the lower flow unit. The presence of jointing in the lower unit is likely a function of slow cooling, due to thermal insulation by the upper flow unit.

Pumiceous pyroclastic flows possibly triggered by dome collapse deposited the pumice lapilli deposits overlying the block and ash flow deposits. Poorly vesicular lithic rhyolite lapilli within these deposits represent dome-derived lithics.

BAF2

Overlying the previously described block and ash flow deposits, and forming most of the Waiohau pyroclastic fan northeast of Mt Tarawera (Fig. 1), is a volcanic breccia, variable in both component size and concentration, but with no identified time breaks. Exposure is discontinuous, and there is no complete section through the sequence, but a schematic log is given in Figure 3.

The deposit cannot be divided easily either laterally or vertically, but may comprise several flow units with distinct characteristics. Vertical changes in grainsize and clast concentration and type give a layered appearance (Fig. 4), however changes are always gradual and the deposit is generally unbedded. Both normal and reverse grading were observed and are a common feature of this deposit.

The breccia is poorly sorted, but individual horizons are locally sorted to moderately sorted. Although clast concentration is high, estimated at up to 60%, it is matrix supported throughout. Clasts comprise flow-banded lithic rhyolite, poorly to moderately vesicular rhyolite and highly vesicular obsidian blocks and lapilli. Presence of vesicular obsidian is a characteristic feature of these deposits and is ubiquitous throughout the observed sequence. Grainsize is variable throughout and ranges over almost four orders of magnitude, from the coarse ash matrix to the largest clasts over 1m (longest dimension). Clasts are angular to sub-rounded with rounding increasing with decreasing grainsize.

Figure 3: Schematic section through Waiohau Pyroclastics volcanic breccia exposed in escarpment south of Tarawera River

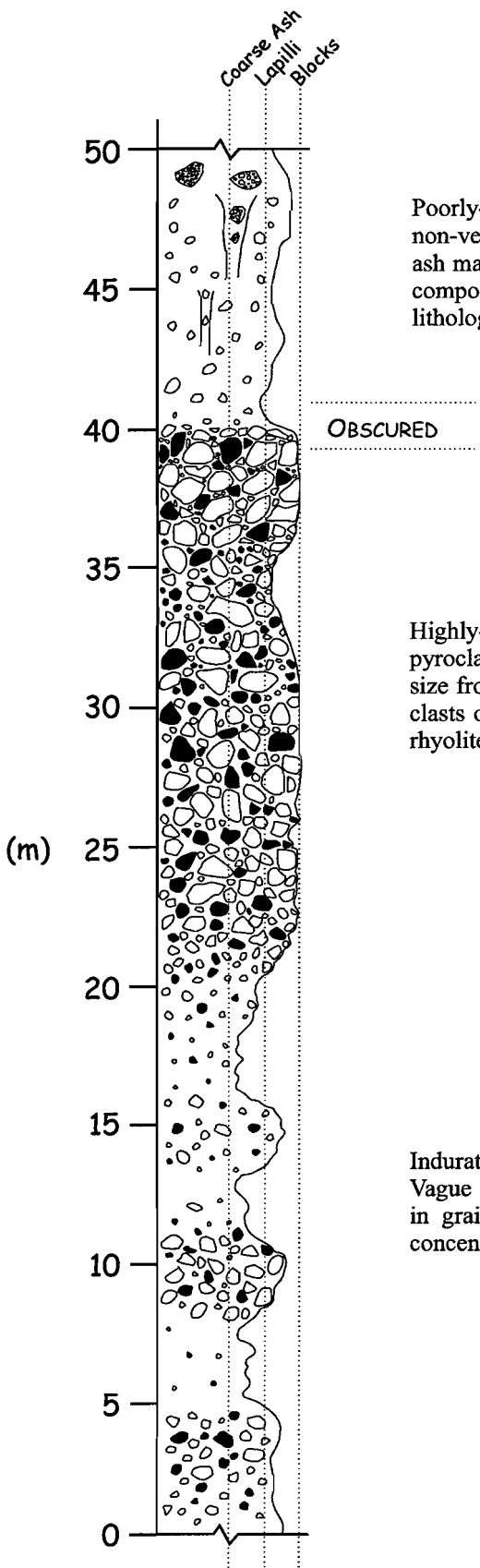

Poorly-indurated, poorly sorted. Moderately to non-vesicular angular rhyolite clasts in a coarse ash matrix. Gas escape pipes concentrate coarser components and contain fragments of clastogenic lithology.

Highly-indurated (incipient welding?) Clast-rich pyroclastic breccia. Poorly sorted, clasts range in size from 10mm to 1m. Angular to sub-rounded clasts of non-vesicular to poorly vesicular lithic rhyolite and highly vesicular obsidian.

Indurated, poorly sorted, pyroclastic breccia. Vague layering defined by vertical changes in grainsize of clast component and clast concentration.

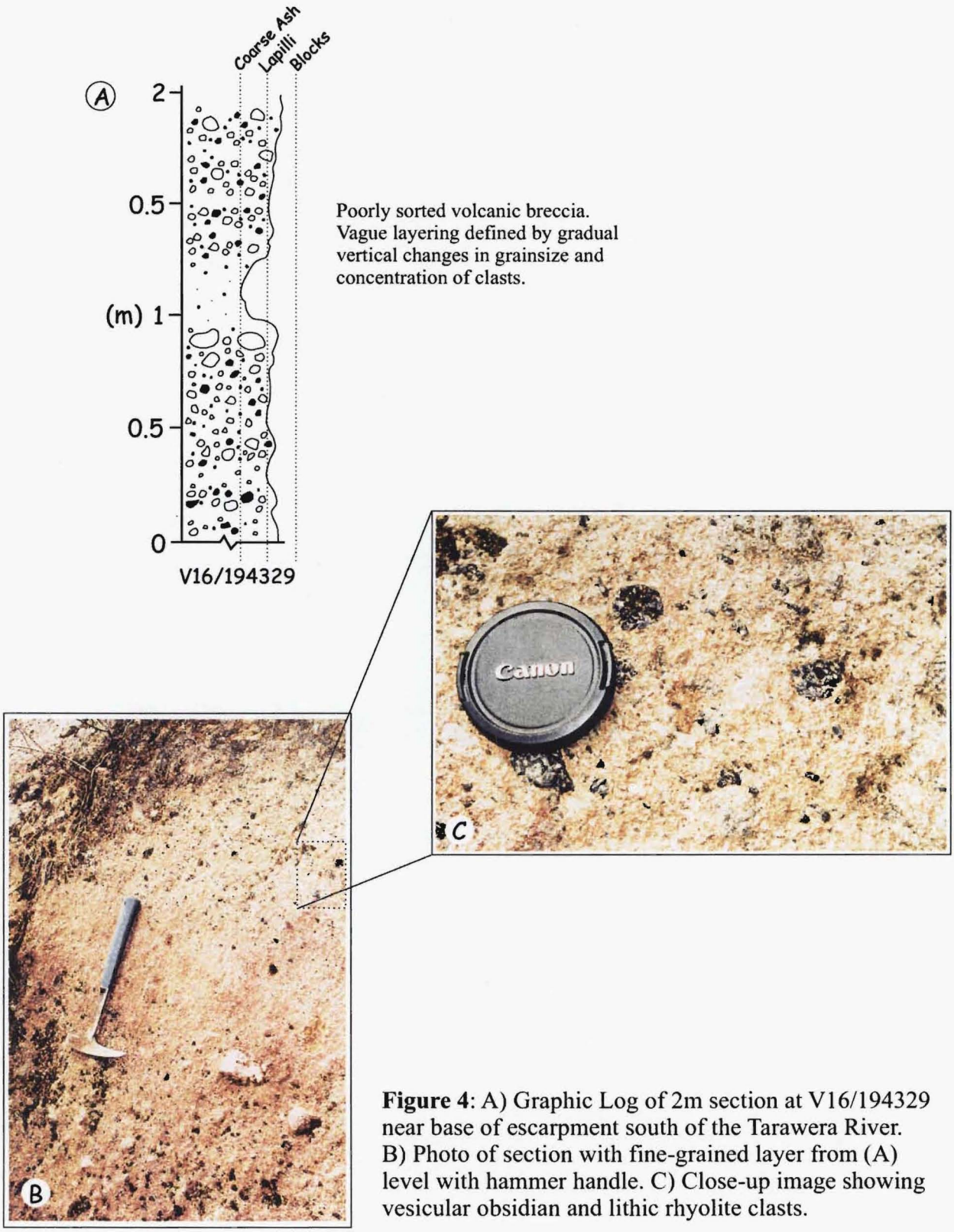

Figure 4: A) Graphic Log of 2m section at V16/194329 near base of escarpment south of the Tarawera River. B) Photo of section with fine-grained layer from (A) level with hammer handle. C) Close-up image showing vesicular obsidian and lithic rhyolite clasts.

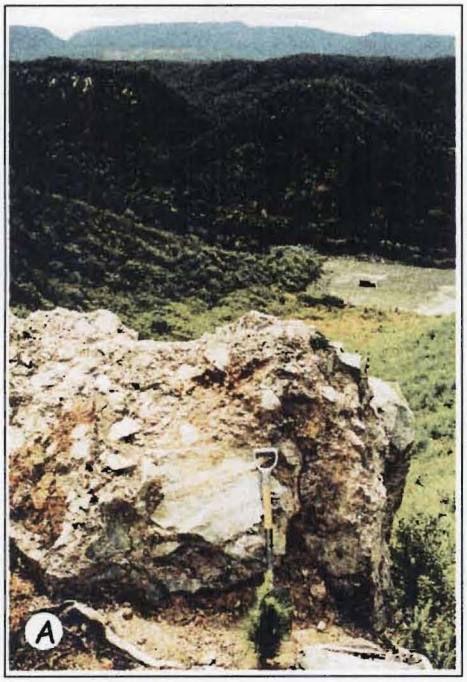

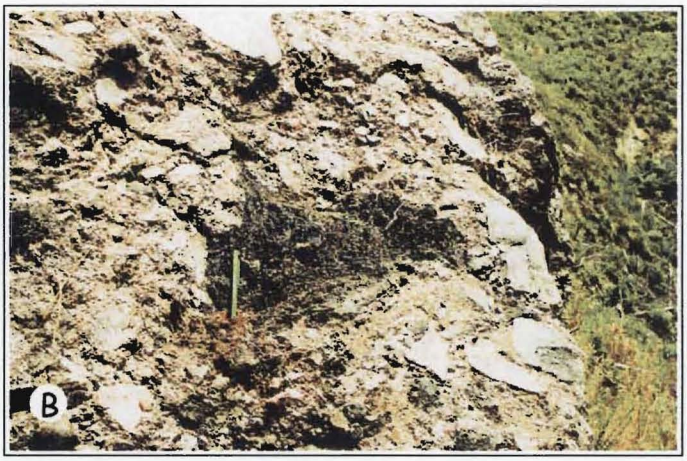

Figure 5: A) Looking north from Bluff outcrop at V16/225326. B) Same outcrop as in (A) showing large vesicular obsidian clast (pencil for scale). See text for discussion.

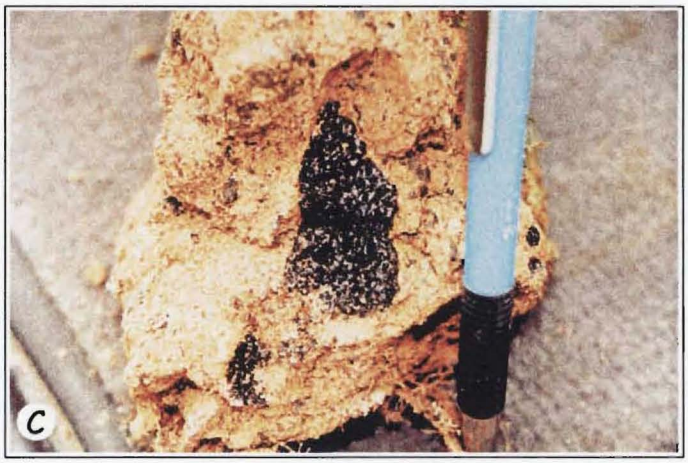

C) Sample of Waiohau volcanic breccia from V16/98325 showing vesicular obsidian clast.

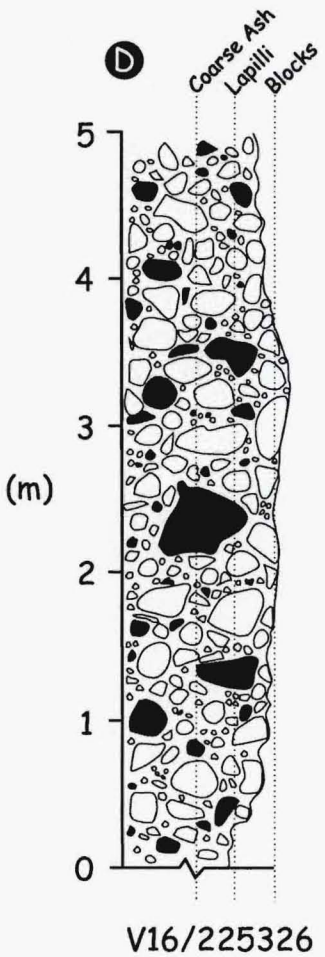

Well indurated, poorly sorted, clast-rich volcanic breccia. Clast grain size range 10mm < 1m. Clasts are variably vesiculated lithic rhyolite and highly vesicular obsidian.

D) Graphic Log of section at V16/225326 (as in photos A and C).

Particular horizons within the deposit are significantly more indurated, contain larger clasts, and are more clast-rich than the bulk of the sequence. Bluff-forming horizons approximately 5m thick within the deposit (See Map) are highly indurated and commonly jointed, and contain the largest of the clasts (Figure 5).

Interpretation

Features of the deposit described here are consistent with a block and ash flow origin. Characteristics may not individually be indicative of a particular genesis, however the properties of the deposit as a whole reflect the mode of fragmentation and deposition.

The clast population is thought to almost entirely juvenile clasts derived from the collapse of part of a growing dome. Without the benefit of geochemical or detailed petrographic analysis, it is impossible to determine the proportion of accidental lithics derived from pre-existing domes or lavas. The clast population is dominated by poorly vesiculated, lithic rhyolite, which occurs in the core of domes and flows (Figure X) where heat retention is greatest and complete crystallisation can occur (Richnow, 1999).

The dominance of crystalline rhyolite indicates that collapse was large enough to sample the interior zone of the dome, and that crystallisation had occurred prior to collapse. Rhyolite domes and lava flows start to cool prior to the onset of crystallisation (the result of the 'nucleation lag time' Manley, 1992); this may help constrain the timing of dome collapse to after cooling had proceeded enough such that crystallisation could occur.

The coarsely vesicular pumice zone is the likely source of the more vesiculated clasts, while the finely vesicular zone would have been crushed during transport and is represented by the ash matrix.

Vesicular obsidian is not typically a common lithology in either domes or block and ash flows.. Cole (1970) first described a flow breccia on the Mt Tarawera access road as an unsorted breccia containing large blocks of vesiculated obsidian in an ash matrix and interpreted it as the result of a nuee ardente eruption. The vesicular obsidian clasts were thought to have formed by re-heating and subsequent gas expansion of pre-existing clasts. The source of the obsidian remains unclear, but its proximity and relationship to

lithic rhyolite in the dome model (Fig. 6) suggests it was derived from here. If collapse occurred while still hot, then vesiculation may result from sudden decompression.

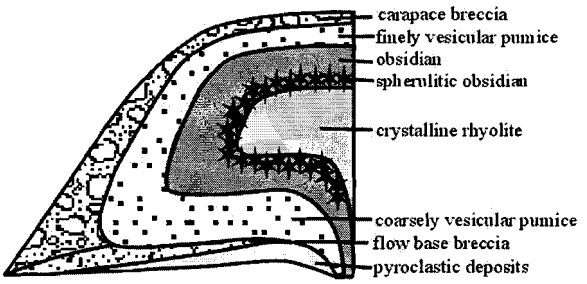

Figure 6: Idealised representation of lithological zonation in a rhyolite dome. After Richnow (1999)

Indurated horizons within the deposit may have formed by deposition from much hotter flow units, caused by collapse into the hot interior of a dome. These indurated or incipiently welded units are associated with an increase in clast size and concentration. Larger clasts may retain their heat for longer and cause partial welding (?) of the ash matrix, resulting in a more coherent deposit. If this theory is correct, then collapse and generation of block and ash flows formed while dome lavas were still hot, but had cooled enough to allow crystallisation. Richnow (1999) in a study of Wahanga Dome at Mt Tarawera, estimated the time needed for the entire dome to cool below the glass-transition temperature at 40 years.

Source

The distribution and stratigraphic position of the block and ash flow deposits confirms their eruption late in the Waiohau eruptive phase, but burial by younger lavas of the same phase makes their precise source location impossible to determine. High density pyroclastic flows are heavily constrained by topography, and the current distribution may in part be due to the position of the Hawea Lava flows (Fig. 1) of the Okareka eruptive phase, and Eastern Dome, which extruded earlier in the same phase.

Vents within the vicinity of Kanakana Dome (Fig. 1) are the source for most of the Waiohau Pyroclastics, and the location of the block and ash flow deposits of this study are consistent with this source area. However, the block and ash flows may also have been generated further north, from either dome collapse or collapse of the steep leading

edge of a lava flow. The Pokohu Lava forms a relatively thin cap over the pyroclastic fan northeast of Mt Tarawera and is ruled out as a source based on its lack of obsidian and stratigraphic position. Older lavas beneath the Pokohu lava flow (ie those which form the escarpment at Tarawera Falls, V16/186317) must be regarded as a possible source but this is unresolvable based on field evidence.

Clast size and concentration, and the volume of the block and ash flow deposits (estimated at 2.44km^3 by Speed, 2001) suggest large-scale failure of a dome. Welded clastogenic blocks found near the top of the sequence (Figure X) within pumiceous pyroclastic flow deposits suggest incorporation of vent-derived lithics during an explosive phase. This is in agreement with Speed (2001) who suggests that eruption of the block and ash flow (referred to as debris avalanche) caused sudden decompression at the vent, leading to more explosive eruptions and the development of pyroclastic surges.

Most of the features of the deposit are consistent with generation by large-scale dome collapse. Continuous but pulsatory collapse fed block and ash flows of varying competence leading to variation in clast size and concentration within the sequence.

Significance and Further Work

While Block and ash flows are commonplace, and have been well documented as the products of dome collapse, some features of the deposits within the Waiohau sequence are more complex and deserving of special attention. The highly indurated and jointed horizons within both the BAF1 and BAF2 sequences indicate that cooling occurred as a deposit, rather than individual clasts, suggesting that little heat was lost during transport. Although no textural evidence for welding was observed, clasts are dense and mostly non-vesicular and therefore can't collapse. In the absence of a significant compactional load, the indurated nature of the deposits is hard to explain without inducing some welding process. As welded block and ash flow deposits have not been reported in the literature this is an interesting feature and worth further work.

While the level of exposure will constrain any further work on these deposits, geochemical and petrographic data may help define a source and define more clearly the

eruptive mechanism. Extensive block and ash flow deposits suggest dome collapse has been a common feature in the growth of the Tarawera massif, and are an important process to understand in any hazard assessment.

REFERENCES

CAS, R.A. F & WRIGHT, J.V. (1987) Volcanic Successions modern and ancient. Chapman and Hall, London, 528p.

COLE, J.W. (1970) Description and correlation of Holocene Volcanic Formations in the Tarawera-Rerewhakaaitu Region. Transactions of the Royal Society of New Zealand 8: 93-108

FISHER, R.V., SMITH, A.L., ROOBOL, M.J. (1980) Destruction of St. Pierre, Martinique, by ash-cloud surge, May 8 and 20, 1902. Geology 8: 472-476

LA CROIX, A. (1904) La Montagne Pelee ses eruptions. Masson, 662pp

MANLEY, C. (1992) Extended cooling and viscous flow of large, hot rhyolite lavas: Implications of numerical modelling results. Journal of Volcanology and Geothermal Research 53: 27-46

MELLORS, R.A., WAITT, R.B., SWANSON, D.A. (1988) Generation of pyroclastic flows and surges by hot-rock avalanches from the dome of Mt St Helens volcano, USA. Bulletin of Volcanology 50: 14-25

NAIRN, I.A (1981) Some studies of the geology, volcanic history, and geothermal resources of the Okataina Volcanic Centre, Taupo Volcanic Zone, New Zealand. Unpublished PhD thesis, Victoria University, New Zealand.

NAIRN, I.A (1989) Sheet V16 AC, Mount Tarawera, Rotorua. New Zealand Geological survey, Department of Scientific and Industrial Research.

NEUMANN VAN PADANG, M. (1993) De uitbarstang van den Merapi (midden Java) in de jaren 1930-1931. Ned. Indies. Dienst Mijnbouwk. Vulkan. Seism. Mededel, 12.

RICHNOW, J (1999) Eruptional and post-eruptional processes in rhyolite domes. Unpublished PhD thesis, University of Canterbury, New Zealand.

SATO, H., FUJII., T. NAKADA.S. (1992) Crumbling of dacite dome lava and generation of pyroclastic flows at Unzen Volcano. Nature 360, 664-666.

SPEED, J. A (2001) The 11.9 ka Waiohau Eruptive Episode, Okataina Volcanic Centre. Unpublished Masters thesis, University of Auckland, New Zealand.

TAKAHASHI, T. AND TSUJIMOTO, H. (2000) A mechanical model for Merapi-type pyroclastic flow. Journal of Volcanology and Geothermal Research 98: 91-115

Ui, T., Matsuwo, N., Sumita, M. and Fujinawa, A. (1999) Generation of block and ash flows during the 1990-1995 eruption of Unzen Volcano, Japan. Journal of Volcanology and Geothermal Research 89: 123-137

VAN BEMMELEN, R.W. (1949) The geology of Indonesia and adjacent archipelago. The Hague, Government Printing Office.